Special Issue Reprint

Innovative Food Products and Processing

Edited by
Bhesh R. Bhandari and Hasmadi Mamat

www.mdpi.com/journal/applsci

MDPI

Innovative Food Products and Processing

Innovative Food Products and Processing

Editors

Bhesh R. Bhandari
Hasmadi Mamat

Editors

Bhesh R. Bhandari
The University of Queensland
St. Lucia, QLD, Australia

Hasmadi Mamat
Universiti Malaysia Sabah
Kota Kinabalu, Malaysia

This is a reprint of articles from the Special Issue published online in the open access journal *Applied Sciences* (ISSN 2076-3417) (available at: https://www.mdpi.com/journal/applsci/special_issues/YDA4G578W3).

For citation purposes, cite each article independently as indicated on the article page online and as indicated below:

Lastname, A.A.; Lastname, B.B. Article Title. *Journal Name* **Year**, *Volume Number*, Page Range.

Cover image courtesy of Hasmadi Mamat

Contents

About the Editors

Bhesh R. Bhandari

Prof Bhandari is a Professor of Food Processing Technology and Engineering at the University of Queensland, Australia. He obtained his PhD from ENSIA (France) in Food Process Engineering in 1992. His major research focus is on food materials science/engineering, including the microencapsulation of food ingredients, nanotechnology, glass-transition-related issues in food processing and product systems, and the 3D printing of food materials. Prof Bhandari invented a patented continuous process to produce microgel particles that can be used to encapsulate various food functional ingredients and pharmaceutical drugs. Professor Bhandari has been listed as a "Highly Cited Researcher" every year from 2019 to 2022 by Clarivate (Web of Science) in his subject field. Professor Bhandari is a recipient of the Lifetime Achievement Award (2023), Distinguished Alumini Award (2019), Bolaike Outstanding Drying Research Award 2017, Bruce Chandler Book Award 2015 and Excellence on Drying–Applying Fundamentals to Practice 2012. Professor Bhandari also won "Top 25 Q-index" award among more than 2500 researchers at the University of Queensland. Prof Bhandari has co-authored more than 500 papers, including 9 co-edited books and 35 book chapters.

Hasmadi Mamat

Hasmadi Mamat is a Senior Lecturer at the Faculty of Food Science and Nutrition at Universiti Malaysia Sabah (UMS) in Malaysia. He earned his Ph.D. in Food Science from the University of Nottingham in the United Kingdom. He is currently the Dean of the Faculty of Food Science and Nutrition. His research interests include the characterization of food biopolymers and the production of bread items employing composite flour derived from local raw materials. With over two decades of academic experience, he has published 79 articles in high-impact journals and presented over 30 talks at national and international conferences. He is also a Research Fellow at the UMS Food Safety and Quality Unit and the UMS Seaweed Research Unit. He holds the title of Professional Technologist with the Malaysia Board of Technologists (MBOT).

Preface

Due to the change in consumption habits and the catastrophic effects of climate change, feeding the growing world population will be a significant problem for our current food systems in the coming decades. According to projections, climate change will impede the advancement of global food security by interrupting production, resulting in local availability restrictions and price increases. Demand for functional foods, special-purpose meals, convenience foods, and more palatable foods has increased due to rising food allergies, rising food consciousness, and changing consumer demographics. New food processing and preservation methods are being investigated and implemented in order to meet some of these demands.

This Special Issue focuses on R&D linked to novel food products (functional foods or functional components) or processes that fuse the development of contemporary processing and preservation technologies with fundamental understandings of food science and technology. The articles that have been published in this Special Issues address a wide range of subjects and applications, including the utilization of food chemistry, biochemistry, fermentation, microbiology, new modern processing and preservation technologies, as well as new processing techniques for efficient waste management and green technology for the food processing industry.

The launch of this Special Issue coincided with the International Conference on Food Science and Nutrition 2022 (ICFSN 2022), which was successfully hosted by the Faculty of Food Science and Nutrition, Universiti Malaysia Sabah on the 24th and 25th of August 2022. The conference, themed "Future Food: Emerging Trends, Health, and Diversity," provided an invaluable platform for experts and specialists from around the world to share knowledge, experiences, innovative ideas, and the most recent research in food science and technology, food service, and nutrition. We extend our heartfelt gratitude to the entire Organizing Committee of ICFSN 2022 for their unwavering commitment and dedication, ensuring the smooth execution of the conference.

Finally, we would like to take this opportunity to express our sincere appreciation for the hardworking staff of the MDPI Book, the outstanding editorial board of the *Applied Sciences* journal, with special mention to Ms. Freda Wu, the assistant editor of this remarkable Special Issue, as well as our brilliant authors and diligent, highly-skilled reviewers. This Special Issue would not have been possible without your vital efforts, and we sincerely appreciate your continuous support throughout.

Bhesh R. Bhandari and Hasmadi Mamat
Editors

Editorial

Special Issue on Innovative Food Products and Processing

Hasmadi Mamat [1],* and Bhesh R. Bhandari [2]

[1] Faculty of Food Science and Nutrition, Universiti Malaysia Sabah (UMS),
   Kota Kinabalu 88400, Sabah, Malaysia
[2] School of Agriculture and Sustainability, The University of Queensland, St. Lucia, QLD 4072, Australia
* Correspondence: idamsah@ums.edu.my

The food industry is experiencing a significant transformation, driven by evolving consumer preferences, sustainability concerns, and technological advancements. This revolution involves introducing innovative food products and processing techniques that cater to changing tastes, improve nutritional value, ensure food safety, better utilize food waste as well as byproducts, and reduce environmental impact.

In this Special Issue, much focus has been placed on research and development (R&D) related to innovative food products, including functional foods or ingredients, as well as processes that integrate fundamental knowledge of food science and technology with emerging processing and preservation technologies. For instance, encapsulation techniques are used to protect sensitive nutrients during food processing and storage, targeted delivery preserving their effectiveness and nutritional benefits [1]. Emulsifiers derived from soybean lecithin and pea protein isolate are being studied for their capacity to encapsulate as well as emulsify antimicrobial molecules under different pH conditions and drying methods [2].

The increasing emphasis on healthy lifestyles has influenced the food and beverage industry. A formulation for a potentially functional beverage mixture with low energy content has been developed to cater to personalized nutrition, children, athletes, and older individuals [3]. Additionally, there is a consumer preference for reduced salt content in food and beverages. Incorporating seaweed into reduced salt patties has been found to enhance textural properties while maintaining an acceptable taste profile [4].

Emerging modern processing techniques are revolutionizing the food industry by enhancing quality, safety, and sustainability. Process optimization plays a crucial role in improving efficiency, product quality, safety, and sustainability. For example, there have been proposed optimizations of oligosaccharide preparation from underutilized red seaweed through thermal hydrolysis [5] and the study of factors that influence stabilization processes in amaranth purees and brandies [6,7]. Furthermore, research has explored the potential of using bambangan, a tropical fruit, as a cocoa butter replacer, offering an alternative fat source for food applications [8].

Advancements have also been made in gluten-free bakery products to improve their taste, texture, and nutritional profiles. New flours and ingredients are being utilized to create gluten-free alternatives that closely resemble traditional wheat-based products [9]. Bakery items can also be transformed into functional foods by incorporating ingredients and fortification techniques that provide additional health benefits beyond basic nutrition [10,11].

Additionally, the utilization of byproducts as food ingredients is gaining attention for its potential to reduce waste, enhance sustainability, and create value-added products. Byproducts from various food processing industries can be upcycled into valuable ingredients, supporting a circular and efficient food system. For example, byproducts of canned pulse liquids have shown promise as egg white replacers in the development of various food products, and needlefish skin collagen possesses potential industrial applications [12,13].

Overall, these innovations are reshaping the food industry, offering improved products, sustainable practices, and novel approaches to meet the evolving needs and preferences of consumers.

References

1. Koh, W.Y.; Lim, X.X.; Tan, T.-C.; Kobun, R.; Rasti, B. Encapsulated Probiotics: Potential Techniques and Coating Materials for Non-Dairy Food Applications. *Appl. Sci.* **2022**, *12*, 10005. [CrossRef]
2. Baghi, F.; Ghnimi, S.; Dumas, E.; Gharsallaoui, A. Microencapsulation of Antimicrobial trans-Cinnamaldehyde: Effect of Emulsifier Type, pH, and Drying Technique. *Appl. Sci.* **2023**, *13*, 6184. [CrossRef]
3. Habschied, K.; Nišević, J.; Krstanović, V.; Lončarić, A.; Valek Lendić, K.; Mastanjević, K. Formulation of a Wort-Based Beverage with the Addition of Chokeberry (*Aronia melanocarpa*) Juice and Mint Essential Oil. *Appl. Sci.* **2023**, *13*, 2334. [CrossRef]
4. Pindi, W.; Qin, L.W.; Sulaiman, N.S.; Mohd Zaini, H.; Munsu, E.; Wahab, N.A.; Mohd Noor, N.Q.I. Effects of Salt Reduction and the Inclusion of Seaweed (*Kappaphycus alvarezii*) on the Physicochemical Properties of Chicken Patties. *Appl. Sci.* **2023**, *13*, 5447. [CrossRef]
5. Padam, B.S.; Siew, C.K.; Chye, F.Y. Optimization of an Innovative Hydrothermal Processing on Prebiotic Properties of Eucheuma denticulatum, a Tropical Red Seaweed. *Appl. Sci.* **2023**, *13*, 1517. [CrossRef]
6. Mohd Amin, S.F.; Karim, R.; Yusof, Y.A.; Muhammad, K. Effects of Metal Concentration, pH, and Temperature on the Chlorophyll Derivative Content, Green Colour, and Antioxidant Activity of Amaranth (*Amaranthus viridis*) Purees. *Appl. Sci.* **2023**, *13*, 1344. [CrossRef]
7. Muñoz-Redondo, J.M.; Puertas, B.; Valcárcel-Muñoz, M.J.; Rodríguez-Solana, R.; Moreno-Rojas, J.M. Impact of Stabilization Method and Filtration Step on the Ester Profile of "Brandy de Jerez". *Appl. Sci.* **2023**, *13*, 3428. [CrossRef]
8. Ridhwan, N.M.; Mamat, H.; Akanda, M.J.H. Fatty-Acid Profiles, Triacylglycerol Compositions, and Crystalline Structures of Bambangan-Seed Fat Extracted Using Different Solvents. *Appl. Sci.* **2022**, *12*, 8180. [CrossRef]
9. Lee, J.-S.; Yusoff, N.; Ho, A.L.; Siew, C.K.; Akanda, J.H.; Tan, W.X. Quality Improvement of Green Saba Banana Flour Steamed Cake. *Appl. Sci.* **2023**, *13*, 2421. [CrossRef]
10. Ronie, M.E.; Abdul Aziz, A.H.; Mohd Noor, N.Q.I.; Yahya, F.; Mamat, H. Characterisation of Bario Rice Flour Varieties: Nutritional Compositions and Physicochemical Properties. *Appl. Sci.* **2022**, *12*, 9064. [CrossRef]
11. Zakaria, M.K.; Matanjun, P.; George, R.; Pindi, W.; Mamat, H.; Surugau, N.; Seelan, J.S.S. Nutrient Composition, Antioxidant Activities and Glycaemic Response of Instant Noodles with Wood Ear Mushroom (*Auricularia cornea*) Powder. *Appl. Sci.* **2022**, *12*, 12671. [CrossRef]
12. Donatus, F.; Sintang, M.D.B.; Julmohammad, N.; Pindi, W.; Ab Wahab, N. Physicochemical and Sensory Properties of Bahulu and Chocolate Mousse Developed from Canned Pulse and Vegetable Liquids. *Appl. Sci.* **2023**, *13*, 4469. [CrossRef]
13. Ramle, S.Z.; Oslan, S.N.H.; Shapawi, R.; Mokhtar, R.A.M.; Noordin, W.N.M.; Huda, N. Biochemical Characteristics of Acid-Soluble Collagen from Food Processing By-Products of Needlefish Skin (*Tylosurus acus* melanotus). *Appl. Sci.* **2022**, *12*, 12695. [CrossRef]

Microencapsulation of Antimicrobial *trans*-Cinnamaldehyde: Effect of Emulsifier Type, pH, and Drying Technique

Fatemeh Baghi [1,2], Sami Ghnimi [1,2], Emilie Dumas [1] and Adem Gharsallaoui [1,*]

[1] Univ Lyon, Université Claude Bernard Lyon 1, CNRS, LAGEPP UMR 5007, 69622 Villeurbanne, France
[2] ISARA, Higher Institute of Agriculture and Agri-Food Rhone-Alpes, 23 Rue Jean Baldassini, 69007 Lyon, France
* Correspondence: adem.gharsallaoui@univ-lyon1.fr

Abstract: Two plant-based emulsifiers, soybean lecithin and pea protein isolate, were studied for their emulsifying and encapsulating capacities of an antimicrobial molecule, *trans*-cinnamaldehyde (TC), at two different pH values, three and seven, and after drying with two different techniques, spray-drying and freeze-drying. To characterize the obtained capsules, various physicochemical tests were conducted to examine particle size, encapsulation efficiency, thermal and moisture stability, and powder morphology. The spray-dried (SD) and freeze-dried (FD) powders had an average particle size of 8.35 μm and 144.49 μm, respectively. The SD powders showed similar encapsulation efficiency (EE) for soybean lecithin and pea protein isolate with an average value of 95.69%. On the other hand, the FD powders had lower EE compared to SD powders, with an average of 58.01% for lecithin-containing powders and 83.93% for pea-protein-containing powders. However, the water content of FD powders (2.83%) was lower than that of SD powders (4.72%). The powders prepared at pH 3 showed better thermal stability. Morphological analysis showed spherical particles for SD powders and irregular shapes for FD powders. Nanoemulsions as well as dried powders showed interesting antimicrobial activities against *Escherichia coli* and *Listeria innocua*, confirming their potential use as natural preservatives in foods.

Keywords: microencapsulation; nanoemulsion; *trans*-cinnamaldehyde; spray-drying; freeze-drying

1. Introduction

The use of essential oils (EOs) as natural bioactive agents to reduce the use of synthetic preservatives in the food industry has gained much attention recently. EOs can be extracted from different parts of plants and have promising biological properties including antimicrobial, antioxidant, and antifungal activities. The effect of different EOs on extending the shelf life of foodstuff has long been recognized [1]. However, the use of EOs has some limitations because they are aromatic and volatile substances that are sensitive to oxygen, light, and high temperatures undergone during certain food processes [2]. Encapsulation is a promising technique to overcome these drawbacks through encasing substances in a solid or liquid wall material. Encapsulation has been widely used for the protection of bioactive compounds [3]. It is an interesting technique that has many advantages, such as the possibility of controlled release of the bioactive agent, targeted delivery, and increased biological function of the active substances [4–6]. Further, it is reported that the antimicrobial activity of essential oils increases via encapsulation into surfactant micelles due to their enhanced dispersibility in the aqueous phase [7]. Therefore, encapsulation is used to preserve the EOs against harsh conditions and mask their undesirable tastes and odors. There is evidence that the biological activities of EOs are enhanced via micro- and nanoencapsulation due to the larger active surface area formed [8]. Among about 3000 EOs estimated, trees and shrubs of cinnamon (*Cinnamomum verum*) are an important source of EOs. While many parameters can influence the composition of cinnamon EO,

trans-cinnamaldehyde (TC) (trans-3-phenyl-2-propenal) is generally the major component in the extracted oil (60–75% of the total oil) and demonstrates good antimicrobial activity against pathogenic microorganisms [9]. *trans*-Cinnamaldehyde emulsions applied to real food systems such as watermelon juice showed significant growth inhibition of *Salmonella typhimurium* and *Staphylococcus aureus* [10].

Certain factors must be considered in designing an appropriate encapsulation technique. Appropriate encapsulating agents, temperature, and drying methods are the most important factors for the encapsulation process [11]. Wall material is one of the main factors in the design of an encapsulation system. Maltodextrin is a hydrolyzed starch produced through the partial hydrolysis of starch with acid or enzymes. It is commonly used as a wall material in the microencapsulation of food ingredients. It is a substance with neutral aroma and taste that protects bioactive molecules against oxidation [12]. Low viscosity at high solids concentrations and relatively low cost are the other advantages of maltodextrin that make it a good choice to carry EOs. However, maltodextrin possesses a low emulsifying capacity and marginal retention of volatiles; that is why an emulsifier is needed when this wall material is used to encapsulate oily compounds. Soybean lecithin is a natural amphiphilic molecule that is a mixture of phospholipid derivatives and has recently received much attention as a potential natural emulsifier [13]. Lecithin has both hydrophilic and lipophilic properties, and its hydrophobic part could adsorb to the surface of oil droplets, while its hydrophilic heads tend to interact with water to promote dispersion [14]. Therefore, lecithin can improve the dispersion of the oil phase in water and create a stable emulsion [15,16]. Furthermore, the use of pea protein as an emulsifier has been previously investigated as an attractive seed storage protein source for emulsifying applications due to its nutritional value, good functional properties, and non-allergic nature. In addition, there is evidence that pea protein can be used to produce stable emulsions [17]. To obtain dry microcapsules, the two most appropriate methods to preserve bioactive compounds are spray-drying and freeze-drying. Processing the emulsions into powders increases their stability and their ease of storage and expands their range of applications [18]. Other studies have shown that both drying methods can preserve heat-sensitive bioactive components [11,19,20].

The present study investigated the effect of emulsifier type, pH, and drying method on the production of TC microcapsules. Soybean lecithin and pea protein isolate were used as emulsifiers at different pHs (pH 3 and pH 7). SD and FD powders were produced from the nanoemulsions, and their physical, thermal and antimicrobial properties were assessed to identify the most suitable microencapsulation strategy to produce TC microcapsules with high potential for use as a natural preservative in foods.

2. Materials and Methods

2.1. Materials

Granular soybean lecithin was obtained from Acros Organics (Geel, Belgium). Powdered pea protein isolate and maltodextrin (DE28) were obtained from Roquette-frères SA (Lestrem, France). *trans*-cinnamaldehyde (CA, 99%) was purchased from Sigma-Aldrich (St Quentin Fallavier, France). Analytical grade imidazole, acetic acid, sodium hydroxide, and hydrochloric acid were purchased from Sigma Chemical Co. (Schnelldorf, Germany). Hydranal coulomat was obtained from Fluka Analytical, Sigma Chemical Co. (Germany). Distilled water was used for the preparation of all solutions and emulsions.

2.2. Preparation of Nanoemulsions (NE)

For the preparation of lecithin-based emulsions, 5% (w/w) TC was mixed with 1% (w/w) soybean lecithin and dispersed in buffer solutions (imidazole/acetate, 5 mmol/L) at two different pHs, 3 and 7, and then emulsified separately. For pea protein emulsions, 1% (w/w) of pea protein isolate was first added into buffer solutions through adjusting the pH (3 or 7) and stirring at room temperature until the proteins were completely dissolved. Then, the insoluble part of the pea proteins was separated via centrifuging at 5000 rpm for 5 min. The coarse emulsions stabilized using lecithin or pea protein were prepared using a

high-speed homogenizer (Polytron Pt 2500 E, Kinematica, Switzerland) for 6 min under 18,000 rpm. Finally, fine emulsions were obtained via passing coarse emulsions through a microfluidizer (Microfluidizer LM20, Microfluidics Corp, Newton, MA, USA) twice at 500 bar and once at 1000 bar. At the end, four different emulsions were obtained: two of them were emulsified using soybean lecithin at pH 3 and pH 7, and two other emulsions were emulsified using pea protein at pH 3 and pH 7. Table 1 shows the abbreviations of the emulsion samples.

Table 1. Abbreviations for samples of emulsions and dried powders.

Sample Abbreviation		Buffer pH	Emulsifier	Drying Method
Emulsions	L3	3	Lecithin	-
	L7	7	Lecithin	-
	P3	3	Pea protein	-
	P7	7	Pea protein	-
Powders	L3S	3	Lecithin	Spray-dryer
	L7S	7	Lecithin	Spray-dryer
	P3S	3	Pea protein	Spray-dryer
	P73	7	Pea protein	Spray-dryer
	L3L	3	Lecithin	Freeze-dryer
	L7L	7	Lecithin	Freeze-dryer
	P3L	3	Pea protein	Freeze-dryer
	P7L	7	Pea protein	Freeze-dryer

2.3. Preparation of Microcapsules

Nanoemulsions were mixed for at least 30 min with 30% (w/w) maltodextrin solution in buffer solution (imidazole/acetate, 5 mmol/L) at two different pHs, 3 and 7, at ratio 1:1 (w/w). Each emulsion was mixed with a maltodextrin solution having the same pH. Next, the emulsion–maltodextrin mixture solution was divided into two parts for drying with two different techniques. The moiety of this mixture solution was dried in a laboratory-scale spray-dryer equipped with a 0.5 mm nozzle atomizer (Mini spray-dryer B-290, BUCHI, Buchegg, Switzerland). The mixture solution was pumped to the spray-dryer at a feed rate of 1 L/h at room temperature and dried at an inlet temperature of 180 °C and an outlet temperature of 80 °C with an air pressure of 3.2 bar. The other moiety of the mixture solution was dried with a laboratory-scale freeze dryer (Lyovapor™ L-200 Pro, BUCHI, Buchegg, Switzerland) operating at a vacuum pressure of 0.08 mbar and condensing temperature of −54 °C. Before freeze-drying, the mixture solution was frozen at −20 °C for at least 12 h. The freeze-drying process took 4 days to completely dry the samples. All dried powders were collected and stored in airtight containers at 4 °C for further analysis. Figure 1 shows a schematic representation of the preparation procedure and Table 1 shows the abbreviations of the SD and FD samples.
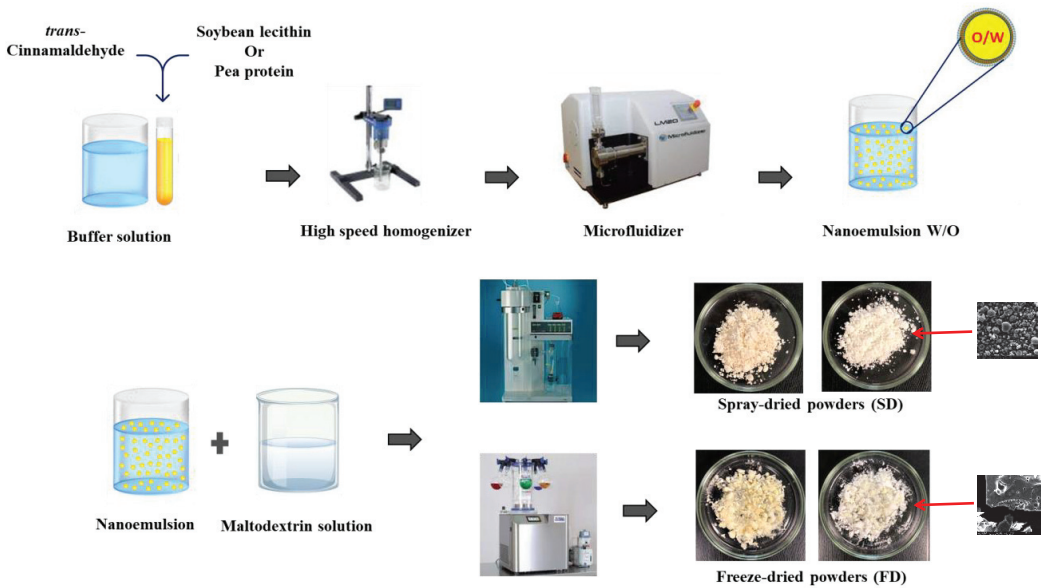
Figure 1. Schematic representation of the different steps of the TC microcapsule preparation procedure.

2.4. Characterization of Nanoemulsions and Microcapsules

2.4.1. Size Distribution of Emulsions and Microcapsules

Droplet size and size distribution of nanoemulsions were determined via dynamic light scattering (DLS) using a Zetasizer Nano-ZS90 (Malvern Instruments Ltd., Worcestershire, UK) at a fixed angle of 90°. One mL of the emulsion was added into 10 mL of distilled water and homogenized in order to eliminate multiple scattering effects. After 90 s of equilibrium, the measurement was performed. The measurements were repeated three times and the average droplet size and average polydispersity index (PDI) were calculated.

The diameter of dried powders was measured via low-angle laser light scattering using a Malvern Mastersizer 3000 instrument (Malvern Instruments Ltd., Worcestershire, UK). The samples were dispersed in absolute ethanol via vortexing before analyses. Particle size distributions were calculated from Mie's theory using the refractive indices of ethanol (1.361) and Maltodextrin (1.673). Mean size was expressed as the mean diameter $D[4,3]$ of the particle size distribution. To give more information about the size distributions, the values of D_{10}, D_{50}, and D_{90}, which indicate diameters of 10%, 50%, and 90% of the volume of the particle group, were recorded. To calculate the width of the size distribution, Equation (1) was used. All measurements were performed at least in triplicate for each sample.

$$\text{Span} = \frac{(D_{90} - D_{10})}{D_{50}} \tag{1}$$

where D_{90}, D_{10}, and D_{50} are the equivalent volume diameters at 90%, 10%, and 50% cumulative volume, respectively.

2.4.2. Zeta Potential (ζ)

The Zeta potential of emulsions was measured using Zetasizer equipment (Malvern Instruments Ltd., Worcestershire, UK) with disposable cuvettes for electrophoretic mobility measurement. The samples were prepared through diluting 1 mL of the emulsion in 10 mL of distilled water and homogenized completely. Zeta potential measurement was performed in triplicate and the mean value was calculated.

2.4.3. Encapsulation Efficiency of TC

Encapsulation efficiency (EE) of powders was measured according to the method described by Hogan et al. [21] with some modifications. Non-encapsulated TC was measured via mixing 5 g of dried powder in 25 mL of pure ethanol for 60 s. The ethanol-dissolved TC was obtained via filtration through Whatman filter paper (grade 4). The ethanol was then removed through drying at 103 °C for 24 h. The non-encapsulated TC was determined gravimetrically. The total TC content in microcapsules was obtained via dissolving 5 g of dried powder into 50 mL of HCL (1 mol/L) through stirring into a boiling water bath for 30 min. Total TC was recovered via filtration using a Whatman filter paper (grade 1). The filter was washed with ethanol in order to collect TC. Another filtration step was performed for removing the remaining residual using Whatman filter paper (grade 4). Total TC was determined through removing ethanol at 103 °C and weighing precisely. To calculate EE, this Equation (2) was used:

$$EE(\%) = \frac{(\text{Total TC} - \text{Non encapsulat TC})}{\text{Total TC}} \times 100 \qquad (2)$$

2.4.4. Surface Morphology of the Microcapsules

Scanning electron microscopy (SEM) (FEI Quanta 250 FEG, Thermo Fisher Scientific, Hillsboro, OR, USA) was used to obtain the morphology of the microcapsules. Measurements were performed at the "Centre Technologique des Microstructures" (CTμ) at the University of Lyon 1 (Villeurbanne, France). Powders were deposited on a flat steel holder. The samples were coated under a vacuum via cathodic sputter before microscopy analysis at magnification of 3000×.

2.4.5. Water Content

Water content determination for dried microcapsules was realized using the Karl Fischer (KF) titration technique. This technique was performed using an 899 KF Coulometer (Metrohm, Villebon Courtaboeuf, France) coupled with an 860 KF Thermoprep oven (Metrohm, Herisau, Switzerland). Hydranal coulomat was used as a reagent. Samples were weighed at approximately 40 mg, and the standard deviation was calculated from at least three replicate measurements.

2.4.6. Thermogravimetric Analysis (TGA)

The thermal behavior of TC microcapsules was determined via thermogravimetric analysis (TGA) using a thermogravimetric analyzer (TG 209, Netzsch Co., Selb, Germany). Alumina crucibles were filled with accurately weighed samples of about 10 mg. The temperature program ranged from 20 °C to 600 °C at a heating rate of 10 °C/min. All experiments were conducted under a nitrogen atmosphere of 20 mL/min flow rate. The weight loss was recorded as a function of temperature and time.

2.4.7. Attenuated Total Reflectance Fourier Transform Infrared (ATR-FTIR) Spectroscopy

The samples were analyzed using an FTIR spectrophotometer coupled with ATR (FTIR: Nicolet iS50, Thermo Scientific, Waltham, MA, USA). All FTIR spectra were carried out at a resolution of 4 cm^{-1} with 64 scans in the spectral range of 4000–400 cm^{-1}.

2.4.8. Antimicrobial Activity

The antimicrobial activity of emulsions and powders was investigated using the agar well diffusion method on the Gram-positive bacteria *Listeria innocua* (DSM20649) and the Gram-negative bacteria *Escherichia coli* (DSM613). Strains were stored at −20 °C in Tryptone Soy Broth (TSB) (Biokar diagnostics, Beauvais, France) with 20% (*v/v*) of glycerol. One milliliter of the stock culture was transferred to 9 mL of TSB and incubated for 7 h at 37 °C. One milliliter of this pre-culture was transferred into 9 mL of TSB and incubated overnight at 37 °C. Finally, one milliliter of this culture was transferred to 9 mL of TSB and incubated

for 5 h at 37 °C. The culture was then diluted to a concentration of 10^{-5} CFU/mL and incorporated at 5% in Tryptone Soy Agar (TSA, Biokar, Allonne, France). A hole with a diameter of 6 mm was punched aseptically with a sterile tip. Amounts of 30 mg of powder samples or 80 μL of each emulsion, which contains the same mass equivalent of TC, were introduced into the wells. Then, the agar plates were incubated at 37 ± 1 °C for 24 h. The diameter of the inhibition zone around the hole was measured. The measurement was performed in triplicate for each sample.

2.5. Statistical Analysis

All tests were performed at least in triplicate. The data were presented as means $\pm$ standard deviation for different samples. One-way analysis of variance (ANOVA) was used, followed by Fisher's test (F) to compare the means. The difference was considered significant at $p < 0.05$.

3. Results

3.1. Characterization of Nanoemulsions

3.1.1. Particle Size and Homogeneity of Emulsions

Particle size and size distribution of emulsions are important parameters to consider because of their effect on the activity and stability of loaded compounds and their release [22]. The average particle size and the polydispersity index (PDI) of the tested emulsions are shown in Table 2. Whatever the pH value, the emulsions stabilized using lecithin had a smaller particle size compared to those stabilized using pea protein. Lecithin resulted in an average size of about 0.11 μm and 0.09 μm at pH 3 and 7, respectively, whereas the average size of pea protein emulsions was 0.22 μm at pH 3 and 0.62 μm at pH 7. The smaller particle size of emulsions stabilized using lecithin could be attributed to the high efficiency of lecithin as an amphiphilic molecule to form water-in-oil (W/O) emulsions [23]. Furthermore, the same concentration of lecithin and pea protein was used in each emulsion. However, pea protein contains a non-soluble portion with no emulsifying effect that was separated before the emulsion was prepared. This reduced the final concentration of pea protein as an emulsifying agent compared to emulsions made with lecithin. Similar results were obtained by [24], who studied the effect of the emulsifier and obtained the smallest particle with lecithin compared to pea protein. A slight difference in particle size was observed depending on the pH. Among the four tested emulsions, the smallest particle size (0.09 μm) was obtained with lecithin at pH 7. For emulsions prepared with pea protein, the smallest particle size (0.22 μm) was obtained at pH 3, and particle size at pH 7 was significantly bigger (0.62 μm). In fact, the pH could be decreased during the dispersion of TC to approach the isoelectric point of pea protein (PI = 4.3), leading to droplet aggregation and an increase in the measured size. Indeed, despite the pH adjustment to 7 after emulsification, the droplets might not completely dissociate [25].

Table 2. Physical properties of nanoemulsions. For results with the same letter, the difference between the means is not statistically significant.

Sample	Size (μm)	PDI	Zeta Potential (mV)
L3	0.11 $\pm$ 0.02 [c]	0.17 $\pm$ 0.02 [c]	-39.96 ± 1.16 [c]
L7	0.09 $\pm$ 0.01 [d]	0.21 $\pm$ 0.02 [bc]	-47.83 ± 1.36 [d]
P3	0.22 $\pm$ 0.02 [b]	0.25 $\pm$ 0.04 [b]	28.93 $\pm$ 1.13 [a]
P7	0.62 $\pm$ 0.06 [a]	0.61 $\pm$ 0.03 [a]	-29.73 ± 0.58 [b]

3.1.2. Zeta Potential of Emulsions

Zeta potential was measured in order to assess emulsion stability. Zeta potential analysis is used as an indicator of the surface charge of particles. The value of the zeta potential provides an indication of the potential stability of the colloidal system. When the particles in the suspension have a high negative or positive zeta potential, they tend to

repel each other, which prevents the aggregation of the droplets and the flocculation of the emulsion. It is generally considered that emulsions having zeta potential values higher than 30 mV (absolute value) are stable [26]. The zeta potential values of the tested emulsions are presented in Table 2, and results show that the average zeta potential (absolute value) measured for all emulsions is high enough to induce emulsion stability. The emulsions stabilized using lecithin had a zeta potential of -39.96 ± 1.16 and -47.83 ± 1.36 mV at pH 3 and 7, respectively, and tended to be more stable than those emulsified using pea protein with a zeta potential of $+28.93 \pm 1.13$ and -29.73 ± 0.58 mV at pH 3 and 7, respectively. The emulsion prepared at pH 7 had a higher value of zeta potential, indicating that this pH is more appropriate for the preparation of emulsions. This result is in accordance with those of the study by Yang et al. [14] that measured zeta potential values comprised between -33.7 and -58.6 mV for different formulations of emulsions prepared with 2% soybean lecithin and 10% essential oils.

3.2. Characterization of Microcapsules
3.2.1. Particle Size and Homogeneity of Microcapsules

The effect of emulsifier type, pH, and drying method on the particle size of dried capsules was evaluated. Table 3 illustrates the volume-weighted average size D[4,3] and some further information about size distribution. The width of the size distribution is shown with span DX values that signify the point in the size distribution, indicating how far the 10 percent and 90 percent points are apart, normalized with the midpoint. The values of these parameters differed depending on the drying method. In contrast, different emulsifying agents and pH did not result in a significant difference in particle size. All SD powders had significantly smaller sizes compared to those dried via FD. SD powders had an average size between 8.00 μm and 8.87 μm. However, FD powders showed an average size between 140.82 μm and 148.21 μm. This is due to the dispersion of the emulsion under pressure during the spray-drying process, which certainly induced a smaller particle size and a smaller width of the size distribution presented by span, whereas for freeze-dried powders, the emulsions were frozen and then the ice was evaporated *via* sublimation without having a dispersion step.

Table 3. Particle size, size distribution, encapsulation efficiency, and water content of microcapsules. For results with the same letter, the difference between the means is not statistically significant.

Sample	D[4,3] (μm)	Dx (10) (μm)	Dx (50) (μm)	Dx (90) (μm)	Span	EE%	Water Content %
L3S	8.87 ± 0.94 [c]	3.14 ± 0.17 [e]	7.42 ± 0.16 [d]	16.04 ± 0.73 [c]	1.73 ± 0.06 [d]	95.46 ± 0.02 [ab]	5.02 ±0.16 [a]
L7S	8.29 ± 0.04 [c]	3.30 ± 0.01 [e]	7.31 ± 0.05 [d]	14.8 ± 0.10 [c]	1.56 ± 0.004 [d]	97.28 ± 0.60 [a]	4.85 ± 0.07 [a]
P3S	8.27 ± 0.03 [c]	3.11 ±0.08 [e]	7.19 ± 0.01 [d]	15.06 ± 0.08 [c]	1.66 ± 0.009 [d]	95.84 ± 1.84 [ab]	4.84 ± 0.06 [a]
P7S	8.00 ± 0.4 [c]	3.28 ±0.01 [e]	6.98 ± 0.05 [d]	14.24 ± 0.05 [c]	1.56 ± 0.004 [d]	94.16 ± 1.19 [ab]	4.18 ± 0.09 [b]
L3L	148.21 ± 14.82 [a]	30.58 ± 2.38 [a]	106.84 ± 5.51 [b]	337 ± 45.02 [a]	2.85 ± 0.28 [b]	51.91 ± 8.58 [d]	2.29 ± 0.17 [d]
L7L	140.82 ± 11.18 [a]	25.26 ± 1.69 [c]	102 ± 4.51 [c]	321.21 ± 33.07 [a]	2.89 ± 0.18 [b]	64.09 ± 6.93 [c]	2.03 ± 0.01 [e]
P3L	141.12 ± 2.49 [b]	28.16 ± 0.78 [b]	111.2 ± 2.49 [a]	248.25 ± 6.05 [b]	1.97 ± 0.01 [c]	84.07 ± 9.12 [ab]	3.47 ± 0.06 [c]
P7L	147.83 ± 14.07 [a]	22.80 ± 0.93 [d]	99.62 ± 3.49 [c]	354.8 ± 47.74 [a]	3.32 ± 0.37 [a]	83.78 ± 13.19 [b]	3.54 ± 0.31 [c]

3.2.2. Encapsulation Efficiency

Encapsulation efficiency is the main parameter to evaluate the best combination of the three factors to encapsulate TC, namely acidity, emulsifier type, and drying method. The percentage of EE is presented in Table 3. As shown, the SD powders possessed a good encapsulation efficiency of over 94%. This efficiency was slightly higher for lecithin than for pea protein, which could be attributed to the smaller size of lecithin-stabilized emulsions compared to that of emulsions stabilized using pea protein. The SD powders had higher EE% than FD powders. This result could be explained by the good re-dispersibility of particles during spray-drying. In addition, this technique is a quick process and water evaporation happens instantly, which allows for better encapsulation efficiency. There were no significant differences between the EE of SD powders, whatever the used emul-

sifier. However, the EEs of FD pea protein emulsions (84.07 and 83.78% at pH 3 and 7, respectively) were higher ($p < 0.05$) than those of the lecithin-emulsified FD powders (51.91 and 64.09% at pH 3 and 7, respectively). This result indicates that the type of emulsifier did not have significant effect on the EE% of SD powders, while pea protein allowed a better EE% than lecithin for FD powders. These results are in agreement with the research study conducted by Talon et al. [27] that showed encapsulation efficiencies of about 95–98% when encapsulating eugenol via spray-drying using whey protein or soy lecithin and maltodextrin in combination with oleic acid and chitosan. In addition, SD citral microcapsules containing dextrin as an encapsulating agent and soy lecithin as emulsifier presented EEs ranging from 97.70 to 99.9% for different ratios of dextrin and citral [28]. In contrast, Murali et al. [29] demonstrated that the EE of black carrot juice with maltodextrin using SD ranged between 60 to 87% depending on the different temperatures applied, compared to FD, which resulted in an EE of 98.5%. Among all the powders we obtained, there were no big differences in EE between powders made at pH 3 or 7 except for the L3L and L7L samples. This could be due to a greater stability of the L7 emulsion compared to the L3 emulsion, according to the zeta potential values.

3.2.3. Water Content

Drying conditions have an important effect on the moisture content of dried capsules. However, the composition of the formulations can also lead to changes in the water content, which will affect the properties of the dried product [30]. Indeed, the moisture content is an important variable in the shelf life of powders. Table 3 shows the percentage of water content in dried powders. The powders that were dried via SD contained more water compared to the powders dried via FD. Among SD powders, no considerable difference in water content was observed. The water content of SD powders ranged from 4.18% for P7S to 5.02% for L3S. This indicates that the emulsifier tested in this study does not have a big effect on the final water content of powders, except for P7S, which contains a slightly lower amount of water of 4.18%. Monteiro Filho et al. [31] showed that the water content of SD microparticles containing essential oils from *Varronia Verbenaceae* and *Achyrocline satureioides* ranged from 3.4 to 5.2% in various storage conditions. In another study [30], SD microcapsules of clove extract with different formulations, two surfactants, and three drying carriers were obtained, and the sample with maltodextrin as the drying carrier showed a moisture content of 4.06%. Among the obtained FD powders, powders prepared using lecithin as emulsifier contained lesser amounts of water. Indeed, L7L and L3L contained 2.03 and 2.29% water, respectively. This is about half of the water content of powders emulsified using pea protein. However, there was no significant difference ($p > 0.05$) between pea protein-emulsified FD powders at different pHs. The obtained water content was 3.53 and 3.59% for P7L and P3L, respectively, which is in agreement with the EE results. In fact, emulsions stabilized using lecithin and dehydrated via freeze-dryer had lower encapsulation efficiency than those emulsified using pea protein. Small variations were observed between powders produced at different pHs for all powders dried using the same drying method. The powders prepared at pH 3 had slightly more water content compared to the powders prepared at pH 7. In general, spray-drying and freeze-drying processes produce powders with lower water content for a longer storage period. In addition, this property is also important in our case because when microcapsules are added to food matrices, they should not significantly modify the water activity of these foods and, consequently, their physicochemical properties. Another study reported similar results with moisture content ranging from 2.7% to 5.0% in the encapsulation process of orange oil using freeze-drying [32]. This result related to water/encapsulating material interactions will be confirmed using thermogravimetric analysis (next section).

3.2.4. Thermogravimetric Analysis (TGA)

The thermal stability of the dried powders was determined using thermogravimetric analysis (Figure 2). The powders' weight loss data are summarized in Table 4. All dried

powder samples generally exhibited the same dehydration trend and decomposition phases as the conventional thermogravimetric profile of carbohydrates. Weight loss occurred in three main stages. The initial weight loss up to 100 °C corresponds to the evaporation of water and adsorbed volatile compounds or non-encapsulated oil from the powders. The weight loss of this first stage varied between 6.31% and 7.07%. There is no significant difference between the different powders. The second stage of thermal degradation corresponds to the decomposition of the carrier. It coincides with the loss of essential oil. The powders prepared at pH 3 presented higher temperatures in this step. This could be due to the higher concentrations of H$^+$ ions in acidic solutions that could cause more hydrogen-bonding interactions. Finally, the third stage of thermal degradation corresponds to the thermal decomposition of the organic compounds or inert carbonaceous residues. The principal weight loss occurred during this last step for all samples. The average weight loss for all powders was 58.72 ± 0.68%. These results are similar to the data reported by Volić et al. [33], who encapsulated thyme essential oil via freeze-drying using whey protein nanocarriers. They observed the weight loss over three stages, of which the third stage corresponded to a weight loss of about 80% of their mass.
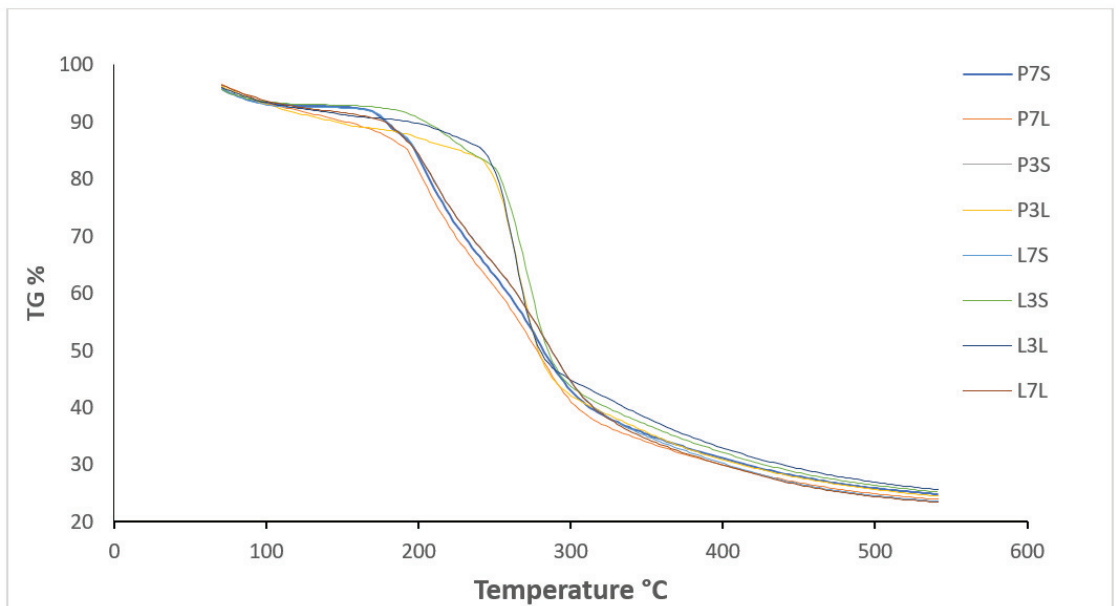
Figure 2. TG curves of microcapsules of *trans*-cinnamaldehyde (SD and FD powders).

Table 4. The weight loss temperature (Tm) and mass loss (%) of microcapsules. For results with the same letter, the difference between the means is not statistically significant.

Sample	Step 1		Step 2		Step 3	
	T (°C)	Mass Loss (%)	T (°C)	Mass Loss (%)	T (°C)	Mass Loss (%)
L3S	100.62	6.53 ± 0.02 [d]	245.37	16.49 ± 0.7 [a]	297.95	57.58 ± 0.21 [f]
L7S	100.67	7.07 ± 0.02 [a]	194.46	12.46 ± 0.37 [d]	313.12	59.37 ± 0.06 [b]
P3S	100.47	6.92 ± 0.02 [b]	257.93	18.56 ± 0.18 [a]	311.16	59.83 ± 0.08 [a]
P7S	100.57	6.79 ± 0.01 [e]	192.95	13.12 ± 0.04 [d]	308.04	59.10 ± 0.07 [bc]
L3L	100.47	6.80 ± 0.02 [c]	242.88	15.21 ± 0.03 [c]	313.16	58.10 ± 0.14 [e]
L7L	100.49	6.29 ± 0.02 [c]	197.46	14.50 ± 0.37 [c]	308.11	58.16 ± 0.45 [e]
P3L	100.49	6.87 ± 0.08 [bc]	242.85	16.75 ± 0.11 [b]	305.46	58.60 ± 0.23 [d]
P7L	100.57	6.60 ± 0.02 [d]	192.41	14.88 ± 0.14 [c]	300.52	58.95 ± 0.11 [c]

The total weight loss of all powders ended at 600 °C. At the end, all powders completely degraded and turned into gray ash. As we observed, the drying method and the different emulsifying agents did not cause a considerable change in the thermal stability of the dried powders. Thermal stability varied only slightly with the pH at which the emulsions were prepared prior to drying, with thermal stability being higher at pH 3 than at pH 7. TGA was used as an indicator of thermal stability to determine decomposition kinetics according to the rate of sample weight loss and then to estimate sample stability. The results demonstrated the thermal stability of SD and FD powders during low temperature storage. In addition, encapsulation can be considered to protect TC from thermal degradation, and the TGA diagram could be useful to inform about temperatures at which powders can be used for food and beverage applications.

3.2.5. Structural Characterization Using Fourier Transform Infrared Spectroscopy (FTIR)

The FTIR spectra of dried samples are depicted in Figure 3. All the powders showed rather similar peaks with some differences in the intensity of the peaks. The peak around 3300 cm^{-1} comes from the phenolic hydroxyl groups, and the peak at about 2900 cm^{-1} comes from the aromatic C–H groups of the samples. The band at 1600 cm^{-1} belongs to the C=C stretching vibration. The peaks at 1373 and 1451 cm^{-1} represent the C–H bending vibration. The peak at 1013 cm^{-1} refers to C–O–C stretching vibrations. The stretching vibrations of anhydrous glucose are lower than 1000 cm^{-1} and the C–O bond stretching appears between 800 and 1500 cm^{-1}.
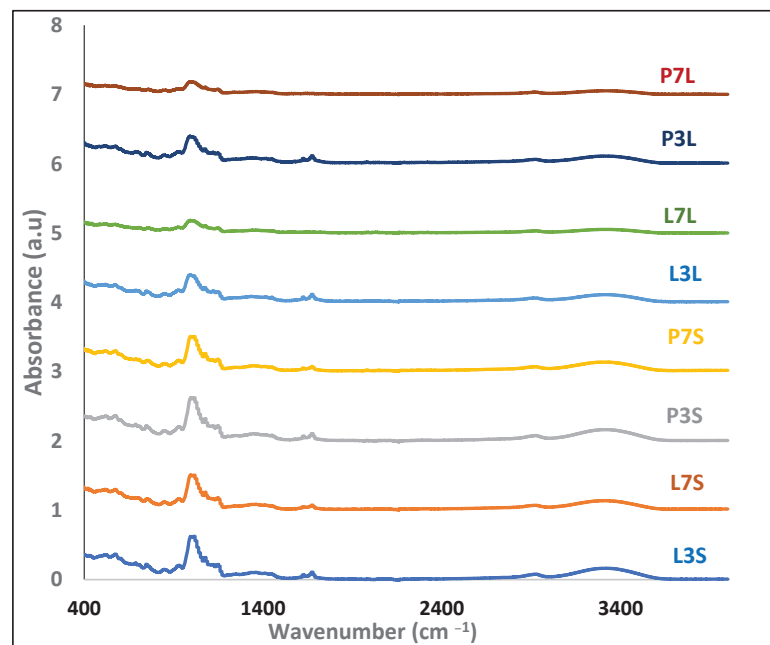
Figure 3. FTIR spectra of microcapsules.

The intensity of the peak around 3300 cm^{-1} is different according to the tested sample. In fact, the intensity of this peak became slightly higher for powders prepared at pH 3. The modification of the absorbance intensity of this rather broad peak due to the O–H bond could also highlight the presence of hydrogen bonds between the molecules within the capsules. The intensity of the peak at around 3400 cm^{-1} corresponding to residual humidity presented less intensity for FD powders. This result is in agreement with water content results that showed FD powders contain less humidity content.

In addition, between powders with the same pH, those that were spray-dried showed a slightly higher intensity of peaks around 1000 cm^{-1} (Figure 3). This suggests that spray-drying may improve the interactions between the different constituents of the microcapsules and at the oil–water interface of emulsions during water evaporation, resulting in better protection of the active compound. This result is similar to the study by Lin et al. [34], who used maltodextrin and lecithin to encapsulate squid oil via spray-drying.

3.2.6. Antimicrobial Activity

The antimicrobial activity of all emulsions and dried powders was tested on two foodborne bacteria, *Escherichia coli*, a Gram-negative bacteria, and *Listeria innocua*, a Gram-positive bacteria, as a surrogate of the pathogenic *Listeria monocytogenes*. The emulsions were added to wells created in media inoculated with one of the test bacteria. After 24 h, the inhibition zones were measured. Emulsions containing sunflower oil instead of TC (control) showed no inhibition zone. The diameters of the inhibition zone for the different emulsions are shown in Figure 4. All emulsions and dried powders exhibited antimicrobial activity on both tested bacteria. In addition, all samples showed a smaller inhibition zone against *E. coli* than against *L. innocua***.** This result can be explained by the fact that Gram-negative bacteria have an additional hydrophilic membrane embedded with lipopolysaccharide molecules that prevent the penetration of hydrophobic compounds such as essential oils. Among the emulsions, L3 and L7 showed larger inhibition zones than those emulsified using pea protein (P3 and P7). This result is consistent with that of particle size. Indeed, the emulsions prepared with lecithin exhibited smaller sizes than those emulsified with pea protein. This smaller size could provide a higher active surface area and efficiency of EOs to destroy the cell wall of microorganisms [1]. The antimicrobial activity of emulsions prepared with lecithin was reduced after drying. In contrast, powders containing pea protein showed relatively the same antimicrobial activity as their emulsion before drying. Among the spray-dried powders, L3S and L7S exhibited larger inhibition zones than P3S and P7S. This could also be attributed to the smaller particle size of the emulsion (0.09 μm) at pH 7 prepared using lecithin rather than the particle size of the emulsion prepared at pH 3 (0.11 μm).

Different results were obtained for freeze-dried powders. P3L and P7L, containing pea protein, exhibited a larger inhibition zone compared to freeze-dried powders containing lecithin (L3L and L7L). This can be explained by the effect of encapsulation efficiency. Because lecithin-emulsified emulsions had lower encapsulation efficiency, the antimicrobial activity of the freeze-dried lecithin-containing powders was changed. In addition, the powders were prepared at different pH values. This parameter did not have a significant effect on the diameters of the inhibition zone. One can conclude that the pH of emulsions before drying had no significant effect on the antimicrobial activity of powders after drying. In addition, the drying methods applied in this study successfully preserved the antimicrobial activity of *trans*-cinnamaldehyde. Spray-drying and freeze-drying processes could provide the possibility of fabricating antimicrobial powders that can be applied for food preservation applications.
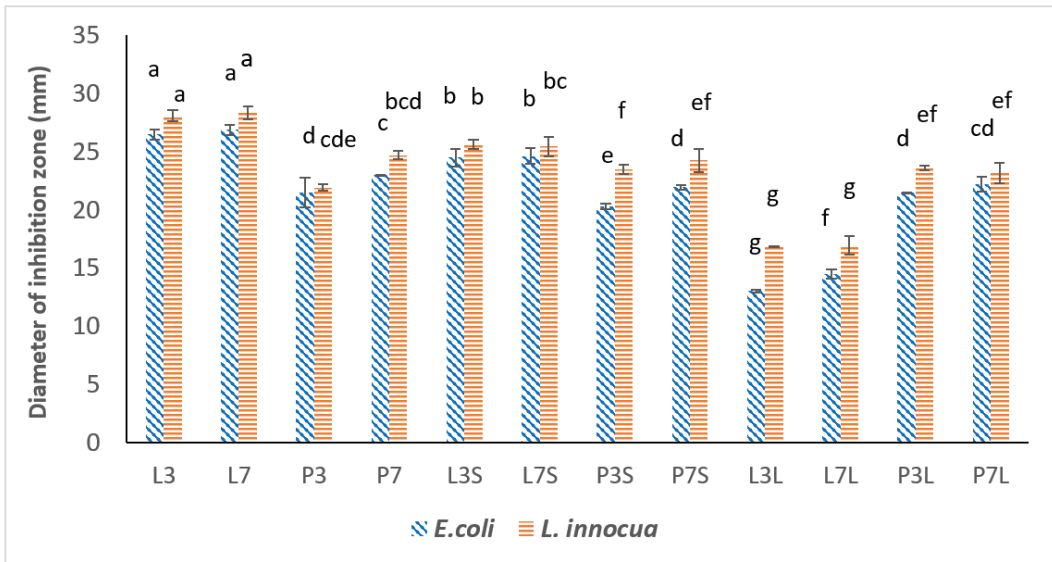
Figure 4. Antimicrobial activity of encapsulated *trans*-cinnamaldehyde before and after drying (spray-drying and freeze-drying). For results with the same letter, the difference between the means is not statistically significant.

3.2.7. Microstructural Features of the Dried Powders via Scanning Electron Microscopy

The morphology of all powders was studied using a scanning electron microscope (SEM). The micrographs shown in Figure 5 reveal a noticeable variation in structure and particle size between the SD and FD powders. All the analyzed SD samples were found to be almost spherical with some surface dents. Size polydispersity was observed and is consistent with the results obtained from laser light scattering using a Mastersizer instrument, which showed the presence of particles of different sizes. Some cracks were also observed, indicating the loss of essential oils as volatile compounds. Similar results have been reported by several authors [35–37]. The micrographs of FD powders showed an irregular shape similar to broken glass. Porosity was also observed in FD powders. The porosity could be explained by the formation of essential oil cavitations resulting in volatilization of the oil during air exposure. This result is in agreement with the encapsulation of rosemary oil performed by Turasan et al. [38]. They observed more pores in a formulation with maltodextrin compared to whey protein. The same results were observed by Pudziuvelyte et al. [39], who used freeze-drying for microencapsulation of polyphenol compounds using different wall materials. The particles presented a structure with porosity and a smooth surface which could be attributed to the degree of polymerization of the maltodextrin as encapsulating wall [40]. No significant difference was observed in the morphology of the particles obtained with different formulations of the samples that were dried with the same drying method.
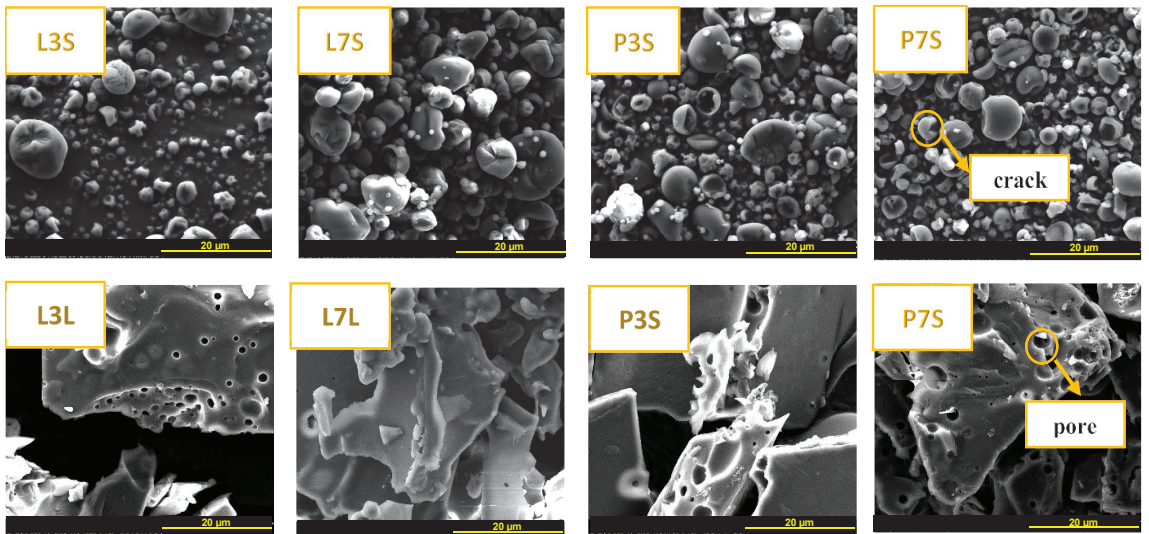
Figure 5. SEM image and particle analysis. First line: spray-dried powders (L3S, L7S, P3S, P7S). Second line: freeze-dried powders (L3L, L7L, P3S, P7S).

4. Discussion

To produce dry microcapsules, i.e., powders from which an oil-in-water emulsion can easily be reconstituted when exposed to an aqueous solution, the emulsions used must exhibit small droplets of oil before the drying step. Moreover, the particle size distribution and the stiffness of the interfacial membrane could have significant effects on the TC release profile from the microcapsules as well as on the encapsulation efficiency upon drying of the emulsion. The different structural properties of the two emulsifiers used may explain the differences observed in the characteristics of the emulsions formed before drying. Indeed, lecithin is a natural small-molecule emulsifier composed of many different phospholipids, and the two most abundant phospholipid species are phosphatidylcholine and phosphatidylethanolamine. However, the two major components of pea protein are 11S legume protein and 7S vicilin protein. They have a regular quaternary structure, hexameric for legumin protein and trimeric for vicilin protein. The total molecular weight of a legumin unit is about 380 kDa. It is a very compact globular protein in which the acidic polypeptides are located outside and the basic polypeptides constitute the hydrophobic core of the protein. 7S vicilin is a glycoprotein with a molecular weight of approximately 150 kDa. The quaternary structure of pea globulins depends on pH and salt concentration. Given these structural differences, the two emulsifiers have different interfacial properties, such as adsorption kinetics, interfacial tension-lowering kinetics, interfacial rheology, and concentration at the interfacial membrane. If the absorption of lecithin molecules is quite fast, that of globular proteins is slower because it requires a phase of dissociation and unfolding before integrating the oil–water interface. This phenomenon results in a difference in the size of the droplets in favor of the emulsions stabilized with lecithin [17].

The absolute value of the zeta potential for all emulsions was high enough to induce emulsion stability whatever emulsifier was used, but emulsions prepared with lecithin showed slightly higher values, indicating better stability. This result can be interpreted in terms of the higher final concentration of lecithin at interfacial membranes, since a part of pea protein was insoluble and separated before emulsification. Moreover, the emulsions stabilized using lecithin had smaller average particle size than those emulsified using pea protein.

The average size of spray-dried powders did not change significantly according to the type of emulsifier and pH, as all emulsions were pulverized under the same conditions, while the average size of freeze-dried particles was significantly bigger. These differences may be due to the fact that spray-drying includes a step of spraying into fine spherical droplets whereas freeze-drying is a sublimation of a frozen emulsion in static mode. Moisture content is an important parameter because of its effect on the powder stability, flowability, stickiness, microbial growth, and oxidation of bioactive compounds. FD powders contain less water content compared to the SD powders; however, both drying processes applied in this study provided acceptable water content ranging from 2.03 to 5.02%, offering the possibility of long storage lifetimes of these antimicrobial powders. In fact, moisture contents ranging between 4 and 6% could be considered suitable for long-term storage [41]. The attainment of microcapsules with interesting properties is the main outcome of this study because the direct application of liquid emulsions in food processing is limited and the encapsulation techniques applied supplied powders with acceptable EE for food applications.

5. Conclusions

The main objective of this study was to develop antimicrobial capsules containing *trans*-cinnamaldehyde via spray-drying or freeze-drying using two plant-based emulsifiers, namely lecithin and pea protein, at pH 7 or pH 3. The spray-drying process is much more satisfactory than freeze-drying for emulsions stabilized with lecithin due to the better encapsulation efficiency. In addition, spray-drying reduced the particle size by more than 16 times compared to freeze-drying. However, the freeze-dried powders contained less water. From the SEM micrographs, the SD powders have a spherical morphology, and crystal shapes were observed for the FD powders. The powders prepared at pH 3 had better thermal stability, and all powders presented interesting antimicrobial activity. These powders possess appropriate properties to use as potentially natural antimicrobial agents in food industries. Future research should be carried out to investigate the preservative potential of microcapsules of *trans*-cinnamaldehyde in extending the shelf life of meat and dairy products.

References

1. Sharma, S.; Barkauskaite, S.; Jaiswal, A.K.; Jaiswal, S. Essential Oils as Additives in Active Food Packaging. *Food Chem.* **2020**, *343*, 128403. [CrossRef]
2. Turek, C.; Stintzing, F.C. Stability of Essential Oils: A Review. *Compr. Rev. Food Sci. Food Saf.* **2013**, *12*, 40–53. [CrossRef]
3. Smaoui, S.; Ben Hlima, H.; Ben Braïek, O.; Ennouri, K.; Mellouli, L.; Mousavi Khaneghah, A. Recent Advancements in Encapsulation of Bioactive Compounds as a Promising Technique for Meat Preservation. *Meat Sci.* **2021**, *181*, 108585. [CrossRef] [PubMed]
4. Aljaafari, M.N.; AlAli, A.O.; Baqais, L.; Alqubaisy, M.; AlAli, M.; Molouki, A.; Ong-Abdullah, J.; Abushelaibi, A.; Lai, K.-S.; Lim, S.-H.E. An Overview of the Potential Therapeutic Applications of Essential Oils. *Molecules* **2021**, *26*, 628. [CrossRef] [PubMed]
5. Majeed, H.; Bian, Y.-Y.; Ali, B.; Jamil, A.; Majeed, U.; Khan, Q.F.; Iqbal, K.J.; Shoemaker, C.F.; Fang, Z. Essential Oil Encapsulations: Uses, Procedures, and Trends. *RSC Adv.* **2015**, *5*, 58449–58463. [CrossRef]
6. Wang, Q.; Gong, J.; Huang, X.; Yu, H.; Xue, F. In Vitro Evaluation of the Activity of Microencapsulated Carvacrol against *Escherichia Coli* with K88 Pili. *J. Appl. Microbiol.* **2009**, *107*, 1781–1788. [CrossRef] [PubMed]

7. Gaysinsky, S.; Taylor, T.M.; Davidson, P.M.; Bruce, B.D.; Weiss, J. Antimicrobial Efficacy of Eugenol Microemulsions in Milk against Listeria Monocytogenes and *Escherichia Coli* O157:H7. *J. Food Prot.* **2007**, *70*, 2631–2637. [CrossRef]
8. Alehosseini, E.; Jafari, S.M. Micro/Nano-Encapsulated Phase Change Materials (PCMs) as Emerging Materials for the Food Industry. *Trends Food Sci. Technol.* **2019**, *91*, 116–128. [CrossRef]
9. Chen, H.; Hu, X.; Chen, E.; Wu, S.; McClements, D.J.; Liu, S.; Li, B.; Li, Y. Preparation, Characterization, and Properties of Chitosan Films with Cinnamaldehyde Nanoemulsions. *Food Hydrocoll.* **2016**, *61*, 662–671. [CrossRef]
10. Jo, Y.-J.; Chun, J.-Y.; Kwon, Y.-J.; Min, S.-G.; Hong, G.-P.; Choi, M.-J. Physical and Antimicrobial Properties of Trans-Cinnamaldehyde Nanoemulsions in Watermelon Juice. *LWT Food Sci. Technol.* **2015**, *60*, 444–451. [CrossRef]
11. Eun, J.-B.; Maruf, A.; Das, P.R.; Nam, S.-H. A Review of Encapsulation of Carotenoids Using Spray Drying and Freeze Drying. *Crit. Rev. Food Sci. Nutr.* **2020**, *60*, 3547–3572. [CrossRef] [PubMed]
12. Kurek, M.A.; Pratap-Singh, A. Plant-Based (Hemp, Pea and Rice) Protein–Maltodextrin Combinations as Wall Material for Spray-Drying Microencapsulation of Hempseed (*Cannabis Sativa*) Oil. *Foods* **2020**, *9*, 1707. [CrossRef]
13. Mazo Rivas, J.C.; Schneider, Y.; Rohm, H. Effect of Emulsifier Type on Physicochemical Properties of Water-in-Oil Emulsions for Confectionery Applications. *Int. J. Food Sci. Technol.* **2016**, *51*, 1026–1033. [CrossRef]
14. Yang, Q.-Q.; Sui, Z.; Lu, W.; Corke, H. Soybean Lecithin-Stabilized Oil-in-Water (O/W) Emulsions Increase the Stability and in Vitro Bioaccessibility of Bioactive Nutrients. *Food Chem.* **2021**, *338*, 128071. [CrossRef] [PubMed]
15. Chiplunkar, P.P.; Pratap, A.P. Ultrasound Assisted Synthesis of Hydroxylated Soybean Lecithin from Crude Soybean Lecithin as an Emulsifier. *J. Oleo Sci.* **2017**, *66*, 1101–1108. [CrossRef]
16. Li, J.; Li, Y.; Guo, S. The Binding Mechanism of Lecithin to Soybean 11S and 7S Globulins Using Fluorescence Spectroscopy. *Food Sci. Biotechnol.* **2014**, *23*, 1785–1791. [CrossRef]
17. Gharsallaoui, A.; Cases, E.; Chambin, O.; Saurel, R. Interfacial and Emulsifying Characteristics of Acid-Treated Pea Protein. *Food Biophys.* **2009**, *4*, 273–280. [CrossRef]
18. Kandasamy, S.; Naveen, R. A Review on the Encapsulation of Bioactive Components Using Spray-Drying and Freeze-Drying Techniques. *J. Food Process Eng.* **2022**, *45*, e14059. [CrossRef]
19. Fang, Z.; Bhandari, B. 4—Spray Drying, Freeze Drying and Related Processes for Food Ingredient and Nutraceutical Encapsulation. In *Encapsulation Technologies and Delivery Systems for Food Ingredients and Nutraceuticals*; Woodhead Publishing Series in Food Science, Technology and Nutrition; Garti, N., McClements, D.J., Eds.; Woodhead Publishing: Sawston, UK, 2012; pp. 73–109, ISBN 978-0-85709-124-6.
20. Rezvankhah, A.; Emam-Djomeh, Z.; Askari, G. Encapsulation and Delivery of Bioactive Compounds Using Spray and Freeze-Drying Techniques: A Review. *Dry. Technol.* **2020**, *38*, 235–258. [CrossRef]
21. Hogan, S.; McNamee, B.; O'Riordan, D.; O'Sullivan, M. Emulsification and Microencapsulation Property of Sodium Caseinate/Carbohydrate Blends. *Int. Dairy J.* **2001**, *11*, 137–144. [CrossRef]
22. Haghju, S.; Beigzadeh, S.; Almasi, H.; Hamishehkar, H. Chitosan Films Incorporated with Nettle (*Urtica Dioica* L.) Extract-Loaded Nanoliposomes: I. Physicochemical Characterisation and Antimicrobial Properties. *J. Microencapsul.* **2016**, *33*, 438–448. [CrossRef] [PubMed]
23. Balcaen, M.; Steyls, J.; Schoeppe, A.; Nelis, V.; Van der Meeren, P. Phosphatidylcholine-Depleted Lecithin: A Clean-Label Low-HLB Emulsifier to Replace PGPR in w/o and w/o/w Emulsions. *J. Colloid Interface Sci.* **2021**, *581*, 836–846. [CrossRef] [PubMed]
24. Donsì, F.; Annunziata, M.; Vincensi, M.; Ferrari, G. Design of Nanoemulsion-Based Delivery Systems of Natural Antimicrobials: Effect of the Emulsifier. *J. Biotechnol.* **2012**, *159*, 342–350. [CrossRef] [PubMed]
25. Muijlwijk, K.; Colijn, I.; Harsono, H.; Krebs, T.; Berton-Carabin, C.; Schroën, K. Coalescence of Protein-Stabilised Emulsions Studied with Microfluidics. *Food Hydrocoll.* **2017**, *70*, 96–104. [CrossRef]
26. Duffy, J.; Larsson, M.; Hill, A. Suspension Stability; Why Particle Size, Zeta Potential and Rheology Are Important. *Annu. Trans. Nord. Rheol. Soc.* **2012**, *20*, 6.
27. Talón, E.; Lampi, A.-M.; Vargas, M.; Chiralt, A.; Jouppila, K.; González-Martínez, C. Encapsulation of Eugenol by Spray-Drying Using Whey Protein Isolate or Lecithin: Release Kinetics, Antioxidant and Antimicrobial Properties. *Food Chem.* **2019**, *295*, 588–598. [CrossRef]
28. Yoplac, I.; Vargas, L.; Robert, P.; Hidalgo, A. Characterization and Antimicrobial Activity of Microencapsulated Citral with Dextrin by Spray Drying. *Heliyon* **2021**, *7*, e06737. [CrossRef]
29. Murali, S.; Kar, A.; Mohapatra, D.; Kalia, P. Encapsulation of Black Carrot Juice Using Spray and Freeze Drying. *Food Sci. Technol. Int.* **2015**, *21*, 604–612. [CrossRef]
30. Cortés-Rojas, D.; Souza, C.; Oliveira, W. Encapsulation of Eugenol Rich Clove Extract in Solid Lipid Carriers. *J. Food Eng.* **2014**, *127*, 34–42. [CrossRef]
31. Monteiro Filho, J.C.K.; Rodrigues, R.A.F. *Varronia Verbenacea* and Achyrocline Satureioides Essential Oils in Granules and Microparticles: Stability and in Vitro Release Studies. *Dry. Technol.* **2021**, *39*, 1895–1911. [CrossRef]
32. Dinakaran, A. Optimal Spray-Drier Encapsulation Process of Orange Oil. In Proceedings of the 14th International Drying Symposium, Sao-Paulo, Brazil, 22–25 August 2004; pp. 621–627.

33. Volić, M.; Pećinar, I.; Micić, D.; Đorđević, V.; Pešić, R.; Nedović, V.; Obradović, N. Design and Characterization of Whey Protein Nanocarriers for Thyme Essential Oil Encapsulation Obtained by Freeze-Drying. *Food Chem.* **2022**, *386*, 132749. [CrossRef] [PubMed]
34. Lin, S.Y.; Hwang, L.S.; Lin, C.C. Thermal Analyser and Micro FT-IR/DSC System Used to Determine the Protective Ability of Microencapsulated Squid Oil. *J. Microencapsul.* **1995**, *12*, 165–172. [CrossRef] [PubMed]
35. Alvarenga Botrel, D.; Vilela Borges, S.; Victória de Barros Fernandes, R.; Dantas Viana, A.; Maria Gomes da Costa, J.; Reginaldo Marques, G. Evaluation of Spray Drying Conditions on Properties of Microencapsulated Oregano Essential Oil. *Int. J. Food Sci. Technol.* **2012**, *47*, 2289–2296. [CrossRef]
36. Gharsallaoui, A.; Saurel, R.; Chambin, O.; Voilley, A. Pea (*Pisum Sativum*, L.) Protein Isolate Stabilized Emulsions: A Novel System for Microencapsulation of Lipophilic Ingredients by Spray Drying. *Food Bioprocess Technol.* **2012**, *5*, 2211–2221. [CrossRef]
37. Escobar-Avello, D.; Avendaño-Godoy, J.; Santos, J.; Lozano-Castellón, J.; Mardones, C.; von Baer, D.; Luengo, J.; Lamuela-Raventós, R.M.; Vallverdú-Queralt, A.; Gómez-Gaete, C. Encapsulation of Phenolic Compounds from a Grape Cane Pilot-Plant Extract in Hydroxypropyl Beta-Cyclodextrin and Maltodextrin by Spray Drying. *Antioxidants* **2021**, *10*, 1130. [CrossRef]
38. Turasan, H.; Sahin, S.; Sumnu, G. Encapsulation of Rosemary Essential Oil. *LWT Food Sci. Technol.* **2015**, *64*, 112–119. [CrossRef]
39. Pudziuvelyte, L.; Marksa, M.; Sosnowska, K.; Winnicka, K.; Morkuniene, R.; Bernatoniene, J. Freeze-Drying Technique for Microencapsulation of *Elsholtzia ciliata* Ethanolic Extract Using Different Coating Materials. *Molecules* **2020**, *25*, 2237. [CrossRef]
40. Campelo, P.H.; Sanches, E.A.; Fernandes, R.V.d.B.; Botrel, D.A.; Borges, S.V. Stability of Lime Essential Oil Microparticles Produced with Protein-Carbohydrate Blends. *Food Res. Int.* **2018**, *105*, 936–944. [CrossRef]
41. Šavikin, K.; Nastić, N.; Janković, T.; Bigović, D.; Milićević, B.; Vidović, S.; Menković, N.; Vladić, J. Effect of Type and Concentration of Carrier Material on the Encapsulation of Pomegranate Peel Using Spray Drying Method. *Foods* **2021**, *10*, 1968. [CrossRef]

Effects of Salt Reduction and the Inclusion of Seaweed (*Kappaphycus alvarezii*) on the Physicochemical Properties of Chicken Patties

Wolyna Pindi *, Lim Wei Qin, Nurul Shaeera Sulaiman, Hana Mohd Zaini, Elisha Munsu, Noorakmar Ab Wahab and Nor Qhairul Izreen Mohd Noor

Faculty of Food Science and Nutrition, Universiti Malaysia Sabah, Jalan UMS, Kota Kinabalu 88400, Sabah, Malaysia
* Correspondence: woly@ums.edu.my; Tel.: +60-88-320000 (ext. 101388)

Abstract: This study investigates the effect of salt reduction through the inclusion of seaweed (*Kappaphycus alvarezii*) on the physicochemical and sensory qualities of chicken patties. A control sample (1.5% salt and without seaweed) and four chicken patty formulations were used with two levels of salt (1% and 1.5%) and two levels of seaweed (2% and 4%). Adding seaweed improves water holding capacity and minimized cooking loss in reduced-salt patties. In addition, adding seaweed decreases the shrinkage of the diameter and thickness of chicken patties ($p > 0.05$). However, adding seaweed made the patties darker, as shown by lower L* values ($p > 0.05$). Additionally, the incorporation of seaweed significantly increased ($p < 0.05$) the hardness, chewiness, cohesiveness, and elasticity of patties. Reduced-salt chicken patties with the addition of 2–4% of seaweed showed lower extracted water than 1.5% salt chicken patties with seaweed ($p < 0.05$), indicating a higher water holding capacity. The sensory evaluation showed that the chicken patty with 1.5% salt and 4% seaweed had the highest overall acceptability. However, the overall acceptability of the chicken patties with 1% salt and 4% seaweed was significantly higher ($p < 0.05$) than the control. In conclusion, the addition of *Kappaphycus alvarezii* to reduced salt patties improved textural properties with acceptable taste profiles.

Keywords: seaweed; reduced salt; meat emulsion; physicochemical properties; sensory; meat products; patty

1. Introduction

Specific population groups widely consume comminuted meat products such as sausages and patties, positively impacting the food sector's economy [1]. However, some processed meat products have high salt content. Due to its low cost and various technological properties, salt is a multipurpose ingredient in processing meat [2]. Table salt (NaCl) is mostly used in meat formulations to improve shelf life, sensory properties, and convenience [3]. However, other additives of sodium salts, such as phosphates, glutamates, lactases, and nitrites, could add to the sodium burden [4].

About 75% of the daily sodium globally comes from processed food items, with 20–30% from meat products [5]. Excessive sodium intake can lead to hypertension, increasing the risk of cardiovascular illnesses, a significant public health issue [6]. The World Health Organization (WHO) have set an adult intake of NaCl limit to less than 5 g/day to overcome health-related issues [7]. The food sector has been encouraged to develop low-salt meat products due to health recommendations and customers' awareness of their health.

Meat products normally contain 7 to 39 g/kg of sodium chloride since most meat formulations require at least 2% salt content for the ionic strength necessary for solubilising and extracting the salt-soluble proteins [8]. Therefore, a decrease in salt content can deteriorate the flavour intensity because NaCl provides features necessary in meat products [8].

The low-salt formulation also tends to have higher cooking loss owing to lower water holding capacity and poor solubilisation of myofibrillar proteins [9].

Various strategies have been considered to minimise salt content and create meat products that meet nutritional recommendations. In processing Chinese bacon, NaCl was partially replaced with potassium chloride to promote the growth of *Lactobacillus* and impacted proteolysis and lipid oxidation [10]. During salami processing, replacing the NaCl with a mixture of KCl, CaCl$_2$, and MgCl$_2$ decreases the sodium content by 40%, with minor effects on sensory qualities. Still, there was a significant increase in lipid oxidation. Other alternatives include incorporating naturally salty-tasting ingredients such as seaweed [2].

Seaweeds contain nutrients and biological compounds, such as proteins, polysaccharides, omega-3 fatty acids, and vitamins [11]. The fatty acid contents of red seaweed were primarily made up of palmitic acid (31.62–41.71%), oleic acid (9.21–10.33%), and arachidonic acid (29.40–38.33%) [12]. *K. alvarezii* also exhibited high amount of soluble (16.73 g/100 g), insoluble (42.24 g/100 g), and total dietary fibre (58.97 g/100 g) [13]. In addition, seaweed contains minerals, including Ca (262.98 mg/100 g), Fe (11.34 mg/100 g), and Zn (0.29 mg/100 g) [14]. Due to their high mineral content, seaweeds can serve as salt substitutes in meat products, reducing sodium intake while increasing the consumption of other minerals unavailable in NaCl-salted processed meat [15]. Seaweeds have a low Na/K ratio, ideal for avoiding hypertension and cardiovascular disorders [2].

The red seaweed *Kappaphycus alvarezii* belongs to the phylum *Rhodophyta* and serves as a source of kappa carrageenan, a phyllocoloid used as a stabilising and thickening agent in food [16]. The phenolic compounds found in abundance in *K. alvarezii* have antioxidant, anti-allergenic, anti-inflammatory, and cardioprotective properties [17]. The antioxidant potency composite index of *K. alvarezii* was 87.93%, owing to the presence of hydroxybenzoic acid, hydroxycinnamic acid, and flavonoid [18,19].

As the research shows [20], adding 4% of *K. alvarezii* to chicken sausage increased the overall phenolic content, reduced lipid oxidation, and showed acceptable sensory results. Additionally, the incorporation of red seaweeds (*Poryphyra umbilicalis* and *Palmaria palmata*) in frankfurters showed decreased ash and estimated shelf-life similar to the control [21]. However, little is known about the effects of *K. alvarezii* addition to reduced-salt patty. Thus, the objective of this study was to develop a chicken patty that could satisfy the need for meat products with lower salt content while promoting consumer acceptance of functional food through different inclusion levels of *K. alvarezii*. The reformulated patties were assessed based on their rheological, physicochemical, and sensory parameters.

2. Materials and Methods

2.1. Preparation of Seaweed Powder

K. alvarezii seaweed purchased from a local market in Kota Kinabalu was rinsed with tap water to remove the dirt, sand, adhesives and epiphytes and dried for 48 h at 45 °C in a drying cabinet (TD-150F, Thermoline Scientific, Wetherill Park, NSW, Australia) [22]. The dried sample was ground into powder using a grinder (WSG30E, Waring, Zhengzhou, China) for 5 min and filtered using a refiner machine (R50, TEM, Modena, Italy). The samples were kept at 4 °C in an airtight container for further analyses [23].

2.2. Preparation of Chicken Patty

Boneless chicken breasts were purchased from Desa Hatchery Sdn. Bhd. and ground using a 4 mm hole plate meat grinder (4812, Hobart, Offenburg, Germany). Four batches of patties were prepared with different salt levels ranging from 1% to 1.5% and *K. alvarezii* (dry matter basis) levels ranging from 2% to 4%, as shown in Table 1. One batch of the patty was prepared at a normal salt (dry matter basis) level without adding seaweed as a control. The patty preparation was modified based on the formulations described by [24]. The ground chicken breast was mixed with other ingredients, such as seaweed powder, potato starch, ice water, and spices, by a mixer (KM331, Kenwood Chef Classic, Petaling

Jaya, Malaysia) for 3 min. Next, 70 g portions of batter were moulded in a hamburger maker with a diameter of 100 and a 10 mm height.

Table 1. Chicken patty formulation with seaweed.

Ingredients	Formulation (%)				
	Control	F1	F2	F3	F4
Chicken breast	65.0	65.0	65.0	65.0	65.0
Seaweed	0	2	2	4	4
Ice water	25.0	23.5	23.0	21.5	21.0
Potato starch	6.0	6.0	6.0	6.0	6.0
Salt	1.5	1.0	1.5	1.0	1.5
Sugar	1.0	1.0	1.0	1.0	1.0
Black pepper	0.5	0.5	0.5	0.5	0.5
White pepper	0.5	0.5	0.5	0.5	0.5
Garlic	0.5	0.5	0.5	0.5	0.5
Total	100	100	100	100	100

Control (without seaweed), F1 (2% seaweed and 1.0% salt), F2 (2% seaweed and 1.5% salt), F3 (4% seaweed and 1.0% salt), F4 (4% seaweed and 1.5% salt).

2.3. Texture Profile Analysis

The texture profile of the patty was analysed using a texture analyser machine (TA. XT Plus, Stable Micro Systems, Surrey, UK) [23]. The test condition was set at a speed of 1.5 mm/s and a height of 2.0 cm. The patty sample was sliced into a 2.0 cm cylindrical shape and compressed to 40% of the original thickness using a 3.5 cm cylindrical probe. The texture profile results were obtained, and the hardness, cohesiveness, chewiness, and elasticity were analysed.

2.4. Colour Analysis

The surfaces of the patty samples were evaluated using a HunterLab Colorimeter (Colorflex-EZ, HunterLab, Reston, VA, USA) [25]. The CIELAB colour system (L* = 0, black; L* = 100, white; +a* = redness; −a* = greenness; +b* = yellowness; −b* = blueness) was measured. The colorimeter was calibrated using a white tile as reference (L* = 93.97; a* = −0.08, and b* = 1.21).

2.5. pH Determination

A total of 10 g of sample was mixed with 90 mL of distilled water for 30 s. The pH of the chicken patty was measured using a pH meter (340, Mettler-Toledo, Greifensee, Switzerland) using the method described in [26].

2.6. Water Activity

The water activity analysis for the chicken patty was carried out using a water activity indicator (HYGROLAB C1, Rotronic, South Burlington, VT, USA) at 25 °C. About 2 g of chicken patty batter was placed into a 3 mm sized cell [27]. Water activity samples were analysed twice, and the average results were recorded.

2.7. Water Holding Capacity

The water holding capacity of the chicken patty was determined by the modified method [28]. A total of 10 g of chicken patty sample was placed in a beaker and heated in a water bath at 90 °C for 1 h. The cooled sample was centrifuged (X3R, Thermo Scientific, USA) at 4 °C and 4000 rpm for 15 min. The water holding capacity is the weight loss after centrifugation and calculated using Equation (1):

$$\text{Water holding capacity } (\%) = \frac{1 - B - A}{M} \times 100 \tag{1}$$

where A is the weight of the chicken patty before heating, B is the weight after centrifugation, and M is the total water content in the sample.

2.8. Cooking Loss

Patty samples were cooked in a steamer for 30 min at 80 °C and then cooled for 30 min [20]. The weight of patty samples before and after cooking was recorded. Cooking loss is the difference in the weight of uncooked and cooked samples as shown in Equation (2):

$$\text{Cooking loss (\%)} = \frac{\text{A} - \text{B}}{\text{A}} \times 100 \tag{2}$$

where A is the weight of the chicken patty before cooking, and B is the weight of the chicken patty after cooking.

2.9. Shrinkage in Diameter and Thickness

The shrinkage in diameter and thickness of raw and cooked chicken patty was measured using a vernier callipers (530-122, Mitutoyo, Japan) [25]. The results were calculated by using Equations (3) and (4):

$$\text{Diameter shrinkage (\%)} = \frac{\text{Diameter of raw patty} - \text{Diameter of cooked patty}}{\text{Diameter of raw patty}} \times 100 \tag{3}$$

$$\text{Thickness shrinkage (\%)} = \frac{\text{Thickness of raw patty} - \text{Thickness of cooked patty}}{\text{Thickness of raw patty}} \times 100 \tag{4}$$

2.10. Rheological Properties

Dynamic rheological properties of the patty sample were examined using an AR500 rheometer (AR500 TA Co., Ltd., New Castle, DE, USA) equipped with a 50 mm parallel plate [24]. A strain sweep test was performed at 20 °C to measure the storage modulus (G′), loss modulus (G″), and loss factor (tan δ). Angular frequency, shear strain, and amplitude were set at 6.283 rad/s, 0.5%, and 0.1–100 Hz, respectively.

2.11. Sensory Evaluation

The sensory evaluation of the chicken patty was conducted using a 7-point hedonic scale (1 = extremely dislike, 7 = extremely like). About 30 untrained panellists aged 20–26 years (15 males and 15 females) of the Faculty of Food Science and Nutrition, Universiti Malaysia Sabah were selected to evaluate the patty samples' colour, aroma, taste, elasticity, and overall acceptance. The patty was grilled until the internal temperature reached 80 °C. The sample was then uniformly cut into rectangular pieces (5.0 cm × 5.0 cm × 2.0 cm) and served to each panellist at the Sensory Evaluation Laboratory along with a random three-digit code. Water at room temperature was provided for mouth rinsing before trying a new sample [20]. Panellists were instructed and reminded to rinse their mouth prior to testing a new sample formulation.

2.12. Statistical Analysis

The statistical analysis was performed using a one-way Analysis of Variance (ANOVA) to evaluate the effects of salt reduction and seaweed addition on the patty's physicochemical and sensory properties. Data were analysed using the SPSS statistical processor software version 26.0 (IBM Corp., Armonk, NY, USA). Tukey HSD test was used to evaluate the significant difference between the means for the various attributes ($p < 0.05$). All analyses were performed in triplicate.

3. Results and Discussion

3.1. Texture Profile Analysis

Texture profile analysis was conducted on patty samples with and without the addition of *K. alvarezii*, as shown in Table 2. Adding seaweed into the chicken patty significantly

increased the hardness ($p < 0.05$). Hardness is the maximum force during the first compression of the food sample on the texture analyser [29,30]. The greatest hardness value (2.86 N, Table 2) was obtained in F4 containing 4% *Kappaphyccus alvarezii* and a similar salt content to the control formulation. The protein from the seaweed created a more rigid protein network, creating a harder and coarse texture patty. The low-salt meat was faced with a lack of protein aggregation to form a strong protein network. However, the increased hardness indicated that *Kappaphycus alvarezii* can overcome texture issues in low salt patties.

Table 2. Textural properties of chicken patties with and without the addition of seaweed at different salt levels.

Formulation	Hardness (N)	Chewiness (N)	Cohesiveness	Elasticity (mJ)
Control (C)	1.32 ± 0.06 [d]	1.06 ± 0.02 [b]	0.76 ± 0.02 [c]	0.93 ± 0.01 [b]
F1 (2KA, 1.0S)	1.81 ± 0.18 [c]	1.41 ± 0.02 [b]	0.78 ± 0.01 [bc]	0.95 ± 0.03 [ab]
F2 (2KA, 1.5S)	2.44 ± 0.07 [b]	1.98 ± 0.18 [a]	0.79 ± 0.02 [bc]	0.96 ± 0.02 [ab]
F3 (4KA, 1.0S)	2.62 ± 0.08 [ab]	2.01 ± 0.18 [a]	0.82 ± 0.03 [ab]	0.98 ± 0.03 [ab]
F4 (4KA, 1.5S)	2.86 ± 0.18 [a]	2.20 ± 0.30 [a]	0.86 ± 0.01 [a]	1.01 ± 0.03 [a]

Mean ± standard deviation (SD) with different lowercase superscripts showed significant differences for different formulation of samples ($p < 0.05$). Control = 0% *Kappaphycus alvarezii*, 1.5% salt; F1 = 2% *Kappaphycus alvarezii*, 1.0% salt; F2 = 2% *Kappaphycus alvarezii*, 1.5% salt; F3 = 4% *Kappaphycus alvarezii*, 1.0% salt; F4 = 4% *Kappaphycus alvarezii*, 1.5% salt.

In addition, F4 (2.20 N) showed a significantly higher ($p < 0.05$) chewiness value than the control sample (1.06 N). The effort to chew the food product is positively associated with the food's hardness value, increasing the chewiness value [31]. A similar finding was also reported by [32], in which the sausage with a higher salt content tended to be harder to chew. The cohesiveness and elasticity values also rose as more seaweed was added to the patty (Table 2). However, there was no significant difference ($p > 0.05$) in the cohesiveness of F1 (0.78) and F2 (0.79) from the control (0.76). The result demonstrates the ability of *Kappaphycus alvarezii* as a meat extender at reduced-salt content.

3.2. Cooking Loss, Water Holding Capacity, and pH of Patty

Cooking loss in meat products is closely related to the water holding capacity of meat [23]. A high percentage of water holding capacity indicates a high percentage of cooking yield. Whereas meat with low water holding capacity results in more water and cooking losses. In this study, adding seaweed powder significantly ($p < 0.05$) reduced the cooking loss (Table 3). F4 had the lowest (10.02%) cooking loss, while the control patty showed the highest (16.85%) cooking loss. Seaweed is a rich source of dietary fibre [33], affecting meat properties, including water and fat binding ability. As the dietary fibre was hydrated, the water molecules were retained and occupied in the pore space of fibre, which eventually minimised the cooking loss [34]. The results were in agreement with [23], which reported that adding seaweed (*Kappaphycus alvarezii*) powder in mechanically deboned chicken meat (MDCM) sausages reduced the percentage of cooking loss compared to those without seaweed ($p < 0.05$).

The water holding capacity (WHC) is expressed as the percentage of extracted water, as presented in Table 3. The results showed that the F2, F3, and F4 samples retained more water than the control patty ($p < 0.05$). At similar seaweed content, treatments containing higher levels of salt (F2 and F4) showed lower percentages of extracted water, which were 10.03% and 8.25%, respectively. A low salt concentration affected the heat-induced gelation in meat products due to low myofibrillar protein dissolution. On the contrary, a high amount of salt minimized the extracted water by increasing the solubility and strength of myofibrillar proteins network [3]. However, F1 (11.26%) and F3 (8.50%) showed lower extracted water than the control (12.60%, $p < 0.05$), despite having lower salt content, indicating that *K. alvarezii* could retain water in meat products.

Table 3. Cooking loss, percentage of extracted water, and pH reading for a different formulation of the chicken patty.

Formulation	Cooking Loss (%)	Extracted Water (%)	pH
Control (C)	16.85 ± 0.01 [a]	12.60 ± 0.66 [a]	5.47 ± 0.10 [c]
F1 (2KA, 1.0S)	15.19 ± 0.03 [b]	11.26 ± 1.01 [ab]	5.64 ± 0.20 [bc]
F2 (2KA, 1.5S)	12.37 ± 0.02 [c]	10.03 ± 0.31 [bc]	5.92 ± 0.02 [ab]
F3 (4KA, 1.0S)	10.38 ± 0.04 [d]	8.50 ± 0.50 [cd]	6.05 ± 0.02 [a]
F4 (4KA, 1.5S)	10.02 ± 0.02 [e]	8.25 ± 0.23 [d]	6.06 ± 0.08 [a]

Mean ± standard deviation (SD) with different lowercase superscripts showed significant differences for different formulations of samples ($p < 0.05$). Control = 0% *Kappaphycus alvarezii*, 1.5% salt; F1 = 2% *Kappaphycus alvarezii*, 1.0% salt; F2 = 2% *Kappaphycus alvarezii*, 1.5% salt; F3 = 4% *Kappaphycus alvarezii*, 1.0% salt; F4 = 4% *Kappaphycus alvarezii*, 1.5% salt.

pH is an important factor associated with the meat's water-holding capacity. Except for F1, the addition of *Kappaphycus alvarezii* significantly increased ($p < 0.05$) the pH of the patty, with F4 showing the highest pH value of 6.06. The pH of meat products affects their texture, as low pH indicates a decreased water holding capacity [35]. The pH value shown in Table 3 agreed with the texture profile analysis (Table 2), as the addition of seaweed increased the hardness, chewiness, cohesiveness, and elasticity of the patties.

3.3. Colour Evaluation

Colour is an important parameter that determines the meat wholesomeness and consumer acceptance of a product [31]. The colour distinguishes the water content, meat pigments, and fat of processed meat products. The colour analysis results were expressed as L*(0) = black, L*(100) = white, +a* = redness, −a* = greenness, +b* = yellowness, and −b* = blueness [30]. It was observed that the brightness (L*) and yellowness (b*) of a patty did not show any significant difference among the F1, F2, F3, and F4 samples. Based on the report by [34,36], the L* value is influenced by the moisture content and pH value of meat products. In the present study, it could be concluded that higher pH values (Table 3) resulted in lower brightness (Table 4) of patty samples.

Table 4. Colour of different formulation of chicken patty.

Formulation	L*	a*	b*
Control (C)	54.37 ± 0.98 [a]	3.69 ± 0.19 [c]	19.17 ± 0.91 [a]
F1 (2KA, 1.0S)	52.20 ± 1.93 [ab]	3.74 ± 0.19 [c]	15.52 ± 0.34 [b]
F2 (2KA, 1.5S)	50.45 ± 6.40 [ab]	4.15 ± 0.55 [bc]	18.45 ± 0.41 [ab]
F3 (4KA, 1.0S)	47.99 ± 1.37 [ab]	4.51 ± 0.13 [ab]	17.91 ± 1.18 [b]
F4 (4KA, 1.5S)	44.80 ± 0.68 [b]	5.06 ± 0.10 [a]	17.44 ± 1.73 [b]

Mean ± standard deviation (SD) with different lowercase superscripts showed significant differences for a different formulation of samples ($p < 0.05$). Control = 0% *Kappaphycus alvarezii*, 1.5% salt; F1 = 2% *Kappaphycus alvarezii*, 1.0% salt; F2 = 2% *Kappaphycus alvarezii*, 1.5% salt; F3 = 4% *Kappaphycus alvarezii*, 1.0% salt; F4 = 4% *Kappaphycus alvarezii*, 1.5% salt.

The a* value of F1 and F2 were similar ($p > 0.05$) with the control, while F3 and F4 showed higher redness ($p < 0.05$). *K. alvarezii* falls under the Rodophyte division, which contains high phycoerythrin and phycocyanin [16]. The colours of these compounds are stronger than other pigments such as chlorophyll and beta-carotene [16]. In terms of yellowness (b*), [37] associated the reduced b* value with the higher WHC of meat products caused by the addition of seaweed in the formulations.

3.4. Water Activity

Water activity (a_w) is a physicochemical parameter that can control the food quality by determining the growth capacity of microorganisms and measuring the ratio between water pressure in the material and air pressure outside the material [38,39]. Table 5 shows that water activity decreased with the addition of seaweed, but only F4 showed a significant

difference ($p < 0.05$) with the control sample. The presence of seaweed acts as a humectant, reducing the a_w. This finding agrees with [40], stating that dietary fibre from a nonmeat ingredient can act as a humectant in meat products.

Table 5. The water activity of different chicken patty formulations.

Formulation	Water Activity
Control (C)	0.947 ± 0.00 [a]
F1 (2KA, 1.0S)	0.940 ± 0.01 [ab]
F2 (2KA, 1.5S)	0.936 ± 0.00 [ab]
F3 (4KA, 1.0S)	0.933 ± 0.01 [ab]
F4 (4KA, 1.5S)	0.920 ± 0.00 [b]

Mean $\pm$ standard deviation (SD) with different lowercase superscripts showed significant differences for different formulations of samples ($p < 0.05$). Control = 0% *Kappaphycus alvarezii*, 1.5% salt; F1 = 2% *Kappaphycus alvarezii*, 1.0% salt; F2 = 2% *Kappaphycus alvarezii*, 1.5% salt; F3 = 4% *Kappaphycus alvarezii*, 1.0% salt; F4 = 4% *Kappaphycus alvarezii*, 1.5% salt.

Additionally, higher salt content reduced ($p > 0.05$) the a_w, as proved by F2 (0.936) and F4 (0.920). Salt plays an important role in maintaining the quality of meat products by reducing the water activity in meat products. Previous research reported that a reduction in salt from 1.5% to 1.0% might alter the shelf life of meat products [41]. Most pathogens require a minimum a_w of 0.95, while the growth of *Clostridium botulinum E* required a minimum a_w of 0.97. However, some bacteria can produce toxins in even in low a_w conditions, such as *Listeria monocytogenes* ($a_w = 0.92$) and *Staphylococcus aureus* ($a_w = 0.86$) [42].

3.5. Shrinkage of Diameter and Thickness of Chicken Patty

The diameter and thickness shrinkages of chicken patties are closely associated with fat levels. The decreasing of fat levels caused a significant decrease in the diameter and thickness of the chicken patty ($p < 0.05$). Table 6 listed the diameter and shrinkage thickness of different chicken patty formulation types.

Table 6. Shrinkage of diameter and thickness of chicken patties with different formulations.

Formulation	Shrinkage of Diameter (%)	Shrinkage of Thickness (%)
Control (C)	31.33 ± 3.21 [a]	53.00 ± 3.61 [a]
F1 (2KA, 1.0S)	18.00 ± 3.46 [ab]	36.67 ± 11.55 [a]
F2 (2KA, 1.5S)	14.67 ± 1.53 [c]	26.67 ± 15.28 [ab]
F3 (4KA, 1.0S)	13.33 ± 1.53 [c]	20.67 ± 9.29 [ab]
F4 (4KA, 1.5S)	6.33 ± 3.51 [d]	15.33 ± 6.11 [b]

Mean $\pm$ standard deviation (SD) with different lowercase superscripts showed significant differences for different formulations of samples ($p < 0.05$). Control = 0% *Kappaphycus alvarezii*, 1.5% salt; F1 = 2% *Kappaphycus alvarezii*, 1.0% salt; F2 = 2% *Kappaphycus alvarezii*, 1.5% salt; F3 = 4% *Kappaphycus alvarezii*, 1.0% salt; F4 = 4% *Kappaphycus alvarezii*, 1.5% salt.

A significant decrease in diameter and thickness shrinkage was shown in the patties with added seaweed. F4 had the lowest diameter and thickness shrinkage of 6.33 mm and 15.33 mm, followed by F3, F2, F1, and the control sample. Seaweed containing cation concentrations such as potassium and calcium ions could retain the gel structure of carrageenan in situ and link with the meat protein matrix to absorb the water and had fat-holding properties [43]. In addition, the salt content of F4 was 1.5%, which can bind water and form a more stable gel. In contrast, a salt reduction in 1.0% in F1 showed a significant difference in diameter and thickness shrinkage ($p < 0.05$) but adding seaweed as a substitute could reduce the shrinkage of the diameter and thickness of chicken patties [44]. The formation of carrageenan gel structure by potassium and calcium ions in *Kappaphycus alvarezii* can increase the linkages with the meat–protein matrix to absorb and improve the water and fat-holding properties, which resulted in a reduction in the shrinkages of the patties [43].

3.6. Dynamic Rheological Properties of Chicken Patty

The high storage modulus (G′) compared to the loss modulus (G″) indicate the solid-like texture of the profile. High G′ indicated a harder emulsion texture. Based on Figure 1, F4 had the highest G′, validating the findings in Table 2. The sample with shorter linear G′ when shear stress is applied indicated a weak protein–protein myofibrillar interaction, which indicated a brittleness. F4 had a shorter linear G′, while the control sample had a more constant G′ linear. A high seaweed concentration improved the chicken patty's hardness but slightly altered the matrix's protein interaction.
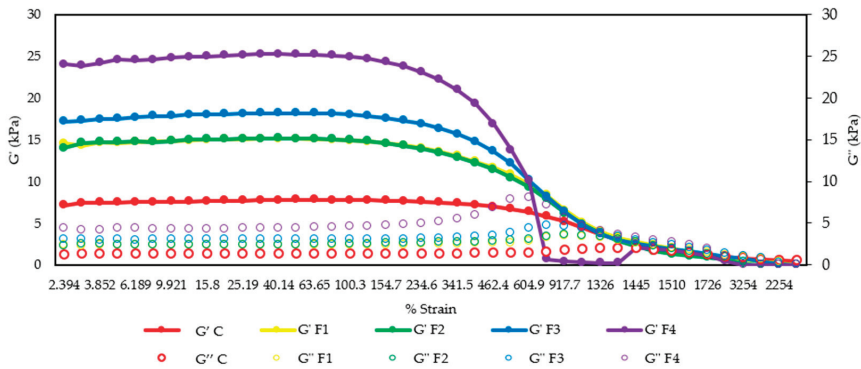
Figure 1. Strain sweep test for the effect of salt reduction and addition of seaweed (*K. alvarezii*) on the chicken patty.

Table 7 shows the maximum range of the Linear Viscoelastic Region (LVR) value and loss tangent (tan δ). The G′ and G″ values were directly proportional. The higher the G′ value, the higher the G″ chicken patty's value. The increased shear rate was required to break a harder G′, as supported in Figure 1. Although F4 had the highest G′ value of 17.24 kPa, the deformation was found under a low strain percentage of 527.6%. F4 was brittle and unable to restrain the applied stress. A stable protein network exhibits a high tangent value [21]. F4 had the lowest tangent value, while F3 had the highest tangent value, as shown in Table 7. A higher tangent indicates higher elasticity properties than viscosity, forming a more orderly gel network structure to increase the water-holding capacity of the low-salt chicken patty. Thus, F3 exhibited a strong protein network, while a weak protein network was shown in F4 [45].

Table 7. Strain sweep analysis for different formulations of chicken patty samples.

Formulation	Strain Oscillation Test	
	G′ (kPa)	G″ (kPa)
Control (C)	4.76 ± 0.40 [a]	1.48 ± 0.05 [a]
F1 (2KA, 1.0S)	7.23 ± 0.98 [a]	2.09 ± 0.42 [a]
F2 (2KA, 1.5S)	7.27 ± 1.51 [a]	2.30 ± 0.51 [a]
F3 (4KA, 1.0S)	12.87 ± 1.21 [b]	4.84 ± 4.41 [a]
F4 (4KA, 1.5S)	17.24 ± 0.49 [c]	4.50 ± 3.37 [a]

Mean ± standard deviation (SD) with different lowercase superscripts showed significant differences for different formulation of samples ($p < 0.05$). Control = 0% *Kappaphycus alvarezii*, 1.5% salt; F1 = 2% *Kappaphycus alvarezii*, 1.0% salt; F2 = 2% *Kappaphycus alvarezii*, 1.5% salt; F3 = 4% *Kappaphycus alvarezii*, 1.0% salt; F4 = 4% *Kappaphycus alvarezii*, 1.5% salt.

3.7. Sensory Evaluation of Low-Salt Chicken Patty with Seaweed

A 7-scale Hedonic test determined consumer acceptance of the sensory attributes of the *Kappaphycus alvarezii* seaweed-mixed low-salt chicken patty. The sensory attributes tested consisted of colour, aroma, hardness, elasticity, juiciness, and overall acceptance, as shown in Table 8.

Table 8. Sensory attributes for different formulations of chicken patty.

Formulation	Sensory Attributes					
	Colour	Aroma	Hardness	Elasticity	Juiciness	Overall Acceptance
Control (C)	4.70 ± 1.58 ᵃ	5.60 ± 1.40 ᵃ	3.97 ± 1.27 ᵃ	4.03 ± 1.54 ᵃ	5.37 ± 1.43 ᵃ	4.33 ± 1.37 ᵃ
F1 (2KA, 1.0S)	4.97 ± 1.10 ᵃᵇ	5.03 ± 1.35 ᵃ	4.50 ± 1.11 ᵃᵇ	4.43 ± 1.17 ᵃ	5.13 ± 1.41 ᵃᵇ	4.40 ± 1.28 ᵃ
F2 (2KA, 1.5S)	5.10 ± 1.03 ᵃᵇᶜ	5.00 ± 1.31 ᵃ	5.20 ± 1.24 ᵇ	4.60 ± 1.59 ᵃᵇ	4.60 ± 1.04 ᵃᵇ	4.70 ± 0.88 ᵃᵇ
F3 (4KA, 1.0S)	5.60 ± 1.07 ᵇᶜ	4.83 ± 1.18 ᵃ	5.30 ± 1.06 ᵇᶜ	5.50 ± 1.20 ᵇᶜ	4.40 ± 1.19 ᵇ	5.27 ± 0.94 ᵇ
F4 (4KA, 1.5S)	5.87 ± 0.97 ᶜ	4.73 ± 1.66 ᵃ	6.03 ± 1.13 ᶜ	5.67 ± 1.24 ᶜ	4.33 ± 1.42 ᵇ	6.10 ± 1.02 ᶜ

Mean ± standard deviation (SD) with different lowercase superscripts showed significant differences for different formulation of samples ($p < 0.05$). Control = 0% *Kappaphycus alvarezii*, 1.5% salt; F1 = 2% *Kappaphycus alvarezii*, 1.0% salt; F2 = 2% *Kappaphycus alvarezii*, 1.5% salt; F3 = 4% *Kappaphycus alvarezii*, 1.0% salt; F4 = 4% *Kappaphycus alvarezii*, 1.5% salt.

F4 received the highest score in colour likeness compared to other formulations ($p < 0.05$). Although the seaweed-treated patty was darker than the control sample, the panellist favoured the seaweed-treated patty. The control sample received the lowest colour acceptance with a brownish-white colour. This finding is supported by the colour analysis of the redness value a*, as shown in Table 4. A high redness a* value of the patty was commonly perceived as positive and is observed in most commercial patties.

There is no significant difference ($p > 0.05$) in aroma attributes. F4 received the highest acceptance score for its hardness and elasticity attributes with values of 6.03, signicantly higher than the control patty ($p < 0.05$). The high hardness and elasticity acceptance score in the seaweed-treated patty agreed with the texture profile improvement described in Table 4.

Juiciness, or the amount of water in meat products, is an important element for taste enhancement and meat tenderness, making it easy to chew. The decreased trend in juiciness with higher seaweed concentrations is shown in Table 8 F4 received the lowest score value among the five formulations ($p < 0.05$). However, there was no significant difference in juiciness score ($p > 0.05$) for the control sample, F1, and F2. Although the WHC improved as more seaweed was added to the patty, the seaweed patty perceived a drier mouth feel, reducing the juiciness acceptance in a patty with a high concentration of seaweed [46].

F4 received the highest score for overall acceptance and was closely followed by F3. Despite a low score for juiciness, F4 received a high score for acceptance in most other sensory attributes such as colour, hardness, and elasticity. Furthermore, salt is commonly used to enhance the organoleptic properties of meat products. Therefore, reducing salt contents deteriorated sensorial properties, although the addition of seaweed did compensate for some attributes such as hardness and elasticity.

4. Conclusions

This study investigates the effect of adding *Kappaphycus alvarezii* seaweed on the low-salt chicken patty in terms of its physicochemical properties. Adding *K. alvarezii* lowered the percentage of cooking loss, shrinkage of diameter and thickness while improving the water holding capacity. *K. alvarezii* could also improve the texture attributes such as the hardness, elasticity, chewiness, and cohesiveness of the patty. In addition, seaweed addition influenced the colour of sample by increasing the brightness (L*) and redness (+a*), while decreasing the yellowish value (+b*). The water activity remained unchanged despite the increased addition of seaweed. Additionally, *K. alvarezii* improved the dynamic rheological properties, owing to the presence of the kappa carrageenan and salt-binding properties between the meat protein matrices. The sensory evaluation results showed that salt reduction to 1.0% with the addition of 4% *K. alvarezii* into the chicken patty sample (F3) was still acceptable and preferred, despite the highest overall acceptance of F4. Future studies will concentrate on increasing the health advantages of the patty through the combination of salt and fat reduction, using *K. alvarezii* at the acceptable inclusion levels identified in the present study.

References

1. Gullón, B.; Gagaoua, M.; Barba, F.J.; Gullón, P.; Zhang, W.; Lorenzo, J.M. Seaweeds as promising resource of bioactive compounds: Overview of novel extraction strategies and design of tailored meat products. *Trends Food Sci. Technol.* **2020**, *21*, 1–18. [CrossRef]
2. Gullón, P.; Astray, G.; Gullón, B.; Franco, D.; Campagnol, P.C.B.; Lorenzo, J.M. Inclusion of seaweeds as healthy approach to formulate new low-salt meat products. *Curr. Opin. Food Sci.* **2021**, *40*, 20–25. [CrossRef]
3. Jo, K.; Lee, J.; Jung, S. Quality characteristics of low-salt chicken sausage supplemented with a winter mushroom powder. *Korean J. Food Sci. Anim. Resour.* **2018**, *38*, 769. [CrossRef]
4. Kameník, J.; Saláková, A.; Vyskočilová, V.; Pechová, A.; Haruštiaková, D. Salt, sodium chloride or sodium? Content and relationship with chemical, instrumental and sensory attributes in cooked meat products. *Meat Sci.* **2017**, *131*, 196–202. [CrossRef] [PubMed]
5. Aaslyng, M.D.; Vestergaard, C.; Koch, A.G. The effect of salt reduction on sensory quality and microbial growth in hotdog sausages, bacon, ham and salami. *Meat Sci.* **2014**, *96*, 47–55. [CrossRef] [PubMed]
6. Bhat, Z.F.; Morton, J.D.; Mason, S.L.; Bekhit, A.E.D.A. The application of pulsed electric field as a sodium reducing strategy for meat products. *Food Chem.* **2020**, *306*, 125622. [CrossRef]
7. Kloss, L.; Meyer, J.D.; Graeve, L.; Vetter, W. Sodium intake and its reduction by food reformulation in the European Union—A review. *NFS J.* **2015**, *1*, 9–19. [CrossRef]
8. Inguglia, E.S.; Zhang, Z.; Tiwari, B.K.; Kerry, J.P.; Burgess, C.M. Salt reduction strategies in processed meat products—A review. *Trends Food Sci. Technol.* **2017**, *59*, 70–78. [CrossRef]
9. O'Flynn, C.C.; Cruz-Romero, M.C.; Troy, D.; Mullen, A.M.; Kerry, J.P. The application of high-pressure treatment in the reduction of salt levels in reduced-phosphate breakfast sausages. *Meat Sci.* **2014**, *96*, 1266–1274. [CrossRef]
10. Gan, X.; Zhao, L.; Li, J.; Tu, J.; Wang, Z. Effects of partial replacement of NaCl with KCl on bacterial communities and physicochemical characteristics of typical Chinese bacon. *Food Mircobiol.* **2021**, *93*, 103605. [CrossRef]
11. Lafarga, T.; Acién-Fernández, F.G.; Garcia-Vaquero, M. Bioactive peptides and carbohydrates from seaweed for food applications: Natural occurrence, isolation, purification, and identification. *Algal Res.* **2020**, *48*, 101909. [CrossRef]
12. Capillo, G.; Savoca, S.; Costa, R.; Sanfilippo, M.; Rizzo, C.; Lo Giudice, A.; Albergamo, A.; Rando, R.; Bartolomeo, G.; Spanò, N.; et al. New insights into the culture method and antibacterial potential of Gracilaria gracilis. *Mar. Drugs* **2018**, *16*, 492. [CrossRef] [PubMed]
13. Alcantara, J.D.S.; Lazaro-Llanos, N. Mineral availability, dietary fiber contents, and short-chain fatty acid fermentation products of *Caulerpa lentillifera* and *Kappaphycus alvarezii* seaweeds. *Kimika* **2020**, *31*, 1–10. [CrossRef]
14. Lorenzo, J.M.; Agregán, R.; Munekata, P.E.; Franco, D.; Carballo, J.; Şahin, S.; Barba, F.J. Proximate composition and nutritional value of three macroalgae: *Ascophyllum nodosum*, *Fucus vesiculosus* and *Bifurcaria bifurcate*. *Mar. Drugs* **2017**, *15*, 360. [CrossRef]
15. Circuncisão, A.R.; Catarino, M.D.; Cardoso, S.M.; Silva, A.M. Minerals from macroalgae origin: Health benefits and risks for consumers. *Mar. Drugs* **2018**, *16*, 400. [CrossRef]
16. Mohammad, S.M.; Razali, S.M.; Rozaiman, N.M.; Laizani, A.N.; Zawawi, N. Application of seaweed (*Kappaphycus alvarezii*) in Malaysian food products. *Int. Food Res. J.* **2019**, *26*, 1677–1687.
17. Cox, S.; Abu-Ghannam, N.; Gupta, S. Effect of processing conditions on phytochemical constituents of edible Irish seaweed *Himanthalia elongate*. *J. Food Process. Preserv.* **2012**, *36*, 348–363. [CrossRef]
18. Mutiarahma, S.; Putra, V.G.; Chaniago, W.; Carrera, C.; Anggrahini, S.; Palma, M.; Setyaningsih, W. UV-Vis Spectrophotometry and UPLC–PDA Combined with Multivariate Calibration for *Kappaphycus alvarezii* (Doty) Doty ex Silva Standardization Based on Phenolic Compounds. *Sci. Pharm.* **2021**, *89*, 47. [CrossRef]

19. Araújo, P.G.; Nardelli, A.E.; Fujii, M.T.; Chow, F. Antioxidant properties of different strains of *Kappaphycus alvarezii* (*Rhodophyta*) farmed on the Brazilian coast. *Phycologia* **2020**, *59*, 272–279. [CrossRef]
20. Munsu, E.; Mohd Zaini, H.; Matanjun, P.; Ab Wahab, N.; Sulaiman, N.S.; Pindi, W. Physicochemical, sensory properties and lipid oxidation of chicken sausages supplemented with three types of seaweed. *Appl. Sci.* **2021**, *11*, 11347. [CrossRef]
21. Vilar, E.G.; Ouyang, H.; O'Sullivan, M.G.; Kerry, J.P.; Hamill, R.M.; O'Grady, M.N.; Kilcawley, K.N. Effect of salt reduction and inclusion of 1% edible seaweeds on the chemical, sensory and volatile component profile of reformulated frankfurters. *Meat Sci.* **2020**, *161*, 108001. [CrossRef] [PubMed]
22. Matanjun, P.; Mohamed, S.; Mustapha, N.M.; Muhammad, K. Nutrient content of tropical edible seaweeds, *Eucheuma cottonii*, *Caulerpa lentillifera* and *Sargassum polycystum*. *J. Appl. Phycol.* **2009**, *21*, 75–80. [CrossRef]
23. Pindi, W.; Mah, H.W.; Munsu, E.; Ab Wahab, N. Effects of addition of *Kappaphycus alvarezii* on physicochemical properties and lipid oxidation of mechanically deboned chicken meat (MDCM) sausages. *Br. Food J.* **2017**, *119*, 2229–2239. [CrossRef]
24. Wan Rosli, W.I.; Solihah, M.A.; Aishah, M.; Nik Fakurudin, N.A.; Mohsin, S.S.J. Colour, textural properties, cooking characteristics and fibre content of chicken patty added with oyster mushroom (*Pleurotus sajor-caju*). *Int. Food Res. J.* **2011**, *18*, 621–627.
25. Kumari, A.; Mane, B.G.; Thakur, D.; Khurana, S.K. Effect of incorporation of Lungru (*Diplazium esculentum*) on physicochemical, microbiological and sensory quality of chicken patties. *J. Meat Sci. Technol.* **2015**, *3*, 28–31.
26. Cegiełka, A.; Gniewosz, M.; Hać-Szymańczuk, E.; Chlebowska-Śmigiel, A. Effect of the addition of pullulan on the quality of low-fat homogenized scalded sausages. *CYTA J. Food* **2017**, *15*, 147–154. [CrossRef]
27. Serdaroglu, M.; Ozsumer, M.S. Effects of soy protein, whey powder and wheat gluten on quality characteristics of cooked beef sausages formulated with 5, 10 and 20% fat. *Electron. J. Pol. Agric. Univ.* **2003**, *6*, 3.
28. Huo, M.; Guo, Y. Electric field enhances shear resistance of polymer melts via orientational polarization in microstructures. *Polymers* **2020**, *12*, 335. [CrossRef]
29. Lis, A.; Staniewski, B.; Ziajka, J. A comparison of butter texture measurements with the AP 4/2 penetrometer and TA. XT. Plus texture analyzer. *Int. J. Food Prop.* **2021**, *24*, 1744–1757. [CrossRef]
30. Cofrades, S.; Benedí, J.; Garcimartin, A.; Sánchez-Muniz, F.J.; Jimenez-Colmenero, F. A comprehensive approach to formulation of seaweed-enriched meat products: From technological development to assessment of healthy properties. *Food Res. Int.* **2017**, *99*, 1084–1094. [CrossRef]
31. Barretto, A.C.d.S.; Pacheco, M.T.B.; Pollonio, M.A.R. Effect of the addition of wheat fiber and partial pork back fat on the chemical composition, texture and sensory property of low-fat bologna sausage containing inulin and oat fiber. *Food Sci. Technol.* **2015**, *35*, 100–107. [CrossRef]
32. Ventanas, S.; Puolanne, E.; Tuorila, H. Temporal changes of flavour and texture in cooked bologna type sausages as affected by fat and salt content. *Meat Sci.* **2010**, *85*, 410–419. [CrossRef] [PubMed]
33. Wong, K.H.; Cheung, P.C. Nutritional evaluation of some subtropical red and green seaweeds: Part I-proximate composition, amino acid profiles and some physicochemical properties. *Food Chem.* **2000**, *71*, 475–482. [CrossRef]
34. Cox, S.; Abu-Ghannam, N. Enhancement of the phytochemical and fibre content of beef patties with *Himanthalia elongata* seaweed. *Int. J. Food Sci. Technol.* **2013**, *48*, 2239–2249. [CrossRef]
35. Debrecéni, O.; Lípová, P.; Bučko, O.; Cebulska, A.; Kapelánski, W. Effect of pig genotypes from Slovak and Polish breeds on meat quality. *Arch. Anim. Breed.* **2018**, *61*, 99–107. [CrossRef]
36. Ferrini, G.; Comaposada, J.; Arnau, J.; Gou, P. Colour modification in a cured meat model dried by Quick-Dry-Slice process and high pressure processed as a function of NaCl, KCl, K-lactate and water contents. *Innov. Food Sci. Emerg. Technol.* **2012**, *13*, 69–74. [CrossRef]
37. Aleson-Carbonell, L.; Fernandez-Lopez, J.; Perez-Alvarez, J.A.; Kuri, V. Functional and sensory effects of fibre-rich ingredients on breakfast fresh sausages manufacture. *Food Sci. Technol. Int.* **2005**, *11*, 89–97. [CrossRef]
38. Zhong, H.; Gao, X.; Cheng, C.; Liu, C.; Wang, Q.; Han, X. The structural characteristics of seaweed polysaccharides and their application in gel drug delivery systems. *Mar. Drugs* **2020**, *18*, 658. [CrossRef]
39. Choi, Y.S.; Choi, J.H.; Han, D.J.; Kim, H.Y.; Kim, H.W.; Lee, M.A.; Chung, H.J.; Kim, C.J. Effects of *Laminaria japonica* on the physico-chemical and sensory characteristics of reduced-fat pork patties. *Meat Sci.* **2012**, *91*, 1–7. [CrossRef] [PubMed]
40. Biswas, A.K.; Kumar, V.; Bhosle, S.; Sahoo, J.; Chatli, M.K. Dietary fibers as functional ingredients in meat products and their role in human health. *Int. J. Livest. Prod.* **2011**, *2*, 45–54.
41. Roohinejad, S.; Koubaa, M.; Barba, F.J.; Saljoughian, S.; Amid, M.; Greiner, R. Application of seaweeds to develop new food products with enhanced shelf-life, quality and health-related beneficial properties. *Food. Res. Int.* **2017**, *99*, 1066–1083. [CrossRef] [PubMed]
42. Petit, G.; Jury, V.; de Lamballerie, M.; Duranton, F.; Pottier, L.; Martin, J.L. Salt intake from processed meat products: Benefits, risks and evolving practices. *Compr. Rev. Food Sci. Food Saf.* **2019**, *18*, 1453–1473. [CrossRef] [PubMed]
43. Leandro, A.; Pereira, L.; Gonçalves, A.M. Diverse applications of marine macroalgae. *Mar. Drugs* **2019**, *18*, 17. [CrossRef]
44. Jeong, J.Y.; Lim, S.T.; Kim, C.J. The quality characteristics of salted ground pork patties containing various fat levels by microwave cooking. *Korean J. Food Sci. Anim. Resour.* **2016**, *36*, 538. [CrossRef] [PubMed]

45. Sun, X.D.; Holley, R.A. Factors influencing gel formation by myofibrillar proteins in muscle foods. *Compr. Rev. Food Sci. Food Saf.* **2011**, *10*, 33–51. [CrossRef]

46. Babji, A.S.; Ramachandran, R.; Ismail, N.H. Effects of Addition of Seaweed (*Kappaphycus alvarezii*), Fish Gelatin and Chicken Feet Gelatin on the Quality Characteristics of Chicken Sausages. In Proceedings of the International Seminar on Tropical Animal Production (ISTAP), Yogyakarta, Indonesia, 12–14 September 2017; pp. 414–418.

Article

Physicochemical and Sensory Properties of Bahulu and Chocolate Mousse Developed from Canned Pulse and Vegetable Liquids

Floris Donatus [1], Mohd Dona Bin Sintang [2], Norliza Julmohammad [1], Wolyna Pindi [1] and Noorakmar Ab Wahab [1,*]

[1] Faculty of Food Science and Nutrition, Universiti Malaysia Sabah, Kota Kinabalu 88400, Sabah, Malaysia
[2] Nestle Research and Development Centre, Singapore 618802, Singapore
* Correspondence: aqemanur@ums.edu.my

Abstract: Egg white is the most commonly used foaming agent in various aerated foods. Malaysia has been experiencing an egg crisis due to lower production and increased egg consumption rates since the COVID-19 restrictions were lifted. Thus, finding an alternative functional ingredient to address the egg shortage is essential. Liquids discarded from commercially plant-based canned foods have the potential to replace eggs in food products as an alternative foaming agent. Therefore, this study aims to investigate the physicochemical and sensory properties of bahulu and chocolate mousse using canned liquids of green peas (pulses N and P), lentils (pulse R), chickpeas (pulse X), button mushrooms (vegetable A), and straw mushrooms (Vegetable D). Canned liquids were incorporated into bahulu and mousse formulations to replace egg whites. The developed bahulu and mousse were baked for 25 min at 180 °C and chilled for 3 hours at 4 °C, respectively. The texture profile of bahulu and the viscosity properties of the chocolate mousse were determined in this study. Furthermore, the research examines the proximate analysis and sensory acceptance of both products. According to the findings, bahulu A, produced from canned vegetable liquids, had the lowest hardness, springiness, and chewiness ($p < 0.05$) levels. In contrast, canned pulse liquid, which was used in bahulu N, produced comparable hardness, fracturability, adhesiveness, springiness, cohesiveness, and chewiness with the control sample ($p > 0.05$). Moreover, the viscosity values of mousses A (2238.33 ± 2.89 cP) and D (2778.33 ± 2.89 cP) were lower than the control mousse (8005.00 ± 0.00 cP) ($p < 0.05$). Bahulu and mousse contain 6.58–6.83% and 1.52–1.90% of protein, respectively. The protein content of canned pulse liquid products was higher than that of canned vegetable liquids ($p < 0.05$). The lowest taste acceptance was observed in samples Bahulu N and P as well as mousses N and P ($p < 0.05$). This outcome could be due to the saltiness derived from the canned green pea liquid. The appearance, odor, and overall acceptability of the bahulu and mousse were comparable to the control samples and well-accepted by the panelists ($p > 0.05$). The findings demonstrate that canned pulse liquids (green peas, lentils, and chickpeas) can potentially mimic egg white in the development of bahulu and chocolate mousse.

Keywords: egg white; pulses; foaming agent; aerated foods; canned liquid

1. Introduction

Aerated foods contain air or gas, which makes the finished products lighter and more voluminous [1]. Aerated foods can have both positive and negative consequences for the food industry. Extra cost and effort are required to create the desired aerated products with lower allergenicity levels of β-lactoglobulin that remains unaffected, even when heated [2]. Furthermore, the overbeating effect of liquid egg whites is permanent [3]. Advantageously, aerated foods add variety to food products, ranging from baked to chilled, resulting in a novel texture and sensory appeal [1]. The incorporation of air into food

products produces foods with a softer texture. Mousses are the classic example of aerated food widely consumed, in which the incorporation and retention of bubbles are crucial in the success of the dish [4]. Mousse highly depends on its texture, which is supposed to be fluffy, soft, and airy. Good-quality mousse is when the foam is produced with an even distribution of smaller bubbles, resulting in a more stable and creamier mousse [5]. Bahulu is another example of an aerated food, which is very popular among Malaysians. Bahulu is prepared by baking in various shapes [6]. The most common shape of bahulu is bahulu cermai (button bahulu) and bahulu ikan emas (goldfish bahulu). Moreover, some of the aerated foods provide extra nutritional benefits to consumers. For instance, bread is high in fiber, which is good for human health. The foam inside food can enhance the food's texture, color, and novelty, thus increasing consumers' excitement towards a specific food product [7]. These include producing aerated foods, such as ice cream, cakes, soft drinks, and more.

Over the years, egg white has been extensively applied as an excellent foaming agent in many aerated foods, including mousse [8]. Egg white contains protein albumen that can rapidly absorb on the air–liquid interface during whipping and form a cohesive viscoelastic film through intermolecular interactions [9]. Some aerated foods' reliance on egg white may cause the demand for eggs to increase further. Situations, such as high feed costs, an unstable economy, and disease outbreaks disrupting egg production rates, will eventually have an impact on egg demand fulfilment. Recently, egg scarcity has emerged as one of Malaysia's most pressing issues, particularly following the relaxation of COVID-19 restrictions [10]. Thus, plant-based foods have gained significant attention from the community as an alternative foaming agent to replace egg whites [11]. Various plant proteins, such as pulses, are commercially available for the further development of plant-based products, including aerated foods [12]. A study was conducted on the proximate meringue composition and sensory evaluation of haricot beans, garbanzo chickpeas, whole green lentils, and split yellow pea liquids [13]. The meringue produced from these liquids had a lower moisture content than egg white meringue. However, the meringue from garbanzo chickpeas and whole green lentils produced comparable hardness compared to egg white meringue. Furthermore, the overall preference did not significantly vary from the liquids to egg whites. Another study showed that replacing egg whites with aquafaba did not considerably affect the physicochemical parameters of a sponge cake [14]. Thus, this research aims to investigate the physicochemical properties and sensory acceptance of bahulu and chocolate mousse developed from selected canned pulse and vegetable liquids. Aeration characterization is used to test the ability of various canned pulse and vegetable liquids to form foam. Based on the overrun results [15], liquids from green peas (pulses N and P), lentils (pulse R), chickpeas (pulse X), button mushrooms (vegetable A), and straw mushrooms (vegetable D) obtained overruns higher than 1000% and were chosen as potential foaming agents for bahulu and chocolate mousse development.

2. Materials and Methods

2.1. Materials

The commercial canned samples and eggs were obtained from Bataras Supermarket, Sabah. Other materials utilized were all-purpose flour, baking powder, cooking chocolate, butter, and sugar that were also obtained from Bataras Supermarket, Papar. Table 1 shows the types of canned pulse and vegetable liquid samples used and their symbols. Meanwhile, the nutritional information of the canned products as specified by the manufacturers is shown in Table 2.

Table 1. Canned pulse and vegetable liquid samples.

Materials	Manufacturers	Symbols
Button Mushroom	Myxo, China	Vegetable A, Bahulu A, Mousse A
Straw Mushroom	Rex, Malaysia	Vegetable D, Bahulu D, Mousse D
Green Pea	Sunstar, Malaysia	Pulses N, Bahulu N, Mousse N
Green Pea	Marina, Malalysia	Pulses P, Bahulu P, Mousse P
Lentils	Cirio, Italy	Pulses R, Bahulu R, Mousse R
Chickpea	Coppola, Italy	Pulses X, Bahulu X, Mousse X

Table 2. Nutritional composition of canned products.

Sample	Nutritional Composition					
	Protein (g)	Fat (g)	Carbohydrate (g)	Salt (mg)	Fiber (g)	Sugar (g)
Vegetable A (Button Mushroom)	1	0	4	330	2	2.2
Vegetable D (Straw Mushroom)	4	1	6.3			
Pulse N (Green Pea)	19	0	60	2400	25	
Pulse P (Green Pea)	5	1	10		4	
Pulse R (Lentils)	5.9		0.9	600	4.2	
Pulse X (Chickpea)	5.4	1.6	10.8	25	5.6	

2.2. Product Development

2.2.1. Bahulu

The process of making bahulu desserts was referred to and modified [6]. The formulation of bahulu developed from liquid egg whites as the control is shown in Table 3. Firstly, 100 g of all-purpose flour and 7 g of baking powder were prepared in a bowl (Mixture A). The flour was sifted for several minutes. Then, 110 g of liquid egg whites were beaten to form foam (Mixture B). Then, about 25 g of sugar was blended and whisked with mixture B for three minutes. Then, mixture A was added to and mixed with the sugar-foam ingredient by using a scraper, and placed in a bahulu mould. Lastly, the batter was baked under a preheated oven (Sinmag SM-994f, New Taipei City, Taiwan) at 180 °C for 25 min. The end-product was kept in an air-tight container at room temperature for a day prior to the texture profile analysis, proximate analysis, and sensory evaluation. The steps were repeated by replacing 100% of egg whites presented in the Table 3 formulation with pulses N, P, R, and X, and vegetables A and D liquids.

Table 3. Formulation of Bahulu control.

Material	Weight (g)
All-Purpose Flour	100
Baking Powder	7
Liquid Egg Whites	110
Sugar	25

2.2.2. Chocolate Mousse

For the chocolate mousse [16], the formulation of the mousse developed from liquid egg whites as the control is shown in Table 4. A total of 150 g of dark chocolate (Bakerchoize, Malaysia) was melted using the double-boiling method, and 50 g of butter was added to the melted chocolate. A total of 110 g of liquid egg whites was produced to form foam and

25 g of sugar was added to the foam. The chocolate and egg white foam were mixed and 5 g of lemon zest was then added. Lastly, the mixture was poured into a suitable container and stored in a chiller at 0–4 °C for three hours. The final product of the chocolate mousse was examined for viscosity, proximate analysis, and sensory evaluation. The stages were repeated by substituting the liquid from pulses N, P, R, and X, and vegetables A and D for 100% of the egg whites presented in Table 4's formulation.

Table 4. Formulation of mousse control.

Material	Weight (g)
Dark Chocolate	150
Butter	50
Liquid Egg Whites	110
Sugar	25
Lemon Zest	5

2.3. Texture Profile Analysis of Bahulu

TA.XT.Plus (Stable Micro Systems, Godalming, UK) with a 36 mm diameter cylinder was used to describe the bahulu's texture in terms of hardness, fracturability, adhesiveness, cohesiveness, springiness, gumminess, and chewiness [17]. The bahulu control and samples baked the day before were prepared by removing the bahulu's outer layer and crust and cutting it into a size of 25 mm × 25 mm × 25 mm. The test was performed by a measuring force on compression of 5 g, with the speed set at 2 mm/minute at a distance of 10 mm. Triplicate results were obtained for each sample [18].

2.4. Viscosity of Chocolate Mousse

The viscosity [19] values of the control and chocolate mousse samples were measured using a rotational viscometer (Brookfield DV-II+PRO, Middleboro, MA, USA). Speed and spindle were determined at the start of the experiment. The speed and spindle values were determined by observing the percentage values of the results. The percentage must be between 10–100%. Spindle 4, with a speed of 0.5 rpm, was the best option to determine the egg and samples' viscosity values. The time taken to measure the viscosity was two minutes. Triplicate results were obtained for all samples.

2.5. Proximate Analysis

The proximate composition of bahulu and chocolate mousse desserts was determined according to the methods described by the Association of Official Analytical Chemists [20]. Protein content was measured using the Kjeldahl method, N × 6.25 (FOSS Kjeltec^{TM} 2300, Hillerød, Denmark), fat content (FOSS Soxtec^{TM} 8000, Hillerød, Denmark), ash content by a muffle furnace (Thermo Scientific, Waltham, MA, USA) at 550 °C, and moisture content by the oven-drying method in an incubator oven (Fisher Scientific, Waltham, MA, USA) at 105 °C. The crude fiber content was determined through the gravimetric method by using a fiber bag, Fibretherm (Gerhardt, Germany), dried in an oven at 105 °C overnight, and incinerated at 550 °C overnight. Carbohydrate content was calculated as 100% (protein content %—fat content %—moisture content %—ash content %—fiber content %). The results are expressed in percentages (%). Lastly, the caloric value (Cal) of bahulu was estimated: Calorie (kcal) = (Crude Protein × 4 kcal) + (Crude Fat × 9 kcal) + (Crude Carbohydrate × 4 kcal) [21].

2.6. Sensory Evaluation

A sensory evaluation was conducted to determine the preference and acceptance of the dessert, according to the methods of Lawless and Heymann [22]. A laboratory sensory test to determine the degree of liking and disliking both bahulu and chocolate mousse was conducted using a 9-point rating scale (extremely dislike to extremely like). About 10 g of bahulu and chocolate mousse samples were weighed and labeled randomly with a

3-digit-code sample prior to food tasting. Water was provided for each panelist to cleanse their mouths. About 40 untrained panelists from the Faculty of Food Science and Nutrition, Universiti Malaysia Sabah, were selected to evaluate the appearance, color, odor, taste, texture, and overall acceptability of the bahulu and chocolate mousse desserts.

2.7. Statistical Analysis

The data were represented as mean ± standard deviation. The means of collected data were analyzed by advanced analysis in the Statistical Package (SPSS Inc., version 26.0) application for Windows and ANOVA tests. The differences between the mean values were calculated using Duncan's multiple comparison tests at a 95% confidence level ($p < 0.05$). The bivariate Pearson's correlation was used for the linear relationship between the determination of two variables.

3. Results and Discussions

3.1. Physicochemical and Sensory Properties of Bahulu

3.1.1. Texture Profile Analysis of Bahulu

Table 5 shows the texture profile analysis result of bahulu composed of canned liquid samples and egg whites. Bahulu developed from vegetable D and pulses N, P, and X had a hardness profile comparable to the Bahulu control ($p > 0.05$), while bahulu developed from vegetable A and pulse R had lower and higher levels of hardness, respectively, compared to the Bahulu control ($p < 0.05$). Hardness can be defined as the first mastication of food redesigned by a uniaxial compression test, where stress is required to deform a food in an approximately linear way to be reproduced [23]. A similar pattern can be observed in the hardness result for meringue, where the meringue created from garbanzo chickpeas had a comparable hardness profile to those produced from egg whites [13]. Vegetable A had the lowest foam stability with a drainage ratio of 1.14, resulting in a weak and less elastic foam. Because of these factors, foam created from canned vegetable liquids had a decreased ability to retain an aerated structure than the other samples, resulting in a softer texture for Bahulu A [23]. Similarly, sponge cake developed from aquafaba [14] had a lower hardness result than an egg white sponge cake. This result could be attributed to the differences in the foam stability of aquafaba and egg whites. It has been reported that the interaction of protein and insoluble carbohydrates during the canning process affects the viscosity of aquafaba [24]. The liquid for pulse R had a higher viscosity of 41.1 cP when compared to the liquids for pulses N and P, as well as vegetables A and D. Because the higher viscosity improved the foaming stability, Bahulu R was slightly harder than the other samples. Foam stability is determined by the thickness and strength of the interface film, which is related to the high viscosity of the continuous phase [25]. The protein contents of vegetable A and pulse N, as specified by the manufacturer, were lower and higher, respectively, when compared to the other types of commercial vegetable and pulse cans (Table 2). Furthermore, when compared to other canned liquid samples, pulse N had the highest protein (2.18%), salt (7.70%), and sugar (8.90%) contents, according to our study (unpublished data). As the protein concentration increases, so does the foaming stability [26]. Similarly, higher salt and sugar contents increase the liquid's viscosity, resulting in a more stable foam for pulse N [26].

The fracturability of Bahulu samples A, D, N, P, R, and X were comparable to the Bahulu control ($p > 0.05$). Fracturability is the tendency for the bahulu to break during the instrumental test [27]. Bahulu produced from potential canned liquid samples breaks at the same rate as bahulu created from egg whites when it is eaten. Therefore, all the canned liquid samples possessed similar brittleness levels as egg whites, which is necessary for consumers' eating experience. High fracturability and hardness levels with low cohesiveness are important texture characteristics for crispy, baked, or dry aerated foods [28].

Table 5. Texture profile analysis of Bahulu.

Sample	Hardness (g)	Fracturability	Adhesiveness (mJ)	Springiness (mm)	Cohesiveness	Chewiness (mJ)
Control	4.03 ± 0.01 [b]	4.11 ± 0.04 [a,b,c]	−0.08 ± 0.03 [e]	0.99 ± 0.01 [e]	0.87 ± 0.02 [c]	3.49 ± 0.09 [f]
Bahulu A	3.91 ± 0.01 [a]	4.03 ± 0.01 [a]	−1.89 ± 0.02 [c]	0.38 ± 0.04 [a]	0.57 ± 0.02 [a,b]	0.89 ± 0.02 [a]
Bahulu D	4.11 ± 0.02 [b,c]	4.22 ± 0.07 [b,c]	−2.52 ± 0.02 [a]	0.61 ± 0.05 [b]	0.51 ± 0.01 [a]	1.34 ± 0.02 [c]
Bahulu N	4.03 ± 0.01 [b]	4.13 ± 0.01 [a,b,c]	−0.04 ± 0.02 [e]	0.99 ± 0.01 [e]	0.86 ± 0.01 [c]	3.49 ± 0.09 [f]
Bahulu P	4.08 ± 0.12 [b,c]	4.13 ± 0.13 [a,b,c]	−2.19 ± 0.08 [b]	0.58 ± 0.08 [b]	0.51 ± 0.05 [a]	1.19 ± 0.04 [b]
Bahulu R	4.15 ± 0.03 [c]	4.23 ± 0.01 [c]	−0.01 ± 0.01 [e]	0.83 ± 0.02 [d]	0.60 ± 0.05 [b]	2.18 ± 0.06 [e]
Bahulu X	4.10 ± 0.09 [b,c]	4.09 ± 0.08 [a,b]	−1.56 ± 0.06 [d]	0.73 ± 0.05 [c]	0.55 ± 0.07 [a,b]	1.92 ± 0.16 [d]

Different letters in the same column indicate significant differences ($p < 0.05$); mean ± S.D., $n = 3$.

As for the adhesiveness, there were no significant differences in the bahulu developed from pulses N and R to the Bahulu control ($p > 0.05$). Meanwhile, the bahulu developed from pulse P and vegetables A and D had a higher level of adhesiveness compared to the control sample ($p < 0.05$). Adhesiveness represents the ability of the cake to adhere to the teeth when chewed. Therefore, a higher negative value of adhesiveness results in greater adhesive [29]. A low level of adhesiveness is preferable as bahulu is a solid food and should be easier to chew and swallow without it adhering too much to the teeth. Bahulu samples N and R had a better texture in terms of adhesiveness compared to other bahulu developed from canned liquids. The high level of adhesiveness in other bahulu samples might be attributed to the higher moisture content, as displayed in Table 6. Sucrose, which was added to the bahulu formulation, has a high water affinity due to its hygroscopic properties [30]. As a result, sugar prevents baked goods from drying out and becomes more adhesive.

Table 6. Proximate composition of bahulu.

Sample	Protein (%)	Fat (%)	Ash (%)	Fiber (%)	Moisture (%)	Carbohydrate (%)	Caloric Value (kcal)
Bahulu Control	10.43 ± 0.31 [c]	0.49 ± 0.01 [b]	4.21 ± 0.02 [a]	0.22 ± 0.01 [a]	35.40 ± 0.01 [c]	49.26 ± 0.31 [a]	243.13 ± 0.20 [c]
Bahulu A	0.35 ± 0.04 [a]	1.24 ± 0.03 [d]	4.42 ± 0.01 [b]	0.20 ± 0.02 [a]	36.45 ± 0.02 [d]	57.34 ± 0.05 [d]	241.88 ± 0.20 [b]
Bahulu D	0.44 ± 0.01 [a]	1.26 ± 0.01 [d]	4.43 ± 0.02 [b]	0.20 ± 0.01 [a]	36.43 ± 0.01 [d]	57.23 ± 0.02 [d]	242.01 ± 0.09 [b]
Bahulu N	6.83 ± 0.26 [b]	0.09 ± 0.01 [a]	4.49 ± 0.05 [c]	0.22 ± 0.01 [a]	35.42 ± 0.02 [c]	52.95 ± 0.29 [b]	239.95 ± 0.14 [a]
Bahulu P	0.67 ± 0.49 [a]	1.29 ± 0.09 [d]	4.52 ± 0.02 [c]	0.22 ± 0.01 [a]	36.43 ± 0.01 [d]	56.90 ± 0.57 [d]	241.87 ± 0.37 [b]
Bahulu R	6.58 ± 0.54 [b]	0.06 ± 0.02 [a]	4.45 ± 0.01 [bc]	0.22 ± 0.01 [a]	34.05 ± 0.01 [b]	54.64 ± 0.50 [c]	245.44 ± 0.03 [d]
Bahulu X	6.70 ± 0.36 [b]	0.71 ± 0.01 [c]	4.20 ± 0.03 [a]	0.21 ± 0.01 [a]	33.58 ± 0.01 [a]	55.59 ± 0.37 [c]	251.57 ± 0.15 [e]

Different letters in the same column indicate significant differences ($p < 0.05$); mean ± S.D., $n = 3$.

Springiness is the rate at which the bahulu recovers from a deforming force [31]. Bahulu N recovered more rapidly and did not break as easily as the other bahulu developed from canned liquid samples, similar to the control sample. When foam is stable, it assists in holding the structure of a food product. Foam with sugar is stable and appears less stiff [32], thus enhancing food attributes and increasing product acceptance. On the other hand, cohesiveness measures the strength of internal bonds composing the bahulu product [33]. The deformation rate depends on the strength of the bahulu and the difficulty level of breaking the inner bonds [34]. Therefore, a certain level of cohesiveness in bahulu is preferable, especially its internal bonds, similar to egg white bahulu. The internal bond strength of Bahulu N was comparable to the egg white bahulu, which resulted from the foaming stability of pulse N. Only bahulu produced from pulse N had similar springiness, cohesiveness, and chewiness characteristics as the Bahulu control ($p > 0.05$). Meanwhile, bahulu developed from vegetables A and D, and pulses P, R, and X had reduced springiness, cohesiveness, and chewiness values compared to the control sample ($p < 0.05$).

Bahulu composed of pulse P and vegetables A and D had a reduced chewiness value compared to the bahulu composed of pulses R and X ($p < 0.05$). Chewiness can be described as the energy needed to chew solid food [35], in this case bahulu, until it is ready to be

swallowed. It is the relation between hardness X cohesiveness X springiness. In all three parameters, Bahulu N had the most similarities to the Bahulu control. Pulse N had the highest protein and salt contents (Table 2), which contributed to the formation of a stable foam from its liquid, resulting in a more chewable product. The chewiness level of bahulu produced from pulse P (1.19 ± 0.04 mJ) and vegetables A (0.89 ± 0.02 mJ) and D (1.34 ± 0.02 mJ) was too low, which may reduce consumers' enjoyment of chewing the bahulu before swallowing it. In a previous study [36], chickpea flour decreased gluten-free muffins' springiness, cohesiveness, and chewiness levels. Similarly, bahulu made from chickpeas and other pulse and vegetable liquids in this study had lower springiness, cohesiveness, and chewiness. Pulse N was an exception, where its bahulu had similar springiness, cohesiveness, and chewiness levels compared to the Bahulu control ($p > 0.05$). The chewiness parameter showed a positive correlation in the bivariate Pearson's correlation ($R^2 = 0.859$) to the hardness parameters of bahulu. A similar positive-correlation trend of chewiness and hardness was also observed in eggless cake containing soy milk [37].

3.1.2. Proximate Composition of Bahulu

The Bahulu control contained the highest protein content of 10.43% (Table 6) among the bahulu developed from canned liquid samples ($p < 0.05$). The protein content of bahulu produced from canned pulse liquids ranged from 6.58 to 6.83%, which was higher than that of canned vegetable liquids, but lower than that of the Bahulu control. This suggested that using canned liquids may reduce the protein content of bahulu when compared to egg whites. A previous study [11] showed that aquafaba contained heat-stable proteins, which might delay protein denaturation and coagulation during baking, contrary to liquid egg whites that are heat-sensitive. Therefore, canned pulse liquid foams were able to hold their protein content after the baking process.

All bahulu samples had different amounts of fat than the control sample ($p < 0.05$). The fat contents of the Bahulu control (0.49%), N (0.09%), R (0.06%), and X (0.71%) were lower than the bahulu developed from pulse P (1.29%) and vegetables A (1.24%) and D (1.26%). Nevertheless, all the samples contained a low fat content. This outcome might be because the canned pulse and vegetable liquids contained less than 1% of fat. Moreover, the nutritional information specified by the manufacturers also indicated the fat content of the product was about 1 g (Table 2). In another study [6], rice bran had a high fat content (16–22%), contributing to the fat content in bahulu. The fat content of the bahulu developed from canned liquid samples was much lower, between 0%–1.3%. Thus, canned liquid samples are proven to be a good choice for an alternative foaming agent, as bahulu with a reduced fat content was able to be produced.

Ash levels in bahulu developed from vegetables A and D, as well as pulses N, P, and R, were higher in the range of 4.42–4.45% than in Bahulu X (4.20%) and the Bahulu control (4.21%) ($p < 0.05$). Meanwhile, the amount of crude fiber in all bahulu samples was comparable to the egg white bahulu ($p > 0.05$). All bahulu composed of canned pulse and vegetable liquids contained a significant amount of ash and fiber as the control variables, which made the canned liquid samples beneficial for food-product development. Most of the ash content resulted from the other products used to make bahulu, such as flour and sugar. A higher ash content in the bahulu produced from canned liquids was probably attributed to the flour used. Wheat flour contains ash that becomes a major indicator of wheat flour's quality and use [38]. Therefore, it was suggested that the usage of flour in making bahulu desserts in this study contributed to the ash and fiber contents. The presence of fiber in bahulu improved its texture. This was demonstrated in a study in which fiber increased the elasticity of cake or muffin batter, resulting in a firmer and less cohesive cake or muffin [39].

There were no significant differences in the moisture content between Bahulu N and the Bahulu control ($p > 0.05$), both of which had a moisture content of around 35.4%. However, with the addition of vegetables A and D, and pulse P, the moisture content of the bahulu products slightly increased to 36.4%. ($p < 0.05$). In contrast, for pulses R and X,

the moisture content slightly decreased, ranging from 33.5 to 34.0% ($p < 0.05$). Moisture in a food product is crucial as food needs to have a certain level of moisture to maintain its texture, shape, and taste, and remain safe from microbial growth. Extra water in a food product can increase the rate of microbial growth [40]. All the samples had a moisture content of around 30%, the same as the egg white bahulu's moisture level. Similarly, a cake made with aquafaba has a moisture content of 21.44%, which is around 20%, comparable to a cake made with egg whites (22.18%) [14]. Therefore, the bahulu composed of canned liquid samples had a moisture content suitable for maintaining its texture and shape as the Bahulu control.

The amount of protein in the bahulu developed from canned liquids was much lower than in the Bahulu control. Therefore, the carbohydrate percentage was higher in the bahulu produced from canned liquid samples. The carbohydrate content of the egg white bahulu was the lowest compared to the bahulu developed from vegetables A and D and pulses N, P, R, and X ($p < 0.05$). Carbohydrates are important as the main source of energy [41]. Similar to the Bahulu control, bahulu produced from pulses N, P, R, and X and vegetables A and D can be consumed as a source of energy. Moreover, a higher carbohydrate content might improve the foaming properties of bahulu composed of canned liquid samples. For instance, the foaming capacity is significantly increased when sucrose (carbohydrate) is present in whey protein isolates [42]. Finally, the caloric value of the Bahulu control (243.13 kcal) was higher than that of Bahulu samples A (241.88 kcal), D (242.01 kcal), N (239.95 kcal), and P (241.87 kcal), but lower than that of Bahulu samples R (245.44 kcal) and X (245.44 kcal) (251.57 kcal) ($p < 0.05$). The calories in fat, protein, and carbohydrates vary depending on the food [43]. In the bahulu products, egg white bahulu had the highest amount of protein, which contributed to the higher number of calories than Bahulu samples A, D, N, and P.

3.1.3. Sensory Properties of Bahulu

Table 7 shows the results of the sensory test for bahulu made from selected canned liquids and control egg whites. There was no significant difference between the Bahulu control and Bahulu samples A, D, N, P, R, and X ($p > 0.05$) in appearance. The original appearance of bahulu is commonly bahulu cermai (star-shaped button) [44]. All the bahulu samples looked identical to the Bahulu control (Figure 1a). Figure 1b,c represent a picture of bahulu developed from canned pulse (Bahulu X) and vegetable (Bahulu A) liquids.

Table 7. Sensory properties of Bahulu samples.

Sample	Appearance	Color	Odor	Taste	Texture	Overall Acceptability
Bahulu Control	6.30 ± 1.86 [a]	6.30 ± 2.00 [b]	6.43 ± 1.53 [a]	6.60 ± 1.53 [b]	6.20 ± 1.64 [a]	7.35 ± 1.19 [a]
Bahulu A	6.15 ± 1.70 [a]	6.23 ± 2.07 [b]	6.53 ± 1.57 [a]	6.60 ± 1.53 [b]	6.03 ± 1.54 [a]	7.03 ± 1.46 [a]
Bahulu D	6.20 ± 1.80 [a]	6.13 ± 2.03 [b]	6.50 ± 1.59 [a]	6.60 ± 1.53 [b]	6.05 ± 1.54 [a]	7.35 ± 1.19 [a]
Bahulu N	6.25 ± 2.00 [a]	4.40 ± 2.05 [a]	6.53 ± 1.62 [a]	4.73 ± 2.69 [a]	6.18 ± 1.57 [a]	7.40 ± 0.93 [a]
Bahulu P	6.25 ± 2.00 [a]	4.30 ± 2.07 [a]	6.50 ± 1.59 [a]	4.73 ± 2.69 [a]	6.20 ± 1.56 [a]	7.23 ± 1.19 [a]
Bahulu R	6.35 ± 1.90 [a]	4.38 ± 2.08 [a]	6.43 ± 1.53 [a]	6.60 ± 1.53 [b]	6.13 ± 1.59 [a]	7.10 ± 1.53 [a]
Bahulu X	6.30 ± 1.86 [a]	6.30 ± 2.00 [b]	6.43 ± 1.53 [a]	6.60 ± 1.53 [b]	6.10 ± 1.61 [a]	7.18 ± 1.24 [a]

Different letters in the same column indicate significant differences ($p < 0.05$).

The colors of Bahulu A, D, and X were similar to the Bahulu control ($p > 0.05$). Meanwhile, the bahulu produced from pulses N, P, and R had a significantly different color compared to the Bahulu control ($p < 0.05$). The color of the original Bahulu control was brown. The color was the result of the flour, sugar, and baking powder being mixed and baked at 180 °C. The browning effect was caused by the Maillard reaction, which was triggered by the presence of amino acids in the flour protein, sugar, and a high temperature [45]. In addition to the Maillard reaction, caramelization occurred when the carbohydrate content of the bahulu was exposed to high temperatures [45]. Liquid egg whites, vegetables A and D, and pulse X produced a white-colored foam, and thus did not affect the bahulu's

color. The liquid color of Bahulu samples N and P was green, producing light-green foam. As for Bahulu R, the canned liquid was produced from pulse R with a red color; hence, the foam was light red. The color of the foam affected the color of the end product, with Bahulu samples N and P being a slightly greenish, while Bahulu R appeared red. Similarly, a study showed that the appearance of whole-green-lentil meringues was rated lower than others due to the color of the whole green lentils [13]. Nevertheless, the color change was not significant to the panelists' preferences of bahulu as the shape was still the same as the Bahulu control.
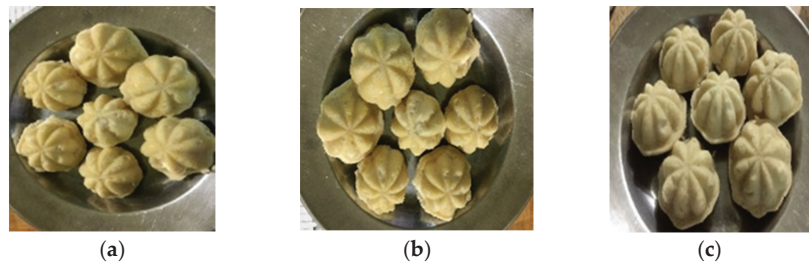
Figure 1. (**a**) Bahulu control; (**b**) Bahulu X; (**c**) Bahulu A.

The aroma or odor is sensed by olfactory receptors in the nasal epithelium [46]. This aroma or volatile molecule is usually inhaled into the nose or during chewing through the back of the throat. A particular volatile molecule then produces a specific smell. All of the bahulu products developed from canned liquid samples had the same odor or aroma as the Bahulu control ($p > 0.05$). Using canned liquid samples to produce bahulu desserts did not affect the original aroma or odor. Bahulu samples N and P were significantly different from the control sample ($p < 0.05$), while Bahulu samples A, D, R, and X were not significantly different ($p > 0.05$) in terms of taste. Taste is the most decisive criterion to be considered when making a dessert [47]; thus, it has a major impact on the final decision. Bahulu samples N and P were composed of the selected green pea liquids that could be influenced by the salt content, as specified by the manufacturer, particularly in pulse P, which contained of 2400 mg of salt (Table 2). Both bahulu tastes were slightly salty, resulting in a poor taste value. The presence of more salt decreased the moisture content [48] in Bahulu samples N and P, making the products taste saltier. Originally, bahulu has a sweet taste [44] similar to the Bahulu control and other bahulu samples in this study.

Furthermore, all the bahulu samples were not significantly different from the control sample ($p > 0.05$) in terms of texture. Foam stability is crucial for the good texture of a food product [49]. As bahulu is classified as an aerated food, the structure of the food, or texture, strongly depends on its foamability and foam stability. The bahulu samples developed from canned liquid samples were successfully created with a similar texture as the Bahulu control. Overall, the panelists provided positive feedback for all the bahulu desserts ($p > 0.05$). A similar result was obtained for the study of meringues [13]. The overall preference did not significantly vary across the meringues produced from pulse liquids. Therefore, the pulse and vegetable liquids used in this study could produce successful solid–aerated foods, although the liquid samples had different stability rates.

3.2. Physicochemical and Sensory Properties of Chocolate Mousse
3.2.1. Viscosity of Chocolate Mousse

The viscosity properties of mousses N, P, and X were not significantly different to egg whites ($p > 0.05$) (Table 8). Meanwhile, the viscosity value of chocolate mousse developed from vegetables A and D was lower than egg whites ($p < 0.05$). Food texture depends on viscosity, especially for liquid or semi-liquid foods [50]. The lower viscosity levels of mousses A and D (2238.33cP and 2778.33cP) might have been due to the lower viscosity of the canned liquids from vegetables A and D (20.67cP and 23.17cP). Differences in viscosity

cause differences in texture [51]. Vegetable-based chocolate mousses were more watery than pulse-based chocolate mousses, which were more solid. This outcome was due to the differences in the viscosity levels of the mousses developed from canned vegetable and pulse liquids. Mousses N, P, R, and X had viscosity levels ranging from 8001 to 8005cP, which were much higher than mousses A and D. Thus, mousses A and D were less accepted in the viscosity analysis.

Table 8. Viscosity of chocolate mousses.

Sample	Viscosity (cP)
Mousse Control	8005.00 ± 0.00 [d]
Mousse A	2238.33 ± 2.89 [a]
Mousse D	2778.33 ± 2.89 [b]
Mousse N	8004.33 ± 0.58 [cd]
Mousse P	8002.33 ± 1.53 [cd]
Mousse R	8001.67 ± 0.58 [c]
Mousse X	8004.33 ± 0.58 [cd]

Different letters in the same column indicate significant differences ($p < 0.05$); mean ± S.D., $n = 3$.

3.2.2. Proximate Composition of Chocolate Mousse

The mousse control had the highest protein content of 4.69%, which was higher than the mousses produced from canned liquid samples ($p < 0.05$) (Table 9). Chocolate mousse produced from canned pulse liquids contained more protein, ranging from 1.52–1.90%, than the canned vegetable liquids (0.68–0.80%). This was also due to the heat-stable protein in the pulse liquids. Meanwhile, the protein content of the egg white mousse was lower than the egg white bahulu (Table 6). The double-boiling method used in making egg white mousse to melt the chocolate and butter, then folded with egg white and canned liquid foams, caused the protein inside the egg white foam to denature as there was a change in the temperature. Egg white protein is sensitive to high temperatures as it can easily denature and coagulate [52].

Table 9. Proximate compositions of chocolate mousses.

Sample	Protein (%)	Fat (%)	Ash (%)	Fiber (%)	Moisture (%)	Carbohydrate (%)	Caloric Value (kcal)
Mousse Control	4.69 ± 1.18 [c]	28.62 ± 0.01 [b]	1.01 ± 0.01 [c]	2.07 ± 0.12 [a]	28.95 ± 0.01 [b]	34.65 ± 1.15 [c]	423.26 ± 0.01 [b]
Mousse A	0.80 ± 0.10 [a]	49.04 ± 0.01 [d]	0.88 ± 0.01 [b]	2.06 ± 0.05 [a]	27.70 ± 0.01 [a]	19.53 ± 0.12 [b]	531.60 ± 1.28 [d]
Mousse D	0.68 ± 0.50 [a]	49.02 ± 0.02 [d]	0.88 ± 0.02 [b]	2.06 ± 0.04 [a]	27.72 ± 0.01 [a]	19.64 ± 0.52 [b]	531.96 ± 2.18 [d]
Mousse N	1.90 ± 0.18 [b]	25.31 ± 0.08 [a]	0.80 ± 0.01 [a]	2.10 ± 0.02 [a]	30.01 ± 0.01 [c]	39.89 ± 0.25 [d]	403.88 ± 0.59 [a]
Mousse P	0.92 ± 0.06 [ab]	49.07 ± 0.01 [d]	0.79 ± 0.01 [a]	2.02 ± 0.04 [a]	27.71 ± 0.05 [a]	19.50 ± 0.13 [b]	530.55 ± 1.42 [d]
Mousse R	1.52 ± 0.43 [ab]	48.03 ± 0.01 [c]	1.01 ± 0.01 [c]	2.08 ± 0.08 [a]	30.00 ± 0.01 [c]	17.36 ± 0.44 [a]	514.44 ± 2.90 [c]
Mousse X	1.82 ± 0.17 [b]	25.35 ± 0.01 [a]	1.00 ± 0.01 [c]	2.07 ± 0.06 [a]	29.98 ± 0.02 [c]	39.78 ± 0.13 [d]	403.36 ± 0.81 [a]

Different letters in the same column indicate significant differences ($p < 0.05$); mean ± S.D., $n = 3$.

The fat contents of mousses N (25.31%) and X (25.35%) were less than the mousse control (28.62%) ($p < 0.05$), whereas the fat contents of mousses A (49.04%), D (49.02%), P (49.07%), and R (48.03%) were higher than the control sample ($p < 0.05$). The stability of oil foam in chocolate aeration greatly depends on drainage [53]. Increasing the level of egg yolk would decrease the foam stability of the egg white [54]. This outcome suggests that foam stability is crucial, especially in food products, such as chocolate mousse, and fat content decreases foam's stability. Additionally, other studies reported that high-fat milk may decrease the foaming ability, stability, and functionality of aerated dairy products [55]. A stable foam maintains its initial properties, forming a viscoelastic film to surround air bubbles, thus making it difficult to collapse [56]. Therefore, a higher foam stability in egg whites (drainage ratio: 0.00), pulse N (drainage ratio: 0.02), and pulse X (drainage ratio: 0.00) produced a stable mousse texture in the control mousse and mousses N and X

so that the oil or fat was not separated from the product. A higher drainage ratio for pulse P (0.06), pulse R (0.14), vegetable A (1.14), and vegetable D (1.14) caused the lower stability of mousses P, R, A, and D, which altered the mousses' properties, and high-fat mousses were produced.

Mousses A (0.88%), D (0.88%), N (0.80%), and P (0.79%) contained a significant amount of ash, albeit slightly less than the mousse control (1.01%) ($p < 0.05$). As for the fiber, all mousses had a comparable amount of fiber content to the mousse control ($p > 0.05$). The ash and fiber contents in all the mousse samples might be attributed to the chocolate and sugar used. This outcome shows that pulses N, P, R, and X, and vegetables A and D were beneficial when used as foaming agents in making chocolate mousses, similar to liquid egg whites. Furthermore, the hydrophilic surface of fiber can combine well with bubbles at the interface, strengthening the liquid sample's film and increasing the surface viscosity, thereby increasing the foaming stability [57]. Fiber and viscosity in this study showed a positive correlation in the bivariate Pearson's correlation, $R^2 = 0.732$, where a higher fiber content leads to greater viscosity. From Table 9, it can be observed that mousses A, D, and P have moisture contents ranging from 27.70–27.72% that are lower than the mousse control (28.95%), whereas mousses N, R, and X have moisture contents ranging from 29.98–30.01% that are higher than the mousse control (28.95%) ($p < 0.05$). The food moisture appears in two forms: first, water bound to ingredients in the food, such as protein, salt, and sugar; second, free or unbound water that is available for microbial growth [48]. Mousses N, R, and X had a similar texture as the mousse control, where the texture was soft and smooth. Meanwhile, for mousses A, D, and P, due to their lower viscosity values (Table 8) stability, the texture was seen to be slightly watery as the water was not fully incorporated into the mousses. These available, unbound waters were susceptible to microbial growth [40].

In bahulu, the carbohydrate content was lower when the protein content was higher. Contrarily, mousses A, D, P, and R had a low carbohydrate content, although the protein was low as fat was higher in these mousses. Mousses A, D, P, and R had carbohydrate contents ranging from 17.36 to 19.64% lower than the mousse control of 34.65%, while mousses N (39.89%) and X (39.78%) had carbohydrate contents higher than the mousse control ($p < 0.05$). Mousses N and X had a higher carbohydrate content as the protein and fat contents were low. The mousse control (423.26 kcal) had a higher caloric value than mousses N (403.88 kcal) and X (403.88 kcal). Mousses A (531.60 kcal), D (531.96 kcal), P (530.55 kcal), and R (514.44 kcal) had higher caloric values than the mousse control ($p < 0.05$), which could be attributed to their fat content. Fat has more calories per gram than protein and carbohydrates combined [58].

3.2.3. Sensory Properties of Chocolate Mousse

For the chocolate mousse, all of the mousse samples' appearance were not significantly different to the mousse control ($p > 0.05$) (Table 10). All the mousses looked the same as they did not have a fixed shape. The shape of the chocolate mousse was formed by the container used. All mousse samples' colors were similar to the mousse control ($p > 0.05$). Usually, chocolate mousse appears to be brown to darker brown in color, imitating the color of the chocolate. The dominant brown color of the chocolate was not affected by the color of the canned liquid samples. Mousse A was a slightly darker shade of brown because of the mousse's lower viscosity level and higher moisture content, as presented in Tables 8 and 9, respectively. Most panelists could not differentiate between the smell of the desserts; thus, there was no significant difference ($p > 0.05$) between the samples and control samples. All the mousse samples had a sweet smell similar to the mousse control. Originally, chocolate mousses should have a sweet to bittersweet taste depending on the amount of cocoa in the chocolate.

Table 10. Sensory properties of chocolate mousses.

Sample	Appearance	Color	Odor	Taste	Texture	Overal Acceptability
Mousse Control	6.30 ± 1.57 [a]	6.85 ± 1.69 [a]	6.08 ± 1.61 [a]	7.18 ± 1.41 [b]	6.18 ± 1.68 [c]	7.40 ± 0.87 [ab]
Mousse A	6.00 ± 2.10 [a]	6.90 ± 1.66 [a]	5.98 ± 1.66 [a]	7.18 ± 1.41 [b]	4.95 ± 1.06 [a]	7.65 ± 0.62 [b]
Mousse D	6.00 ± 2.10 [a]	6.90 ± 1.66 [a]	6.18 ± 1.71 [a]	7.18 ± 1.41 [b]	5.15 ± 1.19 [b]	7.40 ± 0.87 [ab]
Mousse N	6.35 ± 1.56 [a]	6.90 ± 1.66 [a]	6.05 ± 1.61 [a]	5.10 ± 2.66 [a]	6.23 ± 1.69 [c]	7.00 ± 1.55 [a]
Mousse P	6.30 ± 1.57 [a]	6.90 ± 1.66 [a]	6.03 ± 1.81 [a]	5.10 ± 2.66 [a]	6.20 ± 1.71 [c]	7.65 ± 0.62 [b]
Mousse R	6.30 ± 1.57 [a]	6.90 ± 1.66 [a]	6.15 ± 1.63 [a]	7.18 ± 1.41 [b]	6.20 ± 1.73 [c]	7.25 ± 1.26 [ab]
Mousse X	6.20 ± 1.52 [a]	6.90 ± 1.66 [a]	6.08 ± 1.61 [a]	7.18 ± 1.41 [b]	6.20 ± 1.70 [c]	7.13 ± 1.22 [ab]

Different letters in the same column indicate significant differences ($p < 0.05$).

Mousses N and P were significantly different ($p < 0.05$), while other samples were not significantly different ($p > 0.05$) to the mousse control in terms of taste. Similar to bahulu, Mousses N and P were made using canned green pea liquids; thus, the mousses were slightly salty. From the result, it can be observed that all mousses' textures were acceptable to the panelists ($p < 0.05$), except for mousses A and D that were less acceptable compared to the control sample ($p < 0.05$). Mousses A's and D's slightly watery texture was coherent with their previous low-viscosity result of vegetable-liquid mousses. Therefore, it was less accepted by the consumers. The texture of mousse is important as it affects the consumers' acceptability and desire to buy it again [29]. Nevertheless, most panelists believed that if improvements were made towards the samples, they would be as good as the original or the control. Overall, the majority of the panelists provided positive feedback for the mousse samples as a whole ($p > 0.05$).

4. Conclusions

The results show that the canned pulse liquids have more potential to imitate egg whites in bahulu and chocolate mousse development compared to canned vegetable liquids. Bahulu N developed from canned green pea (pulse N) liquids had comparable hardness, fracturability, adhesiveness, springiness, cohesiveness, and chewiness qualities to egg white bahulu. Moreover, chocolate mousse produced from green pea (pulse N) liquid exhibited comparable viscosity to egg white mousse but contained less fat and higher carbohydrates. Despite having a positive effect on the texture profile and viscosity, green pea liquids had a significant impact on the color and taste of the products. However, both Bahulu N and mousse N, which used green pea liquids, demonstrated similar acceptance in terms of appearance, odor, texture, and overall acceptability as Bahulu and mousse controls.

Author Contributions: Conceptualization, N.A.W. and M.D.B.S.; methodology, F.D.; software, W.P.; validation, N.A.W. and W.P.; formal analysis, F.D.; investigation, F.D.; resources, N.A.W.; data curation, F.D.; writing—original draft preparation, F.D.; writing—review and editing, N.A.W., M.D.B.S., N.J. and W.P.; visualization, N.A.W., N.J. and W.P.; supervision, N.A.W., M.D.B.S. and N.J.; project administration, N.A.W.; funding acquisition, N.A.W. All authors have read and agreed to the published version of the manuscript.

Institutional Review Board Statement: Not applicable.

Informed Consent Statement: Not applicable.

Data Availability Statement: Not applicable.

Conflicts of Interest: The authors declare no conflict of interest.

References

1. Campbell, G.M. Aerated Foods. In *Encyclopedia of Food and Health*; Elsevier: Amsterdam, The Netherlands, 2016; pp. 51–60.
2. Shin, M.; Han, Y.; Ahn, K. The influence of the time and temperature of heat treatment on the allergenicity of egg white proteins. *Allergy Asthma Immunol. Res.* **2013**, *5*, 96–101. [CrossRef]
3. Nastaj, M.; Mleko, S.; Terpiłowski, K.; Tomczy´nska-Mleko, M. Effect of Sucrose on Physicochemical Properties of High-Protein Meringues Obtained from Whey Protein Isolate. *Appl. Sci.* **2021**, *11*, 4764. [CrossRef]
4. Orrego, M.; Troncoso, E.; Zúñiga, R.N. Aerated whey protein gels as new food matrices: Effect of thermal treatment over microstructure and textural properties. *J. Food Eng.* **2015**, *163*, 37–44. [CrossRef]
5. Duquenne, B.; Vergauwen, B.; Capdepon, C.; Boone, M.A.; De Schryver, T.D.; Hoorebeke, L.V.; Weyenberg, S.V.; Stevens, P.; Block, J.D. Stabilising frozen dairy mousses by low molecular weight gelatin peptides. *Food Hydrocoll.* **2016**, *60*, 317–323. [CrossRef]
6. Rosniyana, A.; Hazila, K.K.; Hashifah, M.A.; Norin, S.A.S.; Zain, A.M. Nutritional composition and sensory properties of *kuih baulu* incorporated stabilised rice bran. *J. Trop. Agric. Food Sci.* **2011**, *39*, 1–9.
7. Murray, B.S. Recent developments in food foams. *Curr. Opin. Colloid Interface Sci.* **2020**, *50*, 101394. [CrossRef]
8. Duan, X.; Li, J.; Zhang, Q.; Zhao, T.; Li, M.; Xu, X. Effect of a multiple freeze-thaw process on structural and foaming properties of individual egg white proteins. *Food Chem.* **2017**, *228*, 243–248. [CrossRef]
9. Lomakina, K.G.; Míková, K. A study of the factors affecting the foaming properties of egg white—A review. *Czech J. Food Sci.* **2018**, *24*, 110–118. [CrossRef]
10. Kar, S. As Malaysia Faces Egg Shortage, PM Anwar Ibrahim Advises People against Panic Buying. Republicworld.com. Available online: https://www.republicworld.com/world-news/rest-of-the-world-news/as-malaysia-faces-egg-shortage-pm-anwar-ibrahim-advises-people-against-panic-buying-articleshow.html (accessed on 23 February 2023).
11. Shim, Y.Y.; Mustafa, R.; Shen, J.; Ratanapariyanuch, K.; Reaney, M. Composition and Properties of Aquafaba: Water Recovered from Commercially Canned Chickpeas. *J. Vis. Exp.* **2018**, *132*, 56305.
12. Amagliani, L.; Silva, J.V.C.; Saffon, M.; Dombrowski, J. On the foaming properties of plant proteins: Current status and future opportunities. *Trends Food Sci. Technol.* **2021**, *118*, 261–272. [CrossRef]
13. Stantiall, S.E.; Dale, K.J.; Calizo, F.S.; Serventi, L. Application of pulses cooking water as functional ingredients: The foaming and gelling abilities. *Eur. Food Res. Technol.* **2017**, *244*, 97–104. [CrossRef]
14. Mustafa, R.; He, Y.; Shim, Y.Y.; Reaney, M.J.T. Aquafaba, wastewater from chickpea canning, functions as an egg replacer in sponge cake. *Int. J. Food Sci. Technol.* **2018**, *53*, 247–2255. [CrossRef]
15. Donatus, F.; Sintang, M.D.; Julmohammad, N.; Noorakmar, A.W. Potential application of unconsumed liquid from commercial canned food products in fabrication and characterisation of non-dairy edible foam. *Int. J. Agric. For. Plant.* **2020**, *10*.
16. Treat Dreams. Chocolate Mousse (without Heavy Cream). Available online: https://treatdreams.com/chocolate-mousse-without-heavy-cream/ (accessed on 21 January 2023).
17. Hosseini Ghaboos, S.H.; Seyedain Ardabili, S.M.; Kashaninejad, M. Physicochemical, textural and sensory evaluation of sponge cake supplemented with pumpkin flour. *Int. Food Res. J.* **2018**, *25*, 854–860.
18. Stable Micro Systems. Texture: Measure and Analyse Properties Stable Micro Systems. Available online: https://www.stablemicrosystems.com/TextureAnalysisProperties.html (accessed on 23 January 2023).
19. Sheng, L.; Wang, Y.; Chen, J.; Zou, J.; Wang, Q.; Ma, M. Influence of high-intensity ultrasound on foaming and structural properties of egg white. *Food Res. Int.* **2018**, *108*, 604–610. [CrossRef]
20. AOAC. *Official Methods of Analysis*; Association of Official Analytical Chemists: Arlington, VA, USA, 2005.
21. Fernandes, S.S.; Filipini, G.; Salas-Mellado, M.d.l.M. Development of cake mix with reduced fat and high practicality by adding chia mucilage. *Food Biosci.* **2021**, *42*, 101148. [CrossRef]
22. Lawless, H.T.; Heymann, H. *Sensory Evaluation of Food: Principles and Practices*, 2nd ed.; Springer: New York, NY, USA, 2010.
23. Funami, T.; Nakauma, M. Instrumental food texture evaluation in relation to human perception. *Food Hydrocoll.* **2022**, *124*, 107253. [CrossRef]
24. He, Y.; Meda, V.; Reaney, M.J.T.; Mustafa, R. Aquafaba, a new plant-based rheological additive for food applications. *Trends Food Sci. Technol.* **2021**, *111*, 27–42. [CrossRef]
25. Hwang, J.; Shyu, Y.S.; Yeh, L.; Sung, W. Study on Sponge Cake Qualities Made from Hen, Duck and Ostrich Eggs. *J. Food Nutr. Res.* **2018**, *6*, 110–115. [CrossRef]
26. Wang, Z.; Zhang, S.; Vardhanabhuti, B. Foaming properties of whey protein isolate and λ-carrageenan mixed systems. *J. Food Sci.* **2015**, *80*, 1893–1902. [CrossRef] [PubMed]
27. Paula, A.M.; Conti-Silva, A.C. Texture profile and correlation between sensory and instrumental analyses on extruded snacks. *J. Food Eng.* **2014**, *121*, 9–14. [CrossRef]
28. Jiang, H.; Hettiararchy, N.S.; Horax, R. Quality and estimated glycemic profile of baked protein-enriched corn chips. *J. Food Sci. Technol.* **2019**, *56*, 2855–2862. [CrossRef]
29. Lu, R.; Cen, H. 8 Non-destructive methods for food texture assessment. In *Instrumental Assessment of Food Sensory Quality*; Woodhead Publishing: Sawston, UK, 2013; pp. 230–254.
30. Milner, L.; Kerry, J.P.; O'Sullivan, M.G.; Gallagher, E. Physical, textural, and sensory characteristics of reduced sponge cakes, incorporated with clean-label sugar-replacing alternative ingredients. *Innov. Food Sci. Emerg. Technol.* **2020**, *59*, 102235. [CrossRef]

31. Faber, T.J.; Jaishankar, A.; McKinley, G.H. Describing the firmness, springiness, and rubberiness of food gels using fractional calculus. Part II: Measurements on semi-hard cheese. *Food Hydrocoll.* **2017**, *62*, 325–339. [CrossRef]
32. StudyCorgi. Effects of Different Compounds on Egg White Foam Stability. Available online: https://studycorgi.com/effects-of-different-compounds-on-egg-white-foam-stability/ (accessed on 1 February 2023).
33. Nishinari, K.; Turcanu, M.; Nakauma, M.; Fang, Y. Role of fluid cohesiveness in safe swallowing. *NPJ Sci. Food* **2019**, *3*, 5. [CrossRef] [PubMed]
34. Hamedi, F.; Mohebbi, M.; Shahidi, F.; Azarpazhooh, E. Ultrasound assisted osmotic treatment of model food impregnated with pomegranate peel phenolic compounds: Mass transfer, texture and phenolic evaluations. *Food Bioprocess. Technol.* **2018**, *11*, 1061–1074. [CrossRef]
35. Kasapis, S.; Bannikova, A. Chapter 2—Rheology and food microstructure. In *Woodhead Publishing Series in Food Science, Technology and Nutrition*; Ahmed, J., Ptaszek, P., Basu, S., Eds.; Woodhead Publishing: Sawston, UK, 2017; pp. 7–46.
36. Herranz, B.; Canet, W.; Jimenez, M.J.; Fuentes, R.; Alvarez, M.D. Characterisation of chickpea flour-based gluten-free batters and muffins with added biopolymers: Rheological, physical and sensory properties. *Int. J. Food Sci. Technol.* **2016**, *51*, 1087–1098. [CrossRef]
37. Rahmati, N.F.; Tehrani, M.M. Influence of different emulsifiers on characteristics of eggless cake containing soy milk: Modeling of physical and sensory properties by mixture experimental design. *J. Food Sci. Technol.* **2014**, *51*, 1697–1710. [CrossRef]
38. Cardoso, R.V.C.; Fernandes, A.; Heleno, S.A.; Rodrigues, P.; Gonzalez-Paramas, A.M.; Barros, L.; Ferreira, I. Physicochemical characterization and microbiology of wheat and rye flours. *Food Chem.* **2019**, *280*, 123–129. [CrossRef]
39. Foschia, M.; Peressini, D.; Sensidoni, A.; Brennan, C.S. The effects of dietary fibre addition on the quality of common cereal products. *J. Cereal Sci.* **2013**, *58*, 216–227. [CrossRef]
40. Moore, S. Why is Moisture Content Analysis of Food Important? Available online: https://www.news-medical.net/life-sciences/Why-is-Moisture-Content-Analysis-of-Food-Important.aspx# (accessed on 29 January 2023).
41. Ludwig, D.S.; Hu, F.B.; Tappy, L. Dietary carbohydrate: Role of quality and quantity in chronic disease. *BMJ* **2018**, *361*, 2340. [CrossRef] [PubMed]
42. Ghanimah, M.; Ibrahim, E. Effect of pH, carbohydrates, and NaCl on functional properties of whey proteins. *J. Sustain. Agric. Sci.* **2018**, *44*, 93–99. [CrossRef]
43. Osilla, E.V.; Safadi, A.O.; Sharma, S. Calories. 2022. Available online: https://www.ncbi.nlm.nih.gov/books/NBK499909/ (accessed on 30 January 2023).
44. Nur Afifah, M.J.; Aishah, B. Effect of maltodextrin substitution on physicochemical and sensory properties of Malay traditional cake 'Bahulu'. *Int. J. Eng. Technol.* **2018**, *7*, 239–243. [CrossRef]
45. Zaitoun, M.; Ghanem, M.; Harphoush, S. Sugars: Types and their functional properties in food and human health. *Int. J. Public Health Research.* **2018**, *6*, 93–99.
46. Malnic, B.S.; Saraiva, L.R. Odor coding in the mammalian olfactory epithelium. *Cell Tissue Res.* **2021**, *383*, 445–456.
47. Péneau, S.; Hoehn, E.; Roth, H.-R.; Escher, F.; Nuessli, J. Importance and consumer perception of freshness of apples. *Food Qual. Prefer.* **2006**, *17*, 9–19. [CrossRef]
48. Clemson.edu. Available Moisture in Foods: What Is It Anyway? Available online: https://www.clemson.edu/extension/food/canning/canning-tips/39available-moisture.html (accessed on 23 January 2023).
49. Huppert, T. Milk Foam: Creating Texture and Stability. Available online: https://scanews.coffee/2014/09/15/milk-foam-creating-texture-and-stability/ (accessed on 23 January 2023).
50. Conti-Silva, A.C.; Ichiba, A.K.T.; Silveira, A.L.d.; Albano, K.M.; Nicoletti, V.R. Viscosity of liquid and semisolid materials: Establishing correlations between instrumental analyses and sensory characteristics. *J. Text. Stud.* **2018**, *49*, 569–577. [CrossRef]
51. Gray, D.; Abdel-Aal, E.M.; Seetharaman, K.; Kakuda, Y. Differences in viscosity and textural properties of selected barley cultivars as influenced by pearling and cooking. *Food Chem.* **2010**, *120*, 402–409. [CrossRef]
52. Akkouche, Z.; Aissat, L.; Madani, K. Effect of heat on egg white protein. In *International Conference on Applied Sciences*; IntechOpen: London, UK, 2012; pp. 407–413.
53. Vieira, J. Chocolate Aeration—Art or Science? New Food Magazine. Available online: https://www.newfoodmagazine.com/article/5415/chocolate-aeration-art-or-science/ (accessed on 29 January 2023).
54. Li, X.; Li, J.; Chang, C.; Wang, C.; Zhang, M.; Su, Y.; Yang, Y. Foaming characterization of fresh egg white proteins as a function of different proportions of egg yolk fractions. *Food Hydrocoll.* **2019**, *90*, 118–125. [CrossRef]
55. Ho, T.M.; Bhandari, B.; Bansal, N. Influence of milk fat on foam formation, foam stability and functionality of aerated dairy products. In *Dairy Fat Products and Functionality*; Springer: Cham, Switzerland, 2020; pp. 583–606.
56. Massoud, R.; Hosseini, A.H.; Massoud, A. Functional properties of food proteins; gelation and stable foam. In Proceedings of the 6th International Conference on Science and Engineering (ICES), Paris, France, 7 December 2017; pp. 1–8.
57. Hou, Q.; Xiwen, W. Effect of fiber surface characteristics on foam properties. *Cellulose* **2018**, *25*, 3315–3325. [CrossRef]
58. Mozaffarian, D. Food and weight gain: Time to end our fear of fat. *Lancet Diabetes Endocrinol.* **2016**, *4*, 633–635. [CrossRef] [PubMed]

Article

Impact of Stabilization Method and Filtration Step on the Ester Profile of "Brandy de Jerez"

José Manuel Muñoz-Redondo [1], Belén Puertas [2], Manuel José Valcárcel-Muñoz [3], Raquel Rodríguez-Solana [1] and José Manuel Moreno-Rojas [1,*]

[1] Department of Agroindustry and Food Quality, Andalusian Institute of Agricultural and Fisheries Research and Training (IFAPA), Alameda del Obispo, Avda Menéndez Pidal, 14004 Córdoba, Spain

[2] Department of Agroindustry and Food Quality, Andalusian Institute of Agricultural and Fisheries Research and Training (IFAPA), Cañada de la Loba, 11471 Jerez de la Frontera, Cádiz, Spain

[3] Bodegas Fundador, S.L.U., 11403 Jerez de la Frontera, Cádiz, Spain

*   Correspondence: josem.moreno.rojas@juntadeandalucia.es; Tel.: +34-67-153-2758

Abstract: Brandy stabilization is an important step aimed at decanting the suspended organic and inorganic particles that may cause undesirable turbidity (cloudiness or haze) in brandies, affecting the physico-chemical stability, the organoleptic characteristics, and the consumer's quality perception of the brandy. This phenomenon originates from insoluble salts, volatile compounds (higher alcohols, fatty acid esters, and others), and ethanol-soluble lignins. Among them, ethyl esters of long-chain fatty acids are considered the main cause of haze formation, due to a decrease in their solubility when brandies are stored at low temperatures. For this reason, producers are recommended to intentionally encourage the formation of haze and then to remove it before releasing the brandy to the market. The purpose of this work was to study the influence of two methods of stabilization, the traditional method at room temperature for 1 year, and cold stabilization for 7 days at $-10\ °C$, on the ester profile of "Brandy de Jerez". The results were compared with non-stabilized samples, to determine the main changes in the volatile composition. The use of multivariate statistical analyses made it possible to identify the esters (potential markers) most impacted by the stabilization process. It was observed that traditional stabilization yielded the most distinct ester profile, while brandies stabilized at cold temperature displayed a lower impact on their volatile composition. Furthermore, both stabilization processes produced a significant decrease in ethyl esters of long-chain fatty acids, which are the compounds responsible for haze formation.

Keywords: esters; brandy; HS-SPME/GC-MS; cold stabilization; multivariate statistics

1. Introduction

Brandy is a matured spirit obtained by distillation of wine. Its consumption is extensive throughout the world, and Spain is one of the world's leading producers, with the so-called "Brandy de Jerez". This product is elaborated in the Southern Spanish area known as *Marco de Jerez* under a protected geographical indication [1], following the specification provided by the Technical File [2]. "Brandy de Jerez" is produced from *holandas* (<70% *v/v* of ethanol), spirits (70–86% *v/v* of ethanol) or wine distillates (86–94.8% *v/v* of ethanol), and its organoleptic equilibrium is reached by ageing in American oak (*Quercus alba*) casks of a capacity lower than 1000 L and previously seasoned with Sherry wines. This ageing process follows the traditional dynamic system known as *Criaderas* and *Solera* [3]. Three quality categories can be distinguished according to the regulation of the "Brandy de Jerez" and their ageing: *Solera* brandy (minimum 6 months of ageing), *Solera Reserva* brandy (minimum 1 year), and *Solera Gran Reserva* brandy (more than 3 years).

The final characteristics of this product are determined by the different steps followed during the production process, such as the selection of the raw material, the winemaking, the distillation system (alquitara, charentais alembic, or distillation column) used to distil

the wine, the ageing or maturation in American sherry casks, and finally the stabilization of the drink before bottling [4]. Brandy stabilization is an important step aimed at decanting the suspended organic and inorganic particles that may cause undesirable turbidity (commonly referred to as cloudiness or haze) in brandies. This turbidity can change the physico-chemical properties of the brandy once bottled, and it affects the organoleptic characteristics of the final drink and the perception of consumers about the quality of this product. Cloudiness often appears in fruit brandies when the alcohol content is below 45% v/v, as well as at temperatures below 7 °C, usually reached during storage and transportation [5]. In addition, haze can slowly form in the final product after bottling. For this reason, producers are recommended to intentionally encourage the formation of haze and then to remove it before releasing the brandy to the market [6]. Haze formation originates from insoluble salts (potassium bitartrate, calcium tartrate, calcium oxalate), volatile compounds (including esters), and ethanol-soluble lignins [6]. Among the volatile metabolites, ethyl and isoamyl esters of long-chain fatty acids, phenylethanol, and ethyl lactate have been described to be linked to haze formation [4,7,8].

There are several ways to reduce the cloudiness in spirit beverages, such as the use of activated carbon, an adsorbent and hydrophobic material that is able to trap volatile compounds and adsorb organic compounds [9], or based on filtration materials (cellulose, carbon, diatomaceous earth, or candle filters) that need to be carefully chosen to prevent loss of flavour compounds [7]. A common practice for removing the haze formed in alcoholic beverages (particularly red, sparkling, and sweet fortified wines and brandies) is a stabilization process at room temperature (around 25 °C) for 7–30 days, followed by filtration before bottling. However, this method may not complete all the physicochemical reactions and insolubilizations that can occur in brandies, and the haze may not be completely removed after filtration. Additionally, new insolubilizations may appear in brandies stabilized by means of this method when exposed to low temperatures, due to destabilization of colloidal equilibriums. This can be a problem for those brandies that are exported to regions with cold climates, since during shipping bottles may remain at low temperatures for long periods of time, creating insolubilizations in the final product. In this sense, a common alternative to prevent haze formation is cold stabilization [4,10], by freezing the spirit at temperatures below −5 °C for a few days, followed by subsequent filtration before bottling [7,11,12].

Previous works carried out on fruit brandies (apricot, plum, and rye) studied different conditions of stabilization, such as the temperature and filtration systems [4,5,7,12]. The results showed the influence of these factors on the final turbidity of the samples, obtaining the best results with intermediate values of temperature (from −1 to −4 °C) and filter pore size (filter sheets with a higher nominal retention rate, >0.7 µm, and membranes with 800 nm pore size). However, most of the studies focused on the effect of the stabilization and filtration processes on the physical characteristics of the brandies, ignoring their effect on the aroma quality. In this sense, esters are one of the most important families of volatile compounds impacting the aroma of brandies, being the main known contributors to the flower and fruity notes [13]. In brandies, these compounds are mainly originated during wine fermentation and are modulated during wine maturation, distillation, and brandy ageing [14]. Their relevance for the organoleptic properties of brandies comes from their low perception threshold and their contribution to the brandy aroma through synergistic interactions, even at concentrations below their perception thresholds [15].

Thus, the objective of the present work was to compare the influence of two methods of stabilization on the ester profile of "Brandy de Jerez": the traditional method at room temperature for 1 year, to assure that all physicochemical reactions and insolubilizations that may occur during stabilization have been completed, followed by filtration; and cold stabilization for 7 days at −10 °C, followed by filtration. The ester profile obtained with both stabilization processes was also compared with the ester profile of brandies without stabilization.

2. Materials and Methods

2.1. Brandy Samples

The brandies used in this work were from Jerez de la Frontera (Spain), from the protected geographical indication (PGI) [1] "Brandy de Jerez". The samples were elaborated following the traditional dynamic system called *Criaderas* and *Solera* as is established in the regulations of the Regulatory Council of "Brandy de Jerez" [16]. A total of 27 brandies were prepared: 9 non-stabilized (NonStab), 9 stabilized at cold temperature (ColdT), and 9 stabilized at room temperature (RoomT).

First, 1 brandy *Solera* (36% v/v of alcohol and 6–9 months of ageing), 3 *Solera Reserva* (36% v/v and 12–18 months) and 5 *Solera Gran Reserva* (40% v/v and 6–12 years) were elaborated at Bodegas Fundador, corresponding to the non-stabilized brandies. The formulations of the younger scales of the *Criaderas* and *Solera* from the dynamic ageing systems of the brandies included two or more of the following distillates: holandas (65% v/v), column spirits (77% v/v), and high-grade wine distillates (94.7% v/v). The hydrations of the final *Solera* and *Solera Reserva* brandies were adjusted to 36% v/v and the *Solera Gran Reserva* to 40% v/v in stainless steel tanks.

Then, a total of 50 L from industrially elaborated brandies were taken, to prepare brandies stabilized using two static methods (using 20 L of brandy in each method), which were carried out in darkness and repeated in two consecutive years. The stabilization methods consisted of:

- Traditional stabilization: room temperature ($20 \pm 5\,^\circ$C) for 1 year, followed by filtration with PALL CORPORATION plates (New York, NY, USA) Seitz K-200 series.
- Cold stabilization: low temperature ($-10 \pm 1\,^\circ$C) stabilization for 7 days and filtration using Seitz PALL CORPORATION plates (New York, NY, USA) Seitz K-200 series at $-10\,^\circ$C.

2.2. Chemicals

High-performance liquid chromatography (HPLC)-grade ethanol was obtained from J.T. Baker Chemicals B.V. (Denventer, The Netherlands). Milli-Q water was produced by a Milli-Q Plus water system (Millipore, Madrid, Spain). Ethylenediaminetetraacetic acid (EDTA) was supplied by Panreac Applichem (Barcelona, Spain). Sigma-Aldrich (Madrid, Spain) supplied the following: sodium chloride ACS reagent grade (purity $\geq$99.8%), and the standard compounds ethyl butyrate ($\geq$99%), ethyl hexanoate ($\geq$99%), ethyl octanoate ($\geq$99%), ethyl decanoate ($\geq$99%), ethyl dodecanoate ($\geq$99%), ethyl myristate ($\geq$99%), ethyl palmitate ($\geq$99%), ethyl stearate ($\geq$99%), propyl acetate ($\geq$99%), isobutyl acetate ($\geq$99%), isoamyl acetate ($\geq$99%), hexyl acetate ($\geq$99%), phenylethyl acetate ($\geq$99%), ethyl isobutyrate (98%), ethyl 2-methylbutyrate ($\geq$99%), ethyl isovalerate ($\geq$99%), ethyl phenylacetate (98%), ethyl cinnamate (98%), ethyl dihydrocinnamate (98%), methyl hexanoate ($\geq$99%), methyl octanoate ($\geq$99%), methyl decanoate ($\geq$99%), isoamyl butyrate (98%), ethyl heptanoate (98%), ethyl nonanoate (98%), ethyl propanoate ($\geq$99%), isobutyl hexanoate ($\geq$99%), ethyl valerate ($\geq$99.7%), and acetaldehyde ($\geq$99.5%). The deuterated internal standards [^{2}H$_3$]-ethyl butyrate, [^{2}H$_{11}$]-ethyl hexanoate, [^{2}H$_{15}$]-ethyl octanoate, [^{2}H$_5$]-ethyl trans-cinnamate, [^{2}H$_{23}$]-ethyl dodecanoate, [^{2}H$_{27}$]-ethyl myristate, [^{2}H$_{31}$]-ethyl palmitate, and [^{2}H$_{35}$]-ethyl stearate were supplied by CDN isotopes (Pointe-Claire, QC, Canada).

2.3. HS-SPME-GC-MS

Sample Preparation and Extraction Conditions

A previously developed methodology was used to determine the esters in the brandies [17]. Briefly, 25 mL of brandy sample was spiked with 20 µL of an internal standard mix solution of 8 deuterated compounds at 200 mg/L. The peak integration of each ester was normalized using specific deuterated standards, as follows: ethyl isobutyrate, ethyl 2-methylbutyrate, ethyl isovalerate, ethyl propanoate, ethyl butyrate, isoamyl acetate, ethyl valerate, propyl acetate, and isobutyl acetate were normalized with [^{2}H$_3$]-ethyl butyrate. Ethyl hexanoate, methyl hexanoate, methyl octanoate, isoamyl butanoate,

isobutyl hexanoate, ethyl heptanoate, and hexyl acetate were normalized with $[^2H_{11}]$-ethyl hexanoate. $[^2H_{15}]$-Ethyl octanoate was used to normalize ethyl octanoate, methyl decanoate. Phenylethyl acetate, ethyl dihydrocinnamate, and ethyl cinnamate were normalized with $[^2H_5]$-ethyl trans-cinnamate; while ethyl dodecanoate, ethyl decanoate, ethyl nonanoate, and ethyl phenylacetate were normalized with $[^2H_{23}]$-ethyl dodecanoate. Finally, $[^2H_{27}]$-ethyl myristate, $[^2H_{31}]$-ethyl palmitate, and $[^2H_{35}]$-ethyl stearate were used to normalize ethyl myristate, ethyl palmitate, and ethyl stearate, respectively. Then, the spiked samples were diluted in EDTA solution (200 mM and pH adjusted to 7 with NaOH 1 M), since this chemical prevents oxidation of the compounds [18]. Afterwards, the brandy samples were diluted to reach 7.2% *v/v* ethanol, and 10 mL of this solution was transferred to a 20 mL SPME vial containing 3.5 g of NaCl, to increase the ionic strength of the analytes and release more volatiles into the headspace [18,19]. The vials were capped, and the solution was homogenized using a vortex shaker for 30 s and placed in a Combipal autosampler tray (CTC Analytics, Zwingen, Switzerland).

A 100 μm PDMS fiber (Supelco, Bellefont, PA, USA), previously conditioned according to the supplier recommendation, was used for extraction of esters via HS-SPME. For the equilibrium step, the vials were incubated at 500 rpm for 2 min at 33 °C, while the extraction was performed at the same temperature and agitation conditions for 55 min.

The conditions of the gas chromatograph were as follows: the desorption time and temperature were set at 15 min and 250 °C, respectively, performed in a Trace GC ultragas chromatograph (Thermo Fisher Scientific S. p.A., Rodano, Milan, Italy). The desorbed volatiles passed to an ISQ Single MS spectrometer (Thermo Fisher Scientific, Austin, TX, USA). The injection was performed in splitless mode, and the column used for volatile separation was a BP21 column of 50m × 0.32 mm and 0.25 μm film thickness (SGE Analytical Science, Milton Keynes, UK). The carrier gas was helium at a constant flow rate of 1.7 mL/min. The oven temperature program was set at 40 °C for 5 min, raised to 220 °C at 3 °C/min, and held for 30 min. The MS operated in electron ionization mode at 70 eV using selected-ion-monitoring (SIM) mode. The transfer line and source temperature of the MS were set at 230 °C and 200 °C, respectively. The identification procedure was performed by comparing the retention times and mass spectra with those of the pure standards. All the samples were analyzed in duplicate by repeating the extraction procedure two times for each sample, in order to reduce the contribution of experimental and analytical variability to the final concentration measurements.

2.4. Statistical Analysis

Quantification of the samples was performed by fitting calibration curves with the commercial standard of each ester. Then, to check the structure of the data and to look for grouping of the brandy samples, a principal component analysis (PCA) was fitted [20]. Afterwards, the main differences between samples related to the stabilization process were studied by means of a multilevel partial least squares discriminant analysis (ML-PLS-DA), due to the paired structure of the data [21]. Multilevel decomposition was applied, due to the paired structure of the data, with three measures for the same samples: before and after cold stabilization and filtration, allowing focusing on the effect of this treatment, regardless the initial composition of each brandy. The model was optimized and validated by means of a described previously double cross-validation scheme [22], using leave-one-out cross validation of both nested loops and the balanced error rate (BER) as diagnostic statistics. The *p*-value of the model was obtained from a permutation test ($n = 1000$, since this was large enough to sample the tails of the distribution and to attain a *p*-value up to 0.001) for BER, area under the receiver operating characteristic curve (AUROC), and the average number of misclassified (NMC). The *p*-value of the model was calculated as follows:

$$p\text{-value} = \frac{1 + (\text{Diagnostic}_P \leq \text{Diagnostic})}{N} \tag{1}$$

where ($Diagnostic_P \leq Diagnostic$) is the number of elements in the H_0 distribution that are smaller or equal to the diagnostic (BER, AUROC, or NMC) of the original data.

The most discriminatory metabolites were selected using an iterative process based on previously described variable importance in projection (VIP) scores [23]. Briefly, the method was based on selecting the variables with a VIP value above a changing threshold during an iterative procedure: as long as the model improved, the threshold was increased and a new model with a reduced number of variables was fitted. This process was performed within a double-cross validation scheme repeated 100 times. Finally, the variables with high stability (those that remained in the final model) above 70% were chosen. The statistical analyses were performed using the software R version 4.0.3 and the package *mixOmics* [24].

3. Results and Discussion

Esters in brandies are mainly derived from the initial distillate, which depends on the base wine used for distillation (where its conservation in the presence or absence of lees, has an important influence), although they are modulated during ageing [25,26]. The most abundant family of esters measured in the brandy samples was the ethyl esters of fatty acids, with concentrations ranging from 11.6 to 48.8 mg/L, being in agreement with those found in previous studies with similar samples [27,28]. Among them, ethyl octanoate (that ranged from 9 to 18 mg/L) followed by ethyl decanoate (from 0.034 to 20.1 mg/L) displayed the overall highest concentrations. These compounds are considered important contributors to the aroma of distilled beverages and have been identified as odor active compounds in distillates [27,29]. Meanwhile, higher alcohol acetates and ethyl esters of branched acids were found in concentrations of 1.27–3.81 mg/L and 0.14–1.76 mg/L, respectively, with isoamyl acetate being the most abundant acetate ester, in accordance with the literature [27].

3.1. Effect of Ageing

A principal component analysis (PCA) was carried out to study the main variation sources in the data and to determine the grouping of samples. The first two principal components of the PCA accounted for the 61% of the total sample variability (Figure 1), the main variation source being explained by PC1 (39%), which was related with the ageing of the brandies (Figure 1A). It was observed that *Solera* and *Solera Reserva* brandies with a more similar period of ageing, averaging 6–9 and 12–18 months, respectively (Figure 1A), displayed a similar ester profile, characterized by higher levels of isoamyl acetate, hexyl acetate, isobutyl acetate, ethyl butyrate, methyl hexanoate, propyl acetate, ethyl octanoate, phenylethyl acetate, ethyl valerate, isobutyl hexanoate, methyl octanoate, isoamyl octanoate, ethyl dihydrocinnamate, and ethyl hexanoate (Figure 2A). Meanwhile, the ester profile of the *Solera Gran Reserva* brandies (averaging 6–12 years of ageing) displayed a more differentiated ester profile, with an overall increase of the rest of the esters analyzed, including ethyl 2-methylbutyrate, ethyl nonanoate, ethyl phenylacetate, ethyl isovalerate, ethyl isobutyrate, ethyl decanoate, ethyl dodecanoate, ethyl propanoate, ethyl heptanoate, isoamyl butanoate, ethyl myristate, and ethyl cinnamate. Among these, ethyl isobutyrate, ethyl 2-methylbutyrate and ethyl decanoate have been described as olfactive markers of a similar product (Calvados), as well as isoamyl acetate [30], which, conversely, displayed lower concentrations in the *Solera Gran Reserva* brandies. These results demonstrated the distinctive and exclusive character of the brandies with a longer ageing period. Another study [31] also found that "Brandies de Jerez" *Solera Gran Reserva* displayed a clear difference in phenolic and furanic derivative profile from other brandies produced in different regions, indicating their highly specific character. The higher concentration of esters observed for the *Solera Gran Reserva* brandies may be related to the continuous esterification of fatty acids and ethanol, and losses of water and ethanol through evaporation effects and perspiration through the pores of the wood during ageing [26,32].
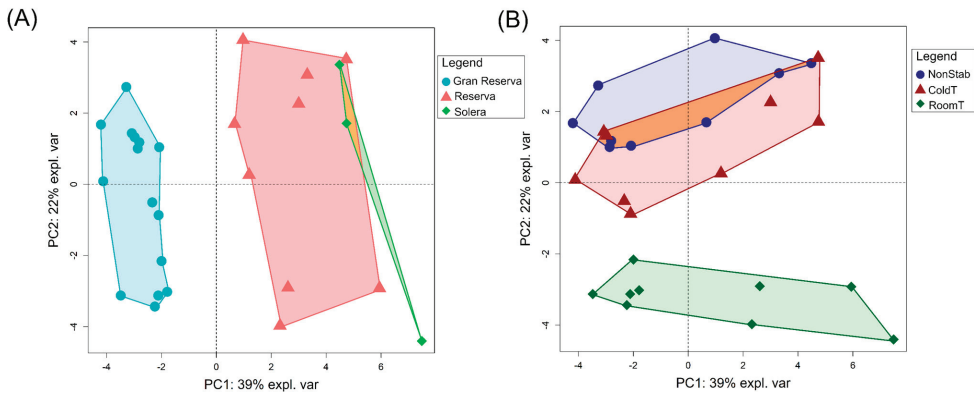
Figure 1. Principal component analysis (PCA) carried out on the brandy samples. Scores plot for the first two principal component highlighting brandies according to the ageing factor (**A**), and before and after cold stabilization and filtration treatment (**B**). NonStab: non-stabilized brandy; ColdT: brandy stabilized at cold temperature; RoomT: brandy stabilized at room temperature.
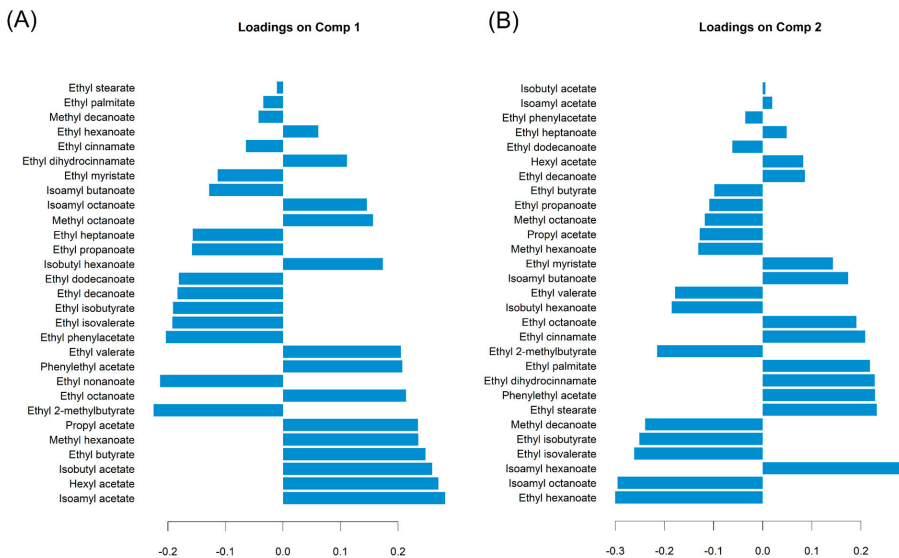
Figure 2. Loadings bar plot on component 1 (**A**) and component 2 (**B**) of the principal component analysis carried out on the brandy samples.

3.2. Effect of the Stabilization Process

Brandies before and after both stabilization processes are highlighted in the scores plot of Figure 1B. The most distinct ester profile was observed for the brandies submitted to room temperature stabilization, as is shown by a clear separation in component 2 of the PCA (Figures 1B and 2B). However, due to the large differences observed between brandies, predominantly related to the ageing and the paired structure of the data [21] with repeated measurements of the same samples (before stabilization, after cold stabilization, and after room temperature stabilization), differences related to stabilization were not clearly highlighted, especially for the samples stabilized at cold temperature. Therefore, a multilevel decomposition was applied, to focus on the effect of the treatment, and a partial least squares discriminant analysis (ML-PLS-DA) was performed for the three

classes: brandies before stabilization, after cold stabilization and filtration, and after room temperature stabilization and filtration (Figure 3).
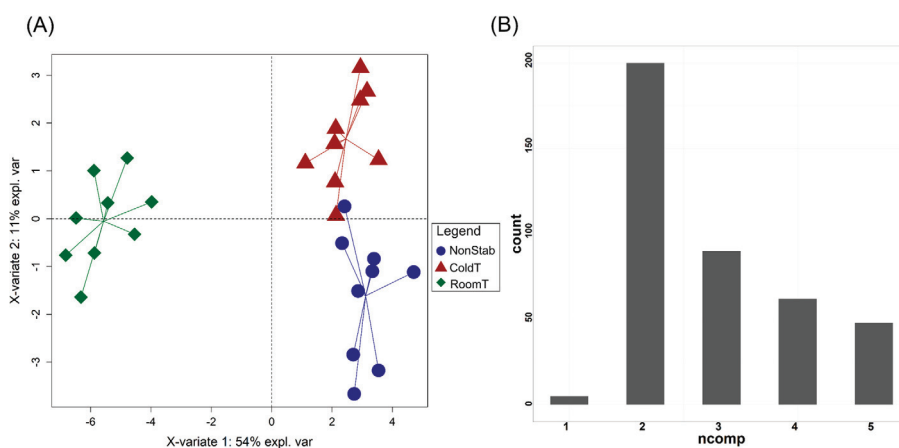
Figure 3. Graphical outputs of the multilevel partial least squares discriminant analysis (ML-PLS-DA) carried out to discriminate between the brandy samples before and after cold stabilization and filtration. (**A**) Scores plot for component 1 (X-variate 1) and component 2 (X-variate 2), and (**B**) histogram of the number of components optimized for the sub-models during the double-cross validation. NonStab: non-stabilized brandies; ColdT: brandy stabilized at cold temperature; RoomT: brandy stabilized at room temperature.

The model was optimized and validated following a double cross-validation scheme. The sub-models were predominantly optimized into two components, revealing the low complexity of the model (also shown during the PCA assessment) and reducing the risk of overfitting (Figure 3B). The ML-PLS-DA displayed a good performance, with a BER of 0.09 ± 0.05 (Table 1). Brandies stabilized at room temperature were correctly assigned in all the cases, supporting a more distinct ester profile, while the error of the model was due to incorrect assignment between brandies without stabilization and after cold stabilization. Therefore, this error suggested a lower impact on the ester profile when cold stabilization was applied. Then, the model was successfully validated using a permutation test. The null distributions calculated from the class label permutation are shown in Figure 4 for the three diagnostics statistics: BER, AUROC and NMC, which displayed an expected Gaussian shape (Figure 4). The average performance of the model fell in the tail of the null distribution for the three diagnostics, obtaining a p-value of the model below 0.05 in all the cases (Table 1). All these results supported the robustness of the ML-PLS-DA, being the most model suitable for analyzing and interpreting the dataset.

Table 1. Multilevel partial least squares discriminant analysis (ML-PLS-DA) performance (from a double cross-validation scheme).

Mean BER	Class	Mean Class Error	Predicted as NonStab	Predicted as ColdT	Predicted as RoomT	*p*-Value (Model)
0.09 ± 0.05	NonStab	0.15 ± 0.11	765	135	0	BER, AUROC, NMC: 0.001
	ColdT	0.14 ± 0.10	122	778	0	
	RoomT	0.00 ± 0.00	0	0	900	

BER: balanced error rate. NonStab: brandies before stabilization. ColdT: brandies with cold stabilization. RoomT: brandies with room temperature stabilization. *p*-value of the model obtained from a permutation test ($n = 1000$) for the balanced error rate (BER), area under the receiver operating characteristic curve (AUROC), and the average number of misclassified (NMC).

(A)

Histogram of BER
(Mean BER: 0.666)

(B)

Histogram of AUROC
(Mean AUROC: 0.504)

(C)

Histogram of NMC
(Mean NMC: 18)
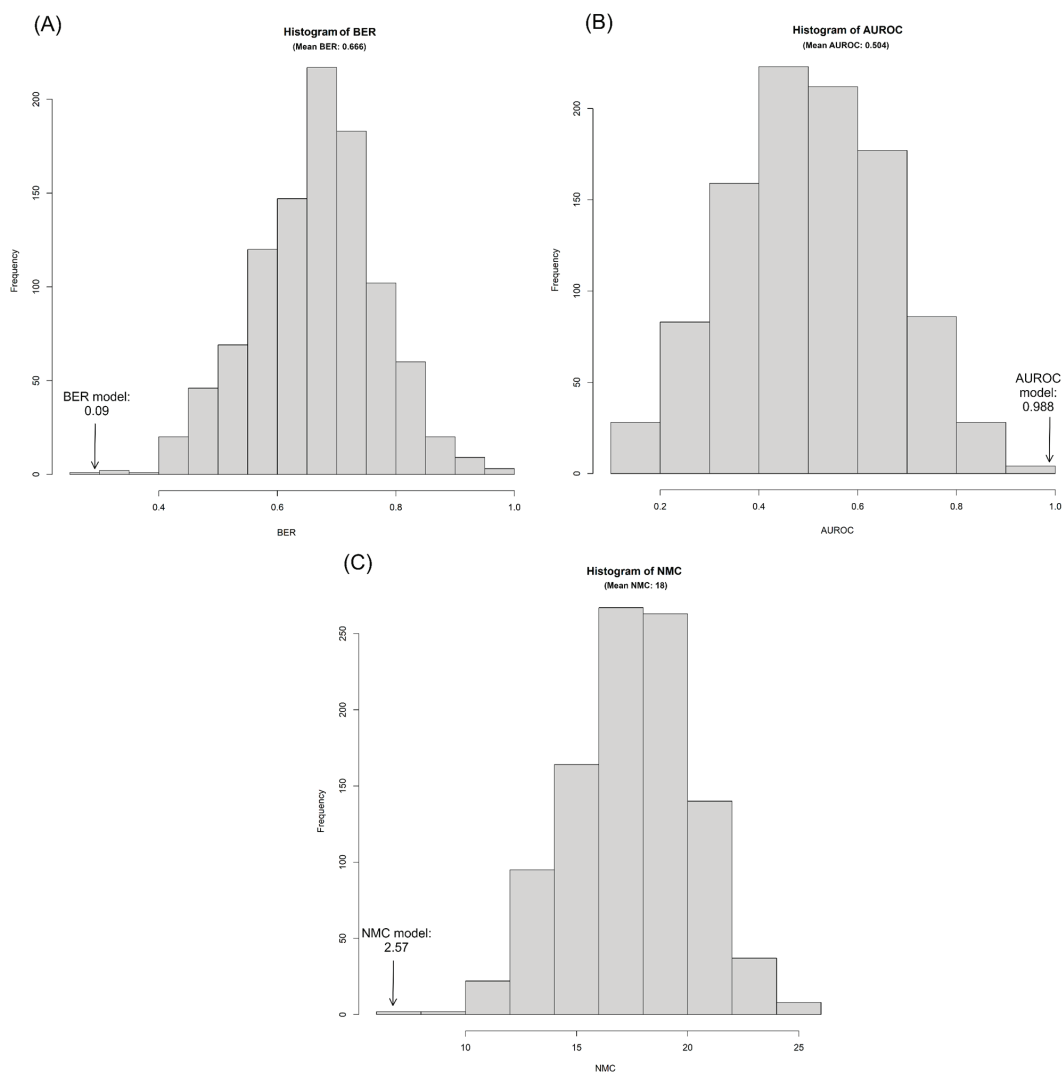
Figure 4. Results from the permutation test ($n = 1000$) performed on the multilevel partial least squares discriminant analysis (ML-PLS-DA). Histogram obtained from the permutation test for (**A**) the balanced error rate (BER), (**B**) area under the receiver operating characteristic curve (AUROC), and (**C**) the average number of misclassified (NMC). The real average performance of the model for the three statistics obtained from the double cross-validation is shown in each plot.

Differences in the ester profile of the brandies related to the stabilization process are shown in the scores and loadings plots of the ML-PLS-DA model (Figures 3A and 5). As was expected from the previous PCA, the brandies submitted to room temperature stabilization and filtration displayed the most distinct ester profile, being separated from the rest in component 1 (X-variate 1), which explained a high 54% of the variance. This stabilization process resulted in higher contents of many esters, such as isoamyl octanoate, ethyl isovalerate, ethyl isobutyrate, isobutyl hexanoate, ethyl 2-methylbutyrate, propyl acetate, ethyl butyrate, isoamyl acetate, methyl hexanoate, ethyl hexanoate, ethyl valerate, methyl decanoate, and isobutyl acetate. The percentage of change related to the control

brandy (before stabilization) is shown in Supplementary Table S1. Meanwhile, other esters such as isoamyl hexanoate, isoamyl butanoate, ethyl octanoate, hexyl acetate, phenylethyl acetate, ethyl cinnamate, ethyl decanoate, ethyl heptanoate, ethyl palmitate, ethyl dihydrocinnamate, ethyl stearate, ethyl nonanoate, and ethyl myristate displayed a significant decrease in their concentration.
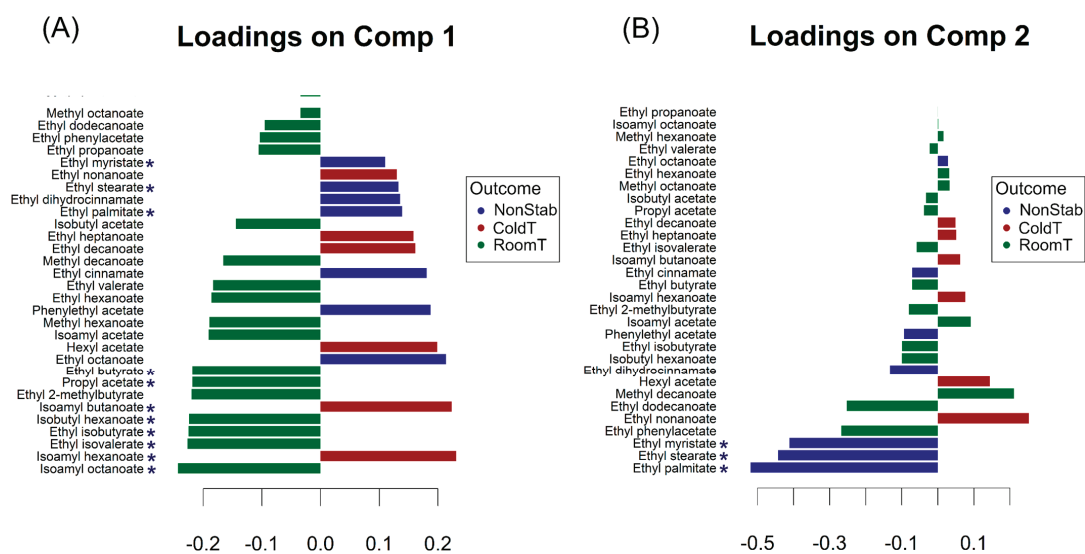
Figure 5. Loadings contribution barplot on component 1 (**A**) and component 2 (**B**) of the multilevel partial least squares discriminant analysis (ML-PLS-DA) carried out to discriminate between brandy samples before and after cold stabilization and filtration. Color indicates the class for which the compound had a maximal mean value. Bar length represents the multivariate regression coefficient, with either a positive or negative sign for that particular feature of each component, i.e., the importance of each variable in the model. NonStab: non-stabilized brandies; ColdT: brandy stabilized at cold temperature; RoomT: brandy stabilized at room temperature. An asterisk highlights the most discriminative compounds selected during a variable reduction procedure (i.e., potential markers related with the stabilization method).

The brandies submitted to cold stabilization were separated from those before stabilization in component 2 (X-variate 2), which explained 11% of the total variance (Figures 3A and 4B). This meant that the volatile profile of these brandies was less impacted by the stabilization process. This was mainly driven by a decrease in ethyl esters of long-chain fatty acids: ethyl palmitate, ethyl stearate, and ethyl myristate, with this method being effective for reducing these undesirable compounds, since turbidity of brandies is associated with ethyl esters of long-chain fatty acids due to decreases in their solubility, mainly related to low storage temperatures [7]. Therefore, a reduction of these compounds is beneficial in terms of ensuring the stability of brandies [33]. However, these ethyl esters displayed a greater decrease in brandies stabilized at room temperature, especially for ethyl stearate (decreasing below the detection limit in all the brandies, Supplementary Table S1). Meanwhile, both stabilization procedures yielded decreases of ethyl palmitate between 70–98% of the initial values and ethyl myristate between 11–87% (Supplementary Table S1). A previous study showed a similar reduction of ethyl myristate after brandy stabilization [7]. These results (lower content of ethyl esters of long-chain fatty acids and similar profile to the rest of the esters present in samples before stabilization) indicated a lower impact on the ester profile when cold stabilization was used, compared to room temperature stabilization.

A variable reduction procedure was performed to determine the esters most impacted by the stabilization process, i.e., the markers of this process. This procedure was repeated 100 times, and the compounds selected in at least the 70% of the iteration are highlighted in Figure 4 with an asterisk. Ethyl esters of long chain fatty acids were among the most impacted esters. The ester compounds selected as markers of room temperature stabilization were isoamyl octanoate, isoamyl hexanoate, ethyl isovalerate, ethyl isobutyrate, isobutyl hexanoate, isoamyl butanoate, propyl acetate, ethyl butyrate, ethyl palmitate, ethyl stearate, and ethyl myristate. As previously addressed, changes in these compounds could not be properly controlled; thus, this stabilization method may not be adequate for obtaining brandies with high quality standards. Meanwhile, none of the esters were selected as markers for the brandies stabilized at cold temperature, providing evidence of the minor impact of this process on the volatile profile of the brandies.

4. Conclusions

This study showed the impact of the cold and room temperature stabilization and subsequent filtration on the ester profile of brandies. Both methods achieved a drastic reduction of the long-chain fatty acids ethyl esters (ethyl palmitate, myristate, and stearate), with these compounds being the major cause of turbidity in brandies that meet consumer specifications. The traditional stabilization was slightly more effective in reducing these undesirable ethyl esters. However, this stabilization method produced important changes to the ester profile of the brandies, with significant increases of isoamyl octanoate, ethyl isovalerate, ethyl isobutyrate, isobutyl hexanoate, propyl acetate, and ethyl butyrate. Thus, using this stabilization method may lead to non-controlled aromatic changes. Meanwhile, cold stabilization produced less changes in the ester profile of brandies, being postulated as method for stabilizing brandies with a reduced impact on its aromatic quality, while achieving a successfully reduction in long-chain fatty acids.

References

1. Union European Parliament and of the Council. *Regulation (EC) No 2019/787 of 17 April 2019, on the Definition, Description, Presentation and Labelling of Spirit Drinks, the Use of the Names of Spirit Drinks in the Presentation and Labelling of Other Foodstuffs, the Protection of Geographical Indications for Spirit Drinks, the Use of Ethyl Alcohol and Distillates of Agricultural Origin in Alcoholic Beverages, and Repealing Regulation (EC) No 110/2008*; Union European Parliament and of the Council: Brussels, Belgium, 2019.
2. Boletín Oficial la Junta Andalucía. Consejería de Agricultura Pesca y Desarrollo Rural. Orden de 28 de Junio de 2018, por la que se aprueba el expediente técnico de Indicación Geográfica "Brandy de Jerez". *BOJA Histórico* **2018**, *127*, 19–20.
3. Schwarz, M.; Rodríguez, M.; Martínez, C.; Bosquet, V.; Guillén, D.; Barroso, C.G. Antioxidant Activity of Brandy de Jerez and Other Aged Distillates, and Correlation with Their Polyphenolic Content. *Food Chem.* **2009**, *116*, 29–33. [CrossRef]
4. Miljić, U.D.; Puškaš, V.S.; Vučurović, V.M.; Razmovski, R.N. The Application of Sheet Filters in Treatment of Fruit Brandy after Cold Stabilization. *Acta Period. Technol.* **2013**, *44*, 87–94. [CrossRef]
5. Puškaš, V.; Miljić, U.; Vasić, V.; Jokić, A.; Manović, M. Influence of Cold Stabilisation and Chill Membrane Filtration on Volatile Compounds of Apricot Brandy. *Food Bioprod. Process.* **2013**, *91*, 348–351. [CrossRef]
6. Piggott, J.R.; Gonzalez Vinas, M.A.; Conner, J.M.; Withers, S.J.; Paterson, A. Effect of Chill Filtration on Whisky Composition and Headspace. *Spec. Publ. R. Soc. Chem.* **1996**, *197*, 319–324.
7. Balcerek, M.; Pielech-Przybylska, K.; Dziekońska-Kubczak, U.; Patelski, P.; Różański, M. Effect of Filtration on Elimination of Turbidity and Changes in Volatile Compounds Concentrations in Plum Distillates. *J. Food Sci. Technol.* **2019**, *56*, 2049–2062. [CrossRef]
8. Bordiga, M. *Post-Fermentation and -Distillation Technology: Stabilization, Aging, and Spoilage*; CRC Press: Boca Raton, FL, USA, 2017.
9. Mukhin, V.M.; Shubina, N.A.; Abramova, I.M.; Zubova, I.D.; Lupascu, T.G. New Carbonic Adsorbents for Industrial Sorting Purification in Vodka Production. *Environ. Eng. Manag. J. EEMJ* **2009**, *8*, 1017–1019. [CrossRef]
10. Nikolov, H.; Marinov, M.; Penov, N. Study on the Stabilization of Wine Brandy Concentrates and Wine Brandy by Cold Treatment II. *Stabilization of Wine Brandy. Food Procces. Ind. Mag.* **2006**, *55*, 25–29.
11. Ribéreau-Gayon, P.; Glories, Y.; Maujean, A. *Handbook of Enology: The Chemistry of Wine Stabilization and Treatments*; Wiley: Hoboken, NJ, USA, 2000.
12. Różański, M.; Pielech-Przybylska, K.; Balcerek, M. Influence of Alcohol Content and Storage Conditions on the Physicochemical Stability of Spirit Drinks. *Foods* **2020**, *9*, 1264. [CrossRef]
13. Duran Guerrero, E.; Cejudo Bastante, M.J.; Castro Mejias, R.; Natera Marin, R.; Garcia Barroso, C. Characterization and Differentiation of Sherry Brandies Using Their Aromatic Profile. *J. Agric. Food Chem.* **2011**, *59*, 2410–2415. [CrossRef]
14. Tsakiris, A.; Kallithraka, S.; Kourkoutas, Y. Grape Brandy Production, Composition and Sensory Evaluation. *J. Sci. Food Agric.* **2014**, *94*, 404–414. [CrossRef]
15. Nascimento, E.S.; Cardoso, D.R.; Franco, D.W. Quantitative Ester Analysis in Cachaça and Distilled Spirits by Gas Chromatography- Mass Spectrometry (GC-MS). *J. Agric. Food Chem.* **2008**, *56*, 5488–5493. [CrossRef]
16. The Consejo Regulador. Available online: https://www.brandydejerez.es/en/our-philosophy/consejo-regulador (accessed on 25 May 2021).
17. Muñoz-Redondo, J.M.; Valcárcel-Muñoz, M.J.; Rodríguez Solana, R.; Puertas, B.; Cantos-Villar, E.; Moreno-Rojas, J.M. Development of a Methodology Based on Headspace Solid-Phase Microextraction Coupled to Gas Chromatography-Mass Spectrometry for the Analysis of Esters in Brandies. *J. Food Compos. Anal.* **2022**, *108*, 104458. [CrossRef]
18. Dziekońska-Kubczak, U.; Pielech-Przybylska, K.; Patelski, P.; Balcerek, M. Development of the Method for Determination of Volatile Sulfur Compounds (Vscs) in Fruit Brandy with the Use of HS–SPME/GC–MS. *Molecules* **2020**, *25*, 1232. [CrossRef]
19. Davis, P.M.; Qian, M.C. Effect of Ethanol on the Adsorption of Volatile Sulfur Compounds on Solid Phase Micro-Extraction Fiber Coatings and the Implication for Analysis in Wine. *Molecules* **2019**, *24*, 3392. [CrossRef]
20. Jolliffe, I.T.; Cadima, J. Principal Component Analysis: A Review and Recent Developments. *Philos. Trans. R. Soc. Math. Phys. Eng. Sci.* **2016**, *374*, 20150202. [CrossRef]
21. Westerhuis, J.A.; van Velzen, E.J.; Hoefsloot, H.C.; Smilde, A.K. Multivariate Paired Data Analysis: Multilevel PLSDA versus OPLSDA. *Metabolomics* **2010**, *6*, 119–128. [CrossRef]
22. Szymańska, E.; Saccenti, E.; Smilde, A.K.; Westerhuis, J.A. Double-Check: Validation of Diagnostic Statistics for PLS-DA Models in Metabolomics Studies. *Metabolomics* **2012**, *8*, 3–16. [CrossRef]
23. Muñoz-Redondo, J.M.; Ruiz-Moreno, M.J.; Puertas, B.; Cantos-Villar, E.; Moreno-Rojas, J.M. Multivariate Optimization of Headspace Solid-Phase Microextraction Coupled to Gas Chromatography-Mass Spectrometry for the Analysis of Terpenoids in Sparkling Wines. *Talanta* **2020**, *208*, 120483. [CrossRef]
24. Rohart, F.; Gautier, B.; Singh, A.; Lê Cao, K.-A. MixOmics: An R Package for 'omics Feature Selection and Multiple Data Integration. *PLoS Comput. Biol.* **2017**, *13*, e1005752. [CrossRef]
25. Campo, E.; Cacho, J.; Ferreira, V. Solid Phase Extraction, Multidimensional Gas Chromatography Mass Spectrometry Determination of Four Novel Aroma Powerful Ethyl Esters: Assessment of Their Occurrence and Importance in Wine and Other Alcoholic Beverages. *J. Chromatogr. A* **2007**, *1140*, 180–188. [CrossRef] [PubMed]
26. Durán-Guerrero, E.; Castro, R.; de Valme García-Moreno, M.; del Carmen Rodríguez-Dodero, M.; Schwarz, M.; Guillén-Sánchez, D. Aroma of Sherry Products: A Review. *Foods* **2021**, *10*, 753. [CrossRef] [PubMed]

27. Nikićević, N.; Velickovic, M.; Jadranin, M.; Vučković, I.; Novaković, M.; Vujisić, L.V.; Stanković, M.; Urosevic, I.; Tešević, V. The Effects of the Cherry Variety on the Chemical and Sensorial Characteristics of Cherry Brandy. *J. Serbian Chem. Soc.* **2011**, *76*, 1219–1228. [CrossRef]

28. Zhao, Y.; Xu, Y.; Li, J.; Fan, W.; Jiang, W. Profile of Volatile Compounds in 11 Brandies by Headspace Solid-Phase Microextraction Followed by Gas Chromatography-Mass Spectrometry. *J. Food Sci.* **2009**, *74*, C90–C99. [CrossRef]

29. Genovese, A.; Ugliano, M.; Pessina, R.; Gambuti, A.; Piombino, P.; Moio, L. Comparison of the Aroma Compounds in Apricot (Prunus Armeniaca, l. Cv. Pellecchiella) and Apple (Malus Pumila, l. Cv. Annurca) Raw Distillates. *Ital. J. Food Sci.* **2004**, *16*, 185–196.

30. Ledauphin, J.; Guichard, H.; Saint-Clair, J.-F.; Picoche, B.; Barillier, D. Chemical and Sensorial Aroma Characterization of Freshly Distilled Calvados. 2. Identification of Volatile Compounds and Key Odorants. *J. Agric. Food Chem.* **2003**, *51*, 433–442. [CrossRef]

31. Rodríguez Dodero, M.C.; Guillén Sánchez, D.A.; Rodríguez, M.S.; Barroso, C.G. Phenolic Compounds and Furanic Derivatives in the Characterization and Quality Control of Brandy de Jerez. *J. Agric. Food Chem.* **2010**, *58*, 990–997. [CrossRef]

32. Christoph, N.; Bauer-Christoph, C. Flavour of Spirit Drinks: Raw Materials, Fermentation, Distillation, and Ageing. In *Flavours and Fragrances*; Springer: Berlin/Heidelberg, Germany, 2007; pp. 219–239.

33. Carrillo, J.C.M. *Feasibility Testing of Chill Filtration of Brown Spirits to Increase Product Stability*; University of Louisville: Louisville, KY, USA, 2015.

Article

Quality Improvement of Green Saba Banana Flour Steamed Cake

Jau-Shya Lee [1],*, NurDiyana Yusoff [2], Ai Ling Ho [1], Chee Kiong Siew [1], Jahurul Haque Akanda [3] and Wan Xin Tan [1]

[1] Faculty of Food Science and Nutrition, University Malaysia Sabah, Jalan UMS, Kota Kinabalu 88400, Sabah, Malaysia

[2] Agriculture Research Centre, Department of Agriculture Sabah, Tuaran 89207, Sabah, Malaysia

[3] Department of Agriculture, School of Agriculture, University of Arkansas, 1200 North University Drive, M/S 4913, Pine Bluff, AR 71601, USA

* Correspondence: jslee@ums.edu.my

Abstract: Gluten avoidance is becoming a popular diet trend around the world. In this study, green Saba banana flour (GSBF) was used to produce a gluten-free (GF) steamed cake. The effects of soy protein isolate (SPI) (0%, 10%, 15%) and Ovalette (0%, 3.5%, 7%) on the quality of the cake were investigated. Physicochemical properties of the flours were measured. The viscosity and specific gravity of the batters; as well as the specific volume, weight loss and texture profile of the resulting cakes were determined. Sensory evaluation was performed to compare the acceptance of the cake formulations. The macronutrient and resistant starch content of the cakes were determined. The use of an appropriate level of SPI and Ovalette was found to effectively enhance the aeration of the cake batter and improved the specific volume and weight loss of the cake. The presence of Ovalette was essential to soften the texture of the cake. GF cake supplemented with 10% SPI and 3.5% Ovalette obtained the highest sensorial acceptance. The nutritional quality of this sample was significantly improved, whereby it contained higher protein than the gluten-containing counterpart. GSBF also contributed to the high dietary fiber and resistant starch content of the cake.

Keywords: green banana flour; soy protein isolate; emulsifier; cake; gluten-free; resistant starch; dietary fiber

1. Introduction

Celiac Disease (CD) is a major public health problem worldwide, the prevalence of this disease is 1.4% based on serologic test results [1]. It is an autoimmune digestive disorder caused by ingestion of gluten (particularly gliadin peptides) that leads to injury of the small bowel of the patients, subsequently causing nutritional deficiency, development of fertility-related complications and malignancy [2,3]. The prevalence of CD is believed to be heavily underestimated due to the frequently misdiagnose with other irritable bowel syndromes and a lack of awareness among medical professionals about the extra-intestinal presentations of the disease [4,5]. Till now, the only effective treatment available to CD patients is a stringent lifetime gluten-free (GF) diet [6]. In addition to the needs of CD patients, GF foods are also in demand by consumers with gluten sensitivity or non-coeliac gluten intolerance [7]. In recent years, GF foods have also become popular among consumers without CD [8]. This has resulted in an upsurge in demand and drastic growth in the global GF food market size.

Gluten refers to a group of storage proteins made up of gliadins and glutenins. Hydrated glutenins are more cohesive and contribute to the dough strength and elasticity, whereas hydrated gliadins behave as a plasticizer for glutenins and are responsible for the viscosity and extensibility of the dough system [9]. Avoidance of gluten in bakery products by switching from using conventional wheat flour to other low protein flours indicates

a loss of technological quality and nutritional quality of the final products. As a result, it is of paramount importance to replace proteins from other sources in the GF product formulations to achieve the desirable properties such as to enhance the Maillard browning and flavor formation while cooking; to improve the viscoelasticity of the dough or batter; as well as to improve the structure of the final products by aiding the gelation and foaming process [10].

Green banana flour is known to contain high resistant starch (RS) which is resistant to digestion. Intake of RS has been reported as able to reduce postprandial insulinemic and elevated glycemic responses. Other metabolic health-associated benefits of RS are increasing satiety, reducing fat storage, improving insulin sensitivity, lowering triglyceride and plasma cholesterol concentrations [11,12]. Through a proper modulation of SCFAs in the human body, the obesity-related metabolic disorders, and their associated diseases, such as type 2 diabetes, hypertension can be prevented [13,14]. These attractive health benefits have called attention to the development of various food products using green banana flour. Segundo et al. (2017) [15] found that the substitution of wheat flour with green banana flour increased the dietary fiber, resistant starch, polyphenol content and antioxidant activity of both layer cakes and sponge cakes. They also found that the particle size of green banana flour affected the nutritional quality of the cakes, where coarse flours yielded cakes with a higher content of dietary fiber, and fine flours yielded cakes with a significantly higher RS content. Another study also disclosed that the fiber content and the antioxidant properties of cake samples were enhanced upon addition of banana flour from 2% to 10%, however, a negative impact on textural and sensory profile was noticed beyond 8% of incorporation [16].

Soy Protein Isolate (SPI) is a highly purified protein that is isolated from soybean. It has good gelling, emulsifying and foaming properties and is often used as a functional ingredient in food industry. SPI was used to replace the protein in GF food such as rice-cassava bread [10] and banana-cassava pasta [17]. SPI could effectively improve the total phenolic content, antioxidant capacities, enhance amino acid profiles and increase the protein digestibility of gluten-free pasta made of mixture of banana flour and cassava flour [17].

Emulsifiers are key ingredients for the successful production of bakery products. They are surface-active, and amphiphilic by nature. They typically improve the aeration and fine dispersion of air bubbles in the batter or dough system. They also have crumb-softening and anti-staling effects and can help improve cake volume [18]. The straight fatty acid-chain of emulsifier molecules can form a complex with the helical structure of amylose in starch, thus reducing the rate of starch retrogradation [18]. Several authors have incorporated emulsifiers in gluten-free formulations to improve the quality of the products [19–22].

Saba banana (ABB triploid hybrid) is a cooking banana most abundantly found in the state of Sabah, Malaysia. The banana is a commercial crop that has been distributed to other parts of Malaysia, and Brunei Darussalam since 2010 [23]. It is commonly consumed as fried banana fritters, steamed, or used to make other local snacks. The downstream industrial applications are still limited. The unripe green Saba banana flour (GSBF) is reported to contain high RS with an estimated glycemic index (GI) of 47.48 [24]; thus, can be classified as a low GI food [25]. With its low digestibility and low cost, green Saba banana flour is an excellent alternative for development of GF foods to increase the food choice for individuals on a GF diet. However, green banana flour lacks the nutritive value, particularly protein, and technological functionality of wheat flour, leading a need to supplement the functional ingredients in the product formulation. This project was aimed at developing a gluten-free cake using GSBF, SPI and a commercial emulsifier, Ovalette. The objective of this study was to characterize the batter and cake quality upon addition of SPI and Ovalette, and subsequently the sensory acceptance and nutritional quality of the final product.

2. Materials and Methods

2.1. Materials

Matured Saba banana (*Musa acuminata × Musa balbisiana*) was collected from an orchard in Keningau, Sabah. Banana fruits without physical defects and with total green color peel (matured but unripe) were immediately processed into flour upon arrival in the laboratory. Soy protein isolate (SPI) with a protein content of 88% was purchased from Thong Sheng Food Technology Sdn. Bhd., Pulau Pinang, Malaysia, Ovalette, a commercial gel phase emulsifier mixture of mono- and diglycerides and polyglycerol esters of fatty acids was bought from Bakels (Malaysia) Sdn Bhd. (Shah Alam, Malaysia). Wheat flour (Cap Sauh, Johor Bahru Flour Bill Sdn. Bhd., Johor, Malaysia), castor sugar (Gula Prai; Malayan Sugar Manufacturing Corporation Bhd., Kuala Lumpur, Malaysia), full cream milk powder (Dutch Lady; Dutch Lady Milk Industries Bhd., Petaling Jaya, Malaysia), palm olein (VeSawit; YL Brands Sdn. Bhd., Kuala Lumpur, Malaysia), baking powder, salt and vanilla essence were locally purchased. Other chemicals were used as received without further purification.

2.2. Preparation of Green Saba Banana Flour

The method of Lee et al. [24] was followed to prepare the green Saba banana flour (GSBF). The freshly received green banana was peeled, sliced (2 mm thick), and immediately soaked in 0.5% (*w/v*) citric acid for 10 min. The banana slices were then dried at 50 °C for 24 h. The dried chips were ground and sieved through 60-mesh screen. The flour was kept in an air-tight container until further use.

2.3. Preparation of Cake

The basic formulation of the cake (based on flour weight) consisted of 100% flour, 100% sugar, 100% egg, 20% full-cream milk powder, 15% palm olein, 4% vanilla essence, 2% baking powder and 1% salt. Two independent variables were the SPI (soy protein isolate) and Ovalette; which were tested at three levels (SPI: 0%, 10% and 15%; Ovalette: 0%, 3.5% and 7%) in the GSBF cakes. The levels of these additives were determined from the preliminary trials in the laboratory. A total of eight cake formulations were investigated. On top of that, two additional cake formulations were also prepared for comparison, namely the standard and the control. The standard (positive reference for comparison) was the gluten-containing cake made of 100% wheat flour; meanwhile, the cake made of 100% GSBF without SPI and Ovalette was used as the control of the experiment. Table 1 shows the cake formulations that underwent comparison.

Table 1. The cake formulations under investigation.

Sample	Ingredient (%) *			
	Wheat Flour	**GSBF**	**Ovalette**	**SPI**
Standard	100	0	0	0
Control	0	100	0	0
O0P10	0	100	0	10
O0P15	0	100	0	15
O35P0	0	100	3.5	0
O35P10	0	100	3.5	10
O35P15	0	100	3.5	15
O7P0	0	100	7	0
O7P10	0	100	7	10
O7P15	0	100	7	15

* The % of the ingredient was based on the % of flour. GSBF—green Saba banana flour; SPI—soy protein isolate.

The steam cake was prepared according to the method of Itthivadhanapong et al. [26] with slight modifications. The egg, sugar, salt and Ovalette were mixed in a cake mixer (KitchenAid 5KsM150 Stand Mixer, KitchenAid, Benton Harbor, MI, USA) at speed No.

5 for 5 min until the batter turned white and became fluffy. After that, the flour, milk powder, SPI and palm olein were added with continuous stirring at speed No. 3 (2 min). After mixing, the batter was poured into a rectangular cooking pan (18 cm length × 9 cm width × 6 cm height) and steamed in a preheated steamer (15 min preheating) for 30 min. After steaming, the cake was removed from the pan and allowed to cool down for 1 h at ambient temperature. The cake was kept in an air-tight container at room temperature (25 °C) prior to further analysis.

2.4. Measurement of Color

The color of the flour was determined by a Minolta colorimeter (Konica CR 400; Osaka, Japan). Results were expressed in the CIE *L*a*b** color space using the D65 standard illuminant and the 10° standard observer. The *L** coordinate is a measure of lightness, with 0 being black and 100 representing white. The *a** coordinate represents the green to red color range, and a positive *a** value indicates redness. The *b** coordinate represents the blue to yellow color range, and a positive *b** value indicates yellowness. Five g of flour sample was firmly pressed into a glass petri dish (outer diameter of 5 cm), and the surface of the flour was leveled before the measurement was taken.

2.5. Water Holding Capacity

The water-holding capacity of the flour was determined according to Mesías and Morales [27] with slight modifications. One g of flour and 25 mL of distilled water were added into a pre-weighed centrifuged tube and vigorously vortexed for 1 min. The tube was held at room temperature for 30 min prior to centrifugation at 3000× *g* for 20 min. The supernatant was discarded, and the tube was weighed. The water-holding capacity was calculated by the following formula:

$$\text{Water holding capacity} \ = \ \frac{W2 - W1}{W0} \times 100 \tag{1}$$

where
- W0 = weight of flour;
- W1 = weight of centrifuge tube with flour;
- W2 = weight of centrifuge tube with sediment.

2.6. Oil Holding Capacity

One g of flour and twenty-five mL of palm oil were added into a pre-weighed centrifuged tube and the content was mixed using a vortex mixer for 2 min. The tube was allowed to stand at room temperature for 30 min prior to centrifugation at 3000× *g* for 20 min. The supernatant was discarded, and the tube was weighed. Oil-holding capacity was calculated by the following formula:

$$\text{Oil holding capacity} \ = \ \frac{W2 - W1}{W0} \times 100 \tag{2}$$

where
- W0 = weight of flour;
- W1 = weight of centrifuge tube with flour;
- W2 = weight of centrifuge tube with sediment.

2.7. Proximate Analysis

The proximate compositions were determined in accordance with AOAC methods [28]. The moisture content of the sample was determined after drying 3 g of sample in a 105 °C oven for 24 h (AOAC 931.01). The loss of weight was recorded as the moisture content. For protein content determination, the Kjeldahl method (AOAC 2001.11) was used, whereby 3 g of sample was first hydrolyzed with 15 mL of concentrated sulfuric acid containing two copper catalyst tablets in a heat block at 400 °C for 2 h. After that, the nitrogen content of the

digested sample was determined by the Kjeldahl analyzer (Kjeltec 2300; FOSS, Hilleroed, Denmark). The total nitrogen content was then multiplied by 6.25 to estimate the total protein content of sample. The fat content was determined by Soxhlet extraction method. The sample (3 g) was extracted with 90 mL of petroleum ether for 1 h 20 min in a Soxhlet extraction system (Soxtec 8000; FOSS, Hilleroed, Denmark) (AOAC 991.36). The ash content of the sample was determined by ashing 3 g of sample in a muffle furnace (Carbolite, Hope Valley, UK) set at 550 °C for 24 h (AOAC 930.05).

2.8. Determination of Total Dietary Fiber

The total dietary fiber content of sample was determined following the procedures provided by Megazyme TDF test kit (K-TDFR; Megazymes, Wicklow, Ireland). Briefly, 1 g of sample was subjected to sequential enzymatic digestion by heat-stable α-amylase, protease, and amyloglucosidase. After enzymatic hydrolysis, pre-heated ethanol (60 °C, 95%) was added to precipitate the dietary fiber in the sample. The precipitation process take place at room temperature for 60 min. The precipitated dietary fiber was recovered by filtering the solution through a celite-filled crucible fitted to Fibertec 1023 (FOSS, Denmark). Then, the crucible was dry overnight in a 105 °C oven. The dried residue was then measured for ash and protein content. Total dietary fiber is the weight of the filtered and dried residue after deducting the weight of protein and ash.

2.9. Determination of Resistant Starch

The Resistant Starch (RS) content was determined using Megazyme RS Kit (K-RSTAR; Megazyme International Ireland Ltd., Co., Wicklow, Ireland). About 100 mg of sample was added with pancreatic α-amylase (10 mg/mL) and amyloglucosidase (3 U/mL), followed by incubation at 37 °C for 16 h under continuous agitation (WB14; Memmert, Schwabach, Germany). Four mL of ethanol (99% *v/v*) was added to terminate the reaction, the RS was recovered as a pellet on centrifugation (3000 rpm for 10 min). The supernatant was decanted and re-suspended in 2 mL of 50% ethanol with vigorous mixing. Six mL of ethanol was further added and subjected to centrifugation at 3000 rpm for another 10 min. The ethanol suspension and centrifugation steps were repeated twice, prior to dissolving the RS pellet in 2 M KOH by vigorous stirring in an ice-water bath. The solution was neutralized with acetate buffer and hydrolyzed with amyloglucosidase (0.1 mL, 3300 U/mL) for 20 min at 50 °C. The solution was then transferred to a 100 mL volumetric flask and adjusted to 100 mL with distilled water and mixed well. 0.1 mL of aliquots was then diluted with 3 mL of Glucose Determination Reagent (GOPOD Reagent) and incubated at 50 °C for 20 min. The absorbance was measured at 510 nm (Lambda 35; Perkin-Elmer, Buckinghamshire, UK) against the reagent blank. The resistant starch content in the test samples was calculated as follows:

$$\text{Resistant starch (g/100 g sample)} = \Delta E \times F \times 100/0.1 \times 1/1000 \times 100/W \times 162/180 \quad (3)$$

where
ΔE = absorbance read against the reagent blank;
F = conversion from absorbance to micrograms;
100/0.1 = volume correction (0.1 mL taken from 100 mL);
1/1000 = conversion from micrograms to milligrams;
W = dry weight of sample;
162/180 = factor to convert from free D-glucose, as determined, to anhydro-D-glucose as occurs in starch.

2.10. Batter Specific Gravity

Batter specific gravity was calculated by dividing the weight of batter over the weight of an equal volume of the water [29]. The specific gravity of the batter was defined as the weight of the batter against the weight of the water.

2.11. Batter Viscosity

The cake batter viscosity was measured using a viscometer (DV-II+ Viscometer; Brook-field, WI, USA). The measurement was carried out after the batter was rested for 10 min after mixing was completed. Two hundred ml of batter was placed into a 500 mL beaker up to a level marked near the brim. Spindle No. 07 and test speed of 30 rpm were used to determine the viscosity at room temperature (25 °C). The viscosity value was recorded after 1 min of shearing.

2.12. Texture Profile Analysis

Texture Profile Analysis (TPA) of the samples was conducted using a TA.XTPlus Texture Analyzer (TA-XT Plus; Stable Micro Systems Ltd., Godalming, Surrey, UK) with as 80 mm aluminum cylindrical probe. The cake samples were cut into $2 \times 2 \times 2$ cm^3 cubes (with the crust removed) and subjected to a programmed double-cycle compression and the texture profile was determined using Texture Expert 1.05 software (Stable Microsystems). The crumb was compressed to 25% of its initial height at 2 mm/s. Thirty s delay was set between the first and second compression. The hardness, springiness, chewiness and resilience were obtained from the force–time curve of the texture profile. The texture parameter of cake was averaged from 10 sub-samples of two replicates (total 20 measurements).

2.13. Sensory Evaluation

Sensory evaluation was conducted on the day after the cakes were prepared in individual booths with cool, natural, fluorescent light. The tests were carried out at the Laboratory of Sensory Evaluation located at the Faculty of Food Science and Nutrition, Universiti Malaysia Sabah. Because of the high number of cake formulations, two types of sensory tests were performed: Ranking Test and Hedonic Test. Ranking Test using Balanced Incomplete Block (BIB) design was first carried out to discriminate the least preferred formulations (total of eight formulations, $t = 8$) to avoid the potential sensory fatigue among the panelists [30] in the subsequent Hedonic Test. In BIB design (Table S1 (Supplementary Materials)), every formulation was replicated seven times ($r = 7$) and all pair of cake formulations occurred three times ($\lambda = 3$) in 14 blocks ($b = 14$) [31]. A total of 42 untrained healthy panelists ranked their preference over 4 samples ($k = 4$) randomly assigned to them (1 = like the most and 4 = dislike the most).

Forty healthy panelists recruited from the students and staff of the faculty were involved in the Hedonic test. They were asked to evaluate the volume, color, aroma, taste, softness, moistness, and overall acceptability of the cake samples assigned. A typical nine-point hedonic scale by Jones et al. [32] was used (1 = dislike extremely, 5 = neither like nor dislike and 9 = like extremely).

In both sensory evaluation sessions, cake slices (approximately 10 g each; equivalent to two-bite portions) coded with three-digit numbers were served along with drinking water for palate cleansing. The panelists were advised to rinse their mouth in between each sample testing. All the cake samples were halved (cross-sectional) and presented to the panelists for the evaluation of the cake volume. The panelists were asked to observe and compare the volume of the cakes prior to evaluation of other attributes.

2.14. Statistical Analysis

The results were the average of at least triplicate measurements except for the data of TPA and Sensory Evaluation. The data were analyzed using one-way analysis of variance (ANOVA) with SPSS ver. 24 (Statistical Package for Social Science). The means were compared at 95% confidence interval. Non-parametric data from Ranking Test were analyzed with Friedman's test. Fisher's Least Significant Difference (*LSD*) test was conducted to determine the difference between the samples when the null hypothesis of Friedman's Test was rejected. The Kruskal–Wallis test and Mann–Whitney U test were employed to examine the statistical difference for the sensory attributes tested in Hedonic Test.

3. Results and Discussion

3.1. Flour Analysis

Several basic chemical compositions of green Saba banana flour (GSBF) were determined and compared to commercial wheat flour (WF) (Table 2). As expected, WF contains higher protein and fat, whereas SGBF contains higher ash, dietary fiber and resistant starch (RS) ($p < 0.05$). The protein, fat, ash, and RS content of GSBF agrees with the earlier reported values [33,34]. RS in green banana flour is the non-digestible polysaccharides that behaves in the same way as dietary fiber. It is resistant to digestion but can be fermented by colonic microbiota to produce short chain fatty acids with positive metabolic effects [35,36]; additionally, it has the ability to prevent obesity, type 2 diabetes and hypertension [14]. The dietary fiber in banana flour consists of mixture of soluble fraction (pectin) and insoluble fraction (cellulose, lignin and hemicellulose) [37]. Other commonly used gluten-free flours such as maize and rice have also been reported to have lower levels of fiber as compared to WF [38,39]; thus, have caused the resultant products to have lower nutritional quality.

Table 2. Chemical compositions of commercial wheat flour and green Saba banana flour.

Composition	Wheat Flour (WF)	Banana Flour (GSBF)
Moisture (%)	13.44 ± 0.37 [b]	11.81 ± 0.24 [a]
Protein * (%)	11.69 ± 0.05 [b]	3.87 ± 0.02 [a]
Fat * (%)	0.91 ± 0.01 [b]	0.41 ± 0.01 [a]
Ash * (%)	0.85 ± 0.03 [a]	1.96 ± 0.02 [b]
Dietary fiber * (%)	2.82 ± 0.02 [a]	10.22 ± 0.16 [b]
Resistant starch * (%)	27.9 ± 0.27 [a]	68.9 ± 0.14 [b]

* Dry matter basis. Means with identical alphabet within the same row indicate insignificant difference ($p > 0.05$).

In raw form, the RS in WF and GSBF was inherently RS2 that was protected from digestion by the crystalline structure of the starch granules. GSBF contained more highly dense starch granules [40] which were more difficult for the digestive enzyme to penetrate, hence a higher RS than in WF.

Apart from basic chemical composition, the color, water and oil-holding capacity of WF and GSBF were also compared (Table 3). The color of the flour is expressed using three values: $L*$ value ranges from 0 to 100, where 0 illustrates black and 100 represents white, $a*$ value corresponds to green (−) and red (+), whereas $b*$ corresponds to blue (−) and yellow (+). GSBF was found to be less white, darker with more intense redness and yellowness than WF ($p < 0.05$). A commercial baking white wheat flour was used in this study, typically, this flour is bleached to remove the yellow pigment (xanthophyll) to make it whiter. Besides not being treated with bleaching agent, the yellowish color of GSBF was also contributed by the tissue browning by enzymatic oxidation of the phenolic compounds in the fruit.

Table 3. Color, water-holding capacity and oil-holding capacity of wheat flour (WF) and green Saba banana flour (GSBF).

Characteristic	Wheat Flour (WF)	Banana Flour (GSBF)
Color		
Brightness ($L*$)	90.74 ± 0.13 [b]	82.72 ± 0.01 [a]
Redness ($a*$)	0.30 ± 0.02 [a]	1.46 ± 0.04 [b]
Yellowness ($b*$)	8.95 ± 0.04 [a]	9.62 ± 0.04 [b]
Water-holding capacity (%)	74.67 ± 3.51 [a]	172.00 ± 4.03 [b]
Oil-holding capacity (%)	85.67 ± 2.08 [b]	64.33 ± 1.53 [a]

Means with identical alphabet within the same row indicate insignificant difference ($p > 0.05$).

3.2. Batter Analysis

The viscosity and specific gravity of the cake batters were measured. Figure 1 shows that the batter prepared using 100% GSBF reported the lowest viscosity and the highest specific gravity ($p < 0.05$) among all tested samples. Gluten in the standard batter (100% WF) provided the desirable, unique rheological properties of the batter by conferring water absorption capacity, cohesivity, viscosity and elasticity [9]. Higher viscosity in the WF batter was attributed to the gluten development [41] after hydration by water and mixing. In the absence of gluten, the control exhibited high fluidity; little air could be incorporated in the batter during mixing, which led to a high batter density. The addition of SPI and Ovalette (O0P10, O0P15, O35P0 and O7P0) significantly increased the batter viscosity and improved the air retention of the batter ($p < 0.05$). SPI was reported to have higher water-adsorption capacity as compared to wheat protein [42] and resulted in an increment of the gluten-free batter viscosity as reported earlier [43]. Compared to the batter formulations containing single additive (O0P10 and O0P15 vs. O35P0 and O7P0), the combination of two additives would further reduce the specific gravity of the batters (Figure 1). Since the introduction of SPI and Ovalette to GSBF was based on an addition basis, the use of 10% and 15% of SPI elevated the total solid content of the formulations and thus their viscosities. It is noteworthy that the presence of Ovalette in the formulation was essential to lower the batter density to a more desirable value, closing to that of the standard (100% WF). Ovalette appeared to enhance the aeration and help stabilize the foams in the batter. Ovalette is a commercial emulsifier consisting of a mixture of α-tending emulsifiers (mono- and diglycerides and polyglycerol esters of fatty acids) that is commonly used in cake production. Blends of monoglycerides and polyglycerol esters of fatty acids bring about synergistic effect in enhancing the formation of firm and stable gels via attractive integrations and forming "bridges" between air bubbles in foams that lead to more solid-like foams [16,44] to effectively retain the entrapped air. Blends of polyglycerol fatty acid esters and monoglycerides are known to improve sponge cake aeration and stability with less mixing time and improved foam and emulsion stability [16,45].
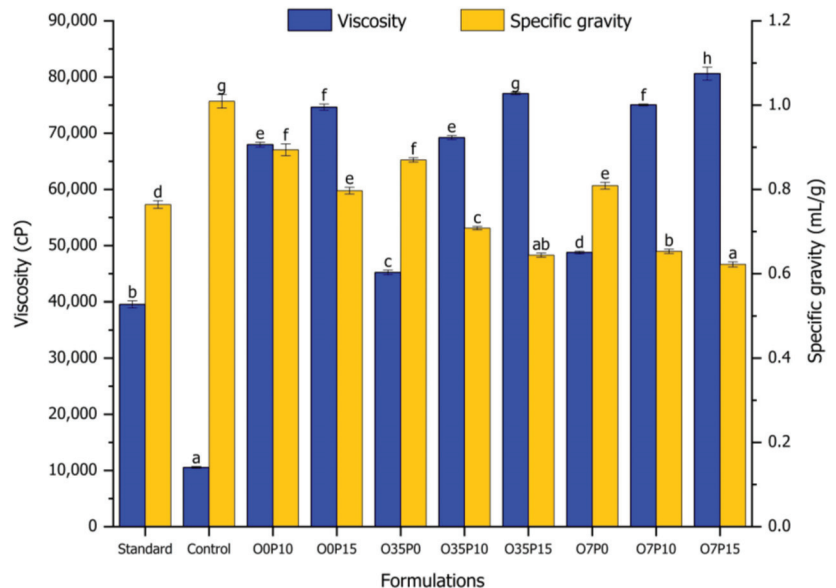
Figure 1. Viscosity (cP) and specific gravity (mL/g) for different formulations of cake batter. Histogram with different alphabet (a–h) indicates significant difference ($p < 0.05$).

3.3. Cake Analysis

3.3.1. Specific Volume and Weight Loss

Specific volume and weight loss were determined for the cakes (Figure 2). Specific volume is the indicator of the strength and extensibility of the food matrix, it is also a critical visual quality for the cake. Weight loss during the cooking of the batter is related to the gas escaping during steaming and it is a crucial parameter for the structural transformation of the cake [39]. Formation of cake structure primarily relies on the aeration and gas bubble stability during cooking [46]. The control sample presented a very compact structure with the lowest degree of expansion (Figure S1). Because of its extremely low batter viscosity (Figure 1), this sample failed to hold the gas bubbles within the food matrix while steaming. The results obtained suggest that the presence of both additives are important for the improvement of the cake volume; though the specific volume of the sample added with SPI alone (O0P10) achieved a similar specific volume to the standard ($p < 0.05$), but the weight loss was still far higher than the desirable value. When SPI and Ovalette were incorporated in the formulation at an appropriate ratio, O35P15, the specific volume and weight loss were insignificantly different from the standard ($p > 0.05$). The batter viscosity increments by addition of SPI and Ovalette (Figure 1) created a sufficient batter consistency that is crucial for retaining the air bubble formed during mixing and the CO_2 produced during steaming. However, the progressive addition of SPI was unfavorable because the batter density turned out to be too high to effectively incorporate the desirable amount of gas bubbles. As shown in Figure 2, supplementing 10% of SPI showed enhancement in the cake volume, but when 15% of SPI was used, the volume of the cakes was impaired instead. Apparently, the correct batter viscosity is crucial to ensure the successful aeration of the cake. Majzoobi et al. [29] found that an acceptable sponge cake can be obtained by using 20% SPI, but any further increase in SPI resulted in inferior cake quality. When used in bread batter, emulsifiers promoted the viscosity, which in turn improved the buoyancy of bubbles, preventing their coalescence and producing a uniform distribution [46]. The α-gel phase of the emulsifier would form solid and elastic films at the oil–water interface, which encapsulated oil during air incorporation into cake batter, thus preventing foam destabilization [18,47].
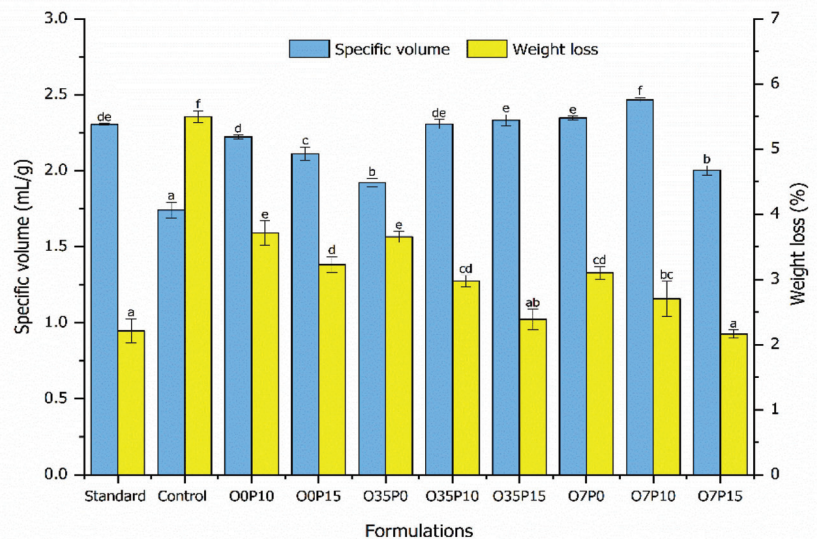
Figure 2. Specific volume (mL/g) and weight loss (%) of different formulations of Saba banana flour cake. Histogram with different alphabet (a–f) indicates significant difference ($p < 0.05$).

3.3.2. Texture Profile Analysis

Apart from visual quality, the texture of the cake is another critical characteristic that may influence consumer acceptability. The hardness, cohesiveness, springiness and chewiness of the cakes were determined (Table 4). As expected, those cakes with a less expanded volume (control, O0P10, O0P15 and O7P15) (Figure S1) recorded higher hardness than the standard ($p < 0.05$). The highly compact stacking of starch particles in these samples required higher external force to cause the structural damage. Even though addition of SPI was able to increase the specific volume in O0P10 and O0P15 (Figure 2), it did not improve the hardness of the cakes ($p < 0.05$); rather, the hardness of the cake increased with the increasing level of SPI in these two samples which may be attributed to the high water binding capacity of SPI that reduced the free water and hence the cake softness [29]. On the other hand, the hardness of the sample supplemented with Ovalette alone (O35P0 and O7P0) showed an insignificant difference from the standard ($p > 0.05$). Results obtained also indicate that Ovalette inclusion softened the banana flour cakes added with SPI such as O35P10, O35P15 and O7P10. The softening effect of Ovalette was credited to the formation of amylose-emulsifier complex that reduced the recrystallization of starch molecules after cooking and upon cooling [19]. These complex structures prevent further physical changes in dissolved amylose and reducing starch retrogradation [18]. The extremely high hardness of O7P15 could be attributed to the highest solid content and relatively low specific volume (dense structure).

Table 4. Texture profile of wheat flour cake (standard) and different formulations of Saba banana flour cakes.

Sample	Texture Profile Parameters			
	Hardness (kg)	**Cohesiveness**	**Springiness**	**Chewiness (kg)**
Standard	2.517 ± 0.129 [a]	0.674 ± 0.018 [f]	0.880 ± 0.009 [c]	1.493 ± 0.086 [d]
Control	3.288 ± 0.224 [c]	0.400 ± 0.014 [e]	0.715 ± 0.163 [b]	0.943 ± 0.240 [c]
O0P10	3.454 ± 0.211 [c]	0.380 ± 0.022 [d]	0.689 ± 0.137 [ab]	0.898 ± 0.162 [bc]
O0P15	3.784 ± 0.177 [d]	0.374 ± 0.011 [d]	0.666 ± 0.151 [ab]	0.944 ± 0.228 [c]
O35P0	2.473 ± 0.159 [a]	0.383 ± 0.018 [d]	0.740 ± 0.070 [b]	0.702 ± 0.099 [a]
O35P10	2.605 ± 0.188 [a]	0.371 ± 0.008 [d]	0.665 ± 0.061 [ab]	0.629 ± 0.075 [a]
O35P15	2.768 ± 0.167 [ab]	0.354 ± 0.015 [c]	0.591 ± 0.116 [a]	0.596 ± 0.102 [a]
O7P0	2.405 ± 0.140 [a]	0.369 ± 0.009 [cd]	0.726 ± 0.072 [b]	0.646 ± 0.092 [a]
O7P10	2.875 ± 0.231 [b]	0.335 ± 0.012 [b]	0.687 ± 0.135 [ab]	0.655 ± 0.116 [a]
O7P15	3.674 ± 0.196 [d]	0.309 ± 0.008 [a]	0.663 ± 0.112 [ab]	0.751 ± 0.128 [ab]

Means (n = 3) in a column with identical alphabet indicate insignificant difference ($p > 0.05$). Standard—cake made of WF; control—cake made of GSBF without SPI and Ovalette.

The results obtained indicating that gluten is the main factor granting the typical cohesiveness, springiness and chewiness of the cake. Cohesivity of gluten is known for providing necessary structuring functionalities in bakery products. In the absence of gluten, these textural properties were totally diminished ($p < 0.05$) as shown in the textural parameters of the control. Cohesiveness represents the ability of a material to stick to itself; thus, it is an indication of how well a product withstands a second deformation relative to its resistance under the first deformation [48]. It also refers to the rate at which food disintegrates under mechanical action, or as the resistance of food to traction [29]. Increasing the level of SPI and Ovalette was found to further reduce the cohesiveness of the GSBF cakes ($p < 0.05$). High springiness values are related to high chewing quality, whereas low springiness reflects the tendency to crumble upon external forces [49–51]. Comparatively, this textural parameter seemed to be least influenced by SPI and Ovalette where almost all the cake formulations showed similar springiness to the control ($p > 0.05$). Chewiness is defined as the energy required to masticate a solid food product [52]. Without Ovalette, the chewiness of O0P10 and O0P15 were insignificantly different to the control, but other cake samples supplemented with both Ovalette and SPI required much lower

energy to chew with no difference among them ($p < 0.05$). The use of SPI and Ovalette was incapable of improving the cohesiveness and chewiness of GSBF cake, instead causing an appreciable reduction in these parameters.

3.3.3. Sensory Evaluation

Ranking Test was conducted to screen the eight formulations of GSBF-based cake formulations supplemented with SPI and Ovalette, and the rank sum obtained for each sample is shown in Table 5. Comparatively, the formulations without SPI (O35P0 and O7P0) were least preferred by the panelists. The four top-ranked samples with insignificant statistical difference ($p > 0.05$) were identified as O35P10, O35P15, O7P10 and O0P10. These four samples were then subjected to the Hedonic Test to compare the degree of satisfaction and acceptance regarding the cake appearance, color, aroma, taste, softness, moistness and overall acceptability. The control was deliberately included in the Hedonic Test to be compared with these four samples.

Table 5. Rank sum for green Saba banana flour-based cakes obtained in Ranking Test.

Sample	Rank Sum
O35P10	36 [a]
O35P15	39 [a]
O7P10	40 [ab]
O0P10	45 [ab]
O7P15	56 [c]
O0P15	64 [cd]
O35P0	70 [cd]
O7P0	72 [d]

Rank sums with identical alphabet indicates insignificant difference ($p > 0.05$). *LSD* rank = 15.18.

Table 6 shows the mean scores for the seven tested sensory attributes. In agreement with the results of the cake analysis and TPA, the control obtained the lowest degree of satisfaction for all the tested attributes ($p < 0.05$). In brief, the control was disliked by the panelists, whereby the mean scores for all the attributes fell between 2—dislike very much and 3—dislike moderately. The results of the Hedonic Test show that the poor eating quality of the control was effectively overcome by the addition of SPI and Ovalette. It is notable that the cakes supplemented with both additives (O35P10, O35P15, O7P10) were more preferred to the one that received SPI alone (O0P10). An appreciable increase in preference was observed in all the supplemented samples except for color. This is because the color of the cakes was affected by the darker color of the green banana flour (Table 3), the crumbs turned out to be brownish, differing from the golden yellowish of normal cake (Figure S1). Cakes with a higher volume exhibited a higher preference, possibly due to the brighter color as affected by the degree of expansion. Sample O35P15 was the most preferred sample that obtained the highest score for all the tested attributes ($p < 0.05$), hence was rated with the highest overall acceptability. It should, however, be borne in mind that the sensory quality for O35P15 may require further enhancement in future as the mean score for overall acceptability only lay between 7—like moderately and 8—like very much.

3.4. Chemical Composition of Selected Cake Formulations

The effect of SPI and Ovalette on the macronutrient content of GSBF cake in the most preferred formulation (O35P15) was determined by comparing it to the composition of the standard and the control (Table 7).

Table 6. Mean score for sensory attributes of five formulations of Saba banana flour cake obtained from Hedonic Test.

Attribute	Sample				
	Control	O0P10	O35P10	O35P15	O7P10
Cake Volume	2.43 ± 0.78 [a]	4.11 ± 0.27 [b]	6.73 ± 0.86 [c]	7.38 ± 0.29 [c]	6.83 ± 0.55 [c]
Color	2.78 ± 0.55 [a]	3.38 ± 0.44 [b]	5.10 ± 0.29 [c]	5.40 ± 0.38 [d]	5.38 ± 0.47 [d]
Aroma	2.68 ± 1.03 [a]	6.73 ± 0.29 [b]	7.15 ± 0.61 [bc]	7.83 ± 0.35 [c]	6.98 ± 0.33 [b]
Taste	2.55 ± 1.32 [a]	6.00 ± 0.36 [b]	7.02 ± 0.09 [c]	7.65 ± 0.12 [d]	6.70 ± 0.45 [c]
Softness	2.16 ± 0.41 [a]	6.48 ± 0.20 [b]	7.38 ± 0.59 [d]	7.75 ± 0.11 [d]	7.11 ± 0.88 [c]
Moistness	2.88 ± 0.39 [a]	6.20 ± 0.61 b	7.78 ± 0.58 [d]	7.58 ± 0.43 [d]	7.25 ± 0.63 [c]
Overall Acceptability	2.48 ± 0.65 [a]	5.38 ± 0.72 [b]	6.55 ± 0.27 [c]	7.30 ± 0.31 [d]	6.35 ± 0.41 [c]

Means (n = 40) in a row with identical alphabet indicate insignificant difference ($p > 0.05$). Control—cake made of GSBF without SPI and Ovalette. Descriptor for 9-point Hedonic Scale: 1—dislike extremely; 5—neither like nor dislike; 9—like extremely.

Table 7. Chemical composition of standard (100% WF), control (100% SGBF) and O35P15.

Composition	Standard	Control	O35P15
Moisture (%)	33.74 ± 0.24 [b]	31.44 ± 0.16 [a]	31.58 ± 0.15 [a]
Protein * (%)	10.79 ± 0.04 [b]	7.16 ± 0.03 [a]	12.67 ± 0.06 [c]
Fat * (%)	10.70 ± 0.25 [c]	8.32 ± 0.02 [a]	10.13 ± 0.17 [b]
Ash * (%)	1.53 ± 0.11 [a]	1.69 ± 0.09 [a]	1.84 ± 0.10 [b]
Dietary fiber * (%)	3.57 ± 0.09 [a]	13.66 ± 0.17 [c]	12.70 ± 0.11 [b]
Resistant starch * (%)	2.10 ± 0.17 [a]	13.02 ± 0.35 [c]	8.51 ± 0.34 [b]

* Dry matter basis. Means with identical alphabet within the same row indicate insignificant difference ($p > 0.05$). Standard—cake made of WF; control—cake made of GSBF without SPI and Ovalette.

The nutrient profile, particularly protein and resistant starch content, of O35P15 was significantly improved as compared to the control ($p < 0.05$). SPI was reported to contain 8.41% protein [17], thus resulted in an almost 77% increment in protein when compared to the control. The protein content in O35P15 is even higher than that of the standard ($p < 0.05$). The high percentage of SPI in O35P15 is also believed to contribute to the higher fat content ($p < 0.05$), in which the SPI used in this study was reported to contain 5% of crude fat (acid hydrolysis). It is remarkable that the dietary fiber and resistant starch in both of the banana flour-based cakes were much higher than the standard ($p < 0.05$), owing to the nutrient profile of SGBF (Table 1). The RS in banana cakes was much lower than that of GSBF possibly ascribed to the presence of different types of RS in the materials. RS is classified into five subtypes, RS1 (physically inaccessible starch), RS2 (raw starch with B-type crystalline), RS3 (retrograded starch), RS4 (chemically modified starch) and RS5 (amylose-lipid complexes) [52,53]. The RS in GSBF is primarily comprised of RS2 the indigestibility of which is inherently due to the more perfectly arranged crystalline molecular structure [40]. Steaming caused disruption of the starch granules in the batter and destroyed the majority of RS2 in raw GSBF to increase the starch digestibility. Upon cooling of the cake, part of the gelatinized starch experienced retrogradation to yield RS3. These newly rearranged crystals were resistant to the enzymatic attack during digestion. Retrogradation of amylose molecule was identified as the main mechanism for the formation of RS3 but banana starch also contained long outer amylopectin α-1,6-linked side chains that were an excellent source for producing RS3 [54,55]. According to Codex Alimentarius International Food Standards [56], the food is considered a source of dietary fiber if the dietary fiber content is at least 3 g of fiber per 100 g of food, and high in fiber if it contains 6 g of fiber per 100 g of food. Equally, a food that contains 10 g of protein per 100 g of food can be considered as high in protein. With regards to this, O35P15 can be claimed as a food high in protein and high in dietary fiber.

4. Conclusions

This study demonstrated the feasibility of employing SPI and Ovalette in overcoming the technological drawbacks of SGBF in cake making. These two additives significantly

improved the technological characteristics of the batter and hence the cake. Noticeable enhancement of nutritional quality was also observed in the best formulated GSBF cake produced, particularly in the protein, dietary fiber and resistant starch contents. This finding confirmed the potential of green Saba banana flour to be included as an ingredient to rectify the low dietary fiber intake in human diet. However, the results of TPA and sensory evaluation suggest that the texture and color of the cake did not achieve the expected level of acceptance. Based on the results of the Hedonic Test, the overall acceptability of the best cake formulation was rated in between the score "like moderately" and the score "like very much", therefore, future work looking into further improvement of the texture and color of the cake is recommended.

Supplementary Materials: The following supporting information can be downloaded at: https://www.mdpi.com/article/10.3390/app13042421/s1, Figure S1: Cross sectional view of standard (100% wheat flour), the control (100% GSBF) and other GSBF cakes supplemented with different levels of soy protein isolate (SPI) and Ovalette; Table S1: The plan for arranging GSBF cakes for Ranking Test generated by Balanced Incomplete Block (BIB) Design.

Author Contributions: Conceptualization, J.-S.L.; methodology, A.L.H.; validation, J.-S.L. and N.Y.; formal analysis, W.X.T.; investigation, W.X.T.; resources, J.H.A. and N.Y.; data curation, J.-S.L. and W.X.T.; writing—original draft preparation, J.-S.L. and C.K.S.; writing—review and editing, J.-S.L. and A.L.H.; visualization, W.X.T. and J.H.A.; supervision, J.-S.L.; project administration, N.Y. and C.K.S.; funding acquisition, J.-S.L. All authors have read and agreed to the published version of the manuscript.

Institutional Review Board Statement: Not applicable.

Informed Consent Statement: Informed consent was obtained from all sensory panelists involved in the study.

Data Availability Statement: Not applicable.

Conflicts of Interest: The authors declare no conflict of interest.

References

1. Singh, P.; Arora, A.; Strand, T.A.; Leffler, D.A.; Catassi, C.; Green, P.H.; Kelly, C.P.; Ahuja, V.; Makharia, G.D. Global prevalence of Celiac Disease: Systematic review and meta-analysis. *Clin. Gastroenterol. H.* **2018**, *16*, 823–836. [CrossRef] [PubMed]
2. Dicke, W.K.; Van De Kamer, J.H.; Weijers, H.A. Celiac disease. *Adv. Pediatr.* **1957**, *9*, 277–318. [PubMed]
3. Fuchs, V.; Kurppa, K.; Huhtala, H.; Mäki, M.J.; Kekkonen, L.; Kaukinen, K. Delayed celiac disease diagnosis predisposes to reduced quality of life and incremental use of health care services and medicines: A prospective nationwide study. *United Eur. Gastroenterol. J.* **2018**, *6*, 567–575. [CrossRef] [PubMed]
4. Jinga, M.; Popp, A.; Balaban, D.V.; Dima, A.M.; Jurcut, C. Physicians' attitude and perception regarding celiac disease: A questionnaire-based study. *Turk. J. Gastroenterol.* **2018**, *29*, 419–426. [CrossRef] [PubMed]
5. Molder, A.; Balaban, D.V.; Jinga, M.; Molder, C.-C. Current evidence on computer-aided diagnosis of Celiac Disease: Systematic review. *Front. Pharmacol.* **2020**, *11*, 341. [CrossRef] [PubMed]
6. Yoosuf, S.; Makharia, G.K. Evolving therapy for celiac disease. *Front. Pediatr.* **2019**, *7*, 193. [CrossRef] [PubMed]
7. Gaesser, G.A.; Angadi, S.S. Gluten-free diet: Imprudent dietary advice for the general population? *J. Acad. Nutr. Diet.* **2012**, *112*, 1330–1333. [CrossRef]
8. Bulka, C.M.; Davis, M.A.; Karagas, M.R.; Ahsan, H.; Argos, M. The unintended consequences of a gluten-free diet. *Epidemiology* **2017**, *28*, e24–e25. [CrossRef] [PubMed]
9. Wieser, H. Chemistry of gluten proteins. *Food Microbiol.* **2007**, *24*, 115–119. [CrossRef] [PubMed]
10. Crockett, R.; Ie, P.; Vodovotz, Y. Effects of soy protein isolate and egg white solids on the physicochemical properties of gluten-free bread. *Food Chem.* **2011**, *129*, 84–91. [CrossRef]
11. Haralampu, S.G. Resistant starch—A review of the physical properties and biological impact of RS3. *Carbohydr. Polym.* **2000**, *41*, 285–292. [CrossRef]
12. Das, M.; Rajan, N.; Biswas, P.; Banerjee, R. A novel approach for resistant starch production from green banana flour using amylopullulanase. *LWT* **2022**, *153*, 112391. [CrossRef]

13. Fernández, J.; Redondo-Blanco, S.; Gutiérrez-del-Río, I.; Miguélez, E.M.; Villar, C.J.; Lombó, F. Colon microbiota fermentation of dietary prebiotics towards short-chain fatty acids and their roles as anti-inflammatory and antitumour agent: A review. *J. Funct. Foods* **2016**, *25*, 511–522. [CrossRef]

14. Pingitore, A.; Gonzalez-Abuin, N.; Ruz-Maldonado, I.; Huang, G.C.; Frost, G.; Persaud, S.J. Short chain fatty acids stimulate insulin secretion and reduce apoptosis in mouse and human islets in vitro: Role of free fatty acid receptor 2. *Diabetes Obes. Metab.* **2019**, *21*, 330–339. [CrossRef] [PubMed]

15. Segundo, C.; Román, L.; Gómez, M.; Martínez, M.M. Mechanically fractionated flour isolated from green bananas (*M. cavendishii* car. nanica) as a tool to increase the dietary fibre and phytochemical bioactivity of layer and sponge cakes. *Food Chem.* **2017**, *219*, 240–248. [CrossRef] [PubMed]

16. Bharathi, N.D.; Dasgupta, P.; Venkatachalam, C.D. Studies on the formulation of cake using green banana flour. In Proceedings of the AIP Conference—4th National Conference on Current and Emerging Process Technologies e-CONCEPT-2021, Kongu Engineering College, Erode, India, 20 February 2021; Volume 2387.

17. Rachman, A.; Brennan, M.A.; Morton, J.; Torrico, D.; Brennan, C.S. In-vitro digestibility, protein digestibility corrected amino acid, and sensory properties of banana-cassava gluten-free pasta with soy protein isolate and egg while protein addition. *Food Sci. Hum. Wellness* **2023**, *12*, 520–527. [CrossRef]

18. Wang, F.C.; Marangoni, A.C. Advances in the application of food emulsifier α-gel phases: Saturated monoglycerides, polyglycerol fatty acid esters, and their derivatives. *J. Colloid Interf. Sci.* **2016**, *483*, 394–403. [CrossRef] [PubMed]

19. Onyango, C.; Unbehend, G.; Lindhauer, M.G. Effect of cellulose-derivatives and emulsifiers on creep-recovery and crumb properties of gluten-free bread prepared from sorghum and gelatinised cassava starch. *Food Res. Int.* **2009**, *42*, 949–955. [CrossRef]

20. Purhagen, J.K.; Sjöö, M.E.; Eliasson, A.-C. The anti-staling effect of pre-gelatinized flour and emulsifier in gluten-free bread. *Eur. Food Res. Technol.* **2012**, *235*, 265–276. [CrossRef]

21. Sciarini, L.S.; Ribotta, P.D.; León, A.E.; Pérez, G.T. Incorporation of several additives into gluten free breads: Effect on dough properties and bread quality. *J. Food Eng.* **2012**, *111*, 590–597. [CrossRef]

22. Aguilar, N.; Albanell, E.; Miη, B.; Capellas, M. Chickpea and tiger nut flours as alternatives to emulsifier and shortening in gluten-free bread. *LWT Food Sci. Technol.* **2015**, *62*, 225–232. [CrossRef]

23. Sabah Agriculture Department. *Pisang Sabah-Ikon Tanaman Buah-buahan Negeri Sabah*; Sabah Agriculture Department: Kota Kinabalu, Sabah, Malaysia, 2022.

24. Lee, J.-S.; George, R.; Yusoff, N.; Fong, J.A. Enhancing enzymatic resistance of green Saba banana flour by pullulanase debranching and autoclave-cooling treatment. *Trans. Sci Tech.* **2021**, *8*, 552–559.

25. International Standards Organization. *Food Products–Determination of the Glycaemic Index (GI) and Recommendation for Food Classification*; International Organization for Standardization: Geneva, Switzerland, 2010.

26. Itthivadhanapong, P.; Jantathai, S.; Schleining, G. Improvement of physical properties of gluten-free steamed caked based on black waxy rice flour using different hydrocolloids. *J. Food Sci. Technol.* **2016**, *53*, 2733–2741. [CrossRef] [PubMed]

27. Mesías, M.; Morales, F.J. Effect of different flours on the formation of hydroxymethylfurfural, furfural, and dicarbonyl compounds in heated glucose/flour systems. *Foods* **2017**, *6*, 14. [CrossRef]

28. AOAC. *Official Methods of Analysis of AOAC International*, 17th ed.; AOAC International: Gaithersburg, MD, USA, 2000.

29. Majzoobi, M.; Ghiasi, F.; Habibi, M.; Hedayati, S.; Farahnaky, A. Influence of soy protein isolate on the quality of batter and sponge cake. *J. Food Process. Preserv.* **2014**, *38*, 1164–1170. [CrossRef]

30. Best, D.J.; Rayner, J.C.W.; Allingham, D. A statistical test for ranking data from partially-balance incomplete block designs. *J. Sens. Stud.* **2011**, *26*, 81–84. [CrossRef]

31. Cochran, W.G.; Cox, G.M. *Experimental Design*, 2nd ed.; John Wiley & Sons, Inc.: Hoboken, NJ, USA, 1957.

32. Jones, L.V.; Peryam, D.R.; Thurstone, L.L. Development of a scale for measuring soldier's food preferences. *Food Res.* **1955**, *20*, 512–520. [CrossRef]

33. Sardá, F.A.H.; de Lima, F.N.R.; Lopes, N.T.T.; Santos, A.D.O.; de C. Tobaruela, E.; Kato, E.T.M.; Menezes, E.W. Identification of carbohydrate parameters in commercial unripe banana flour. *Food Res. Int.* **2016**, *81*, 203–209. [CrossRef]

34. Huang, S.; Martinez, M.M.; Bohrer, B.M. The compositional and functional attributes of commercial flours from tropical fruits (Breadfruit and banana). *Foods* **2019**, *8*, 586. [CrossRef] [PubMed]

35. Sánchez-Zapata, E.; Viuda-Martos, M.; Fernández-López, J.; Pérez-Alvarez, J.A. Resistant starch as functional ingredient. In *Polysaccharides*; Ramawat, K.G., Mérillon, J.M., Eds.; Springer International Publishing: Cham, Switzerland, 2015; pp. 1911–1931.

36. Batista, A.L.D.; Silva, R.; Cappato, L.P.; Ferreira, M.V.S.; Nascimento, K.O.; Schmiele, M.; Esmerina, E.A.; Balthazar, C.F.; Silva, H.L.A.; Moraes, J.; et al. Developing a synbiotic fermented milk using probiotic bacteria and organic green banana flour. *J. Funct. Foods* **2017**, *38*, 242–250. [CrossRef]

37. Thebaudin, J.Y.; Lefebvre, A.C.; Harrington, M.; Bourgeois, C.M. Dietary fibres: Nutritional and technological interest. *Trends Food Sci. Technol.* **1997**, *8*, 41–48. [CrossRef]

38. Hosseini, S.M.; Soltanizadeh, N.; Mirmoghtadaee, P.; Banavand, P.; Mirmoghtadaie, L.; Shojaee-Aliabadi, S. Gluten-free products in celiac disease: Nutritional and technological challenges and solutions. *J. Res. Med. Sci.* **2018**, *23*, 109. [PubMed]

39. Ammar, I.; Gharsallah, H.; Ben Brahim, A.; Attia, H.; Ayadi, M.A.; Hadrich, B.; Felfoul, I. Optimization of gluten-free sponge cake fortified with whey protein concentrate using mixture design methodology. *Food Chem.* **2021**, *343*, 128457. [CrossRef]

40. Liao, H.-J.; Hung, C.-C. Chemical composition and invitro starch digestibility of green banana (cv. Giant Cavendish) flour and its derived autoclaved/debranched powder. *LWT Food Sci. Technol.* **2015**, *64*, 639–644. [CrossRef]
41. Loewe, R. Role of ingredients in batter systems. *Cereal Foods World* **1993**, *38*, 673–677.
42. Roccia, P.; Ribotta, P.D.; Perez, G.T.; Leon, A.E. Influence of soy protein on rheological properties and water retention capacity of wheat gluten. *LWT Food Sci. Technol.* **2009**, *42*, 358–362. [CrossRef]
43. Ronda, F.; Oliete, B.; Gomez, M.; Caballero, P.A.; Pando, V. Rheological study of layer cake batters made with soybean protein isolate and different starch sources. *J. Food Eng.* **2011**, *102*, 272–277. [CrossRef]
44. Richardson, G.; Langton, M.; Fäldt, P.; Hermansson, A.-M. Microstructure of α-crystalline emulsifiers and their influence on air incorporation in cake batter. *Cereal Chem.* **2002**, *79*, 546–552. [CrossRef]
45. Silva, R.F. Use of alpha-crystalline emulsifiers in the sweet goods industry. *Cereal Foods World* **2000**, *45*, 405–4110.
46. Sahi, S.S.; Alava, J.M. Functionality of emulsifiers in sponge cake production. *J. Sci. Food Agric.* **2003**, *83*, 1419–1429. [CrossRef]
47. Stauffer, C.E. Emulsifier for the Food Industry. In *Bailey's Industrial Oil and Fat Products*, 6th ed.; Shahidi, F., Ed.; John Wiley & Sons, Inc.: Hoboken, NJ, USA, 2005; Volume 4, pp. 229–268.
48. Bourne, M.C. *Food Texture and Viscosity: Concept and Measurement*, 2nd ed.; Academic Press: New York, NY, USA, 2002; pp. 183–184.
49. McCarthy, D.F.; Gallagher, E.; Gormley, T.R.; Schober, T.J.; Arendt, E.K. Application of response surface methodology in the development of gluten-free bread. *Cereal Chem.* **2005**, *82*, 609–615. [CrossRef]
50. Matos, M.E.; Rosell, C.M. Relationship between instrumental parameters and sensory characteristics in gluten-free breads. *Eur. Food Res. Technol.* **2012**, *235*, 107–117. [CrossRef]
51. Feng, W.; Zhang, H.; Wang, R.; Zhou, X.; Wang, T. Modifying the internal structures of steamed rice cakes by emulsifiers for promoted textural and sensory properties. *Food Chem.* **2021**, *354*, 129469. [CrossRef] [PubMed]
52. Wu, T.-Y.; Tsai, S.-J.; Sun, N.-N.; Dai, F.-J.; Yu, P.-H.; Chen, Y.-C.; Chau, C.-F. Enhanced thermal stability of green banana starch by heat-moisture treatment and its ability to reduce body fat accumulation and modulate gut microbiota. *Int. J. Biol. Macromol.* **2020**, *160*, 915–924. [CrossRef] [PubMed]
53. Gutierrez, T.J.; Tovar, J. Update of the concept of type 5 resistant starch (RS5): Self-assembled starch V-type complexes. *Trends Food Sci. Technol.* **2021**, *109*, 711–724. [CrossRef]
54. Lehmann, U.; Jacobasch, G.; Schmiedl, D. Characterization of resistant starch type III from banana (Musa acuminata). *J. Agric. Food Chem.* **2002**, *50*, 5236–5240. [CrossRef] [PubMed]
55. Kaur, L.; Dhull, S.B.; Kumar, P.; Singh, A. Banana starch: Properties, description and modified variations—A review. *Int. J. Biol. Macromol.* **2020**, *165*, 2096–2101. [CrossRef] [PubMed]
56. Codex Alimentarius International Food Standards. Guidelines for Use of Nutrition and Health Claims. Available online: https://www.fao.org/fao-who-codexalimentarius/thematic-areas/nutrition-labelling/en/ (accessed on 11 November 2022).

Article

Formulation of a Wort-Based Beverage with the Addition of Chokeberry (*Aronia melanocarpa*) Juice and Mint Essential Oil

Kristina Habschied [1], Jelena Nišević [1], Vinko Krstanović [1], Ante Lončarić [1], Kristina Valek Lendić [2] and Krešimir Mastanjević [1,*]

[1] Faculty of Food Technology, Josip Juraj Strossmayer University of Osijek, 31000 Osijek, Croatia
[2] Institute of Public Health of the Osijek-Baranja County, F. Krežme 1, 31000 Osijek, Croatia
* Correspondence: kmastanj@gmail.com; Tel.: +385-31-224-373

Featured Application: This research resulted in a potentially functional non-alcoholic beverage applicable to all age groups. With the addition of chokeberry juice, a potent antioxidative beverage with no added sugars, this drink has the potential to become a functional beverage. This preparation could have a promising application in the food and beverage industries, providing health benefits due to its high antioxidant potential.

Abstract: In Croatia, the production of non-alcoholic wort-based beverages is in its initial stages. The main goal of this research was to produce wort that could be then used in the production of a wort-based beverage with the addition of chokeberry (*Aronia melanocarpa*) juice. Sensory characteristics and consumer acceptance was also analyzed. Worts were prepared by the standard mashing process, using Munich and pale ale malt. Chokeberry juice was added to the cooled worts. For the purpose of this research, two versions of wort with different concentrations of chokeberry juice (10%, 20%, 30%) were formulated, and all of the beverages were subjected to sensory analysis. Sensory analysis showed that wort with the addition of 30% chokeberry juice was the most accepted. This concentration of chokeberry juice gave the beverage a pleasant taste, but needed some improvement. To address this, mint essential oil was added to the mixture and carbonation using gaseous CO_2 was conducted. This beverage received better acceptance when carbonated and mixed with mint essential oil. In addition to the sensory analysis, the polyphenol content of the chosen beverage was also analyzed, along with its nutritional value. Polyphenol content was 2621.47 mg/L and antioxidative activity was 2.28 mmol Trolox/L. The energy value was determined to be 57 kcal. However, in order to optimize the production of this wort-based beverage, further research should be conducted.

Keywords: chokeberry; wort; mint essential oil; malt; polyphenols; anthocyanins; antioxidant capacity

1. Introduction

Beer production has been practiced for more than 5000 years, as evidenced by numerous legends and records on clay tablets of the inhabitants of former Mesopotamia. Additionally, Greek and Roman literature refer to beer, mocking people who drank beer instead of wine. This point of view regarding beer as a less valuable drink than wine changed during the reign of Charlemagne, with beer production even extending to monasteries. It was at this time, at the turn of the seventh century, that beer hopping began [1].

Modern times demand modern approaches and innovations in the food and beverage industries. Recent decades have imposed certain choices regarding the health demands of consumers. Increases in food allergies, food intolerance, and healthy food and lifestyle choices have led to a rise in healthy food production. Functional foods and beverages that aid and preserve the health of consumers is a current trend [2]. Since cereals are such a great source of various beneficial components such as phenols, vitamins B and E, fibers,

carbohydrates, and phytoestrogens, it is reasonable to employ them in the production of food and beverages [3–5].

Wort is a semi-product in the production of beer, obtained after the thermal and enzymatic decomposition of basic raw materials, i.e., barley or wheat malt. Standard all-malt wort commonly contains around 12% monosaccharides, 5% sucrose, 47% maltose, 15% maltotriose, and 25% higher saccharides, such as dextrins [6]. Wort does not contain alcohol since no yeasts have been added to it, omitting the fermentation process. However, it does contain many minerals and vitamins such as vitamin C. Interestingly, Captain Cook is known to have used wort to suppress the occurrence of scurvy during his long voyages at sea. After his second voyage (1772–1775), he reported that wort was effective as an antiscorbutic medicine [7]. Thus, wort is a great beverage that can potentially and easily be transformed into a functional drink.

As for chokeberry (*Aronia melanocarpa*), its products are recognized as foods that have a beneficial effect on health and are designated as functional food. Due to its antioxidant properties, such as its rich polyphenols content, chokeberry is used as a medicine. Polyphenolic compounds are commonly found in all plants. They are a significant antioxidant available in food [8]. Many studies have investigated polyphenols due to their therapeutic effects related to oxidative stress [9]. Among polyphenols, anthocyanins and proanthocyanidins are the most biologically active components in *A. melanocarpa* berries [9,10]. Chokeberry is also a source of glucose, fructose, sucrose, sorbitol and pectic, K and Zn, along with certain amounts of Na, Ca, Mg and Fe. Vitamins B1, B2, B6, and C, niacin, pantothenic acid, folic acid, alpha and beta tocopherol and carotenoids are also found in chokeberry fruits, in addition to citric, malic, shikimic, and ascorbic acid [9,11]. The antioxidative activity of black chokeberry have also been confirmed, as well as its other related benefits such as antihypertensive, lipid-lowering, and anti-inflammatory effects [12–14]. Most importantly, no harmful effects from chokeberry juice, fruit and extracts have been reported [9]. The aim of this study was to produce a polyphenol-rich beverage based on the combination of wort and chokeberry that has no added sugars or sweeteners and is suitable for everyone (children, sportsmen and older people). Since wort is a naturally sweet beverage and chokeberry juice is rich in polyphenols and antioxidative activity, it was reasonable to assume such a mixture would result in a drink acceptable to consumers. The combination of wort and chokeberry juice resulted in a product with an increased content of polyphenols, anthocyanins, and antioxidant activity.

2. Materials and Methods

2.1. Production of Wort

For the purpose of this research, light and dark worts were produced. Grounded malt was mashed at 69 °C for 1 h in a 20 L Speidel Braumeister (Speidel Tank- und Behälterbau GmbH, Ofterdingen, Germany). The first batch was produced with 5 kg of Munich malt (Badass barley malt, Nova Gradiška, Croatia) with the addition of 50 g black wheat malt (Wheat chocolate—Weyermann®, Bamberg, Germany) to achieve a darker color. The second batch was produced using pale ale malt (Badass barley malt, Nova Gradiška, Croatia), also 5 kg. The production process was the same for both worts. Water for mashing was prepared by reverse osmosis and hardness was adjusted by adding 1 g $CaSO_4$, 2.5 g $CaCl_2$, and 2 g $MgSO_4$ for darker wort and 6.5 g $CaSO_4$, 14 g $CaCl_2$, and 9 g $MgSO_4$ for pale ale wort. At the end of the mashing process, spent grains were rinsed with 4 L of the same water used for mashing. The rinsing water temperature was 72 °C. After the separation of spent grains, worts were boiled at 100 °C for 1 h. This step was followed by cooling to 23 °C, using a Speidel cooling coil. Worts were then transferred to a container. The obtained volume of worts was 19 L each. Chokeberry juice (Encian d.o.o. Donji Stupnik, Croatia) was then added in each keg in concentrations of 30% to the volume of wort. For example, since keg has the volume of 18 L, the volume of wort was 13.8 L and the added juice was 4.2 L for 30% beverage mixture.

The optimal amount of chokeberry juice was determined previously, testing out the three mixtures with the addition of chokeberry juice in 10, 20, and 30% to 5 L of lighter and darker non-carbonated wort mixtures.

In order to improve the sensory properties of the prepared wort-based drink with the addition of chokeberry juice to soften the taste of the wort itself, 0.25 mL of mint essential oil was added to 18 L of the prepared drinks. The beverages were then left in the cooler at 2 °C. The prepared wort-based drinks were then carbonized using CO_2 at 2.5 bar.

2.2. Sensory Evaluation

Upon production, a sensory evaluation was needed to decide which beverage is more appealing to consumers. Primarily, the addition of chokeberry juice in concentrations of 10, 20 or 30% in darker and lighter wort was subjected to evaluation to decide which drink would be the most acceptable. An evaluation was conducted as described in Section 2.2.1. A table presenting the evaluated properties can be found in the Supplementary Material.

After determining the most suitable addition of chokeberry juice, another sensory evaluation was carried out to determine which mixture would be better accepted among consumers. A drinkability test was conducted to determine which version of the prepared mixture would be accepted better among consumers, as described in Section 2.2.2.

2.2.1. Sensory Evaluation of Basic Characteristics

A sensory evaluation was conducted by 20 untrained consumers (13 females and 7 males). The panel consisted of beer consumers of different age groups (aged 21–59). The test and sensory descriptors were adjusted from the general evaluation sheer for beer [15]. The scoring of each sensory attribute was conducted on a five- or four-point intensity scale, where 1 point means "fault" and higher points mean "excellent", as can be seen from the Supplementary Material, Table S1. Smell, taste, bitterness, astringency, carbonation, and mouthful were determined in the second round of testing, as opposed to the first round of testing where carbonation was omitted since the beverages were not carbonated. Tastings were performed in an appropriate room. Samples were kept at room temperature for 10 min before the test and poured into a clean transparent glass. All samples were served under a number and every sample was tested in triplicate. Evaluators were offered flat mineral water between the samples, together with plane white bread. Tastings were conducted twice; the first tasting was carried out with the beverage being offered to the consumers at room temperature, and for the second tasting, the evaluators were offered a cold (4 °C) beverage.

2.2.2. Drinkability Test

After the sensory evaluation, a drinkability test was performed in order to determine which version of the beverage would be more acceptable. The drinkability test involved the two produced beverages. The same panelists who participated in the sensory evaluation were called up again (20 consumers, aged 21–58). Panelists were initially offered to try all beverages (200 mL in a glass marked with numbers), cooled at 4 °C. The tasting atmosphere provided a relaxed environment, with a person waiting on the participants. After the initial tasting of the beverages, panelists were left to choose on their own between the samples. The test lasted for 2 h and was conducted in the afternoon (5–7 PM) and was performed as described by Habschied et al. [16].

2.3. Determination of Polyphenols Index

The total polyphenolic index (TPI) was determined using Folin–Ciocalteu reagent (FC) according to a procedure described by [17]. The changes in the color of the radical from light blue to dark blue were measured after 30 min at 760 nm using a UV-Vis spectrophotometer (Shimadzu UVmini-1240, Kyoto, Japan). The TP was quantified from gallic acid calibration curve (3–20 mg/L, R^2 = 0.9961). The TPI was calculated and expressed as mg gallic acid equivalent (GAE) per L of beverage.

2.4. Determination of Antioxidant Activity

The antioxidant activity was measured using a DPPH radical according to a modified method described by [18]. The reaction mixture consisted of 0.2 mL of the beverage sample and 3 mL of DPPH radical solution 0.1 mM in methanol. The changes in the color of the radical from deep violet to light violet were measured after 30 min at 515 nm using a UV-ViS spectrophotometer (Shimadzu UVmini-1240, Kyoto, Japan). The antiradical activity (AA) was determined using the following equation (y = 0.9548x + 0.0294; R^2 = 0.9914) obtained from linear regression after plotting the A515 nm of known solutions of trolox against concentration (0.1–0.9 mM). The results were expressed as mmol of Trolox® equivalents (TE) per one liter of beverage (mmol TE/L).

2.5. Determination of Anthocyanins and Flavonoid Content

Monomeric anthocyanins were determined using the method described by Giusti et al. [19]. Total monomeric anthocyanins were expressed as cyanidin-3-glucoside, and the obtained values were expressed as mg/L.

The total flavonoid content was determined according to Makris et al. [20]. Briefly, 0.5 mL of the beverage sample was mixed with 4 mL of distilled water, then 0.3 mL 5% $NaNO_2$ was added and allowed to react for 5 min. Following this, 0.3 mL 10% $AlCl_3$ was added and the mixture was allowed to react for a further 5 min. At the end, 2 mL 1 M Na_2CO_3 and 2.4 mL distilled water were added to the reaction mixture and the absorbance at 510 nm was read against a blank. For each sample, the measurements were performed in triplicates and values were interpolated on a calibration curve using catechin as a standard and expressed as g catechin equivalents per L of beverage (g CE/L).

2.6. Nutritional Value Determination

All analyses are in-house methods and can be retrieved from the Institute of Public Health of the Osijek-Baranja County upon request; however, a short description the analyses carried out in this study is provided here. Fat content was determined using the Röse–Gottlieb method. The method is commonly used to determine fats in foods that mainly also contain proteins (milk, butter, cheese, meat, whole meal, etc.) [21].

Ash was determined according to the standard method based on burning the sample at a temperature of 550 ± 10 °C and weighing the obtained residue [22].

Crude fiber determination was carried out using the Scharrer–Kürschner method [23]. Sugar content was determined according to Luff [24].

Salt was determined as follows: 10–50 g of the homogenized sample was transferred to a 250 mL volumetric flask and filled to the mark with distilled water. Then, it was shaken and filtered. Twenty-five mL of the filtrate was transferred into a 100 mL flask and subjected to titration with 0.1 M $AgNO_3$ with the addition of 10 drops of potassium chromate until the color changed from yellow to red, using an in-house method.

Brix, dry matter and refraction index was determined using a refractometer (Carl Zeiss Abbe, Oberkochen, Germany), which is part of an in-house method.

Protein content was determined as described by Lim [25].

2.7. Statistical Analysis

Analysis of variance (ANOVA) and Fisher's least significant difference test (LSD) were conducted, with the least statistical significance set to $p < 0.05$. Statistica 13.1. (TIBCO Software Inc., Palo Alto, CA, USA) was the software of choice for this data set.

3. Results and Discussion

To determine which version of the beverage would be preferred among the consumers, a sensory evaluation was conducted. Upon preliminary sensory evaluation, as shown in Table 1, it appeared that the addition of 30% chokeberry juice is more acceptable than other combinations (10 and 20%) for both versions of wort. Smell, taste, bitterness, astringency,

and mouthful were evaluated for all mixtures, but the overall result was taken into account and is presented in Table 1.

Table 1. Table presenting evaluating scores/acceptance of formulated beverages.

Formulation	Score
Temperature	20 °C
Munich 30%	26.50 [a]
Pale ale 30%	23.05 [b]
Munich 20%	22.65 [b]
Pale ale 20%	20.95 [bc]
Munich 10%	21.55 [bc]
Pale ale 10%	20.00 [c]

Means within rows with different superscripts [a,b,c] are significantly different ($p < 0.05$).

From this table, it is visible that for both worts, lighter and darker, the addition of 30% of chokeberry juice gave a pleasant taste to the wort, and scored the highest. The highest score of 26.50 points was received for Munich malt wort, with 30% of added chokeberry juice. The similar formulation with pale ale malt and 30% chokeberry juice followed with a slightly but statistically significantly lower score of 23.05 points. In general, the darker beverage received better scores than the pale ale malt beverage, as can be seen from Table 1. However, the panelists noted that the addition of mint, cooling, and carbonation would probably add t a more enjoyable and refreshing kick to the beverage. In further evaluations, mint essential oil and carbonation were added. Such beverages, prepared as described in the Section 2, were then offered to the panelists in order to determine the preferable mixture.

The next stage of this research was set up as a second sensory analysis performed in order to evaluate the consumers' preference among the produced wort mixtures. According to the results presented in Table 2 and Figures 1 and 2, sample M (Munich malt with 30% chokeberry juice and mint oil) had an overall better result in all evaluated categories than sample P (pale ale malt with chokeberry juice and mint oil). Since the panelists previously declared that a cooled beverage would provide a more refreshing kick, we served them the same beverages at two temperatures (20 °C and 4 °C).

Table 2. Table presenting evaluating scores/acceptance of formulated beverages drank at different temperatures.

Temperature	20 °C	4 °C
Sample	Score	
Munich 30%	24.60 [aB]	26.50 [aA]
Pale ale 30%	21.40 [bB]	24.50 [bA]

Means within rows with different superscripts [a,b] are significantly different ($p < 0.05$); Means within columns with different superscripts [A,B] are significantly different ($p < 0.05$).

Smell, bitterness, taste, carbonation, and mouthful all received higher scores in sample M, while astringency received a lower score, as opposed to the sample P, where astringency was rated a higher score. Astringency is an important property in this research since the intention was to achieve a moderate bitterness with just a hint of astringency originating from chokeberry. The results indicate that consumers prefer drinks stored at lower temperatures (4 °C), as can be seen in Table 2 and Figures 1 and 2.
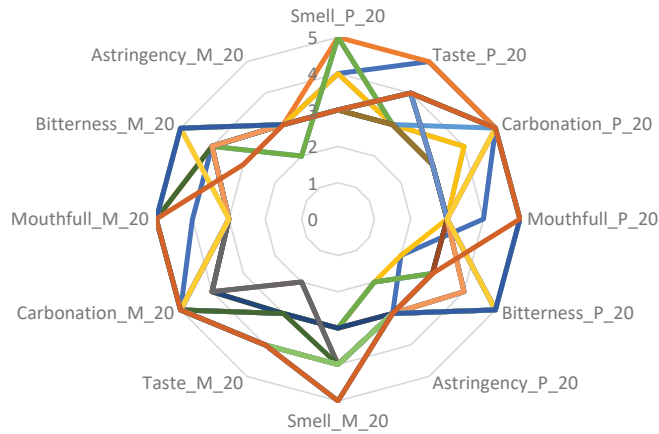
Figure 1. Sensory analysis of samples at 20 °C; Sample produced with pale ale malt is marked as "P" and sample produced with Munich malt is marked with "M".
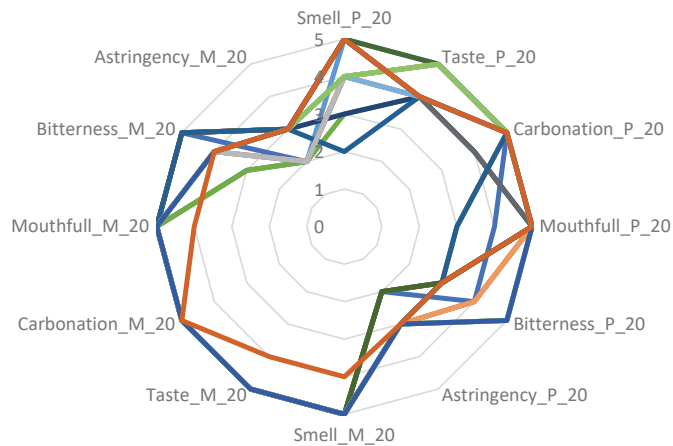
Figure 2. Sensory analysis of samples at 4 °C; Sample produced with pale ale malt is marked as "P" and sample produced with Munich malt is marked with "M".

Consumers prefer a less bitter, more carbonated drink, which is provided with a beverage formulated with Munich malt. During storage at a lower temperature, the feeling of astringency and the feeling of bitterness decreased, which is evident from Figures 1 and 2. Additionally, there were tasters who commented that they liked the sweetness, i.e., that the drink was not too sweet for them, unlike commercially available soft drinks. Lower temperature (4 °C) also contributed to the mouthful score and the feeling of carbonation for both mixtures.

The taste of wort was dominant in this drink, and most of the tasters had never tasted wort. However, this research showed that potential consumers, who had the opportunity to try a similar wort-based drink earlier (the tested drink was commercially available as a wort-based beverage with lemon or orange juice), exhibited a better acceptance of the wort-based drink with the addition of chokeberry juice and mint essential oil. This indicates that the taste of wort, or wort-based drinks, is a habit-forming taste in the sense that consumers can develop a fondness for this drink over time through more frequent consumption of the product. As mentioned before, the sweetness of this drink was acceptable to individuals who follow a healthier way of life, with reduced or no-sugar content in their diet.

This narrowed the choice to two possible mixtures that were acceptable to consumers: lighter and darker versions of wort enriched with chokeberry juice (30%), and mint essential oil and carbonated, which were tested using the drinkability test. This test was set up to determine which drink was more acceptable to consumers. The drinkability test revealed that, as shown in Table 3, the darker mixture (marked as sample 2) prepared with Munich malt was better accepted among users than the lighter color version prepared with pale ale malt (sample 1). It appeared that the darker wort was more acceptable to the eyes of the end consumers when mixed with chokeberry juice and was more pleasant in taste than the lighter color version.

Table 3. Drinkability test results.

Sample	V (L) of Consumed Beer
1	7.8 [a]
2	10.8 [b]

Means within rows with different superscripts [a,b] are significantly different ($p < 0.05$). Sample 1—pale ale malt wort with the addition of 30% chokeberry juice and mint oil; sample 2—Munich malt wort with the addition of 30% chokeberry juice and mint oil.

The drinkability test was performed in order to determine which version of the wort mixture would provide a better, more pleasant beverage. According to the results (Table 3), consumers seemed to prefer sample 2 (darker wort mixture), as they drank 10.8 L of beer, while sample 1 was less desirable, with 7.8 L of consumed beverage.

Research conducted by Habschied et al. [26] reported that dark and black beers contain higher amounts of polyphenols and exhibit higher antioxidative activity. According to this report, a darker wort formulation would presumably contain a higher amount of antioxidative activity and polyphenols.

Since it was statistically confirmed that the more desirable beverage mixture was darker wort with chokeberry, additional analyses were carried out accordingly, as described in the following sections.

The values of antioxidant activity and polyphenols obtained from the analysis of wort-based drinks with the addition of chokeberry juice and mint essential oil are presented in Table 4. Since there are no scientific literature data about wort-based beverages in that regard, the obtained results were compared with the antioxidant activity and polyphenol value of industrially-produced dark and black beer [26]. The hypothesis was that the prepared beverage would have higher antioxidant activity, i.e., a higher proportion of polyphenols, than the dark or black beers. This is especially anticipated due the additions of potent antioxidant chokeberry juice. The results shown in Table 4 confirmed the stated hypothesis, i.e., the antioxidant activity of dark, i.e., black of beer, is lower than determined in this beverage by an average of four times. Maximal values for dark and black beer were around 0.6 mmol Trolox/100 mL, while for this beverage, the antioxidative activity was determined to be 2.28 mmol Trolox/100 mL. As for the content of polyphenols, their content in dark beers averaged to 682.79 mg/L (maximal value was determined for black beer sample and amounted to 855 mg/L), which is also four times lower than the value found in the prepared wort-based beverage with the addition of chokeberry juice and mint essential oil. The proportion of polyphenols in black beers was slightly higher than in dark beers, i.e., the average value of polyphenols in the analyzed samples of dark beer is 809.43 mg/L, which shows that the proportion of polyphenols in the prepared drink is three times higher than in black beer. Namely, the content of polyphenols in the mixture was 2621.47 mg/L. Anthocyanins and flavonoids have also been analyzed. The content of anthocyanins was 87.67 mg/L, while flavonoids reached 1110.00 g/kg. These concentrations are significant and surely add to the biological value of the chosen mixture. Anthocyanins in chokeberry juice can be found in concentrations of 200–480 mg/L [27–29]. The results obtained in this research are within these values, considering this is a 30% chokeberry juice solution. Chokeberry juice can have a wide range of polyphenol content; according to several authors,

it can range from 3000 mg GAE/L to 11,000 mg GAE/L [30,31]. Antioxidative activity in commercially available juices was 19.02–106.13 mmol Trolox/L [32]. The obtained results of our research fit with the values of polyphenols and antioxidative activity that can be found in the literature. Namely, since this beverage contains 30% chokeberry juice, the values for polyphenols are within the range reported in the aforementioned literature. However, antioxidative activity falls slightly short in comparison to the 100% chokeberry juice, probably due to the dilution with wort.

Table 4. Determined antioxidative activity, polyphenols, anthocyanins and flavonoids content in the best-chosen beverage, Munich malt beverage with 30% of chokeberry juice.

	Value
Polyphenols	2621.47 mg/L
Anthocyanins	87.67 mg/L
Antioxidative activity	2.28 mmol Trolox/L
Flavonoids	1110.00 mg/L

Since there is no alcohol in this drink, it is rich in antioxidants, and there are no added sugars or sweeteners, it can also be recommended for children.

Similar research, using caramel and darker malts, was conducted by Shopska et al. [33], who developed a wort-based beverage with increased biological value. They developed a beverage using 24.2% Vienna, 51.8% Melanoidin, 20% Caramel pils, and 4% Special X malts. This formulation was rated as optimal in regard of antioxidative activity. Additionally, research by Latifova et al. [34] investigated the production of a lactic acid beverage based on wort and mint (*Menta piperita* L.), which resulted in increased antioxidant activity.

To determine the nutritive value of the composed beverage, an analysis of nutritional properties was also carried out. The results are presented in Table 5. The caloric or energy value of the produced drink was 239 kJ or 57 kcal. Artificial flavors and sweeteners have not been added to this drink; all carbohydrates and sugars originate from malt and chokeberry juice.

Table 5. Determined nutritive value of the best-chosen beverage, Munich malt beverage with 30% of chokeberry juice.

Energy Value (in 100 g of Sample)	239 kJ/57 kcal
Dry matter	14.5%
Ashes	0.25%
Raw fibers	0.00%
Fat	0.00%
Proteins	0.28%
Salt	0.09%
Total sugars	6.65%
Carbohydrates	13.97%

A small amount of salt (0.09%) and no fat content provides a good nutritional option for consumers who wish to avoid such ingredients. Additionally, as mentioned before, the sweetness of the beverage was rated as pleasant, especially by individuals who choose to avoid sugars in their diet.

4. Conclusions

Trends in the food and beverage industry are dependent on the increase in healthy lifestyles of the public, especially among younger people. Thus, novel formulations are being developed and subjected to research. No sugar, no alcohol and the efficient addition

of the potent antioxidative juice of chokeberry is a desirable formulation, accessible to younger and older people.

Dark wheat malt was added to increase the number of polyphenols in the drink, but also to improve the color of the drink itself. Namely, as reported in the preliminary conducted sensory evaluation, using only light, pale ale malt, for the formulation, the drink was not visually appealing to consumers. After determining the acceptable formulation with 30% chokeberry juice and the addition of mint essential oil and CO_2, the taste significantly improved. The fizziness provided by CO_2 contributes to the feeling of refreshment during consumption. This beverage is rich in polyphenols, mainly anthocyanins, and it can be consumed by children, older people, or even sportsmen, as it is a non-alcoholic beverage.

This research resulted in the formulation of a potentially functional beverage mixture with an energy value of only 239 kcal, which makes it ideal for use in personalized nutrition, nutrition for children, sportsmen, and older people, as was set in the objectives of the study. However, further research is needed to determine the true functionality of this beverage.

References

1. Marić, V. *Tehnologija Piva*, 1st ed.; Karlovac University of Applied Sciences: Karlovac, Croatia, 2009.
2. Cardinali, F.; Osimani, A.; Milanović, V.; Garofalo, C.; Aquilanti, L. Innovative Fermented Beverages Made with Red Rice, Barley, and Buckwheat. *Foods* **2021**, *10*, 613. [CrossRef] [PubMed]
3. Coda, R.; Montemurro, M.; Rizzello, C.G. Yogurt-like beverages made with cereals. In *Yogurt in Health and Disease Prevention*; Shah, N.P., Ed.; Elsevier: Amsterdam, The Netherlands, 2017; pp. 183–201.
4. Katina, K.; Laitila, A.; Jovonen, R.; Liukkonen, K.H.; Kariluoto, S.; Piironen, V.; Landgerg, R.; Åman, P.; Poutanen, K. Bran fermentation as a means to enhance technological properties and bioactivity of rye. *Food Microbiol.* **2007**, *24*, 175–186. [CrossRef] [PubMed]
5. Basinskienne, L.; Cizeikiene, D. Cereal-Based Nonalcoholic Beverages. In *Trends in Nonalcoholic Beverages*; Galanakis, C.M., Ed.; Academic Press: Cambridge, MA, USA, 2020; pp. 63–99.
6. Wort. Available online: https://beerandbrewing.com/dictionary/nfffzoYQNF/ (accessed on 5 February 2023).
7. Stubbs, B.J. Captain Cook's beer: The antiscorbutic use of malt and beer in late 18th century sea voyages. *Asia Pac J Clin Nutr.* **2003**, *12*, 129–137. [PubMed]
8. Daskalova, E.; Delchev, S.; Vladimirova-Kitova, L.; Kitov, S.; Denev, P. Black Chokeberry (*Aronia melanocarpa*) Functional Beverages Increase HDL-Cholesterol Levels in Aging Rats. *Foods* **2021**, *10*, 1641. [CrossRef] [PubMed]
9. Denev, P.; Kratchanov, C.; Ciz, M.; Lojek, A.; Kratchanova, M. Bioavailability and antioxidant activity of black chokeberry (*Aronia melanocarpa*) polyphenols: In vitro and in vivo evidences and possible mechanisms of action: A review. *Comp. Rev. Food Sci. Food Saf.* **2012**, *11*, 471–489. [CrossRef]
10. Kokotkiewicz, A.; Jaremicz, Z.; Luczkievicz, M. Aronia plants: A review of traditional use, biological activities, and perspectives for modern medicine. *J. Med. Food* **2010**, *13*, 255–269. [CrossRef]
11. Skoczyñska, A.; Jêdrychowska, I.; Porêba, R. Influence of chokeberry juice on arterial blood pressure and lipid parameters in men with mild hypercholesterolemia. *Pharm. Rep.* **2007**, *59*, 177–182.

12. Zapolska-Downar, D.; Hajdukiewicz, K.; Bryk, D. *Aronia melanocarpa* fruit extract exhibits anti-inflammatory activity in human aortic endothelial cells. *Eur. J. Nutr.* **2012**, *51*, 563–572. [CrossRef]
13. Cebova, M.; Klimentova, J.; Janega, P.; Pechanova, O. Effect of bioactive compound of *Aronia melanocarpa* on cardiovascular system in experimental hypertension. *Oxid. Med. Cell. Longev.* **2017**, *2017*, 8156594. [CrossRef]
14. Valcheva-Kuzmanova, S.; Kuzmanov, A.; Kuzmanova, V.; Tzaneva, M. *Aronia melanocarpa* fruit juice ameliorates the symptoms of inflammatory bowel disease in TNBS-induced colitis in rats. *Food Chem. Toxicol.* **2018**, *113*, 33–39. [CrossRef]
15. Middle European Brewing Analysis Commission (MEBAK); Band II.n Brautechnische Middle European Brewing Analysis Commission (MEBAK). *Band II.n Brautechnische Analysenmethoden*, 3rd ed.; Selbstverlag der MEBAK: Freising-Weihenstephan, Germany, 1997.
16. Habschied, K.; Krstanović, V.; Šarić, G.; Ćosić, I.; Mastanjević, K. Pseudo-Lager—Brewing with Lutra® Kveik Yeast. *Fermentation* **2022**, *8*, 410. [CrossRef]
17. Singleton, V.L.; Rossi, J.A., Jr. Colorimetry of total phenolics with phosphomolybdic–phosphotungstic acid reagents. *Am. J. Enol. Viticult.* **1965**, *16*, 144–158.
18. Brand-Williams, W.; Cuvelier, M.E.; Berset, C. Use of a free radical method to evaluate antioxidant activity. *LWT* **1995**, *28*, 25–30. [CrossRef]
19. Giusti, M.; Wrolstad, R.E. Characterization and Measurement of Anthocyanins by UV-Visible Spectroscopy. *Curr. Protoc. Food Anal. Chem.* **2001**, *5*, 1–13. [CrossRef]
20. Makris, D.P.; Boskou, G.; Andrikopoulos, N.K. Polyphenolic content and in vitro antioxidant characteristics of wine industry and other agri-food solid waste extracts. *J. Food Compos. Anal.* **2007**, *20*, 125–132. [CrossRef]
21. Available online: https://hive.blog/hive-196387/@yusvelasquez/determination-of-fat-content-in-milk-rose-gottlieb-method (accessed on 20 December 2022).
22. Available online: https://people.umass.edu/~{}mcclemen/581Ash&Minerals.html (accessed on 20 December 2022).
23. Thaler, H. Determination of crude fibre by Scharrer's method. *Vorratspfl. Lebensm.* **1938**, *1*, 350–352.
24. Available online: https://www.gafta.com/write/MediaUploads/Contracts/2018/METHOD_10.1_SUGAR_-_LUFF_SCHOORL_METHOD.pdf (accessed on 5 November 2022).
25. Lim, P.Y. Available online: https://aquadocs.org/bitstream/handle/1834/40994/B-1.pdf?sequence=1&isAllowed=y (accessed on 3 December 2022).
26. Habschied, K.; Lončarić, A.; Mastanjević, K. Screening of Polyphenols and Antioxidative Activity in Industrial Beers. *Foods* **2020**, *9*, 238. [CrossRef] [PubMed]
27. Popović, K.; Pozderović, A.; Jakobek, L.; Rukavina, J.; Pichler, A. Concentration of chokeberry (*Aronia melanocarpa*) juice by nanofiltration. *J. Food Nutr. Res.* **2016**, *55*, 159–170.
28. Pozderović, A.; Popović, K.; Pichler, A.; Jakobek, L. Influence of processing parameters on permeate flow and retention of aroma and phenolic compounds in chokeberry juice concentrated by reverse osmosis. *Cyta-J. Food* **2016**, *14*, 382–390.
29. Sainova, I.; Pavlova, V.; Alexieva, B.; Vavrek, I.; Nikolova, E.; Valcheva-Kuzmanova, S.; Markova, T.; Krachanova, M.; Denev, P. Chemoprotective, antioxidant and immunomodulatory in vitro effects of Aronia melanocarpa total extract on laboratory-cultivated normal and malignant cells. *J. Biosci. Biotechnol.* **2012**, *35*, 43.
30. Tolić, M.T.; Krbavčić, I.P.; Vujević, P.; Milinović, B.; Jurčević, I.L.; Vahčić, N. Effects of weather conditions on phenolic content and antioxidant capacity in juice of chokeberries (*Aronia melanocarpa* L.). *Pol. J. Food Nutr. Sci.* **2017**, *67*, 67–74. [CrossRef]
31. Tolić, M.T.; Jurčević, I.L.; Krbavčić, I.P.; Marković, K.; Vahčić, N. Phenolic content, antioxidant capacity and quality of chokeberry (*Aronia melanocarpa*) products. *Food Technol. Biotechnol.* **2015**, *53*, 171–179. [CrossRef] [PubMed]
32. Sosnowska, D.; Podsędek, A.; Kucharska, A.Z.; Redzynia, M.; Opchowska, M.; Koziołkiewicz, M. Comparison of in vitro anti-lipase and antioxidant activities, and composition of commercial chokeberry juices. *Eur. Food Res. Technol.* **2016**, *242*, 505–515. [CrossRef]
33. Shopska, V.; Teneva, D.; Denkova-Kostova, R.; Ivanova, K.; Denev, P.; Kostov, G. Modelling of Malt Mixture for the Production of Wort with Increased Biological Value. *Beverages* **2022**, *8*, 44. [CrossRef]
34. Latifova, G.; Nedyalkov, P.; Denkova-Kostova, R.; Teneva, D.; Goranov, B.; Denkova, Z.; Kostov, G.; Shopska, V.; Kaneva, M. Lactic acid beverage based on wort and mint (*Menta piperita* L.). *Bulg. Chem. Commun.* **2022**, *54*, 49–56.

Article

Optimization of an Innovative Hydrothermal Processing on Prebiotic Properties of *Eucheuma denticulatum*, a Tropical Red Seaweed

Birdie Scott Padam [1], Chee Kiong Siew [1] and Fook Yee Chye [1,2,*]

[1] Faculty of Food Science and Nutrition, Universiti Malaysia Sabah, Jalan UMS,
Kota Kinabalu 88400, Sabah, Malaysia
[2] Seaweed Research Unit, Universiti Malaysia Sabah, Jalan UMS, Kota Kinabalu 88400, Sabah, Malaysia
* Correspondence: fychye@ums.edu.my

Featured Application: This study provides key factors for the efficient subcritical low-acid hydrolysis of oligosaccharides from red seaweed having potential prebiotic properties, a sought-after functional food ingredient. Extraction of marine oligosaccharides from sustainable seaweed biomass with minimal loss is a green effort to cater to the huge global functional food demand.

Abstract: Seaweed is a sustainable source of marine oligosaccharides that potentially could be used as a prebiotic ingredient for functional food development. The study aims to optimize the oligosaccharide preparation through thermal hydrolysis of an under-utilized red seaweed, *Eucheuma denticulatum*. Response surface methodology (RSM) applying Box–Behnken design (BBD) was used on three parameters including temperature (105–135 °C), hydrolysis time (15–35 min) and sulfuric acid concentration (0.05–0.2 M). Optimized fractions with good prebiotic activity were characterized using high-performance size-exclusion chromatography (HP-SEC) and Fourier transform infrared spectroscopy (FT-IR). *Eucheuma denticulatum* oligosaccharides fraction 1 (ED-F1) was shown to promote the growth of beneficial gut microbiota including *Lactobacillus plantarum*, *L. casei*, *L. acidophilus*, *Bifidobacterium animalis* and *B. longum* with the highest prebiotic activity score of 1.64 ± 0.17. The optimization studies showed that hydrolysis time was the most significant parameter for the oligosaccharides yield. Optimal hydrolysis conditions for ED-F1 were 120 °C, 21 min, 0.12 M H_2SO_4 with the highest yield achieved (11.15 g/100 g of dry weight). The molecular weight of ED-F1 was determined at 1025 Da while FT-IR analysis revealed the presence of sulfated oligosaccharides with similar characteristics of *i*-carrageenan. These findings signify the innovative method for the efficient production of seaweed derived prebiotic oligosaccharides, which could be a promising source of functional food ingredients for the development of health foods and beverages.

Keywords: optimization; response surface methodology; lactobacillus; bifidobacterium; *Eucheuma denticulatum*; seaweed oligosaccharide; HMF

1. Introduction

Seaweeds are one of the most consumed marine products, especially in Asia, where it has been cultivated and used since time immemorial. It is estimated that the global seaweed industry produced 32.7 million tonnes in volume in 2020, with revenue of about USD 13.3 billion [1,2]. About 85% of the seaweed produced is directly consumed as food. These unique marine macroalgae attract consumers due to the numerous known nutritional and health benefits containing bioactive ingredients showing properties such as anti-cancer, anti-cholesterol and anti-hypertension [3–5] as well as anti-inflammatory [6]. It is also reported to be a sustainable source for potential prebiotics [7,8]. Among the many components available from seaweeds, the polysaccharides and oligosaccharides from these

marine biomasses are known to be unique and have gained a tremendous research interest for food and pharmaceutical applications.

The diverse number of species within the three major groups of seaweed (red, green and brown), provides a huge variation in the types and properties of their polysaccharides (carrageenan, alginate, agar) which have different applications in the food industry [9]. Polysaccharides are generally deposited in the seaweed cell matrix, mainly for structural purposes. Conventionally, polysaccharides are extracted from seaweeds through physical and chemical degradation of biomass tissues using the hydrothermal method, alkaline and acid hydrolysis, as well as enzymatic preparation, while further degradation of the extracted polysaccharide or prolonged degradation of the seaweed biomass yields low molecular weight polysaccharides and oligosaccharides [10]. Some seaweed polysaccharides are heavily sulfated and vary tremendously in their monosaccharide composition as well as polymer linkage [11]. A typical polysaccharide such as agarose has an average molecular weight of more than 100,000 Da and 0.15% sulfate content, while a low molecular weight agaropectin has a mass below 20,000 Da with up to 8% sulfate content [12].

Current studies showed that some seaweeds' non-digestible polysaccharides and hydrolysed low molecular weight polysaccharides and oligosaccharides promote the growth of beneficial gut microbiota such as lactobacilli and bifidobacterium. These include alginate and agar polysaccharides from *Grateloupia filicina*, *Eucheuma spinosum, Kappaphycus alvarezii* [13,14] as well as commercially available laminaran (*Laminaria* sp.), ulvan (*Ulva* sp.) and porphyran (*Propia* sp.) [11]. Agaro-oligosaccharides derived from the hydrolysis *Gracillia lemaneiformis* polysaccharides also exhibit similar activity in promoting significant abundance in beneficial microbiota population while *Sargassum confusum* oligosaccharides display potential anti-diabetic properties through regulating the gut microbiota [15,16]. Low molecular weight oligosaccharides with such activities are much sought after not only for their physicochemical properties, but also for their bioactivity, with the potential to create huge impact in the industry [17].

Extraction of oligosaccharide is the first and most challenging step in determining the composition and properties of the compounds, in which the recovery is affected by several factors such as temperature, solvent, and extraction technique. Conventional extraction methods using high temperatures for a prolonged period is always detrimental to sample as the decomposition of polysaccharide backbone yields by-products such as hydroxymethyl furfural and furfural derivatives that can be toxic at high concentrations [18,19]. Diluted acid hydrolysis coupled with high temperature extraction by far is still the low-cost method for the recovery of oligosaccharides from lignocellulosic material. However, there is very little study of the utilization of low acid hydrolysis and its effects on the degree of recovery of oligosaccharides from seaweeds, especially for the less-cultivated varieties.

Response surface methodology (RSM) through Box–Behnken design (BBD) is a powerful tool to predict the best extraction conditions leading to optimal desired experimental responses. Recent published literatures have demonstrated this method combination for the efficient extraction of seaweed phytosterols [20], plant antioxidants [21] and mushroom peptides [22]. A minimum of three levels of each shortlisted parameter is required for the BBD to fit a second-order regression model (quadratic model) [21]. In this context, the current study aimed to investigate the effects of temperature, time and acid concentration on the oligosaccharides extraction from red seaweed *Eucheuma denticulatum* and optimizing the extraction parameters using RSM for higher recovery of the oligosaccharide fractions while reducing the formation of by-product 5-hydroxymethyl furfural (HMF).

2. Materials and Methods

2.1. Materials

All solvents, reagents, chemical standards and microbiological medium were purchased from Merck (Darmstadt, Germany) unless otherwise stated. *Lactobacillus paracasei* (LC01), bifidobacterium lactis BB12 (BB12) and *Bifidobacterium longum* BB46 (BB46) cultures were from Chrs. Hansen (Hørsholm, Denmark). *Lactobacillus plantarum* ATCC 8014

(LP8014), and *Escherichia coli* ATCC 11775 (EC11775) were from American Type Culture Collection (ATCC, Manassas, VA, USA). Commercial prebiotic (Fibrulose F97™) was from Cosucra (Pecq, Belgium).

2.2. Seaweed Sample Preparation

Red seaweed (*Eucheuma denticulatum*) was collected from Semporna, Sabah Malaysia with the assistance from the Seaweed Research Unit, Universiti Malaysia Sabah. Seaweeds were washed from impurities, dried at 50 °C until reaching approximately 10% moisture content, milled and were kept in an airtight container in −20 °C. Species verification was performed by the Seaweed Research Unit, Universiti Malaysia Sabah.

2.3. Hydrolysis and Extraction of Seaweed Oligosaccharide Fraction

The seaweed oligosaccharide fraction was extracted using the modified autoclave method (130 °C, 15 psi, 15 min) (Hirayama, Japan) [23] with low acid hydrolysis (0.2 M H_2SO_4). Dried and defatted seaweed powder were used (25 g, 1:20 solid–liquid ratio) and placed in 1 L blue-cap Schott™ bottles. Recovered liquor was neutralized with calcium carbonate and the supernatant was recovered through centrifugation (5000 rpm, 5 min). The supernatant was concentrated under vacuum until 10% of its initial volume at 60 °C and was deproteinized through the removal of precipitates (8000 rpm, 5 min). Sequentially, two volumes and five volumes of ethanol (95%) were added to the supernatant under constant stirring and both precipitates were removed through centrifugation. The supernatant obtained after the removal of the ethanol precipitate were concentrated again to 5% volume and were precipitated using nine volumes of pure ethanol (99.9%) to obtain low molecular weight oligosaccharides. Oligosaccharide precipitates were washed with pure ethanol twice and vacuum dried at 50 °C. Bradford's protein assay was used to check for residual protein. Oligosaccharide precipitates were fractionated through anion exchange column (DEAE-Sepharose® Fast Flow Column, 20 mm × 100 cm) (Sigma-Aldrich, St. Louis, MO, USA) and gradient eluted with distilled water, 0.1, 0.2, 0.4 M, 0.8 M and 1.6 M NaCl solutions [24]. Each fraction was collected and the phenol–sulfuric acid assay [25] was used to determine the sulfated sugar content. Fractions which contained oligosaccharides were pooled, concentrated, desalted (Sephadex® G-10 column, 2.0 × 25 cm) (Sigma-Aldrich, St. Louis, MO, USA), vacuum dried and weighed. Fractions were subjected to size exclusion chromatography (HP-SEC) (Agilent 1200, Santa Clara, CA, USA) using BIOSEP-SEC S2000 column (Phenomenex, Torrance, CA, USA). Elution took place at 30 °C with 50 mM sodium nitrate and the elution was monitored using a refractive index detector (RID) [26]. Calibration was performed using galactose, maltose, maltotriose, and dextrans with molecular weight ranging between 1 and 25 kDa as standards.

2.4. Prebiotic Activity Assay and Prebiotic Activity Score

The assay was conducted by adding bacterial suspensions (final inoculum concentrations of 6 log CFU/mL) to separate tubes containing MRS basal broth (probiotic) or M9 broth (EC) (with 1% (wt/vol) glucose or 1% (wt/vol) prebiotic). Cultures were incubated under anaerobic conditions at 37 °C. After 0 h and 24 h of incubation, bacterial samples were enumerated on MRS and TSA, respectively. Each assay was performed in triplicate. The prebiotic activity score was calculated using the Equation (1) according to Huebner et al. 2007 [27]:

$$\text{Prebiotic activity score} = \text{probiotic } (\Delta \log \text{CFU/mL prebiotic}/\Delta \log \text{CFU/mL glucose}) - \text{enteric } (\Delta \log \text{CFU/mL prebiotic}/\Delta \log \text{CFU/mL glucose}) \tag{1}$$

2.5. Quantification of HMF

Briefly, the chromatographic separation was performed using an Agilent 1200 Series HPLC, equipped with a diode array detector (DAD) (Agilent, Santa Clara, CA, USA). Extraction liquor containing 5-hydroxy-2-methylfurfural (HMF) was injected through a

Phenomenex column (Luna C18, 5.0 μm, 4.6 × 150 mm) at 30 °C. The mobile phase consisted of water (with 0.5% formic acid) and acetonitrile in the ratio 90:10 (vol/vol) under isocratic conditions, at a flow rate of 0.8 mL/min with an injection volume of 30.0 μL. The detection was carried out at 285 nm and the total run time was 8 min. All aqueous samples solutions were filtered on 0.45 μm nylon filters before injection on chromatographic system [28].

2.6. Selection of Three Levels of Independent Variables (X_1, X_2, X_3)

Extraction of oligosaccharide fraction ED-F1 was done at different temperatures (95 °C to 135 °C hours) at constant time (15 min) and 0.2 M H_2SO_4 concentration. The best extraction temperatures were forwarded down and were used as a constant for the next extraction procedure in which the time is varied (15 min to 55 min) while applying a constant 0.2 M H_2SO_4 concentration. The best extraction temperatures applied with the best extraction time were forwarded down as constant variables for the next extraction procedure varying the H_2SO_4 concentration (0.05 M to 0.25 M). All extraction liquors were similarly purified according to the previous method to obtain fraction ED-F1. Parameters with the highest fraction yield were selected as center points.

2.7. Experimental Design and Validation of Models

The optimization approach was carried out using The Design Expert (Version 11.0.0, Stat-Ease Inc, Minneapolis, MN, USA) according to a three level, three variable Box–Behnken design with 17 design points. Three independent variables consist of hydrolysis temperature (°C, X_1), time (min, X_2) and sulfuric acid concentration (M H_2SO_4, X_3). A narrowed three levels of each variable were selected based on the results from the single factor experimentation, denoted as lower level (−1), upper level (+1) and including the center point (0). Levels were assigned accordingly for X_1: 115 °C(−1), 125 °C(0), to 135 °C(+1); X_2: 15 min(−1), 25 min(0), 35 min(+1); X_3: 0.05 M(−1), 0.125 M(0), 0.2 M(+1). Responses (Y) are based on the recovered yield of oligosaccharide fraction in grams and hydroxymethyl furfural concentration in the reaction liquor (g/L). Experimental data were fitted to the following second order polynomial equation proposed for the analysis of each response (Y) shown by Equation (2):

$$Y = \beta 0 + \sum_{i=1}^{3} \beta i X i + \sum_{i=1}^{3} \beta i i X i^2 + \sum_{i \neq j=1}^{3} \beta i j X i X j \qquad (2)$$

In the equation, Y is the yield of oligosaccharide fraction and hydroxymethyl furfural concentration, predicted response; β_0, β_i, β_{ii}, and β_{ij} are regression coefficients for intercept, linear, quadratic and interaction terms respectively; X_i and X_j are independent variables. The significance of the model was calculated in terms contributing to the regression sum of squares. The reduced model was then acquired through the exclusion of the non-significant coefficients from the initial model after the analysis the regression model coefficients (R^2) and evaluating the model lack of fit using ANOVA ($p < 0.05$) and the Fisher test value (F-value). Response surface plots were developed to explain the effects of independent variables (temperature, time and H_2SO_4 concentration) on the response variables (ED-F1 fraction, HMF) [29].

2.8. FT-IR Spectra Acquisition

The Fourier transform infrared (FT-IR) spectrum of the ED-F1 was detected on the FT-IR spectrometer (Spectrum 100, Perkin Elmer, Waltham, MA, USA), recorded in a transmittance mode over a wavelength range between 4000 and 400 cm^{-1} [30]. Iota-carrageenan was used as a reference standard. Triplicates of each sample were scanned to get an average spectrum.

2.9. Statistical Analysis

All determinations were performed at least in triplicate. Data were expressed as mean values ± standard deviation. Comparison of means was performed by one-way analysis of variance (ANOVA) with a significance level of $p < 0.05$. The Design Expert software (ver.12) (Stat-Ease, Inc., Minneapolis, MN, USA) was used for constructing the regression model, designing the Box–Behnken and predicting the optimal parameters.

3. Results

3.1. Purification and Prebiotic Activity Score of Red Seaweed Oligosaccharide Fractions

Red seaweed oligosaccharide fractions undergoing anion-exchange column yielded three distinct fractions assigned ED-F1, ED-F2 and ED-F3 (Figure 1). The first fraction eluted out with water resulted in the major peak, followed by a peak eluted using 0.2 M and 0.4 M NaCl, while no peak was detected through the elution using 0.8 M–1.6 M (results not shown). Monitoring was conducted using the phenol–sulfuric assay and similar fractions were pooled together into one single fraction. Anion-exchange chromatography was extensively used to fractionate oligosaccharides including fucooligosaccharides derived from the enzymatic hydrolysis of brown seaweed Sargassum honeri [31] as well as ulvan oligosaccharides from green seaweed *Ulva* sp. [32]. Gradient increase in the ionic strength of the mobile phase (Cl⁻), competes with the binding site of the positively charged DEAE sepharose resin that will gradually enable the release of negatively charged molecules that binded earlier [33]. Ionized sulphate ester groups are the prime contributors to the natural anionic properties of the seaweed oligosaccharides [34].
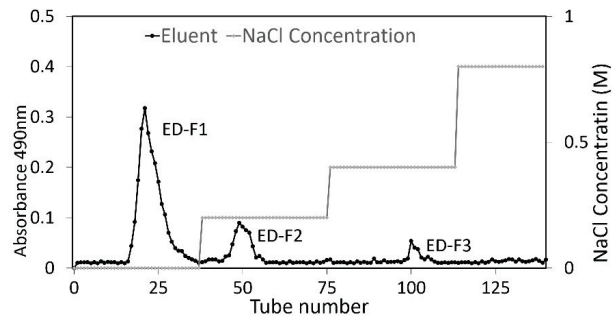
Figure 1. *E. denticulatum* low molecular weight oligosaccharide fractions obtained through anion exchange chromatography (DEAE-Sepharose® Fast Flow).

The three oligosaccharide fractions subjected to prebiotic assay showed positive prebiotic activity score values against five different commercial probiotics (Figure 2). ED-F1 displayed the highest prebiotic activity score against all probiotics with the highest value against *L. paracasei* LC01 at 1.64 ± 0.17. The prebiotic activity score values of ED-F1 were significantly higher compared to commercial prebiotic F97 against *B. animalis* BB12, *B. longum* BB46, *L. paracasei* LC01 and *L. acidophilus* LA05. These values are higher than the reported prebiotic activity score of pectic oligosaccharide fractions from citrus peel against *L. paracasei* (0.17–0.38) and *Bifidobacterium bifidum* (0.09–0.93) [35], but comparable to the score of seaweed polysaccharides extracted from *Sargassum withii* (1.42) and *Enteromorpha compressa* (1.44) against *Lactobacillus plantarum* [36]. The current study displayed a slightly lower prebiotic activity score values of ED-F1 against *L. plantarum* LP8014. The variation observed in the prebiotic activity score of different fractions for both bifidobacteria and lactobacilli strain relates to its metabolic diversity [27] and their different preferential utilization of various oligosaccharides in the fraction [27,37,38]. Depending on the species, lactobacilli strains have been known to possess a great variety of genes involved in the metabolism of both complex oligosaccharides and simple sugars which can be switched on depending on the availability of the type of carbohydrates available [39].
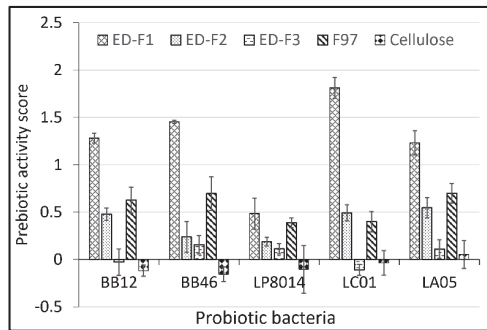
Figure 2. Prebiotic activity score of *E. denticulatum* fractions obtained through anion exchange chromatography (ED-F1, ED-F2, ED-F3) compared against commercial prebiotic Fibrulose (F97) and a negative control (Cellulose).

3.2. Selection of Factor Levels

Both ED-F1 fraction yield and HMF concentration in the extraction liquor showed a positive linear relationship affected by extraction temperature from 95 °C to 135 °C (Figure 3a) with the yield of ED-F1 fraction increased by 6.52 g/100 g at extraction temperature of 125 °C compared to 95 °C. It has been shown previously that water at subcritical level (>100 °C) has the tendency to produce hydronium ions (H_3O^+), which resulted in the rapid hydrolysis of macromolecules into smaller molecules [40]. It was observed that the increment of temperature in the hydrolysis of passion fruit peel and oat is proportionate to the gradual increase in solid loss percentage of the raw material as well as the increase in detectable smaller carbohydrates such as oligosaccharides and monosaccharides as well as acids and HMF by-products [21,40]. For optimization, a shorter temperature range from 115 °C to 135 °C was selected based on significance increase in the yield of ED-F1 fraction at temperatures 125 °C to 135 °C. The temperatures 115 °C and 135 °C were selected for the lower and upper level, respectively, to be applied in the optimization design using RSM.
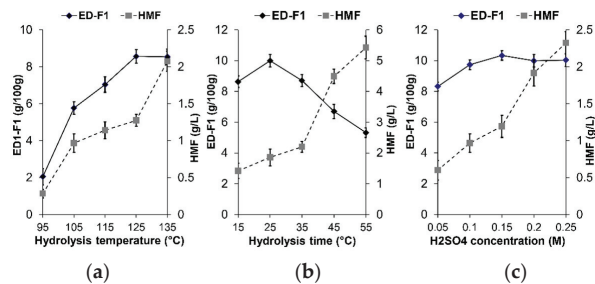
Figure 3. The yield of ED-F1 fraction and HMF by-product as affected by (**a**) hydrolysis temperature, (**b**) hydrolysis time and (**c**) H_2SO_4 concentration.

When the temperature of 125 °C was brought down for further application in varying the time of hydrolysis, the results were observed showing an inverse linear relationship between the yield of ED-F1 fraction and hydrolysis time 25 to 55 min while HMF increased gradually from 15 to 55 min. Liu et al. (2020) [41], showed that the degree of hydrolysis of fucosylated glycosaminoglycan using mild acid increase exponentially against time at temperatures below 100 °C over the span from 1 to 36 h while Sophonputtanaphoca et al. (2018) [42], reported that oligosaccharides can be produced within 30 to 60 min at temperatures between 100–121 °C. In the current study, a gradual decrease of ED-F1 yield observed at temperature 125 °C against a timespan of 35 to 55 min suggested a preferable shorter hydrolysis time. The gradual decrease of ED-F1 could be due to the hydrolysis of

the oligosaccharide components generating more HMF as shown in (Figure 3b). It is also important to note that time of hydrolysis may also be affected by the plant matrix itself made up of different glycan backbones between the current and previous studies. Time of hydrolysis at 15 min to 35 min was selected based on the observed peak increase of the ED-F1 fraction yield at 25 min.

Incrementing the H_2SO_4 concentration in the hydrolysis solvent showed an increasing trend of ED-F1 fraction yield with a plateauing trend at 0.2 M–0.25 M concentration at constant 25 min time (Figure 3c). In contrast, Wang et al. (2019) [43], demonstrated that mild sulfuric acid concentration (0.3–0.7 M) had a significantly increasing trend in the hydrolysis of press-lye waste hemicelluloses to xylo-oligosaccharides. This could be explained by the difference in the other factors used such as hydrolysis time and temperature as well as the difference in the type of carbohydrates in the raw material in the current study. It is also shown in the previous study by Sophonputtanaphoca et al. (2018), acid concentration beyond a certain range with the effect of time and temperature favours the production of monosaccharide over the oligosaccharide fraction with the oligosaccharide completely undetectable at hydrolysis using sulfuric acid concentration at 2 M for 1 h [42]. A range of 0.05 M to 0.2 M H_2SO_4 concentration was selected for the lower and upper level for optimization.

3.3. RSM Model and Analysis of Variance

RSM was used to investigate the effects of hydrolysis temperature (115–135 °C), extraction time (15 min–35 min) and H_2SO_4 concentration (0.05 M–0.2 M) on the oligosaccharides fraction ED-F1 with potential prebiotic from *E. denticulatum*. Several studies have successfully employed this method in optimizing hydrolysis parameters to obtain corncob xylooligosaccharides from a microwave-assisted hydrolysis [44], deriving glucomanno-oligosaccharides from copra meal hydrolysis [45] and enzymatic hydrolysis to obtain galacto (arabino)-oligosaccharide from potato rhamnogalacturonan [46]. ED-F1 fraction was selected to be optimized due to its significant and highest prebiotic activity score against five commercial probiotics. HMF was also measured as it is directly associated with the decomposition of hexoses under heat treatment and was known to be a potential carcinogen at high amounts.

Three hydrolysis parameters were selected as factors and the operating range were narrowed. These parameters have been shown to significantly affect ED-F1 fraction yield. The factors were assigned as hydrolysis temperature (X_1), hydrolysis time (X_2) and H_2SO_4 concentration (X_3) (Table 1). Several researchers also have emphasized these to be vital factors that highly affect low or mild acid hydrolysis procedures to obtain oligosaccharides [44,47,48]. The Box–Behnken model was selected for the design of the experiment considering the restriction of operability in the selected factor (maximum heating temperature of the autoclave). Not only does the Box–Behnken design accommodate for a minimum number of experiments, but it also efficiently allows estimating first order and second order coefficients of the model and provides supportive analysis on the interactions between the variables [49]. The three selected factors were assigned a lower, center point and upper level designated in code of −1, 0, +1, respectively, in which the central point and the experimental points are equidistant.

From the 17 experiments, a quadratic model was adjusted to the responses (ED-F1 and HMF), and the regression coefficients for the linear, quadratic, and interaction terms were calculated and statistically evaluated using ANOVA. Table 2 shows the statistical analysis of the regression coefficients of the complete polynomial models for the yield of ED1-F1 and HMF. Based on the ANOVA ($p \leq 0.05$), the linear first-order effect was significant for all factors (temperature X_1, time X_2, H_2SO_4 concentration X_3), the quadratic second-order effect was significant only for temperature and H_2SO_4 concentration for both ED-F1 yield and HMF.

Table 1. Box–Behnken experimental design layout and observed responses of oligosaccharide fraction yield (ED-F1) and HMF by-product.

Std. Order	Independent Variables [1]			Responses [2]	
	X_1 Temperature (°C)	X_2 Time (Min)	X_3 H_2SO_4 (M)	ED-F1 Yield (g/100 g)	HMF (g/L)
1	115 (−1)	15 (−1)	0.13(0)	8.58	0.67
2	135 (+1)	15 (−1)	0.13(0)	9.52	1.94
3	115 (−1)	35 (+1)	0.13(0)	9.64	1.75
4	135 (+1)	35 (+1)	0.13(0)	9.12	2.10
5	115 (−1)	25 (0)	0.05 (−1)	7.78	0.64
6	135 (+1)	25 (0)	0.05 (−1)	8.64	1.28
7	115 (−1)	25 (0)	0.2 (+1)	8.15	1.50
8	135 (+1)	25 (0)	0.2 (+1)	7.65	2.14
9	125 (0)	15 (−1)	0.05 (−1)	8.41	0.73
10	125 (0)	35 (+1)	0.05 (−1)	9.26	0.96
11	125 (0)	15(−1)	0.2 (+1)	8.55	1.26
12	125 (0)	35 (+1)	0.2 (+1)	8.77	2.10
13	125 (0)	25 (0)	0.13(0)	9.86	1.36
14	125 (0)	25 (0)	0.13 (0)	10.11	1.47
15	125 (0)	25 (0)	0.13 (0)	9.85	1.35
16	125 (0)	25 (0)	0.13 (0)	10.05	1.51
17	125 (0)	25 (0)	0.13 (0)	9.87	1.32

[1] X_1 Temperature: hydrolysis temperature; X_2 Time: hydrolysis time and X_3 H_2SO_4: sulfuric acid concentration.
[2] ED-F1: *E. denticulatum* fraction 1; HMF: 5-hydroxymethyl furfural.

Table 2. Regression coefficients for the polynomial model for oligosaccharides hydrolysis from *E. denticulatum*.

Model Parameters	Regression Coefficients [1]			
	ED-F1 Yield		HMF	
	Full Quadratic Model	Reduced Quadratic Model	Full Quadratic Model	Reduced Quadratic Model
Intercept	9.97	9.98	5.88	5.88
X_1-Temperature (°C)	−0.098 *	−0.098 *	0.72 ***	0.72 ***
X_2-Time (Min)	−0.216 ***	−0.216 ***	0.39 ***	0.39 ***
X_3-H_2SO_4 (M)	−0.121 *	−0.121 *	1.37 ***	1.37 ***
X_1X_2	−0.365 ***	−0.365 ***	0.23 **	0.23 **
X_1X_3	−0.34 ***	−0.34 ***	−0.23	-
X_2X_3	−0.158 ***	−0.158 ***	−0.0063 *	−0.0063 *
X_1^2	−0.722 *	0.722 *	0.90 **	0.90 **
X_2^2	−0.029	-	−0.043	-
X_3^2	−1.19 ***	−1.19 ***	−1.05 **	−1.05 **
Polynomial model *F* value	98.47	121.19	41.18	58.16
p value	0.0012	<0.0001	<0.0001	<0.0001
Lack of fit *F* value	0.804	0.6738	0.472	0.464
p value	0.553	0.6443	0.718	0.789
Standard deviation	0.108	0.103	0.1	0.095
R^2	0.9922	0.9918	0.9815	0.9784
Mean	9.05	9.05	1.41	1.41
Adjusted R^2	0.9821	0.9836	0.9576	0.9616
Coefficient of variation (CV)(%)	1.19	1.14	7.10	6.77
Predicted R^2	0.9452	0.9607	0.901	0.926
Adeq precision	27.522	30.3894	20.466	24.02

[1] ED-F1: *E. denticulatum* fraction 1; HMF: 5-hydroxymethyl furfural. *** $p < 0.001$, ** $p < 0.01$, * $p < 0.05$.

The effect of the interaction between any two factors (X_1, X_2 and X_3) was significant for ED-F1 yield. Similar occurrence was observed for HMF by-product except for the non-significance between interactions of X_1X_3. The insignificant coefficients were removed from the second-order polynomial model.

Thus, the reduced regression equation with the coded values was established as the following:

$$\text{ED-F1 yield (g)} = 9.97 - 0.098X_1 - 0.216X_2 - 0.121X_3 - 0.722X_1{}^2 - 1.19X_3{}^2 - 0.365X_1X_2 - 0.34X_1X_3 - 0.158X_2X_3; \quad (3)$$

$$\text{HMF by-product (g/L)} = 5.88 + 0.72X_1 + 0.39X_2 + 1.37X_3 + 0.90X_1{}^2 - 1.05X_3{}^2 + 0.23X_1X_2 - 0.0063X_2X_3; \quad (4)$$

where X_1 is hydrolysis temperature, X_2 is hydrolysis time and X_3 is H_2SO_4 concentration.

The reduced quadratic models were statistically significant with the *p*-value for both responses (ED-F1 yield and HMF) shows <0.0001, indicating the model is statistically significant at 95.0% confidence interval ($p < 0.05$). Furthermore, the aptness of the second-order polynomial model was confirmed by the insignificant lack of fit F-values ($p > 0.05$), indicating the lack of fit is not significant relative to the pure error in this experiment [50]. The regression coefficient (R^2) was well adjusted for the experimental data (ED-F1 yield adjusted $R^2 = 0.9836$, HMF adjusted $R^2 = 0.9616$) which indicates that the quality of the models was retained even after the removal of some terms. Based on the adjusted R^2 value for both models, only 1.74% and 3.94% of the total variation is not explained by both ED-F1 yield and HMF models, respectively, with the variations in the ED-F1 yield (98.36%) and HMF content (96.16%) are direct results to changes in the temperature, time and H_2SO_4 concentration. The difference between the predicted R^2 and the adjusted R^2 for both models were in reasonable agreement (less than 0.2) while the model fitting was better as R^2 value observed is closest to 1 [51]. Moreover, the lower value of CV (<5) for ED-F1 implies the low deviations between the experimental data values and the predicted data values. Models with low CV values (<10) are still considered to have good reliability and reproducibility [52]. The "Adeq Precision" which implies the signal-to-noise ratio, indicates an adequate signal (>4) for all models and can be used to navigate the design space [49,50,53].

3.4. Effects of Hydrolysis Parameters on the Yield of Oligosaccharides Fraction ED-F1 and HMF By-Products

Based on Table 1, ED-F1 yield ranged from 7.65 to 10.11 g according to the changes in the levels of extraction parameters. The lowest yield was obtained under the conditions of X_1: 135 °C, X_2: 25 min and X_3: 0.2 M H_2SO_4, while the highest yield was observed in X_1: 125 °C, X_2: 25 min and X_3: 0.13 M H_2SO_4. Time of extraction (X_2) (β: −0.216) exhibited the highest significance ($p < 0.001$) for the yield of ED-F1 as compared to both temperature (X_1) (β: −0.098) and H_2SO_4 concentration (X_3) (β: −0.121) ($p < 0.05$, respectively), while for the HMF production in the extraction liquor, all three parameters are equally significant ($p < 0.001$) with all positive values of the regression coefficients (Table 2). Positive regression coefficients imply that the increment of the parameter levels will have a direct proportion to the production of the product, vice-versa [54]. Interaction between any two parameters X_1, X_2 and X_3 are highly significant to the yield of ED-F1 ($p < 0.001$), but on the opposite, interaction of X_1-X_3 is not significant for the formation of HMF. Similar occurrence was reported by [55] in optimizing the hydrolysis conditions for xylans from beech wood and corn cob. Their results indicated that temperature and time of hydrolysis plays a pivotal factor in the conversion of hemicelluloses to oligosaccharides using the minimum concentration of sulfuric acid, thus reducing the degradation of xylose monomers to furfural by-product.

Temperature and H_2SO_4 concentration also showed a significant effect on the hydrolysis yield of ED-F1 mainly with the temperature around 120–130 °C and H_2SO_4 concentration around 0.9–1.6 M (Figure 4). Temperatures below 120 °C and higher than 130 °C showed reduction in hydrolysis yield of ED-F1 which can be confirmed by the negative quadratic

term of temperature in the reduced mathematical model. Similarly, H_2SO_4 concentration range below 0.09 M and higher than 0.16 M showed negative impact on ED-F1 yield. Subcritical temperatures beyond the boiling point of water with the addition of mild acid have been shown to efficiently reduce the hydrolysis time for a higher yield of oligosaccharide fraction. According to Wang et al. (2018), the highest yield (45.18%) of xylooligosaccharide (XOS) fraction using subcritical water with 1% (0.1 M) sulfuric acid from hemicellulose was the highest at 120 °C for 60 min [56]. Temperatures beyond 120 °C have been noted to produce more xylose monomers. This observation could be explained by the different hydrolysis rate constant of the substrate at different temperature and acid concentration that affects the scission of terminal-nonreducing bonds, interior glycosidic bonds and terminal-reducing C-O bonds; the chain length of the produced oligosaccharides and the constant have been shown to be proportionally related [57].
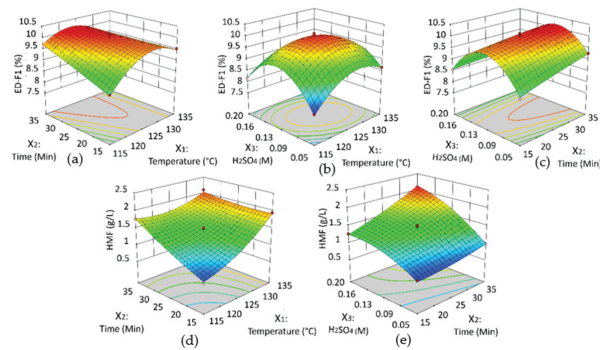
Figure 4. Three-dimensional response surface plots showing the effects of temperature, time and H_2SO_4 on ED-F1 yield (**a–c**) and HMF (**d,e**).

3.5. Validation of the Model and Optimal Extraction Condition of ED-F1 Oligosaccharide Fraction

Based on the response surfaces, the yield of ED-F1 is highly influenced by the hydrolysis parameters. Hence, it is important to get the most desirable parameter conditions to obtain the optimum ED-F1 yield. Since HMF production is directly proportional to the reduction of ED-F1, the goal is set to reduce the production of HMF in the extraction liquor. The reduced quadratic models were used to generate optimal hydrolysis conditions for ED-F1 oligosaccharide fraction yield and the values were 121 °C, 21 min and 0.12 M H_2SO_4 concentration (Table 3). The desirability value was close to 1 and calculated to be 0.844. All the hydrolysis parameters were set in range while the ED-F1 fraction yield and HMF concentration were both set at maximum and at minimum, respectively. The experimental validation of the mathematical model was performed in triplicate. The ED-F1 yield obtained through the optimization procedure was 11.15 ± 0.03 g/100 g dw. Both ED-F1 yield and HMF by-product produced values were close to the predicted by the mathematical model in optimal conditions with a low percentage of relative error (3.15% and 4.72%, respectively) reflects the adequacy of the developed quadratic models [52]. The optimization procedure increased the yield of ED-F1 by 31.41% compared to initial extraction and hydrolysis methods.

Table 3. Validation of conditions for the optimum yield of ED-F1.

Optimum Conditions [1]			Responses [2]	Desirability = 0.844		
Temperature (°C) (In range)	Time (Min) (In range)	H_2SO_4 (M) (In range)		Predicted	Actual	% Relative error
121	21	0.12	ED-F1 Yield (g/100 g) (Maximize)	10.81	11.15 ±0.03	3.15
			HMF (g/L) (Minimize)	1.06	1.11 ±0.08	4.72

[1] X_1 Temperature: hydrolysis temperature; X_2 Time: hydrolysis time and X_3 H_2SO_4: sulfuric acid concentration. [2] ED-F1: *E. denticulatum* fraction 1; HMF: 5-hydroxymethyl furfural.

3.6. Characterization of ED-F1

3.6.1. Size-Exclusion Chromatography

ED-F1 was subjected to HP-SEC to determine the homogeneity of the fraction as well as its molecular weight. Figure 5 shows a single symmetrical peak eluted at 13.84 min depicting that the sample is highly homogenous containing oligosaccharides of similar or close in terms of their molecular weight [58]. The regression equation obtained from the oligosaccharide and dextran standards was LogMW = −0.2252X + 6.1281 with a correlation coefficient (R2) of 0.9826. The average molecular weight was represented by Mw, and the elution time was represented by X. According to the equation, the average molecular weight of ED-F1 was calculated as 1.025×10^3 Da. Low molecular weight manno-oligosaccharides and galacto-oligosaccharide (<1.0 KDa) was shown to promote the growth of *Bifidobacteria* and *Lactobacilli* in an in vitro fermentation [59]. Based on the earlier study, these low molecular weight oligosaccharides are easily metabolized in a pure culture study and efficiently being converted to lactate by *Lactobacilli* species. Oligosaccharides derived from agaran and carrageenan with the molecular weight in the range of 0.4–1.4 and 1.0–7.0 KDa has also been shown to promote the beneficial gut microflora of pigs namely Ruminococcaceae, *Coprococcus*, *Roseburia*, and *Faecalibacterium* [60].
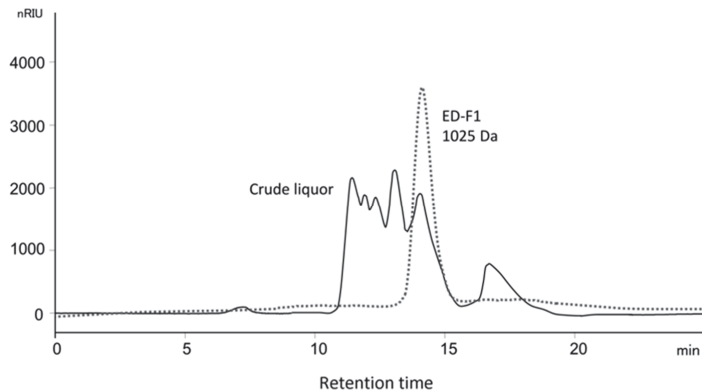
Figure 5. *E. denticulatum* ED-F1 fraction observed under size-exclusion chromatography (HP-SEC).

3.6.2. Fourier Transform Infrared Spectra Analysis

ED-F1 was subjected to FT-IR spectroscopy to determine the characteristic absorption bands and *i*-carrageenan was used as a standard. In both samples, two similar bands were observed in the 4000–2000 cm^{-1} region of the FT-IR spectra (Figure 6). The broad absorption appeared at 3200–3500 cm^{-1} represents hydrogen bonded O–H stretching vibrations while a weak signal at 2926 cm^{-1} is due to C–H stretching vibrations. The FT-IR absorption band observed around the region of 1075–1041 cm^{-1} was attributed to glycosidic linkages connecting sugar molecules and a common trait to all polysaccharides

and oligosaccharides. The band around 930 cm^{-1} were ascribed to the vibration of C–O–C bridge of 3,6-anhydrogalactose. These bands were also observed in earlier studies in both agaro-oligosaccharides from enzymatic hydrolysis of agar [61], sulfated polysaccharides extracted from red seaweeds [62]. The 3,6-anhydrogalactose polymer unit is one of the unique features that distinguished agaran and carrageenan type oligosaccharides from other common seaweed derived polymer such as alginate type oligosaccharide [63,64]. However, the 930 cm^{-1} peak is known to be absent in both *mu* and *lambda* carrageenan as the C-O-C bridge is replaced by a sulfate group RO-SO$_3$ [64].
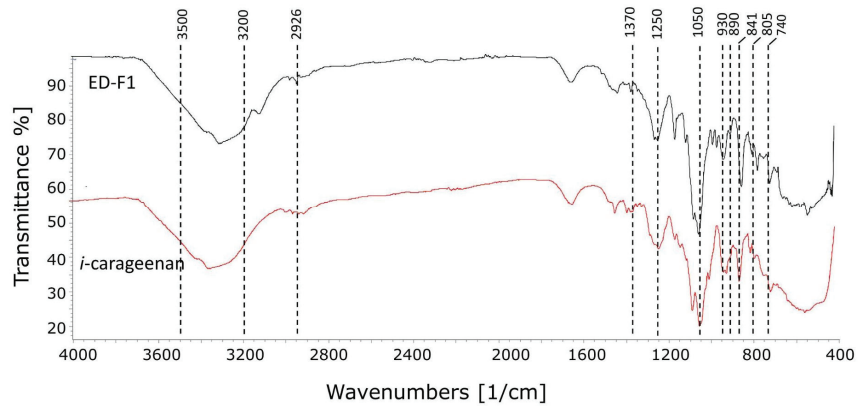
Figure 6. FT-IR spectroscopy of *E. denticulatum* ED-F1 fraction in comparison with *i*-carrageenan standard (4000–400 cm^{-1}).

Sulfation observed in ED-F1 was similar to the *i*-carrageenan standard designated at C4 of the galactose unit (841 cm^{-1}) and C2 of the 3,6-anhydrogalactose (805 cm^{-1}) [63]. A small peak near 1370 cm^{-1} also indicates the presence of sulfate groups in both samples. A broad IR peak was also observed between 1120 and 1270 cm^{-1} and is indicative of the S = O stretching vibration of sulfate groups on both sample [62]. A slightly higher intensity of 890 cm^{-1} peak was observed in ED-F1 but almost unobservable at *i*-carrageenan. This peak represents the stretching vibration of the anomeric C-H of unsulfated β-galactopyranosyl residues implying the presence of this residue in ED-F1 but very minimal in *i*-carrageenan. A previous study by [60] compared the prebiotic activity of sulfated and non-sulfated seaweed derived oligosaccharides namely alginate oligosaccharide, agaro- oligosaccharide and *k*-carrageenan oligosaccharides. Sulfated and non-sulfated oligosaccharides have been shown to have distinct effects on the gut microbiota in terms of the types of beneficial bacteria groups promoted, opportunistic pathogen population and production of different ratios of short chain fatty acids (SCFAs). Thus, the prebiotic efficacy of ED-F1 having both sulfated and non-sulfated β-galactopyranosyl residues in comparison with other either sulfated or non-sulfated marine oligosaccharides need further verification.

4. Conclusions

E. denticulatum seaweed has been shown to be a potential source of low molecular weight prebiotic oligosaccharides with the observed prebiotic activity scores of ED-F1 (against five different probiotic) that are significantly higher compared to a commercial prebiotic. Thermal hydrolysis with low acid concentration has been proven to be a suitable method to derive these prebiotic oligosaccharides from the macroalgae matrix. The temperature, time of hydrolysis and H$_2$SO$_4$ concentration significantly affected the hydrolysis of *E. denticulatum* cell matrix. Based on the regression coefficient and *p*-value of all models, time of hydrolysis (X_2) was shown to be the most significant factor in determining the yield of ED-F1 oligosaccharide fraction while the further degradation towards the production of by-product HMF was equally affected all factors. Box–Behnken design and response

surface methodology was successfully employed to optimize the hydrolysis procedure and the maximum yield of oligosaccharides ED-F1 fraction from *E. denticulatum* was derived under the following conditions: temperature 121 °C, time 21 min and 0.12 M H_2SO_4. The optimized parameter yielded 11.15 g of ED-F1 fraction per 100 g of dry seaweed material. Initial characterization of the fraction revealed a composition similar to a carrageenan type oligosaccharide. Results obtained from this study further support the possibility of utilizing an underutilized seaweed as a potential source of a functional ingredient in the food industry with a rapid hydrolysis and extraction process potentially applicable to other macroalgae species. However, further work needs to be done in order to identify individual oligosaccharide components within the fraction as well as their prebiotic efficacy in an animal model.

Author Contributions: Writing—original draft preparation, B.S.P.; conceptualization, methodology, supervision, F.Y.C.; writing—review and editing, C.K.S. and F.Y.C.; project administration and funding acquisition, F.Y.C. All authors have read and agreed to the published version of the manuscript.

Institutional Review Board Statement: Not applicable.

Informed Consent Statement: Not applicable.

Data Availability Statement: Not applicable.

Conflicts of Interest: The authors declare no conflict of interest.

References

1. FAO. *The State of World Fisheries and Aquaculture 2022. Towards Blue Transformation*; FAO: Rome, Italy. Available online: https://www.fao.org/3/cc0461en/cc0461en.pdf (accessed on 4 July 2022).
2. Chopin, T.; Tacon, A.G.J. Importance of seaweeds and extractive species in global aquaculture production. *Rev. Fish. Sci. Aquac.* **2021**, *29*, 139–148. [CrossRef]
3. Gómez-Guzmán, M.; Rodríguez-Nogales, A.; Algieri, F.; Gálvez, J. Potential role of seaweed polyphenols in cardiovascular-associated disorders. *Mar. Drugs* **2018**, *16*, 250. [CrossRef]
4. Shimoda, H. Seaweed fucoxanthin supplementation improves obesity parameters in mildlyobese Japanese subjects. *J. Funct. Food Health Dis.* **2017**, *7*, 246–262. [CrossRef]
5. Lopes-Costa, E.; Abreu, M.; Gargiulo, D.; Rocha, E.; Ramos, A.A. Anticancer effects of seaweed compounds fucoxanthin and phloroglucinol, alone and in combination with 5-fluorouracil in colon cells. *J. Toxicol. Environ. Health* **2017**, *80*, 776–787. [CrossRef] [PubMed]
6. Wu, S.; Zhang, X.; Liu, J.; Song, J.; Yu, P.; Chen, P.; Lio, Z.; Wu, M.; Tong, H. Physicochemical characterization of *Sargassum fusiforme* fucoidan fractions and their antagonistic effect against P-selectin-mediated cell adhesion. *Int. J. Biol. Macromol.* **2019**, *15*, 656–662. [CrossRef] [PubMed]
7. Charoensiddhi, S.; Abraham, R.E.; Su, P.; Zhang, W. Chapter four-seaweed and seaweed-derived metabolites as prebiotics. In *Advances in Food and Nutrition Research*; Toldrá, F., Ed.; Academic Press: Cambridge, MA, USA, 2020; pp. 97–156. [CrossRef]
8. Cherry, P.; Yadav, S.; Strain, C.R.; Allsopp, P.J.; McSorley, E.M.; Ross, P.; Stanton, C. Prebiotics from seaweeds: An ocean of opportunity? *Mar. Drugs* **2019**, *17*, 327. [CrossRef] [PubMed]
9. Porse, H.; Rudolph, B. The seaweed hydrocolloid industry: 2016 updates, requirements, and outlook. *J. Appl. Phycol.* **2017**, *29*, 2187–2200. [CrossRef]
10. Zhu, B.; Ni, F.; Xiong, Q.; Yao, Z. Marine oligosaccharides originated from seaweeds: Source, preparation, structure, physiological activity and applications. *Crit. Rev. Food Sci. Nutr.* **2020**, *61*, 60–74. [CrossRef]
11. Seong, H.; Bae, J.-H.; Seo, J.S.; Kim, S.-A.; Kim, T.-J.; Han, N.S. Comparative analysis of prebiotic effects of seaweed polysaccharides laminaran, porphyran, and ulvan using in vitro human fecal fermentation. *J. Funct. Foods* **2019**, *57*, 408–416. [CrossRef]
12. Antonio, M.S.; Andrea, S.; Nunziacarla, S.; Valbona, A.; Marilena, S.; Gioele, C. Gracilaria gracilis, source of agar: A short review. *Curr. Org. Chem.* **2017**, *21*, 380–386.
13. Bajury, D.M.; Rawi, M.H.; Sazali, I.H.; Abdullah, A.; Sarbini, S.R. Prebiotic evaluation of red seaweed (*Kappaphycus alvarezii*) using in vitro colon model. *Int. J. Food Sci. Nutr.* **2017**, *68*, 821–828. [CrossRef]
14. Chen, X.; Sun, Y.; Hu, L.; Liu, S.; Yu, H.; Xing, R.; Li, P. In vitro prebiotic effects of seaweed polysaccharides. *J. Oceanol. Limnol.* **2018**, *36*, 926–932. [CrossRef]

15. Yang, C.; Lai, S.; Chen, Y.; Liu, D.; Liu, B.; Ai, C.; Wan, X.; Gao, L.; Chen, X.; Zhao, C. Anti-diabetic effect of oligosaccharides from seaweed *Sargassum confusum* via JNK-IRS1/PI3K signalling pathways and regulation of gut microbiota. *Food Chem. Toxicol.* **2019**, *131*, 110562. [CrossRef] [PubMed]

16. Zhang, X.; Aweya, J.J.; Huang, Z.-X.; Kang, Z.-Y.; Bai, Z.-H.; Li, K.-H.; He, X.-T.; Liu, Y.; Chen, X.-Q.; Cheong, K.-L. In vitro fermentation of *Gracilaria lemaneiformis* sulfated polysaccharides and its agaro-oligosaccharides by human fecal inocula and its impact on microbiota. *Carbohydr. Polym.* **2020**, *234*, 115894. [CrossRef] [PubMed]

17. Trincone, A. Short bioactive marine oligosaccharides: Diving into recent literature. *Curr. Biotechnol.* **2015**, *4*, 212–222. [CrossRef]

18. Klinchongkon, K.; Khuwijitjaru, P.; Wiboonsirikul, J.; Adachi, S. Extraction of oligosaccharides from passion fruit peel by subcritical water treatment. *J. Food Process Eng.* **2017**, *40*, e12269. [CrossRef]

19. You, Y.; Zhang, X.; Li, P.; Lei, F.; Jiang, J. Co-production of xylooligosaccharides and activated carbons from Camellia oleifera shell treated by the catalysis and activation of zinc chloride. *Bioresour. Technol.* **2020**, *306*, 123131. [CrossRef]

20. Chen, Z.; Shen, N.; Wu, X.; Jia, J.; Wu, Y.; Chiba, H.; Hui, S. Extraction and quantitation of phytosterols from edible brown seaweeds: Optimization, validation, and application. *Foods* **2023**, *12*, 244. [CrossRef]

21. Hosni, S.; Gani, S.S.A.; Orsat, V.; Hassan, M.; Abdullah, S. Ultrasound-assisted extraction of antioxidants from *Melastoma malabathricum* Linn, modeling and optimization using Box–Behnken design. *Molecules* **2022**, *28*, 487. [CrossRef]

22. Zou, X.-G.; Chi, Y.; Cao, Y.-Q.; Zheng, M.; Deng, Z.-Y.; Cai, M.; Yang, K.; Sun, P.-L. Preparation process optimization of peptides from *Agaricus blazei* Murrill, and comparison of their antioxidant and immune enhancing activities separated by ultrafiltration membrane technology. *Foods* **2023**, *12*, 251. [CrossRef]

23. Meinita, M.D.; Hong, Y.K.; Jeong, G.T. Comparison of sulfuric and hydrochloric acids as catalysts in hydrolysis of *Kappaphycus alvarezii* (cottonii). *Bioprocess Biosyst. Eng.* **2011**, *35*, 123–128. [CrossRef]

24. Jiang, X.; Zhang, Z.; Chen, Y.; Zhenteng Cui, Z.; Liangen Shi, L. Structural elucidation and in vitro antitumor activity of a novel oligosaccharide from Bombyx batryticatus. *Carbohydr. Polym.* **2014**, *103*, 434–441. [CrossRef] [PubMed]

25. Masuko, T.; Minami, A.; Iwasaki, N.; Majima, T.; Nishimura, S.; Lee, Y.C. Carbohydrate analysis by a phenol–sulfuric acid method in microplate format. *Anal. Biochem.* **2005**, *339*, 69–72. [CrossRef] [PubMed]

26. Moniz, P.; Ho, A.L.; Duarte, L.C.; Kolida, S.; Rastall, R.A.; Pereira, H.; Carvalheiro, F. Assessment of the bifidogenic effect of substituted xylo-oligosaccharides obtained from corn straw. *Carbohydr. Polym.* **2016**, *136*, 466–473. [CrossRef]

27. Huebner, J.; Wehling, R.L.; Hutkins, R.W. Functional activity of commercial prebiotics. *Int. Dairy J.* **2007**, *17*, 770–775. [CrossRef]

28. De Andrade, J.K.; Komatsu, E.; Perreault, H.; Torres, Y.R.; Da Rosa, M.R.; Felsner, M.L. In house validation from direct determination of 5-hydroxymethyl-2-furfural (HMF) in Brazilian corn and cane syrups samples by HPLC–UV. *Food Chem.* **2016**, *190*, 481–486. [CrossRef] [PubMed]

29. Altemimi, A.B.; Mohammed, M.J.; Yi-Chen, L.; Watson, D.G.; Lakhssassi, N.; Cacciola, F.; Ibrahim, S.A. Optimization of ultrasonicated kaempferol extraction from *Ocimum basilicum* using a box–Behnken design and its densitometric validation. *Foods* **2020**, *9*, 1379. [CrossRef]

30. Sellimi, S.; Younes, I.; Ayed, H.B.; Maalej, H.; Montero, V.; Rinaudo, M.; Dahia, M.; Mechichi, T.; Hajji, M.; Nasri, M. Structural, physicochemical and antioxidant properties of sodium alginate isolated from a Tunisian brown seaweed. *Int. J. Biol. Macromol.* **2015**, *72*, 1358–1367. [CrossRef]

31. Silchenko, A.S.; Rasin, A.B.; Kusaykin, M.I.; Kalinovsky, A.I.; Miansong, Z.; Changheng, L.; Malyarenko, O.; Zueva, A.O.; Zvyagintseva, T.N.; Ermakova, S.P. Structure, enzymatic transformation, anticancer activity of fucoidan and sulphated fucooligosaccharides from *Sargassum horneri*. *Carbohydr. Polym.* **2017**, *175*, 654–660. [CrossRef]

32. Fournière, M.; Latire, T.; Lang, M.; Terme, N.; Bourgougnon, N.; Bedoux, G. Production of active poly- and oligosaccharidic fractions from *Ulva sp.* by combining enzyme-assisted extraction (eae) and depolymerization. *Metabolites* **2019**, *9*, 182. [CrossRef] [PubMed]

33. Duong-Ly, K.C.; Gabelli, S.B. Salting out of proteins using ammonium sulfate precipitation. *Methods Enzymol.* **2014**, *541*, 85–94.

34. Cosenza, V.A.; Navarro, D.A.; Stortz, C.A.; Ana, M.; Rojas, A.M. Rheology of partially and totally oxidized red seaweed galactans. *Carbohydr. Polym.* **2020**, *230*, 115653. [CrossRef] [PubMed]

35. Zhang, S.; Hu, H.; Wang, L.; Liu, F.; Pan, S. Preparation and prebiotic potential of pectin oligosaccharides obtained from citrus peel pectin. *Food Chem.* **2018**, *244*, 232–237. [CrossRef] [PubMed]

36. Praveen, M.; Karthika Parvathy, K.R.; Jayabalan, R.; Balasubramanian, P. Dietary fiber from Indian edible seaweeds and its in-vitro prebiotic effect on the gut microbiota. *Food Hydrocoll.* **2019**, *96*, 343–353. [CrossRef]

37. Fuhren, J.; Schwalbe, M.; Peralta-Marzal, L.; Rosch, C.; Schols, H.A.; Kleerebezem, W. Phenotypic and genetic characterization of differential galacto-oligosaccharide utilization in *Lactobacillus plantarum*. *Sci. Rep.* **2020**, *10*, 21657. [CrossRef]

38. Singh, B.P.; Vij, S. α-Galactosidase activity and oligosaccharides reduction pattern of indigenous lactobacilli during fermentation of soy milk. *Food Biosci.* **2018**, *22*, 32–37. [CrossRef]

39. Zúñiga, M.; Yebra, M.J.; Monedero, V. Complex oligosaccharide utilization pathways in lactobacillus. *Curr. Issues Mol. Biol.* **2021**, *40*, 49–80. [CrossRef]

40. Yoo, H.-U.; Ko, M.-J.; Chung, M.-S. Hydrolysis of beta-glucan in oat flour during subcritical-water extraction. *Food Chem.* **2020**, *308*, 125670. [CrossRef]

41. Liu, X.; Zhang, Z.; Mao, H.; Wang, P.; Zuo, Z.; Gao, L.; Shi, X.; Yin, R.; Gao, N.; Zhao, J. Characterization of the hydrolysis kinetics of fucosylated glycosaminoglycan in mild acid and structures of the resulting oligosaccharides. *Mar. Drugs* **2020**, *18*, 286. [CrossRef]
42. Sophonputtanaphoca, S.; Pridam, C.; Chinnak, J.; Nathong, M.; Juntipwong, P. Production of non-digestible oligosaccharides as value-added by-products from rice straw. *Agric. Nat. Resour.* **2018**, *52*, 169–175. [CrossRef]
43. Wang, T.; Li, C.; Song, M.; Fan, R. Xylo-oligosaccharides preparation through acid hydrolysis of hemicelluloses isolated from press-lye. *Grain Oil Sci. Technol.* **2019**, *2*, 73–77. [CrossRef]
44. Lin, Q.; Li, H.; Ren, J.; Deng, A.; Li, W.; Liu, C.; Sun, R. Production of xylooligosaccharides by microwave-induced, organic acid-catalyzed hydrolysis of different xylan-type hemicelluloses: Optimization by response surface methodology. *Carbohydr. Polym.* **2017**, *157*, 214–225. [CrossRef] [PubMed]
45. Rungruangsaphakun, J.; Keawsompong, S. Optimization of hydrolysis conditions for the mannooligosaccharides copra meal hydrolysate production. *3 Biotech* **2018**, *8*, 169. [CrossRef]
46. Khodaei, N.; Karboune, S. Optimization of enzymatic production of prebiotic galacto/galacto(arabino)-oligosaccharides and oligomers from potato rhamnogalacturonan I. *Carbohydr. Polym.* **2018**, *181*, 1153–1159. [CrossRef]
47. Xu, Y.; Shen, M.; Chen, Y.; Lou, Y.; Luo, R.; Chen, J.; Zhang, Y.; Li, J.; Wang, W. Optimization of the polysaccharide hydrolysate from *Auricularia auricula* with antioxidant activity by response surface methodology. *Int. J. Biol. Macromol.* **2018**, *113*, 543–549. [CrossRef] [PubMed]
48. Yang, C.; Hu, C.; Zhang, H.; Chen, W.; Deng, Q.; Tang, H.; Huang, F. Optimation for preparation of oligosaccharides from flaxseed gum and evaluation of antioxidant and antitumor activities in vitro. *Int. J. Biol. Macromol.* **2020**, *153*, 1107–1116. [CrossRef] [PubMed]
49. Danish, M.; Khanday, W.A.; Hashim, R.; Sulaiman, N.S.B.; Akhtar, M.N.; Nizami, M. Application of optimized large surface area date stone (*Phoenix dactylifera*) activated carbon for rhodamin B removal from aqueous solution: Box-Behnken design approach. *Ecotoxicol. Environ. Saf.* **2017**, *139*, 280–290. [CrossRef]
50. Manmai, N.; Unpaprom, Y.; Ramaraj, R. Bioethanol production from sunflower stalk: Application of chemical and biological pretreatments by response surface methodology (RSM). *Biomass Convers. Biorefin.* **2021**, *11*, 1759–1773. [CrossRef]
51. Savic-Gajic, I.M.; Savic, I.M.; Nikolic, V.D. Modelling and optimization of quercetin extraction and biological activity of quercetin-rich red onion skin extract from Southeastern Serbia. *J. Food Nutr. Res.* **2018**, *57*, 15–26.
52. Fawzy, M.A.; Gomaa, M. Optimization of citric acid treatment for the sequential extraction of fucoidan and alginate from *Sargassum latifolium* and their potential antioxidant and Fe(III) chelation properties. *J. Appl. Phycol.* **2021**, *33*, 2523–2535. [CrossRef]
53. Guo, Z.; Zhao, B.; Li, H.; Miao, S.; Zheng, B. Optimization of ultrasound-microwave synergistic extraction of prebiotic oligosaccharides from sweet potatoes (*Ipomoea batatas* L.). *Innov. Food Sci. Emerg. Technol.* **2019**, *54*, 51–63. [CrossRef]
54. Prasad, S.; Malav, M.K.; Kumar, S.; Singh, A.; Pant, D.; Radhakrishnan, S. Enhancement of bio-ethanol production potential of wheat straw by reducing furfural and 5-hydroxymethylfurfural (HMF). *Bioresour. Technol. Rep.* **2018**, *4*, 50–56. [CrossRef]
55. Beckendorff, A.; Lamp, A.; Kaltschmitt, M. Optimization of hydrolysis conditions for xylans and straw hydrolysates by HPLC analysis. *Biomass Convers. Biorefin.* **2021**. [CrossRef]
56. Wang, Y.; Cao, X.; Zhang, R.; Xiao, L.; Yuan, T.; Shi, Q.; Sun, R. Evaluation of xylooligosaccharide production from residual hemicelluloses of dissolving pulp by acid and enzymatic hydrolysis. *RSC Adv.* **2018**, *8*, 35211–35217. [CrossRef] [PubMed]
57. Ebikade, E.; Lym, J.; Wittreich, G.; Saha, B.; Vlachos, D.G. Kinetic studies of acid hydrolysis of food waste-derived saccharides. *Ind. Eng. Chem. Res.* **2018**, *57*, 17365–17374. [CrossRef]
58. He, B.-L.; Zheng, Q.-W.; Guo, L.-Q.; Huang, J.-Y.; Yun, F.; Huang, S.-S.; Lin, J.-F. Structural characterization and immune-enhancing activity of a novel high-molecular-weight polysaccharide from *Cordyceps militaris*. *Int. J. Biol. Macromol.* **2020**, *145*, 11–20. [CrossRef] [PubMed]
59. Wei, X.; Fu, X.; Xioa, M.; Liu, Z.; Zhang, L.; Mou, H. Dietary galactosyl and mannosyl carbohydrates: In-vitro assessment of prebiotic effects. *Food Chem.* **2020**, *329*, 127179. [CrossRef]
60. Han, Z.-L.; Yang, M.; Fu, X.-D.; Chen, M.; Su, Q.; Zhao, Y.-H.; Mou, H.-J. Evaluation of prebiotic potential of three marine algae oligosaccharides from enzymatic hydrolysis. *Mar. Drugs* **2019**, *17*, 173. [CrossRef] [PubMed]
61. Kang, O.L.; Yong, P.F.; Ma'aruf, A.G.; Osman, H.; Nazaruddin, R. Physicochemical and antioxidant studies on oven-dried, freeze-dried and spray-dried agaro-oligosaccharide powders. *Int. Food Res. J.* **2014**, *21*, 2363–2367.
62. Fernando, I.; Sanjeewa, K.; Samarakoon, K.W.; Lee, W.W.; Kim, H.S.; Kang, N.; Ranasinghe, P.; Lee, H.S.; Jeon, Y.J. A fucoidan fraction purified from *Chnoospora minima*; a potential inhibitor of LPS-induced inflammatory responses. *Int. J. Biol. Macromol.* **2017**, *104*, 1185–1193. [CrossRef] [PubMed]
63. Duan, F.; Yu, Y.; Liu, Z.; Tian, L.; Mou, H. An effective method for the preparation of carrageenan oligosaccharides directly from Eucheuma cottonii using cellulase and recombinant κ-carrageenase. *Algal Res.* **2016**, *1*, 93–99. [CrossRef]
64. Pereira, G.A.; Arruda, H.S.; Molina, G.; Pastore, G.M. Extraction optimization and profile analysis of oligosaccharides in banana pulp and peel. *J. Food Process Preserv.* **2017**, *42*, e13408. [CrossRef]

Article

Effects of Metal Concentration, pH, and Temperature on the Chlorophyll Derivative Content, Green Colour, and Antioxidant Activity of Amaranth (*Amaranthus viridis*) Purees

Siti Faridah Mohd Amin [1,2], Roselina Karim [2], Yus Aniza Yusof [3] and Kharidah Muhammad [2,*]

[1] Faculty of Food Science and Nutrition, Universiti Malaysia Sabah, Jalan UMS, Kota Kinabalu 88400, Sabah, Malaysia

[2] Faculty of Food Science and Technology, Universiti Putra Malaysia, UPM Serdang, Serdang 43400, Selangor, Malaysia

[3] Faculty of Engineering, Universiti Putra Malaysia, UPM Serdang, Serdang 43400, Selangor, Malaysia

* Correspondence: kharidah@upm.edu.my

Abstract: The thermal process of green amaranth leads to the partial or complete degradation of chlorophyll pigments and loss of green colour due to the formation of chlorophyll derivatives. This study aimed to evaluate a stabilisation process utilising metal ions to obtain a stable green colour of metal-chlorophyll derivative complexes. In this study, the effects of $CuSO_4$ (0–240 ppm), $ZnCl_2$ (0–1800 ppm) ions, pH (4–9), and temperature (60–100 °C) on green amaranth purees with a constant time of 15 min were investigated. In tapered leaf amaranths, the sample depicted higher contents of chlorophyll *a* (0.33 mg/g), chlorophyll *b* (0.34 mg/g), and total chlorophyll (0.68 mg/g) than round leaf amaranths (chlorophyll *a* = 0.28 mg/g, chlorophyll *b* = 0.29 mg/g, and total chlorophyll = 0.58 mg/g). A higher chlorophyll derivative content (0.62 mg/g), DPPH scavenging activity (93 mM TE/g), and FRAP value (54 mM TE/g) of Cu-amaranth purees were successfully achieved using 210 ppm of $CuSO_4$ after heating at pH 6 and 80 °C. Zn-amaranth purees were produced using 1500 ppm of $ZnCl_2$ at pH 8 and 90 °C for 15 min with chlorophyll derivative content of 0.39 mg/g, DPPH scavenging activity of 79 mM TE/g, and FRAP value of 57 mM TE/g. In HPLC chromatograms, two major peaks were identified as chlorophylls *a* and *b* in fresh amaranths. Nevertheless, these two peaks disappeared in Cu- and Zn-amaranth purees, presumably due to the formation of metallo-chlorophyll derivatives.

Keywords: chlorophylls; green colour; antioxidant activity; amaranth; metal ions

1. Introduction

The amaranth plant species belong to the genus Amaranthus and the family of Amaranthaceae [1]. Additionally, the genus Amaranthus comprises 60 to 70 species with over 400 varieties in temperate and tropical climates [2]. Three species are typically grown for their edible grains, while 17 species are planted for their edible leaves, such as *A. blitum*, *A. cruentus*, *A. dubius*, *A. tricolor*, and *A. viridis* [3]. Only three species of amaranths are discovered in Malaysia, which are "bayam itik" (*A. blitum*), "bayam putih" (*A. paniculatus*), and "bayam panjang" or "bayam hijau" (*A. viridis*). Nonetheless, these species are abundantly available in the market with round or tapered leaf characteristics [4].

The green amaranth (*Amaranthus viridis* L.) is an excellent source of phytochemicals, which include chlorophylls. Moreover, green amaranths are the least expensive vegetable compared to other local leafy vegetables, such as kale, mustard green, celery, pak choy, and cabbage. Amaranths have been reported to produce 1504 mg/kg of total chlorophyll as they are significantly higher in magnesium (Mg), calcium (Ca), potassium (K), copper (Cu), phosphorus (P), zinc (Zn), iron (Fe), and manganese (Mn) [5,6]. In addition, chlorophylls typically produce a natural green colour while exhibiting high antioxidant activity,

and anti-inflammatory, anti-carcinogenic, anti-bacterial, and wound healing characteristics [7,8]. There are two primary forms of chlorophylls in plants consisting of chlorophyll *a* (blue-green) and chlorophyll *b* (yellow-green), which contain a methyl or formyl group, respectively.

Although green vegetables demonstrate excellent benefits, the chlorophyll pigments are unstable during extraction and thermal processing. The instability occurs in unfavourable temperatures and pH, contact with oxygen, and exposure to light [9,10]. In Malaysia, green amaranth is consumed directly, or its puree is incorporated into food products. However, this may involve some handling delay, which can be detrimental to its colour and chlorophyll content. Amaranth puree rapidly turns brown after thermal processing but remains green at chilling and frozen temperatures.

Nevertheless, its colour degrades on thawing. According to Schwartz et al., temperature and pH are the most critical factors affecting the stability of chlorophylls [11]. The authors reported that chlorophylls *a* and *b* could convert to magnesium ions (Mg^{2+})-free derivatives at pH less than 7 and 60 °C or higher temperatures. Furthermore, the converted products of the conversion process include pheophytin, pheophorbide, pyropheophytin, and pyropheophorbide [12]. Consequently, the conversion process reduced green colour intensity and antioxidant activity.

A study by Erge et al. indicated that the visual green colour loss in green peas occurred at a temperature range of approximately 70 to 100 °C [13]. Furthermore, the study observed that chlorophyll *a* degraded about 12 to 18 times more than chlorophyll *b*. Additionally, Edelenbos et al. reported that cooking green peas (*Pisum sativum*) in water for three minutes increased the amount of pheophytins *a* and *b* while decreasing the contents of chlorophylls *a* and *b* [14].

The formation of stable chlorophyll molecules in green amaranths can be produced to overcome these drawbacks by substituting divalent cations, such as Zn or Cu, in the porphyrin ring of Mg-free chlorophyll derivatives [15]. The stabilising process can form metallo-chlorophyll derivatives, similar in colour to chlorophylls. Furthermore, these metallo-chlorophyll derivatives are more stable and thermally resistant when compared to Mg-chlorophylls in low-pH foods [15–17]. The stabilisation process of chlorophyll derivatives using metal ions, such as Zn and Cu was also reported to improve the colour of pears, avocados, pandans, pennyworts, peas, and grapes [18–24].

A study by Senklang et al. reported the reaction process of fresh leaves with 300 mg/L of $ZnCl_2$ at pH 5, 110 °C, and a reaction time of 15 min [25]. The study leads to the formation of Zn-chlorophyll derivatives in pandan leaves, such as Zn-pheophytin and Zn-pyropheophytin. Similar to native chlorophylls, these derivatives are green in colour but more stable to acid and heat while functioning as antioxidants [26]. Meanwhile, Guzmán et al. proved that the heating process of avocado purees added with Cu or Zn produced a higher puree colour than non-treated samples at approximately 87 to 89 °C [19]. The results agreed with those reported by Canjura et al. and Salama et al., in which the colour stability of Zn- and Cu-based chlorophylls in vegetables was improved by temperature values higher than 85 °C [22,27]. Rahayuningsih et al. [28] reported that the optimum stabilisation conditions of suji leaves (*Pleomele Angustifolia* Roxb.) were obtained using 700 mg/L of $ZnCl_2$. The study was performed at pH 7, at a temperature of 85 °C, and with a total chlorophyll content of 47.29 mg/100 g fresh weight.

In Cu and Zn complexes, they are known not to be absorbed by the body and are removed as excretion products. Hence, these complexes are safe and permitted to be utilised in most countries as food additives. Nevertheless, the Food and Drug Administration (FDA) regulation limits that only 75 mg/L of Zn can remain in the final product, while the concentration of free ionisable Cu must be kept below 200 mg/L [17,29,30]. Furthermore, these metal ions, such as Cu, Zn, Mg, Ca, and Fe, play an important role in biological and biomedical processes [31]. A study by de Vogel et al. and Ferruzzi et al. discovered that in vitro anti-mutagenic activity of natural chlorophylls and commercial-grade derivatives, such as sodium copper chlorophyllin (SCC) was associated with a decreased risk of colon

cancer and numerous dietary and environmental mutagens [12,32]. Gomes et al. [33] further proved that SCC has been utilised in several countries as a food colourant and nutritional supplement without adverse effects for over 50 years. Moreover, SCC is promoted for its anti-bacterial and anti-viral properties [34,35].

Another study by Ferruzzi et al. [16] discovered substantially higher antioxidant capacities of metallo-chlorophyll derivatives (such as Cu-pheophytin a, Cu-chlorophyllin, Zn-pheophytin, and Zn-pyropheophytin) than natural chlorophylls and Mg-free derivatives. Other researchers also reported similar results on the antioxidant activities of metal ions containing chlorophylls, such as Cu-pheophytin, Cu-chlorophyllin, Zn-pheophytin, Zn-pyropheophytin, and Mg-chlorophyll [36–38].

Although the method of stabilising chlorophylls has been successfully employed with several vegetables, there is still a lack of information on the use of Zn and Cu to stabilise the chlorophylls in green amaranth purees. Thus, this research aims to investigate the stabilisation process of chlorophylls in amaranth purees, which includes the effect of various metal concentrations, pH, and temperatures. Furthermore, the obtained results were further utilised to evaluate the colour intensities, chlorophylls and their derivative contents, and antioxidant activities of the metal-stabilised amaranth purees. The research suggests that stabilization of green amaranth with different metal ions and conditions has the potential to preserve the green colour and antioxidant activity of amaranth for further use in food processing.

2. Materials and Methods

2.1. Materials

Fresh green amaranths (tapered and round leaves) were purchased from a local market in Kuala Lumpur, Malaysia, and were processed immediately.

2.2. Chemicals

The 2,2-Diphenyl-1-picrylhydrazyl (DPPH), methanol, 2,4,6-Tripyridyl-s-Triazine (TPTZ), $ZnCl_2$, $CuSO_4$, and acetone chemicals were purchased from Sigma Chemical Co. (St. Louis, MO, USA). Additionally, the chlorophyll *a* (MW = 893.5 g/mol) and chlorophyll *b* (MW = 907.5 g/mol) standards (HPLC grade) were purchased from Sigma Co. (St Louis, MO, USA). All other chemicals used in this study were either HPLC or analytical grades and purchased from Merck (Darmstadt, Germany).

2.3. Stabilisation of Amaranth Purees

The single-factor experiments were used for the stabilisation process of chlorophylls in green amaranths (*A. viridis*). A total of three factors were studied, which are different metal concentrations ($CuSO_4$ and $ZnCl_2$), pH, and temperature. Three responses were selected, which are colour value (priority), chlorophyll derivative content, and antioxidant activity (free radical DPPH) with ferric reducing antioxidant power (FRAP) assay. The steps involved in the stabilisation process of chlorophylls are further explained.

In Step 1, the stabilisation process of chlorophylls in green amaranths was performed according to Siti Faridah Mohd Amin et al. and Senklang et al. with slight modifications [25,39]. In brief, fresh amaranths were washed, drained, chopped, and the roots were discarded. The cleaned amaranth leaves with stalks were blended in a Waring blender for 5 min at high speed to obtain amaranth puree. The purees were then divided and mixed with varying concentrations of $CuSO_4$ (0, 30, 60, 90, 120, 150, 180, 210, and 240 ppm) or $ZnCl_2$ (0, 300, 600, 900, 1200, 1500, and 1800 ppm). Subsequently, the amaranth purees were kept constant at pH 6 (adjusted using citric acid or NaOH) before being incubated at a constant temperature of 80 °C for 15 min. The optimum values of $CuSO_4$ and $ZnCl_2$ concentrations were selected based on the purees with the highest green colour, chlorophyll derivative content, and antioxidant activity.

In Step 2, the chlorophylls in the green amaranth were stabilised using the optimum concentrations of $CuSO_4$ and $ZnCl_2$ obtained from Step 1. In addition, the chlorophyll

stabilisation process was carried out at a pH range of approximately 4 to 9 at a constant temperature of 80 °C for a reaction time of 15 min. The optimum stabilisation pH value was selected based on the purees with the highest green colour, chlorophyll derivative content, and antioxidant activity.

In Step 3, the stabilisation process was performed at various temperatures (60 to 100 °C) using the optimum values of $CuSO_4$ and $ZnCl_2$ concentrations obtained from Step 1, and the optimum pH as determined in Step 2. Similarly, the optimum temperature was also chosen based on the purees with the highest green colour, chlorophyll derivative content, and antioxidant activity.

2.4. Physicochemical Properties

2.4.1. Determination of Colour

The colour parameters of the purees were determined using a Hunter Lab Ultra-Scan Colorimeter (Sphere Spectrocolorimeter, Hunter Association Inc., Reston, VA, USA) in the reflectance mode and with illuminant D65 to measure a* (+a* = red, −a* = green) and b* (+b* = yellow, −b* = blue). The −a*/b* ratio was used as an index of apparent changes in greenness, as described by Larrauri García et al. [40]. The high negative values of a*/b* ratios indicate that the amaranth puree is greener and less yellow.

2.4.2. Extraction and Determination of Total Chlorophylls

The measurement of chlorophylls and chlorophyll derivative contents in control (fresh amaranth puree) and amaranth purees stabilised with Cu or Zn were determined according to Senklang et al. with slight modifications [25]. In brief, the extraction process of chlorophylls from the purees was performed in dim light using stoppered tubes covered with aluminium foil to reduce the photo-destruction effect on the chlorophylls. Each lot of amaranths (1 g) was ground with 100% acetone using a mortar and pestle until the residue became colourless. The content of the mortar was then transferred into a centrifuge tube and washed several times with 100% acetone. The total amount of 100% acetone used in this extraction process was 50 mL. Subsequently, the mixture was centrifuged at $3500 \times g$ for 10 min. The absorbance values of the extracted chlorophylls in the supernatant were collected at 662 and 645 nm wavelengths for chlorophyll *a* and chlorophyll *b*, respectively. The absorbance measurements were performed using 100% acetone as the reference in the UV-Vis spectrophotometer (Shimadzu, Japan). The chlorophylls *a* and *b* and total chlorophyll (mg/g fresh weight) were then calculated according to the method of Costache et al. based on Equations (1)–(3), respectively [41]. Moreover, the absorbance spectra of the acetone extract of fresh amaranths and metal-treated amaranths were recorded using a wavelength range of approximately 300 to 700 nm.

$$\text{Chlorophyll } a = 11.75A_{662} - 2.350A_{645} \tag{1}$$

$$\text{Chlorophyll } b = 18.61A_{645} - 3.960A_{662} \tag{2}$$

$$\text{Total chlorophylls} = (16.26\ A_{645} + 7.790\ A_{642}) \times \text{Dilution factor}/1000 \tag{3}$$

2.4.3. Preparation of Amaranth Puree Extracts for Antioxidant Activity Measurements

The stabilised amaranth purees were dried at 45 °C for 24 h in a convection oven (Venticell 111, MMM Group, Munich, Germany). Subsequently, the dried purees were ground to a fine powder using a Pulverisette 14-rotor mill (Fritsch, GmbH, Oberstein, Germany). The powders (0.25 g) were extracted with 10 mL of 80% methanol. The extraction process was performed in a test tube at 40 °C in a water bath with a continuous shaking process for 24 h. The tubes were then cooled to room temperature (27 ± 2 °C) and centrifuged at $3500 \times g$ for 15 min. Finally, the supernatants were placed in airtight glass vials and stored in a refrigerator until further use for antioxidant activity measurements [42].

2.4.4. Free Radical DPPH Assay Measurements

The antioxidant activity of the extracts from the stabilised purees was measured using the free radical DPPH assay through slight modifications of the spectrophotometric method by Brand-Williams [43]. In brief, a 3.9 mL aliquot of 0.1 mM methanolic DPPH solution (prepared using 80% v/v methanol) was mixed with 0.1 mL of amaranth puree extract in a test tube. The tube was vortexed for 15 s and incubated in the dark for 15 min at room temperature. Subsequently, the absorbance of the solution in the test tube was measured using a UV-Vis spectrophotometer (Shimadzu, Japan) using a wavelength of 515 nm with 80% methanol (v/v) as the reference. The Trolox solutions were used to construct the standard curves, and the results were expressed in mM of Trolox Equivalents (TE).

2.4.5. FRAP Assays for the Antioxidant Activity Study

The FRAP assays were performed according to Benzie et al. with minor modifications [44]. In brief, a FRAP reagent was prepared from sodium acetate buffer (300 mM, pH 3.6), 10 mM of 2,4,6-Tripyridyl-s-Triazine (TPTZ) solution in 40 mM HCl, and 20 mM $FeCl_3$ solutions in proportions of 10:1:1 (v/v), respectively. Furthermore, the FRAP reagent was prepared daily and warmed to 37 °C with a water bath before further use. The FRAP reagent (2.85 mL) was combined with the sample extracts (150 L), and the mixture was left for 30 min at room temperature. Subsequently, the reaction mixture absorbances were measured at a wavelength of 593 nm, and the assay measurements were carried out in triplicate. The standard curves were constructed using the Trolox solutions, and the results were presented in mM of Trolox Equivalents (TE).

2.5. Identification of Chlorophylls and Their Derivatives in Fresh, Zn-, and Cu-Amaranth Purees Using Reversed-Phase High-Performance Liquid Chromatography (HPLC)

2.5.1. Extraction of Chlorophylls and Chlorophyll Derivatives

The extraction process of the chlorophylls from fresh, Cu- and Zn-amaranth purees was conducted by following the method of Canjura et al. [45]. In brief, 34 mL of acetone was added to 5 g of the amaranth puree. The mixture was homogenised with Ultra-Turrax homogeniser (IKA Werke, Labortechnik, Staufen, Germany) for 2 min. The homogenate was then filtered under vacuum through a Whatman 42 filter paper. Subsequently, the filtrate was brought to volume with acetone in a 25 mL volumetric flask.

2.5.2. Chromatographic Separation and Identification of Chlorophylls and Chlorophyll Derivatives

The chlorophylls *a* and *b* and metallo-chlorophyll derivatives in fresh and metal-stabilised amaranth purees were separated by HPLC using an Agilent system equipped with an autosampler, column thermostat, and diode array detector (DAD). The isocratic elution was performed with the mobile phase of ethyl acetate/methanol/water (40:54:10 $v/v/v$) as described by Ngo et al. [18]. In brief, the triplicate 20 μL of fresh and metal-amaranth extracts in acetone were injected into a Zorbax Eclipse Plus C18 reverse-phase column (5 μm particle size, 4.6 mm in internal diameter × 250 mm in length) (Agilent Technologies, Santa Clara, CA, USA) and maintained at 30 °C. All extracts were handled in the dark throughout the extraction, concentration, and injection processes. Furthermore, all extracts were filtered through a 13 mm diameter and 0.45 μm nylon filter (Captiva Econofilters, Agilent Technologies) before being injected into the HPLC system. All chlorophylls and their derivatives were detected at a wavelength of 658 nm. Finally, the identification of peaks was confirmed by comparing retention times (tret) obtained from chlorophyll *a* and *b* standards.

2.5.3. Preparation of Calibration Curves for Chlorophylls *a* and *b* Determined using HPLC

Chlorophyll *a* and *b* standards were each (1 g) dissolved in 20 mL of 100% acetone to obtain 0.05 mg/mL stock solutions. Eight concentrations from 0.002 to 0.010 mg/mL in 10 mL acetone were prepared from the stock solution of each standard. Each standard

solution (20 µL) was injected into an Agilent 1200 series HPLC (Agilent, Santa Clara, CA, USA). The calibration curves were prepared by plotting the peak area against the concentration ratio. The concentrations were then calculated using the standard calibration curves of chlorophylls *a* and *b*. The chromatographic conditions employed in this measurement were as previously mentioned.

2.6. Statistical Analysis

MINITAB (version 16) statistical software was employed for one-way analysis of variance (ANOVA). Tukey's test was performed to determine the significant differences among means at the 5% level. The data were expressed as means ± standard deviations of three replicate determinations.

3. Results and Discussion

3.1. Chlorophyll Content of Amaranth Leaves

The chlorophylls *a* and *b* and the total chlorophyll content in acetone extracts were estimated and tabulated in Table 1. The highest content of chlorophylls *a* and *b* and total chlorophyll was observed from amaranths with tapered leaves than round leaves. Therefore, the amaranths with tapered leaves were selected for further analysis.

Table 1. The chlorophyll content (mg/100 g fresh weight) of green amaranth varieties.

Parameter	Amaranth with Round Leaves	Amaranth with Tapered Leaves
Chlorophyll *a*	28.90 [b] ± 1.47	33.54 [a] ± 1.77
Chlorophyll *b*	29.04 [b] ± 1.52	34.37 [a] ± 1.93
Total chlorophyll	57.94 [b] ± 2.99	67.91 [a] ± 3.66

Each value is expressed as mean ± standard deviation ($n = 3$) of triplicate analysis. [a,b] Means followed by different superscript lowercase letters indicate significant differences ($p < 0.05$) within a row by Tukey's HSD test.

3.2. Stabilisation Process of Chlorophylls

3.2.1. Effect of $CuSO_4$ and $ZnCl_2$ Concentrations

Compared to the chlorophyll content (0.30 mg/g) treated with 60 mg/L of $CuSO_4$, only 0.21 mg/g of total chlorophyll content was achieved by the 300 mg/L of $ZnCl_2$ (Figure 1). Moreover, the greenness ($-a*/b*$) of amaranth purees increased with increasing concentrations of both Cu and Zn. For Cu-amaranth purees (Figure 1a), the maximum level of greenness was reached when 210 mg/L of $CuSO_4$ was added. Additionally, no significant ($p > 0.05$) differences were observed in the greenness values when 210 to 240 mg/L of $CuSO_4$ was added. Thus, the results implied that 210 mg/L of $CuSO_4$ resulted in the complete formation of Cu-chlorophyll derivatives in the amaranth puree.

In Figure 1a, the chlorophyll derivative contents of the Cu-amaranth purees increased with increasing metal concentrations. Furthermore, no significant ($p > 0.05$) differences were depicted at 180, 210, and 240 mg/L of $CuSO_4$. Therefore, stabilization at 210 mg/L of $CuSO_4$ was chosen due to its highest greenness value and chlorophyll derivative contents (0.46 mg/g FW). For Zn-amaranth purees (Figure 1b), no significant ($p > 0.05$) differences were observed when the a*/b* value reached its maximum from 1200 to 1800 mg/L of $ZnCl_2$. Meanwhile, chlorophyll derivatives content was significantly highest (0.27 mg/g fresh weight) in Zn-amaranth puree treated with 1500 mg/L of $ZnCl_2$. Hence, 1500 mg/L of $ZnCl_2$ concentration was selected for subsequent experiments. The Zn concentration obtained in this study was close to the finding of Ngo et al., which retained the green colour of pears using 1300 mg/L of Zn ions [18]. In this study, the $ZnCl_2$ concentrations were higher than $CuSO_4$ concentrations. Hence, the higher $ZnCl_2$ concentrations were due to Zn salts being less reactive than Cu salts [22,25]. In addition, the formation of Zn complexes with chlorophyll derivatives occurred much slower than Cu complexes [46]; therefore, more Zn ions are required to form metallo-chlorophyll complexes in amaranth purees.

Figure 1a,b, demonstrate that the green pigments of the control purees (0 mg/L of Cu or Zn and heated at 80 °C for 15 min) have mostly degraded. Both control purees turned

brownish with a*/b* values of −0.05 and −0.04, respectively; therefore, the colour changes could be due to the formation of chlorophyll degradation compounds, which changed from bright green to brownish [47,48]. In addition, the chlorophyll degradation compounds are Mg-free derivatives, while the control puree had only 0.19 mg/g of total chlorophyll derivative content [49]. Previous studies reported that the formation of metallo-chlorophyll complexes depends on the metal and pigment concentrations, pH [50], temperature [51], and duration of contact between the metal solution and vegetable tissues [22]. Thus, Cu and Zn were used for subsequent studies with concentrations of 210 mg/L and 1500 mg/L, respectively.
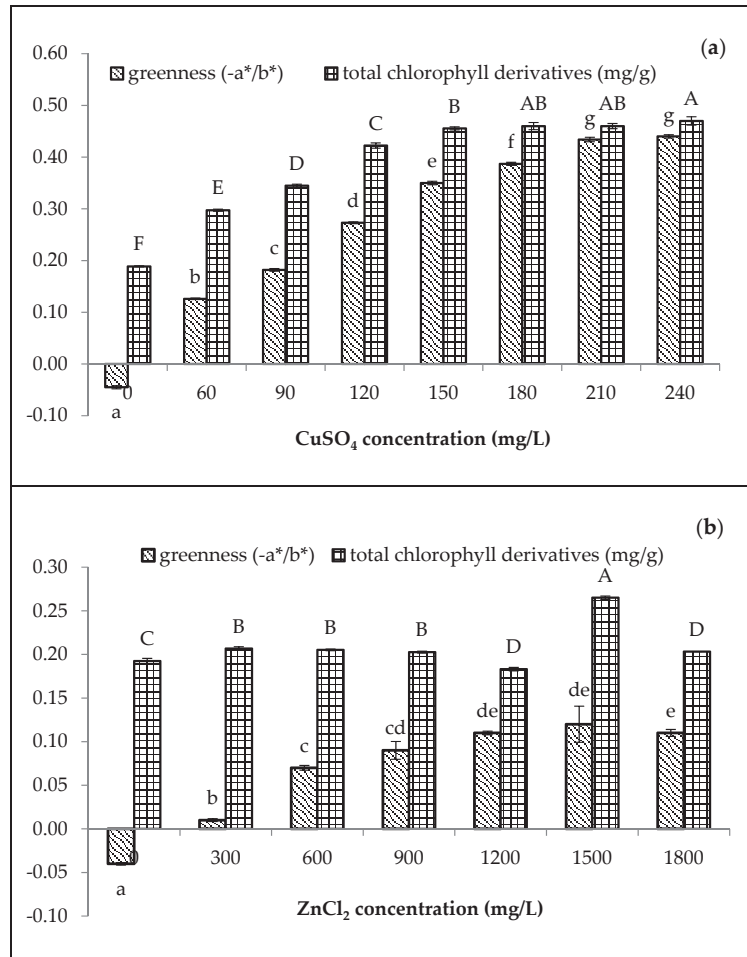
Figure 1. Effect of metal (**a**) CuSO$_4$ and (**b**) ZnCl$_2$ concentrations on greenness (−a*/b*) and total chlorophyll derivative content (mg/g) of amaranth purees. The study was performed at pH 6 after heating at 80 °C for 15 min. Each value is expressed as mean ± standard deviation (*n* = 3) of triplicate analysis. The bars with different lowercase (a–g) and uppercase letters (A–F) indicate significant differences (*p* < 0.05) in Tukey's HSD test.

3.2.2. Effect of pH

Figure 2 presents the effect of various pH values (4–9) on the amaranth purees stabilised with Cu and Zn concentrations of 210 mg/L and 1500 mg/L, respectively, at 80 °C

for 15 min. Thus, the results indicated that the pH value significantly affected the greenness and chlorophyll derivative content of both Cu- and Zn-amaranth purees ($p < 0.05$). Moreover, these results are consistent with the findings of LaBorde et al., that the formation of metallo-chlorophyll derivatives in heated vegetables was a pH-dependent process [52].
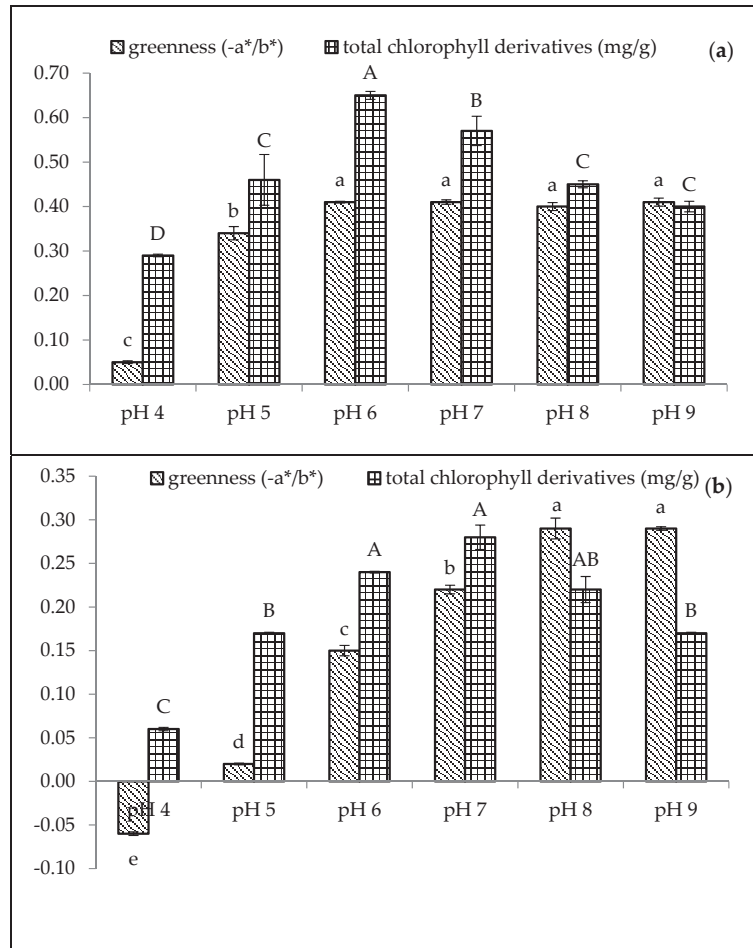
Figure 2. Effect of pH on greenness ($-a^*/b^*$) and total chlorophyll derivative content (mg/g) in (**a**) 210 mg/L of $CuSO_4$ and (**b**) 1500 mg/L of $ZnCl_2$ stabilised amaranth purees after heating at 80 °C for 15 min. Each value is expressed as mean $\pm$ standard deviation ($n = 3$) of triplicate analysis. The bars with different lowercase (a–e) and uppercase (A–D) letters indicate significant differences ($p < 0.05$) in Tukey's HSD test.

In Figure 2a, Cu-amaranth purees produced the highest greenness value (-0.41) with no significant difference ($p > 0.05$) between pH from 6 to 9. Comparatively, Zn-amaranth purees are significantly ($p < 0.05$) the highest greenness value (-0.29) at pH 8. Subsequently, the greenness value reached a plateau above pH 8. Guzmán et al. reported similar results that the avocado purees treated with copper chloride showed larger negative values of a^*/b^* (greener colour) than the avocado purees treated with $ZnCl_2$ [19]. In contrast, Senklang et al. reported that the green colour of pandan leaf extracts was highest at pH 5 and lower at pH 7 and 8 [25]. Hence, the contradicting results of pH may be associated with variations in the plants' raw materials and chlorophyll derivative contents.

The highest chlorophyll derivative content (0.65 mg/g FW) was observed in Cu-amaranth purees (prepared with 210 mg/L of $CuSO_4$) at pH 6. Nevertheless, the value decreased at pH > 6 (Figure 2a). Based on these results, metallo-chlorophyll complexes rapidly formed when the pH was increased from 4 to 8.5. On the contrary, these formations decreased at pH 10 [49]. Therefore, the Cu-amaranth purees at pH 6 were used for subsequent experiments. Meanwhile, the chlorophyll derivative content of Zn-amaranth purees at pH 7 and 8 were 0.28 and 0.22 mg/g FW, respectively. However, the colour of the puree at pH 8 was brighter than the puree at pH 7 (Figure 2b). Based on these observations, the Zn-amaranth puree treated at pH 8 was selected for subsequent experiments.

3.2.3. Effect of Temperature

The greenness and chlorophyll derivative content of the Cu-amaranth and Zn-amaranth purees increased with the increasing temperature in Figure 3. Based on the results, the Cu-amaranth puree produced the highest chlorophyll derivative content (0.62 mg/g FW) at 80 °C and greenness value (−0.40) at 80 to 100 °C (Figure 3a). The thermal treatment process was also reported as essential when using metals to retain green pigments. The heat is important in removing carbomethoxy at the C10 carbon position on the isocyclic ring of chlorophyll, transforming the pyrrole nucleus into a cation [44]. Thus, the transformation improves the diffusion of divalent metal ions (Cu^{2+} or Zn^{2+}) in dislodging Mg^{2+} ions to form metal complexes with chlorophylls [17]. The highest greenness value was depicted with the Zn-amaranth purees at 90 °C. Meanwhile, the highest chlorophyll derivative content was observed at 90 °C (0.39 mg/g FW) and 100 °C (0.37 mg/g FW).

In this study, the findings were in line with Guzmán et al., which reported that avocado purees treated with Cu or Zn at 87 to 89 °C produced greener colour than untreated samples [19]. Similarly, Canjura et al. and Salama et al. reported that treating green vegetables with Cu and Zn and heating them at higher temperatures (>85 °C) would result in colour improvements [22,27]. Canjura et al. also reported that peas blanched in Zn solution (50–500 mg/L) showed increased complex formation during the heat process (121–125 °C) [22]. The heat treatment process causes chlorophyll derivatives, such as pheophytin, to react with metal ions to form metal-pheophytin complexes with a stable green colour [22,44]. Therefore, heat treatments at 80 °C (Cu-amaranth puree) and 90 °C (Zn-amaranth puree) were selected as the optimum stabilisation temperatures.

Figure 4 displays the three absorbance spectra of acetone extracts of fresh and metal-stabilised amaranth purees. The amaranth purees are mostly absorbed in the blue and red regions of visible light due to the presence of chlorophylls and their derivative forms [53]. All acetone extracts of fresh and metal-stabilised amaranth purees have two major absorption bands in the visible range, which are "red" (Q-) and "blue" (Soret- or B-) bands [53]. The "red" and "blue" bands of chlorophyll *a* (Q- and B-bands) were located at wavelengths of 662 and 430 nm for acetone solutions, respectively [54]. A difference in the maximum absorption of the amaranth extracts at wavelengths from 350 to 500 nm was displayed in Figure 5 due to the colour differences between fresh amaranth and metal-stabilised purees [18].

The maximum absorption peaks of fresh amaranth puree were located at 433.77 and 668.86 nm wavelengths. Hence, the results were closely related to Von Elbe et al. [52], which concluded that the absorption maxima of chlorophyll *a* were at 428.5 and 660.5 nm wavelengths. Furthermore, Ngo et al. also reported that the fresh pear peel absorption peaks occurred at wavelengths of 430 and 660.5 nm [18]. Thus, these results indicated that the green colour of fresh amaranth puree was dominated by chlorophyll *a* [18].

For Cu-stabilised purees, the absorption maxima peaks were at wavelengths of 424.93 and 656.85 nm, respectively. The results were consistent with the findings of Scotter et al., in which the absorption maxima at the Soret (S-) and Q-bands of Cu chlorophyll *a* were at wavelengths of 422 and 652 nm [55], respectively. Based on the amaranth stabilised with Zn, the extracts revealed absorption maxima at 413.28 and 667.48 nm wavelengths.

In addition, Zheng et al. elucidated that the absorption maxima of Thomson seedless grape purees occurred at 664 to 670 nm wavelengths for the complexes with $ZnCl_2$ [23]. Nonetheless, these data contradict the data of Von Elbe et al., who reported that the absorption maxima for the Zn stabilization process were at wavelengths of 655 and 423 nm [52]. The contradicting results were probably due to the different concentrations of Zn and the heat treatment processes used.
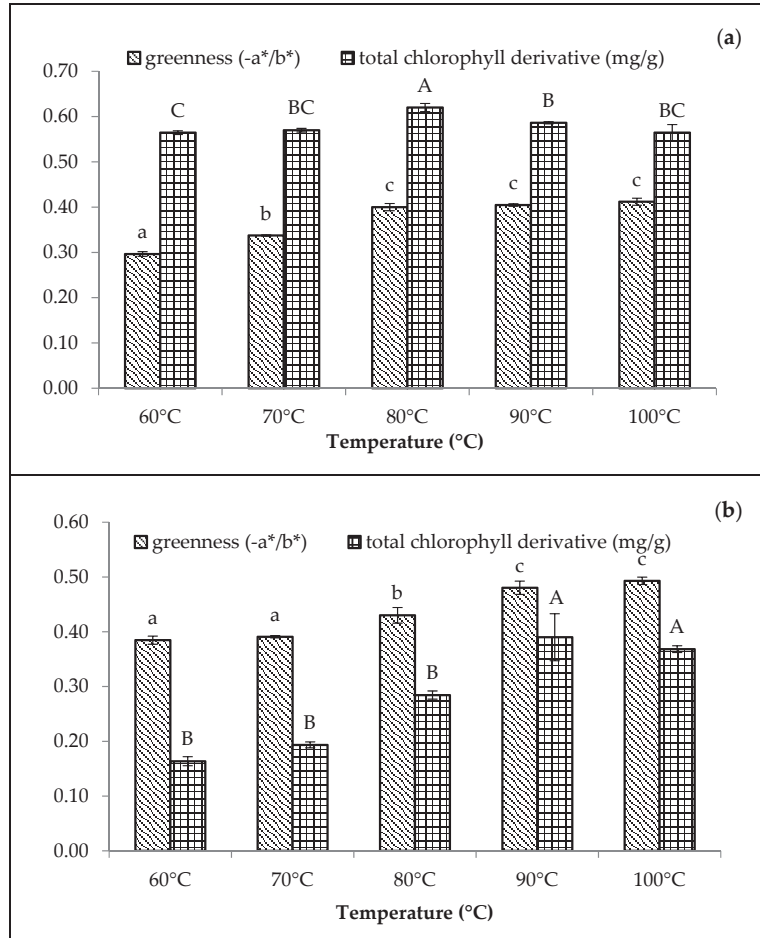
Figure 3. Effect of temperatures (reaction time of 15 min) on colour ($-a*/b*$) and total chlorophyll derivative content (mg/g) of (**a**) 210 mg/L of $CuSO_4$ stabilised amaranth purees at pH 6 and (**b**) 1500 mg/L of $ZnCl_2$ stabilised amaranth purees at pH 8. Each value is expressed as mean $\pm$ standard deviation ($n = 3$) of triplicate analysis. The bars with different lowercase (a–c) and uppercase (A–C) letters indicate significant differences ($p < 0.05$) in Tukey's HSD test.
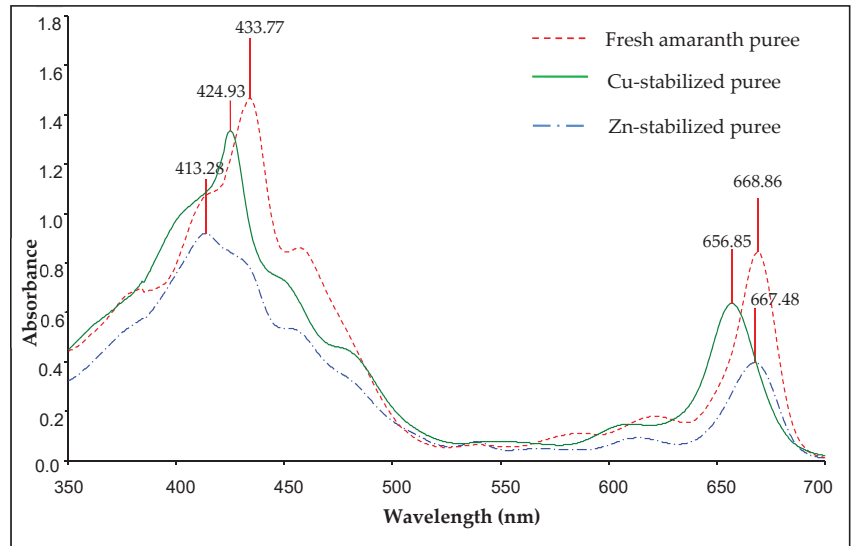
Figure 4. Absorbance spectra of acetone extracts of fresh and metal-stabilised amaranth purees (Cu-amaranth puree: 120 mg/L of CuSO$_4$ at 80 °C for 15 min, Zn-amaranth puree: 1500 mg/L of ZnCl$_2$ at 90 °C for 15 min.
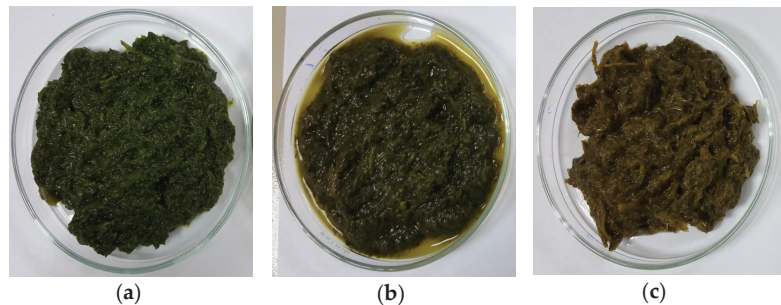
Figure 5. Amaranth purees of (**a**) Cu-amaranth puree stabilised at pH 6 and 80 °C for 15 min with 210 mg/L of CuSO$_4$, (**b**) Zn-amaranth puree stabilised at pH 8 and 90 °C for 15 min with 1500 mg/L ZnCl$_2$, and (**c**) control amaranth puree (0 mg/L of Zn or Cu and heated at 80 °C for 15 min).

3.3. Antioxidant Activities of Cu- and Zn-Amaranth Purees

3.3.1. Effect of Metal Concentration

Figure 6 displays the significant effects of metal concentrations on the antioxidant activity of methanolic extracts of Cu- and Zn-amaranth purees. Based on the Cu-amaranth purees, the DPPH antioxidant activities reached their maximum levels when the puree was stabilised with 210 and 240 mg/L of CuSO$_4$. Furthermore, the FRAP values were highest when treated with CuSO$_4$ above 120 mg/L. The Zn-amaranth purees depicted no significant differences at the highest value of the DPPH antioxidant activity (300 and 1500 mg/L of ZnCl$_2$). Nevertheless, the FRAP values increased when ZnCl$_2$ was above 1200 mg/L.
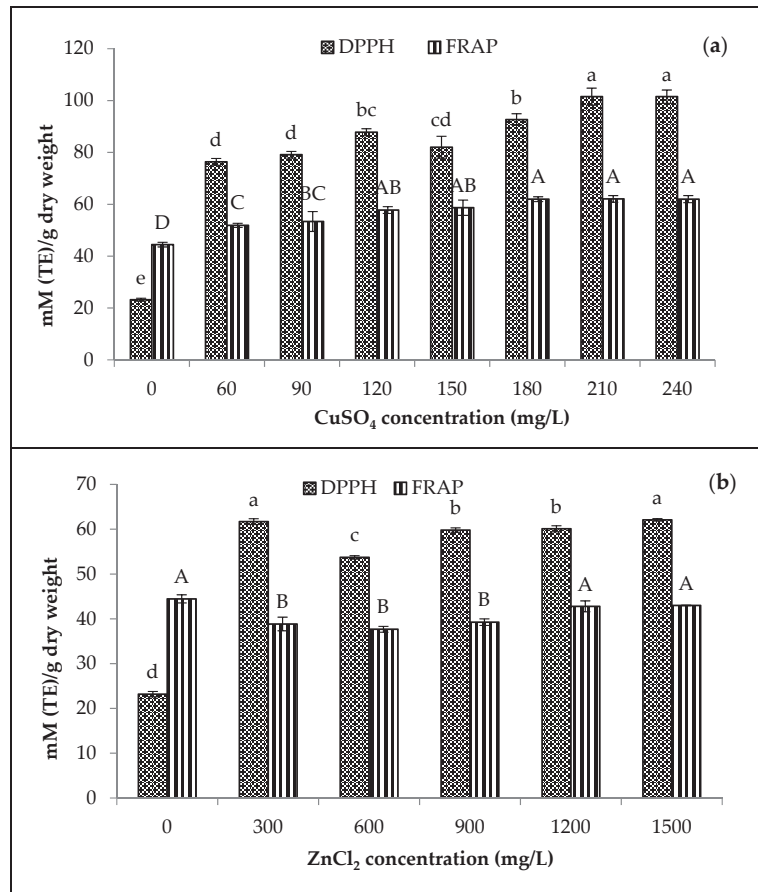
Figure 6. Effect of metal (**a**) $CuSO_4$ and (**b**) $ZnCl_2$ concentrations on antioxidant activity of amaranth puree at pH 6 after heating at 80 °C for 15 min. Each value is expressed as mean ± standard deviation (*n* = 3) of triplicate analysis. The bars with different lowercase (a–e) and uppercase (A–D) letters indicate significant differences (*p* < 0.05) in Tukey's HSD test.

Figure 6 shows lower antioxidant activity in amaranth puree with metal-free deriva-tives (at 0 mg/L of $CuSO_4$ and $ZnCl_2$) than in amaranth puree containing metallo-chlorophyll derivatives. Interestingly, the FRAP values of amaranth purees were significantly (*p* < 0.05) higher than Zn-amaranth purees in the range of approximately 300 to 900 mg/L of $ZnCl_2$. The higher FRAP values could be related to the other components in amaranth purees, which contributed to their higher antioxidant activity. According to Hoshina et al. and Ferruzzi et al., the antioxidant content was related to metal-treated samples [16,56].

In another study, Wrolstad et al. elucidated that metallo-chlorophyll derivatives, such as Cu-pyropheophytin and Zn-pheophytin produced higher antioxidant activities than metal-free derivatives (pheophytin and pyropheophytin) [57]. The findings in Figure 6 supported the higher antioxidant activity. Furthermore, the $CuSO_4$ (210 mg/L) and $ZnCl_2$ (1500 mg/L) stabilisation process on amaranth purees revealed the highest chlorophyll derivative contents. Thus, the relationship between antioxidant activity and chlorophyll derivative content of metal-treated amaranth purees was observed. Furthermore, metallo-chlorophyll derivatives, such as Cu- and Zn- pheophytin or phyropheophytin were re-ported to exhibit significantly higher antioxidant capacity than metal-free chlorophyll derivatives [57].

3.3.2. Effect of pH

The DPPH and FRAP values of stabilised amaranth purees affected by pH are presented in Figure 7. The results depicted that the Cu-amaranth puree at pH 6 had the highest DPPH (105.33 mM TE/dry weight) and FRAP (43.75 mM TE/dry weight) values. Additionally, the antioxidant activity of Zn-amaranth puree increased when treated at above pH 6. The DPPH and FRAP values of Zn-amaranth purees ranged from 76 to 80 mM TE/dry weight and 30 to 47 mM TE/dry weight, respectively. Hence, these values were lower than the values of Cu-amaranth purees.
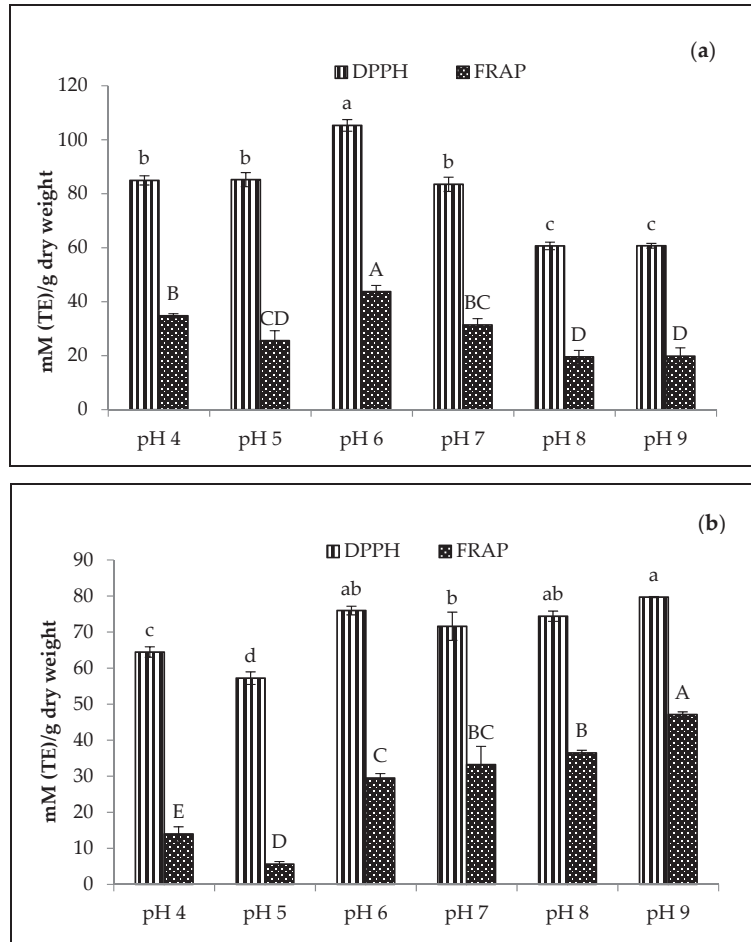
Figure 7. Effect of pH on antioxidant activities of (**a**) 210 mg/L of CuSO$_4$ and (**b**) 1500 mg/L of ZnCl$_2$ stabilised amaranth purees after heating at 80 °C for 15 min. Each value was expressed as mean $\pm$ standard deviation (n = 3) of triplicate analysis. The bars with different lowercase (a–d) and uppercase (A–E) letters indicate significant differences ($p < 0.05$) in Tukey's HSD test.

3.3.3. Effect of Temperature

In Figure 8, the Zn-amaranth purees significantly ($p < 0.05$) displayed the highest DPPH values at 88 mM TE/dry weight at 100 °C. Conversely, the highest FRAP values range from 57 to 58 mM TE/dry weight at 80 to 100 °C. A similar trend was also observed for Cu-amaranth purees with the highest DPPH values ranging from 93 to 95 mM TE/dry weight at 80 to 100 °C. Moreover, the DPPH values were higher than Zn-amaranth purees. Thus, these

findings confirmed that the antioxidant activities increased with increasing temperatures, probably due to the formation of firm bonds between Zn or Cu with chlorophyll derivatives. In addition, the metallo-chlorophyll derivatives complexes are more resistant to acid and heat treatments than natural Mg^{2+}-chlorophyll complexes [58].
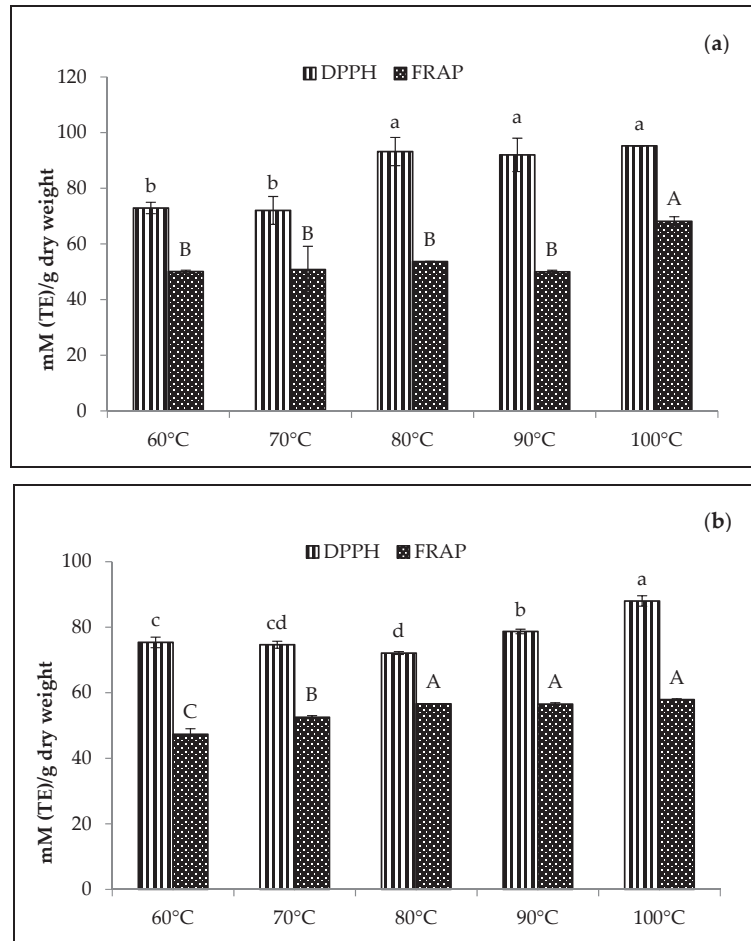
Figure 8. Effect of temperatures for the reaction time of 15 min on antioxidant activities of (**a**) 210 mg/L of $CuSO_4$ stabilised amaranth purees at pH 6 and (**b**) 1500 mg/L of $ZnCl_2$ stabilised amaranth purees at pH 8. Each value was expressed as mean $\pm$ standard deviation ($n = 3$) of triplicate analysis. The bars with different lowercase (a–d) and uppercase (A–C) letters indicate significant differences ($p < 0.05$) in Tukey's HSD test.

3.4. Identification of Chlorophylls and Their Derivatives in Fresh, Cu-, and Zn-Amaranth Purees Using Reversed-Phase HPLC

The identification of peaks was confirmed by comparing retention times (t_{ret}) of the peaks in the sample with standard chlorophylls *a* and *b* (Figure 9a,b). As shown in Figure 9c, the HPLC chromatogram of the chlorophyll fraction from the fresh amaranth extract depicted two major peaks at retention times (t_{ret}) of 16.73 (peak 1) and 27.65 min (peak 2). Hence, these peaks corresponded to chlorophyll *b* and chlorophyll *a*, respectively.
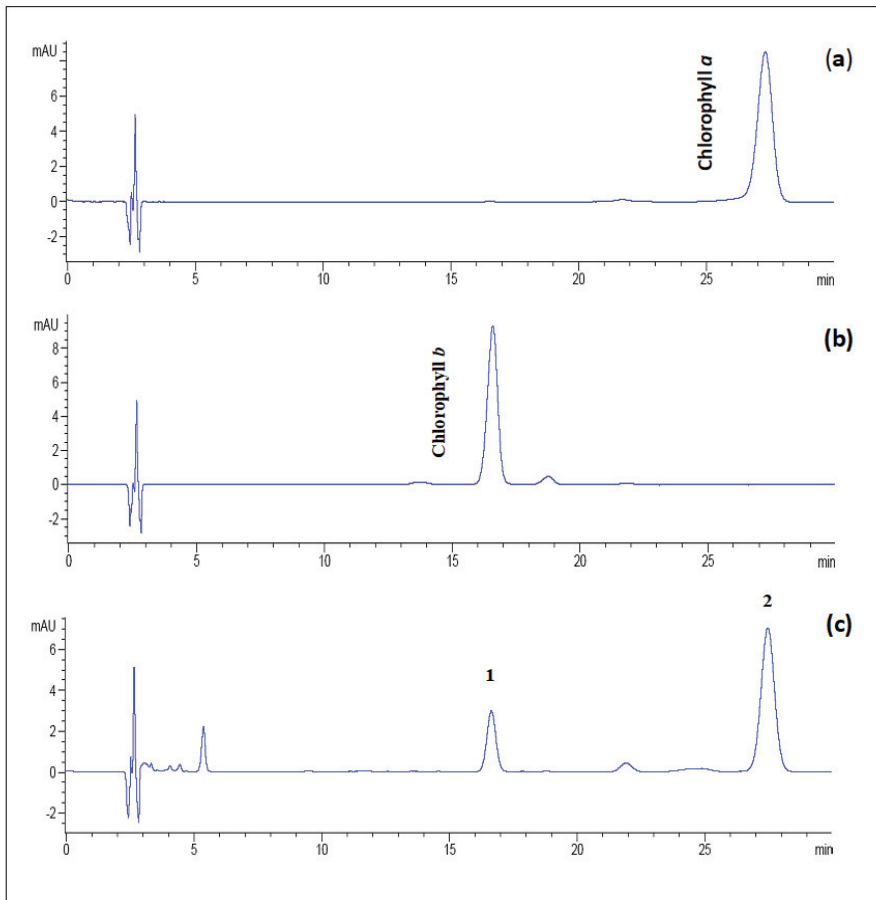
Figure 9. The reversed-phase HPLC chromatograms of (**a**) standard chlorophyll *a*, (**b**) standard chlorophyll *b*, and (**c**) fresh amaranth puree extracts (peaks identification: 1 = chlorophyll *b* and 2 = chlorophyll *a*) were detected at a wavelength of 658 nm. The separation process was carried out using a reversed-phase C$_{18}$ column with an isocratic mobile phase of ethyl acetate/methanol/water (40:54:10 *v/v/v*).

Chlorophyll *b* appeared to have a shorter retention time in the non-polar C$_{18}$ type of column, which is more polar and eluting than chlorophyll *a* [59,60]. The elution order of chlorophylls *a* and *b* of fresh amaranth extracts coincided with green bean and spinach extracts [51]. Additionally, chlorophylls *a* and *b* in fresh amaranths were 5.01 mg/g and 1.26 mg/g, respectively. In this study, the chlorophyll content of fresh amaranth puree recorded was higher than green beans (chlorophyll *a*: 1.11 mg/g, b: 0.74 mg/g) and peas (chlorophyll *a*: 0.8 mg/g, b: 0.51 mg/g) [61]. Nevertheless, the chlorophyll content of chlorophylls *a* and *b* in spinach leaves (chlorophyll *a*: 14.1 mg/g, *b*: 6.2 mg/g DW) was higher than the amaranth purees reported in this study [62].

4. Conclusions

In conclusion, the findings of this study established that metal concentration, pH, and temperature can influence the stabilisation process of the green colour, chlorophyll derivative content, and antioxidant activity of amaranth purees. The optimal stabilisation process conditions for the formation of Cu-amaranth purees were successfully achieved at

pH 6 and a temperature of 80 °C for a reaction time of 15 min using 210 mg/L of $CuSO_4$. Alternatively, Zn-amaranth occurred more readily at pH 8 and a temperature of 90 °C for a reaction time of 15 min using 1500 mg/L of $ZnCl_2$. The chromatograms in both Cu- and Zn-amaranth extracts showed no peaks, which corresponded to the complete degradation of chlorophylls *a* and *b* due to the formation of metallo-chlorophyll derivatives. The colour of Cu-amaranth puree was olive-green, while Zn-amaranth puree was bluish-green. Based on the results obtained in this study, the outcome will be useful in developing stable green vegetables with antioxidant activity to be applied in the food processing industry.

Author Contributions: Supervision, project administration, funding acquisition, and writing—review and editing, K.M.; conceptualization, methodology, and resources, K.M., R.K., and Y.A.Y.; formal analysis, data curation, writing—original draft preparation, and writing—review and editing, S.F.M.A. and K.M. All authors have read and agreed to the published version of the manuscript.

Institutional Review Board Statement: Not applicable.

Informed Consent Statement: Not applicable.

Data Availability Statement: Not applicable.

Conflicts of Interest: The authors declare no conflict of interest.

References

1. Sarker, U.; Hossain, M.M.; Oba, S. Nutritional and antioxidant components and antioxidant capacity in green morph Amaranthus leafy vegetable. *Sci. Rep.* **2020**, *10*, 1336. [CrossRef] [PubMed]
2. Alegbejo, J.O. Nutritional value and utilization of Amaranthus (*Amaranthus* spp.)—A Review. *Bayero J. Pure Appl. Sci.* **2013**, *6*, 136–143. [CrossRef]
3. Achigan-Dako, E.G.; Sogbohossou, O.E.D.; Maundu, P. Current knowledge on *Amaranthus* spp.: Research avenues for improved nutritional value and yield in leafy amaranths in sub-Saharan Africa. *Euphytica* **2014**, *197*, 303–317. [CrossRef]
4. Amin, I.; Norazaidah, Y.; Hainida, K.I.E. Antioxidant activity and phenolic content of raw and blanched Amaranthus species. *Food Chem.* **2006**, *94*, 47–52. [CrossRef]
5. Vivek, P.; Prabhakaran, S.; Shankar, S.R. Assessment of nutritional value in selected edible greens based on the chlorophyll content in leaves. *Res. Plant Biol.* **2013**, *3*, 45–49.
6. Sarker, U.; Islam, M.T.; Rabbani, M.G.; Oba, S. Genotypic variability for nutrient, antioxidant, yield and yield contributing traits in vegetable amaranth. *J. Food Agric. Environ.* **2014**, *12*, 168–174.
7. Sarker, U.; Islam, M.T.; Rabbani, M.G.; Oba, S. Phenotypic divergence in vegetable amaranth for total antioxidant capacity, antioxidant profile, dietary fiber, nutritional and agronomic traits. *Acta Agric. Scand. B Soil Plant Sci.* **2018**, *68*, 67–76. [CrossRef]
8. Hosikian, A.; Lim, S.; Halim, R.; Danquah, M.K. Chlorophyll extraction from microalgae: A review on the process engineering aspects. *Int. J. Chem. Eng.* **2010**, *2010*, 1–11. [CrossRef]
9. Schoefs, B. Chlorophyll and carotenoid analysis in food products. Properties of the pigments and methods of analysis. *Trends Food Sci. Technol.* **2002**, *13*, 361–371. [CrossRef]
10. Lanfer-Marquez, U.M.; Sinnecker, P. Chlorophylls: Properties, biosynthesis, degradation and functions. In *Food Colorants: Chemical and Functional Properties*; Socaciu, C., Ed.; CRC Press: Boca Raton, FL, USA, 2007; pp. 25–45.
11. Schwartz, S.J.; Lorenzo, T.V. Chlorophylls in foods. *Crit. Rev. Food Sci. Nutr.* **1990**, *29*, 1–17. [CrossRef]
12. Ferruzzi, M.G.; Blakeslee, J. Digestion, absorption, and cancer preventative activity of dietary chlorophyll derivatives. *Nutr. Res.* **2007**, *27*, 1–12. [CrossRef]
13. Erge, H.S.; Karadeniz, F.; Koca, N.; Soyer, Y. Effect of heat treatment on chlorophyll degradation and color loss in green peas. *Gida Derg.* **2008**, *33*, 225–233.
14. Edelenbos, M.; Christensen, L.P.; Grevsen, K. HPLC determination of chlorophyll and carotenoid pigments in processed green pea cultivars (*Pisum sativum* L.). *J. Agric. Food Chem.* **2001**, *49*, 4768–4774. [CrossRef] [PubMed]
15. Kang, Y.R.; Park, J.; Jung, S.K.; Chang, Y.H. Synthesis, characterization, and functional properties of chlorophylls, pheophytins, and Zn-pheophytins. *Food Chem.* **2018**, *245*, 943–950. [CrossRef] [PubMed]
16. Ferruzzi, M.G.; Böhm, V.; Courtney, P.D.; Schwartz, S.J. Antioxidant and antimutagenic activity of dietary chlorophyll derivatives determined by radical scavenging and bacterial reverse mutagenesis assays. *J. Food Sci.* **2002**, *67*, 2589–2595. [CrossRef]
17. Ngo, T.; Zhao, Y. Retaining Green Pigments on Thermally Processed Peels-on Green Pears. *J. Food Sci.* **2005**, *70*, C568–C574. [CrossRef]
18. Ngo, T.; Zhao, Y. Formation of Zinc-Chlorophyll-Derivative Complexes in Thermally Processed Green Pears (*Pyrus communis* L.). *J. Food Sci.* **2007**, *72*, C397–C404. [CrossRef]

19. Guzmán, G.R.; Dorantes, A.L.; Hernández, U.H.; Hernández, S.H.; Ortiz, A.; Mora, E.R. Effect of zinc and copper chloride on the color of avocado puree heated with microwaves. *Innov. Food Sci. Emerg. Technol.* **2002**, *3*, 47–53. [CrossRef]
20. Porrarud, S.; Pranee, A. Microencapsulation of Zn-chlorophyll pigment from Pandan leaf by spray drying and its characteristic. *Int. Food Res. J.* **2010**, *17*, 1031–1042.
21. Chaiwanichsiri, S.; Dharmsuriya, N.; Sonthornvit, N.; Janjarasskul, T. Process improvement to preserve the color of instant pennywort *Centella asiatica* (Linn.) *Urban. J. Sci. Res. Chula. Univ.* **2000**, *25*, 233–243.
22. Canjura, F.L.; Watkins, R.H.; Schwartz, S.J. Color Improvement and Metallo-chlorophyll Complexes in Continuous Flow Aseptically Processed Peas. *J. Food Sci.* **1999**, *64*, 987–990. [CrossRef]
23. Zheng, Y.; Shi, J.; Pan, Z.; Cheng, Y.; Zhang, Y.; Li, N. Effect of heat treatment, pH, sugar concentration, and metal ion addition on green color retention in homogenized puree of Thompson seedless grape. *LWT-Food Sci. Technol.* **2014**, *55*, 595–603. [CrossRef]
24. Ngo, T.X. Understanding the Principles and Procedures to Retain Green and Red Pigments in Thermally Processed Peels-on Pears (*Pyrus Communis* L.). Ph.D. Thesis, Oregon State University, Corvallis, OR, USA, 2008.
25. Senklang, P.; Anprung, P. Optimizing Enzymatic Extraction of Zn–Chlorophyll Derivatives from Pandan Leaf Using Response Surface Methodology. *J. Food Process. Preserv.* **2010**, *34*, 759–776. [CrossRef]
26. Tonucci, L.H.; Von Elbe, J.H. Kinetics of the formation of zinc complexes of chlorophyll derivatives. *J. Agric. Food Chem.* **1992**, *40*, 2341–2344. [CrossRef]
27. Salama, M.F.; Moharram, H.A. Relationship between colour improvement and metallo-chlorophyll complexes during blanching of peas and broccoli. *Alex. J. Food Sci. Technol.* **2007**, *4*, 11–18.
28. Rahayuningsih, E.; Pamungkas, M.S.; Olvianas, M.; Putera, A.D.P. Chlorophyll extraction from suji leaf (*Pleomele angustifolia* Roxb.) with $ZnCl_2$ stabilizer. *J. Food Sci. Technol.* **2018**, *55*, 1028–1036. [CrossRef]
29. FDA. *Listing of Color Additives Exempt from Certification; Sodium Copper Chlorophyllin*; Food and Drug Administration: Silver Spring, MD, USA, 2002; pp. 35429–35431.
30. EFSA. Scientific Opinion on re-evaluation of copper complexes of chlorophylls (E 141(i)) and chlorophyllins (E 141(ii)) as food additives. *EFSA J.* **2015**, *13*, 4151.
31. Soldatović, T. Mechanism of interactions of Zinc(II) and Copper(II) complexes with small biomolecules. In *Basic Concepts Viewed from Frontier in Inorganic Coordination Chemistry*; Intechopen: London, UK, 2018.
32. de Vogel, J. Green Vegetables and Colon Cancer: The Mechanism of a Protective Effect by Chlorophyll. Ph.D. Thesis, Wageningen University and Research Centre, Wageningen, The Netherlands, 2006; p. 151.
33. Gomes, B.B.; Barros, S.B.M.; Andrade-Wartha, E.R.S.; Silva, A.M.O.; Silva, V.V.; Lanfer-Marquez, U.M. Bioavailability of dietary sodium copper chlorophyllin and its effect on antioxidant defence parameters of Wistar rats. *J. Sci. Food Agric.* **2009**, *89*, 2003–2010. [CrossRef]
34. Ulbricht, C.; Bramwell, R.; Catapang, M.; Giese, N.; Isaac, R.; Le, T.D. An evidence-based systematic review of chlorophyll by the Natural Standard Research Collaboration. *J. Diet. Suppl.* **2014**, *11*, 198–239. [CrossRef]
35. Solymosi, K.; Mysliwa-Kurdziel, B. Chlorophylls and their derivatives used in food industry and medicine. *Mini-Rev. Med. Chem.* **2017**, *17*, 1194–1222. [CrossRef]
36. Zhan, R.; Wu, J.; Ouyang, J. In vitro antioxidant activities of sodium zinc and sodium iron chlorophyllins from pine needles. *Food Technol. Biotechnol.* **2014**, *52*, 505. [CrossRef] [PubMed]
37. Praveena, B.; Murthy, S. Role of photosynthetic pigments in protection against oxidative damage. *Int. J. Plant Anim. Environ. Sci.* **2013**, *4*, 167–171.
38. Hsu, C.Y.; Chao, P.Y.; Hu, S.P.; Yang, C.M. The antioxidant and free radical scavenging activities of chlorophylls and pheophytins. *Nutr. Food Sci.* **2013**, *4*, 1–8. [CrossRef]
39. Amin, S.F.M.; Karim, R.; Yusof, Y.A.; Muhammad, K. Effects of enzymatic liquefaction, drying techniques, and wall materials on the physicochemical properties, bioactivities, and morphologies of Zinc-amaranth (*Amaranthus viridis* L.) powders. *Int. J. Food Sci* **2021**, *2021*, 1–13. [CrossRef] [PubMed]
40. Larrauri García, J.A.; Saura Calixto, F. Evaluation of CIE-lab colour parameters during the clarification of a sugar syrup from Mesquite pods (*Prosopis Pallida* L.). *Int. J. Food Sci. Technol.* **2000**, *35*, 385–389. [CrossRef]
41. Costache, M.A.; Campeanu, G.; Neata, G. Studies concerning the extraction of chlorophyll and total carotenoids from vegetables. *Rom. Biotechnol. Lett.* **2012**, *17*, 7703–7708.
42. Li, H.B.; Wong, C.C.; Cheng, K.W.; Chen, F. Antioxidant properties in vitro and total phenolic contents in methanol extracts from medicinal plants. *LWT-Food Sci. Technol.* **2008**, *41*, 385–390. [CrossRef]
43. Brand-Williams, W.; Cuvelier, M.; Berset, C. Use of a free radical method to evaluate antioxidant activity. *LWT-Food Sci. Technol.* **1995**, *28*, 25–30. [CrossRef]
44. Benzie, I.F.; Strain, J. The ferric reducing ability of plasma (FRAP) as a measure of "antioxidant power": The FRAP assay. *Anal. Biochem.* **1996**, *239*, 70–76. [CrossRef]
45. Canjura, F.L.; Schwartz, S.J. Separation of chlorophyll compounds and their polar derivatives by high-performance liquid chromatography. *J. Agric. Food Chem.* **1991**, *39*, 1102–1105. [CrossRef]
46. Gaur, S.; Shivhare, U.; Ahmed, J. Degradation of chlorophyll during processing of green vegetables: A review. *Stewart Postharvest Rev.* **2006**, *2*, 1–8.

47. Weemaes, C.A.; Ooms, V.; Loey, A.M.V.; Hendrickx, M.E. Kinetics of chlorophyll degradation and colour loss in heated broccoli juice. *J. Agric. Food Chem.* **1999**, *47*, 2404–2409. [CrossRef] [PubMed]
48. Östbring, K.; Rayner, M.; Sjöholm, I.; Otterström, J.; Albertsson, P.Å.; Emek, S.C.; Erlanson-Albertsson, C. The effect of heat treatment of thylakoids on their ability to inhibit in vitro lipase/co-lipase activity. *Food Funct.* **2014**, *5*, 2157–2165. [CrossRef] [PubMed]
49. Heaton, J.W.; Marangoni, A.G. Chlorophyll degradation in processed foods and senescent plant tissues. *Trends Food Sci. Technol.* **1996**, *7*, 8–15. [CrossRef]
50. LaBorde, L.F.; Von Elbe, J.H. Zinc complex formation in heated vegetable purees. *J. Agric. Food Chem.* **1990**, *38*, 484–487. [CrossRef]
51. Lin, Z.; Schyvens, E. Influence of blanching treatments on the texture and colour of some processed vegetables and fruits. *J. Food Process. Preserv.* **1995**, *19*, 451–465. [CrossRef]
52. LaBorde, L.F.; Von Elbe, J.H. Chlorophyll degradation and zinc complex formation with chlorophyll derivatives in heated green vegetables. *J. Agric. Food Chem.* **1994**, *42*, 1100–1103. [CrossRef]
53. Von Elbe, J.; Schwartz, S. Colourants. *Food Chem.* **1996**, *3*, 651–723.
54. Hoff, A.J.; Amesz, J. *Chlorophylls*; Scheer, H., Ed.; CRC Press: Boca Raton, FL, USA, 1991; p. 723.
55. Scotter, M.J.; Castle, L.; Roberts, D. Method development and HPLC analysis of retail foods and beverages for copper chlorophyll (E141 [i]) and chlorophyllin (E141 [ii]) food colouring materials. *Food Addit. Contam.* **2005**, *22*, 1163–1175. [CrossRef]
56. Hoshina, C.; Tomita, K.; Shioi, Y. Antioxidant activity of chlorophylls: Its structure-activity relationship. In *Photosynthesis: Mechanisms Effects*; Springer: Dordrecht, The Netherlands, 1998; Volume 4, pp. 3281–3284.
57. Wrolstad, R.E.; Acree, T.E.; Decker, E.A.; Penner, M.; Reid, D.; Schwartz, S.; Shoemaker, C.; Smith, D.; Sporns, P. Pigments, Colorants, Flavors, Texture, and Bioactive Food Components. In *Handbook of Food Analytical Chemistry*; John Wiley and Sons, Inc.: Hoboken, NJ, USA, 2005.
58. Leunda, M.; Guerrero, S.; Alzamora, S. Color and chlorophyll content changes of minimally processed kiwifruit. *J. Food Process. Preserv.* **2000**, *24*, 17–38. [CrossRef]
59. Lim, C.K. *High-Performance Liquid Chromatography and Mass Spectrometry of Porphyrins, Chlorophylls and Bilins*; World Scientific Publishing Co., Pte Ltd.: Singapore, 2009.
60. Gökmen, V.; Savaş Bahçeci, K.; Serpen, A.; Acar, J. Study of lipoxygenase and peroxidase as blanching indicator enzymes in peas: Change of enzyme activity, ascorbic acid and chlorophylls during frozen storage. *LWT-Food Sci. Technol.* **2005**, *38*, 903–908. [CrossRef]
61. Turkmen, N.; Poyrazoglu, E.S.; Sari, F.; Sedat Velioglu, Y. Effects of cooking methods on chlorophylls, pheophytins and colour of selected green vegetables. *Int. J. Food Sci. Technol.* **2005**, *41*, 281–288. [CrossRef]
62. Teng, S.S.; Chen, B.H. Formation of pyrochlorophylls and their derivatives in spinach leaves during heating. *Food Chem.* **1999**, *65*, 367–373. [CrossRef]

Article

Biochemical Characteristics of Acid-Soluble Collagen from Food Processing By-Products of Needlefish Skin (*Tylosurus acus melanotus*)

Siti Zulaikha Ramle [1], Siti Nur Hazwani Oslan [1], Rossita Shapawi [2], Ruzaidi Azli Mohd Mokhtar [3], Wan Norhana Md. Noordin [4] and Nurul Huda [5,*]

[1] Faculty of Food Science and Nutrition, Universiti Malaysia Sabah, Jalan UMS, Kota Kinabalu 88400, Sabah, Malaysia
[2] Borneo Marine Research Institute, Universiti Malaysia Sabah, Jalan UMS, Kota Kinabalu 88400, Sabah, Malaysia
[3] Biotechnology Research Institute, Universiti Malaysia Sabah, Jalan UMS, Kota Kinabalu 88400, Sabah, Malaysia
[4] Fisheries Research Institute, Batu Maung 11960, Penang, Malaysia
[5] Faculty of Sustainable Agriculture, Universiti Malaysia Sabah, Sandakan 90509, Sabah, Malaysia
* Correspondence: drnurulhuda@ums.edu.my

Abstract: The by-product of needlefish (*Tylosurus acus melanotus*) waste possesses important characteristics that could be used in food applications. Fish by-product collagen may be used in place of mammalian collagen due to ethical and religious considerations over environmental degradation. Different forms of acid-soluble collagen (ASC) were successfully extracted from needlefish skin. Based on dry weight, the collagen extracted using acetic acid (AAC), lactic acid (LAC), and citric acid (CAC) treatments was 3.13% with a significantly difference ($p < 0.05$), followed by 0.56% and 1.03%, respectively. Based on proximate analysis, the needlefish skin composition was found to be significantly different ($p < 0.05$) between compositions, with the highest moisture content at 61.65%, followed by protein (27.39%), fat (8.59%), and ash (2.16%). According to the SDS-PAGE results, all extracted collagen were identified as a type 1 collagen. Additionally, ATR-FTIR revealed that all collagens had amide A, B, amide I, II, and III peaks. AAC significantly outperforms LAC and CAC in terms of yield following physicochemical characterisation, including pH determination, colour (L* value), and hydroxyproline content. All collagens demonstrated strong heat resistance and structural stability with T_{max} above 38 °C. Collagen was most soluble at pH 5 for AAC, pH 3 for LAC, and pH 7 for CAC. The effect of collagen solubility on NaCl concentration was discovered to be significantly reduced to 50 g/L for all collagen samples. All collagens can be used as alternatives to terrestrial collagen in a diverse range of applications.

Keywords: by-product; needlefish (*Tylosurus acus melanotus*); acid-soluble collagen extraction; physicochemical; characterization

1. Introduction

Nowadays, fishing is an important sector of the world economy, producing a wide range of by-products from fish processing, including over 196 million tonnes of fish expected to be processed by 2025, making fish production a potentially profitable industry [1]. As an outcome, needlefish (*Tylosurus acus melanotus*) can be found in abundance in Malaysia, particularly in Sabah and Sarawak. Generally, needlefish are processed into surimi and utilised to manufacture fish balls. Wastes from needlefish, such as skin, bones, fins, and heads are eliminated during the preparation of surimi. However, by-products can be recovered and turned into a range of useful substances, including collagen [2]. As collagen is made from fish wastes, the resulting collagen will be halal, as Muslims are barred from consuming pig collagen and its use is therefore prohibited [3]. According to Schmidt et al. [4],

fish by-products such as scales, bones, fins, and skin are the most secure sources for collagen production, and no fish-related diseases have been reported. Furthermore, crude protein levels in fish by-products can reach up to 35%, and depending on the species, age and season, collagen can constitute up to 70% of the fish's dry weight [2]. As a result, these have the potential to serve as a source of collagen, polyunsaturated fatty acids (PUFA), gelatine, enzymes, and essential amino acids [5]. Therefore, there is a need for collagen that can be made from marine sources that has been demonstrated to be comparable to traditional collagen made from mammalian sources in terms of amino acid content and biocompatibility [6]. Wastes often created by fish processing that have been utilised; include the skin, bone and muscle of leather jackets (*Odonus niger*) [7]; skin, scales and fins of *Catla catla* and *Cirrhinus mrigala* [8]; skin of tilapia (*Oreochromis niloticus*) [9]; and several other parts which have texture and are promising sources of collagen.

Due to its unique properties, collagen is important to many sectors, including those that provide healthy meals, cosmetics, tissue engineering, and wound-care products [10]. Collagen makes up nearly 30% of the total protein in mammalian skin and bone connective tissue [6] and governs tissue growth, supports structural integrity, and offers texture, shape, thickening, durability, and gel function [11]. Recently, Oslan et al. [2] discovered a range of techniques for extracting collagen from fish, including acid solubilization, enzyme solubilization, ultrasound, and the extrusion-hydro-extraction (EHE) approaches. In order to extract collagen, acids and enzymes are commonly used. Generally, collagen dissolves in acidic liquids; however, when exposed to a very acidic pH, its solubility diminishes, and certain chemicals can be hazardous or toxic [12]. By attaching an amine group (-COOH) on the collagen protein, weak acids or organic acids, such as acetic acid, citric acid, and lactic acid, are utilised to facilitate the collagen extraction process [13]. In addition, studies on collagen extraction from fish have revealed that the yield of collagen and the optimal conditions required vary depending on the type of raw material, type of acid, concentration, time, and temperature [14,15]. However, excessive acid concentrate destroys peptides, lowering the quantity and quality of the collagen [15]. In terms of thermal stability, fish collagen has less thermal stability than mammalian collagen, which may be attributable to the short amino acid (proline and hydroxyproline) residues [16]. However, hydroxyproline improves with heat stability by stabilising the triple helix structure of collagen. Fish with lower hydroxyproline concentrations have been shown to have lower denaturation temperatures than fish with greater hydroxyproline concentrations [2]. Furthermore, several strategies for enhancing cross linking and thermal stability of fish collagen have been used. The denaturing temperature of salmon atelocollagen (SC) has been enhanced from 18.6 °C to 47 °C after employing a modified approach in which a neutral buffer was combined with an acidic SC solution at 4 °C during collagen fibril development [16]. Therefore, the goal of this work was to extract and analyse acid soluble collagen from needlefish skin (*Tylosurus acus melanotus*) for the use in food and other industries.

2. Materials and Methods

2.1. Raw Materials Preparation

The needlefish (*Tylosurus acus melanotus*) was obtained at a fish market in Kota Kinabalu, Sabah. The needlefish were chilled and delivered to the laboratory within 40 min of purchase, then washed with cold distilled water. The fish were deboned using mechanical equipment (SFD-8, 137 Taiwan). The skins were thoroughly cleaned under running tap water before being trimmed into 0.5 cm pieces using a scalpel [11]. Additionally, skin samples were cleaned, placed in polyethylene bags, and stored at −20 °C until collagen extraction. Analytical-grade reagents were employed in all experiments.

2.2. Sample Pre-Treatment and Defatting Process

The needlefish skin was immersed in a 0.1 N NaOH (1:10) (w/v) solution at 4 °C for 6 h, with the solution being replaced every 3 h to eliminate non-collagen protein. Subsequently, they were rinsed with tap water to achieve a pH of 7.0 neutrality [17]. The samples were

then submerged in a 10% (1:10) butyl alcohol solution at 4 °C for 24 h. This solution was changed every 6 h to remove fat, and then the skin was washed again with cold distilled water until the pH level was neutralize.

Proximate Analysis

Proximate analysis of moisture, fat, protein and ash content of skin needlefish was performed using established techniques developed by the Association of Official Analytical Chemists (AOAC) [18].

2.3. Extraction of Collagen Using Different of Organic Acid

The preparation of the acid-soluble collagen (ASC) extraction method was based on Zaelani et al. [19] with slight modifications. Extraction was carried out utilising various forms of organic acids. After pre-treatment and defatting, skin samples were extracted with 0.5 M organic acid. This study utilized acetic acid, lactic acid, and citric acid. All procedures were conducted at 4 °C, with samples immersed in a different solution for 72 h at a ratio of 1:15 (w/v). Afterwards, the mixture was passed through two layers of gauze fabric in order to collect the supernatant. Next, the salting-out process was done by adding NaCl solution to the resultant supernatant until the supernatant's final concentration reached 2.5 M at a pH of 7.0. This was carried out in the presence of 0.05 M Tris–HCl. The mixture was centrifuged at 15,000× g for 30 min at 4 °C (Eppendorf, Centrifuge 5804, Hampton, VA, USA) in order to generate a precipitate. After removing the supernatant, the residue was collected, re-dissolved in a 0.5 M ratio of 1:9 (w/v) of organic acid and then washed. The residue was then dialyzed in 0.1 M acetic acid, lactic acid, or citric acid for 24 h and then cold distilled water for 48 h, changed every 12 h. The generated collagen was subsequently frozen at −80 °C and freeze-dried (Labconco, South Kansas City, KS, USA) for 72 h by following the freeze-dry technique. The produced collagen was classified as acetic acid collagen (AAC), lactic acid collagen (LAC), or citric acid collagen (CAC) and was stored at 4 °C until further examination. The collagen extraction yield was examined and characterised using a variety of methods.

2.3.1. Extraction Yield

The collagen extraction yield was estimated according to Normah and Maidzatul [20], its dry basis was used in the calculation of the percentage of the following equation:

$$\text{Yield (\%)} = \frac{\text{Weight of collagen (g)}}{\text{Weight of skin (g)}} \times 100 \tag{1}$$

2.3.2. Percentage of Swelling

The needlefish skin that had undergone the non-collagenous protein removal technique was filtered and allowed to rest for 15 min before being weighed on a digital scale. The following equation was used from Huda et al. [21] to determine the rate (%) of swelling:

$$\text{Swelling (\%)} = \frac{\text{Weight after immersed 0.1 N NaOH (g)}}{\text{Weight of raw material (g)}} \times 100 \tag{2}$$

2.4. Characterization of Collagen
2.4.1. Recognition of the Colour

The colour of all collagen samples was determined using the Huda et al. [22] technique using a colorimeter (Konica Minolta, Tokyo, Japan) based on the International Commission de I'Éclairage (CIE) scale. It was necessary to use the colour values of L*, a*, and b* as arguments. L* indicates brightness; 0 was darkest and 100 was the brightest. a* represented redness, from red +60 to green −60, while b* represented yellowness.

2.4.2. Hydroxyproline Content

The hydroxyproline concentration in the ASC powders of all extracted collagens was determined using a flexible method described by Nalinanon et al. [23]. Initially, collagen samples were dissolved in 6 M hydrochloric acid at 115 °C for 24 h at a concentration of 5 mg/mL. Then, the hydrolysed collagen was dissolved in distilled water, and the pH was adjusted until it reached 6–6.5. The mixture was then incubated for 20 min at room temperature after 2 mL of hydrolysate and 1 mL of chloramine reagent were added. Next, 1 mL of perchloric acid was added, and the mixture remained at room temperature for 5 min. Following the addition 1 mL of Ehrlich's reagent to the hydrolysate, the sample was incubated for 20 min at 60 °C. The sample was then analysed with a UV–Vis spectrophotometer at 558 nm wavelength.

2.4.3. Fourier Transform Infrared Spectroscopy (ATR-FTIR)

ATR-FTIR spectra were acquired using a previously described approach by Matmaroh et al. [24], with a few minor adjustments to identify the structural properties of collagen. A 30-mg collagen sample was combined with 100 mg potassium bromide (KBr) and shaped into a tablet, which was placed into the FTIR spectrometer's sample container. All spectra were captured using an infrared spectrophotometer (Nicolet, Thermo Electron, Waltham, MA, USA) with a resolution of 2 cm^{-1} between 400 to 4000 cm^{-1}.

2.4.4. Ultraviolet–Visible Spectroscopy (UV–Vis) Measurement

Based on the study by Chinh et al. [25], an ultraviolet–visible spectroscopy UV–Vis spectrophotometer (Agilent Cary 60) was used to measure the UV–Vis spectra of collagen solutions between 200 and 400 nm.

2.4.5. Sodium Dodecyl Sulphate-Polyacrylamide Gel Electrophoresis (SDS-PAGE)

SDS-PAGE was used to analyse the protein patterns of ASC samples using a modified approach by Jeong et al. [26]. Samples of collagen were dissolved in 0.1 M acetic acid with 5% sodium dodecyl sulphate before being heated for 1 h at 85 °C. The mixture was centrifuged at 5000 rpm for 5 min at room temperature to remove undissolved debris. After centrifugation, the supernatants were pipetted into a second tube. The sample buffers (with and without 5% mercaptoethanol) were mixed at 1:1 (v/v) with extracted collagens and heated at 85 °C for 3 min. After heat incubation, 15 μL of the mixture was put into a 5% stacking and 12% resolving acrylamide gel. Electrophoresis was set at a constant voltage of 120 V for 1.5 h, and the molecular weight markers were determined using a dual colour protein standard (10–250 kDa). The soluble sample was mixed 4:1 (v/v) with 60 mM Tris–HCl at pH 8 containing 10% sodium dodecyl sulphate, 25% glycerol, and 0.1% blue bromophenol. 25% glycine, 20% SDS, 5% mercaptoethanol, and 0.1% bromophenol blue were used to create loading dyes. Wide range molecular weight markers were used to estimate the molecular weight of proteins. The gel was stained with Coomassie Brilliant Blue R-250 staining solution after electrophoresis. The Mini-PROTEAN electrophoresis equipment was used to run the SDS-PAGE gel.

2.4.6. Thermal Transition Measurement

The temperature transition of collagen was evaluated using a differential scanning calorimeter (DSC Q200 V24.4 Build 116, TA Instruments, Water LLC, New Castle, DE, USA) following the method of Zeng et al. [27]. Lyophilized collagens were rehydrated in deionized water for 48 h at 4 °C. The rehydrated samples (5–10 mg) were carefully weighed into sealed aluminium pans (PerkinElmer, Waltham, MA, USA) and scanned over the temperature range of 20–50 °C at a rate of 10 °C/min. An empty sealed aluminium pan was utilised as a reference. The device was calibrated for temperature and enthalpy using indium as the standard, and samples were continuously purged at a rate of 50 mL/min with ultrahigh-purity nitrogen. The device was equilibrated at 20 °C for 5 min before scanning; ice water was employed as a cooling medium. The area on the DSC thermo-

gram was utilised to assess total denaturation enthalpy (H). The thermogram determined the transition temperature (T_{max}). The findings were analysed using TA software (TA Instruments, New Castle, DE, USA).

2.4.7. Effect of pH and NaCl on Solubility

The solubility of collagens at various pH and NaCl concentrations was investigated using the Jamilah et al. [28] technique with slight modified. All collagen was dissolved in 0.5 M acetic acid at 4 °C and the solution was stirred for 18 h to obtain a final concentration of 3 mg/mL. The solution was centrifuged at a speed of $10,000\times g$ for 30 min (Eppendorf, Centrifuge 5804, USA) at a temperature of 4 °C before the pH was altered to 1, 3, 5, 7, 9, or 11 with 2 mol/L HCl or 2 mol/L NaOH. The amount of protein in the supernatant was determined, with bovine serum albumin as the standard. The relative solubility was estimated using the solubility value at each pH using the following Equation (3): Relative solubility (%) = (protein content of supernatant at current pH/total protein content in sample) × 100. In order to carry out the solubility test pertaining to the impact of NaCl concentration, 5 mL of collagen solution with a concentration of 6 mg/mL was mixed with 5 mL of NaCl solution. In this study, the NaCl solution was dissolved in 0.5 M acetic acid at concentrations of 0, 10, 20, 30, 40, 50, and 60 g/L. The mixture of collagen solution and NaCl solution was stirred continuously for 60 min at 4 °C, followed by centrifugation at $10,000\times g$ for 30 min at 4 °C. Protein content in the supernatants was then determined. All samples were tested for protein using the Enhanced BCA Protein Assay Kit, with bovine serum albumin as the standard. The relative solubility at each NaCl concentration was measured and the relative solubility was calculated according to Equation (4): relative solubility (%) = (protein content of supernatant/total protein content in sample) × 100. The relative solubility was evaluated in terms of the highest pH and NaCl concentration values recorded. The relative solubility of both substances was estimated using the following Equations (3) and (4):

$$Relative\ solubilty\ (\%) = \frac{Current\ concentration\ of\ protein\ at\ current\ pH}{The\ highest\ concentration\ of\ protein} \times 100 \quad (3)$$

$$Relative\ solubilty\ (\%) = \frac{Current\ concentration\ of\ protein\ at\ current\ NaCl}{The\ highest\ concentration\ of\ protein} \times 100 \quad (4)$$

2.5. Statistical Analysis

The values for the various parameters examined are reported as the mean ± standard deviation, assayed in triplicate. One-way analysis of variance (ANOVA) was used for statistical analysis, and IBM SPSS Statistics version 27.0 software was used (IBM Corp., Armonk, NY, USA).

3. Results and Discussion

3.1. Proximate Analysis

According to Table 1, the highest proximate needlefish skin composition was moisture at 61.65%, followed by protein (27.39%), lipid composition (8.59%), and ash (2.16%) with a significant difference ($p < 0.05$) between the proximate compositions that were analysed. The proportion of moisture is a reliable measure for the relative content of energy, protein, and lipids. The higher the protein and lipid composition and the higher the energy density of the fish, the lower the percentage of moisture [29]. According to the previous analyses, fish moisture contributes for 70 to 80% of its weight. In this study, moisture content was below 61.65%. This may be influenced by differences in fish species, habitat, genetics, and dietary habits [3]. Furthermore, in terms of protein content, marine fish tend to outperform freshwater fish. Proteins and lipids are major nutrients in fish and their levels help define the nutritional status of particular organisms.

Table 1. Proximate composition of needlefish skin.

Composition (%)	Skins Sample
Moisture	61.65 ± 1.15 [d]
Protein	27.39 ± 0.08 [c]
Lipid	8.59 ± 0.07 [b]
Ash	2.16 ± 0.03 [a]

Values are reported as mean ± SD (n = 3). Different lowercase letters indicate significant difference ($p < 0.05$).

Moreover, a high protein content was recorded, which is regarded as a most crucial ingredient in the food sector. However, the presence of lipids in this component can prompt food producers to use these wastes while processing foods. Moreover, different parts of the fish have different composition to other sections, such as the scales, fins, and bones. According to Maktoof et al. [30], the amount of proteins and lipids in *Cyprinus carpi* fish scales ranged between 22.1–23.99% and 1.9–2.3%, respectively. The fish's protein, lipid, and calorie density affect its moisture content. This is because proteins have high biological value and contain essential amino acids, whereas fish lipids contain both fatty acids and omega-3 fatty acids [31]. Following this, the swordfish ash content of its skin sample was reported at 2.16%. A significant excess of essential minerals in the skin may result in high ash levels [32].

3.2. Extraction Yield, Hydroxyproline Content, pH, Colour and Thermal Transition Measurement

Table 2 shows that the collagen yields of needlefish skin samples treated with different organic acids AAC, LAC, and CAC, all of which were significantly different at ($p < 0.05$). AAC produced the most collagen (3.13%), followed by CAC (1.03%) and LAC (0.56%). Due to the use of different acids during the extraction, the interaction of aldehydes with lysine and hydroxylin at the telopeptide helix region may account for differences in collagen yield among AAC, LAC, and CAC [15]. This may be due to the fact that various types of acids were employed to extract collagen from fish skin, and the pH of the combination was not kept at the same level as it was at the beginning of the process. This resulted in a shift in the amount of collagen that was extracted from the fish skin. A major reason that organic acids are used so frequently in collagen production studies is that the acid–collagen molecule interaction can split collagen crosslinks and is able to boost extraction efficiency. For instance, homogenization, mixing, acid dissolution, and extraction time can affect collagen yield [7]. Furthermore, based on previous studies, AAC should extract more collagen than CAC because the acid employed has a high capacity for collagen extraction [33]. This may be connected to the excess salt left behind after cellulose-tube dialysis, which increases collagen mass. This is clear when CAC has a rough surface and removable crystals. In addition, Skierka and Sadowska [34] reported that synthesised collagen from Baltic cod skin (*Gadus morhua*) using various acids produced different percentages of collagen, with the greatest collagen content formed from acetic acid and lactic acid, with a maximum yield of 90%, followed by citric acid with a yield of 60%. In contrast, the production of collagen with hydrochloric acid yielded the lowest percentage (18%). The yield of collagen extracted from marine fish skin has been reported in ranges from 49.8% to 51.4% [35]. However, Govindharaj et al. [36] revealed a final yield of eel skin collagen was around 4.2%.

In collagen extraction, the swelling percentage is as significant as the collagen yield content. This is because collagen can swell when the pH is decreased to 4 or elevated to 10 due to its inability to connect between portions of its molecular structure [37]. According to Table 1, there was a significant difference at ($p < 0.05$), indicating that the largest swelling percentage for CAA (226.37%), followed by CAC (210.41%), and LAC (198.37%). This significant swelling percentage indicates that the weight of the needlefish skin expanded fourfold from its original weight of 50 g. Furthermore, swelling is an important factor to consider in collagen extraction because it can impact the ability of collagen's internal molecular structure to connect to other proteins and enhance protein fragmentation by breaking non-covalent interactions [38]. Furthermore, according to Table 1, the value of

hydroxyproline content for all collagens demonstrated a significant difference ($p < 0.05$). AAC had a slightly higher hydroxyproline content of 81.69 mg/g, than LAC (79.07 mg/g) and CAC (79.95 mg/g). Kittiphattanabawon et al. [39] determined the hydroxyproline concentration in the skin and bones of a giant eye fish (*Priacanthus tayenus*) to be 58.5 mg/g and 42.4 mg/g, respectively. Additionally, hydroxyproline is an amino acid marker that supports collagen's triple helical structure and a substance used to quantify tissue collagen [40]. The hydroxyproline component is likewise found exclusively in collagen and is in negligible quantities compared to other proteins. As a result, it can provide a quantitative estimate of the amount of collagen present. Furthermore, the more the hydroxyproline content value, the greater the extractable collagen content [2].

Table 2. Extraction yield and physicochemical properties of acid-soluble collagen from the skin of needlefish (*Tylosurus acus melanotus*) extracted using different acid extraction methods.

Parameters	AAC	LAC	CAC
Yield (% dry weight basis)	3.13 ± 0.02 [c]	0.56 ± 0.011	1.03 ± 0.03 [b]
Swelling (%)	226.37± 0.03 [c]	198.37± 0.03 [a]	210.41± 0.16 [b]
Hydroxyproline content (mg/g dry sample)	81.69 ± 2.01 [b]	79.07 ± 0.3 [a]	79.95 ± 0.09 [a]
pH	4.85 ± 0.49 [a]	4.81 ± 0.19 [a]	4.51 ± 0.07 [a]
Colour scale, L*	69.77 ± 4.04 [b]	71.89 ± 1.52 [c]	57.14 ± 4.13 [a]
a*	0.15 ± 0.16 [a]	0.92 ± 0.22 [b]	0.73 ± 0.09 [b]
b*	5.52 ± 1.23 [a]	5.20 ± 0.02 [a]	4.69 ± 0.65 [a]
T_{max} (°C)	39.00± 0.25 [a]	38.60± 0.19 [a]	38.15 ± 0.12 [a]
Enthalpy (ΔH) (mJ/g)	0.0398	0.0346	0.0218

Values are reported as mean ± SD (n = 3). Different lowercase letters indicate significant difference ($p < 0.05$). The colour scale: L* (brightness), a* (green-reddish), and b* (brightness) (blue-yellowish). AAC: acetic acid collagen; LAC: lactic acid collagen; CAC: citric acid collagen.

Table 1 shows the results of the pH test for acid-soluble collagen, which indicates that there were no appreciable differences between the various types of acid extraction. The pH value of AAC was 4.85, which was higher than that of LAC (4.81) and CAC (4.51). Typically, a pH measurement of between 6 and 7 is considered ideal for collagen [41]. In contrast, the measurements of the pH of AAC, LAC, and CAC in this study did not exceed pH 6, which indicates that these compounds are acidic. This means that during the dialysis process, salts and acids could be removed completely, so there are still salts and acids left [42]. Additionally, the type of acid utilised and the amount of acid during the extraction process may contribute to differences in the pH of collagen [30]. This could also be the result of a pH neutralisation process that is not working to its full capacity. Another factor that could contribute to the low pH is that the pH of the collagen in the fish varies according to species [15].

In terms of colour, the quality of collagen can be measured. There are three values on the colour scale: L* (brightness), a* (green–reddish), and b* (brightness) (blue–yellowish). Table 1 shows the L* a* b* values for AAC, LAC, and CAC collagen samples. LAC had a higher L* colour scale value than AAC and CAC, with significant differences at ($p < 0.05$) of 71.89, 69.77, and 57.14, respectively. The colour scale a* revealed that LAC had the greatest value of 0.92, followed by CAC (0.73) and AAC (0.15), with a significant difference of ($p < 0.05$) between them. Furthermore, b* colour showed that the AAC sample recorded a reading of 5.52 that was slightly higher than CAC (5.20) and LAC (4.69), with no significant difference at ($p < 0.05$). In the thermal conversion of collagen, when collagen is heated, its triple helix breaks up into a random coil through a series of changes in viscosity, sedimentation, diffusion, light scattering, and other properties [43]. Protein denaturation is associated with the breakdown of tertiary structure and the loss of biological activity. Collagen denatures by detaching from its alpha chain and melting from its triple helix crystal [44]. According to several studies, marine collagen has less heat stability than mammalian collagen. The thermal stability of collagen is also closely connected to the environment and body temperature [45]. According to Table 1, the maximal transition

temperature, T_{max}, and the enthalpy (ΔH) for collagen AAC, LAC, and CAC were 39.00 °C, 38.60 °C, and 38.15 °C, respectively, and producing (ΔH) 0.0398 J/g, 0.0346 J/g, and 0.0218 J/g, respectively. These were slightly higher than the maximum temperatures recorded for collagens from catla skin, which were 34.99 °C, and 35.19 °C for collagens from rohu skin. Collagen has different thermal properties because its molecular structure breaks down when heated to high temperatures [46]. In the DSC, collagen absorbs heat when the temperature rises, and at a certain temperature, it starts to break down [15]. This study showed that the T_{max} values were greater than those typically found in fish collagen, which are usually less than 30 °C. This reveals that AAC, LAC, and CAC have great heat resistance and structural stability and could be utilised to replace mammalian collagen [47]. Generally, the collagen of fish species that inhabit high-temperature regions contains a higher concentration of amino acids and is more resistant to heat than the collagen of fish species that inhabit high-temperature regions with low elevations [45,48]. Another possible explanation is the intramolecular hydrogen bonds that stabilise collagen's triple helix shape may also break into many levels in the presence of acidity, leading to the repulsion of collagen molecules in an acidic solution [49].

3.3. Characterization Structure of Collagen

3.3.1. UV-VIS Absorption Spectra

Figure 1 represents the ultraviolet (UV) absorption spectra of collagen after treatment with three different acids ranging 210 nm to 400 nm in wavelength: AAC, LAC, and CAC. The absorption of needlefish skin collagen was measured at 231.5 nm (Figure 1). This was aligned with the normal absorption of collagen. Therefore, triple helix collagen has a prominent absorption peak near 230 nm [11]. Through peptide bonds and side chains, protein molecules, particularly collagen, absorb UV light. This indicates that peptide bonds are incorporated into the collagen polypeptide chain via n* transitions of C=O, -COOH, and -CO-NH2-groups [50]. Moreover, as the principal functional component in collagen with the ability to absorb UV and visible light, collagen is a potent antioxidant [51]. All extracted collagen had no absorption peaks at 250–280 nm (Figure 1). This is related to type I collagen that lacks aromatic residues, such as tryptophan, tyrosine, and phenylalanine, which are detected at wavelengths of 280 nm in collagen samples [11]. Based on the UV–VIS spectrum of AAC, LAC, and CAC samples (231.5 nm), samples had an absorption peak that is about the same as the study by Liao et al. [52], in which skin samples from Barramundi and Tilapia had absorption peaks of 230.3 nm and 230.9 nm, respectively. Furthermore, these values were equivalent to those obtained from the skins of Horse Mackerels (*Magalaspis cordyla*), Croaker (*Otolithes ruber*) [50] and Shabout (*Arabibarbus grypus* Heckel, 1843) [53].

3.3.2. Fourier Transform Infrared Spectroscopy (ATR-FTIR)

Figure 2 shows the FTIR spectra absorption rate measurements for ASC in the range 4000–800 cm^{-1}, which are comparable. All collagens contain a primary absorption band in the amide band region, however the FTIR spectra for AAC, LAC, and CAC differ slightly, suggesting that their secondary structures varied. Five major absorption peaks have been identified, amide A, amide B, amide I, amide II, and amide III [15].
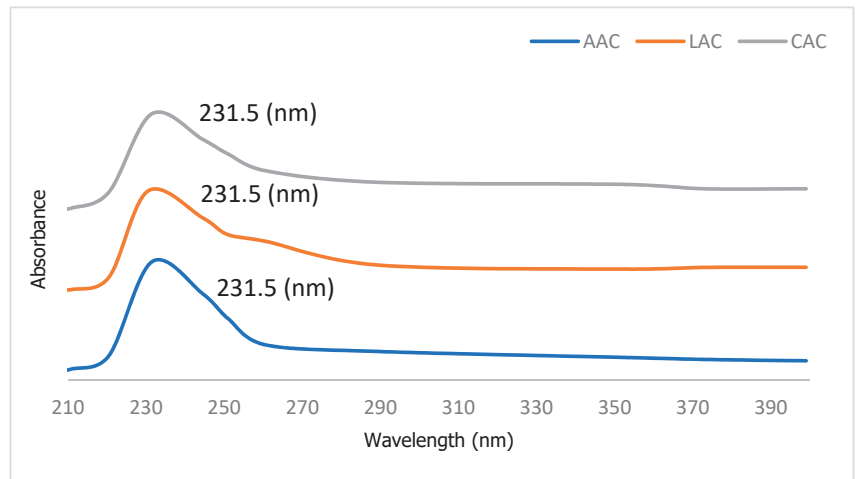
Figure 1. UV absorption of needlefish skin collagens extracted with different acids. AAC: acetic acid collagen; LAC: lactic acid collagen; CAC: citric acid collagen.
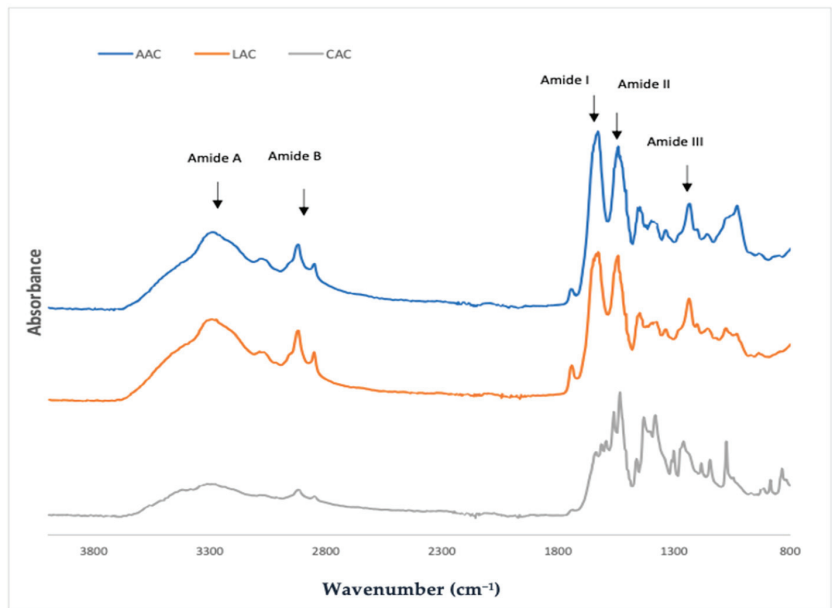
Figure 2. ATR-FTIR patterns of needlefish skin collagen extracted with different acids. AAC: acetic acid collagen; LAC: lactic acid collagen; CAC: citric acid collagen.

Previous studies have found that amide A peaks are typically recorded between 3400 and 3440 cm^{-1} and are frequently associated with N-H stretching vibrations. Nonetheless, in this study the amide A peak was the most prominent peak at (3289.46 cm^{-1}) for all collagen extractions, which were lower than previously reported. This is because the N-H stretching functional group of amide A interacts with amines of several proteins and complex molecules, shifting the amide A band to a lower frequency range than usual. It also suggests that hydrogen bonding exist in every collagen [39]. When the CH$_2$ group is stretched asymmetrically [36], amide B peaks are frequently observed in collagen. Amide B

readings for AAC were 2939.08 cm^{-1}, those for CAC were 2920.44 cm^{-1}, and the reading for LAC was marginally lower than those for AAC and CAC recorded at 2918.58 cm^{-1}. Amide I peaks are typically found between 1600 and 1700 cm^{-1} due to their strong absorption, which is principally caused by C=O stretching vibrations along the polypeptide spine [54]. Lower frequency number peaks are associated with a decrease in molecular organisation, making it a sensitive predictor of the secondary structure of peptides [55].

Amide I was found at the peak of this study, and the absorption rates of AAC, LAC, and CAC were all within the same range (1640.07 cm^{-1}). In addition, assessments of the amide II absorption rate for all extracted collagen remained within a similar range, 1541.30 cm^{-1}. The amide II peaks have wavelengths between 1500 and 1600 cm^{-1} and are associated with N-H bending and C-N stretching vibrations, as well as the helical shape of three collagens. Since the NH group in the peptide chain is involved in hydrogen bonding, CAC had a low value. As a result, the amide group's position moves to a lower intensity. When the wavelength decreases, the number of hydrogen bonds in collagen increases [54]. The amide peak of the peptide III bond indicates complicated interactions between molecules. As shown in Figure 2, it arises due to the C-N stretching and N-H bending vibrations of the peptide group. Amide III is detected for normal collagen range between 1200 cm^{-1} and 1350 cm^{-1} for maximum absorption. According to the data, the absorption rate of amide III was within the normal range for AAC (1231.92 cm^{-1}), CAC (1235.64 cm^{-1}) and LAC (1231.92 cm^{-1}). As amide III was in the standard range, a collagen triple helix structure could be observed [56].

3.3.3. Sodium Dodecyl Sulphate-Polyacrylamide Gel Electrophoresis (SDS-PAGE)

SDS-PAGE was performed to determine the protein pattern of collagen extracted with various acids. Figure 3 shows that the SDS-PAGE pattern demonstrated that all acid-treated collagens from swordfish skin were recognised as type I collagen. Figure 3 demonstrates collagen extracted using AAC, LAC, and CAC by a distinct 250 kDa band that is connected to two other bands to form a beta band, suggesting the presence of chain crosslinking links. Bands ranging from 130 to 100 kDa corresponded to the different chains—type I collagen containing two α1(I) chains and one α2(I) chain [57]. There were no variations in protein patterns found under reducing and non-reducing conditions (with or without beta-mercaptoethanol) for the collagen samples, demonstrating the absence of disulphide connections between chains. This is because cysteine and methionine are present in low levels in collagen type I [35]. Additionally, the lower bands show a lower molecular weight, which could be caused by non-collagenous proteins or collagen peptides made when only part of the collagen was broken down [30]. These results are comparable to previously reported for collagens taken from the skins of southern catfish (*Silurus meridionalis* Chen) [58], and hybrid sturgeon [30].

3.3.4. Effect of NaCl Solubility

Figure 4 shows the percentage relative solubility of all acid-soluble collagens (AAC, LAC, and CAC) with varied concentrations of sodium chloride (NaCl) ranging from 0 to 60 g/L. All collagens had a high relative solubility in the range of 0–10 g/L NaCl. This is because salt ions connect weakly to the surface of charged protein groups at low NaCl concentrations, and as a result, they do not upset any of the hydration loops on the collagen domain [51].
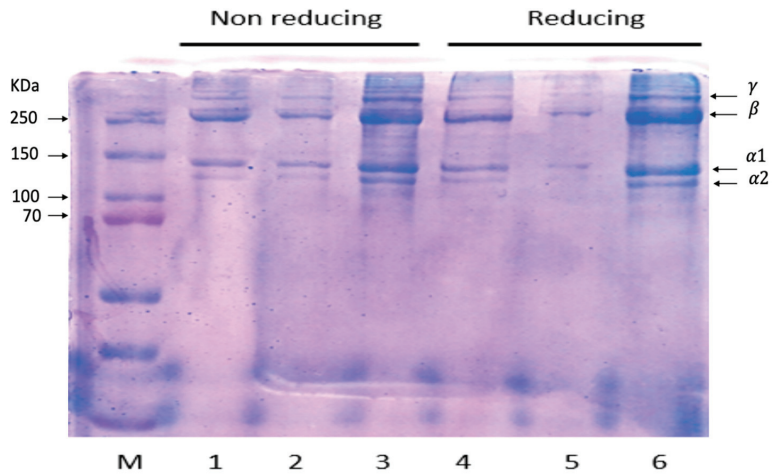
Figure 3. SDS-PAGE protein pattern of acids-soluble collagen for non-reducing and reducing conditions. Lane M: molecular weight marker; Lanes 1 and 4: acetic acid extraction (AAC); Lanes 2 and 5: lactic acid extraction (LAC); Lanes 3 and 6: citric acid extraction (CAC).
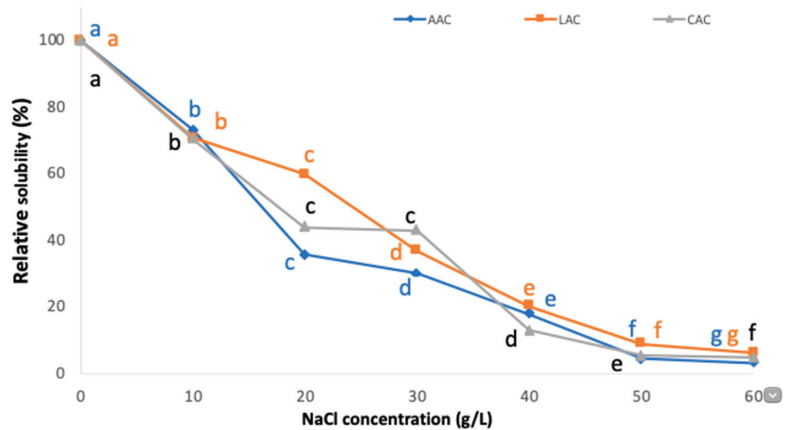
Figure 4. Effect of solubility of needlefish skin collagens extracted with different acids at different concentration of NaCl. AAC: acetic acid collagen; LAC: lactic acid collagen; CAC: citric acid collagen. Different letters indicated significant differences between the samples.

In most instances, the solubility of collagen in acetic acid at a concentration of 0.5 M decreased as the NaCl concentration increased [2]. The results were consistent to Pamungkas et al. [59] of collagen from haruan scales (*Channa striatus*) and Jamilah et al. [28] of collagen from barramundi skin (*Lates calcarifer*). At a NaCl concentration of 30 g/L, however, the graphs for all three acid-soluble collagens showed a substantial decrease in relative solubility to 50 g/L. Reduced collagen solubility may have resulted from the out-salting phenomenon, which occurs at relatively high NaCl concentrations. Increased salt concentration increases hydrophobic–hydrophobic interactions between protein chains and competition for water with salt ions [51]. In addition, this substantial decline can be attributed to the effects of salinization [24]. The solubility of collagen, for instance, is found to decrease with increasing salt chloride concentration. This results in a boost in ion strength, which in turn decreases protein solubility and precipitates stimulated proteins [55].

3.3.5. Effect of pH of Solubility

Figure 5 shows the effect of solubility of needlefish skin collagens extracted with different acids at different pH. The extracted collagen was examined by dissolving them in 0.5 M acetic acid before testing at pH 1, 3, 5, 7, 9 and 11. It was found that all three samples were highly soluble at pH 1.
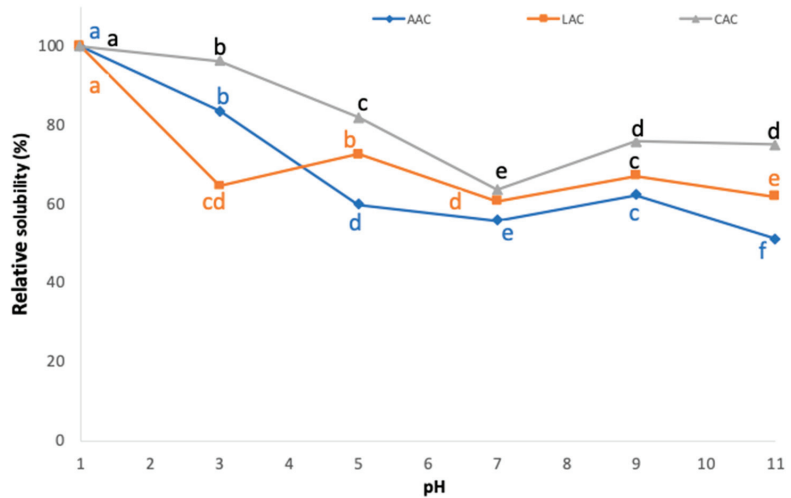
Figure 5. Effect of solubility of needlefish skin collagens extracted with different acids at different concentration of NaCl. AAC: acetic acid collagen; LAC: lactic acid collagen; CAC: citric acid collagen. Different letters indicated significant differences between the samples.

Generally, collagen protein is most soluble at pH values between 2 and 5, where it dissolves more than 80% [23]. Therefore, the solubility of AAC and CAC decreased as the pH rose over 3. Nurkhoeriyati et al. [60] reported pH 5–6 as the lowest solubility of myofibrillar protein. Due to hydrophobic interactions between collagen molecules, collagen becomes less soluble at neutral and alkaline pH values [17]. Based on the obtained solubility values, AAC indicated a drop in pH 5, 7, 9, and 11 when the relative solubility was less than 60%. Furthermore, the isoelectric point (pI) for all the extracted collagen was discovered at pH 7. According to Chen et al. [51], the increased hydrophobic–hydrophobic interactions between molecules in collagen causes the lower relative solubility. In addition, it was observed that the pH increased slightly from 7 to 9. This is due to the fact that relative solubility increases under situations with an acidic pH (pH 1). Moreover, the greater solubility can be attributed to a repulsive force that exists between the chains when the pH is either lower than or higher than the pI [17]. According to the Nalinanon et al. [23], collagen may be subject to molecular degradation, which can lead to reduced solubility.

4. Conclusions

The economical and ecological utilisation of fish skins resulting from industrial processing has attracted increasing interest. The variety of acids utilised influence the extraction of acid soluble collagen (ASC) from needlefish skin. In this study, pre-treatment and extraction with organic acids was found the acid–collagen molecular interaction can split collagen crosslinks and enhance extraction efficiency. The amount of hydroxyproline in each collagen of extracted from needlefish skin presented a significant difference ($p < 0.05$), with AAC (81.69 mg/g) having slightly more hydroxyproline than LAC (79.07 mg/g) and CAC (79.95 mg/g). It showed that extractable collagen was enhanced by the hydroxyproline content. The results revealed that lipid and pigment were eliminated by ASC extraction, and skin fibres were efficiently relaxed by the extraction methods. The yield and purity of

the extracted collagen were clearly increased, with yield percentages of 3.13%, 0.56%, and 1.03% for AAC, LAC, and CAC, respectively. Collagen has been fully characterised in terms of its structure, physicochemical properties, and biological roles. Analysis of the UV spectra, FTIR spectroscopy, and thermal stability identified the collagen obtained from fish skin as type I. Moreover, the collagen recovered from fish skins revealed that its denaturation temperature, T_{max} was comparable to that of collagen taken from terrestrial skin. These results show that needlefish skin collagen can be employed in industrial applications.

References

1. Gao, R.; Yu, Q.; Shen, Y.; Chu, Q.; Chen, G.; Fen, S.; Yang, M.; Yuan, L.; Clements, D.J.M.; Sun, Q. Production, bioactive properties, and potential applications of fish protein hydrolysates: Developments and challenges. *Trends Food Sci. Technol.* **2021**, *110*, 687–699. [CrossRef]
2. Oslan, S.N.H.; Li, C.X.; Shapawi, R.; Mokhtar, R.A.M.; Noordin, W.N.M.; Huda, N. Extraction and characterization of bioactive fish by-product collagen as promising for potential wound healing agent in pharmaceutical applications: Current trend and future perspective. *Int. J. Food Sci.* **2022**, *2022*, 9437878. [CrossRef] [PubMed]
3. Nurilmala, M.; Suryamarevita, H.; Husein Hizbullah, H.; Jacoeb, A.M.; Ochiai, Y. Fish skin as a biomaterial for halal collagen and gelatin. *Saudi J. Biol. Sci.* **2022**, *29*, 1100–1110. [CrossRef]
4. Schmidt, M.; Dornelles, R.C.P.; Mello, R.; Mazutti, M.; Demiate, I. Collagen extraction process. *Int. Food Res. J.* **2016**, *23*, 913–922.
5. Baco, N.; Oslan, S.N.H.; Shapawi, R.; Mohhtar, R.A.M.; Noordin, W.N.M.; Huda, N. Antibacterial activity of functional bioactive peptides derived from fish protein hydrolysate. *IOP Conf. Ser. Earth Environ. Sci.* **2022**, *967*, 012019. [CrossRef]
6. Coppola, D.; Oliviero, M.; Vitale, G.A.; Lauritano, C.; D'Ambra, I.; Iannace, S.; de Pascale, D. Marine collagen from alternative and sustainable sources: Extraction, processing and applications. *Mar. Drugs* **2020**, *184*, 214. [CrossRef]
7. Muralidharan, N.; Jeya, S.R.; Sukumar, D.; Jeyasekaran, G. Skin, bone and muscle collagen extraction from the trash fish, Leather Jacket (*Odonus niger*) and their characterization. *J. Food Sci. Technol.* **2013**, *50*, 1106–1113. [CrossRef]
8. Mahboob, S. Isolation and characterization of collagen from fish waste material-skin, scales and fins of Catla catla and *Cirrhinus mrigala*. *J. Food Sci. Technol.* **2015**, *52*, 4296–4305. [CrossRef]
9. Munawaroh, H.S.H.; Gumilar, G.G.; Berliana, J.D.; Aisyah, S.; Nuraini, V.A.; Ningrum, A.; Susanto, E.; Martha, L.; Kurniawan, I.; Hidayati, N.A.; et al. In Silico proteolysis and molecular interaction of Tilapia (*Oreochromis niloticus*) skin collagen-derived peptides for environmental remediation. *Environ. Res.* **2022**, *212*, 113002. [CrossRef]
10. Furtado, M.; Chen, L.; Chen, Z.; Chen, A.; Cui, W. Development of fish collagen in tissue regeneration and drug delivery. *Eng. Regen.* **2022**, *3*, 217–231. [CrossRef]
11. He, L.; Lan, W.; Wang, Y.; Liu, Y. Extraction and characterization of self-assembled collagen isolated from Grass carp and Crucian carp. *Foods* **2019**, *8*, 396. [CrossRef] [PubMed]
12. Kuwahara, J. Extraction of type I collagen from Tilapia scales using acetic acid and ultrafine bubbles. *Processes* **2021**, *9*, 288. [CrossRef]
13. Liu, D.; Wei, G.; Li, T.; Hu, J.; Lu, N.; Regenstein, J.M.; Zhou, P. Effects of alkaline pretreatments and acid extraction conditions on the acid-soluble collagen from Grass carp (*Ctenopharyngodon idella*) skin. *Food Chem.* **2015**, *172*, 836–843. [CrossRef] [PubMed]
14. Prestes, R.C. Colágeno e seus derivados: Características e aplicações em produtos cárneos. *Rev. Unopar Cíent. Ciênc. Biol. Saúde* **2013**, *1*, 65–74.
15. Jafari, H.; Lista, A.; Siekapen, M.M.; Ghaffari-Bohlouli, P.; Nie, L.; Alimoradi, H.; Shavandi, A. Fish collagen: Extraction, characterization, and applications for biomaterials engineering. *Polymers* **2020**, *12*, 2230. [CrossRef] [PubMed]
16. Subhan, F.; Ikram, M.; Shehzad, A.; Ghafoor, A. Marine collagen: An emerging player in biomedical applications. *J. Food Sci. Technol.* **2015**, *52*, 4703–4707. [CrossRef]
17. Chuaychan, S.; Benjakul, S.; Kishimura, H. Characteristics of acid- and pepsin-soluble collagens from scale of Seabass (*Lates calcarifer*). *LWT-Food Sci. Technol.* **2015**, *63*, 71–76. [CrossRef]

18. AOAC. *Official Maethods of Analysis of AOAC International*, 17th ed.; Association of the Official Analytical Chemists (AOAC) International: Gaithersburg, MD, USA, 2003. Available online: https://ums.on.worldcat.org/oclc/476567963 (accessed on 5 January 2022).

19. Zaelani, B.; Safithri, M.; Tarman, K.; Setyaningsih, I. Collagen isolation with acid soluble method from the skin of Red snapper (*lutjanus* sp.). *IOP Conf. Ser. Earth Environ. Sci.* **2019**, *241*, 012033. [CrossRef]

20. Normah, I.; Maidzatul, A.M. Effect of extraction time on the physico-chemical characteristics of collagen from Sin croaker (*Johniecop sina*) waste. *Int. Food Res. J.* **2018**, *25*, 1074–1080.

21. Huda, N.; Seow, E.K.; Normawati, M.N.; Nik Aisyah, N.M.; Fazilah, A.; Easa, A.M. Effect of duck feet collagen addition on physicochemical properties of surimi. *Int. Food Res. J.* **2013**, *20*, 537–544.

22. Huda, N.; Seow, E.K.; Normawati, M.N.; Nik Aisyah, N.M.; Fazilah, A.; Easa, A.M. Preliminary study on physicochemical properties of duck feet collagen. *Int. J. Poult. Sci.* **2013**, *12*, 615–621. [CrossRef]

23. Nalinanon, S.; Benjakul, S.; Visessanguan, W.; Kishimura, H. Use of pepsin for collagen extraction from the skin of bigeye snapper (*Priacanthus tayenus*). *Food Chem.* **2007**, *104*, 593–601. [CrossRef]

24. Matmaroh, K.; Benjakul, S.; Prodpran, T.; Encarnacion, A.B.; Kishimura, H. Characteristics of acid soluble collagen and pepsin soluble collagen from scale of spotted golden Goatfish (*Parupeneus heptacanthus*). *Food Chem.* **2011**, *129*, 1179–1186. [CrossRef] [PubMed]

25. Chinh, N.T.; Manh, V.Q.; Trung, V.Q.; Lam, T.D.; Huynh, M.D.; Tung, N.Q.; Hoang, T. Characterization of collagen derived from tropical freshwater carp fish scale wastes and its amino acid sequence. *Nat. Prod. Commun.* **2019**, *14*, 1934578X19866288. [CrossRef]

26. Jeong, H.S.; Venkatesan, J.; Kim, S.K. Isolation and characterization of collagen from marine fish (*Thunnus obesus*). *Biotechnol. Bioprocess Eng.* **2013**, *18*, 1185–1191. [CrossRef]

27. Zeng, S.; Yin, J.; Yang, S.; Zhang, C.; Yang, P.; Wu, W. Structure and characteristics of acid and pepsin-solubilized collagens from the skin of Cobia (*Rachycentron canadum*). *Food Chem.* **2012**, *135*, 1975–1984. [CrossRef] [PubMed]

28. Jamilah, B.; Hartina, M.U.; Hashim, D.M.; Sazili, A.Q. Properties of collagen from Barramundi (*Lates calcarifer*) skin. *Int. Food Res. J.* **2013**, *20*, 835–842.

29. Depmson, I.B.; Schwarz, C.J.; Shea, M. Comparative proximate body Atlantic salmon with emphasis on parr from fluvial and lacustrine habitats. *J. Fish. Biol.* **2004**, *64*, 1257–1271.

30. Maktoof, A.A.; Jafar Elherarlla, R.; Ethaib, S. Identifying the nutritional composition of fish waste, bones, scales, and fins. *IOP Conf. Ser. Mater Sci. Eng.* **2020**, *871*, 012013. [CrossRef]

31. Nurnadia, A.A.; Azrina, A.; Amin, I. Proximate composition and energetic value of selected marine fish and shellfish coast of peninsular Malaysia. *Int. Food Res. J.* **2011**, *18*, 137–148.

32. da Trindade Alfaro, A.; Simões Da Costa, C.; Graciano Fonseca, G.; Prentice, C. Effect of extraction parameters on the properties of gelatin from King weakfish (*Macrodon ancylodon*) bones. *Food Sci. Technol. Int.* **2011**, *15*, 553–562. [CrossRef]

33. Wei, P.; Zheng, H.; Shi, Z.; Li, D.; Xiang, Y. Isolation and charazterication of acid-soluble collagen and pepsin-soluble collagen from the skin of hybrid Sturgeon. *J. Wuhan Univ. Technol. Mater. Sci. Ed.* **2019**, *34*, 950–959. [CrossRef]

34. Skierka, E.; Sadowska, M. The influence of different acids and pepsin on the extractability of collagen from the skin of Baltic cod (*Gadus morhua*). *Food Chem.* **2007**, *105*, 1302–1306. [CrossRef]

35. Nagai, T.; Suzuki, N. Isolation of collagen from fish waste material—Skin, bone and fins. *Food Chem.* **2000**, *68*, 277–281. [CrossRef]

36. Govindharaj, M.; Roopavath, U.K.; Rath, S.N. Valorization of discarded Marine Eel fish skin for collagen extraction as a 3D printable blue biomaterial for tissue engineering. *J. Clean. Prod.* **2019**, *230*, 412–419. [CrossRef]

37. Liu, D.C.; Lin, Y.K.; Chen, M.T. Optimum condition of extracting collagen from chicken feet and its characteristics. *Asian-Australas. J. Anim. Sci.* **2001**, *14*, 1638–1644. [CrossRef]

38. Cheng, F.Y.; Hsu, F.W.; Chang, H.S.; Lin, L.C.; Sakata, R. Effect of different acids on the extraction of pepsin-solubilised collagen containing melanin from silky fowl feet. *Food Chem.* **2009**, *113*, 563–567. [CrossRef]

39. Kittiphattanabawon, P.; Benjakul, S.; Visessanguan, W.; Nagai, T.; Tanaka, M. Characterisation of acid-soluble collagen from skin and bone of Bigeye snapper (*Priacanthus tayenus*). *Food Chem.* **2005**, *89*, 363–372. [CrossRef]

40. Blanco, M.; Vázquez, J.A.; Pérez-Martín, R.I.; Sotelo, C.G. Hydrolysates of fish skin collagen: An opportunity for valorizing fish industry byproducts. *Mar. Drugs* **2017**, *15*, 131. [CrossRef]

41. Sionkowska, A.; Kozłowska, J.; Skorupska, M.; Michalska, M. Isolation and characterization of collagen from the skin of Brama australis. *Int. J. Biol. Macromol.* **2015**, *80*, 605–609. [CrossRef]

42. Angel Martínez-Ortiz, M.; Delia Hernández-Fuentes, A.; Pimentel-González, D.J.; Campos-Montiel, R.G.; Vargas-Torres, A.; Aguirre-Álvarez, G. Extraction and characterization of collagen from rabbit skin: Partial characterization. *CYTA J. Food* **2015**, *13*, 253–258. [CrossRef]

43. Usha, R.; Ramasami, T. The effects of urea and n -propanol on collagen denaturation: Using DSC, circular dicroism and viscosity. *Thermochim. Acta* **2004**, *409*, 201–206. [CrossRef]

44. Capella-Monsonís, H.; Coentro, J.Q.; Graceffa, V.; Wu, Z.; Zeugolis, D.I. An experimental toolbox for characterization of mammalian collagen type I in biological specimens. *Nat. Protoc.* **2018**, *13*, 507–529. [CrossRef]

45. Zhang, J.; Tu, X.; Wang, W.; Nan, J.; Wei, B.; Xu, C.; Lang, H.; Yuling, X.; Sheng, L.; Wang, H. Insight into the role of grafting density in the self-assembly of acrylic acid-grafted-collagen. *Int. J. Biol. Macromol.* **2019**, *128*, 885–892. [CrossRef] [PubMed]

46.   Kumar, N.S.S.; Nazeer, R.A. Erratum to: Wound healing properties of collagen from the bone of two marine fishes. *Int. J. Pept. Res. Ther.* **2012**, *18*, 193. [CrossRef]

47.   Liu, D.; Liang, L.; Regenstein, J.M.; Zhou, P. Extraction and characterisation of pepsin-solubilised collagen from fins, scales, skins, bones and swim bladders of Bighead carp (*Hypophthalmichthys nobilis*). *Food Chem.* **2012**, *133*, 1441–1448. [CrossRef]

48.   Wang, J.; Pei, X.; Liu, H.; Zhou, D. Extraction and characterization of acid-soluble and pepsin-soluble collagen from skin of Loach (*Misgurnus anguillicaudatus*). *Int. J. Biol. Macromol.* **2018**, *106*, 544–550. [CrossRef]

49.   Ahmad, M.; Benjakul, S. Extraction and characterisation of pepsin-solubilised collagen from the skin of unicorn Leather jacket (*Aluterus monocerous*). *Food Chem.* **2010**, *120*, 817–824. [CrossRef]

50.   Kumar, N.S.S.; Nazeer, R.A. Characterization of acid and pepsin soluble collagen from the skin of Horse mackerels (*Magalaspis cordyla*) and Croaker (*Otolithes ruber*). *Int. J. Food Prop.* **2013**, *16*, 613–621. [CrossRef]

51.   Chen, S.; Chen, H.; Xie, Q.; Hong, B.; Chen, J.; Hua, F.; Bai, K.; He, J.; Yi, R.; Wu, H. Rapid isolation of high purity pepsin-soluble type I collagen from scales of Red drum fish (*Sciaenops ocellatus*). *Food Hydrocoll.* **2016**, *52*, 468–477. [CrossRef]

52.   Liao, W.; Guanghua, X.; Li, Y.; Shen, X.R.; Li, C. Comparison of characteristics and fibril-forming ability of skin collagen from Barramundi (*Lates calcarifer*) and Tilapia (*Oreochromis niloticus*). *Int. J. Biol. Macromol.* **2018**, *107*, 549–559. [CrossRef]

53.   Göçer, M. Extraction and characterization of collagen from the skin and bone of Shabout (*Arabibarbus grypus* Heckel, 1843). *Iran. J. Fish. Sci.* **2022**, *21*, 671–687.

54.   Hukmi, N.M.M.; Sarbon, N.M. Isolation and characterization of acid soluble collagen (ASC) and pepsin soluble collagen (PSC) extracted from silver Catfish (*Pangasius* sp.) skin. *Int. Food Res. J.* **2018**, *6*, 2601–2607.

55.   Yu, D.; Chi, C.F.; Wang, B.; Ding, G.F.; Li, Z.R. Characterization of acid-and pepsin-soluble collagens from spines and skulls of skipjack tuna (*Katsuwonus pelamis*). *Chin. J. Nat. Med.* **2014**, *12*, 712–720. [CrossRef] [PubMed]

56.   Saallah, S.; Roslan, J.; Julius, F.S.; Saallah, S.; Mohamad Razali, U.H.; Pindi, W.; Sulaiman, M.R.; Pa'ee, K.F.; Mustapa, K.S.M. Comparative study of the yield and physicochemical properties of collagen from Sea cucumber (*Holothuria scabra*), obtained through dialysis and the ultrafiltration membrane. *Molecules* **2021**, *26*, 2564. [CrossRef]

57.   Seixas, M.J.; Martins, E.; Reis, R.L.; Silva, T.H. Extraction and characterization of collagen from elasmobranch byproducts for potential biomaterial use. *Mar. Drugs* **2020**, *18*, 617. [CrossRef]

58.   Xu, S.; Yang, H.; Shen, L.; Li, G. Purity and yield of collagen extracted from southern Catfish (*Silurus meridionalis* Chen) skin through improved pretreatment methods. *Int. J. Food Prop.* **2017**, *20*, S141–S153. [CrossRef]

59.   Pamungkas, B.F.; Murdiati, A.S.; Indrati, R. Characterization of the acid- and pepsin-soluble collagens from Haruan (*Channa striatus*) Scales. *Pak. J. Nutr.* **2019**, *18*, 324–332. [CrossRef]

60.   Nurkhoeriyati, T.; Huda, N.; Ahmad, R. Gelation properties of spent duck meat surimi-like material produced using acid-alkaline solubilization methods. *J. Food Sci.* **2011**, *76*, S48–S55. [CrossRef]

Article

Nutrient Composition, Antioxidant Activities and Glycaemic Response of Instant Noodles with Wood Ear Mushroom (*Auricularia cornea*) Powder

Muhammad Kamil Zakaria [1], Patricia Matanjun [1,*], Ramlah George [1], Wolyna Pindi [1], Hasmadi Mamat [1], Noumie Surugau [2] and Jaya Seelan Sathiya Seelan [3]

[1]   Faculty of Food Science & Nutrition, Universiti Malaysia Sabah, Jalan UMS, Kota Kinabalu 88400, Sabah, Malaysia

[2]   Faculty of Science and Natural Resources, Universiti Malaysia Sabah, Jalan UMS, Kota Kinabalu 88400, Sabah, Malaysia

[3]   Institute for Tropical Biology and Conservation, Universiti Malaysia Sabah, Jalan UMS, Kota Kinabalu 88400, Sabah, Malaysia

*   Correspondence: patsy@ums.edu.my

Abstract: *Auricularia cornea,* or wood ear mushroom (WEM), is an edible macrofungus that is popular as a delicacy and for various biological activities. This study aims to determine the nutrient composition, in vitro antioxidant activities and the effect on postprandial blood glucose in human subjects after consuming instant noodles incorporated with 5% WEM powder. The proximate composition of WEM powder was 9.76% moisture, 2.40% ash, 7.52% protein, 0.15% fat, 37.96% crude fibre, 42.21% carbohydrate, and a total dietary fibre was 69.43%. Meanwhile, the proximate composition of 5% WEM noodles was 10.21% moisture, 2.87% ash, 11.37% protein, 0.16% fat, 5.68% crude fibre and 68.96% carbohydrates, while the total dietary fibre was 13.30%. The mineral content of WEM powder in decreasing order: potassium > calcium > magnesium > sodium > iron > zinc > manganese > copper > selenium > chromium. The incorporation of 5% WEM powder significantly ($p < 0.05$) reduced carbohydrates and increased the ash, crude fibre and total dietary fibre, antioxidant activities and total phenolic content of the instant noodles. Furthermore, the incorporation of 5% WEM significantly increased potassium, calcium, magnesium, iron, and zinc content. The addition of WEM powder reduced the postprandial glycaemic response and produced a moderate glycaemic index (GI). In conclusion, the incorporation with WEM powder could be an effective way of developing nutritious and low GI instant noodles, thus, improving nutrient intake and human health.

Keywords: *Auricularia cornea*; wood ear mushroom; instant noodles; glycaemic response

1. Introduction

The wood ear mushroom (WEM) is a wood-decaying fungi from the genus Auricularia, commonly known as jelly or black fungus. Its distinct gelatinous ear-like shape, fruiting body and brown-to-black colouration have unique sensory features and are rich in medicinal properties [1,2]. Similar to other edible mushrooms, the WEM is low in fat and calories and a good source of protein, fibre, essential elements, and bioactive compounds [3]. The WEM has been reported to exhibit several biological activities, such as antioxidant [4], antimicrobial [5], anti-inflammatory [6], immunomodulatory [7], hypoglycaemic [8], and hypocholesterolemic effects [9], all of which contribute to good health. The WEM is a promising solution for disease prevention through incorporation as an ingredient in supplements or food products in the nutraceutical, pharmaceutical, and food industries [10]. Nonetheless, this novel ingredient remains underutilised because of consumer preferences for other edible mushrooms, such as oyster and button mushrooms. Furthermore, there is limited data on the locally grown WEM as a functional ingredient.

The incorporation of instant noodles with various ingredients to improve minerals, fibre, and vitamin content, is a popular practice [11,12]. Conversely, the use of mushrooms as a functional element in instant noodles is relatively new. Few studies have incorporated edible mushrooms such as oyster and shitake mushrooms, but there have been no reports on WEM utilisation [13–17]. According to the literature, the incorporation of mushroom powder significantly improved the proximate composition of noodles in terms of protein and fibre content, but information regarding antioxidant activities is limited. In terms of sensory quality, several studies that used different types of mushroom species found the incorporation of more than 5% would negatively affect the sensory quality of the noodles, especially the texture and taste [14,15,18]. Furthermore, the potential of WEM polysaccharides to exhibit the hypoglycaemic effect has widely been discussed, but the scientific evidence is limited to animal studies [3,19]. Previous studies have demonstrated that the incorporation of *Auricularia* spp. into the diet could induce hypoglycaemia in genetically diabetic mice [20–22]. Similarly, in vitro studies by Vallee et al. (2017) and Wu et al. (2014) also showed the hypoglycaemic effect of *Auricularia* spp. where 5% of the *Auricularia* mushroom powder was able to attenuate in vitro starch digestion [23,24]. Therefore, this present study examined the nutrient composition, antioxidant activities, and the effect on postprandial blood glucose levels of WEM powder and instant noodles incorporated with WEM powder. The study findings could add value to the product by improving nutrient qualities, hence, providing healthier food choices for consumers.

2. Materials and Methods

2.1. Sample Preparation

The WEM or *A. cornea* (previously known as *A. polytricha*) was cultivated and supplied by the Rural Development Corporation, a government agency under the Sabah Ministry of Agriculture and Fisheries. The fresh WEM was dried at 50 °C for 24 h in a dehydrator (Cabela's 80 L, Sidney, NE, USA), ground into 250 µm powder and stored in an air-tight container for further use.

The instant noodle was formulated based on Sulaiman et al. with slight modifications [25]. The ingredients were purchased from the local supermarket, and filtered tap water from the laboratory was utilised in the making of instant noodles. The formulation of the control instant noodles comprised 100% all-purpose wheat flour (Johor Flour Mill, Johor, Malaysia), 38% water, 2.5% iodide salt (Adabi, Rawang, Malaysia), and 1.2% sodium bicarbonate (Kings, Pulau Pinang, Malaysia). In the modified instant noodle, 5% of the wheat flour was replaced with the WEM powder, while the remaining ingredients were unchanged. All ingredients were weighed accordingly. Water was mixed with salt and sodium bicarbonate before the solution was added gradually into the flour until it formed a dough. The dough was rested for 30 min before the sheeting process to reduce the dough thickness to 2–3 mm and obtain a smooth surface. The dough was cut into equal lengths and air-steamed for 8 min before it was finally dried overnight (24 h) at 50 °C using a dehydrator (Cabela's 80 L, Sidney, NE, USA).

2.2. Proximate Composition Analysis

The moisture, ash, crude fat, crude protein, and crude fibre content, were determined using the standard Association of Analytical Chemists (AOAC) methods [26]. The moisture content was determined after drying the noodles overnight at 105 °C in a universal oven (Binder Inc., Bohemia, NY, USA). The ash content was determined after the dried sample was incinerated in the furnace (Carbolite Gero Ltd., Derbyshire, UK) overnight at a temperature of 550 °C. Meanwhile, the fat content was determined via the Soxhlet method using the Soxhlet Avanti auto system and petroleum ether as the solvent (Soxtec™ 2050, FOSS, Hillerød, Denmark). The protein content was then determined after the sample was digested with concentrated sulphuric acid (H_2SO_4) and selenium tablet using a digester (KJELDATHERM, Gerhardt GmbH, Königswinter, Germany) before being calculated by an automated Kjeldahl machine (Kjeltec, Foss, Hillerød, Denmark). The conversion factor used

to determine the crude protein in the mushroom was 4.38, and 6.25 for general food [27]. The crude fibre content was determined based on the weight of the sample, which was digested and filtered using the machine (Fibertherm, Gerhardt, Brackley, UK), followed by overnight drying in a universal oven (Binder Inc., Bohemia, NY, USA) and 4 h of ashing using furnace (Carbolite Gero Ltd., Derbyshire, UK). Finally, the carbohydrate content was calculated from the sum of percentages of crude protein, ash, fat, and crude fibre subtracted from 100.

2.3. Total Dietary Fibre (TDF)

The TDF was determined using the Total Dietary Fiber Assay Kit (Megazyme International Ireland Limited, Wicklow, Ireland) based on AOAC enzymatic-gravimetric methods 985.29. A sample was mixed with 50 mL phosphate buffer solution (pH 6.0 ± 0.1) before 50 μL a-amylase was added, and the mixture was boiled for 30 min. Then, the pH was adjusted to 7.5 ± 0.1 by adding 0.275 N of sodium hydroxide (NaOH) and 100 μL protease. The mixture was then incubated at 60 °C with continuous agitation for 30 min. Next, 0.325 N hydrochloric acid (HCl) was added to adjust the pH to 4.5 ± 0.2 before adding 200 μL amyloglucosidase, and the solution was incubated at 60 °C for 30 min. The mixture was filtered through a crucible containing fritted glass disk and Celite 545, followed by three washings of 20 mL 75% ethanol, two 10 mL 95% ethanol and two 10 mL portions of acetone before being dried overnight at 105 °C and weighed. Finally, the dried residue was analysed for protein content using the Kjeldahl method and a duplicate residue was analysed for ash. The weights of protein and ash were subtracted from the residue weight obtained to determine the insoluble dietary fibre.

2.4. Mineral Analysis

The mineral quantification of copper, zinc, chromium, calcium, magnesium, potassium, sodium, iron, manganese, and selenium, was performed according to the AOAC method [26]. The dry samples were added with 10 mL of 65% nitric acid (HNO_3) before the mixture was heated until the brown smoke was undetectable. Then, 2 mL of distilled water and 3 mL of hydrogen peroxide (H_2O_2) were added to the solution and heated until the total volume was reduced to 5 mL. Next, 10 mL HCl was added to the solution and reheated for 15 min. Finally, the mixture was filtered and transferred to a volumetric flask for dilution. The quantification of elements was carried out using the Inductive Coupled Plasma-Optical Emission Spectrometer (ICP-OES) (Perkin Elmer, Waltham, MA, USA).

2.5. Antioxidant Activities Analysis

The samples were soaked in methanol for 24 h and agitated at 150 rpm at room temperature twice [28]. Both filtrations were combined, and the solvent was removed via evaporation with a rotary evaporator at 40 °C. The dried extracts were stored in a dark place at 4 °C until further use.

The scavenging activity of 2, 2-diphenyl-2-picryl-hydrazyl (DPPH) inhibition by the extracts was determined based on Teoh et al. with modification [29]. The extract at various concentrations was added to 2.9 mL of methanolic DPPH radical solution (6×10^{-5} M). The mixture was shaken vigorously and left to stand for 45 min at 25 °C in the dark. The mixture absorbance was then measured at 517 nm with a UV-VIS spectrophotometer (Lambda 35 UV–VIS Spectrometer, PerkinElmer, Waltham, MA, USA), and Trolox (Merck, EMD Millipore Corporation, Darmstadt, Germany) was used as the calibration standard while methanol mix with DPPH radical was the negative control. The results were reported as the IC_{50} Of WEM.

Next, the ferric-reducing antioxidant power (FRAP) assay of the WEM extract was determined based on the method by Yim et al. with some modifications [30]. The FRAP reagent was prepared freshly, containing 300 mM acetate buffer (pH 3.6), 10 mM TPTZ in 40 mM HCl and 20 Mm iron (III) chloride ($FeCl_3$) at a ratio of 10:1:1 at a temperature of 37 ± 2 °C. The reagent (200 μL) was mixed with 20 μL methanol extract, and the

absorbance at 593 nm was recorded after 10 min using a UV–VIS spectrophotometer (Lambda 35 UV–VIS Spectrometer, PerkinElmer, Waltham, MA, USA). Iron (II) sulfate heptahydrate ($FeSO_4.7H_2O$) (Systerm, Classic Chemicals Sdn. Bhd., Shah Alam, Selangor, Malaysia) was used as a standard for a calibration curve.

The total phenolic compound (TPC) of the sample extract was determined based on the Folin-Ciocalteu assay by Teoh et al., with some modifications [29]. The methanol extract (200 µL) was transferred into a test tube and mixed thoroughly with 1 mL of Folin-Ciocalteu reagent. After 3 min, 0.8 mL of 7.5% (w/v) sodium carbonate (Na_2CO_3) was added to the mixture and agitated for 30 min in the dark. The absorbance of the extracts and prepared blank were measured at 515 nm using a UV–VIS spectrophotometer (Lambda 35 UV–VIS Spectrometer, PerkinElmer, Waltham, MA, USA). The result was represented as mg of gallic acid equivalents (GAE) per gram extract.

2.6. Glycaemic Analysis (Blood Glucose Measurement and Calculation of Glycaemic Index)

Ethical approval for this study was granted by the Medical Research Ethics Committee of Universiti Malaysia Sabah [JKEtika 2/21(16)]. The analysis was conducted at the Nutrition and Dietetic Laboratory, Faculty of Food Science and Nutrition, Universiti Malaysia Sabah. The protocol for glycaemic analysis was conducted according to Wolever et al. [31].

Ten healthy volunteers participated in this study. Participants were given a subject information sheet with details of the study protocol and had the opportunity to ask questions. They signed an informed consent before participating in the study. Inclusion criteria of study participants are as follows: age 23 to 31 years old and non-smoker, normal body mass index (BMI) (19 and 25 kg/m^2), and has normal fasting blood glucose level (<5.6 mmol/L). Individuals that were pregnant, allergic to food, hypersensitive, restricted or specified diet, inflammatory or metabolic diseases, and prescribed with medications that may interfere with carbohydrate metabolism, were excluded from participating in this study.

Each participant completed five sessions of glycaemic index trials: three sessions for reference carbohydrates (50 g of glucose dissolved in 250 mL of water) and one session for control instant noodles and one session for instant noodles incorporated with 5% WEM as a test food. The sessions were carried out on separate days. The order of the test food, control and reference that were tested by each participant was randomised using online tool Research Randomizer (Version 4.0) [32]. The analysis was conducted in the morning after the participant fasted overnight for a minimum of 10 h. Blood glucose levels were measured in capillary blood obtained by finger prick using a lancet (ACCU-CHEK® Safe T-Pro Plus, Roche, Basel, Switzerland), blood glucose test strip (Freestyle Freedom Lite®, Abbott Laboratories, Chicago, IL, USA) and glucometer (Freestyle Freedom Lite®, Abbott Laboratories, Chicago, IL, USA). Blood sugar levels were measured at seven time points (0, 15, 30, 45, 60, 90, and 120 min). The glycaemic response or the incremental area under the curve (IAUC) for each reference and test food was calculated by the trapezoid rule [33].

The glycaemic index (GI) was calculated by using Equation (1) [31].

$$GI = (IAUC \text{ of the test food}/\text{the IAUC of reference food}) \times 100 \qquad (1)$$

2.7. Data Analysis

The experiments were carried out in triplicates, and the data were presented as average values. Statistical Package for the Social Science (SPSS) version 26 for Windows (SPSS Inc., Chicago, IL, USA) was used in the statistical analysis. First, the independent t-test was used to determine significant differences ($p < 0.05$) in the mean value of proximate composition and mineral content between samples. The analysis of variance (ANOVA) test was then performed to determine the significant differences ($p < 0.05$) in the mean value of antioxidant activities and total phenolic content between samples. A paired T-test was used for the mean comparison of postprandial blood glucose response within 120 min between control and incorporated instant noodles with 5% WEM. The mean of IAUC between reference and test food was compared using ANOVA and Tukey's B post-hoc for multiple comparisons.

3. Results and Discussion

3.1. Proximate Composition

This study aims to utilise edible mushrooms as a functional ingredient for food products, as there are reported studies on the underutilisation of this ingredient [34,35]. Edible mushrooms are considered a superfood that is highly nutritious, low in calories and possesses other biological compounds beneficial to human health [36,37]. The proximate composition of WEM powder is shown in Figure 1, where the highest composition is a carbohydrate, followed by crude fibre, moisture, protein, ash, and fat. The fat content of WEM powder was the lowest as all edible mushrooms are well-known for the low fat content ($\leq$5% dry weight) and were the least nutritive constituents [38].
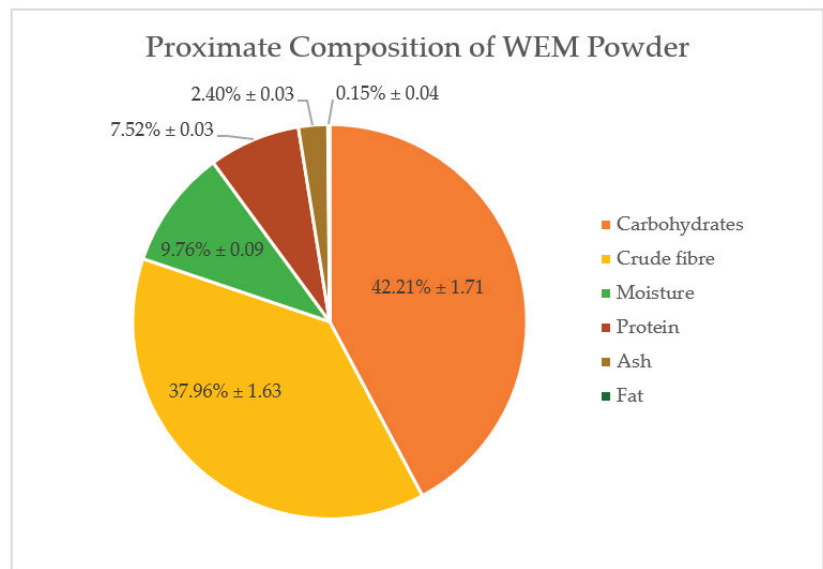
Figure 1. The proximate composition of WEM (*A. cornea*) powder on a dry weight basis was expressed as means $\pm$ standard deviation (*n* = 3), WEM = wood ear mushroom.

The moisture content of dry WEM powder was 9.76 $\pm$ 0.09% which is consistent with earlier studies that reported the moisture content of dried *Auricularia* species ranged between 6 to 15% [39,40]. Most fresh edible mushrooms, including *Auricularia* species, are high in moisture (85–94%), thus providing WEM with a unique gelatinous and smooth texture, but highly perishable [41,42]. Besides mushroom variety, environmental factors such as temperature, relative humidity, and post-harvest condition, can also influence the moisture content [43]. Therefore, most commercial WEM was dried to inhibit microbial and enzymatic activities while improving shelf-life stability [41]. The dried, hard, and brittle WEM can be rehydrated for consumption without altering the flavour and texture.

The ash content recorded in the present study (2.40 $\pm$ 0.03%) was slightly lower than previous studies (3 to 9% dry weight) for cultivated *Auricularia* species in China and India [44,45]. One of the primary factors influencing ash content is the substrate where edible mushrooms grow, which may vary depending on the cultivation technique. Moreover, the substrate composition can differ in organic matter content, pH, and metal concentration [46]. Thus, the ash content of cultivated mushrooms tends to be lower than wild mushrooms, as the latter grows in a nutrient-rich environment [47,48]. Nevertheless, the ash content of cultivated mushrooms can be improved via substrate modification [39]. Mushrooms absorb minerals from the ecosystem through bioaccumulation, hence, promoting the ash content in both wild and cultivated mushrooms [27]. Additionally, climate differences and genetic

factors could alter the ash content of mushrooms [46]. Regardless of whether cultivated or wild, the ash content of edible mushrooms is higher or comparable to most vegetables [47].

The protein content of WEM in the present study was in line with *A. polytricha* (7.2%) grown in Vietnam but lower than *A. auricular* (11.38%) from China [43,45]. In addition, the protein content of *Auricularia* species was lower than other edible mushroom species, such as oyster and shitake mushrooms (wild or cultivated) as reported in a previous study [49]. The difference in protein content might be caused by the mushroom species and strain, the development of the fruiting body, substratum, and location [50]. Furthermore, recent findings reported that there is a significant difference in crude protein content between wild and cultivated mushrooms [39,50].

The WEM powder is high in carbohydrates (42.21 $\pm$ 1.71%), which agrees with the study conducted by Shan et al. (28.38–82.8%) [45]. The carbohydrate content may vary between species, but up to 70% of total carbohydrate content were non-digestible polysaccharides in mushrooms, thus, diminishing fungi as the primary source of energy [51]. In this study, the fibre content of cultivated WEM powder (37.96 $\pm$ 1.63%) was higher than in a previous study (2.11–15.32% dry weight) [49]. Several studies have also reported no differences in fibre content between cultivated and wild WEM, and WEM also recorded the highest fibre content than other edible species [41,45,49]. In addition, the non-digestible polysaccharide of edible mushrooms is an alternative source of dietary fibre that remains underutilised compared to fruits, vegetables, and legumes [34].

Some but not all proximate compositions of WEM powder in the current study are comparable with other findings of cultivated WEM. The slight variation may be due to factors such as strain, the development stages of the fruiting body, nutrient distribution within the fruiting body, post-harvest handling and environmental conditions [47]. However, ensuring the stability of nutritional constituents is critical to incorporate WEM powder in food products [52].

A previous study by Sulaiman et al. found that the 5% of WEM incorporated in instant noodles was the best formulation among five modified formulas ranging from 5% to 25% [25]. The sensory evaluation of the 5% formulation recorded the highest score for colour, aroma, taste, texture, and overall acceptance, and there was no significant difference in any of the sensory attributes when compared with the control. This would be a good indication for the product to be accepted and its suitability for consumption. Table 1 shows the proximate composition of instant noodles incorporated with WEM and without WEM powder (control). The results showed a significant ($p < 0.05$) reduction of carbohydrates, increased ash and crude fibre, and no significant differences in moisture, protein, and fat content between the control instant noodle and noodles incorporated with 5% WEM. Specifically, the moisture content of both noodles was higher than previous findings (<5%), but the values remained within the recommended shelf-life stability (<12%) [53]. Furthermore, the current protein value of noodles did not improve with WEM inclusion, thus, contradicting past studies where the addition of mushroom powder had significantly increased the protein content of the noodles [13–15]. This finding might be attributed to the lower protein content of WEM compared to other edible mushrooms. Meanwhile, the significant increase of ash content in the noodles incorporated with 5% WEM powder indicated that this ingredient is a good source of minerals, as observed in other studies [40,46]. In addition, the current study demonstrated a significant ($p < 0.05$) increase in crude fibre content in WEM noodles, due to the presence of natural fibre in the mushroom [13–15]. Consequently, the addition of WEM powder significantly reduced the carbohydrate content. Nevertheless, according to Shams et al., long storage periods can reduce the fibre content and increase the carbohydrate content caused by the degradation of complex polysaccharides into simple sugar [53].

Table 1. The proximate composition of noodles incorporated with WEM and without WEM (control).

Instant Noodles	Proximate Composition (%)					
	Moisture	Ash	Protein	Fat	Crude Fibre	Carbohydrate
Control	10.61 ± 0.18 [a]	1.36 ± 0.02 [b]	11.86± 0.01 [a]	0.21 ± 0.04 [a]	3.36 ± 0.25 [b]	72.70 ± 0.32 [a]
5% WEM	10.47 ± 0.45 [a]	2.87 ± 0.03 [a]	11.37 ± 0.06 [a]	0.16 ± 0.06 [a]	5.68 ± 1.29 [a]	68.96 ± 1.34 [b]

Values were expressed as means ± standard deviation (n = 3). Different superscripts in the same column were significantly different ($p < 0.05$).

3.2. Total Dietary Fibre (TDF)

Table 2 demonstrates that the incorporation of WEM significantly increased ($p < 0.05$) the TDF of instant noodles due to the high dietary fibre in WEM (69.43 ± 1.12%). The TDF of WEM mushrooms was higher than the crude fibre content as the TDF accounted for soluble and insoluble fibres, thus reflecting the overall mushroom fibre content [34]. Moreover, the current result exhibited higher TDF content than previous studies, and the improvement was attributed to the WEM powder as a rich source of fibre, as stated in earlier findings [13,54]. Resultantly, the addition of WEM powder in noodles will lead to a sufficient intake of dietary fibre that can help improve gut health, weight management, and glycaemic response among consumers [55,56].

Table 2. The dietary fibre of noodles incorporated with WEM and without WEM (control).

Instant Noodles	Dietary Fibre (%)
Control	4.06 ± 0.34 [b]
5% WEM	13.30 ± 3.06 [a]

Values were expressed as means ± standard deviation (n = 3). Different superscripts in the same column were significantly different ($p < 0.05$).

3.3. Mineral Analysis

Table 3 shows the mineral composition of WEM powder, consisting of 10 macro and microelements expressed as mg/kg of the dry weight. Potassium was the highest macro element found in the WEM powder, consistent with earlier studies on the *Auricularia* species [45,57,58]. Meanwhile, the calcium and magnesium in WEM were lower than previous findings from Cameroon at 886.2 mg/kg and 835.4 mg/kg, respectively [59]. The sodium content reported in this study (68.929 ± 1.72 mg/kg) was the lowest macro-element, which was lower than an earlier study (109.1 mg/kg) [59]. Furthermore, WEM contained more potassium and calcium than magnesium and sodium, which agrees with the study by Kadnikova et al. [40].

Table 3. The mineral content of WEM (*A. cornea*).

	Concentration of Macro Element (mg/kg dw)			
	Sodium	Potassium	Calcium	Magnesium
WEM	68.929 ± 1.72	10,136.303 ± 4.70	750.315 ± 0.02	504.305 ± 0.02
	Concentration of Micro Element (mg/kg dw)					
	Iron	Zinc	Manganese	Copper	Chromium	Selenium
WEM	32.015 ± 0.80	11.499 ± 0.29	3.790 ± 0.09	2.104 ± 0.07	0.149 ± 0.00	0.131 ± 0.00

Values were expressed as means ± standard deviation (n = 2); dw = dry weight.

Iron and zinc have been reported as the highest micro elements found in *Auricularia* species (50–100 mg/kg), while the presence of copper, manganese, chromium, and selenium, was less than 20 mg/kg of dry weight. The amount of iron and zinc in this study was the highest for microelements, but at lower levels (50 mg/kg) compared to previous

findings [41]. Likewise, the remaining trace elements have been reported in other species, such as *A. thailandica* and *A. polytricha* [58,59]. In summary, the trend of macro and microelements in the WEM powder in decreasing order is as follows: potassium > calcium > magnesium > sodium > iron > zinc > manganese > copper > selenium > chromium.

Table 4 shows the mineral content of instant noodles with WEM and without WEM (control). There was a significant ($p < 0.05$) increase in potassium, calcium, magnesium, iron, and zinc content, but no significant difference ($p > 0.05$) in the concentration of manganese, copper, and chromium, in noodles incorporated with WEM compared to the control. Moreover, the content of sodium and selenium in incorporated noodles was significantly ($p < 0.05$) lower than the control. The present result demonstrated that all analysed minerals were present in the control noodles made from wheat flour, but the addition of WEM powder increased the prevalent macro and microelements, such as potassium, calcium, magnesium, iron, and zinc. Despite that, no increment was observed for manganese, copper, chromium, and selenium, in the incorporated noodles because of the low levels recorded in the WEM powder. Sodium was the highest constituent in both instant noodles due to salt addition in the noodle-making process. According to Ibrahium et al., the increment of minerals in the incorporated food was attributed to the high contents of mineral salts in the mushroom [60]. In addition, the current potassium, calcium, and iron content were higher than the previous finding by Parvin et al. that included oyster mushrooms in instant noodles (2705.5 mg/kg potassium, 275.8 mg/kg calcium, and 52.6 mg/kg iron) [15]. Therefore, the positive outcomes of this study could be an alternative solution for nutrient deficiencies [3].

Table 4. The mineral element content of noodles incorporated with WEM and without WEM (control).

	Concentration of Macro Element (mg/kg dw)			
	Sodium	Potassium	Calcium	Magnesium
Control	$1.61 \times 10^4 \pm 3.551$ [a]	1442.932 ± 1.323 [b]	418.604 ± 0.384 [b]	269.131 ± 0.247 [b]
5% WEM	$1.52 \times 10^4 \pm 4.450$ [b]	1896.633 ± 2.448 [a]	507.511 ± 0.031 [a]	303.160 ± 1.976 [a]

	Concentration of Micro Element (mg/kg dw)					
	Iron	Zinc	Manganese	Copper	Chromium	Selenium
Control	61.122 ± 0.285 [b]	8.768 ± 0.118 [b]	7.197 ± 0.097 [a]	5.234 ± 0.070 [a]	0.262 ± 0.004 [a]	0.174 ± 0.004 [a]
5% WEM	77.584 ± 0.195 [a]	10.475 ± 0.218 [a]	7.281 ± 0.151 [a]	4.215 ± 0.088 [a]	0.255 ± 0.005 [a]	0.141 ± 0.003 [b]

Values were expressed as means $\pm$ standard deviation ($n = 2$); dw = dry weight. Different superscripts in the same column were significantly different ($p < 0.05$).

Different mushroom species may accumulate minerals at different capacities from the substratum, and various analytical methods could be the factors that explained the variation of minerals [46,57]. Furthermore, high mineral values suggested that WEM is a potential source of good-quality ingredients [44]. The essential elements in WEM are comparable to other edible mushrooms and are required in varying amounts for the proper functioning of the body (biochemical reactions, metabolic growth, and enzymatic activities) [61]. Due to bioaccumulation ability of edible mushrooms, consumer should aware of the excessive mineral intake which could harm the body due to association with increasing cardiovascular risk factor and heart diseases; thus, the guideline of recommended daily intake of minerals and trace elements should be followed for safe consumption [62]. For instance, the safe limit of copper, iron, manganese, and zinc per kg of human body weight set by the World Health Organization are 40 mg/kg, 15 mg/kg, 400–1000 mg/kg, and 60 mg/kg, respectively [46]. However, the recommendation for daily intake of dietary minerals also depends on factors such as sexes, dietary practices, food preparation and processing, bioavailability, mineral interactions, and the chemical forms of the minerals [63].

3.4. Antioxidant Activities and Total Phenolic Contents (TPC)

Methanol was used as the solvent for the extraction, as higher polarity solvents could increase the yield of polar phenolic compounds, leading to higher antioxidant

activity [58,64]. The phenolic compounds are a large group of secondary metabolites in plants and fungi exhibiting antioxidant activities and oxidation protection [44]. Therefore, the high TPC of a mushroom suggests a higher antioxidant capacity [50,65]. Based on Table 5, the WEM powder could exhibit antioxidant activities mediated by free radical scavenging abilities and reducing power due to the presence of total phenolic content [58]. The strong DPPH radical-scavenging activity of the extracts indicated the high hydrogen-donating capacity; thus, the DPPH free radicals scavenging [66]. Meanwhile, the FRAP assay demonstrates the ability of the non-enzymatic antioxidant extract associated with the presence of reductone to break the free radical chain by donating an electron to stabilise and terminate the radical chain reactions [28]. The present data demonstrated that the TPC of WEM powder is higher than the value reported in previous studies, such as ethanolic extract of *A. polytricha* (4.74 mg GAE/g), ethanolic extract of *A. auricula* (2.75 mg GAE/g) and methanolic extract of *A. thailandica* (1.99 mgGAE/g) [29,58,66]. In addition, the wild edible mushroom has been reported to contain higher phenolic compounds than cultivated mushrooms, as the stressful environment enhanced the production of secondary metabolites [44].

Table 5. The antioxidant activities and TPC of wood ear mushroom (WEM) powder and noodles incorporated with WEM and without WEM (control).

	Control Noodles	5% WEM Noodles	WEM Powder
IC_{50} DPPH (mg/mL)	19.53 ± 0.51 [c]	13.00 ± 0.36 [b]	0.85 ± 0.11 [a]
FRAP (μM $FeSO_4$/g)	4.01 ± 0.04 [c]	7.64 ± 0.08 [b]	17.73 ± 0.83 [a]
TPC (mg GAE/g)	0.93 ± 0.08 [c]	1.19 ± 0.24 [b]	5.81 ± 0.09 [a]

Results were expressed as means ± standard deviation. (*n* = 3). Different superscripts in the same row were significantly different (*p* < 0.05).

The present study also demonstrated that the incorporated noodles with 5% WEM powder exhibited significantly (*p* < 0.05) lower IC_{50} for DPPH inhibition than the control noodles. The lower IC_{50} value reflected the strong DPPH scavenging capacity, but a much lower value has been recorded in another study that incorporated noodles with button mushrooms (0.4 mg/mL) [53]. Meanwhile, the FRAP value for the incorporated noodles was significantly (*p* < 0.05) higher than the control noodles, indicating a strong reduction capacity. Nevertheless, the improvement of antioxidant capacity in the incorporated instant noodles was due to the increment of TPC, which agrees with past studies but with different mushroom species and functional ingredients [18,67].

The present study supports the potential of incorporating edible mushrooms in the food product due to the abundance of phytochemicals with potent antioxidant abilities and is associated with health benefits, particularly the implications of diseases caused by oxidative stress and free radicals [68]. Despite that, the impact of processing and cooking may reduce the TPC and antioxidant capacity due to the cutting, steaming, or drying process, or long-term storage, which requires further investigation [69,70]. Besides the phenolic compounds, recent studies found that mushroom polysaccharides demonstrated potent antioxidant abilities, such as free radicals scavenging, a metal chelator, and reducing power [20,71,72]. Antioxidants are essential to protect living organisms from oxidative damage by preventing or inhibiting the oxidation reaction.

3.5. Glycaemic Index

The glycaemic analysis was conducted to observe the effect of incorporating instant noodles with 5% of WEM mushroom on the postprandial blood glucose level among participants in this study. Figure 2 illustrates the mean postprandial blood glucose level within two hours for 10 female subjects with normal body mass index (BMI) who consumed the test food, containing 50 g of carbohydrates. The baseline for the blood glucose level was comparable and started to rise drastically within 15 min after consuming the test meals and peaked at 30 min, whereas the control noodles recorded higher blood glucose levels

than the incorporated noodles with 5% WEM powder ($p < 0.05$). Subsequently, the blood glucose level of the control noodles exhibited a drastic drop between 30 to 60 min before a steady fall at 90 min, and remained constant until 120 min. Meanwhile, the blood glucose level of the incorporated noodles saw a gradual drop from 30 min to 120 min. At 120 min, the average blood glucose level of the control noodles was higher (5.5 mmol/L) than the noodles incorporated with 5% WEM (5.1 mmol/L) ($p < 0.05$). It was confirmed that adding WEM powder reduced the peak and lowered the glucose concentration of digested WEM noodles in blood vessels, hence, exhibiting the hypoglycaemic effect. The observation was in agreement with previous findings that the incorporation of 5% of mushroom powder was able to exhibit a hypoglycaemic effect [23,65].
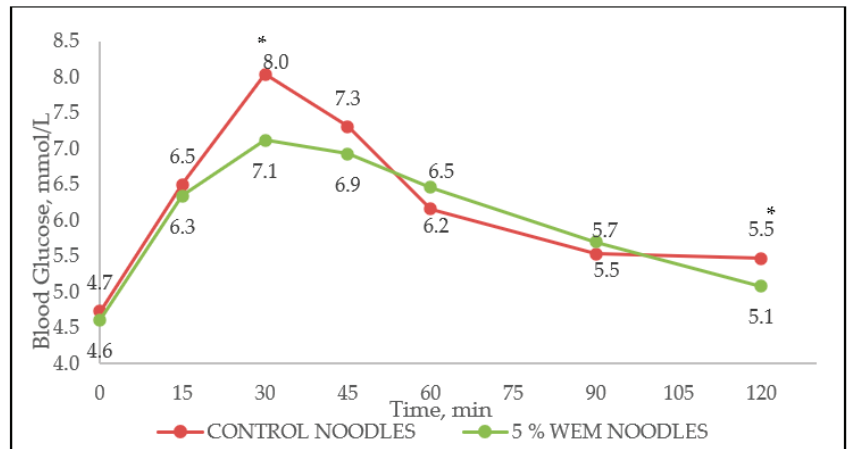
Figure 2. The comparison of postprandial blood glucose response within 120 min between control and 5% WEM instant noodles ($n = 10$), * indicates a significant difference ($p < 0.05$).

Numerous animal studies have demonstrated the hypoglycaemic effect of WEM by observing the effect of powder supplementation in the diet of diabetic mice, which reduces the plasma glucose, insulin, urinary glucose, and food intake [8]. On a normal occasion, carbohydrates were broken down into glucose once the test food was ingested. The blood glucose level would spike drastically until reaching the highest concentration within 30 min and fall back to normal glucose level after 2 h, depending on the type of food consumed [73]. Nonetheless, the presence of fibre-rich ingredients, such as WEM powder, interferes with digestion and delays the gastrointestinal tract emptying process affecting the absorption of nutrients, particularly glucose [74]. An in vitro study mimicking the behaviour of enzymatic digestion was conducted by Wu et al. who observed that the polysaccharides of *Auricularia* mushroom could form highly viscous substances and retard glucose diffusion by forming a barrier that interferes with starch hydrolysis [24]. In addition, another study found a negative correlation between the glycaemic response and total dietary fibre of mushroom powder. High amounts of dietary fibre could lead to the alteration of physicochemical properties and the digestibility of noodles [65]. This condition could explain the graph pattern in Figure 2.

Macronutrients, such as fat and protein, could influence the postprandial blood glucose responses to food, but the effect of those nutrients is more pronounced in mixed meals in a dose-dependent manner [33]. In contrast to one other study, the incorporation of WEM powder did not increase the protein content of instant noodles, which might not contribute to the integrity of protein network in the noodles [65]. Notably, decades of extensive studies have attempted to link certain elements to the modulation of glucose homeostasis [75]. Meanwhile, other studies suggested the hypoglycaemic effect of WEM could be mediated via the polysaccharide interaction with insulin receptors on target

tissues, and partially exhibited via modulation of the anti-oxidative system, but limited knowledge is available to confirm the mechanism [20,76]. Nevertheless, study findings have revealed that adding 5% of WEM powder to noodles could lower the glucose spike, demonstrating the hypoglycaemic effect among consumers.

The glycaemic response was further calculated to obtain the incremental area under the curve (IAUC) for each respondent, which reflected the changes in blood glucose levels within two hours. The mean of IAUC between reference and test foods showed a significant difference ($p = 0.008$). Meanwhile, there was no significant difference in the mean of IAUC between both test food (incorporated noodles with 5% WEM and control). The mean of IAUC of reference food was the highest at 269.83 mmol.min/L, while the mean IAUC of the test food was 196.43 mmol.min/L and 179.78 mmol.min/L for control and incorporated noodles, respectively. Moreover, for a valid GI measurement and high accuracy of GI value, the coefficient variation of reference food should be lower than 30% and for this study, the coefficient variation of reference food that was repeated three times was 15.31%, which was lower than the recommended value [31]. Therefore, the GI value of control noodles containing 50 g of available carbohydrates was high (GI = 75.84), whereas the GI for instant noodles incorporated with 5% WEM were moderate (GI = 68.91).

The GI value of food can be influenced by various factors, particularly methodological and human factors, which are crucial for glycaemic analysis [31,77]. The moderate GI value of 5% WEM noodles indicated that the blood glucose concentration increased moderately within 2 h. Most noodles have been categorized as low GI foods because the digestion process of noodles is slower and incomplete compared to other starch-based foods such as white bread [18]. One of the factors for the discrepancy is the different types of flour used in making instant noodles, where a higher amylose or fibre content can influence the digestibility rate and glycaemic response, resulting in a low GI instant noodle [78]. In addition, food processing can cause physical alterations in the starch structure and promote starch digestibility, but some studies have postulated that the step-in noodle processing, such as mixing, sheeting, and extruding, may cause the protein matrix to continuously entrap starch granules and limit the starch hydrolysis [79]. In addition, the retrogradation process during cooling may increase resistant starch, resulting in low GI food [80]. In a glycaemic study, the control of blood glucose level proves to have a huge benefit for a diabetic patient while it also could lower the risk of cardiovascular heart disease and help in weight management for a healthy individual [81,82]. Nevertheless, this study successfully utilised WEM powder as a functional ingredient in instant noodles and exhibited a hypoglycaemic effect among study participants.

4. Conclusions

The highest composition in WEM powder was carbohydrate, followed by crude fibre, moisture, protein, ash, and fat. The addition of WEM powder in noodles influenced the nutrient composition, significantly reducing carbohydrates and increasing ash, crude fibre, dietary fibre content, and antioxidant activities. Furthermore, the incorporation of WEM powder significantly improved elements such as potassium, calcium, magnesium, iron, and zinc, but not manganese, copper, and chromium. Moreover, adding WEM powder to instant noodles could lower the fluctuation of postprandial blood glucose levels and reduce the GI value. In conclusion, the incorporation of WEM powder is promising in developing nutritious and low GI instant noodles that could increase nutrient intake and improve human health.

Author Contributions: Conceptualization, M.K.Z. and P.M.; investigation, M.K.Z.; writing—original draft preparation, M.K.Z.; writing—review and editing, P.M., R.G., W.P., H.M., N.S. and J.S.S.S.; visualization, M.K.Z.; supervision, P.M. and R.G.; project administration, P.M. and R.G.; funding acquisition, P.M. All authors have read and agreed to the published version of the manuscript.

References

1. Priya, R.U.; Gethaa, D.; Darshan, S. Biology and Cultivation of Black Ear Mushroom—*Auricularia* spp. *Adv. Life Sci.* **2016**, *5*, 10252–10254.
2. Wu, F.; Tohtirjap, A.; Fan, L.F.; Zhou, L.W.; Alvarenga, R.L.M.; Gibertoni, T.B.; Dai, Y.C. Global Diversity and Updated Phylogeny of *Auricularia* (Auriculariales, Basidiomycota). *J. Fungi* **2021**, *7*, 933. [CrossRef] [PubMed]
3. Bandara, A.R.; Rapior, S.; Mortimer, P.E.; Kakumyan, P.; Hyde, K.D.; Xu, J. A Review of the Polysaccharide, Protein and Selected Nutrient Content of *Auricularia*, and Their Potential Pharmacological Value. *Mycosphere* **2019**, *10*, 579–607. [CrossRef]
4. Kozarski, M.; Klaus, A.; Jakovljevic, D.; Todorovic, N.; Vunduk, J.; Petrović, P.; Niksic, M.; Vrvic, M.M.; van Griensven, L. Antioxidants of Edible Mushrooms. *Molecules* **2015**, *20*, 19489–19525. [CrossRef] [PubMed]
5. Avci, E.; Cagatay, G.; Alp Avci, G.; Suicmez, M.; Coskun Cevher, S. An Edible Mushroom With Medicinal Significance; *Auricularia polytricha*. *Hittite J. Sci. Eng.* **2016**, *3*, 111–116. [CrossRef]
6. Li, Z.-Y.; Yao, X.-P.; Liu, B.; Reheman, H.N.; Gao, Y.; Sun, Z.; Ma, Q. *Auricularia auricula-judae* Polysaccharide Attenuates Lipopolysaccharide-Induced Acute Lung Injury by Inhibiting Oxidative Stress and Inflammation. *Biomed. Rep.* **2015**, *3*, 478–482. [CrossRef]
7. Zhang, Y.; Zeng, Y.; Men, Y.; Zhang, J.; Liu, H.; Sun, Y. Structural Characterization and Immunomodulatory Activity of Exopolysaccharides from Submerged Culture of *Auricularia auricula-judae*. *Int. J. Biol. Macromol.* **2018**, *115*, 978–984. [CrossRef]
8. De Silva, D.D.; Rapior, S.; Hyde, K.D.; Bahkali, A.H. Medicinal Mushrooms in Prevention and Control of Diabetes Mellitus. *Fungal Divers* **2012**, *56*, 1–29. [CrossRef]
9. Chiu, W.C.; Yang, H.H.; Chiang, S.C.; Chou, Y.X.; Yang, H.T. *Auricularia polytricha* Aqueous Extract Supplementation Decreases Hepatic Lipid Accumulation and Improves Antioxidative Status in Animal Model of Nonalcoholic Fatty Liver. *Biomed. Pharmacother.* **2014**, *4*, 29–38. [CrossRef]
10. Hyde, K.D.; Xu, J.; Rapior, S.; Jeewon, R.; Lumyong, S.; Niego, A.G.T.; Abeywickrama, P.D.; Aluthmuhandiram, J.V.S.; Brahamanage, R.S.; Brooks, S.; et al. The Amazing Potential of Fungi: 50 Ways We Can Exploit Fungi Industrially. *Fungal Divers.* **2019**, *97*, 1–136. [CrossRef]
11. Gulia, N.; Dhaka, V.; Khatkar, B.S. Instant Noodles: Processing, Quality, and Nutritional Aspects. *Crit Rev Food Sci Nutr* **2014**, *54*, 1386–1399. [CrossRef] [PubMed]
12. Adejuwon, O.H.; Jideani, A.I.O.; Falade, K.O. Quality and Public Health Concerns of Instant Noodles as Influenced by Raw Materials and Processing Technology. *Food Rev. Int.* **2020**, *36*, 276–317. [CrossRef]
13. Arora, B.; Kamal, S.; Sharma, V.P. Nutritional and Quality Characteristics of Instant Noodles Supplemented with Oyster Mushroom (*P. ostreatus*). *J Food Process. Preserv.* **2018**, *42*, e13521. [CrossRef]
14. Wahyono, A.; Novianti; Bakri, A. Kasutjianingati Physicochemical and Sensorial Characteristics of Noodle Enriched with Oyster Mushroom (*Pleorotus ostreatus*) Powder. *J. Phys. Conf. Ser.* **2018**, *953*, 012120. [CrossRef]
15. Parvin, R.; Farzana, T.; Mohajan, S.; Rahman, H.; Rahman, S.S. Quality Improvement of Noodles with Mushroom Fortified and Its Comparison with Local Branded Noodles. *NFS J.* **2020**, *20*, 37–42. [CrossRef]
16. Heo, S.; Jeon, S.; Lee, S. Utilization of *Lentinus edodes* Mushroom β-Glucan to Enhance the Functional Properties of Gluten-Free Rice Noodles. *LWT Food Sci. Technol.* **2014**, *55*, 627–631. [CrossRef]
17. Wang, L.; Zhao, H.; Brennan, M.; Guan, W.; Liu, J.; Wang, M.; Wen, X.; He, J.; Brennan, C. *In Vitro Gastric Digestion Antioxidant and Cellular Radical Scavenging Activities of Wheat-Shiitake Noodles*; Elsevier Ltd.: Amsterdam, The Netherlands, 2020; Volume 330, ISBN 0000000242943.
18. Wang, J.; Brennan, M.A.; Serventi, L.; Stephen, C.; Wang, J.; Brennan, M.A.; Serventi, L.; Stephen, C. Impact of Functional Vegetable Ingredients on the Technical and Nutritional Quality of Pasta. *Crit. Rev. Food Sci. Nutr.* **2022**, *62*, 6069–6080. [CrossRef]
19. Chen, N.; Zhang, H.; Zong, X.; Li, S.; Wang, J.; Wang, Y.; Jin, M. Polysaccharides from *Auricularia auricula*: Preparation, Structural Features and Biological Activities. *Carbohydr. Polym.* **2020**, *247*, 116750. [CrossRef]

20. Hu, X.; Liu, C.; Wang, X.; Jia, D.; Lu, W.; Sun, X.; Liu, Y.; Yuan, L. Hpyerglycemic and Anti-Diabetic Nephritis Activities of Polysaccharides Separated from *Auricularia auricular* in Diet-Streptozotocin-Induced Diabetic Rats. *Exp. Med.* **2017**, *13*, 352–358. [CrossRef]

21. Lu, A.; Yu, M.; Shen, M.; Xu, S.; Xu, Z.; Zhang, Y.; Lin, Z.; Wang, W. Preparation of the *Auricularia auricular* Polysaccharides Simulated Hydrolysates and Their Hypoglycaemic Effect. *Int. J. Biol. Macromol.* **2018**, *106*, 1139–1145. [CrossRef]

22. Shen, M.; Fang, Z.; Chen, Y.; Xiao, B.; Guo, L.; Xu, Y.; Wang, G.; Wang, W.; Zhang, Y. Hypoglycemic Effect of the Degraded Polysaccharides from the Wood Ear Medicinal Mushroom *Auricularia auricula-judae* (Agaricomycetes). *Int. J. Med. Mushrooms* **2019**, *21*, 1033–1042. [CrossRef] [PubMed]

23. Vallée, M.; Lu, X.; Narciso, J.O.; Li, W.; Qin, Y.; Brennan, M.A.; Brennan, C.S. Physical, Predictive Glycaemic Response and Antioxidative Properties of Black Ear Mushroom (*Auricularia auricula*) Extrudates. *Plant Foods Hum. Nutr.* **2017**, *72*, 301–307. [CrossRef] [PubMed]

24. Wu, N.J.; Chiou, F.J.; Weng, Y.M.; Yu, Z.R.; Wang, B.J. In Vitro Hypoglycemic Effects of Hot Water Extract from *Auricularia polytricha* (Wood Ear Mushroom). *Int. J. Food Sci. Nutr.* **2014**, *65*, 502–506. [CrossRef] [PubMed]

25. Sulaiman, D.S.; Zakaria, M.K.; George, R.; Matanjun, P. Sensory Evaluation and Nutrient Composition of Noodles Enriched with Wood Ear Mushroom (*Auricularia polytricha*) Powder. *Trans. Sci. Technol.* **2021**, *8*, 172–177.

26. AOAC. *Official Methods of Analysis*, 17th ed.; Association of Analytical Communities: Gaithersburg, MD, USA, 2000.

27. Kalač, P. A Review of Chemical Composition and Nutritional Value of Wild-Growing and Cultivated Mushrooms. *J. Sci. Food Agric.* **2013**, *93*, 209–218. [CrossRef] [PubMed]

28. Wen Yuh, L.; Mars, J.Y.; Lien Tsung, H.; Liang Chuan, L. Antioxidant Properties of Methanol Extract of a New Commercial Gelatinous Mushrooms (White Variety of *Auricularia fuscosuccinea*) of Taiwan. *Afr. J. Biotechnol.* **2013**, *12*, 6210–6221. [CrossRef]

29. Teoh, H.L.; Ahmad, I.S.; Johari, N.M.K.; Aminudin, N.; Abdullah, N. Antioxidant Properties and Yield of Wood Ear Mushroom, *Auricularia polytricha* (Agaricomycetes), Cultivated on Rubberwood Sawdust. *Int. J. Med. Mushrooms* **2018**, *20*, 369–380. [CrossRef]

30. Yim, H.S.; Chye, F.Y.; Koo, S.M.; Matanjun, P.; How, S.E.; Ho, C.W. Optimization of Extraction Time and Temperature for Antioxidant Activity of Edible Wild Mushroom, *Pleurotus porrigens*. *Food Bioprod. Process.* **2012**, *90*, 235–242. [CrossRef]

31. Wolever, T.M.S.; Meynier, A.; Jenkins, A.L.; Brand-Miller, J.C.; Atkinson, F.S.; Gendre, D.; Leuillet, S.; Cazaubiel, M.; Housez, B.; Vinoy, S. Glycemic Index and Insulinemic Index of Foods: An Interlaboratory Study Using the ISO 2010 Method. *Nutrients* **2019**, *11*, 2218. [CrossRef]

32. Urbaniak, G.C.; Plous, S. Research Randomizer (Version 4.0) [Computer Software]. Available online: http://www.randomizer.org/ (accessed on 1 June 2021).

33. Ballance, S.; Knutsen, S.H.; Fosvold, Ø.W.; Fernandez, A.S.; Monro, J. Predicting Mixed-Meal Measured Glycaemic Index in Healthy Subjects. *Eur. J. Nutr.* **2019**, *58*, 2657–2667. [CrossRef]

34. Cheung, P.C.K. Mini-Review on Edible Mushrooms as Source of Dietary Fiber: Preparation and Health Benefits. *Food Sci. Hum. Wellness* **2013**, *2*, 162–166. [CrossRef]

35. Stachowiak, B.; Reguła, J. Health-Promoting Potential of Edible Macromycetes under Special Consideration of Polysaccharides: A Review. *Eur. Food Res. Technol.* **2012**, *234*, 369–380. [CrossRef]

36. Assemie, A.; Abaya, G. The Effect of Edible Mushroom on Health and Their Biochemistry. *Int. J. Microbiol.* **2022**, *2022*, 8744788. [CrossRef] [PubMed]

37. Samsudin, N.I.P.; Abdullah, N. Edible Mushrooms from Malaysia; a Literature Review on Their Nutritional and Medicinal Properties. *Int Food Res J* **2019**, *26*, 11–31.

38. Islam, T.; Ganesan, K.; Xu, B. Insights into Health-Promoting Effects of Jew's Ear (*Auricularia auricula-judae*). *Trends Food Sci. Technol.* **2021**, *114*, 552–569. [CrossRef]

39. Yao, H.; Liu, Y.; Ma, Z.F.; Zhang, H.; Fu, T.; Li, Z.; Li, Y.; Hu, W.; Han, S.; Zhao, F.; et al. Analysis of Nutritional Quality of Black Fungus Cultivated with Corn Stalks. *J. Food Qual.* **2019**, *2019*, 9590251. [CrossRef]

40. Kadnikova, I.A.; Costa, R.; Kalenik, T.K.; Guruleva, O.N.; Yanguo, S. Chemical Composition and Nutritional Value of the Mushroom *Auricularia auricula-judae*. *J. Food Nutr. Res.* **2015**, *3*, 478–482. [CrossRef]

41. Afiukwa, C.A.; Ebem, E.C.; Igwe, D.O. Characterization of the Proximate and Amino Acid Composition of Edible Wild Mushroom Species in Abakaliki, Nigeria. *Am. Assoc. Sci. Technol. J. Biosci.* **2015**, *1*, 20–25.

42. Liu, Y.T.; Sun, J.; Luo, Z.Y.; Rao, S.Q.; Su, Y.J.; Xu, R.R.; Yang, Y.J. Chemical Composition of Five Wild Edible Mushrooms Collected from Southwest China and Their Antihyperglycemic and Antioxidant Activity. *Food Chem. Toxicol.* **2012**, *50*, 1238–1244. [CrossRef]

43. Hung, P.V.; Nhi, N.N.Y. Nutritional Composition and Antioxidant Capacity of Several Edible Mushrooms Grown in the Southern Vietnam. *Int. Food Res. J.* **2012**, *19*, 611–615.

44. Ao, T.; Deb, C.R. Nutritional and Antioxidant Potential of Some Wild Edible Mushrooms of Nagaland, India. *J. Food Sci. Technol.* **2019**, *56*, 1084–1089. [CrossRef] [PubMed]

45. Shan, H.; Dong Sun, X.; Chun Yang, H.; Yuan Liu, F.; Wang, B.; Chai, L.; Luan, J. Proximate Compositions and Bioactive Compounds of Cultivated and Wild *Auricularia auricular* from Northeastern China. *Eur. J. Nutr. Food Saf.* **2019**, *11*, 175–186. [CrossRef]

46. Obodai, M.; Ferreira, I.C.F.R.; Fernandes, Â.; Barros, L.; Narh Mensah, D.L.; Dzomeku, M.; Urben, A.F.; Prempeh, J.; Takli, R.K. Evaluation of the Chemical and Antioxidant Properties of Wild and Cultivated Mushrooms of Ghana. *Molecules* **2014**, *19*, 19532–19548. [CrossRef] [PubMed]

47. Lu, H.; Lou, H.; Hu, J.; Liu, Z.; Chen, Q. Macrofungi: A Review of Cultivation Strategies, Bioactivity, and Application of Mushrooms. *Compr. Rev. Food Sci. Food Saf.* **2020**, *19*, 2333–2356. [CrossRef] [PubMed]
48. Khan, A.A.; Yao, F.; Idrees, M.; Lu, L.; Fang, M.; Wang, P.; Jiang, W.Z.; Zhang, Y.M. A Comparative Study of Growth, Biological Efficiency, Antioxidant Activity and Molecular Structure in Wild and Commercially Cultivated *Auricularia cornea* Strains. *Folia Hortic.* **2020**, *32*, 255–264. [CrossRef]
49. Srikram, A.; Supapvanich, S. Proximate Compositions and Bioactive Compounds of Edible Wild and Cultivated Mushrooms from Northeast Thailand. *Agric. Nat. Resour.* **2016**, *50*, 432–436. [CrossRef]
50. Thatoi, H.; Singdevsachan, S.K. Diversity, Nutritional Composition and Medicinal Potential of Indian Mushrooms: A Review. *Afr J Biotechnol* **2014**, *13*, 523–545. [CrossRef]
51. Yadav, D.; Negi, P.S. Bioactive Components of Mushrooms: Processing Effects and Health Benefits. *Food Res. Int.* **2021**, *148*, 110599. [CrossRef]
52. Sikander, M.; Malik, A.; Khan, M.S.G.; Qurratul-ain; Khan, R.G. Instant Noodles: Are They Really Good for Health? A Review. *A Review. Electron. J Biol* **2017**, *13*, 222–227.
53. Shams, R.; Jammu, T.; Singh, J.; Rajaram, S.; Hospital, E.; Dar, A.H. Assessment of Shelf Stability of Noodles Fortified with Button Mushroom and Chickpea Starch. *J. Postharvest. Technol.* **2022**, *10*, 122–133.
54. Wandee, Y.; Uttapap, D.; Puncha-arnon, S.; Puttanlek, C.; Rungsardthong, V.; Wetprasit, N. Enrichment of Rice Noodles with Fibre-Rich Fractions Derived from Cassava Pulp and Pomelo Peel. *Int. J. Food Sci. Technol.* **2014**, *49*, 2348–2355. [CrossRef]
55. Khursheed, R.; Singh, S.K.; Wadhwa, S.; Gulati, M.; Awasthi, A. Therapeutic Potential of Mushrooms in Diabetes Mellitus: Role of Polysaccharides. *Int. J. Biol. Macromol.* **2020**, *164*, 1194–1205. [CrossRef] [PubMed]
56. Dhingra, D.; Michael, M.; Rajput, H.; Patil, R.T. Dietary Fibre in Foods: A Review. *J. Food Sci. Technol.* **2012**, *49*, 255–266. [CrossRef]
57. Ekissi, A.C.; Kouame, K.B.; Niaba, K.P.V.; Beugre, G.A.M.; Kati-Coulibaly, S. Physicochemical Characterization of Two Species of Wild Edible Mushrooms: *Lentinus brunneofloccosus pegler* and *Auricularia Auricularia-judae*. *Food Nutr. Sci.* **2021**, *12*, 319–331. [CrossRef]
58. Bandara, A.R.; Karunarathna, S.C.; Mortimer, P.E.; Hyde, K.D.; Khan, S.; Kakumyan, P.; Xu, J. First Successful Domestication and Determination of Nutritional and Antioxidant Properties of the Red Ear Mushroom *Auricularia thailandica* (Auriculariales, Basidiomycota). *Mycol. Prog.* **2017**, *16*, 1029–1039. [CrossRef]
59. Ache, T.N.; Bi, M.E.; Ndam, L.M.; Kinge, T.R. Nutrient and Mineral Components of Wild Edible Mushrooms from the Kilum-Ijim Forest, Cameroon. *Afr. J. Food Sci.* **2021**, *15*, 152–161. [CrossRef]
60. Ibrahim, M.I.; Hegazy, A.I. Effect of Replacement of Wheat Flour with Mushroom Powder and Sweet Potato Flour on Nutritional Composition and Sensory Characteristics of Biscuits. *Researchgate.Net* **2014**, *3*, 8.
61. Liu, E.; Ji, Y.; Zhang, F.; Liu, B.; Meng, X. Review on *Auricularia auricula-judae* as a Functional Food: Growth, Chemical Composition, and Biological Activities. *J. Agric. Food Chem.* **2021**, *69*, 1739–1750. [CrossRef]
62. Mohammadifard, N.; Humphries, K.H.; Gotay, C.; Mena-Sánchez, G.; Salas-Salvadó, J.; Esmaillzadeh, A.; Ignaszewski, A.; Sarrafzadegan, N. Trace Minerals Intake: Risks and Benefits for Cardiovascular Health. *Crit. Rev. Food Sci. Nutr.* **2019**, *59*, 1334–1346. [CrossRef]
63. Freeland-Graves, J.H.; Sachdev, P.K.; Binderberger, A.Z.; Sosanya, M.E. Global Diversity of Dietary Intakes and Standards for Zinc, Iron, and Copper. *J. Trace Elem. Med. Biol.* **2020**, *61*, 126515. [CrossRef]
64. Chan, P.T.; Matanjun, P.; Yasir, S.M.; Tan, T.S. Antioxidant Activities and Polyphenolics of Various Solvent Extracts of Red Seaweed, *Gracilaria changii*. *J. Appl. Phycol.* **2015**, *27*, 2377–2386. [CrossRef]
65. Lu, X.; Brennan, M.A.; Serventi, L.; Liu, J.; Guan, W.; Brennan, C.S. Addition of Mushroom Powder to Pasta Enhances the Antioxidant Content and Modulates the Predictive Glycaemic Response of Pasta. *Food Chem.* **2018**, *264*, 199–209. [CrossRef] [PubMed]
66. Boonsong, S.; Klaypradit, W.; Wilaipun, P. Antioxidant Activities of Extracts from Five Edible Mushrooms Using Different Extractants. *Agric. Nat. Resour.* **2016**, *50*, 89–97. [CrossRef]
67. Kumar, H.; Bhardwaj, K.; Sharma, R.; Nepovimova, E.; Cruz-martins, N.; Dhanjal, D.S.; Singh, R.; Chopra, C.; Verma, R.; Abd-elsalam, K.A.; et al. Potential Usage of Edible Mushrooms and Their Residues to Retrieve Valuable Supplies for Industrial Applications. *J. Fungi* **2021**, *7*, 427. [CrossRef] [PubMed]
68. Rangel-Vargas, E.; Rodriguez, J.A.; Domínguez, R.; Lorenzo, J.M.; Sosa, M.E.; Andrés, S.C.; Rosmini, M.; Pérez-Alvarez, J.A.; Teixeira, A.; Santos, E.M. Edible Mushrooms as a Natural Source of Food Ingredient/Additive Replacer. *Foods* **2021**, *10*, 2687. [CrossRef]
69. Gull, A.; Prasad, K.; Kumar, P. Nutritional, Antioxidant, Microstructural and Pasting Properties of Functional Pasta. *J. Saudi Soc. Agric. Sci.* **2018**, *17*, 147–153. [CrossRef]
70. Choy, A.; Morrison, P.D.; Hughes, J.G.; Marriott, P.J.; Small, D.M. Quality and Antioxidant Properties of Instant Noodles Enhanced with Common Buckwheat Flour. *J Cereal Sci* **2013**, *57*, 281–287. [CrossRef]
71. Nguyen, T.L.; Chen, J.; Hu, Y.; Wang, D.; Fan, Y.; Wang, J.; Abula, S.; Zhang, J.; Qin, T.; Chen, X.; et al. In Vitro Antiviral Activity of Sulfated *Auricularia auricula* Polysaccharides. *Carbohydr. Polym.* **2012**, *90*, 1254–1258. [CrossRef]
72. Su, Y.; Li, L. Structural Characterization and Antioxidant Activity of Polysaccharide from Four Auriculariales. *Carbohydr Polym* **2020**, *229*, 115407. [CrossRef]

73. Giacco, R.; Costabile, G.; Riccardi, G. Metabolic Effects of Dietary Carbohydrates: The Importance of Food Digestion. *Food Res. Int.* **2016**, *88*, 336–341. [CrossRef]
74. Scazzina, F.; Siebenhandl-Ehn, S.; Pellegrini, N. The Effect of Dietary Fibre on Reducing the Glycaemic Index of Bread. *Br. J. Nutr.* **2013**, *109*, 1163–1174. [CrossRef] [PubMed]
75. Ngugi, M.P.; Njagi, J.; Kibiti, C.; Ngeranwa, J.J.N. The Role of Vitamins and Mineral Elements in Management of Type 2 Diabetes Mellitus: A Review. *South As. J. Biol. Sci.* **2012**, *2*, 107–115.
76. Roupas, P.; Keogh, J.; Noakes, M.; Margetts, C.; Taylor, P. The Role of Edible Mushrooms in Health: Evaluation of the Evidence. *J. Funct. Foods* **2012**, *4*, 687–709. [CrossRef]
77. Matthan, N.R.; Ausman, L.M.; Meng, H.; Tighiouart, H.; Lichtenstein, A.H. Estimating the Reliability of Glycemic Index Values and Potential Sources of Methodological and Biological Variability. *Am. Soc. Nutr. Downloaded* **2016**, *104*, 1004–1013. [CrossRef] [PubMed]
78. Jang, H.L.; Bae, I.Y.; Lee, H.G. In Vitro Starch Digestibility of Noodles with Various Cereal Flours and Hydrocolloids. *LWT Food Sci. Technol.* **2015**, *63*, 122–128. [CrossRef]
79. Bharath Kumar, S.; Prabhasankar, P. A Study on Noodle Dough Rheology and Product Quality Characteristics of Fresh and Dried Noodles as Influenced by Low Glycemic Index Ingredient. *J. Food Sci. Technol.* **2015**, *52*, 1404–1413. [CrossRef] [PubMed]
80. Bello-perez, L.A.; Flores-Silva, P.C.; Sifuentes-Nieves, I.; Agama-Acevedo, E. Controlling Starch Digestibility and Glycaemic Response in Maize-Based Foods. *J. Cereal. Sci.* **2021**, *99*, 103222. [CrossRef]
81. Schwingshackl, L.; Hobl, L.P.; Hoffmann, G. Effects of Low Glycaemic Index/Low Glycaemic Load vs. High Glycaemic Index/High Glycaemic Load Diets on Overweight/Obesity and Associated Risk Factors in Children and Adolescents: A Systematic Review and Meta-Analysis. *Nutr. J.* **2015**, *14*, 87. [CrossRef]
82. Mirrahimi, A.; Chiavaroli, L.; Srichaikul, K.; Augustin, L.S.A.; Sievenpiper, J.L.; Kendall, C.W.C.; Jenkins, D.J.A. The Role of Glycemic Index and Glycemic Load In Cardiovascular Disease And Its Risk Factors: A Review of The Recent Literature. *Curr. Atheroscler. Rep.* **2014**, *16*, 381. [CrossRef]

Characterisation of Bario Rice Flour Varieties: Nutritional Compositions and Physicochemical Properties

Macdalyna Esther Ronie [1], Ahmad Hazim Abdul Aziz [1], Nor Qhairul Izzreen Mohd Noor [1], Faridah Yahya [2] and Hasmadi Mamat [1,*]

[1] Faculty of Food Science and Nutrition, University Malaysia Sabah, Jalan UMS,
Kota Kinabalu 88400, Sabah, Malaysia
[2] Faculty of Fisheries and Food Science, Universiti Malaysia Terengganu,
Kuala Nerus 21030, Terengganu, Malaysia
* Correspondence: idamsah@ums.edu.my

Abstract: Gluten-free grains have been intensively studied as alternatives to wheat flour. Bario rice, an indigenous crop from Sarawak, Malaysia, is noted for its excellent aroma and taste. This research examined the nutritional and physicochemical properties of Bario rice flour variations. Four Bario varieties—Bario *Adan Halus* (white), Bario *Tuan* (brown), Bario *Celum* (black), and Bario *Merah Sederhana* (red)—were analysed against the reference sample. The results revealed Bario samples containing moisture contents from 8.35% to 8.69%, ash contents from 0.27% to 1.25%, crude protein contents from 6.89% to 9.43%, crude fat contents from 0.16% to 2.45%, crude fibre contents from 0.21% to 0.87%, and carbohydrate contents from 79.17% to 82.13%. All Bario rice flour contains high amylose contents (26.67% to 36.52%), which positively impact loaf volume. The water absorption capacity (1.20 g/g to 1.26 g/g) of all samples shows no significant difference ($p > 0.05$). The swelling capacity was significantly ($p < 0.05$) high in non-pigmented rice flour. In contrast, pigmented Bario rice flour presented a greater water solubility index than non-pigmented Bario rice flour. The Bario rice flour gelatinisation onset (71.43 °C to 76.49 °C) and peak (77.03 °C to 79.56 °C) temperature were lower than those of the control sample. Higher gelatinisation enthalpy was presented by Bario rice flour (1.23 J/g to 2.59 J/g) than by the control (0.79 J/g). Retrogradation onset (42.65 °C to 50.79 °C), peak (53.64 °C to 56.15 °C) temperatures, and enthalpy (0.19 J/g to 0.87 J/g) were greater in Bario rice flour compared with those in the control. The research suggests that Bario rice flour has potential for use in gluten-free bread mainly due to the relevant carbohydrates, crude proteins, amylose, and swelling capacity.

Keywords: Bario; rice flour; gluten-free; bread; amylose content

1. Introduction

Wheat flour has long been a common ingredient in baked goods and noodles. The presence of gluten proteins in wheat flour greatly influences the structure and texture of wheat based-bakery products. Gluten proteins are the primary determinants of dough because they impart viscoelasticity properties once hydrated and agitated [1]. Due to climatic constraints, wheat is not grown in most Southeast Asian nations, for instance, Malaysia and Indonesia [2]. Hence, those countries have relied on imported wheat to meet their demand for food products based on wheat flour. Recently, the Russia–Ukraine crisis has caused a sudden upsurge in the price of wheat [3]. Therefore, a massive possibility of increments in alternative flour such as rice flours may be in demand instead.

Gluten-related disorders, such as celiac disease, are increasing worldwide. As a result, interest in gluten-free products has intensified among researchers and consumers [4]. A gluten-free diet is the only viable treatment for people with a gluten-related disorder. However, investigations still continue to find the most appropriate and successful therapeutic

options [5]. In celiac disease, adaptive immune response is caused by gluten proteins. Due to their unusual repeating patterns, gastric and pancreatic enzymes are unable to degrade these proteins completely, and their resistance to proteolysis is the leading contributor to their immunogenicity [6,7].

Currently, efforts have been focusing on finding wheat flour alternatives for bakery and food production, consequently saving on foreign exchange by reducing wheat importation [8]. Rice flour is one of the essential raw materials for gluten-free bread due to its global availability and cost-effectiveness [9]. It possesses the properties of being easily digested and absorbed. Moreover, it is well-known for its hypoallergenic properties, colourlessness, and a natural flavour, which rarely negatively affect the end products [10,11]. Previous studies have extensively studied the potential application of rice flour in developing gluten-free bread [12–14]. Most of those studies indicate that rice flour has the potential to be utilised in gluten-free bread. However, several nutritional and physicochemical factors must be considered, such as amylose content [14], particle size [12,13], and water retention capacity [14].

This research focuses on Bario rice varieties. Bario rice is an indigenous crop in Malaysia. It has established its reputation as one of the finest rice varieties due to its soft texture; fine, elongated grains; and superb flavour and aroma [15]. Bario rice varieties are generally cultivated in the Bario highland in the state of Sarawak by the local ethnic community [16]. Bario rice is grown using the conventional method and is devoid of artificial fertilisers [17]. There are four varieties of Bario rice: Bario *Adan Halus*, Bario *Tuan*, Bario *Merah Sederhana*, and Bario *Celum*. It has been remarked that *Adan Halus* is generally classified as white rice; in contrast, Bario *Tuan* is brownish, and Bario *Merah Sederhana* and Bario *Celum* are red and black, respectively [18]. A previous study by Nicholas et al. [18] revealed that Bario *Tuan* and Bario *Celum* are classified as rice with a moderate glycaemic index, which is advantageous for human blood glucose. In addition, a similar study also reported that Bario rice is potentially marketed as healthy food due to its good nutritional content [18]. Thus, due to the eating quality and health benefits of Bario rice, these varieties can potentially be used in the development of gluten-free products. Moreover, past research found that pigmented Bario rice exhibited more outstanding total phenolic content than non-pigmented Bario rice [19].

Currently, there is limited scientific research regarding the nutritional value of these cultivars. In addition, no prior research has focused on the physicochemical properties of Bario rice flour, which is one of the most critical factors for understanding the behaviour of flour for future reference in product development. Therefore, this work aims to provide information on the nutritional compositions and physicochemical properties of local Bario rice varieties. Additionally, the present research is an effort to promote the utilisation of locally grown crops, such as Bario rice, as gluten-free rice flour.

2. Materials and Methods

2.1. Materials

The reference sample, TQR rice, was purchased from a local store in Kota Kinabalu, Sabah, Malaysia. TQR is a local rice variety that is broadly cultivated in Sabah. TQR rice was chosen as a control sample because it is commercial rice often consumed in Sabah. Bario rice samples were obtained from two different suppliers. Bario *Adan Halus* and Bario *Tuan* were obtained from Dagang Mewah Sdn. Bhd., Rawang Selangor, Malaysia. Bario *Merah Sederhana* and Bario *Celum* were obtained from Zulkifli Suli Enterprise, Kuching, Sarawak, Malaysia. Both companies are suppliers that supply authentic Bario rice from Sarawak. In general, the Bario rice varieties were harvested from the highland of Bario, Sarawak, by local farmers.

2.2. Methods

2.2.1. Rice Flour Production

Rice was cleaned individually using tap water for five minutes to ensure that the rice kernels were free from dust and dirt. The rice was then placed on a general flour sifter to remove the remaining water. Upon water draining, the rice was dried in a drying cabinet (Thermoline Scientific TD-78T-SD, Sydney, Australia) at 40 °C approximately for 12 h and above. Dried rice samples were ground to a fine powder using a Waring blender (Panasonic MX-898 M, Selangor, Malaysia) at low speed for 80 s. The grinding process was repeated until fine-sized rice flour could pass through a 250-micron sifter (Endecotts Ltd., London, United Kingdom). The rice flour was sifted using a laboratory sieve shaker (Endecotts Ltd., London, United Kingdom). The fine rice flour was packed in airtight bags and stored at 4 °C until further analysis.

2.2.2. Nutritional Compositions

Determination of moisture content used the 925.10 AOAC (2000) method and the oven drying method. The ash content was determined using the dry weight basis described in the 923.03 AOAC (2000) method. The Fibertherm FT12 (Gerhardt, Brackley, United Kingdom) was utilised to calculate the crude fibre content. Moreover, the Kjeldahl method, detailed in 920.87 (AOAC, 2000), was used to determine the crude protein content of the sample by measuring its protein percentage. This method consists of three parts: digestion, distillation, and titration [20]. Furthermore, the crude fat content was analysed using the fat extraction equipment and the Soxhlet (FOSS Soxhtec™ 2050, Höganäs, Sweden) method described in 920.85 (AOAC, 2000). The carbohydrate content was estimated by deducting the proteins, ash, lipids, and fibre from the samples' dry weight [21].

The amylose content was determined enzymatically using the Megazyme Amylose/Amylopectin assay kit (Megazyme International Ireland Limited, Wicklow, Ireland). In general, this method has two stages of analysis: (1) starch pre-treatment, and (2) con A precipitation of amylopectin and determination of amylose. The wavelength absorbance for the UV–vis spectrophotometer was at 510 nm against the blank reagent.

2.2.3. Physicochemical Properties

The rice flour colour was determined using a colorimeter (Hunterlab CalorFlex EZ, Sunset Hills Road, Reston). The flour sample was inserted into a glass sample cup. The flour sample should entirely cover the bottom surface of a glass sample cup. Colour profiles were expressed in L*, a*, and b*. The L* value indicates the level of light (L = 100) or dark (L = 0), the a* value indicates the amount of redness (+a) or greenness (−a), and the b* value indicates the amount of yellowness (+b) or blueness (−b) [22]. The CalorFlex EZ was standardised using the standard white tile before analysing the sample to prevent errors during colour reading. The result was reported as the mean of triplicates on each sample.

Water absorption capacity and solubility were determined according to the methods described by Coțovanu and Mironeasa, and by Kraithong et al. [23,24] with slight modification. Approximately 1.00 ± 0.02 g of the sample was weighed and recorded as w_0. The sample was then filled into a 50 mL centrifugal tube and weighed again, recorded as w_1. Next, 10 mL of distilled water was added into a centrifugal tube. The dispersions were vortexed every 5 min within 30 min at room temperature, followed by centrifugation for 10 min at 2000 rpm ($359 \times g$). The supernatant was removed from the centrifugal tube, subsequently weighed, and recorded as w_2. The amount of water bound by flour was determined by the difference and expressed as the weight of water bound by dry flour (100 g) [25]. The result was reported as the mean of triplicates on each sample. Water absorption capacity was calculated using Equation (1).

$$\text{Water absorption capacity} = \frac{w_2 - w_1}{w_0} \tag{1}$$

where w_0 = mass of sample (g), w_1 = mass of centrifugal tube + sample (g), and w_2 = mass of centrifugal tube + residue after removing the supernatant (g).

The swelling capacity was determined according to the method described by Anyasi et al. [26] with slight modification. First, 1 g (w_1) of the rice flour sample was moistened with 30 mL of distilled water in a centrifuge tube. The centrifuge tubes containing the sample were heated at 80 °C in the water bath while shaking continuously. The tubes were taken out and allowed to cool down until the temperature decreased to room temperature. After the cooling process, samples were centrifuged at 2200 rpm for 15 min. The supernatant was removed from the centrifuge tube, and the residue weight was recorded (w_2). The swelling capacity (g/g) was determined using Equation (2).

$$\text{Swelling capacity (g/g)} = \frac{w_2}{w_1} \tag{2}$$

where w_1 = mass of dry sample (g) and w_2 = mass of residue (after removing supernatant) (g).

Moreover, the decanted supernatant from the swelling capacity procedure was used to determine the water solubility index of the rice flour. First, the empty crucibles were weighed and recorded as w_4, and the supernatant was poured carefully into the tared crucible. Then, the oven drying method was initiated to the supernatant at 105 °C overnight. On the following day, the dried supernatant was cooled in a desiccator to room temperature and weighed as w_3. The result was reported as the mean of triplicates on each sample. The water solubility index was calculated using Equation (3).

$$\text{Water solubility index, } \% = \frac{w_3 - w_4}{w_1} \times 100 \tag{3}$$

where w_1 = mass of the sample (g), w_3 = mass of crucibles and dried supernatant (g), and w_4 = mass of crucibles (g).

2.2.4. Thermal Properties

The gelatinisation profiles were determined according to the method described by Gunaratne et al. [27] using a different scanning calorimeter (DSC) (Perkin Elmer, Waltham, MA, USA) equipped with a thermal analysis data station (Pyris Software version 9.0.2.0193 (2008), PerkinElmer, Inc., Waltham, MA, United States) with slight modification. First, 2 mg of the rice flour sample was weighed onto the aluminium DSC pan, followed by 6 µL of distilled water with a micropipette. Next, the pan was sealed and kept at room temperature for 1 h. The scanning temperature range and heating rate were 30 °C to 120 °C and 10 °C min^{-1}, respectively, using an empty pan as a reference. In general, the final result of the DSC instrument was expressed as initial temperature value (T_0), peak temperature (T_P), final temperature (T_f), and gelatinisation enthalpy (ΔH) [28].

A retrogradation analysis was conducted according to the method described by Wang et al. [29] with a slight modification. After the gelatinisation in the DSC, the pans were stored at 4 °C for 7 days and rescanned under a constant temperature range from 30 °C to 120 °C and a heating range of 10 °C min^{-1}, similar to the gelatinisation measurement. The final result of the DSC instrument was expressed as initial temperature value (T_0), peak temperature (T_P), final temperature (T_f), and retrogradation enthalpy (ΔH).

2.2.5. Statistical Analysis

All experimental data were analysed using Statistical Packages for the Social Sciences (SPSS) version 26.0 in a completely randomised study design. All experimental values were presented as mean ± standard deviation (mean ± SD). In general, a one-way analysis of variance (ANOVA) was employed to determine the significant differences in data among the experimental units. Tukey's HSD test was utilised for multiple comparisons. Statistical significance was established at $p < 0.05$.

3. Results and Discussion

3.1. Nutritional Compositions

The nutritional compositions of the five rice flours are presented in Table 1.

Table 1. Nutritional compositions of Bario rice flour varieties and TQR rice flour as a reference sample.

Nutritional Compositions	TQR	Bario *Adan Halus*	Bario *Tuan*	Bario *Celum*	Bario *Merah Sederhana*
Moisture	8.47 ± 0.05 [b]	8.35 ± 0.03 [c]	8.69 ± 0.05 [a]	8.67 ± 0.05 [a]	8.50 ± 0.02 [b]
Ash	0.25 ± 0.01 [d]	0.27 ± 0.00 [d]	1.25 ± 0.06 [a]	0.63 ± 0.01 [c]	0.98 ± 0.02 [b]
Crude fiber	0.13 ± 0.03 [c]	0.21 ± 0.03 [c]	0.87 ± 0.05 [a]	0.55 ± 0.07 [b]	0.62 ± 0.09 [b]
Crude protein	7.81 ± 0.45 [c]	8.97 ± 0.08 [ab]	8.66 ± 0.08 [b]	6.89 ± 0.01 [d]	9.43 ± 0.04 [a]
Crude fat	0.22 ± 0.07 [c]	0.16 ± 0.03 [c]	2.45 ± 0.08 [a]	1.13 ± 0.07 [b]	1.32 ± 0.11 [b]
Carbohydrate	83.12 ± 0.35 [ab]	82.04 ± 0.10 [ab]	79.25 ± 1.19 [c]	82.13 ± 0.01 [ab]	79.17 ± 0.29 [c]
Amylose content	32.97 ± 2.96 [a]	26.67 ± 0.49 [b]	36.52 ± 1.37 [a]	26.68 ± 0.69 [b]	32.05 ± 0.81 [ab]

Mean ± standard deviation, ($n = 3$), except for amylose content: mean ± standard deviation, ($n = 2$); Mean values in the same row with different superscripts are significantly different with $p < 0.05$.

3.1.1. Moisture Content

The moisture content was significantly higher for Bario *Tuan* (8.69%) and Bario *Celum* (8.67%). Bario *Adan Halus* (8.35%) had the lowest moisture content. These moisture values are in accordance with past studies, in which the moisture content of various rice ranged from 8% to 9.61% and from 8.44% to 10.04%, respectively [30,31]. However, few previous studies obtained lower moisture contents between 4.25% and 5.06%, and between 5.46% and 7.08%, respectively [32,33]. Generally, a moisture content lower than 14% can be considered safe for an extended storage period, especially for cereal and cereal products [34]. According to USDA Foreign Agricultural Service [35], based on the standard of rice flour production, the moisture content of rice can be more than 10% but less than 15%. In general, a moisture content below 14% can help prevent infestation by insects and microbial growth, which can deteriorate the shelf life of food [36]. As a result, the rice flours in this research should have good shelf lives.

3.1.2. Ash Content

Ash content reflects the total mineral content in the sample [37]. Bario *Tuan* exhibited the highest ash content (1.25%) among other Bario rice flours, followed by Bario *Merah Sederhana* (0.98%) and Bario *Celum* (0.63%), and the lowest ash contents were from Bario *Adan Halus* and TQR rice. TQR and Bario *Adan Halus* indicated no significant difference ($p > 0.05$) in mean ash content. Table 1 shows that the ash content of pigmented rice flour (Bario *Tuan*, *Celum*, and *Merah Sederhana*) is higher than white rice (TQR and Bario *Adan Halus*). Similarly, research by Thomas et al. [16] and Oppong et al. [32] also discovered consistent results, in which the percentage of ash contents of black and brown rice flour is more significant than white rice. The reason for this is that the outer layer of rice grains can influence the rice flour's ash content. In this respect, Bello et al. [38] also speculated that the variation in ash content within rice flours depends on the concentration of compounds within the bran layers of the caryopsis. Another factor, such as the degree of severity during milling for bran separation, can also cause variation in the ash concentration among rice flour varieties [39]. Moreover, variation in the ash content within commodities is also related to the agricultural parameters, such as the soil and irrigation sources [36].

3.1.3. Crude Fibre Content

Bario *Tuan* (0.87%) obtained the highest crude fibre content among the others, followed by Bario *Celum* (0.55%) and Bario *Merah Sederhana* (0.62). The lowest crude fibre content was presented by Bario *Adan Halus* (0.21%) and TQR (0.12%), which exhibited no significant difference from each other ($p > 0.05$). Overall, the crude fibre content among all samples was below 1%. In addition, it can be observed that rice flour produced from pigmented rice

grains contains higher crude fibre than white or polished rice. This finding is comparable with that from past studies by Nicholas et al. [18] and by Thongkaew and Singthong [40]. In general, rice flour's fibre and ash contents increase proportionally with the amount of bran in flour [41].

3.1.4. Crude Protein Content

The highest crude protein content was presented by Bario *Merah Sederhana* (9.43%), and the lowest was from Bario *Celum* (6.89%). In accordance with the present results, previous studies have investigated that rice flour's protein content was from approximately 6% to 9% [24,30,42]. On the contrary, Nicholas et al. [18] reported that the protein content of Bario rice flour ranges from 5.85% to 7.30%. The most likely causes of differences in crude protein content are external factors such as environmental parameters [43] and storage conditions (time and temperature) [33]. The average protein content of rice flour is 7.33% [44]. Based on Table 1, the protein content for the majority of rice flour samples was more than the average value, except for Bario *Celum* (6.89%). Previous research by Paz et al. [45] proposed that it is possible to utilise rice flour with higher protein contents in gluten-free rice flour baked items without altering the qualities of the final products. In addition, the application of high protein rice flour in food development reduces the carbohydrate content, decreasing the glycaemic load during absorption and digestion in the human body. Thus, due to the significant protein content in Bario rice flour, this research suggested that Bario rice flour can potentially be used in gluten-free bread.

3.1.5. Crude Fat Content

Bario *Tuan* had the greatest crude fat content (2.45%), followed by Bario *Merah Sederhana* (1.32%), Bario *Celum* (1.13%), TQR (0.2%), and Bario *Adan Halus* (0.16%). Table 1 shows that the crude fat content for pigmented rice flour is higher than that for white rice (TQR and Bario *Adan Halus*). Likewise, in the study conducted by Puri et al. [46], brown rice (1.73%) flour contained a higher crude fat content than white rice flour (1.13%). The recent study by Oppong et al. [32] revealed the same result; pigmented (brown rice flour) possesses higher fat content than commercial white rice flour. Pigmented rice flour contains a high fat content mainly because of the outer layer known as bran [24,32]. To a large extent, rice bran is the major part of rice that contains lipids or fats, approximately 20% on a dry basis [47]. Thus, rice flour produced from milled and polished rice contains lower fat than pigmented rice flour. On the other hand, the high fat content has been ascertained to improve the sensorial quality of final products, especially tastes [42].

3.1.6. Carbohydrate Content

The carbohydrate content is in the range from 79.17% to 83.12%. TQR has the highest carbohydrate content, 83.12%, and Bario *Merah Sederhana*, 79.17%, shows the lowest carbohydrate value. In addition, there is no significant difference ($p > 0.05$) between Bario *Celum* (82.13%), TQR (83.12%), and Bario *Adan Halus* (82.04%). Similarly, Bario *Merah Sederhana* (79.14%) and Bario *Tuan* (79.25%) show no significant differences ($p > 0.05$). In general, TQR contains the highest carbohydrate value of all. Likewise, in the investigation by Oppong et al. [32], the authors discovered that commercial white rice flour contains more carbohydrates than brown rice varieties. This was expected since pigmented rice varieties are covered by the external layer known as bran, mainly concentrated with crude fat and proteins, ash, and crude fibre [48], which decrease the carbohydrate content within the food.

3.1.7. Amylose Content

Starch is recognised as the main composition of rice flour. Generally, rice starch comprises amylose and amylopectin [49]. The quality of gluten-free rice bread generally relies on the amylose content of rice flour [50,51]. The amylose content of control and Bario rice flour varieties are shown in Table 1. In this research, the highest amylose content was

presented by Bario *Tuan* (36.52%), followed by the control sample (32.97%), Bario *Merah Sederhana* (32.05%), and Bario *Celum* (26.68%), and the lowest amylose content was from Bario *Adan Halus* (26.67%). No significant differences (*p* > 0.05) were exhibited between the three highest amylose contents: Bario *Tuan*, TQR, and Bario *Merah Sederhana*. There are five classifications of amylose content: waxy, very low, low, intermediate, and high. Waxy rice possesses amylose contents in the ranges from 0% to 2%, very low ranges from 2% to 10%, low ranges from 10% to 20%, intermediate ranges from 20% to 25% and high has contents above 25% [52]. Table 1 shows that all samples of Bario rice flour had a high amylose content, with values ranging from 26.67% to 36.53%.

Several studies have examined the role of amylose content in developing gluten-free rice bread. Most researchers reported that amylose positively impacts the development of rice-based products. It has been revealed that amylose content positively impacted specific volumes and the leavening process of the dough [14,53]. High amylose content rice flour possesses good gas-holding properties, resulting in a greater loaf volume in 100% prepared rice bread [51]. The reason for this is that amylose can influence the hydrophobicity of starch granules toward stable Pickering emulsion [54]. On the other hand, a few studies found that softer bread textures were developed from rice flour containing low to medium amylose content; on the contrary, high amylose content rice flour produces rice bread with a sandy texture [55,56]. Even though low-amylose rice flour could develop rice bread with a soft texture, Aoki et al. [55] revealed that the final bread quality is not favourable due to its inferior shape. Hence, Bario rice varieties are predicted to have potential as an ingredient in making rice bread with acceptable quality in terms of loaf volume.

3.2. Physicochemical Properties

The physicochemical properties of the five rice flours are stated in Table 2.

Table 2. Physicochemical properties of Bario rice varieties compared with TQR rice.

Analysis	TQR	Bario *Adan Halus*	Bario *Tuan*	Bario *Celum*	Bario *Merah Sederhana*
Colour					
L*	93.62 ± 0.04 [a]	94.34 ± 0.05 [b]	84.84 ± 0.07 [c]	70.99 ± 0.36 [d]	75.26 ± 0.04 [e]
a*	−0.15 ± 0.01 [d]	−0.21 ± 0.02 [d]	2.12 ± 0.07 [c]	2.75 ± 0.06 [b]	4.80 ± 0.01 [a]
b*	5.27 ± 0.07 [d]	6.21 ± 0.03 [c]	14.46 ± 0.13 [a]	1.20 ± 0.05 [e]	7.91 ± 0.04 [b]
WAC (g/g)	1.20 ± 0.00 [a]	1.26 ± 0.04 [a]	1.24 ± 0.03 [a]	1.21 ± 0.00 [a]	1.21 ± 0.01 [a]
Swelling capacity (g/g)	23.53 ± 0.10 [a]	23.60 ± 0.21 [a]	22.97 ± 0.0 [b]	20.31 ± 0.06 [c]	22.91 ± 0.20 [b]
WSI (%)	2.32 ± 0.01 [c]	1.83 ± 0.08 [d]	2.84 ± 0.04 [b]	2.70 ± 0.10 [b]	3.44 ± 0.22 [a]
Gelatinisation					
T_o	77.41 ± 0.44 [a]	71.43 ± 0.46 [c]	74.04 ± 0.63 [b]	74.89 ± 0.22 [b]	76.49 ± 0.27 [a]
T_p	80.49 ± 0.35 [a]	77.03 ± 0.15 [d]	78.72 ± 0.50 [bc]	78.24 ± 0.41 [c]	79.56 ± 0.21 [ab]
T_f	83.22 ± 0.33 [a]	80.77 ± 0.44 [b]	84.45 ± 0.67 [a]	81.17 ± 0.26 [b]	84.38 ± 0.68 [a]
ΔH_{gel} (J/g)	0.79 ± 0.07 [c]	2.13 ± 0.32 [a]	1.77 ± 0.08 [ab]	2.59 ± 0.61 [a]	1.23 ± 0.16 [bc]
Retrogradation					
T_o	41.80 ± 0.52 [c]	44.50 ± 1.90 [bc]	50.79 ± 1.35 [a]	42.65 ± 1.24 [c]	45.90 ± 0.29 [b]
T_p	44.36 ± 1.55 [b]	54.01 ± 1.33 [a]	56.15 ± 1.27 [a]	53.64 ± 1.63 [a]	54.91 ± 0.63 [a]
T_f	48.71 ± 1.37 [b]	60.19 ± 1.55 [a]	61.02 ± 1.32 [a]	60.19 ± 1.07 [a]	61.25 ± 1.89 [a]
ΔH_{ret} (J/g)	0.13 ± 0.03 [c]	0.76 ± 0.11 [a]	0.19 ± 0.04 [c]	0.87 ± 0.12 [a]	0.42 ± 0.08 [b]

WAC = water absorption index, WSI = water solubility index, T_o = onset temperature, T_p = peak temperature, T_f = final temperature, ΔH_{gel} = gelatinisation enthalpy and ΔH_{ret} = retrogradation enthalpy; Mean ± standard deviation, (*n* = 3); Mean values in the same row with different superscripts are significantly different with *p* < 0.05.

3.2.1. Colour Analysis

The results of the colour analysis of all rice flour samples are shown in Table 2. The L* value expresses the brightness, in which the L* value ranges from 70.99 to 94.34. The brightness of rice flour was more prominent in Bario Adan Halus, followed by TQR. Both varieties exhibited high L* values due to their white appearance. Moreover, Bario Tuan, Bario Merah Sederhana, and Bario Celum rice flour presented lower L* values due to the brown, red, and purple pigmented external layers of the rice grains, respectively. The a* and b* values ranged between −0.15 and 4.80, and between 1.20 and 14.46, respectively. A positive a* value represents red, whereas a negative b* value represents green. Based on the result obtained, a positive a* value was high for Bario Merah Sederhana due to the red pigmentation of the rice bran. On the other hand, b* values ranged from 1.20 to 14.46. Specifically, a positive b* value indicates yellow while a negative b* value represents blue. The colour appearance of TQR and Bario rice flour is shown in Figure 1. In conclusion, the colour profiles of rice flour samples are based on the rice bran's pigment. Rice grains with a brownish-red pigment are typically called red rice, whereas rice kernels with purple pigmentation are renowned as black rice [57]. Anthocyanins and proanthocyanidins or condensed tannins are common pigments in black and red rice, respectively [58].
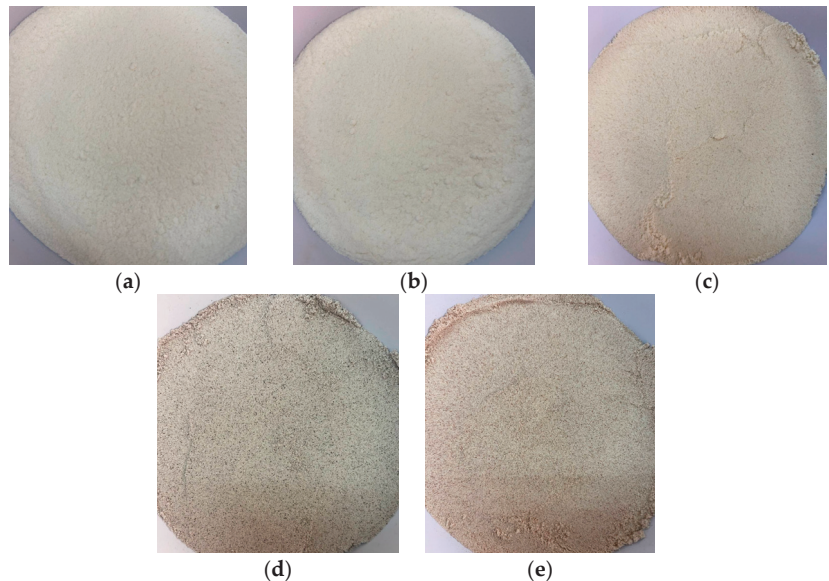
Figure 1. The colour diversity of (**a**) TQR (reference sample) and Bario rice flour, (**b**) Bario *Adan Halus*, (**c**) Bario *Tuan*, (**d**) Bario *Celum*, and (**e**) Bario *Merah Sederhana*.

3.2.2. Water Absorption Capacity

The water absorption capacity (WAC) of food products generally denotes the flour's ability to interact with water [32]. Based on Table 2, WAC ranges from 1.20 g/g to 1.26 g/g. The WAC values among the sample show no significant differences ($p > 0.05$) from each other. The highest WAC value was presented by rice flour made from Bario Adan Halus (1.26 g/g), and the lowest was from TQR (1.20 g/g). Similar values of the WAC rice flour have been stated in previous studies, which is approximately 1.2 g/g [59,60]. Different WACs of rice flour have been associated with starch composition, specifically the amylose and amylopectin ratio; a higher WAC indicates a high amylose content in rice [61]. In this study, Bario Tuan showed the highest amylose concentration; however, Bario Tuan rice flour did not follow that pattern. Alcázar-Alay et al. [62] reported that a high lipid content might decrease WAC because the hydrophobic group of lipids can interfere with the hydration capability of starch granules within rice flour. Based on Table 1, Bario Tuan exhibited the

highest crude fat content; thus, it can be concluded that the possibility of a high crude fat content within Bario Tuan might impedes starch granules' hydration, consequently reducing the WAC. It has been concluded that lower-WAC rice flour (0.99 g/g to 1.07 g/g) provided better rice bread based on its physicochemical properties [63]. Conversely, a study by Cornejo and Rosell [64] discovered that higher-WAC rice flour (1.28 g/g and 1.38 g/g) produced the best gluten-free bread features. According to Han et al. [63], high water absorption decreases stickiness and produces solid dough, and at the bread level, rice flour with low water absorption generates fresh bread.

3.2.3. Swelling Capacity

The swelling of starch granules has occurred during gelatinisation. Starch swelled because the hydroxyl groups within the starch granules formed new hydrogen bonds with water molecules due to the disruption of hydrogen bonds between the hydroxyl group in the double helices of starch molecules [65]. Based on Table 2, the swelling capacity range was between 20.31 g/g and 23.60 g/g. Generally, rice flour produced from Bario Adan Halus (23.60 g/g) exhibited the highest swelling capacity value, and the lowest was presented by Bario Celum (20.32 g/g). Based on the result, pigmented rice flour exhibited significantly ($p < 0.05$) lower swelling capacities compared with white rice flour. These current findings agree with the research performed by Wani et al. [66] and Li et al. [67]. The reason for this is that the outer bran of the pigmented rice grains delayed water penetration into the starch granules, consequently lowering the swelling capacity of the flour. On the other hand, the swelling of granules can also be hindered by lipids [68]. Likewise, in this study, pigmented rice flour generally contained higher lipid content compared with white rice flour, resulting in a lower swelling capacity than white rice flour (TQR and Bario Adan Halus). In bread development, lower swelling capacity flour is not recommended because it might inhibit the swelling process of the final baked products [69]. For that reason, the possibility for Bario rice flour to be used in gluten-free bread production is high.

3.2.4. Water Solubility Index

The water solubility index (WSI) measures a component's capacity to dissolve in water in excess water [70]. Bario Merah Sederhana (3.44%) exhibited a significantly highest WSI value ($p < 0.05$), and the lowest was Bario Adan Halus (1.83%). The greatest WSI rice flour implies a high amount of water-soluble components dispersed aqueously during the cooking process [71]. Based on Table 2, the result indicates that pigmented rice flour has a greater WSI than polished white rice flour. Numerous studies determined that pigmented rice flour usually possesses a lower swelling capacity and a higher WSI compared with white rice flour [66,67,72]. Thiranusornkij et al. [72] have concluded that this might be due to a high concentration of phenolic compounds that has been leached out during processing. However, explanations of the effect of pigmented and non-pigmented rice flour on swelling and water solubility index are still limited; hence further research to be conducted in the future is suggested.

3.2.5. Gelatinitisation

Gelatinisation is identified as a phase transition of starch granules from an ordered to disordered state or known as changes from crystalline to the amorphous structure of starch granules [73]. Gelatinisation occurs in the range from 60 °C to 80 °C with the presence of water during thermal treatment. Figure 2 presents the gelatinisation curve for rice flour samples.
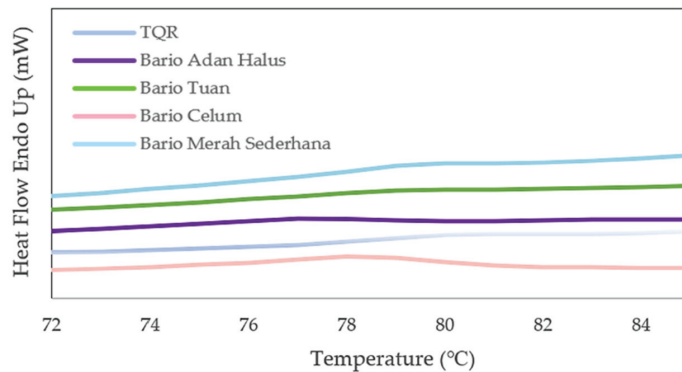
Figure 2. DSC curve of gelatinised rice flour samples for TQR, Bario Adan Halus, Bario Tuan, Bario Celum, and Bario Merah Sederhana.

The gelatinisation onset temperature (T_o) ranges between 71.43 °C and 77.41 °C. The highest value of T_o was presented by TQR rice flour, at 77.41 °C, and the lowest was from Bario Adan Halus (71.43 °C). Moreover, the T_p and T_f ranged between 77.03 °C and 80.49 °C, and between 80.77 °C and 84.45 °C, respectively. The highest T_p and T_f were shown by TQR rice flour, at 80.49 °C and 83.22 °C, respectively, whereas Bario Adan Halus showed the lowest, at 77.03 °C and 80.77 °C, for T_p and T_f, respectively. Nevertheless, the ΔH_{gel} of rice flour samples varies between 0.79 J/g and 2.59 J/g. ΔH_{gel} denotes the thermal energy required to convert the initial crystalline state to an amorphous structure within the starch granules [74]. A high ΔH_{gel} implies high energy required to transform the starch structure from the ordered (crystal) to disordered (amorphous) forms, whereas a low ΔH_{gel} implies the opposite. The ΔH_{gel} of Bario rice flour varied widely, with the highest value found in Bario *Celum* rice flour (2.59 J/g) and the lowest value found in TQR rice flour (0.79 J/g). The variation in ΔH_{gel} can be roughly determined by looking at the area under the DSC curve of gelatinised rice flour in Figure 2.

According to the results, the gelatinisation of TQR rice flour generally requires a higher temperature but less energy to initiate the breakdown of hydrogen bonds in a double-helical amylopectin chain. A previous study by Amini et al. [75] reported that the lower ΔH_{gel} is due to the formation of cracks on the starch surface due to the higher gelatinisation temperature, which facilitate water penetration into the starch granules and further penetration into the starch's crystalline areas, consequently reducing the energy required for gelatinisation. On the other hand, the gelatinisation temperature of Bario Adan Halus was the lowest of all (T_o = 71.43 °C, T_p = 77.03 °C, and T_f = 80.77 °C) but considerably high in ΔH_{gel} (2.13 J/g). A previous study by Farooq et al. [76] also obtained a similar gelatinisation pattern for rice flours. Biliaderis et al. [77] explained that a lower gelatinisation temperature contributes to the upsurge in ΔH_{gel}, and ΔH_{gel} has an inverse proportional relationship with amylose content, in which ΔH_{gel} increases when amylose concentration decreases. Similarly, the amylose contents of Bario Adan Halus (26.67%) and Bario Celum (26.68%) were the lowest possible among all, thus resulting in the highest ΔH_{gel}, 2.13 J/g and 2.59 J/g, respectively. According to Cornejo and Rosell [64], choosing high ΔH_{gel} flours with low T_p is preferable, especially to improve crumb cohesiveness and resilience. Moreover, a positive correlation exists between T_f and the specific volume of the end product. This outcome might be linked to the rising of bread during baking [64]. Bario *Tuan* and Bario *Merah Sederhana* exhibited greater T_f than the control sample, which might have delivered a positive impact on the final product in terms of the specific volume.

3.2.6. Retrogradation

Retrogradation is defined as a process by which amylose and amylopectin molecules reassociate through hydrogen bonding, consequently developing a three-dimensional network structure [78]. Figure 3 shows the retrogradation curve for rice flour samples.
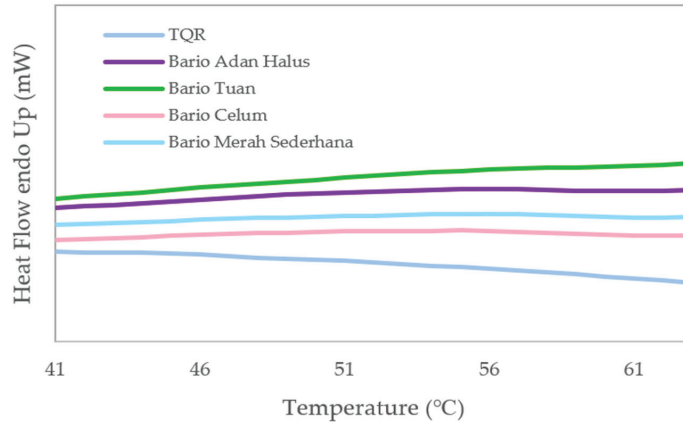
Figure 3. Retrogradation curve of rice flour samples for TQR, Bario Adan Halus, Bario Tuan, Bario Celum, and Bario Merah Sederhana.

Table 2 presents the retrogradation profiles of the control and treatment samples. The T_o range is between 41.80 °C and 50.79 °C. The highest T_o was exhibited by the Bario Tuan variety (50.79 °C), followed in descending order by Bario Merah Sederhana (45.90 °C); Bario Adan Halus (44.50 °C); Bario Celum (42.65 °C); and the control sample, TQR (41.80 °C). There was a significant difference ($p < 0.05$) in the T_o of Bario Tuan compared with other varieties. Moreover, the T_p and T_f ranged between 44.36 °C and 56.15 °C, and between 48.71 °C and 61.25 °C, respectively. The highest T_p was shown by Bario Tuan (56.15 °C), whereas the lowest T_p was showed by the control sample, TQR (44.36 °C). Generally, there are no significant differences ($p > 0.05$) shown by all varieties, except TQR, which had the significantly ($p < 0.05$) lowest T_p. On the other hand, Bario Merah Sederhana (61.25 °C) had the highest T_f, whereas the lowest was presented by TQR (48.71 °C). Similarly, all varieties showed no significant difference ($p > 0.05$), except the TQR variety. In addition, the gap between temperature range (T_f–T_o) can be determined and related to the length of the double helix, so a wider endotherm suggests a wider range of double-helical lengths [79]. The ΔH_{ret} range was between 0.13 J/g and 0.87 J/g. The highest ΔH_{ret} was exhibited by Bario Celum (0.87 J/g), and the lowest was the control sample, TQR (0.13 J/g). A high value of ΔH_{ret} means more energy is required to break down the reassociated amylopectin formed during the storage period, indicating a higher retrogradation process [80]. Thus, Bario Celum (0.87 J/g) and Bario Adan Halus (0.76 J/g) exhibited significantly ($p < 0.05$) higher retrogradation processes compared with the other varieties.

According to Chang et al. [81], amylose content is one of the significant factors influencing starch's retrogradation. Nonetheless, the highest amylose content exhibited by Bario Tuan and ΔH_{ret} of Bario Tuan (0.19 J/g) was lower than that in Bario Adan Halus (0.76 J/g). This indicates that the retrogradation enthalpy was less pronounced in Bario Tuan even though the amylose content was high within this variety. This possibly results from the higher fat content within Bario Tuan (2.45%) than within Bario Adan Halus (0.16%), which might develop starch–lipid complexes, consequently decreasing the amount of starch retrogradation. In general, lipid reduces the movement of amylose due to the development of complexes constructed between amylose and lipid [82]. The starch–lipid complex is developed through a hydrophobic effect due to hydrophilic and hydrophobic groups in lipids. The latter group leads the lipids to move closer to the internal hydrophobic

cavities of amylose [81]. On the other hand, factors such as small molecular sugar and non-polysaccharides, salt ions, granule size, and the ratio of amylose and amylopectin within starch granules could influence the retrogradation profiles [83–86].

4. Conclusions

In conclusion, Bario rice flour possesses a good source of protein content. A significant protein content will increase the nutritional value of gluten-free products. Moreover, the results based on proximate composition (ash, crude fat, and crude fibre content) showed that pigmented Bario rice flour contains a higher value than non-pigmented rice flour, including the control sample. This is primarily due to the external layer of rice kernels. In addition, the carbohydrate content in Bario rice flour varieties is lower than that in the control sample because Bario rice flour generally has higher concentrations of the other proximate compositions. All Bario rice flour classified as having high amylose contents could positively impact the bread volume. The colour profiles of Bario rice flour samples varied depending on the rice bran's pigmentation. The WAC of all samples showed no significant differences ($p > 0.05$) from each other. The swelling capacity was high in all Bario rice flour and can potentially be used in bread-making due to this easy swelling process. The WSI was higher in pigmented Bario rice flour, most probably due to the high concentrations of phenolic compound leached out during processing. The gelatinisation and retrogradation profiles provide information regarding the behaviour of rice flour during and after processing. Bario *Tuan* and Bario *Merah Sederhana* exhibited greater T_f than the control sample. T_f generally correlated positively with the final product's specific volume.

To summarise, this research suggests the application of Bario rice flour in gluten-free bread, especially considering the nutritional content, mainly the carbohydrate, crude protein, and amylose contents, which positively influence the quality of gluten-free bread. Moreover, Bario rice flour offers promising physicochemical properties regarding its swelling capacity, which is beneficial in developing gluten-free bread. Therefore, this study has investigated the nutritional compositions and physicochemical properties of Bario rice flour, which can be helpful information and knowledge for product development. However, future research could extend this study by looking at the quality of the gluten-free bread developed from Bario rice flour. Such research could help increase the scientific knowledge of Bario rice flour varieties as well as promote the utilisation of local crops in developing gluten-free products.

References

1. Ooms, N.; Delcour, J.A. How to impact gluten protein network formation during wheat flour dough making. *Curr. Opin. Food Sci.* **2019**, *25*, 88–97. [CrossRef]
2. Lin, H.I.; Yu, Y.Y.; Wen, F.I.; Liu, P.T. Status of Food Security in East and Southeast Asia and Challenges of Climate Change. *Climate* **2022**, *10*, 40. [CrossRef]
3. Grain and Feed Annual (Annual Report MY2022-0001). Available online: https://apps.fas.usda.gov/newgainapi/api/Report/DownloadReportByFileName?fileName=Grain%20and%20Feed%20Annual_Kuala%20Lumpur_Malaysia_MY2022-0001.pdf (accessed on 11 July 2022).
4. Ren, Y.; Linter, B.R.; Linforth, R.; Foster, T.J. A comprehensive investigation of gluten free bread dough rheology, proving and baking performance and bread qualities by response surface design and principal component analysis. *Food Funct.* **2020**, *11*, 5333–5345. [CrossRef] [PubMed]
5. Asri, N.; Rostami-Nejad, M.; Anderson, R.P.; Rostami, K. The gluten gene: Unlocking the understanding of gluten sensitivity and intolerance. *Appl. Clin. Genet.* **2021**, *14*, 37. [CrossRef]
6. Catassi, C.; Verdu, E.F.; Bai, J.C.; Lionetti, E. Coeliac disease. *Lancet* **2021**, *399*, 2413–2426. [CrossRef]
7. Bascuñán, K.A.; Araya, M.; Roncoroni, L.; Doneda, L.; Elli, L. Dietary gluten as a conditioning factor of the gut microbiota in celiac disease. *Adv. Nutr.* **2020**, *11*, 160–174. [CrossRef] [PubMed]
8. Tharise, N.; Julianti, E.; Nurminah, M. Evaluation of physico-chemical and functional properties of composite flour from cassava, rice, potato, soybean and xanthan gum as alternative of wheat flour. *Int. Food Res. J.* **2014**, *21*, 1642–1643.
9. Feizollahi, E.; Mirmoghtadaie, L.; Mohammadifar, M.A.; Jazaeri, S.; Hadaegh, H.; Nazari, B.; Lalegani, S. Sensory, digestion, and texture quality of commercial gluten-free bread: Impact of broken rice flour type. *J. Texture Stud.* **2018**, *49*, 395–403. [CrossRef]
10. Aleman, R.S.; Paz, G.; Morris, A.; Prinyawiwatkul, W.; Moncada, M.; King, J.M. High protein brown rice flour, tapioca starch & potato starch in the development of gluten-free cupcakes. *Food Sci. Technol.* **2021**, *152*, 112326. [CrossRef]
11. Wu, T.; Wang, L.; Li, Y.; Qian, H.; Liu, L.; Tong, L.; Zhou, S. Effect of milling methods on the properties of rice flour and gluten-free rice bread. *Food Sci. Technol.* **2019**, *108*, 137–144. [CrossRef]
12. Park, J.H.; Kim, D.C.; Lee, S.E.; Kim, O.W.; Kim, H.; Lim, S.T.; Kim, S.S. Effects of rice flour size fractions on gluten free rice bread. *Food Sci. Biotechnol.* **2014**, *23*, 1875–1883. [CrossRef]
13. Luo, S.; Yan, X.; Fu, Y.; Pang, M.; Chen, R.; Liu, Y.; Chen, J.; Liu, C. The quality of gluten-free bread made of brown rice flour prepared by low temperature impact mill. *Food Chem.* **2021**, *348*, 129032. [CrossRef] [PubMed]
14. Gui, Y.; Chen, G.; Tian, W.; Yang, S.; Chen, J.; Wang, F.; Li, Y. Normal rice flours perform better in gluten-free bread than glutinous rice flours. *J. Food Sci.* **2022**, *87*, 554–566. [CrossRef] [PubMed]
15. Wong, S.C.; Yiu, P.H.; Bong, S.T.W.; Lee, H.H.; Neoh, P.N.P.; Rajan, A. Analysis of Sarawak Bario rice diversity using microsatellite markers. *Am. J. Agric. Biol. Sci.* **2009**, *4*, 298–304. [CrossRef]
16. Thomas, R.; Yeoh, T.K.; Wan-Nadiah, W.A.; Bhat, R. Quality evaluation of flat rice noodles (Kway Teow) prepared from Bario and Basmati rice. *Sains Malays.* **2014**, *43*, 339–347. Available online: http://www.ukm.edu.my/jsm/pdf_files/SM-PDF-43-3-2014/03%20Rachel%20Thomas.pdf. (accessed on 14 July 2022).
17. Kevin, M.T.S.; Ahmed, O.H.; Asrina, W.Y.W.; Rajan, A.; Ahzam, M. Towards growing Bario rice on lowland soils: A preliminary nitrogen and potassium fertilization trial. *Am. J. Agric. Biol. Sci.* **2007**, *2*, 99–105. [CrossRef]
18. Nicholas, D.; Hazila, K.K.; Chua, H.P.; Rosniyana, A. Nutritional value and glycemic index of Bario rice varieties. *J. Trop. Agric. Food Sci.* **2014**, *42*, 1–8. Available online: http://jtafs.mardi.gov.my/jtafs/42-1/Bario%20rice.pdf (accessed on 14 July 2022).
19. Sharma, K.; Lee, Y.R. Effect of different storage temperature on chemical composition of onion (*Allium cepa* L.) and its enzymes. *J. Food Sci. Technol.* **2016**, *53*, 1620–1632. [CrossRef]
20. Nielsen, S.S. *Food Analysis Laboratory Manual*, 3rd ed.; Springer International Publishing: Cham, Switzerland, 2017; ISBN 978-3-319-44127-6.
21. Bolea, C.A.; Grigore-Gurgu, L.; Aprodu, I.; Vizireanu, C.; Stănciuc, N. Process-structure-function in association with the main bioactive of black rice flour sieving fractions. *Foods* **2019**, *8*, 131. [CrossRef]
22. Hunter L, a, b Versus CIE 1976 L* a* b*. Available online: https://support.hunterlab.com/hc/en-us/article_attachments/201437795/an02_01.pdf (accessed on 20 July 2022).
23. Coțovanu, I.; Mironeasa, S. Buckwheat Seeds: Impact of milling fractions and addition level on wheat bread dough rheology. *Appl. Sci.* **2021**, *11*, 1731. [CrossRef]
24. Kraithong, S.; Lee, S.; Rawdkuen, S. Physicochemical and functional properties of Thai organic rice flour. *J. Cereal Sci.* **2018**, *79*, 259–266. [CrossRef]
25. Noorfarahzilah, M.; Mansoor, A.H.; Hasmadi, M. Proximate composition, mineral content and functional properties of Tarap (*Artocarpus odoratissimus*) seed flour. *Food Res.* **2017**, *1*, 89–96. [CrossRef]
26. Anyasi, T.A.; Jideani, A.I.; Mchau, G.R. Effects of organic acid pretreatment on microstructure, functional and thermal properties of unripe banana flour. *J. Food Meas. Charact.* **2017**, *11*, 99–110. [CrossRef]
27. Gunaratne, A.; Wu, K.; Collado, L.; Gan, R.Y.; Arachchi, L.V.; Kumara, K.; Corke, H. Physicochemical and functional properties of Caryota urens flour as compared to wheat flour. *Int. J. Food Sci. Technol.* **2016**, *51*, 2647–2653. [CrossRef]

28. Wani, I.A.; Andrabi, S.N.; Sogi, D.S.; Hassan, I. Comparative study of physicochemical and functional properties of flours from kidney bean (*Phaseolus vulgaris* L.) and green gram (*Vigna radiata* L.) cultivars grown in Indian temperate climate. *Legume Sci.* **2020**, *2*, e11. [CrossRef]

29. Wang, S.; Li, C.; Zhang, X.; Copeland, L.; Wang, S. Retrogradation enthalpy does not always reflect the retrogradation behavior of gelatinised starch. *Sci. Rep.* **2016**, *6*, 20965. [CrossRef]

30. Islam, M.Z.; Ud-Din, M.S.; Haque, M.A. Studies on the effect of brown rice and maise flour on the quality of bread. *J. Bangladesh Agric. Univ.* **2011**, *9*, 297–304. [CrossRef]

31. Muttagi, G.C.; Ravindra, U. Chemical and nutritional composition of traditional rice varieties of Karnataka. *J. Pharmacogn. Phytochem.* **2020**, *9*, 2300–2309. [CrossRef]

32. Oppong, D.; Panpipat, W.; Chaijan, M. Chemical, physical, and functional properties of Thai indigenous brown rice flours. *PLoS ONE* **2021**, *16*, e0255694. [CrossRef]

33. Jamal, S.; Qazi, I.M.; Ahmed, I. Comparative studies on flour proximate compositions and functional properties of selected Pakistani rice varieties. *Pak. Acad. Sci.* **2016**, *53*, 47–56. Available online: https://www.paspk.org/wp-content/uploads/2016/0 5/Comparative-Studies-on.pdf (accessed on 26 July 2022).

34. Legal Research Board. Part VIII: Standard and Particular Labelling Requirements for Food (Cereal, Cereal Product, Starch and Bread. In *Food Act 1983 (Act 281) & Regulations (Laws of Malaysia)*; International Law Book Services: Selangor, Malaysia, 2021; p. 99.

35. USDA Foreign Agricultural Service (Rice Flour Standards and Labelling Guidelines Established). Available online: https://apps.fas.usda.gov/newgainapi/api/report/downloadreportbyfilename?filename=Rice%20Flour%20Standards% 20and%20Labelling%20Guidelines%20Established_Tokyo_Japan_6-28-2017.pdf (accessed on 20 July 2020).

36. Verma, D.K.; Srivastav, P.P. Proximate composition, mineral content and fatty acids analyses of aromatic and non-aromatic Indian rice. *Rice Sci.* **2017**, *24*, 21–31. [CrossRef]

37. Rahman, A.N.F.; Bilang, M.; Ikawati, L.N. Physical and proximate analysis of green banana cake premix flour. *IOP Conf. Ser. Earth Environ. Sci.* **2020**, *486*, 12051. [CrossRef]

38. Bello, B.K.; Hou, Y.; Zhao, J.; Jiao, G.; Wu, Y.; Li, Z.; Zhang, J. NF-YB 1-YC 12-bHLH 144 complex directly activates Wx to regulate grain quality in rice (*Oryza sativa* L.). *Plant Biotechnol. J.* **2019**, *17*, 1222–1235. [CrossRef] [PubMed]

39. Czaja, T.; Sobota, A.; Szostak, R. Quantification of ash and moisture in wheat flour by Raman spectroscopy. *Foods* **2020**, *9*, 280. [CrossRef]

40. Thongkaew, C.; Singthong, J. Effect of partial substitution of riceberry rice flour on rice noodles quality. *Food Res.* **2020**, *4*, 9–16. [CrossRef]

41. Varastegani, B.; Zzaman, W.; Yang, T.A. Investigation on physicochemical and sensory evaluation of cookies substituted with papaya pulp flour. *J. Food Qual.* **2015**, *38*, 175–183. [CrossRef]

42. Yuliana, N.D.; Akhbar, M.A. Chemical and physical evaluation, antioxidant and digestibility profiles of white and pigmented rice from different areas of Indonesia. *Braz. J. Food Technol.* **2020**, *23*, 1–13. [CrossRef]

43. Singh, N.; Paul, P.; Virdi, A.S.; Kaur, P.; Mahajan, G. Influence of early and delayed transplantation of paddy on physicochemical, pasting, cooking, textural, and protein characteristics of milled rice. *Cereal Chem.* **2014**, *91*, 389–397. [CrossRef]

44. Hager, A.S.; Wolter, A.; Jacob, F.; Zannini, E.; Arendt, E.K. Nutritional properties and ultra-structure of commercial gluten free flours from different botanical sources compared to wheat flours. *J. Cereal Sci.* **2012**, *56*, 239–247. [CrossRef]

45. Paz, G.M.; King, J.M.; Prinyawiwatkul, W. High Protein Rice Flour in the Development of Gluten-Free Bread. *J. Culin. Sci. Technol.* **2021**, *19*, 315–330. [CrossRef]

46. Puri, S.; Dhillon, B.; Sodhi, N.S. Effect of degree of milling (Dom) on overall quality of rice—A review. *Int. J. Adv. Biotechnol. Res.* **2014**, *5*, 474–489.

47. Priya, T.R.; Nelson, A.R.L.E.; Ravichandran, K.; Antony, U. Nutritional and functional properties of coloured rice varieties of South India: A review. *J. Ethn. Foods* **2019**, *6*, 11. [CrossRef]

48. Sapwarobol, S.; Saphyakhajorn, W.; Astina, J. Biological functions and activities of rice bran as a functional ingredient: A review. *Nutr. Metab. Insights* **2021**, *14*, 11786388211058559. [CrossRef] [PubMed]

49. Araki, E.; Ashida, K.; Aoki, N.; Takahashi, M.; Hamada, S. Characteristics of rice flour suitable for the production of rice flour bread containing gluten and methods of reducing the cost of producing rice flour. *Jpn. Agric. Res. Q. JARQ* **2016**, *50*, 23–31. [CrossRef]

50. Takahashi, M.; Homma, N.; Morohashi, K.; Nakamura, K.; Suzuki, Y. Effect of rice cultivar characteristics on the rice flour bread quality. *Nippon. Shokuhin Kagaku Kogaku Kaishi = J. Jpn. Soc. Food Sci. Technol.* **2009**, *56*, 394–402. [CrossRef]

51. Yano, H.; Koda, T.; Fujita, N.; Nishioka, A. Effect of amylose content in rice flour on batter rheology and bread baking quality. *J. Food Processing Preserv.* **2020**, *44*, e14462. [CrossRef]

52. Zhang, H.; Jang, S.G.; Lar, S.M.; Lee, A.R.; Cao, F.Y.; Seo, J.; Kwon, S.W. Genome-wide identification and genetic variations of the starch synthase gene family in rice. *Plants* **2021**, *10*, 1154. [CrossRef]

53. Aoki, N.; Kataoka, T.; Nishiba, Y. Crucial role of amylose in the rising of gluten-and additive-free rice bread. *J. Cereal Sci.* **2020**, *92*, 102905. [CrossRef]

54. Yano, H.; Fukui, A.; Kajiwara, K.; Kobayashi, I.; Yoza, K.I.; Satake, A.; Villeneuve, M. Development of gluten-free rice bread: Pickering stabilization as a possible batter-swelling mechanism. *LWT-Food Sci. Technol.* **2017**, *79*, 632–639. [CrossRef]

55. Aoki, N.; Umemoto, T.; Hamada, S.; Suzuki, K.; Suzuki, Y. The amylose content and amylopectin structure affect the shape and hardness of rice bread. *J. Appl. Glycosci.* **2012**, *59*, 75–82. [CrossRef]

56. Subba, D.; Katawal, S.B. Effect of particle size of rice flour on physical and sensory properties of Sel-roti. *J. Food Sci. Technol.* **2013**, *50*, 181–185. [CrossRef] [PubMed]

57. Ponjanta, J.; Chomsri, N.O.; Meechoui, S. Correlation of pasting behaviors with total phenolic compounds and starch digestibility of indigenous pigmented rice grown in upper Northern Thailand. *Funct. Foods Health Dis.* **2016**, *6*, 133–143. [CrossRef]

58. Huang, Y.P.; Lai, H.M. Bioactive compounds and antioxidative activity of colored rice bran. *J. Food Drug Anal.* **2016**, *24*, 564–574. [CrossRef] [PubMed]

59. Rosniyana, A.; Hazila, K.K.; Syed, A.S.N. Characteristics of local rice flour (MR 220) produced by wet and dry milling methods. *J. Trop. Agric. Food Sci.* **2016**, *44*, 147–155. Available online: http://jtafs.mardi.gov.my/jtafs/44-1/characteristics.pdf (accessed on 1 August 2022).

60. Martínez, M.M.; Gómez, M. Rheological and microstructural evolution of the most common gluten-free flours and starches during bread fermentation and baking. *J. Food Eng.* **2017**, *197*, 78–86. [CrossRef]

61. Thomas, R.; Bhat, R.; Kuang, Y.T.; Abdullah, W.N.W. Functional and pasting properties of locally grown and imported exotic rice varieties of Malaysia. *Food Sci. Technol. Res.* **2014**, *20*, 469–477. [CrossRef]

62. Alcázar-Alay, S.C.; Meireles, M.A.A. Physicochemical properties, modifications and applications of starches from different botanical sources. *Food Sci. Technol.* **2015**, *35*, 215–236. [CrossRef]

63. Han, H.M.; Cho, J.H.; Kang, H.W.; Koh, B.K. Rice varieties in relation to rice bread quality. *J. Sci. Food Agric.* **2012**, *92*, 1462–1467. [CrossRef]

64. Cornejo, F.; Rosell, C.M. Physicochemical properties of long rice grain varieties in relation to gluten free bread quality. *Food Sci. Technol.* **2015**, *62*, 1203–1210. [CrossRef]

65. Vamadevan, V.; Bertoft, E. Observations on the impact of amylopectin and amylose structure on the swelling of starch granules. *Food Hydrocoll.* **2020**, *103*, 105663. [CrossRef]

66. Wani, A.A.; Singh, P.; Shah, M.A.; Schweiggert-Weisz, U.; Gul, K.; Wani, I.A. Rice starch diversity: Effects on structural, morphological, thermal, and physicochemical properties—A review. *Compr. Rev. Food Sci. Food Saf.* **2012**, *11*, 417–436. [CrossRef]

67. Li, G.; Zhu, F. Physicochemical properties of quinoa flour as affected by starch interactions. *Food Chem.* **2017**, *221*, 1560–1568. [CrossRef] [PubMed]

68. Waziiroh, E.; Schoenlechner, R.; Jaeger, H.; Brusadelli, G.; Bender, D. Understanding gluten-free bread ingredients during ohmic heating: Function, effect and potential application for breadmaking. *Eur. Food Res. Technol.* **2022**, *248*, 1021–1034. [CrossRef]

69. Kusumayanti, H.; Handayani, N.A.; Santosa, H. Swelling power and water solubility of cassava and sweet potatoes flour. *Procedia Environ. Sci.* **2015**, *23*, 164–167. [CrossRef]

70. Suklaew, P.O.; Chusak, C.; Adisakwattana, S. Physicochemical and functional characteristics of RD43 rice flour and its food application. *Foods* **2020**, *9*, 1912. [CrossRef] [PubMed]

71. Shafi, S.; Wani, I.A.; Gani, A.; Sharma, P.; Wani, H.M.; Masoodi, F.A.; Hamdani, A.M. Effect of water and ether extraction on functional and antioxidant properties of Indian horse chestnut (*Aesculus indica* Colebr) flour. *J. Food Meas. Charact.* **2016**, *10*, 387–395. [CrossRef]

72. Thiranusornkij, L.; Thamnarathip, P.; Chandrachai, A.; Kuakpetoon, D.; Adisakwattana, S. Physicochemical properties of Hom Nil (*Oryza sativa*) rice flour as gluten free ingredient in bread. *Foods* **2018**, *7*, 159. [CrossRef]

73. Šárka, E.; Dvořáček, V. New processing and applications of waxy starch (a review). *J. Food Eng.* **2017**, *206*, 77–87. [CrossRef]

74. Hasjim, J.; Li, E.; Dhital, S. Milling of rice grains: Effects of starch/flour structures on gelatinisation and pasting properties. *Carbohydr. Polym.* **2013**, *92*, 682–690. [CrossRef]

75. Amini, A.M.; Razavi, S.M.A.; Mortazavi, S.A. Morphological, physicochemical, and viscoelastic properties of sonicated corn starch. *Carbohydr. Polym.* **2015**, *122*, 282–292. [CrossRef]

76. Farooq, M.A.; Murtaza, M.A.; Aadil, R.M.; Arshad, R.; Rahaman, A.; Siddique, R.; Haq, A.U. Investigating the structural properties and in vitro digestion of rice flours. *Food Sci. Nutr.* **2021**, *9*, 2668–2675. [CrossRef] [PubMed]

77. Biliaderis, C.G.; Page, C.M.; Maurice, T.J.; Juliano, B.O. Thermal characterisation of rice starches: A polymeric approach to phase transitions of granular starch. *J. Agric. Food Chem.* **1986**, *34*, 6–14. [CrossRef]

78. Wang, S.; Li, C.; Copeland, L.; Niu, Q.; Wang, S. Starch retrogradation: A comprehensive review. *Compr. Rev. Food Sci. Food Saf.* **2015**, *14*, 568–585. [CrossRef]

79. Roman, L.; Reguilon, M.P.; Gomez, M.; Martinez, M.M. Intermediate length amylose increases the crumb hardness of rice flour gluten-free breads. *Food Hydrocoll.* **2020**, *100*, 105451. [CrossRef]

80. Shi, M.; Chen, Y.; Yu, S.; Gao, Q. Preparation and properties of RS III from waxy maise starch with pullulanase. *Food Hydrocoll.* **2013**, *33*, 19–25. [CrossRef]

81. Chang, Q.; Zheng, B.; Zhang, Y.; Zeng, H. A comprehensive review of the factors influencing the formation of retrograded starch. *Int. J. Biol. Macromol.* **2021**, *186*, 163–173. [CrossRef] [PubMed]

82. Becker, A.; Hill, S.E.; Mitchell, J.R. Relevance of amylose-lipid complexes to the behaviour of thermally processed starches. *Starch-Stärke* **2001**, *53*, 121–130. [CrossRef]

83. Kang, N.; Reddy, C.K.; Park, E.Y.; Choi, H.D.; Lim, S.T. Antistaling effects of hydrocolloids and modified starch on bread during cold storage. *Food Sci. Technol.* **2018**, *96*, 13–18. [CrossRef]

84. Fu, Z.; BeMiller, J.N. Effect of hydrocolloids and salts on retrogradation of native and modified maise starch. *Food Hydrocoll.* **2017**, *69*, 36–48. [CrossRef]

85. Yamaguchi, Y.; Okawa, Y.; Ninomiya, K.; Kumagai, H.; Kumagai, H. Evaluation and suppression of retrogradation of gelatinised rice starch. *J. Nutr. Sci. Vitaminol.* **2019**, *65*, 134–138. [CrossRef]

86. BeMiller, J.N. Pasting, paste, and gel properties of starch–hydrocolloid combinations. *Carbohydr. Polym.* **2011**, *86*, 386–423. [CrossRef]

Fatty-Acid Profiles, Triacylglycerol Compositions, and Crystalline Structures of Bambangan-Seed Fat Extracted Using Different Solvents

Norazlina Mohammad Ridhwan [1], Hasmadi Mamat [1,*] and Md Jahurul Haque Akanda [2]

[1] Faculty of Food Science and Nutrition, Universiti Malaysia Sabah, Kota Kinabalu 884000, Sabah, Malaysia
[2] Department of Agriculture, School of Agriculture, University of Arkansas, 1200 North University Dr., M/S 4913, Pine Bluff, AR 71601, USA
*   Correspondence: idamsah@ums.edu.my; Tel.: +60-8832-0000

Abstract: Currently, research on the bambangan-fruit seed has become interesting because of its potential application as a cocoa butter alternative. This work aimed to determine the changes in the quality of the extracted bambangan-seed fat (BSF) obtained using hexane, petroleum ether, and ethanol. The extraction solvents affected the total fat content (TFC), physicochemical properties, fatty-acid profile, triacylglycerol composition, and crystalline structure of the extracted BSF. The results showed that BSF has a high content of 1,3-distreoyl-2-oleoyl-glycerol (SOS). The solvent-type significantly ($p < 0.05$) impacts the stearic and oleic acids of the extracts, resulting in apparent changes in the high-melting symmetrical triacylglycerols, such as SOS. Petroleum-ether-extracted BSF has a high stearic acid of 33.40%, followed by that of hexane- and ethanol-extracted BSF at 29.29% and 27.84%, respectively. Moreover, the spherulitic microstructure with needle-like crystals of the extracts also ranges from 30 to 70 μm in diameter. Hexane-extracted BSF illustrated a less-dense, spherulitic, crystalline microstructure with a less-granular centre than those extracted using the other solvents. The results suggested that the quality of the extracted BSF obtained from the nonpolar solvents of hexane and petroleum ether are better than that extracted using ethanol.

Keywords: bambangan; extraction solvents; fatty acid; triacylglycerol; crystalline microstructure

1. Introduction

Mangifera pajang is an indigenous fruit distributed around the Borneo Islands, such as Kalimantan (Indonesia), Sabah and Sarawak (Malaysia), and Brunei [1]. This fruit is locally known as bambangan and has become a prominent, underutilised fruit with significant economic value. Bambangan trees can grow up to 30 m tall, with a cylindrical bole with smooth, broadly fissured, grey bark [2]. It initially grows widely in the forest and is currently cultivated by the local Kadazan–Dusun people, specifically in Sabah [3]. The cultivation of bambangan fruit in Sabah was reported as having a constant growth of 121.6 to 133.03 metric tons from 2016 to 2020, as the trees are currently being planted in orchards or in the backyards of homes, corresponding to the increasing demand for this fruit [4,5]. Bambangan fruit is larger in size, and it has a thick peel (of a brown colour, with rough skin), fibrous flesh. Each fruit can weigh up to 1.5 kg [6].

The local community prefers mature bambangan fruit for consumption and utilises this fruit in functional food-forms, including juice and processed fruit, and as a health drink, and it can be added to food as a flavouring ingredient. However, the seed is not consumed, but rather disposed of as a waste by-product. This waste by-product has been reported to have significant health benefits, based on the considerable number of antioxidant compounds found in the seed and in the peel [2,4,7]. The seed is made up of 9.8–11% fat, 3.08–4.1% protein, and 38.68–72.9% carbohydrate, indicating that the seed has nutritional potential as a source of protein and carbohydrates [7–11]. Bambangan-seed fat (BSF) is

mainly composed of palmitic (7.29–15.8%), stearic (32.37–40.39%), oleic (39.24–48.05%), and linoleic (4.95–8.11%) fatty acids (FAs), which corresponds to the presence of three main triacylglycerols (TG): SOS, SOO, and POS (8.7–40.70%, 11.20–26.87%, and 11.60–11.93%, respectively) [1,9,12,13]. BSF has also become an interest for researchers due to its similarities with cocoa-butter-like fats: illipe butter, mango-seed fat, kokum butter, sal fat, and shea butter [4,8,10,12,14]. Moreover, BSF is SOS-rich, which makes it applicable as an SOS-rich fat resource to increase the hardness of soft fats, which is desirable in a country with a high climate.

The extraction of BSF can be performed in various ways, including using Soxhlet extraction. Soxhlet extraction is economical, simple, and allows several extractions to be carried out simultaneously with high oil-recovery as compared to the other method [15]. The operational cost is also lower because the solvent can be recovered after the extraction, creating reusable solvents to be used for another extraction process [16]. Soxhlet extraction is an economical method that lowers operational costs by using reusable solvents with higher extraction efficiencies than the other method. Using different solvents in Soxhlet extraction gives variation to the oil-quality parameter and thus could extend the applicability of the oil based on its properties, and it offers the best option for extraction. Moreover, fresh solvents are repeatedly brought into contact with the sample, thus supplanting the equilibrium transfer [17]. The extraction's efficacy depends on the temperature, oil nature, particle size, sample pre-treatment conditions, time, and solvent type [18]. The choice of solvents for the extraction is essential for determining the quality of the extracted fat. Different studies have reported on the ways that extraction solvents influence oil quality, specifically the yield and bioactive compound levels [17,19,20]. The process of the Soxhlet extraction of oil can be performed using ethanol; the polar protic solvents or hexane and petroleum ether; the nonpolar solvents [20].

Hexane is commonly preferred among solvents due to its low-melting properties, high availability, and polarity, which lead to high solubility [21–23]. In comparison, petroleum ether has been used for the extraction of lipophilic compounds, and ethanol has been used because of its low-toxicity properties and high availability, as well as its being bio-based [24,25]. Hexane has been classified as a toxic chemical by the US Environmental Protection Agency because it can react with air pollutants to produce ozone and other environmental pollutants [26]. Hence, it is only permitted in maximum amounts of 5 ppm and 10 ppm in meal and oil, respectively, under the PFA Act of 1954 [27]. Several replacement solvents have been found to extract oil from oilseeds without utilising hexane due to safety, health, and environmental concerns [28,29]. Thus, hexane substitutes, for instance, ethanol, water, petroleum ether, and other potential solvents, have been developed and used for oil extraction [25].

However, the work of comparing the fatty acid (FA) composition, triacylglycerol (TG) content, and crystalline microstructure of BSF, as extracted using different solvents, is still in the early stage. Thus, this study aimed to evaluate the changes in the physicochemical properties (iodine value and Slip melting point), FA and TG compositions, and the crystalline microstructure of the extracted BSF using different solvents, as well as the efficiency of the extraction solvents.

2. Materials and Methods

2.1. Materials

Ripe bambangan fruits were provided by a local farmer in Ranau, Sabah, Malaysia. The following items were acquired from Sigma–Aldrich: acetone, acetonitrile, cyclohexane, ethanol, hexane, n-hexane, methanol, potassium hydroxide, petroleum ether, potassium iodide, sodium thiosulfate, starch indicator, Wijs solution, triacylglycerols, and fatty acid methyl esters standard. The analytical chemicals, reagent-grade chemicals, and extraction solvents used were of the highest possible quality.

2.2. Extraction of Bambangan-Seed Fat (BSF) Using Hexane, Petroleum Ether, and Ethanol

Each bambangan seed was separated from the flesh and then cut into small pieces (10 mm × 10 mm × 5 mm) for sample preparation. Next, it was stored in a drying cabinet (48 h at 45 °C) for drying processes. Each dried seed was ground into a powdered form using a grinding mill and kept at −20 °C before the analysis. The extraction was conducted using the AOAC [30] official method of analysis for Soxhlet extraction (Method 945.16), using petroleum ether with slight modifications. A total of 80.0 ± 0.00 g of seed powder was extracted for 8 h at 40 °C using 3 different solvents: hexane, petroleum ether, and ethanol. Ethanol was used as a hexane substitute for oilseed-extraction because of health, safety, and environmental concerns [28,31]. The remaining solvent in the extracted BSF was removed using a rotary evaporator (40 °C) (HEIDOLPH LABORTA 4001) and then filtered in an oven (at 45 °C) to remove any impurities. The total fat content (TFC) for the fat is expressed as the following equation:

$$\text{TFC (\%)} = \frac{Extracted\ crude\ fat\ (g)}{Bambangan\ seed\ powder\ (g)} \times 100 \tag{1}$$

2.3. Physicochemical Properties

The changes in the physicochemical properties, such as the iodine value (IV) and the Slip melting point (SMP), of the extracted BSF were determined according to the AOCS [32] official methods, Cc 3b-92 and Cd 1b-87, respectively. For IV analysis, 0.5 g of melted BSF (at 60 °C) were homogenised with 20 mL of cyclohexane and 25 mL of Wijs solution (iodine solution) and left in the dark for 1 h. Next, 20 mL of 15% KI and 100 mL of distilled water were added to the mixture. A quantity of 0.1 N sodium thiosulfate solution was used to titrate the mixture. After the yellow solution became colourless, 2 mL of the starch indicator was added, and the mixture was titrated until the blue solution became colourless. The following calculation was used to calculate the IVs of the fat samples:

$$\text{IV (g iodine/g)} = \frac{(Vol\ of\ blank\ titrant - vol\ of\ sample\ titrant) \times Normality\ of\ titrant \times 12.69}{mass\ (g)} \tag{2}$$

The SMP of the hexane-, petroleum-ether-, and ethanol-extracted BSF was determined using an open-ended capillary glass tube. Before analysis, the glass tube was dipped into the fat samples to a depth of 10 mm, and the fat was chilled and solidified in an ice bath. Using a rubber band, the BSF samples were attached to the bottom of the thermometer and then immersed in the glass test tube before being placed in a water bath (10 °C) for analysis. The hot-plate temperature (SP131320-33-V, Thermo Scientific, Shanghai, China) was gradually increased by 1 °C to increase the water-bath temperature until the fat column ascended. When the fat column reached a height of 30 mm, the SMP of the fat samples was determined.

2.4. Profile of FA

The FA content of the extracted BSF was determined using a gas chromatography–flame ionisation detector (6890 N, Agilent, Santa Clara, CA, USA) as described by Norazlina et al. [9]. The FA methyl esters (FAMEs) for the extracted BSF were prepared before being injected into the BPX70 column (30 m × 0.25 μm × I.D. 0.25). A quantity of 0.5 g of BSF was dissolved using 2.5 mL of n-hexane and 0.5 mL of potassium hydroxide in methanol (2 N), vortexed (1 min at 1200 rpm), and left to stand at room temperature. After 10 min, the translucent upper-layer was injected into the GC for analysis. The following condition was used to identify the FAMEs: an initial temperature of 90 °C (hold for 5 min), then raise by 8 °C at a time to 185 °C (hold for 1 min), then raise by 2 °C to reach a final temperature of 250 °C (hold for 5 min). Using split-mode, maintain a temperature of 250 °C for the injector and detector (1:20). The FA profile was determined using the FAMEs standard. The results were presented in % concentrations and compared with the FAME standard.

2.5. TG Content

The TG composition of the extracted BSF was measured according to AOCS [32] official method Ce 5c-93, using high-performance liquid chromatography (HPLC; 1200, Agilent, Mississauga, ON, Canada) equipped with a refractive index detector (RID) with slight adjustments. For sample preparation, 0.1 g of the melted fat samples (at 60 °C) was diluted to 10 mL of mobile-phase solution (acetone: acetonitrile, premixed) to make a 10% solution. The mixture was then filtered through a 0.45 μm PTFE syringe filter (47 mm millipore diameter) and placed into the HPLC vial for analysis. A C18-HPLC column (Kromasil C18, Merck, Germany) was used for the study. An injection volume of 5 μL, a column temperature of 30 °C, a detector temperature of 40 °C, a pressure of 8–9 mPa, and mobile-phase acetone: acetonitrile (70:30, v/v) were utilised in the studies. The results were presented in % concentrations and compared with the TG standard

2.6. Crystalline Structure

The changes in the crystalline structure for the 3 extracted BSFs were observed using polarised light microscopy (DM2500P, Leica, Wetzlar, Germany), a method developed by Narine and Marangoni [33]. The crystalline structure of the fat crystals helps define the texture of a product for use in confectionery because it is directly related to the polymorphic behaviour of a fat [34]. A quantity of 15 μL of melted BSF was placed on the microscopic slide (heated at 80 °C), covered with a coverslip, and then chilled at 4 °C for 1 h. The samples were then incubated at 25 °C for 2 days for proper crystallisation before being observed under a polarised light microscope at 40× magnification.

2.7. Statistical Analysis

The total fat content (TFC) analysis and all other studies were conducted in triplicate, and the results are expressed as means and standard deviations (±). The Tukey test and one-way analysis of variance (ANOVA) were used to find any significant differences in the treatment means. A $p < 0.05$ significance value was used to define the significance level.

3. Results

3.1. Extraction of BSF and Its IV and SMP Properties

Figure 1 shows the differences in the physical appearance of the extracted BSFs obtained using hexane, petroleum ether, and ethanol. BSF extracted using a nonpolar solvent is lighter in colour than is polar-solvent-extracted BSF. The hexane and petroleum-ether extracts showed similar appearances, with a common yellow oil-colour, and they solidified faster than did the ethanol extracts. A similar observation was reported in the extraction of kariya seed oil: nonpolar solvents produced yellow oil extracts, and the polar solvent produced a cloudy, dark-golden oil extract [35]. The variation in the extracted BSF appearances was presumably associated with the acid value and free-fatty-acid content, in which free fatty acid is more soluble in the polar solvent [36]. Therefore, the ethanol-extracted BSF had a darker-golden appearance than the hexane and petroleum-ether extracts.

The TFC, IV, and SMP properties of the extracted BSFs are shown in Table 1. The solvents selected, such as hexane and petroleum ether for the current study, are typically used to extract oil from plant kernels [17], while ethanol is considered a green solvent in chemical extraction because of its low toxicity. Among the extraction solvents, hexane produced a high TFC, followed by the petroleum-ether and ethanol extracts. It can be seen that the hexane had a higher level of efficiency for extracting the BSF. The solutes and solvent interactions, boiling temperature, and solvent polarity might be the prominent factors that influenced the BSF's yield, extraction efficacy, and composition [17]. The hexane's low-polarity properties caused rapid molecule-transfer between the solvents, thus leading to a high TFC in the hexane-extracted BSF as compared to the petroleum-ether- and ethanol-extracted BSFs [37]. The presence of the antioxidant compounds and other extract compounds, soluble primarily in polar solvents, presumably led to the low yield of TFC

in the ethanol-extracted BSF. The extraction yield for the 3 extracts was comparable to the reported fat content of mango seed fat, with values of 5.73–7.74% in a previous study [38]. On the other hand, the extracted BSFs' physicochemical properties, such as the IV and the SMP, also showed variation in their values.
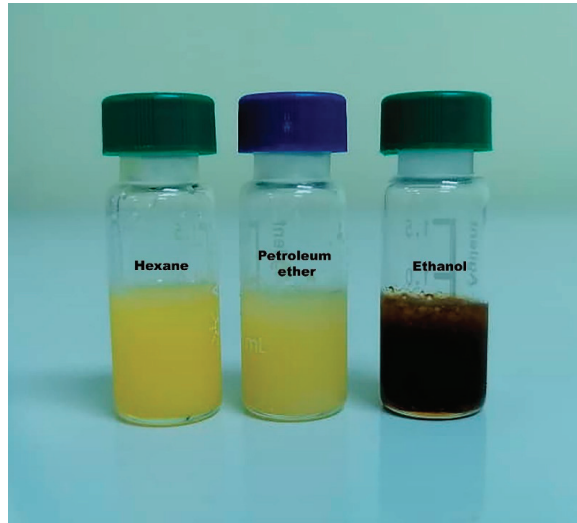
Figure 1. Physical appearance of the extracted BSFs using hexane, petroleum ether, and ethanol.

As seen in Table 1, petroleum-ether-extracted BSF has the lowest IV, followed by the hexane- and ethanol-extracted BSFs. The IV is used to determine the unsaturation levels and the stability of oil for industrial applications [39]. A low IV in the petroleum-extracted BSF indicates that it is prone to better resist oxidation, and it has a higher quality and longer shelf-life than the other two extracts. This behaviour is supported by the results of our previous study, in which the petroleum-ether extracts with low IVs showed a low acidity, with a value of 3.74 mg KOH/g, and had better thermal profiles than the ethanol extracts, with a 7.41 mg KOH/g acid value [40]. The changes in the IV also are associated with the FA composition. A low unsaturation value indicates a low presence of unsaturated FA (UFA); thus, petroleum-ether extracts have more saturated FA (SFA) than hexane and ethanol extracts. The extraction solvents also influence the SMP for the extracted BSFs. The petroleum-ether-extracted BSF showed high SMP values followed by the hexane and ethanol extracts. The low IVs in the petroleum-ether extracts indicate more SFAs and a higher melting-point-TG content than the other solvents; thus, the SMP is higher. The trends in the efficacy of the extraction solvents and the changes in the physicochemical properties for the extracted BSF align with the results reported by Kittiphom and Sutasinee [17] and Jedidi et al. [20].

Table 1. Physicochemical properties of BSFs extracted from hexane, petroleum ether and ethanol.

Physicochemical Properties	Hexane	Petroleum Ether	Ethanol	Bambangan-Seed Fat [9,12]	Mango-Seed Fat [39–41]
Total fat content (%)	7.70 ± 0.00 [a]	6.40 ± 0.10 [b]	2.21 ± 0.01 [c]	-	5.73–7.74
Iodine value (g iodine/g)	56.40 ± 0.00 [b]	52.96 ± 0.00 [c]	59.84 ± 0.00 [a]	50.3–53.5	40.9–44.36
Slip melting point (°C)	31.57 ± 0.51 [c]	31.40 ± 0.52 [b]	28.4 0 ± 0.5 1 [a]	32.0–32.2	30.03–35.7

Values are the mean ± standard deviation of three replicates; means with a different letter (a, b, or c, with a showing the highest value) within a column are significantly different ($p < 0.05$) as measured by the Tukey test.

3.2. Characterisation of FA Profiles in BSF Extracts

Vegetable fats and oils are beneficial for industrial and food purposes, and their quality is closely related to their FA composition [20]. As shown in Table 2, significant ($p < 0.05$) changes in the FA profiles of the 3 extracts were influenced by the solvents used. Obvious changes can be seen in the extracts' stearic and oleic acid compositions. About 52.32–59.70% of the BSFs' FA composition was dominated by the UFA, primarily oleic (43.90–48.31%), with a significant presence of linoleic (8.04–9.72%) acid. This result explains the high unsaturation value of all extracts, especially the ethanol-extracted BSF. The extracts obtained in this study showed softer properties with high UFA compositions as compared to the BSF reported in the previous study [1], in which 56.19% of the FA composition was saturated. The variation obtained in this study was presumably correlated with the geographical latitude, thus showing variation in their compositions. The composition and quality of the fat may vary depending on the fruit's growth condition. According to Varnham [42], the type of a plant, the environment, and the degree to which the seeds ripen determine the FA and the unsaponifiable components of oilseeds. The bambangan fruit used in the study was ripening but over-softening due to transportation and storage, which made the fruit spoil, resulting in variations in the quality parameter.

Table 2. Fatty-acid composition of BSF extracted from hexane, petroleum ether, and ethanol.

Composition (%)	Hexane	Petroleum Ether	Ethanol	Bambangan-Seed Fat [1,9,12]	Mango-Seed Fat [12–38]
$C_{16:0}$ (Palmitic)	8.24 ± 0.00 [b]	9.32 ± 0.00 [a]	8.67 ± 0.00 [b]	8.35–14.91	4.9–14.91
$C_{16:1}$ (Palmitoleic)	0.32 ± 0.00 [a]	0.17 ± 0.00 [b]	0.06 ± 0.00 [c]	-	-
$C_{18:0}$ (Stearic)	29.29 ± 0.00 [b]	33.40 ± 0.00 [a]	27.84 ± 0.00 [c]	36.35–40.39	24.2–47.6
$C_{18:1}$ (Oleic)	46.94 ± 0.00 [b]	43.90 ± 0.00 [c]	48.31 ± 0.00 [a]	39.24–44.5	37.0–58.6
$C_{18:2}$ (Linoleic)	8.51 ± 0.00 [b]	8.04 ± 0.00 [c]	9.72 ± 0.00 [a]	4.95–5.4	3.7–10.4
$C_{18:3}$ (Linolenic)	0.37 ± 0.00 [b]	0.38 ± 0.00 [c]	0.48 ± 0.00 [a]	0.3–0.37	0.4–1.2
C_{20} (Arachidic)	1.87 ± 0.00 [a]	1.77 ± 0.00 [b]	1.67 ± 0.00 [c]	-	-
$C_{20:1}$ (Eicosenoic acid)	0.23 ± 0.00 [a]	0.18 ± 0.00 [c]	0.21 ± 0.00 [b]	-	-
C_{22} (Behenic acid)	0.36 ± 0.00 [a]	0.31 ± 0.00 [b]	0.30 ± 0.00 [c]	-	-

Values are the mean ± standard deviation of 3 replicates; means with a different letter (a, b, or c, with a showing the highest value) within a column are significantly different ($p < 0.05$) as measured by the Tukey test.

Additionally, the temperature also significantly impacts the content of FA, particularly the UFA [43]. On the other hand, the results obtained in this study are in agreement with the FA profiles of BSF extracted by Jahurul et al. [12] and Norazlina et al. [9] and the mango-seed fat extracted by Jahurul et al. [44] and Munchiri, Mahungu, and Gituanja [45]. The SFA and UFA for the reported BSF and mango-seed fat ranged from 44.7 to 44.8% and from 29.1 to 58.6%, from 49.2 to 50.2%, and from 41.1 to 70.2%, respectively. Petroleum-ether-extracted BSF has higher quantities of palmitic and stearic acids, followed by the hexane and ethanol extracts. This shows that petroleum-ether-extracted BSF is harder than the other two extracts. In contrast, ethanol extracts have more oleic acid than do hexane and petroleum-ether extracts. The changes in the FA composition for the 3 extracts can be supported by Kittiphom & Sutasinee [17], who reported similar changes in the extraction of mango-seed oil using hexane (palmitic: 8.97%, stearic: 37.37%, oleic: 43.77%, and linoleic: 6.78%), petroleum ether (palmitic: 8.73%, stearic: 37.70%, oleic: 44.75%, and linoleic: 5.67%) and ethanol (palmitic: 8.50%, stearic: 38.50%, oleic: 43.45%, and linoleic: 6.48%). Moreover, BSF produced by the Soxhlet extraction in this study exhibited an FA-type similar to commercial cocoa butter (CB) (palmitic: 24.5–33.7%, stearic: 33.3–40.2%, oleic:

26.3–36.5%, and linoleic: 1.7–3.56% acids) reported by Gunstone [46], Sonwai et al. [47], Kadivar et al. [48], and Norazura, Sivaruby, and Noor Lida [49], indicating that the extracts are applicable as potential CB alternatives.

3.3. TG Profiles

The TG fat composition is essential for determining the potential application of the extracts, as well as providing information on the polymorphic behaviour. Table 3 summarises the TG content for all extracts, where it can be seen that the TG content was significantly ($p < 0.05$) affected by the extraction solvents. All extracts were dominated by SOS (30.22–44.29%), SOO (20.19–24.18%), and POS (9.57–12.48%) with a significant presence of OOO (5.18–7.09%), POP (2.44–3.83 %), SSS (1.25–3.40%), OLO (2.90–4.56%), and POL (3.16–3.65%). Based on these values, 39.79–56.77% of the composition is high-melting TG (POS and SOS), thus explaining the solidification process of BSF at an ambient temperature. Petroleum-ether-extracted BSF (56.77%) has a high content of high-melting TG, followed by hexane (48.54%) and ethanol (39.79%). This behaviour results in the high SMP value of petroleum-ether extracts, and it increases the hardness of the fat. The variation in the high-melting composition of the extracts was associated with the solubility of the low-melting TG; low-melting TG is more soluble in a polar solvent [50]. Therefore, the ethanol extracts have more low-melting TG than the other extracts.

In addition, the high-melting TG in the hexane extracts is closer to 50% of the TG composition, thus showing a comparable SMP with the petroleum-ether-extracted BSF. The unsaturation value of the hexane extracts is comparable to the petroleum-ether extracts due to the comparable FA and TG compositions. Therefore, this indicates that the quality of the hexane extracts is comparable to that of the petroleum-ether extracts. The relation between the high-melting TG and the SMP obtained in this study also agrees with the melting point of the POS (23.50–43.0 °C) and SOS (19.50–35.50 °C), as reported by a previous study [51–53]. The TG content in the study is also in line with the TG profiles of the reported BSFs and mango-seed fats [8,12,13,34,54–58]. The BSF extracted using different solvents also showed a noticeable amount of OLL, PLL, OLO, POL, PLP, and SSS, as in a previous study [12].

Table 3. Triacyglycerol content of BSF extracted from hexane, petroleum ether, and ethanol.

Composition (%)	Hexane	Petroleum Ether	Ethanol	Bambangan-Seed Fat [8,12,13]	Mango-Seed Fat [41,53–57]
OLL	1.80 ± 0.00 [b]	1.34 ± 0.00 [c]	2.07 ± 0.00 [a]	Traceable	Traceable
PLL	1.19 ± 0.00 [b]	0.71 ± 0.00 [c]	1.42 ± 0.00 [a]	Traceable	Traceable
OLO	3.83 ± 0.00 [b]	2.90 ± 0.00 [c]	4.56 ± 0.00 [a]	Traceable	Traceable
POL	3.02 ± 0.00 [c]	3.16 ± 0.00 [b]	3.65 ± 0.00 [a]	Traceable	Traceable
PLP	1.27 ± 0.00 [b]	0.98 ± 0.00 [c]	1.56 ± 0.00 [a]	Traceable	Traceable
OOO	6.57 ± 0.00 [b]	5.18 ± 0.00 [c]	7.09 ± 0.00 [a]	3.6–5.89	2.5–5.7
POO	2.68 ± 0.00 [a]	2.30 ± 0.00 [b]	2.18 ± 0.00 [c]	3.8–4.57	2.4–10.8
POP	3.83 ± 0.00 [a]	2.95 ± 0.00 [b]	2.44 ± 0.00 [c]	0.75–5.90	1.3–8.9
SOO	23.84 ± 0.00 [b]	20.19 ± 0.00 [c]	24.18 ± 0.00 [a]	11.20–26.88	5.7–30.8
POS	11.78 ± 0.00 [b]	12.48 ± 0.00 [a]	9.57 ± 0.00 [c]	11.35–11.94	5.7–14.8
SOS	36.79 ± 0.00 [b]	44.29 ± 0.00 [a]	30.22 ± 0.00 [c]	28.67–40.71	14.3–51.6
SSS	3.40 ± 0.00 [b]	3.52 ± 0.00 [a]	1.25 ± 0.00 [c]	Traceable	Traceable

Values are the mean ± standard deviation of three replicates; means with a different letter (a, b, or c, with a showing the highest value) within a column are significantly different ($p < 0.05$) as measured by the Tukey test.

3.4. Crystalline Microstructure

Figure 2 shows the crystalline microphotograph of BSFs extracted using hexane, petroleum ether, and ethanol. All fat structures showed spherulite crystals, consisting of needle-like crystals branching outwards with a diameter of 40–70 µm. This structure is commonly associated with the β polymorphic form of a CB [59]. Such a crystalline structure is desirable for making chocolate and confectionery products. The crystalline structure of the extracted BSFs was significantly changed after exposure to the extraction solvents. Petroleum-ether- and ethanol-extracted BSFs showed a compact cluster of fat crystal compared to the hexane-extracted BSF. The spherulite structure of the petroleum-ether-extracted BSF was disrupted after exposure to the solvent, making the structure oval and compact. The ethanol-extracted BSF showed a smaller crystal structure than the hexane-extracted BSF. These findings are similar to the microphotograph reported by Norazlina et al. [9] The changes in the crystalline microstructure (polymorphism, distribution size, size, surface of a structure, and shape) occurred because of the variety in the textural properties of fat and the TG composition [60]. The crystalline microstructure was also potentially influenced by the different FA and TG contents [9], resulting in the difference in the crystallisation state.
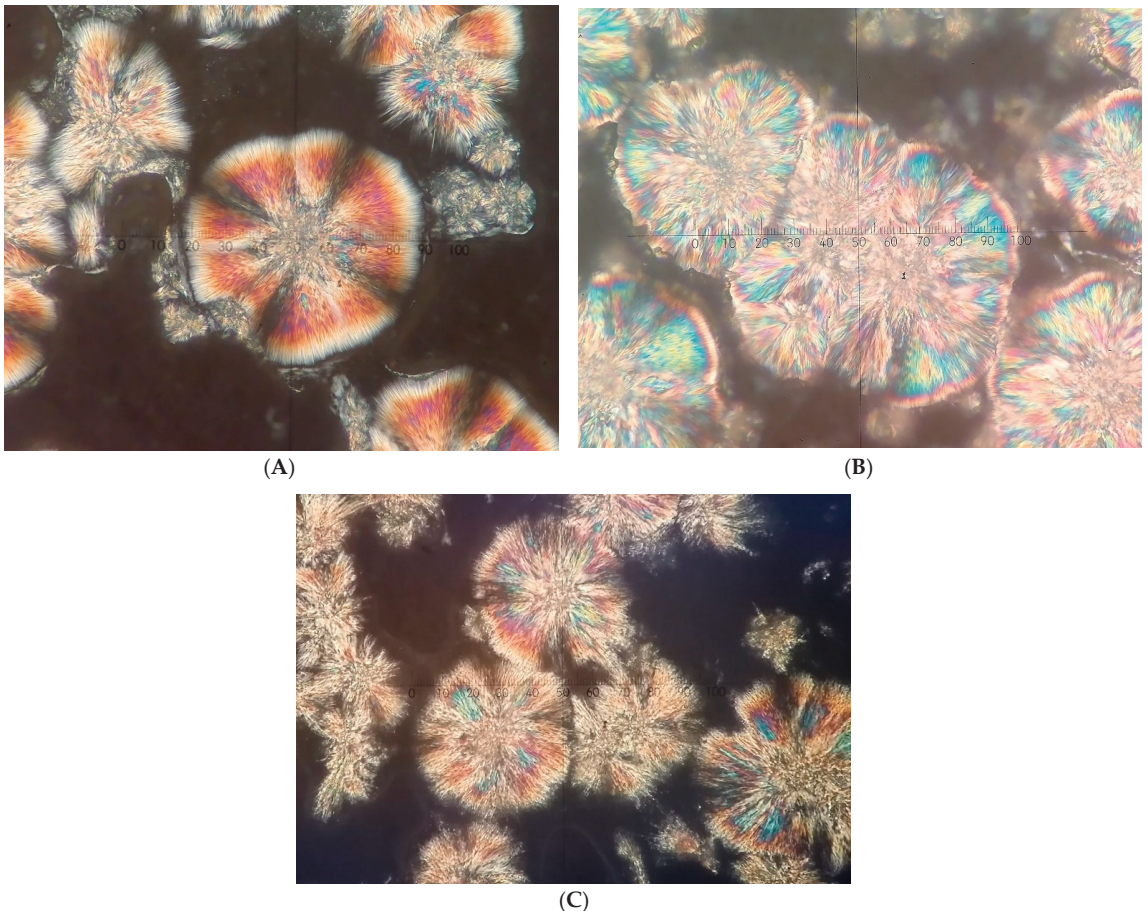

Figure 2. Crystalline microstructure of (**A**) hexane-, (**B**) petroleum-ether-, and (**C**) ethanol-extracted BSF.

Moreover, the saturation-degree of the fat also affected the crystalline microstructure [52]. The unsaturated ethanol-extracted BSF has crystals with a small, densely packed centre, a loose and scattered structure similar to the crystalline microstructure of the mangoseed fat (Thai cultivar) reported by Sonwai and Ponprachanuvut [38]. On the other hand, hexane-extracted BSF exhibited a loosely scattered, spherulite structure similar to that of CB, as reported by Asep et al. [61], thus suggesting that hexane-extracted BSF is similar to CB-like fats and may be applicable as CB alternative.

4. Discussion

This study analysed the FA profiles, TG compositions, and the crystalline microstructures of BSFs obtained using different extraction solvents. To achieve this goal, three different organic solvents were used to obtain the best extraction solvents. Interestingly, the findings showed the solvents affect the composition of the BSF, in which the BSFs extracted using nonpolar solvents (hexane and petroleum ether) are of better quality than those extracted using the polar solvent. Besides that, a previous study also reported that the seed oils extracted using the nonpolar solvents have a high-quality parameter [17,19,20]. The results showed that the characteristics of the extracted BSFs in this study are also in agreement with the reported properties of the BSF reported by Azrina et al. [1], Jahurul et al. [12], and Norazlina et al. [9,13], but the TFC is very low. The unsaturation value (59.84 g iodine/g), UFA (more than 50%) content, and the low-melting TG (33.45%) were high in the ethanol-extracted BSF.

The oil's lower solubility could explain the differences in the extracted BSF's quality parameters, such as the TFC, in the polar solvents compared to the nonpolar solvents. The extracted BSF in the polar solvent was mainly disturbed by another component, such as the antioxidant-extract compounds and free fatty acids, which were co-extracted during the extraction process; thus, a low TFC was obtained in the ethanol oil-extracts. The final results, such as the oil yield, FA profile, and the physicochemical qualities, were significantly influenced by the solvents used for extraction, which have been previously reviewed [61,62]. In fact, hexane and petroleum ether, commonly used as the extraction solvents for lipid-extraction in seed oils [22,25], are supposed to have similar properties. However, these solvents showed significant differences in the properties of the extracted BSF.

Although petroleum-ether-extracted BSF shows high-quality parameters; it has a low unsaturation value, a high SFA, and a high-melting TG composition, the extracts' crystalline microstructure is dense and oval and has a low yield. Concerning the TFC, FA, and TG compositions and the crystalline microstructure, hexane seems to be the most efficient among the extraction solvents studied, with a TFC of 7.7%. Still, it has a low POP (3.83%) and POS (11.78%) content and a high SOO (23.83%) level, which could result in the softening effect. The toxicity of the hexane solvents could also become a concern, such that the solvents' traces should be analysed and not exceed the permitted maximum amount in edible oil, as mentioned above. Nevertheless, petroleum ether is an alternative solvent choice known to have less toxicity than hexane, and it could also be used as an extraction solvent as it has comparable properties with hexane-extracted BSF but with a significantly lower yield.

5. Conclusions

This report is the first study to explore how different organic solvents affect the composition of BSF. This work successfully performed BSF extraction using polar (ethanol) and nonpolar (hexane and petroleum-ether) solvents. The changes in the physicochemical properties, FA and TG compositions, and the crystalline structures of the BSFs extracted from different solvents are presented in this report. The results suggest that the hexane-extracted BSF had better overall fat quality, including a high TFC and IV and SMP values comparable to the petroleum-ether extracts. Although petroleum-ether-extracted BSF has a stearic-acid content similar to that of CB, the FA profiles are close to those of the hexane-extracted BSF. Both extracts showed FA-types similar to those of CB, and only the hexane

extracts exhibited a similarly less-dense crystalline structure. Therefore, hexane-extracted BSF is applicable as a CB alternative due to its similarities with CB. Therefore, hexane is suitable for the extraction of BSF. This research is beneficial for providing the solvent's choice information for BSF extraction and speciality-fat production.

Author Contributions: Data curation, N.M.R.; methodology, H.M. and M.J.H.A.; formal analysis, N.M.R.; software, N.M.R.; writing—original draft preparation, N.M.R. and H.M.; writing—review and editing, N.M.R., H.M. and M.J.H.A.; supervision, H.M. and M.J.H.A.; project administration, H.M. and M.J.H.A.; funding acquisition, H.M. All authors have read and agreed to the published version of the manuscript.

Conflicts of Interest: The authors declare no conflict of interest.

References

1. Azrina, A.; Aznira, A.R.; Khoo, H.E. Chemical properties and fatty acid composition of *Mangifera pajang* and *Mangifera indica* kernel fats. *Malays. J. Nutr.* **2015**, *21*, 355–363.
2. Tangah, J.; Bajau, F.E.; Jilimin, W.; Chan, H.T.; Wong, S.K.; Chan, E.W.C. Phytochemistry and pharmacology of *Mangifera pajang*: An iconic fruit of Sabah, Malaysia. *Syst. Rev. Pharm.* **2017**, *8*, 86–91. [CrossRef]
3. Abu Bakar, M.F.; Mohamed, M.; Rahmat, A.F.; Fry, J.R. Bambangan (*Mangifera pajang*) seed kernel: Antioxidant properties and anti-cancer effects. In *Nuts and Seed in Health and Disease Prevention*; Elsevier Inc.: Amsterdam, The Netherlands, 2011; pp. 183–187.
4. Jahurul, M.H.A.; Zaidul, I.S.M.; Beh, L.; Sharifudin, M.S.; Siddiquee, S.; Hasmadi, M.; Jinap, S. Valuable components of bambangan fruit (*Mangifera pajang*) and its co-products: A review. *Food Res. Int.* **2018**, *115*, 105–115. [CrossRef] [PubMed]
5. Department of Agriculture. *Fruits Crops by State and Type Malaysia: Department of Agriculture*; Department of Agriculture: Kuala Lumpur, Malaysia, 2020; pp. 7–177.
6. Bakar, M.F.A.; Fry, J.F. A review on underutilised indigenous bambangan (*Mangifera pajang*) fruit as a potential novel source for functional food and medicine. *J. Med. Plants Res.* **2013**, *7*, 3292–3297.
7. Abu Bakar, M.F.; Mohamed, M.; Rahmat, A.; Fry, J. Phytochemicals and antioxidant activity of different parts of bambangan (*Mangifera pajang*) and tarap (*Artocarpus odoratissimus*). *Food Chem.* **2009**, *113*, 479–483. [CrossRef]
8. Jahurul, M.H.A.; Ping, L.L.; Sharifudin, M.S.; Hasmadi, M.; Mansoor, A.H.; Lee, J.S.; Noorakmar, B.W.; Amir, H.M.S.; Jinap, S.; Mohd Omar, A.K.; et al. Thermal properties, triglycerides and crystal morphology of bambangan (*Mangifera pajang*) kernel fat and palm stearin blends as cocoa butter alternatives. *LWT-Food Sci. Technol.* **2019**, *107*, 64–71. [CrossRef]
9. Norazlina, M.R.; Jahurul, M.H.A.; Hasmadi, M.; Sharifudin, M.S.; Patricia, M.; Mansoor, A.H.; Lee, J.S. Characteristics of bambangan kernel fat fractions produced by solvent fractionation and their potential industrial applications. *J. Food Proces. Preserv.* **2020**, *44*, e14446. [CrossRef]
10. Jahurul, M.H.A.; Soon, Y.; Sharifudin, M.S.; Hasmadi, M.; Mansoor, A.H.; Zaidul, I.S.M. Optimization of fat yield of bambangan (*Mangifera pajang*) kernel using response surface methodology and its antioxidant activities. *J. Food Meas. Charact.* **2018**, *12*, 1427–1438. [CrossRef]
11. Haron, H.; Said, M. Determination of the nutrient and anti-nutrient contents in seed of *Mangifera pajang* kostermans. *Malays. J. Health Sci.* **2004**, *2*, 1–11.
12. Jahurul, M.H.A.; Soon, Y.; Shaarani Sharifudin, M.; Hasmadi, M.; Mansoor, A.H.; Zaidul, I.S.M. Bambangan (*Mangifera pajang*) kernel fat: A potential new source of cocoa butter alternatives. *Int J. Food Sci. Technol.* **2018**, *53*, 1687–1697. [CrossRef]
13. Norazlina, M.R.; Jahurul, M.H.A.; Hasmadi, M.; Sharifudin, M.S.; Patricia, M.; Lee, J.S.; Amir, H.M.S.; Noorakmar, A.W.; Riman, I. Effects of fractionation technique on triacylglycerols, melting and crystallisation and the polymorphic behavior of bambangan kernel fat as cocoa butter improver. *LWT-Food Sci. Technol.* **2020**, *129*, 109558. [CrossRef]
14. Al-Sheraji, S.H.; Ismail, A.; Manap, M.Y.; Mustafa, S.; Yusof, R.M. Viability and activity of bifidobacteria during refrigerated storage of yoghurt containing *Mangifera pajang* fibrous polysaccharides. *J. Food Sci.* **2012**, *77*, 624–630. [CrossRef]
15. Oladipo, B.; Betiku, E. Process optimisation of solvent extraction of seed oil from *Moringa oleifera*: An appraisal of quantitative and qualitative process variables on oil quality using D-optimal design. *Biocatal. Agric. Biol.* **2019**, *20*, 101187. [CrossRef]
16. Handa, S.S. An overview of extraction techniques for medicinal and aromatic plants. In *Extraction Technologies for Medicinal and Aromatic Plants*; Handa, S.S., Khanuja, S.P.S., Longo, G., Rakesh, D.D., Eds.; International Centre for Science and High Technology: Trieste, Italy, 2008.
17. Kittiphoom, S.; Sutasinee, S. Mango seed kernel oil and its physicochemical properties. *Int. Food Res. J.* **2013**, *20*, 1145–1149.
18. Mani, S.; Jaya, S.; Vadivambal, R. Optimization of solvent extraction of moringa (*Moringa oleifera*) seed kernel oil using response surface methodology. *Food Bioprod. Process.* **2007**, *85*, 328–335. [CrossRef]
19. Stevanato, N.; da Silva, C. Radish seed oil: Ultrasound-assisted extraction using ethanol as solvent and assessment of its potential for ester production. *Ind. Crops Prod.* **2019**, *132*, 283–291. [CrossRef]

20. Jedidi, B.; Mokbli, S.; Sbihi, H.M.; Nehdi, I.A.; Younes, M.R.; Al-Resayes, S.I. Effect of extraction solvents on fatty acid composition and physicochemical properties of *Tecoma stans* seed oils. *J. King Saud Uni. Sci.* **2020**, *32*, 2468–2473. [CrossRef]

21. Liu, S.X.; Mamidipally, P.K. Quality comparison of rice bran oil extracted with d-limonene and hexane. *Cereal Chem.* **2005**, *82*, 209–215. [CrossRef]

22. Danlami, J.M.; Arsad, A.; Zaini, M.A.A.; Sulaiman, H. A comparative study of various oil extraction techniques from plants. *Rev. Chem. Eng.* **2014**, *30*, 605–626. [CrossRef]

23. Mujdalipah, S.; Sasmita, A.H.; Amalia, I.K.; Suryani, A. Separation of glycerolysis product using hexane. In *IOP Conference Series: Materials Science and Engineering*; IOP Publishing: Bandung, Indonesia, 2016.

24. Perrier, A.; Delsart, C.; Boussetta, N.; Grimi, N.; Citeau, M.; Vorobiev, E. Effect of ultrasound and green solvents addition on the oil extraction efficiency from rapeseed flakes. *Ultrasonics Sonochem.* **2017**, *39*, 58–65. [CrossRef]

25. Feng, W.; Li, M.; Hao, Z.; Zhang, J. Analytical Methods of Isolation and Identification. In *Phytochemicals in Human Health*; Rao, V., Mans, D., Rao, L., Eds.; IntechOpen: London, UK, 2019.

26. Hanmoungjai, P.Y.L.E.; Pyle, D.L.; Niranjan, K. Enzymatic process for extracting oil and protein from rice bran. *J. Am. Oil Chem. Soc.* **2001**, *78*, 817–821. [CrossRef]

27. Sawada, M.M.; Venâncio, L.L.; Toda, T.A.; Rodrigues, C.E. Effects of different alcoholic extraction conditions on soybean oil yield, fatty acid composition and protein solubility of defatted meal. *Food Res. Int.* **2014**, *62*, 662–670. [CrossRef]

28. Ahmadi Kamazani, N.; Mortazavi, S.A.; Ebrahimi Tajabadi, M.; Hasani, M.; Ghotbi, M. The Effect of Different Solvent Systems on Some Chemical Properties of Pistachio Nut Oil Contaminated with Aflatoxin. *J. Food Biosci. Technol.* **2015**, *5*, 1–13.

29. Kumar, S.J.; Prasad, S.R.; Banarjee, R.; Agarwal, D.K.; Kulkarni, K.S.; Ramesh, K.V. Green solvents and technologies for oil extraction from oil seeds. *Chem. Cent. J.* **2017**, *11*, 9. [CrossRef]

30. AOAC Official Method of Analysis. *Method 945.16, Oil in Cereal Adjuncts*, 18th ed.; AOAC International: Gaithersburg, MD, USA, 2005.

31. Abdolshahi, A.; Majd, M.H.; Rad, J.S.; Taheri, M.; Shabani, A.; Da Silva, J.A.T. Choice of solvents extraction technique affects fatty acid composition of pistachio (*Pistacia vera* L.) oil. *J. Food Sci. Technol.* **2015**, *52*, 2422–2427. [CrossRef]

32. American Oil Chemists' Society. *Official Methods and Recommended Practices of the American Oils Chemists' Society*, 5th ed.; American Oil Chemists' Society: Champaign, IL, USA, 2003.

33. Narine, S.S.; Marangoni, A.G. The difference between cocoa butter and Salatrim lies in the microstructure of the fat crystal network. *J. Am Oil Chem. Soc.* **1999**, *76*, 7–13. [CrossRef]

34. Rios, R.V.; Pessanha, M.D.F.; Almeida, P.F.; de Viana, C.L.; Lannes, S.C. Applications of fats in some food products. *Food Sci. Technol.* **2014**, *34*, 3–15. [CrossRef]

35. Okeleye, A.A.; Betiku, E. Kariya (*Hildegardia barteri*) seedd oil extrcation: Comparative evaluatin of solvents, modeling and optimisation techniques. *Chem. Eng. Commun.* **2019**, *206*, 1181–1198. [CrossRef]

36. Bhatnagar, A.S.; Krishna, A.G.G. Effect of extraction solvent on oil and bioactives composition of commercial Indian niger (*Guizotia abyssinica* (Lf) class.) seed. *J. Am. Oil Chem.* **2013**, *90*, 1203–1212. [CrossRef]

37. Yang, X.; Lyu, H.; Chen, K.; Zhu, X.; Zhang, S.; Chen, J. Selective extraction of oil from hydrothermal liquefaction of *Salix psammophila* by organic solvents with different polarities through multistep extraction separation. *BioResources* **2014**, *9*, 5219–5233. [CrossRef]

38. Sonwai, S.; Ponprachanuvut, P. Studies of fatty acid composition, physicochemical and thermal properties and crystallisation behaviour of mango kernel fats from various Thai varieties. *J. Oleo Sci.* **2014**, *63*, 661–669. [CrossRef] [PubMed]

39. Xu, Y.X.; Hanna, M.A.; Josiah, S.J. Hybrid hazelnut characteristics and its potential oleochemical application. *Ind. Crops Prod.* **2007**, *26*, 69–76. [CrossRef]

40. Norazlina, M.R.; Tan, Y.S.; Hasmadi, M.; Jahurul, M.H.A. Effect of solvent pre-treatment on the physicochemical, thermal profiles and morphological behavior of *Mangifera pajang* seed fat. *Heliyon* **2021**, *7*, e08073. [CrossRef] [PubMed]

41. Lieb, V.M.; Schuster, L.K.; Kronmüller, A.; Schmarr, H.G.; Carle, R.; Steingass, C.B. Fatty acids, triacylglycerols, and thermal behaviour of various mango (*Mangifera indica* L.) kernel fats. *Food Res. Int.* **2018**, *116*, 527–537. [CrossRef]

42. Varnham, A. *Seed Oil: Biological Properties: Health Benefits and Commercial Applications*; Nova Science Publisher Inc.: New York, NY, USA, 2015.

43. Hou, G.; Ablett, G.R.; Pauls, K.P.; Rajcan, I. Environmental effects on fatty acid levels in soybean seed oil. *J. Am. Oil Chem. Soc.* **2006**, *83*, 759–763. [CrossRef]

44. Jahurul, M.H.; Zaidul, I.S.; Norulaini, N.N.; Sahena, F.; Jaffri, J.M.; Omar, A.M. Supercritical carbon dioxide extraction and studies of mango seed kernel for cocoa butter analogy fats. *CyTA-J. Food* **2014**, *12*, 97–103. [CrossRef]

45. Munchiri, D.R.; Mahungu, S.M.; Gituanja, S.N. Studies on mango (*Mangifera indica* L.) kernel fat of some Kenyan varieties in Meru. *J. Am. Oil Chem. Soc.* **2012**, *89*, 1567–1575. [CrossRef]

46. Gunstone, F.D. *Vegetable Oils in Food Technology Composition, Properties and Use*; Willy-Blackwell: New York, NY, USA, 2011; pp. 291–343.

47. Sonwai, S.; Kaphuekngam, P.; Flood, A. Blending of mango kernel fat and palm oil mid-fraction yo obtain cocoa butter equivalent. *J. Food Sci. Technol.* **2014**, *51*, 2357–2369. [CrossRef]

48. Kadivar, S.; De Clercq, N.; Mokbul, M.; Dewettinck, K. Infulence of enzymatically produced sunflower oil based cocoa butter equivalents on the phase behavior of cocoa butter and quality of dark chocolate. *LWT-Food Sci. Technol.* **2016**, *66*, 48–55. [CrossRef]

49. Norazura, A.M.H.; Sivaruby, K.; Noor Lida, H.M.D. Blended palm fractions as confectioenry fats: A preliminary study. *J. Oil Palm Res.* **2020**, *33*, 360–380. [CrossRef]
50. Kang, K.K.; Kim, S.; Kim, I.H.; Lee, C.; Kim, B.H. Selective enrichment of symmetric monounsaturated triacylglycerols from palm stearin by double solvent fractionation. *LWT-Food Sci. Technol.* **2013**, *51*, 242–252. [CrossRef]
51. Arishima, T.; Sagi, N.; Mori, H.; Sato, K. Polymorphism of POS. I. Occurrence and polymorphic transformation. *J. Am. Oil Chem.* **1991**, *68*, 710–715. [CrossRef]
52. Koyona, T.; Hachiya, I.; Sato, K. Phase behavior of mixed system of SOS and OSO. *J. Phys. Chem.* **1992**, *96*, 10514–10520. [CrossRef]
53. Minato, A.; Ueno, S.; Yano, J.; Smith, K.; Seto, H.; Amemiya, Y.; Sato, K. Thermal and structural properties of sn-1,3-dipalmitoyl-2-oleoylglycerol and sn-1,3-dioleoyl-2-palmitoylglycerol binary mixtures examined with synchroton radiation X-Ray diffraction. *J. Am. Oil. Chem.* **1997**, *74*, 1213–1220. [CrossRef]
54. Jin, J.; Mu, H.; Wang, Y.; Pembe, W.; Liu, Y.; Huang, J.; Jin, Q.; Wang, X. Production of high-melting symmetrical monounsaturated triacylglycerol-rich fats from mango kernel fat by acetone fractionation. *J. Am. Oil Chem. Soc.* **2016**, *94*, 201–213. [CrossRef]
55. Kaphuekngam, P.; Flood, A.; Sonwai, S. Production of cocoa butter equivalent from mango seed almond fat and palm oil midfraction. *J. Food Agro-Ind.* **2009**, *2*, 441–447.
56. Lidefelt, J.O. *Handbook of Vegetable Oils and Fats*, 2nd ed.; Aarhus Karlshamn: Karlshmn, Sweden, 2007.
57. Halcopek, M.; Lisa, M.; Jandera, P.; Kabatova, N. Quantitation of triacylglycerols in plant oils using HPLC with APCI-MS, evaporative light-scattering and UV detection. *J. Sep. Sci.* **2005**, *28*, 1315–1333.
58. Ramel, P.R.; Campos, R.; Marangoni, A.G. Effect of shear and cooling rate on the crystallisation behavior and structure of cocoa butter: Shear applied during the early stages of nucleation. *Cryst. Growth Des.* **2017**, *18*, 1002–1011. [CrossRef]
59. Çiftçi, O.N.; Fadiloğlu, S.; Göğüş, F. Conversion of olive pamoce oil to cocoa butter-like fat in a packed-bed enzyme reactor. *Biores. Technol.* **2009**, *100*, 324–329. [CrossRef]
60. Salvatore, M.M.; Elvetico, A.; Gallo, M.; Salvatore, F.; DellaGreca, M.; Naviglio, D.; Andolfi, A. Fatty acids from *Ganoderma lucidum* Spores: Extraction, identification and quantification. *Appl. Sci.* **2020**, *10*, 3907. [CrossRef]
61. Asep, E.; Jinap, S.; Tan, T.J.; Russly, A.; Harcharan, S.; Nazimah, S. The effects of particle size, fermentation and roasting of cocoa nibs on supercritical fluid extraction of cocoa butter. *J. Food Eng.* **2008**, *85*, 450–458. [CrossRef]
62. Ajala, S.O.; Betiku, E. Yellow oleander seed oil extraction modeling and process parameters optimisation: Performance evaluation of artificial neural network and response surface methodology. *J. Food Process. Preserv.* **2015**, *39*, 1466–1474. [CrossRef]

Review

Encapsulated Probiotics: Potential Techniques and Coating Materials for Non-Dairy Food Applications

Wee Yin Koh [1],*, Xiao Xian Lim [2], Thuan-Chew Tan [2,3], Rovina Kobun [1] and Babak Rasti [4]

[1] Faculty of Food Science and Nutrition, Universiti Malaysia Sabah, Jalan UMS, Kota Kinabalu 88400, Sabah, Malaysia

[2] Food Technology Division, School of Industrial Technology, Universiti Sains Malaysia, Minden 11800, Penang, Malaysia

[3] Renewable Biomass Transformation Cluster, School of Industrial Technology, Universiti Sains Malaysia, Minden 11800, Penang, Malaysia

[4] Australasian Nanoscience and Nanotechnology Initiative, Monash University, Melbourne, VIC 3168, Australia

* Correspondence: weeyin@ums.edu.my; Tel.: +60-8832-0000 (ext. 210900); Fax: +60-8832-0259

Abstract: The growing health awareness among consumers has increased the demand for non-dairy-based products containing probiotics. However, the incorporation of probiotics in non-dairy matrices is challenging, and probiotics tend to have a low survival rate in these matrices and subsequently perform poorly in the gastrointestinal system. Encapsulation of probiotics with a physical barrier could preserve the survivability of probiotics and subsequently improve delivery efficiency to the host. This article aimed to review the effectiveness of encapsulation techniques (coacervation, extrusion, emulsion, spray-drying, freeze-drying, fluidized bed coating, spray chilling, layer-by-layer, and co-encapsulation) and biomaterials (carbohydrate-, fat-, and protein-based) on the viability of probiotics under the harsh conditions of food processing, storage, and along the gastrointestinal passage. Recent studies on probiotic encapsulations using non-dairy food matrices, such as fruits, fruit and vegetable juices, fermented rice beverages, tea, jelly-like desserts, bakery products, sauces, and gum products, were also included in this review. Overall, co-encapsulation of probiotics with prebiotics was found to be effective in preserving the viability of probiotics in non-dairy food matrices. Encapsulation techniques could add value and widen the application of probiotics in the non-dairy food market and future perspectives in this area.

Keywords: encapsulation; non-dairy; probiotics; stability; storage

1. Introduction

The growing awareness among consumers regarding healthy lifestyles has increased the demand for food that could provide additional specific health benefits beyond nutrition. Functional food is one of the leading trends in today's food industry. The term "functional food" refers to foods containing (either present naturally or added by manufacturers) ingredients or bioactive compounds that provide extra health benefits over its adequate nutritional effects, which can beneficially affect one or more physiological mechanisms in the body, resulting in an enhancement in health and reduction in risk for disease, in the amount consumed in a diet [1]. For example, probiotics are one of the dominant groups of functional foods [2].

Probiotics, from the Greek word, "for life", are defined as "live microorganisms that, when administered in adequate amounts, confer a health benefit to the host" by a joint United Nations Food and Agricultural Organization/World Health Organization working group in 2001 and The International Scientific Association for Probiotics and Prebiotics (IS-APP). Probiotics have also been considered functional foods due to their health-promoting abilities [3]. Among probiotic strains in use today, strains from genera of *Lactobacillus* and

Bifidobacterium are the most frequently used. In addition, other non-pathogenic microorganisms that occur within the host gut or tissues have also been developed as probiotics. These include strains from genera *Propionibacterium*, *Pediococcus*, *Bacteroides*, *Bacillus*, *Streptococcus*, *Escherichia*, *Enterococcus*, and *Saccharomyces*. Lately, *Faecalibacterium prausnitzii*, *Akkermansia muciniphila*, and *Eubacterium hallii* have also been identified as potential next-generation probiotics with promising health-promoting functionalities [1,4].

By regulating the natural balance of gut bacteria in the human gastrointestinal tract, probiotics have been shown to promote a wide range of health benefits such as improving intestinal health, improving lactose digestion, enhancing the host's immune response, reducing serum cholesterol, diarrhea diseases, and inflammatory bowel disease, counteracting allergies, and lowering the risk of certain cancers [5]. For a potential probiotic strain to exert therapeutic effects on the host, the viability of probiotics in food should be at least 6 to 7 log CFU/mL (or CFU/g) when reaching the small intestine and colon. In this regard, the viability of at least 8 to 9 log CFU/mL (or CFU/g) of probiotics in food before ingestion is necessary [3,6].

Probiotics must be stable throughout the digestive tract and able to adhere to human epithelial cells when they reach the intestine. However, the survival of probiotics is greatly affected by the harsh conditions of the gastrointestinal tract, including the acidic pH of the gastric environment and bile acids (a loss of around 2 log CFU/mL or CFU/g during digestion) [7]. Several intrinsic (e.g., pH, water activity, molecular oxygen, the composition of the food, food additives added, and oxidation-reduction potential) and extrinsic factors (e.g., temperature, relative humidity, and gas composition) have also been observed to negatively affect the viability and stability of probiotics during food preparation and food processing, as well as over a prolonged storage period [5,7,8].

Traditionally, dairy products have been recognized as the best carriers of probiotics. Current probiotics have been formulated into numerous dairy products, such as fermented milk, yogurt, cheese, and ice cream. However, consumers' preferences today lie more with non-dairy-based probiotic products because of the ongoing trend of vegetarianism and awareness of drawbacks associated with the intake of dairy products, such as lactose intolerance, high cholesterol content, and milk protein allergy [2,9]. In recent years, non-dairy matrices, such as fruits [10–12], fruit and vegetable juices [7,11–26], fermented rice beverages [27], tea [28,29], jelly-like desserts [30], bakery products [31–33], cereal bars [34], sauces [35], gum products [36], and powdered functional drink [37] have been explored as vehicles to deliver probiotics. Although non-dairy food matrices are more versatile (absent of lactose, dairy allergens, and cholesterol) than dairy food matrices, the delivery of probiotics using non-dairy food matrices is more challenging. As an example of a dairy food matrix, milk, which is rich in proteins and fats, could effectively act as a protective matrix to protect the probiotics throughout the digestive tract [38]. In contrast, non-dairy food matrices, such as fruit and vegetable juices, have considerable amounts of organic acids, dissolved oxygen, and inherently low pH values that could negatively affect the viability of inoculated probiotics [9]. Dairy food matrices are usually stored at refrigerated temperature (4 °C), and therefore, the viability of probiotics can be well-maintained throughout the product's shelf life. In contrast to dairy food matrices, non-dairy food matrices are often stored at ambient temperature, which could adversely affect the viability of probiotics [2]. The sensory qualities of non-dairy food matrices could also be enhanced or deteriorated by the metabolic compounds produced through the interaction between the probiotics and food matrices [2,9].

To address these challenges, encapsulation techniques have been implemented to preserve the viability of probiotics. Encapsulation can be defined as "a process in which small solid particles, liquid droplets, or gases are entrapped by a coating layer, or incorporated into a homogeneous or heterogeneous matrix, yielding small capsules with useful properties in immobilization, protection, controlled release, structuration, and functionalization" [39]. In other words, encapsulation is a technique of retaining a substance (core material, such as probiotics) within another (wall material). When applied successfully,

the encapsulation technique may improve the resistance of probiotics to the harsh gastric environment and hence, facilitate the controlled release and successful delivery of probiotics to the site of action. By restricting the probiotics from being directly in contact with food components, encapsulation could maintain the viability of probiotics during the food manufacturing process and long-term storage. Through encapsulation techniques, probiotic cultures can be transformed into concentrated dry powder form, which is more stable and easier to incorporate into many food matrices [1,40–42]. This article aims to review and analyze the effectiveness of encapsulation techniques and supplementation of coating materials on the viability of probiotics in non-dairy food and beverage products during storage, as well as while transiting through our gastrointestinal tract.

2. Encapsulation

To date, encapsulation is one of the most promising techniques in protecting active compounds against adverse environments. Encapsulation technology has been widely used in the pharmaceutical, medicine, nutritional, food science, biological, agriculture, toiletries, and cosmetics industries for over 50 years. The goal of encapsulation is to protect the encapsulated active compound (core material) against unfavorable or adverse environments (such as light, moisture, temperature, and oxygen). In food industries, a broad range of products (including probiotics, antioxidants, antimicrobials, flavors, enzymes, and nucleic acids) are encapsulated to (a) prevent the core material from degradation, (b) slow down the evaporation rate of volatile core material, (c) separate the components that would otherwise react with each other, (d) modify the nature of the core material for easier handling, (e) increase the stability, (f) to mask undesired tastes, colors, and odors, (g) enable sustained and controlled release (release slowly over time at a constant rate), (h) control oxidative reactions, (i) use with bacteriophages to control foodborne pathogens, and (j) extend the shelf life. Indeed, encapsulation is one of the new and effective methods to protect probiotics from the harsh conditions they encounter throughout food processing, shelf storage, and gastrointestinal transit [1,40–42].

3. Probiotic Encapsulation Techniques

Numerous encapsulation technologies have been developed and adopted to protect probiotics. All the techniques aim to protect the viability and stability of probiotics. However, their concepts, operation methods, and properties of produced capsules are different. Each technique also has its own strengths and drawbacks. Figure 1 illustrates different types of probiotics encapsulation techniques and the morphologies of corresponding microcapsules obtained. Various aspects must be taken into consideration before the selection of encapsulation techniques. Selecting a suitable encapsulation technique depends on several parameters, such as the nature of the probiotics, the operational conditions of the encapsulation technique, the properties of the biomaterials used, the particle size needed to deliver the adequate probiotics load without affecting the sensory properties, the release mechanism and release rate, the composition of the target food application, the storage conditions of the food products before consumption, and lastly, the cost limitation of production [43,44].

3.1. Extrusion

Extrusion (also known as external ionic gelation, which produces capsules with sizes of 100 μm to 5 mm) is the oldest and the most common physical technique for encapsulating the probiotic cell. In the extrusion technique, probiotics are first suspended in a biopolymer solution. The suspension is then fed into an extruder (pilot scale) or a syringe needle (laboratory scale) and drips off into a hardening solution (most commonly, calcium chloride) with gentle stirring [40,45].
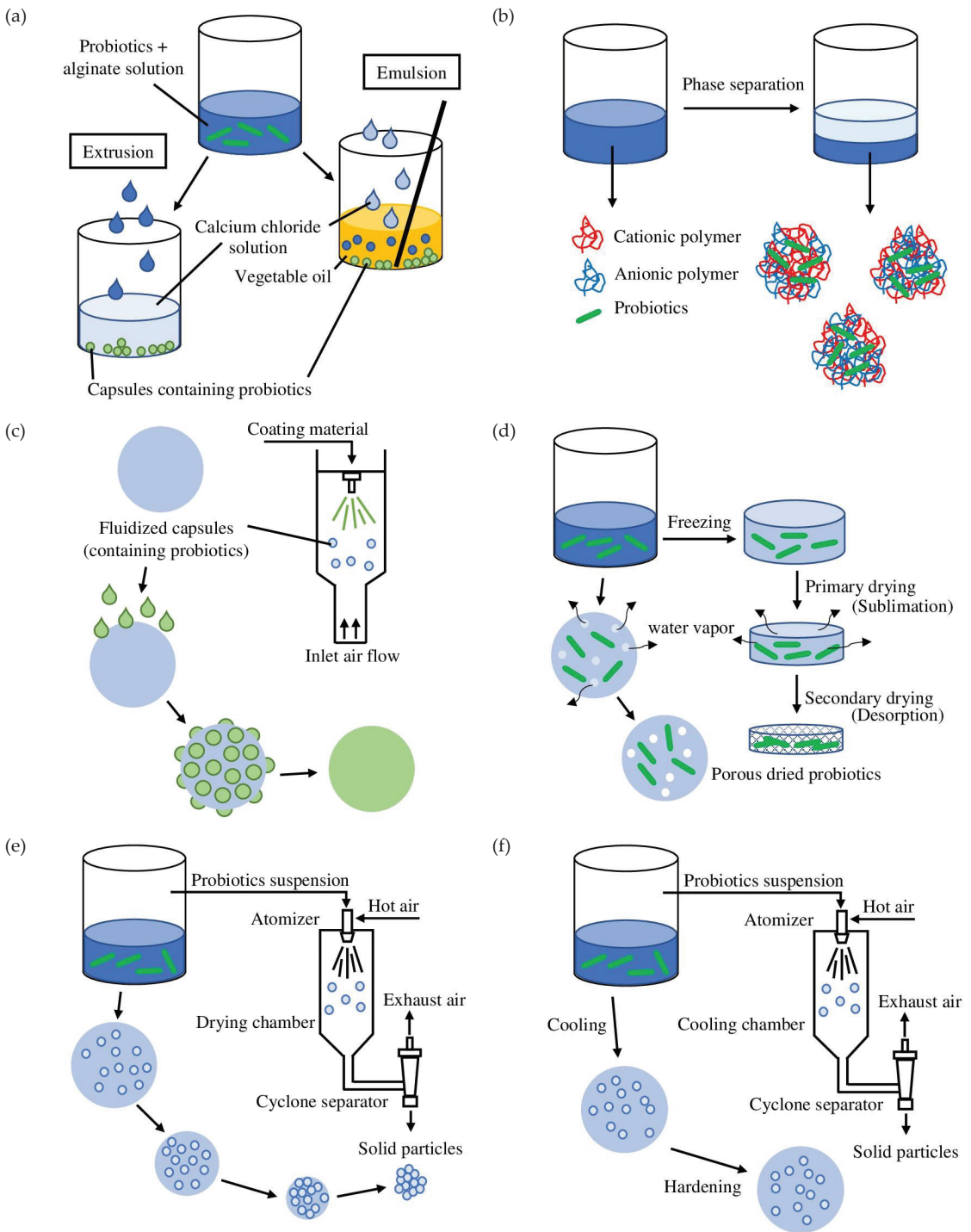
Figure 1. *Cont.*
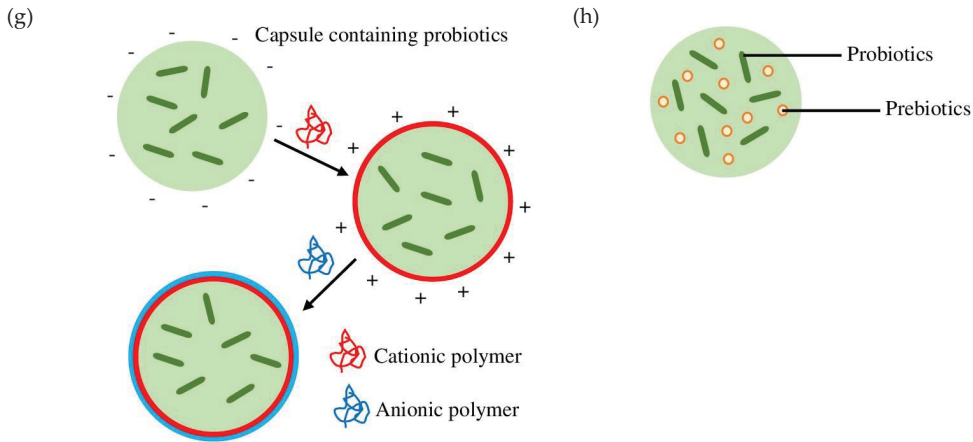
Figure 1. Different types of probiotics encapsulation techniques and the morphologies of corresponding microcapsules obtained: (**a**) ionic gelation (emulsion, extrusion); (**b**) coacervation; (**c**) fluidized bed coating; (**d**) freeze-drying; (**e**) spray-drying; (**f**) spray chilling; (**g**) layer-by-layer method; (**h**) co-encapsulation.

The extrusion technique is relatively simple, direct, straightforward, and gentle (does not involve extreme temperature, pH condition, and organic solvents), thus resulting in relatively high viability (low cell harm) of probiotic microorganisms and requiring a lower operational cost. This technique can be conducted under both aerobic and anaerobic conditions. It is biocompatible and flexible as it does not require any harmful solvents. Using alginate/shellac blend and sunflower oil as wall and core materials, respectively [40,41,43,45], Silva et al. [46] demonstrated that the co-extrusion encapsulation technique increased the probiotic survival of *L. acidophilus* LA3 by about 80% in simulated gastrointestinal conditions and 83% of the probiotics loaded into dried particles were viable after 60 days storage at room temperature (25 °C). Kim et al. [47] also demonstrated that encapsulation of probiotic *L. acidophilus* by ionic gelation between phytic acid and chitosan followed by the addition of calcium carbonate and starch with electrostatic extrusion provided buffering effects and protection against acid injury during simulated gastric conditions and refrigerated storage. The extrusion technique has also been utilized in non-dairy probiotic foods such as *E. faecium* in cherry juice [13], *L. lactis* ABRIINW-N19 in orange juice [17], *L. casei* DSM 20011 in pineapple, raspberry, and orange juices [18], *L. acidophilus* TISTR 2365 in sweet fermented rice sap beverage [27], *L. acidophilus* NCFM in mulberry tea [29], *L. casei* Lc-01 and *L. acidophilus* La5 in mayonnaise [35], and *L. reuteri* in chewing gum [36].

However, the size of beads produced through the extrusion technique is relatively big (up to 5 mm), and the process of bead solidification is also relatively slow. Hence, this technique is not suitable to be used in large-scale production [40,43,45]. Over the last decades, an evolving extrusion technique (vibrating nozzle method) has been focused on and studied. This new extrusion technique uses vibrating technology (mechanical principle), in which, when a defined amplitude is enforced, the vibrational frequency will break the extruded fluid into pre-defined-sized droplets. The size of the droplets generated using this technique can be controlled through the diameter of the jet, the velocity of the extrusion process, the viscosity and the surface tension of the fluid, and the frequency of disturbance [41].

3.2. Emulsion

In the emulsion (also known as internal ionic gelation, which produces capsules with sizes of 200 nm to 1 mm) encapsulation processes, the suspension containing probiotics cell and polymer (disperse phase) is first dispersed into vegetable oil (continuous phase) and

homogenized to form a water-in-oil (W/O) emulsion in the presence of a surfactant (emulsifier). After emulsification, calcium chloride (cross-linking agent) is added to insolubilize and harden (fast gelling process) the water-soluble biopolymer. The gel beads can then be harvested by filtration or centrifugation [40,43].

Compared to the extrusion technique, the emulsion technique is easier to scale up for mass production. Hence, it is more suitable for application at the industrial level [45]. Additionally, high survival of probiotics was also reported after encapsulation using the emulsion technique [43]. Singh et al. [48] found that probiotic *L. rhamnosus* GG encapsulated in a homogeneous system of carboxymethyl cellulose/gelatin blend survived better under simulated intestinal tract conditions compared to free probiotics. Picone et al. [49] revealed that encapsulated *L. rhamnosus* in gelled water-in-oil emulsions had a survival rate of more than 77% against in vitro digestion. Probiotics (*B. bifidum* [7], *L. acidophilus* PTCC1643, *B. bifidum* PTCC 1644 [15], *L. plantarum*, *L. fermentum*, *L. casei*, *L. sphaericus*, *S. boulardii* [16], and *Lactobacillus salivarius* spp. *salivarius* CECT 4063 [10]) encapsulated using the emulsion technique have also been reported as suitable to be used in non-dairy food matrices such as grape [7,15], tomato, and carrot [16] juices, and apple matrix [10]. Furthermore, the emulsion encapsulation technique is flexible since it can adjust and control the beads' size. According to Oberoi et al. [40], the diameter of the beads produced through the emulsion technique can be reduced to 25 μm, which cannot be achieved using extrusion methods. However, the emulsion technique has a high operational cost due to the high price of vegetable oil (such as soy, sunflower, corn–millet, and light paraffin oil) [40,45]. In addition, the microcapsule produced is not suitable for use in low-fat food products due to the oil residual in the capsule [39].

Considering that conventional emulsions are thermodynamically unstable, advanced emulsion technologies such as nano-emulsion, Pickering emulsion, and Pickering high internal phase emulsion are implemented for efficient probiotics encapsulation. Nano-emulsion is a relatively stable emulsion system with smaller droplet sizes ranging from 50 to 200 nm. In the study by Vaishanavi and Preetha [50], nano-emulsions containing soy protein isolate, Tween 80, and gum Arabic were prepared for encapsulating *L. delbrueckii* subsp. *bulgaricus*. The stability and survivability of the probiotics loaded in nano-emulsions were well-maintained throughout the storage period of 40 days. Contrary to nano-emulsions, Pickering emulsion is an emulsion system that does not require emulsifiers in the stabilization process. Pickering emulsion is stabilized rather by solid particles (more effective with hydrophobic particles). Pickering-type double emulsion (water-in-oil-in-water, stabilized with polyglycerol polyricinoleate) has also been used to encapsulate probiotics (*L. acidophilus*) [51]. The viability (gastric digestion = 93.59%, intestinal digestion = 84.24%) and colon-adhesion efficiency (43.27%) of probiotics entrapped in the double emulsion were higher than the free probiotics (viability after 1 h gastric digestion = 0%, colon-adhesion efficiency = 14.20%) during storage (14 days) and after exposure to simulated gastrointestinal conditions. Pickering high internal phase emulsion is a Pickering-type emulsion with a high internal oil phase fraction. By limiting the probiotics from contact with water and oxygen, Pickering high internal phase emulsion is known to possess high encapsulation efficiency and serve as a promising delivery system for probiotics. In a study conducted by Qin et al. [52], Pickering high internal phase emulsion stabilized with the covalent conjugates of whey protein isolate and (-)-epigallocatechin-3-gallate was used to encapsulate and protect probiotics (*L. Plantarum*). The probiotics encapsulated in the emulsion showed higher viability after storage (14 days) and were more resistant to acidic medium, bile salts, and digestive enzyme digestion when compared to the free probiotics.

3.3. Coacervation

Coacervation (phase separation, which produces capsules with sizes of 1 μm to 1 mm) is a process whereby an initial solution is separated into a polymer-rich phase (coacervate) and a polymer-poor phase (coacervation medium). Coacervation techniques can be further categorized into simple and complex coacervations. Simple coacervation involves only a

single polymer. In simple coacervation, phase separation can be induced when a strongly hydrophilic substance, water-miscible non-solvent, or inorganic salt (desolvation of the polymer) is added into a colloid solution. On the other hand, complex coacervation refers to the ionic interactions between two or more polymers (usually a protein and a polysaccharide) of opposite charges. During complex coacervation, when the charge is neutralized, the polymers separate, deposit on the droplet, and form coacervates [41,53]. Therefore, complex coacervation is preferable in probiotics encapsulation and the food industry [43].

Complex coacervation is known to produce capsules with high loading capacity that can incorporate a high number of probiotics. This technique provides high encapsulation efficiency, even at a very high (99%) payload. Complex coacervation is a simple process that does not involve high temperatures and hence, is safe for probiotics. Sharifi et al. [54] showed that probiotic *L. plantarum* and phytosterols, co-entrapped by heteroprotein complex coacervation utilizing whey protein isolate and gum Arabic, resulted in increased probiotic viability in Iranian white cheese. Silva et al. [46] demonstrated improved resistance to simulated gastrointestinal tract conditions of the microcapsules of probiotic *L. acidophilus* encapsulated by complex coacervation followed by transglutaminase crosslinking (up to 9.07 log CFU/g survival) and maintained probiotic viability (up to 9.59 log CFU/g) for 60 days at freezing ($-18\,^{\circ}$C) temperature.

The complex coacervation technique also produces microcapsules with water immiscibility which leads to optimal controlled-release properties. Complex coacervation can produce microcapsules with sizes ranging from 1 to 100 µm. However, complex coacervation is hard to scale up, as the solute used to form coacervates must be in liquid form. The range of polymers employed in this technique is also limited as coacervates are only stable within a range of pH, ionic strength, and temperature. Gelatin is the most common polymer employed in complex coacervation. However, the use of animal-based protein is limited in certain situations [55]. Zhao et al. [56] demonstrated that in comparison with the protein/polysaccharide complex coacervation, the encapsulated probiotic in water/water emulsion via type-A gelatin/sodium caseinate coacervation had a better survival rate after heating, ambient storage, and simulated digestion. The authors indicated that the increased protection of the type-A gelatin/sodium caseinate matrix was associated with lower hygroscopicity, solubilization, and wettability and could also be caused by the significantly higher hydrophobicity. Complex coacervation is also regarded as a costly technique because an additional hardening process is required.

Complex coacervation is suitable for non-dairy probiotic foods. In the study by Silva et al. [22], probiotic orange and apple juices were produced with the aid of complex coacervation associated with enzymatic crosslinking. As indicated by the results, encapsulated *L. acidophilus* LA-02 incorporated in fruit juices can survive throughout a storage period of 63 days (4 $^{\circ}$C). In addition, complex coacervation was also used by Holkem et al. [14] to encapsulate *B. animalis* subsp. *lactis* in the development of probiotic sugar cane juice. The viability of *B. animalis* during storage and delivery was enhanced through complex coacervation.

3.4. Drying Method

3.4.1. Spray-Drying

In food industries, spray-drying is the most used method to dry the encapsulated mixture into powdered probiotics (capsule sizes: 5–150 µm). The principle in spray-drying is the simultaneous mass and heat transfer processes between hot air and droplets. There are three main processes involved in the spray-drying process (i) atomization of a solution comprising probiotics and core material into fine droplets, (ii) droplets evaporation in a heated gas stream, and finally, (iii) separation and collection of spray-dried powder [43,44].

The advantages of this drying technique include (i) the process is rapid and continuous, (ii) this technique does not require a high operational cost (10 times cheaper compared to freeze-drying), (iii) highly reproducible, easy for scaling up and suitable for industrial

application, and (iv) the spray-dried products are typically dry, low in water activity, highly stable, and have low bulk density. Studies about the encapsulation of probiotics by spray-drying have been extensively reported. For example, Arslan et al. [57] showed that probiotic *Saccharomyces cerevisiae* var. *boulardii* microencapsulated with gum Arabic, pea protein, and gelatin by spray-drying were more resistant to simulated stomach solution. Jantzen et al. [58] also demonstrated that probiotic *L. reuteri* cultivated in whey slurry microencapsulated by direct spray-drying showed a 32% greater survival rate upon exposure to simulated digestive juice than those without encapsulation. Numerous studies have used spray-drying encapsulation in non-dairy probiotic food. Vivek et al. [20] demonstrated that spray-dried Sohiong juice fermented with *L. plantarum* remained viable (6.12 log CFU/g) for 36 days of storage at 25 °C. A study by Hernández-Barrueta et al. [28] showed that the viability of spray-dried *L. rhamnosus* GG in a matrix of whey protein isolate and hydrolyzed extruded huauzontle starch was stable in a ready-to-drink green tea beverage during the 5 weeks refrigerated storage.

The drawback of this technique is the harsh processing conditions, which can cause adverse effects on the stability, viability, and survivability of the probiotics [1,40,43]. For instance, the high temperature and osmotic stress applied during spray-drying can kill the probiotics. Furthermore, high air velocities during spray-drying can result in microcapsules formed with poor uniformity in terms of particle size and morphology.

3.4.2. Freeze-Drying

Freeze-drying, also known as lyophilization or cryodesiccation, is a process whereby the water vapor in the frozen sample is removed through the sublimation of ice. This technique produces capsules with sizes of 1–1.5 mm. It is commonly used to preserve thermosensitive components such as probiotics. The process of freeze-drying can be divided into three phases, (i) the initial freezing process of the probiotics (together with the carrier material), (ii) the primary drying (sublimation) phase, and (iii) secondary drying to eliminate the remaining traces of water due to absorption [43].

Rishabh et al. [23] used freeze-drying and spray-drying to encapsulate *E. faecalis* incorporated in carrot juice using gum Arabic and maltodextrin as coating materials. Compared to spray-drying, heat injuries to the probiotics are lower in the freeze-drying technique. Raddatz et al. [59] reported that *L. acidophilus* microencapsulated in the form of emulsification/internal gelation followed by freeze-drying using a blend of pectin micro-particles with prebiotic rice bran maintained probiotic viability for 120 days at 25 °C. In another study, Massounga Bora et al. [25] used freeze-drying to encapsulate *L. acidophilus* and *L. casei* using whey protein isolate and fructooligosaccharides as wall material in the development of probiotics-enriched freeze-dried banana powder. During the 30 days of refrigerated (at 4 °C) storage, the encapsulated probiotics had higher survivability compared to the free cells. The encapsulated probiotics were also more resistant to simulated gastric intestinal fluid.

However, in another investigation by Shoji et al. [60], the authors did not obtain the same positive findings using microencapsulation of *L. acidophilus* Lac-04 through complex coacervation followed by freeze-drying. The authors observed a significant decrease in viability ($p < 0.05$) after 30 days at 37 °C. The microencapsulated probiotics failed to withstand the pH condition of the human stomach. Although the freeze-drying technique has been reported to provide shelf stability to probiotics, sometimes the crystal formation during the freezing process can result in cell injury and eventually lead to cell death. Therefore, cryoprotectants that exert protection for the probiotics are necessary [61]. Cryoprotectants protect probiotics from freezing damage by inhibiting rapid cellular dehydration and ice formation during freeze-drying. Furthermore, freeze-drying is an expensive procedure with high operational and maintenance costs and is not easy to scale up [40].

3.4.3. Spray Chilling

Spray chilling (cooling or congealing, which produces capsules with sizes of 20–200 μm) is like spray-drying, but it injects cold air to atomize and solidify the particles instead of hot air. In the spray chilling process, the encapsulated agent is first dispersed in a molten lipid matrix before atomization in a chamber with cold air injection [62]. In this technique, lipids are utilized as the encapsulation material. During the passage through the gastrointestinal tract, when the temperature reaches the melting point of the carrier material (lipid), the lipases in the intestines digest the lipid wall materials and release the probiotics. Therefore, spray chilling was found to be very promising in the controlled release of probiotics. Spray chilling is reported to be the cheapest encapsulation technique as it provides a high process yield regardless of continuous or batch production. Spray chilling has also been recognized as more environmentally friendly as it requires only mild processing conditions, low operation energy, and time. Since spray chilling does not require heat, the viability of probiotics can be retained. Furthermore, this technique can be operated continuously with the elimination of hold times between manufacturing steps, making it suitable to be scaled up for industrial-scale production [43,48].

S. boulardii, *L. acidophilus*, and *B. bifidum* have been encapsulated using the spray chilling technique [63]. The results showed that the survivability of spray-chilled (*S. boulardii*, 97.89%; *L. acidophilus*, 83.57%; *B. bifidum*, 88.50%) and spray-dried (*S. boulardii*, 97.51%; *L. acidophilus*, 84.05%; *B. bifidum*, 90.10%) probiotics under simulated gastric conditions were similar. The spray chilling technique has also been used to encapsulate probiotics in probiotics-enriched cream-filled cakes [31] and savory cereal bars [34]. Spray chilling improved the survivability of *S. boulardii*, *L. acidophilus*, and *B. bifidum* incorporated in cream-filled and marmalade-filled cake samples during refrigerated storage [31]. Similarly, the viabilities of spray-chilled *L. acidophilus* and *B. animalis* subsp. *lactis* were higher than freeze-dried and free probiotics in the savory cereal bars after being stored for 90 days at 4 °C [34]. However, low encapsulation capacities on the beads produced through this technique have been reported. A lower load (10–20%) was obtained when compared to spray-drying (5–50%) [64]. The beads produced through the spray chilling technique have low melting points (32–42 °C). Probiotics encapsulated using the spray chilling technique were also found to protrude from the beads during storage. Hence, proper handling and storage conditions are required to preserve spray-chilled probiotics [43,44].

3.4.4. Fluidized Bed Drying

Fluidized bed drying, or fluidized bed coating, is a modified spray-drying method that involves intensive, simultaneous heat and mass transfers between solid particles in a suspension (produces capsules with sizes of 5–5000 μm). In the fluidized bed drying process, dried pre-encapsulated probiotics are first suspended in a hot air flow. Subsequently, the surfaces of the particles are fluidized with the biopolymer solution. The biopolymer coating is then solidified into a homogeneous layer surrounded by the pre-encapsulated probiotics [44,50]. In the fluidized bed drying process, the aqueous medium is dried in a uniform airflow, and the dried particles are suspended in the heated air. Hence, the particles are evenly dried with much less agglomeration and are uniformly coated. Compared with spray and freeze-drying processes, fluidized bed drying requires less energy consumption, and therefore, it is comparatively economical. Compared to other techniques, a lower drying temperature (ranges from ambient temperature to 120 °C) can be set and used in fluidized bed drying. Hence, it can preserve heat-sensitive probiotics. For example, Sánchez-Portilla et al. [65] proved that the viability of *Bifidobacterium* sp. was retained for more than 2 years, with a concentration exceeding 5 log CFU/g, as well as resistance to acid and complete enteric-targeted release, through the fluidized bed drying technique. The fluidized bed drying technique is ideal for food industries as it is easy to scale up and can be prepared in large batch volumes and high throughputs. Fluidized bed drying can provide multi-coating layers. Thus, it can contribute to a variety of functional properties. Nevertheless, this technique is time-consuming (~2 h), likely to kill the probiotics, and

it is not easy to master. Therefore, probiotics should be encapsulated before drying in a fluidized bed dryer [43,44,62,66].

Fluidized bed drying techniques have been successfully used by Galvão et al. [11], Mirzamani et al. [32], and Nilubol and Wanchaitanawong [26] to preserve the viability of probiotics in non-dairy food matrices. Galvão et al. [11] dried and coated apple cubes with a mixture containing hydroxyethyl cellulose and polyethylene glycol containing *B. coagulans* using the fluidized bed drying technique. The viability of probiotics in the dried apple snacks was well preserved during the storage period. The fluidized bed drying technique has also been used by Mirzamani et al. [32] to develop probiotic bread. The double-layered (first layer: microcrystalline cellulose powder and alginate or xanthan gum; second layer: gellan or chitosan) microcapsules produced through the fluidized bed drying technique had higher heat resistance and could protect the encapsulated probiotics (*L. Sporogenes*) under baking conditions. In the study of Nilubol and Wanchaitanawong [26], carrot tablets containing *L. plantarum* TISTR 2075 were produced using a fluidized bed drying technique employing gelatin. The finding indicated that the *L. plantarum* TISTR 2075 encapsulated in carrot tablets (survivability: 77.68–87.30%) had higher tolerance against heat digestion treatments than free cells (39.52%).

3.5. Layer-by-Layer Method (Multilayer Technique)

For better performance, encapsulated probiotics are coated with more than one layer, using different polymers for each layer. The layer-by-layer method (multilayer technique) was proven to increase the survivability of probiotics against the conditions of processing, storage, and along the gastrointestinal tract [50,67]. For instance, Beldarrain-Iznaga et al. [68] revealed that microencapsulation of *L. casei* using a combination of layer (canola oil)-by-layer (sodium caseinate) double emulsion and ionic gelation technique could enhance the thermal stability and cell viability of *L. casei* during storage and digestion. The functional characteristics of *L. casei* C24 were also retained through microencapsulation using the layer (alginate)-by-layer (chitosan) double emulsion technique [68]. In another study, layer (carboxymethyl cellulose)-by-layer (zein protein) encapsulating *L. plantarum* 299v was applied to apple slices [12]. The two-layer coating was able to protect the probiotics both under storage and during simulated gastrointestinal conditions.

The layer-by-layer technique involves the alternative adsorption of positively and negatively charged materials on surfaces through the chemical electrostatic deposition technique. This technique produced a protective outer layer on a microencapsulated probiotic by immersing the capsule in a biopolymer solution. This layer coating process can be repeated several times until the desired number of layers or thickness is obtained. The strength of the multilayer-coated capsule can be enhanced by increasing the interaction intensity between the charged materials. This is made possible by modification of the pH, concentration, and ionic strength of the polymer solution [31,45,60].

This technique does not involve high operational costs, as only mild conditions, aqueous solutions, and naturally charged materials are used in the coating process. The thickness, permeability, strength, and morphology of the layers can be tailored depending on the desired application. However, the adhesion times of each layer are between 1 and 60 min, which is not instantaneous. This leads to a certain degree of aggregation of the capsules during the adhesion of the subsequent layer, reducing the available surface area for consecutive layer adhesions [53,69].

3.6. Co-Encapsulation

Co-encapsulation is an encapsulation method that utilizes the synergistic effect of two or more bioactive substances that can positively influence each other to enhance the function/viability of the encapsulated substances. This technique has been used in drugs and bioactive components in pharmaceutical industries [62]. However, in recent years, considerable attention has been given to co-encapsulation processes in food indus-

tries. Co-encapsulation has been proven to be able to sustain and enhance the viability of probiotics [17,18,27,29,35,36,70].

Co-encapsulation of probiotics together with prebiotics has received attention from food researchers. The effect of co-encapsulation of probiotics with arrowroot starch for yogurt was investigated in the study of Samedi and Charles [71]. After being stored in ambient and refrigerated conditions for 90 days, the co-encapsulated probiotics had higher viability when compared to the free probiotics. The probiotics co-encapsulated with arrowroot starch with low digestibility and prebiotic potential were more resistant to the harsh conditions in the gastrointestinal tract and acidic conditions in yogurt. Furthermore, Zaeim et al. [72] investigated the protective role of polysaccharide matrix (inulin or resistant starch in calcium-alginate/chitosan microcapsules) on the co-encapsulated probiotics (*L. plantarum* ATCC 8014 and *B. animalis* subsp. *lactis*) under gastrointestinal conditions and storage at -18, 4, and 25 °C. The presence of inulin and resistant starch in the microcapsules improved the survivability of these probiotics. Shinde et al. [73] also demonstrated that co-extrusion encapsulation of probiotic *L. acidophilus* with apple skin polyphenol extract using an aqueous delivery system possessed >96% microencapsulation efficiency and improved viability under low pH conditions (pH 2, 37 °C, 120 min) and after 50 days refrigeration storage (4 °C) in milk. Overall, encapsulated probiotics with resistant starch had stronger resistance against gastrointestinal conditions compared to the ones with inulin. Resistant starch could prevent gastrointestinal acid from diffusing into the microcapsules by entrapping within the porous alginate matrix. As the carbon source, resistant starch could improve the survival of probiotics during storage and also enhance the colonization and proliferation of probiotics in the intestines [72].

Table 1 shows the main properties, advantages, and disadvantages of encapsulation techniques that can be applied in multilayer and co-encapsulation techniques of probiotics.

Table 1. Overview of common probiotic encapsulation techniques.

Methods	Properties of Encapsulation	Advantages	Disadvantages	References
Extrusion (external ionic gelation)	Produces capsules with sizes of 100 μm to 3 mm. Can encapsulate hydrophilic and hydrophobic/lipophilic compounds.	Monodispersity. Simple and mild process. Can be conducted under both aerobic and anaerobic conditions. Low operation cost. High survival rate of probiotics.	Produces relatively large beads. Slow solidification process. Not suitable for mass production. Additional drying process is required.	[40,41,43,45]
Emulsion (internal ionic gelation)	Produces capsules with sizes of 200 nm to 1 mm. Can encapsulate hydrophilic and hydrophobic compounds.	Simple process. Produces relatively small beads. Suitable for mass production. High survival rate of bacteria.	Polydispersity. High operation cost. Conventional emulsions are thermodynamically unstable. Not suitable for low-fat food matrices. Additional drying process is required.	[39,40,43,45]
Coacervation (complex coacervation)	Produces capsules with sizes of 1 μm to 1 mm. Encapsulates hydrophobic compounds.	Simple and mild process. Suitable for the food industry. High encapsulation efficiency. Controlled release potential.	High operational cost. Not suitable for mass production. Animal-based protein is commonly used. Only stable at a narrow pH, ionic strength, and temperature range.	[43,55]
Spray-drying	Produces capsules with sizes of 5–150 μm. Encapsulates hydrophilic and hydrophobic compounds.	Monodispersity. Fast, continuous process. Low operation cost. Suitable for mass production. Produces dry beads with low bulk density, water activity, and high stability.	Low cell viability. Produces beads with low uniformity. Biomaterials used have to be water-soluble.	[1,40,43,44]
Freeze-drying	Produces capsules with sizes of 1–1.5 mm. Encapsulates hydrophilic and hydrophobic/lipophilic compounds.	Suitable for temperature-sensitive probiotics. Dried end product is suitable for most food applications.	High operation cost. Not suitable for mass production. Cryoprotectants are needed.	[40,61]

Table 1. *Cont.*

Methods	Properties of Encapsulation	Advantages	Disadvantages	References
Spray chilling	Produces capsules with sizes of 20–200 μm. Encapsulates hydrophobic compounds.	Monodispersity. Fast, continuous, mild process. Low operation cost. Suitable for mass production.Promising in controlled release of probiotics.	Low encapsulation efficiency. Rapid release of the encapsulated probiotics. Special storage conditions can be required.	[43,44,48,64]
Fluidized bed coating	Produces capsules with sizes of 5–5000 μm. Encapsulateshydrophilic and hydrophobic compounds.	Mild process.Low operation cost. Suitable for mass production. Can provide multi-coating layers. Suitable for temperature-sensitive probiotics.	Slow process. Probiotics have to be pre-encapsulated and dried.	[43,44,62,66]

4. Biomaterials Utilized for Probiotics Encapsulation

To be an effective encapsulation material (core or wall material), the biomaterial used must be able to protect the encapsulated probiotics along the gastrointestinal tract until reaching the target site (small intestine/large intestine), where they can exert their health-promoting effects. The encapsulation material should only release the encapsulated probiotics when it is exposed and triggered by certain environmental conditions (such as temperature, pH, and enzyme activity). In other words, the capsules containing probiotics should remain protected inside the encapsulation material during the passage through the stomach and only decompose after reaching the target site to release the probiotics. The commonly used biomaterials in probiotic encapsulation include carbohydrates, proteins, and lipids, which will be discussed in detail in the coming subsections. Their specific advantages and limitations in probiotic encapsulation are also summarized in Table 2.

Table 2. Common biomaterials for encapsulating probiotics.

Category	Biomaterial	Characteristics and Advantages	Limitations	Remarks	References
Carbohydrate	Alginates	Anionic character, non-toxic, biocompatibility, biocompostability, cell affinity, strong bioadhesion, absorption characteristics, antioxidative, anti-inflammatory, and low in cost. Stable (shrink) in the low acidic stomach gastric solution and gradually dissolve (swell and release encapsulated probiotics) under alkaline conditions in the small intestine.	Sensitive to heat treatment, highly porous, poor stability and barrier properties.	Technique: extrusion, emulsion.Could form a strong gel network by interacting with cationic material (e.g., chitosan). Combination: pectin, starch, chitosan.	[74,75]
	Chitosan	Cationic character, non-toxic, biodegradability, bioadhesiveness, antimicrobial, antifungal, low in cost, high film-forming properties, great probiotics biocompatibility, resistance to the damaging effects of calcium chelating and anti-gelling agent, generate strong beads.	Degrade easily in low pH conditions, water-insoluble at pH > 5.4. Pose inhibitory effect against lactic acid bacteria.	Technique: extrusion, layer-by-layer (LbL), emulsion.Normally used as a coating rather than as a capsule. Combination: alginate, pectin.	[67,75]
	Starch and starch derivatives	GRAS is abundant, low in cost, non-allergenic, and biodegradable. Could produce gels with strong but flexible structure, transparent, colorless, flavorless, and odorless gel that is semi-permeable to water, carbon dioxide, and oxygen. Resistant to pancreatic enzymes. Pose prebiotic properties.	Exhibit high viscosity in solution.	Technique: extrusion, emulsion. Combination: alginate.	[67,76]
	Cellulose and cellulose derivatives	Abundant, low in cost, biodegradability, biocompatibility, tunable surface properties. Insoluble at pH ≤ 5 but soluble at pH ≥ 6, effective in delivering probiotics to the colon.	Cannot form gel beads by extrusion technique	Technique: emulsion, spray-drying. Combination: alginate, protein.	[77]
	Maltodextrin	Non-toxic, bland in taste, abundant, low in cost, good solubility, low viscosity even at high solid content. Excellent thermal stability. Pose (moderate) prebiotic properties.	Low emulsifying capacity.	Technique: spray-drying. Combination: gum Arabic, sodium caseinate.	[41,78]

Table 2. *Cont.*

Category	Biomaterial	Characteristics and Advantages	Limitations	Remarks	References
	Carrageenan (κ-carrageenan)	Pose thermosensitive and thermoreversible characteristics, the probiotic release can be controlled with temperature.	The gel beads produced are irregular in shape, brittle and weak, and their probiotic release rate is much slower than alginate beads.	Technique: extrusion, emulsion. Dissolves at 80–90 °C. Addition of probiotics at 40–50 °C. Gelation at room temperature. Combination: milk protein, alginate, locust bean gum (LBG), carboxymethyl cellulose.	[41,79]
	Pectin	Anionic character, abundant, non-toxic, water-soluble, biocompatibility, biodegradability, bioadhesiveness, antimicrobial, antiviral, good gelling, emulsifying, thickening and water binding properties, prebiotic effect.	Low in thermal stability, poor mechanical properties. High water solubility. High concentration of sucrose contents.	Technique: spray-drying. Combination: a variety of carbohydrate-based biomaterials.	[75,80,81]
Gums	Xanthan gum	Anionic character, non-toxic, biodegradable, biocompatible, excellent gelling properties, highly soluble in both cold and hot water. Excellent heat and acid stability. Resistant to gastrointestinal digestion and enzymatic decomposition. Could also act as a source prebiotic.	High susceptibility to microbial contamination, unstable viscosity, and uncontrollable hydration rate. Gels produced solely using xanthan gum are relatively weak.	Technique: spray and freeze-drying. Combination: alginate, chitosan, gellan, and β-cyclodextrin.	[41,82,83]
	Gellan gum	Anionic character, non-toxic, biocompatible, biodegradable, water-soluble, and low in cost. High resistance against heat, acidic environments, and enzymatic degradation. Swell at high pH.	High gel-setting temperatures (80–90 °C) cause heat injuries to probiotics.	Technique: spray-drying. Combination: gelatin, sodium caseinate, and alginate.	[41,44,84]
	Gum Arabic	Anionic character, acid stability, highly water soluble, low in viscosity. Exhibit surface activity, foaming, and emulsifying abilities. Could prevent complete dehydration of probiotics during the drying process and storage.	Restricted availability and high cost. Show only partial protection against oxygen.	Technique: spray-drying. Combination: maltodextrin, gelatin, whey protein isolates.	[41,78,84]
Animal-based proteins	Gelatin	Amphoteric character, could form complexes with anionic polymers. Could produce beads with strong structure and impermeable to oxygen.	High solubility.	Technique: extrusion, complex coacervation, spray chilling, spray-drying, lyophilization. Combination: alginate, pectin.	[1,41,85]
	Whey protein	Amphoteric character, highly nutritious, high resistance and stability against pepsin digestion, great gelation properties, thermal stability, hydration, and emulsification properties.	The gel beads or matrices produced are weak.	Technique: extrusion. Combination: gum Arabic, pectin, maltodextrin.	[41,86,87]
	Milk protein (casein)	Amphiphilic character, abundant, low in cost, possess excellent gelling and emulsifying properties, self-assembling properties, biocompatibility, biodegradability, produce gel beads with varying sizes (range from 1 to 1000 μm), higher density and better protection, high resistance to thermal denaturation (sodium caseinate).	Immunogenicity and allergenicity.	Technique: extrusion, emulsification, spray-drying, enzyme-induced gelation. Combination: a variety of carbohydrate-based biomaterials.	[41,88,89]
Plant-based proteins	Zein protein	Amphiphilic character, biocompatible, biodegradable, water-insoluble, high resistance against gastric juice.	Highly unstable, aggregate in aqueous solutions.	Technique: electro-spinning, electro-spraying, spray-drying. Combination: sodium caseinate, alginate, pectin.	[89]
	Soy protein	High nutritional value, less allergenic, surface active, good emulsifying, absorbing, film forming properties, high resistance against gastric juice.	Heat-induced gel formation.	Technique: extrusion, spray-drying, coacervation. Combination: carrageenan, pectin.	[41,89,90]

Table 2. *Cont.*

Category	Biomaterial	Characteristics and Advantages	Limitations	Remarks	References
Lipids	Natural waxes, vegetable oils, diglycerides, monoglycerides, fatty acids, resins	Low in polarity, excellent water barrier properties, thermally stable, and could encapsulate hydrophilic substances.	Weak mechanical properties, chemically unstable, might negatively affect the sensory characteristics of food products due to lipid oxidation.	Technique: spray chilling, spray coating.Have melting points ranging from 50–85 °C. Combination: polysaccharides or proteins.	[91]

4.1. Carbohydrate Polymers

4.1.1. Alginate

Among the carbohydrate polymers used, the most common biomaterial is alginate. Alginate can be produced by various brown seaweeds (*Laminaria digitata*, *Laminaria hyperborea*, *Laminaria japonica*, *Macrocystis pyrifera*, and *Ascophyllum nodosum*) and two genera of bacteria (*Pseudomonas* and *Azotobacter*), making it abundant and comparatively low in cost [45]. Alginate is the preferred biomaterial in probiotic encapsulation owing to its non-harmful nature, ease in producing strong beads, and being promptly accessible. Alginate has good gelling, balancing out, and thickening properties, and is easy to manipulate, biocompatible, and biodegradable [1,40,45,79]. Alginate is a pH-responsive polymer that is stable at lower pH and unstable in higher pH conditions which is beneficial in customizing release profiles. During the delivery, alginate beads tend to shrink in low acidic gastric environments. Hence, it prevents the release of the encapsulated probiotics from the beads. Once the beads reach the small intestine with alkaline conditions, the alginate transforms into a soluble alginic acid layer. Subsequently, they swell and release the encapsulated probiotics [75]. Unfortunately, alginate is sensitive to heat treatment, porous, unstable, and has poor barrier properties because of its high molecular mobility and weak interaction between the molecular chains [1,45]. The weakness of alginate can be overcome through a crosslinking reaction with divalent cations or co-encapsulation with starch or by coating the alginate capsules with an extra layer (multilayer technique) made of a different type of biomaterial [92]. The ionic crosslinking of alginate chains with calcium cations could result in a strong gel structure. The presence of calcium cations could also disrupt the water coordination of the alginate network [79]. The synergistic effects of alginate and starch of the alginate capsules could protect the entrapped probiotics [45]. With the interaction of the negatively charged carboxylic groups of alginate with positively charged amine groups chitosan, stronger, ordered three-dimensional gel networks can be produced. The resulting capsules also have smoother surfaces with decreased water permeability [67].

4.1.2. Chitosan

Chitosan originates from chitin which is naturally synthesized by algae and the shell waste of crab, shrimp, and crawfish [45]. Chitosan-based hydrogels have been extensively employed to deliver probiotics owing to their unique cationic character, non-toxicity, high biocompatibility, biodegradability, bio-adhesiveness, inexpensive nature, antimicrobial, and antifungal properties [67,75,93]. Chitosan also has high tolerance against the deteriorative effects of calcium chelating and anti-gelling agents [67]. However, chitosan is a pH-sensitive material that tends to degrade in low pH conditions and is water-insoluble at pH > 5.4. Therefore, it is less effective in the delivery of probiotics to the gut [75]. Moreover, using chitosan as a polymer for entrapping live lactic acid bacteria (LAB) could exhibit inhibitory effects on the LAB [1]. Therefore, it is commonly applied as a coating or shell rather than a capsule matrix. Chitosan has been extensively used in combination with other biomaterials, including alginate, starch, whey protein isolate, and xanthan gum [1,45]. Chitosan coating could enhance the porosity of alginate beads, thus, reducing leakage of encapsulated bacteria and improving the pH stability of beads [67]. Chitosan coating increased the release rate of probiotics from alginate/starch beads and enhanced the survivability of probiotics in low pH conditions [94]. The chitosan coating on alginate/whey protein

isolates beads increased the resistance to thermal, storage, and simulated gastrointestinal environment [95]. In addition, the heat resistance of microcrystalline cellulose/Xanthan gum beads has also been enhanced by chitosan coating [32]. Encapsulation of probiotics using microcrystalline cellulose powder and alginate, or Xanthan gum followed by coating with chitosan (0.5%) as the outermost layer is effective in protecting probiotics (*L. Sporogenes*) against the baking process (90 °C for 15 min) in bread making.

4.1.3. Gums

Xanthan gum has been proven as an excellent embodiment in conferring protection against harsh gastrointestinal conditions and elevated temperatures (up to 90 °C for 5 s) to probiotics. It is an exopolysaccharide obtained through fermentation by *Xanthomonas campestris* from agro-industrial wastes [79]. Xanthan gum possesses an anionic character, is non-toxic, biodegradable, biocompatible, highly soluble in cold and hot water, and has excellent gelling properties. Furthermore, it has excellent heat and acid stability and is highly resistant to gastrointestinal digestion and enzymatic decomposition [41,82]. The study of Thang et al. [33] indicated the protective effect of Xanthan gum on the viability of *L. acidophilus* incorporated in bread under simulated gastric and intestinal conditions compared to using alginate alone. Xanthan gum has a negative charge structure that could bind to H^+ ions and minimize the effect of an acidic condition on the probiotics. Unfortunately, it has some limitations. It is susceptible to microbial contamination, unstable viscosity, and uncontrollable hydration rate, as well as producing gels with poor shear resistance, mechanical strength, and thermal properties when used solely [41,83]. Therefore, to enhance the coating properties of Xanthan gum in probiotic encapsulation, it is combined and used with other biomaterials, including alginate, chitosan, gellan, and β-cyclodextrin [41]. In contrast to alginate beads, the combination of xanthan and gellan gums produces capsules with higher resistance toward acid conditions [1,41].

Gellan gum is a microbial polysaccharide, industrially produced through fermentation by *Sphingomonas elodea* and *Pseudomonas elodea*. It is available in two forms, low acyl gellan gum (deacylated; Kelcogel) and high acyl gellan gum (acylated; Gelrite). Upon cooling, gellan gum with lower acyl contents (gel setting temperature: 40 °C) forms a more rigid and brittle gel, whereas gellan gum with higher acyl contents (gel setting temperature: 65 °C) tends to produce gels with a softer and more flexible texture. In probiotic encapsulation, low acyl gellan gum is commonly used [41]. In general, gellan gum is negatively charged, non-toxic, biocompatible, biodegradable, relatively cheap, and water-soluble. Gellan gum has high resistance against heat, enzymatic degradation, acidic environments, and swells in alkaline conditions, allowing it to be suitable as a controlled release polymer. However, the gel formed by gellan gum is considerably poor in mechanical strength and unstable in physiological conditions. The high gel-setting temperature (80–90 °C) of gellan gum also causes heat injuries to probiotics. Usually, it is used in combination with other biomaterials such as gelatin, sodium caseinate, and alginate in probiotic encapsulation [44,84]. Gellan gum has been used to increase the thermal stability of probiotics in a study on probiotic bread [32]. Results demonstrated that the gellan gum (1.5%) coating layer increased the survivability of *L. Sporogenes* encapsulated in alginate beads 24 h after baking.

Gum Arabic (or gum acacia) is another common biomaterial used in probiotic encapsulation. It is an arabinogalactan polysaccharide-protein anionic complex that provides surface activity, foaming abilities, and emulsifying characteristics. Gum Arabic possesses acid stability, high water solubility, and low viscosity even at a high concentration [41]. Gum Arabic has high water solubility, relatively low viscosity, and good film-forming and emulsifying properties, which reduces the hygroscopicity and degree of caking of the obtained powder. At the same time, it can prevent complete dehydration of probiotics during the drying process and storage. Hence, gum Arabic has been extensively used in spray-drying [78]. For instance, gum Arabic provided good protection to *L. acidophilus* from spray-drying damage. The viability of *L. acidophilus* encapsulated with gum Arabic was reduced by only 1 log CFU/g after being treated with spray-drying [70]. Gum Arabic tends

to produce microcapsules with irregular shapes and rough surfaces, which can reduce the ability to retain the probiotics. Gum Arabic is also a comparatively expensive ingredient because of frequent supply shortages. It shows partial protection against oxygen. Hence, it is used together with other biomaterials such as maltodextrin, gelatin, and whey protein isolates [41,84]. The use of gum Arabic in combination with maltodextrin (survivability of probiotics: 71.0%) was proven to provide better protection to probiotics during storage (10 weeks) than gum Arabic (35.3%) or maltodextrin (30.2%) alone [69]. Gum Arabic has also been used with β-cyclodextrin to produce the spray-dried probiotics (*S. boulardii*, *L. acidophilus*, and *B. bifidum*) in the production of probiotics-enriched cream-filled cake, marmalade-filled cake, and chocolate coated cake [31].

4.1.4. Starch

Starches have received great attention in the probiotic encapsulation process because they are generally recognized as safe, abundant, inexpensive, non-allergenic, able to produce a gel with a strong and flexible structure, transparent, colorless, flavorless, and odorless gel that is semi-permeable to water, carbon dioxide, and oxygen [76]. Probiotics can survive in gastrointestinal and colon environments when embodied in the starch granules [40]. Moreover, the utilization of starch with combinations of biomaterials, such as alginate and chitosan, was reported to protect the probiotics [41]. Chemically modified starches (e.g., succinated, cross-linked, substituted, oxidized, and acid-treated) possess higher solubility and better mechanical properties and have also been used in probiotic encapsulation [41,76]. Starch, i.e., resistant starch, can also serve as a potential prebiotic since this type of starch cannot be digested in our small intestines. The prebiotic effects of resistant starch allow a higher release of the probiotics in the large intestine. The adherence of the probiotics is also higher with resistant starch due to its robustness and resilience to environmental stresses [1]. Starch adhesion increases the initial cell load of probiotics and improves the targeted delivery of probiotics. However, starch often exhibits high viscosity in solution. Thus, it negatively affects the efficiency of encapsulation [67]. The starch viscosity can be adjusted through starch modifications.

4.1.5. Cellulose and Cellulose Derivatives

Cellulose is the most abundant biopolymer found in nature. Cellulose and its derivatives have been extensively used in probiotic encapsulation owing to their non-toxic character, biocompatibility, tunable surface properties, and pH-controlled release ability. Cellulose is insoluble at pH ≤ 5 but soluble at pH ≥ 6. Hence, it is effective in delivering probiotics to the colon. Common celluloses used in probiotic encapsulation are carboxymethyl cellulose, methyl cellulose, hydroxyethyl cellulose, hydroxypropyl cellulose, hydroxypropyl methyl cellulose, and microcrystalline cellulose. An optimized delivery with a sustained and slow release of probiotics to the targeted region (intestine tracts) has been developed on cellulose-based gel beads [77]. Youssef et al. [94] reported that the viability of *L. salivarius* subsp. *salivarius* CGMCC No. 1.1881 encapsulated in alginate and coated with cellulose (carboxymethyl cellulose) was higher than the probiotics encapsulated in alginate without coating under thermal treatment, storage, and simulated gastrointestinal conditions. The main limitation of celluloses is that they cannot form gel beads using the extrusion technique [77].

4.1.6. Maltodextrin

Maltodextrin is one of the most common wall materials used in spray-drying to encapsulate probiotics. It is a starch hydrolysate produced from any starch via partial acidic or enzymatic hydrolysis. Maltodextrin is abundant, inexpensive, non-toxic, bland in taste, possesses low hygroscopicity, shows excellent thermal stability, has high water solubility, and low viscosity, even when at a high solid content [41,78]. These properties prevent particle agglomeration and contribute to the easy spray-drying of maltodextrin. It also possesses moderate prebiotic properties and is beneficial in probiotic encapsulation. How-

ever, maltodextrin has a weak emulsifying capacity. Hence, it shows a low encapsulation efficiency. In this regard, maltodextrin is often used together with other biomaterials such as gum Arabic and sodium caseinate [41]. Thang et al. [33] reported that the survivability of *L. acidophilus* during the bread-baking process was increased through the addition of maltodextrin in the encapsulation matrix. A higher protective effect was observed when maltodextrin was used with Xanthan gum.

4.1.7. Carrageenans

Carrageenans are natural hydrophilic polymers extracted from red seaweeds (Rhodophyta). Among the three commercially available carrageenans (κ-, ι-, and λ-carrageenan), κ-carrageenan is the most widely used in the encapsulation of probiotics [1]. This is due to the thermosensitive and thermoreversible characteristics of κ-carrageenan, making it a suitable material to deliver probiotics as the release can be controlled with temperature [79]. In general, encapsulation using κ-carrageenan involves the addition of probiotics to melted (at 80–90 °C) κ-carrageenan during the cooling period (at 40–50 °C). The encapsulation is completed when gelation occurs, i.e., when the reaction mixture is cooled to ambient temperature [1]. Nevertheless, the gels produced using κ-carrageenan are brittle and weak [41]. The properties of the formed gel can be enhanced by combining it with ι-carrageenan, locust bean gum, alginate, and carboxymethyl cellulose [41,79]. κ-carrageenan hydrogels have been used to deliver probiotics. It is observed to increase the viability of probiotics under gastrointestinal conditions and storage at refrigeration conditions (4 °C) and room temperature at 22 °C [79]. However, the rate of probiotic release from carrageenan-based hydrogels is much slower than from alginate-based hydrogels [41]. Carrageenan (κ-carrageenan) has also been used to enhance the viability of *B. bifidum* incorporated in grape juice [7]. The viability of *B. bifidum* encapsulated with carrageenan (7.09 log CFU/mL) was higher than the free probiotics (6.58 log CFU/mL) after being stored for 35 days.

4.1.8. Pectin

Pectin is a heteropolysaccharide that can be extracted from various kinds of fruits but commonly from the peels of citrus fruits. Pectin has been extensively used as a substitute for expensive biomaterials in the encapsulation of probiotics owing to its abundance, affordable price, anionic and non-toxic character, biocompatibility, biodegradability, bioadhesives, antimicrobial, and antiviral properties. Pectin possesses excellent gelling, thickening, and water-binding properties. In addition, it can form emulsions at low concentrations, making it suitable to be incorporated into spray-drying techniques. Pectin has been used with maltodextrins as probiotics (*L. casei* Shirota, *L. casei* Immunitas, and *L. acidophilus* Johnsonii) carrier in the production of probiotic enriched orange powder [24]. The combination of pectin and maltodextrins effectively enhanced the stability of probiotics during the spray-drying process. Pectin is resistant to gastric and intestinal enzymes but can be rapidly fermented by gut microbiota, thus facilitating the controlled release of probiotics in the gut. It is also an effective prebiotic that can enhance growth, increase acid tolerance, and improve the survival of encapsulated probiotics [75,80,81]. However, due to the high solubility of pectin in the aqueous medium, the bead produced by pectin shows limitations in its rate of diffusion and release of probiotics. Pectin beads have high porosity, low thermal stability, and mechanical strength. During the gelation of pectin, sucrose content was observed to increase. Therefore, pectin-based beads were not recommended for patients with diabetes [81].

4.2. Protein

In the past, proteins have been widely used as biomaterials in the encapsulation of probiotics. Potential plant-based proteins include maize (zein) and soy proteins, whereas animal-based proteins include gelatin, whey proteins, and milk proteins. In general, proteins possess an amphiphilic character, high emulsifying capacity, gel-forming ability, film formation capability, water solubility, biocompatibility, and biodegradability, allowing them to be excellent encapsulating materials. However, protein conformation and encapsulation

efficiency depend on the pH, ionic strength, and temperature. For instance, proteins are commonly used in combination with carbohydrate-based biomaterials. The main concern of using proteins as encapsulants is their allergenicity. Usually, plant-based proteins are less allergenic than animal-based proteins. The applications of animal-based proteins have also been limited by vegetarian and kosher trends, lactose intolerance, and other dietary restrictions [41].

4.2.1. Plant-Based Proteins
Zein Proteins

Zein is the major protein of maize. Owing to its amino acid residues with polar and non-polar side chains, zein exhibits an amphiphilic character. It is suitable for use as a biomaterial for encapsulations and delivery of water-insoluble probiotics. In addition, zein has high resistance against gastric juice. Hence, it can extend the release of probiotics in the small intestines. Despite its high surface hydrophobicity, zein is highly unstable and tends to aggregate in aqueous solutions. For instance, zein beads are commonly coated with a layer of emulsifiers such as sodium caseinate and Tween 20 or ionic polysaccharides such as alginate and pectin [89].

Riaz et al. [96] used zein protein-coated alginate microbeads to encapsulate *B. bifidum*. The probiotics encapsulated in zein protein (1, 3, 5, 7, and 9% (*w/v*))-coated alginate microbeads were higher in viability compared to those encapsulated in alginate microbeads (10^5 log CFU/g) and free cells (10^3 log CFU/g) after being stored for 32 days at 4 °C. Zein protein coating also enhanced the resistance of encapsulated *B. bifidum* against the harsh conditions in gastrointestinal transit. Zein protein (5% (*w/v*)) coating was also observed to increase the viability of carboxymethyl cellulose-coated *L. plantarum* 299v in apple slices under simulated gastrointestinal conditions [12].

Soy Proteins

To date, the utilization of soy protein in the encapsulation of probiotics is rare. Protein isolated from soybean is a potential probiotic encapsulation biomaterial owing to its high nutritional value, less allergenic nature, and good emulsifying, absorbing, and film-forming properties [41,89]. Soy proteins also possess high resistance against gastric juice. Therefore, they are efficient in delivering and controlling the release of probiotics to the gut. Nevertheless, heat-induced gel formation of soy proteins can affect the viability of heat-sensitive probiotics. Heat treatment could also cause protein denaturation, resulting in loss of functionality [90].

Soy protein isolates have been used with gum Arabic to prepare nano-emulsion to encapsulate *L. delbreuckii* subsp. *Bulgaricus* [50]. The presence of soy protein isolates in the emulsion can increase the stability and enhance the survival rate of probiotics during storage (at 27 °C for 40 days). In another study, soy protein isolates (20% (*w/v*)) were employed with sodium alginate (4% (*w/v*)) to encapsulate *L. plantarum* using the extrusion technique. The inclusion of soy protein isolates increased the thermal resistance of *L. plantarum*. The viability of *encapsulated L. plantarum* (a slight decrease from 9.10 log to 8.11 log CFU/mL) in mango juice remained high after the pasteurization process [21].

4.2.2. Animal-Based Proteins
Gelatin

Gelatin is a heterogeneous mixture of water-soluble proteins that can be obtained through the partial hydrolysis of collagen derived from various sources, e.g., bones, skin, scales, and connective tissues of animals [85]. When dissolved in hot water, gelatin forms a thermoreversible gel, which has been used (both on its own and with other biomaterials) to encapsulate probiotics [1,85].

Gelatin can combine with many different polysaccharides, making it one of the most studied proteins in probiotic encapsulation [1,41]. Amphoteric gelatin can be used with anionic polysaccharides (synergistic effects) to form capsules that are tolerant against

cracking and breaking. The linear structure of gelatin also provides a better oxygen barrier when compared to globular proteins [1].

Whey Proteins

Whey proteins are a complex mixture of globular proteins isolated from whey, which refers to the liquid part of milk (by-product) that separates during the cheese-making process. Whey is mainly constituted of β-lactoglobulin (85%), α-lactalbumin (10%), and bovine serum albumin (5%). β-lactoglobulin, the major protein in whey, is rich in rigid β-sheet structure and two disulfide bonds. These two unique features of β-lactoglobulin provide whey a high resistance and stability against pepsin digestion, making whey protein a suitable encapsulation material for the controlled release of probiotics [86]. Previously, whey proteins have been found to increase the resistance of probiotics against gastrointestinal conditions for up to 3 h [45,88]. Whey proteins, including whey protein concentrates (35−85% protein) and whey protein isolates (>95% protein), have been used in probiotic food products as encapsulating materials [41]. Whey proteins are a suitable medium to preserve and deliver probiotics owing to their high nutritional composition (containing soluble milk proteins and lactose). Whey proteins also possess amphoteric character, good gelation properties, thermal stability, hydration, and emulsification properties (pre-treated by heat-induced denaturation). Hence, they can interact, entrap, and protect probiotics components [87]. In probiotic encapsulation, whey proteins have been used as wall materials together with gum Arabic, maltodextrin, and pectin. The synergistic effects between whey proteins and polysaccharides have been reported to enhance the encapsulation efficiency of whey proteins [86].

Caseins

Caseins are a promising encapsulating material for probiotics owing to their structural and physicochemical properties. Caseins have excellent gelation properties and can form gels under mild conditions through different techniques, including extrusion, emulsification, spray-drying, and acid- and enzyme-induced gelation. As one of the protein components in milk, casein accounts for almost 80% of milk's total protein content. Moderate viscosities of caseins have contributed to easy dispersion of the probiotics, producing gel beads with high density and better protection for the encapsulated probiotics. The strong amphiphilic character allows caseins to encapsulate both hydrophilic and hydrophobic probiotics. Caseins can also produce gel beads of varying sizes (ranging from 1 to 1000 μm). In probiotic encapsulation, sodium caseinate is most used, owing to its excellent emulsifying properties and high resistance to thermal denaturation [41,88,89].

4.3. Lipids

Lipid matrices, such as fatty acids, diglycerides, monoglycerides, vegetable-based oils, waxes, and resins, are commonly used to encapsulate hydrophilic probiotics [81,82]. Lipid-based biomaterials are naturally low in polarity, exhibit excellent water barrier properties, and are thermally stable [76,92]. However, lipid-based biomaterials have weak mechanical properties and are chemically unstable. Therefore, lipids are often combined with other biomaterials, such as polysaccharides or proteins, to increase their performances in probiotic encapsulation [76]. In addition, when used with other biomaterials, capsules with low gas migration can be produced [41,76]. Compared to free *L. casei* and *B. pseudolongum*, lipid encapsulated probiotics were observed to have higher viability under simulated intestinal conditions [41]. However, this improvement was not observed during storage. In addition, lipid-based biomaterials were reported to have adverse effects on the overall sensory characteristics of the food product carrying the probiotics owing to lipid oxidation [41,76].

5. Application of Probiotics Encapsulation in Non-Dairy-Based Food and Beverage Products

The growing demand for non-dairy probiotic food products has encouraged scientists and researchers to explore more new non-dairy food matrices (Table 3). Recent studies have proved that non-dairy food matrices (known to be free of lactose, dairy allergens, and cholesterol and rich in nutrients) are promising vehicles for probiotic delivery. Furthermore, the probiotics were also observed to adapt well to encapsulation using non-dairy food matrices owing to their richness in nutrients. However, researchers still face some challenges, such as the maintenance of probiotic viability and sensory properties of probiotic food products [2,9]. For instance, the composition, pH value, and storage condition of the non-dairy food substrate could negatively affect the viability of inoculated probiotics. Under certain conditions, the metabolic compounds produced through the interaction between the probiotics and food matrices could negatively affect the sensory qualities of non-dairy food products. While probiotics do not usually replicate in non-dairy matrices, it is necessary to keep the viability of probiotics at an adequate level. In addition, components such as carbohydrates, proteins, and flavoring agents in the food matrix could also negatively affect the viability of probiotics. Encapsulated probiotics with bigger particle sizes were also reported to be adverse to the mouthfeel sensation.

Table 3. Examples of recent application of probiotics encapsulation in non-dairy-based products.

Category	Technology	Probiotic/LAB Strain	Encapsulating Agent	Food Product	Results	Reference
Fruit and vegetable-based	Emulsion	*Bifidobacterium bifidum*	60 mL sodium alginate, κ-carrageenan, 5 g Tween 80	Grape juice	The viability of *B. bifidum* was enhanced from 6.58 log CFU/mL (free) to 8.51 log CFU/mL (sodium alginate-encapsulated) and 7.09 log CFU/mL (κ-carrageenan-encapsulated) after 35 days of storage.	[7]
	Extrusion	*Enterococcus faecium*	2% (w/w) sodium alginate	Cherry juice	Encapsulated probiotics had higher viability during storage (4 and 25 °C) and stronger tolerance against heat, acid, and digestion treatments than free probiotics.	[13]
	Emulsion	*Lactobacillus salivarius* spp. *salivarius* CECT 4063	100 mL of sodium alginate (3%), 1 mL Tween 80	Apple matrix	Encapsulated *L. salivarius* spp. *Salivarius* had higher survivability (3%) than those non-encapsulated (19%) after 30 days of storage.	[10]
	Complex coacervation	*Bifidobacterium animalis* subsp. *lactis*	6% whey protein concentrate, 1% gum Arabic, 5% (w/w) proanthocyanidin-rich cinnamon extract (bioactive compound)	Sugar cane juice	Co-encapsulation of compounds was effective in protecting the viability of *B. animalis* and the stability of proanthocyanidins during storage and allowing simultaneous delivery.	[14]
	Emulsion	*Lactobacillus acidophilus* PTCC1643, *Bifidobacterium bifidum* PTCC 1644	2% (v/w) sodium alginate, 5 g/L Span 80 emulsifier	Grape juice	The survivability of *L. acidophilus* and *B. Bifidum* in the encapsulated samples (8.67 and 8.27 log CFU/mL) was higher than free probiotics (7.57 and 7.53 log CFU/mL) after 60 days of storage at 4 °C.	[15]
	Emulsion followed by coating	*Lactobacillus plantarum*, *Lactobacillus fermentum*, *Lactobacillus casei*, *Lysinibacillus sphaericus*, *Saccharomyces boulardii*	Emulsion: 20 mL of sodium alginate (2%), 0.1% Tween 80 Coating: 0.4% chitosan in acidified distilled water	Tomato and carrot juices	Encapsulated probiotics had higher viability than free probiotics during storage of 5–6 weeks at 4 °C. *Lys. sphaericus* was observed to have higher viability and stability than other probiotics.	[16]

Table 3. *Cont.*

Category	Technology	Probiotic/LAB Strain	Encapsulating Agent	Food Product	Results	Reference
	Co-encapsulation (extrusion)	*Lactococcus lactis* ABRIINW-N19	1.5, 2% alginate-0.5% Persian gum (hydrogels), 1, 1.5, 2% fructooligosaccharides (FOS; prebiotic), and 1, 1.5, 2% inulin (prebiotic)	Orange juice	All formulations used were able to retain the viability of *L. lactis* during 6 weeks of storage at 4 °C. Encapsulated *L. lactis* were only released after 2 h and remained stable for up to 12 h in colonic conditions.	[17]
	Vibrating nozzle method (evolved extrusion)	*Lactobacillus casei* DSM 20011	2% sodium alginate	Pineapple, raspberry, and orange juices	After 28 days of storage at 4 °C, some microcapsules were observed as broken in pineapple juice, but the viability was 100% (2.3×10^7 CFU/g spheres). 91% viability (5.5×10^6 CFU/g spheres) was observed in orange juice. Raspberry juice was not a suitable medium for *L. casei*.	[18]
	Co-encapsulation (spray-drying)	*Lactobacillus reuteri*	60 g maltodextrin, 0−2% gelatin	Passion fruit juice powder	The use of gelatin in combination with maltodextrin was more efficient in maintaining the cellular viability and retention of phenolic compounds than maltodextrin alone.	[19]
	Spray-drying	*Lactobacillus plantarum*	0.5% (w/w) magnesium carbonate, 12% (w/w) maltodextrin	Sohiong (*Prunus nepalensis* L.) juice powder	The quality of probiotic Sohiong juice powder and viability of *L. plantarum* (6.12 log CFU/g) could be maintained for 36 days without refrigeration (25 °C and 50% relative humidity).	[20]
	Fluidized bed drying	*Bacillus coagulans*	Mixture of 0.0125 g/mL hydroxyethyl cellulose and 1.17 μL/mL polyethylene glycol	Dried apple snack	Encapsulated *Bacillus coag-ulans* in dried apple snacks had high viability (>8 log CFU/portion) after 90 days of storage at 25 °C.	[11]
	Extrusion	*Lactobacillus plantarum*	Mixtures (1:2, 1:4, 1:8, 1:12) of 4% (w/v) sodium alginate and 20% (w/v) soy protein isolate	Mango juice	Homogenous aqueous solutions of alginate and soy protein isolate (1:8) increased the thermal resistance of *L. plantarum* against pasteurization process. The viability of *L. plantarum* remained high after the pasteurization process (8.11 log CFU/mL; reduced 0.99 log CFU/mL).	[21]
	Layer-by-layer (Coating)	*Lactobacillus plantarum* 299v	First layer: 1% (w/v) carboxymethyl cellulose (CMC) and 50% w/w (based on CMC weight) glycerol; Second layer: 5% (w/v) zein protein	Apple slices	The viability of CMC-zein protein-coated *L. plantarum* 299v was higher than CMC-coated *L. plantarum* 299v in apple slices under simulated gastrointestinal conditions (120 min digestion; CMC-zein protein-coated: 1.00 log CFU/g reduction, CMC-coated: 2.18 log CFU/g reduction).	[12]
	Complex coacervation (associated with enzymatic crosslinking)	*Lactobacillus acidophilus* LA-02	Complex co-acervation: 2.5% gelatin, 2.5% gum Arabic; Crosslinking: 2.5, 5.0 U/g transglutaminase	Apple and orange juices	Encapsulated *L. acidophilus* LA-02 incorporated in fruit juices was able to survive throughout the storage period of 63 days (4 °C).	[22]

Table 3. *Cont.*

Category	Technology	Probiotic/LAB Strain	Encapsulating Agent	Food Product	Results	Reference
	Freeze-drying, spray-drying	*Enterococcus faecalis* (K13)	Gum Arabic and maltodextrin	Carrot juice powder	Heat injuries to the probiotics are lower in the freeze-drying technique compared to spray-drying. After being stored for 1 month, the viability of freeze-dried *E. faecalis* remained high (6–7 log CFU/g).	[23]
	Spray-drying	*Lactobacillus casei* Shirota, *Lactobacillus casei* Immunitas, *and Lactobacillus acidophilus* Johnsonii	Maltodextrin and pectin at weight ratio of 10:1	Orange juice powder	The combination of pectin and maltodextrins effectively protected the probiotics during the spray-drying process and storage (4 °C)	[24]
	Freeze-drying	*Lactobacillus acidophilus*, *Lactobacillus casei*	Whey protein isolate, fructooligosaccha-rides, and combination of whey protein isolate, fructooligosaccharides (1:1)	Banana powder	*L. acidophilus* and *L. casei* encapsulated with the combination of whey protein isolate and fructooligosaccharides had higher survivability after being stored for 30 days at 4 °C and more resistant to the simulated gastric fluid intestinal fluid than free probiotics.	[25]
	Fluidized bed drying	*Lactobacillus plantarum* TISTR 2075	3% (*w/w*) gelatin and 5% (*w/w*) of monosodium glutamate, maltodextrin, inulin, and fructooligosaccharide	Carrot tablet	Encapsulated *L. plantarum* TISTR 2075 in carrot tablet (survivability: 77.68–87.30%) had higher tolerance against heat digestion treatments than free cells (39.52%).	[26]
Other beverages	Spray-drying	*Lactobacillus rhamnosus* GG (LGG)	Mixtures (1:1.6 (*w/w*)) of 7.5% (*w/v*) whey protein isolate and 20% (*w/v*) modified huauzontle's starch (acid hydrolysis-extrusion), supplemented with ascorbic acid	Green tea beverage	The viability of LGG remained above the recommended 7 log CFU/mL after 5 weeks of storage at 4 °C.	[28]
	Co-encapsulation (extrusion)	*Lactobacillus acidophilus* TISTR 2365	Alginate, egg (0, 0.8, 1, and 3%, *w/v*), and fruiting body of bamboo mushroom (prebiotic)	Sweet fermented rice (Khoa-Mak) sap beverage	All formulations used were able to provide high encapsulation yields (95.72−98.86%) and high viability of *L. acidophilus* (>8 log CFU/g) in Khoa-Mak sap beverages for 35 days of storage at 4 °C. Encapsulation with involvement of 3% egg of bamboo mushroom increased the survival of *L. acidophilus* the most.	[27]
	Co-encapsulation (extrusion)	*Lactobacillus acidophilus* NCFM (L-NCFM)	Co-extrusion: 0–2% (*w/v*) LBG, 0–5% (*w/v*) mannitol (prebiotic) Coating: sodium alginate	Mulberry tea	L-NCFM encapsulated with LBG and mannitol (0.5% (*w/v*) and 3% (*w/v*), respectively) showed microencapsulation efficiency and viability of 96.81% and 8.92 log CFU/mL, respectively. Among other samples, L-NCFM microencapsulated with mannitol showed the highest survivability (78.89%) and viable count (6.80 log CFU/mL) after 4 weeks of storage at 4 and 25 °C.	[29]

Table 3. *Cont.*

Category	Technology	Probiotic/LAB Strain	Encapsulating Agent	Food Product	Results	Reference
Bakery products	Double-layered microencapsulation, combination of spray chilling and spray-drying	*Saccharomyces boulardii, Lactobacillus acidophilus, Bifidobacterium bifidum*	Spray chilling: 5% (*v/w*) blend of gum Arabic and β-cyclodextrin solution (9:1 (*w/w*), 20 g in total), 1% lecithin Spray-drying: 5% (*v/w*) blend of gum Arabic and β-cyclodextrin solution, 20 g hydrogenated palm oil, 2% Tween 80 emulsifier	Cake	The survivability of probiotics during the cake baking process was improved by double-layered microencapsulation.	[31]
	Fluidized bed drying	*Lactobacillus sporogenes*	First layer: 10 g microcrystalline cellulose powder and alginate or xanthan gum Second layer: gellan or chitosan	Bread	Encapsulated *L. sporogenes* in alginate (1%) capsule tolerated the simulated gastric acid condition the best. The incorporation of chitosan (0.5%) as an outer layer improved the heat tolerance of *L. sporogenes*. Encapsulated *L. sporogenes* with an outer layer coated with 1.5% gellan showed the highest survivability 24 h after baking.	[32]
	Emulsion	*Lactobacillus acidophilus* ATCC 4356	1. Alginate 2%; 2. Alginate 2% + maltodextrin 1%; 3. Alginate 2% + xanthan gum 0.1%; 4. Alginate 2% + maltodextrin 1% + 0.1% xanthan gum	Bread	Among the encapsulation agents, probiotics encapsulated using the combination of maltodextrin, xanthan gum, and alginate (4) had the highest survivability under storage (7.7 log CFU/bread) and simulated gastrointestinal conditions.	[33]
Sauce	Co-encapsulation (extrusion)	*Lactobacillus casei* Lc-01, *Lactobacillus acidophilus* La5	4% (*w/v*) sodium alginate and 2% alginate mixture in distilled watercontaining 2% high amylose maize starch (prebiotic), 0.2% Tween 80	Mayonnaise	The viability of *L. casei* and *L. acidophilus* encapsulated with high amylose maize starch (7.204 and 8.45 log CFU/mL, respectively) was higher than free probiotics (6.23 and 6.039 log CFU/mL, respectively) and those without high amylose maize starch (7.1 and 7.94 log CFU/mL, respectively) after 91 days of storage at 4°C.	[35]
Others	Extrusion followed by freeze-drying	*Lactobacillus casei* (*L. casei* 431)	3% (*w/v*) quince seed gum, sodium alginate, quince seed gum-sodium alginate	Powdered functional drink	Quince seed gum-alginate microcapsules provided encapsulation efficiency of 95.20% and increased the survival rate of *L. casei* to 87.56%. The powdered functional drink was shelf stable for 2 months.	[37]
	Spray chilling	*Lactobacillus acidophilus* and *Bifidobacterium animalis* subsp. *lactis*	Vegetable fat (Tri-HS-48)	Savory cereal bars	The viabilities of spray-chilled probiotics were higher than freeze-dried and free probiotics in the savory cereal bars after being stored for 90 days at 4 °C.	[34]
	Co-encapsulation (extrusion)	*Lactobacillus reuteri*	2% (*w/v*) sodium alginate, 5 mL of inulin and lecithin solution (0, 0.5, and 1%)	Chewing gum	After storing for 21 days with encapsulation, *L. reuteri* remained viable. The viability of the probiotic increased with the concentration of inulin and lecithin.	[36]

5.1. Fruit and Vegetable-Based

In contrast to dairy products, fruit and vegetable juices do not contain allergens, lactose, and cholesterol. In addition, the main macronutrients in fruit and vegetable juices are carbohydrates and dietary fibers, and they are rich in vitamins, minerals, polyphenols, phytochemicals, and antioxidants. In the sensory aspect, fruit and vegetable juices are refreshing and usually do not have undesirable tastes and flavors. Therefore, fruit and vegetable juices have been recognized as promising carriers for probiotics for all age and economic groups [2,9].

Several factors could limit the survivability of probiotics in fruit and vegetable juices, including the type of probiotic strain used, the conditions of medium (e.g., pH, water activity, oxygen stress, presence of antimicrobial compounds, dyes, flavors, and preservatives), as well as the process of juice production (e.g., pasteurization process, storage temperature, type of packaging material used, and food handling practices) [9]. Among the factors, the pH condition of the medium used has the most effect on the viability of probiotics. Fruit juices naturally have a low pH value, while vegetable juices are generally less acidic. It has been reported that *Lactobacilli* can resist and survive in pH conditions ranging from 3.7 to 4.3; however, *Bifidobacteria* are less acid tolerant. Recently, encapsulated probiotics (*B. animalis*, *B. bifidum*, *E. faecium*, *L. acidophilus*, *L. casei*, *L. fermentum*, *L. lactis*, *L. plantarum*, *L. sphaericus*, and *S. boulardii*) were incorporated into fruit and vegetable juices, such as carrot, cherry, grape, mandarin fruit, mango, orange, passion fruit, pineapple, raspberry, Sohiong, sugar cane, and tomato juices [7,13–18,20–22].

Sour cherry juice has an approximate pH value of 3.5, rendering it an unsuitable medium for delivering probiotics. Encapsulation (technique: extrusion, material: sodium alginate) increased the viability of *E. faecium* in sour cherry juice during storage (from 2.18 to 5.39 log CFU/mL, 4 °C for 60 days; from 4.30 to 6.25 log CFU/mL, 25 °C for 21 days) and its tolerance against heat, acid, and digestion treatments [13]. Although alginate is the most used biomaterial in protecting probiotics, it is susceptible to low acid conditions. Low-acidic conditions change the particle shape of alginate beads, resulting in adverse effects on the release rate. In a recent study [17], Persian Gum was used with alginate and prebiotics (FOS and inulin) to encapsulate *L. lactis* ABRIINW-N19 before being added to orange juice. Among the formulations tested in the study, alginate–Persian Gum + 2% inulin was the best as it contributed the highest encapsulation efficiency and best protection for the probiotics against harsh gastrointestinal conditions. Alginate–Persian Gum + 2% inulin-encapsulated *L. lactis* also showed the highest viability during the storage period. In addition, it exhibited the best cell release activity and buffering ability in orange juice. The application of evolved extrusion technique (vibrating nozzle method) to encapsulate *L. casei* DSM 20011 was demonstrated by Olivares et al. [18]. However, the vibrating nozzle method and biomaterial used (alginate) were reported to be insufficient in protecting the probiotics as the acidic conditions could still negatively affect the viability of *L. casei* even when encapsulated. According to Olivares et al. [18], the addition of antimicrobial compounds, such as anthocyanins, can affect the viability of probiotics. Praepanitchai et al. [21] also utilized the extrusion technique to encapsulate *L. plantarum* in the developing probiotics-enriched mango juice. Soy protein isolate (20% (*w/v*)) used in encapsulation increased the thermal resistance of *L. plantarum* in mango juice, i.e., a slight decrease in the viability of *encapsulated L. plantarum* was observed after the pasteurization.

Generally, the pH value of grape juice ranges between 3.0 and 4.0. Using the emulsion technique, Mokhtari et al. [15] and Afzaal et al. [7] showed that the survivability of probiotics in grape juice can be improved. Both researchers encapsulated their probiotics in alginate beads, while Afzaal et al. [7] also encapsulated *B. bifidum* with κ-carrageenan. Similar findings were observed in both studies, whereby the viability of encapsulated probiotics in grape juice is higher than those of non-encapsulated. The survivability of *L. acidophilus* and *B. bifidum* with encapsulation (8.67 and 8.27 log CFU/mL, respectively) was higher than free probiotics (7.57 and 7.53 log CFU/mL, respectively) after being kept refrigerated (4 °C) for up to 2 months [15]. The survivability of *B. Bifidum* was enhanced

from 6.58 to 8.51 log CFU/mL (encapsulated with sodium alginate) and 7.09 log CFU/mL (encapsulated with κ-carrageenan) after 35 days of storage [7]. The encapsulated probiotics were also observed to have stronger resistance against simulated GI conditions when compared to free probiotics [7].

Similarly, Naga Sivudu et al. [16] also utilized the emulsion technique to encapsulate probiotics (*L. plantarum*, *L. fermentum*, *L. casei*, *L. sphaericus*, and *S. boulardii*) in juices (tomato and carrot juices), but with an additional of chitosan coating at the outer layer of alginate capsule. Although encapsulated probiotics had higher viability than free probiotics during refrigerated storage (4 °C for 5–6 weeks), the beads negatively influenced the sensory quality of the juice. The vegetable juices with encapsulated probiotics were reported as hard to swallow and highly turbid.

Sugarcane juice is a relatively new matrix used to deliver probiotics. In the study carried out by Holkem et al. [14], *B. animalis* was co-encapsulated with concentrated whey protein, gum Arabic, and proanthocyanidin-rich cinnamon extract through a complex coacervation technique. The encapsulation showed an increment in the probiotics' survivability and retention of the phenolic and proanthocyanidin compounds in the sugarcane juice. However, encapsulated probiotics and proanthocyanidin-rich cinnamon extract altered the viscosity of sugarcane juice. This is adverse to the sensory properties of the juice. The complex coacervation technique has also been used by Silva et al. [22] in probiotic orange and apple juices. The encapsulated *L. acidophilus* LA-02 incorporated in fruit juices survived throughout the refrigerated storage (4 °C for 63 days).

By using the spray-drying technique, Vivek et al. [20], Gervasi et al. [24], and Santos Monteiro et al. [19] successfully obtained fruit powder rich in probiotics. Encapsulation with magnesium carbonate and maltodextrin, the viability of *L. plantarum* (6.12 log CFU/g) in Sohiong juice powder was maintained for 36 days without refrigeration [19]. In the study of Gervasi et al. [24], *L. casei* Shirota, *L. casei* Immunitas, and *L. acidophilus* Johnsonii were encapsulated by using pectin and maltodextrin before spray-drying together with orange juice. The combination of pectin and maltodextrin was reported to enhance the stability of probiotics during the spray-drying process. On the other hand, Santos Monteiro et al. [19] claimed that a blend of gelatin and maltodextrin retained the viability of *L. reuteri* and phenolic compounds in passion fruit pulp against harsh conditions of the spray-drying process. In another study [23], freeze-drying and spray-drying were used to encapsulate *E. faecalis* incorporated in carrot juice using gum Arabic and maltodextrin as coating materials. The results showed that freeze-drying exerted fewer heat injuries on the probiotics than those spray-dried. Massounga Bora et al. [25] also used freeze-drying to encapsulate probiotics (*L. acidophilus* and *L. casei*), using whey protein isolate and fructooligosaccharides as wall material, in the production of banana powder. Freeze-dried probiotics were observed to possess higher survivability under storage (4 °C for 30 days) and simulated gastrointestinal conditions than free probiotics. Probiotics (*L. plantarum* TISTR 2075) enriched carrot tablets were developed using the fluidized bed drying technique [26]. The results showed that the encapsulated probiotics in the tablets were more resistant to heat and digestion treatments when compared to the free probiotics.

Fruit pieces are also potential vehicles to deliver probiotics. In a recent study by Ester et al. [10], *L. salivarius* was encapsulated in alginate beads through the emulsion technique before adding to mandarin juice. The probiotic-supplemented mandarin juice was then used to incorporate *L. salivarius* into apple discs. The probiotics-impregnated apple discs were then dried and stored for 30 days. From the study, the encapsulated *L. salivarius* was found to have higher viability than free cells, indicating that encapsulation had improved the heat resistance properties of the probiotics. The encapsulation also proved to exert stronger resistance onto the probiotics against simulated gastrointestinal conditions. Wong et al. [12] also encapsulated probiotics (*L. plantarum* 299v) in apple slices. The *L. plantarum* 299v was coated with carboxymethyl cellulose followed by zein protein, and the coatings were reported to increase the resistance of probiotics under simulated gastrointestinal conditions. In another study, Galvão et al. [11] utilized a fluidized bed drying technique to

dry and coat apple cubes with a mixture of hydroxyethyl cellulose and polyethylene glycol containing *B. coagulans*. The encapsulation was able to preserve the viability of probiotics in the dried apple snacks throughout the storage period.

Nowadays, non-edible parts of fruits have received much attention from researchers due to their abundance of bioactive compounds and promising functional properties. Recently, a powdered premix was developed using grape pomace, pomegranate, beetroot peel extract powders, and *L. casei* 431 co-encapsulated in quince seed gum-alginate hydrogel beads. Encapsulation increased the survival rate of *L. casei* throughout the freeze-drying process, from 42.16 (free cells) to 86.40% (normal encapsulation without the inclusion of prebiotic) and 87.56% (co-encapsulation with prebiotic). Quince seed gum–alginate hydrogel beads showed high encapsulation efficiency of 95.20% and maintained the viability of *L. casei* for up to 2 months [37].

5.2. Other Non-Dairy Based Products

In addition to fruit and vegetable juices, tea and sap beverages have also been used as vehicles to deliver probiotics. Green tea is rich in polyphenols and was found to have various health-promoting effects. The presence of polyphenols has been reported to be able to improve the survival of oxygen-sensitive probiotics in aqueous solutions [73,97]. During storage, fermentation by the probiotics can occur, affecting the sensory acceptability of green tea. Furthermore, the polyphenols in green tea can also be adversely impacted, leading to the loss of its antioxidant activity. To address these adverse effects, Hernández-Barrueta et al. [28] encapsulated *L. rhamnosus* in a matrix of whey protein isolate in combination with modified huauzontle starch by spray-drying before incorporating it into green tea. After refrigerated storage (4 °C for 23 days), the green tea displayed high viability of probiotics (7 log CFU/mL). There was also no evidence of the occurrence of fermentation and insignificant variation in the antioxidant and polyphenolic contents of green tea.

In another work by Yee et al. [29], *L. acidophilus* NCFM (L-NCFM) was encapsulated in beads prepared using locust bean gum with and without mannitol (prebiotic) to develop a mulberry tea fortified with probiotics. Findings from the study revealed that L-NCFM encapsulated with the presence of mannitol showed the highest survivability (78.89%) and viable count (6.80 log CFU/mL) in the tea after a month of storage at 4 and 25 °C, respectively. Higher survivability was also observed in co-encapsulated L-NCFM under simulated gastrointestinal conditions compared to free and regular encapsulated (extrusion without prebiotic) probiotics. Similarly, using a co-encapsulation technique, Srisuk et al. [27] successfully introduced *L. acidophilus* TISTR 2365 into a sweet fermented rice sap beverage. During the encapsulation of probiotics into alginate beads, egg and fruiting bodies of bamboo mushrooms were added as prebiotics. The incorporation of an egg of bamboo mushroom at 3% was observed to increase the survival of *L. acidophilus* in the beverage most efficiently. The total phenolic contents and DPPH radical scavenging activities were also increased with the addition of the prebiotic.

Bakery products are recognized as staple foods worldwide, commonly consumed as breakfast, afternoon tea, and even evening snacks. However, bakery products are usually perceived as unhealthy as they contain high amounts of simple sugars and fats while being low in dietary fiber [98]. Hence, attempts have been made to improve the negative perception of bakery products, including incorporating probiotics into bakery products. Under typical probiotic incorporation into bakery products, whereby probiotics were added to the dough, a significant loss of viable probiotics in the bakery products is inevitable as these probiotics were killed by the high temperature used during baking. Although the loss of viability can be minimized by incorporating the probiotics directly into the cream filling or spreading them on the surface of the baked bakery product, not all bakery products are cream-filled. Arslan-Tontul et al. [31] investigated using single- and double-layered coated capsules to protect *S. boulardii*, *L. acidophilus*, and *B. bifidum* in cake. Double-layered encapsulation was found able to preserve the probiotics during the baking process. In a recent study, Mirzamani et al. [32] used an encapsulation method (fluidized bed drying) to

protect the *L. Sporogenes* in bread production. The encapsulated *L. sporogenes* in alginate (1%) capsules were observed to tolerate the simulated gastric acid condition. Incorporating chitosan (0.5%) into the outer layer increased the ability of probiotics to withstand heat. The highest survivability 24 h after baking was observed in encapsulated *L. sporogenes* with an outer layer coated with 1.5% gellan. In another study by Thang et al. [33], probiotics were incorporated into bread. It was reported that the survivability of *L. acidophilus* during the bread baking process was enhanced through the addition of maltodextrin and Xanthan gum in the encapsulation matrix.

Mayonnaise is used as an adjunct on salads, vegetables, and sandwiches. The high fat and high water activity of mayonnaise make mayonnaise a suitable carrier for probiotics in the human gut. In the study by Bigdelian and Razavi [35], *L. casei* Lc-01 and *L. acidophilus* La5 were added into mayonnaise in free and encapsulated forms (with and without prebiotic). Both *L. casei* and *L. acidophilus* encapsulated with high amylose maize starch (7.204 and 8.45 log CFU/mL) had higher viability than those without prebiotic added (7.1 and 7.94 log CFU/mL) and free cell (6.23 and 6.039 log CFU/mL) after refrigerated storage (4 °C for 91 days). Co-encapsulated probiotic cells had higher viability in mayonnaise throughout the storage than normal encapsulated (extrusion without prebiotic) probiotics. In addition, fewer chemical changes were observed in the mayonnaise sample supplemented with co-encapsulated probiotics.

Confectionery products are food products with minimal nutritional value and high sugar content. Over the years, the popularity of confectionery products has been on the rise among children. In this case, attempts have been carried out to incorporate probiotics into confectionery products, hoping to bring health benefits to consumers, especially children. Among the confectionery products, jelly and chewing gum are extensively consumed by all age groups. While high thermal treatments and low acidic conditions are unavoidable in producing jelly, Wulandari et al. [30] managed to maintain the viability of *L. plantarum* Mar8 (9 log CFU/mL) in black grass jelly for 14 days during refrigerated storage (4 °C) through microencapsulation using carrageenan. Alternately, a combination of inulin and lecithin was used as prebiotic sources with wall material alginate to co-encapsulate probiotics in the preparation of synbiotic chewing gum [36]. The prebiotics in encapsulation retained the viability of the *L. reuteri* during storage (for 21 days) without affecting the sensory properties of the chewing gum. The viability of *L. reuteri* was also reported to increase with the concentration of inulin and lecithin.

6. Conclusions

With the ongoing popular trend of vegetarianism and an increasing number of lactose-intolerant and dairy-allergic consumers, the development of non-dairy delivery systems without lactose, dairy allergens, and cholesterol for probiotics has shown tremendous growth in recent years. Nevertheless, the development of non-dairy delivery systems is quite challenging because the composition, pH value, and storage condition of the non-dairy food matrices could negatively affect the viability of inoculated probiotics. Although encapsulation has been widely reported to be effective in preserving the viability of probiotics during storage, manufacturing, and gastrointestinal digestion, the techniques and biomaterials used are greatly dependent on the probiotic strain, the food matrix, and the food preparation method. Therefore, it is crucial to select appropriate techniques and biomaterials for the encapsulation and delivery of probiotics. Based on cited studies, co-encapsulation of probiotics with prebiotics was found to be most effective in preserving the viability of probiotics in non-dairy food matrices.

Author Contributions: Project administration, funding acquisition, investigation, supervision, W.Y.K.; writing-original draft, visualization, writing—review and editing, W.Y.K. and X.X.L.; writing—review and editing, T.-C.T., R.K. and B.R. All authors have read and agreed to the published version of the manuscript.

References

1. Sarao, L.K.; Arora, M. Probiotics, prebiotics, and microencapsulation: A review. *Crit. Rev. Food Sci. Nutr.* **2017**, *57*, 344–371. [CrossRef]
2. Min, M.; Bunt, C.R.; Mason, S.L.; Hussain, M.A. Non-dairy probiotic food products: An emerging group of functional foods. *Crit. Rev. Food Sci. Nutr.* **2019**, *59*, 2626–2641. [CrossRef]
3. FAO/WHO. *FAO/WHO Joint Working Group Report on Drafting Guidelines for the Evaluation of Probiotics in Food (30 April 2002 and 1 May 2002)*; Scientific Research Publishing: London, ON, Canada, 2002.
4. Sanders, M.E.; Goh, Y.J.; Klaenhammer, T.R. Probiotics and Prebiotics. In *Food Microbiology: Fundamentals and Frontiers*; ASM Press: Washington, DC, USA, 2019; pp. 831–854.
5. Murua-Pagola, B.; Castro-Becerra, A.L.; Abadia-Garcia, L.; Castano-Tostado, E.; Amaya-Llano, S.L. Protective effect of a cross-linked starch by extrusion on the survival of *Bifidobacterium breve* ATCC 15700 in yogurt. *J. Food Process. Preserv.* **2021**, *45*, e15097. [CrossRef]
6. da Silva, M.N.; Tagliapietra, B.L.; dos Santos Richards, N.S.P. Encapsulation, storage viability, and consumer acceptance of probiotic butter. *LWT* **2021**, *139*, 110536. [CrossRef]
7. Afzaal, M.; Saeed, F.; Saeed, M.; Ahmed, A.; Ateeq, H.; Nadeem, M.T.; Tufail, T. Survival and stability of free and encapsulated probiotic bacteria under simulated gastrointestinal conditions and in pasteurized grape juice. *J. Food Process. Preserv.* **2020**, *44*, e14346. [CrossRef]
8. Thamacharoensuk, T.; Boonsom, T.; Tanasupawat, S.; Dumkliang, E. Optimization of microencapsulated *Lactobacillus rhamnosus* GG from whey protein and glutinous rice starch by spray drying. *Key Eng. Mater.* **2020**, *859*, 265–270. [CrossRef]
9. Aspri, M.; Papademas, P.; Tsaltas, D. Review on non-dairy probiotics and their use in non-dairy based products. *Fermentation* **2020**, *6*, 30. [CrossRef]
10. Ester, B.; Noelia, B.; Laura, C.-J.; Francesca, P.; Cristina, B.; Rosalba, L. Probiotic survival and in vitro digestion of *L. salivarius* spp. *salivarius* encapsulated by high homogenization pressures and incorporated into a fruit matrix. *LWT* **2019**, *111*, 883–888.
11. Galvão, A.M.; Rodrigues, S.; Fernandes, F.A. Probiotic dried apple snacks: Development of probiotic coating and shelf-life studies. *J. Food Process. Preserv.* **2020**, *44*, e14974. [CrossRef]
12. Wong, C.H.; Mak, I.E.K.; Li, D. Bilayer edible coating with stabilized *Lactobacillus plantarum* 299v improved the shelf life and safety quality of fresh-cut apple slices. *Food Packag. Shelf Life* **2021**, *30*, 100746. [CrossRef]
13. Azarkhavarani, P.R.; Ziaee, E.; Hosseini, S.M.H. Effect of encapsulation on the stability and survivability of *Enterococcus faecium* in a non-dairy probiotic beverage. *Food Sci. Technol.* **2019**, *25*, 233–242. [CrossRef]
14. Holkem, A.T.; Neto, E.J.S.; Nakayama, M.; Souza, C.J.; Thomazini, M.; Gallo, F.A.; Favaro-Trindade, C.S. Sugarcane juice with co-encapsulated *Bifidobacterium animalis* subsp. *lactis* BLC1 and proanthocyanidin-rich cinnamon extract. *Probiotics Antimicrob. Proteins* **2020**, *12*, 1179–1192. [CrossRef]
15. Mokhtari, S.; Jafari, S.M.; Khomeiri, M. Survival of encapsulated probiotics in pasteurized grape juice and evaluation of their properties during storage. *Food Sci. Technol.* **2019**, *25*, 120–129. [CrossRef]
16. Naga Sivudu, S.; Ramesh, B.; Umamahesh, K.; Vijaya Sarathi Reddy, O. Probiotication of tomato and carrot juices for shelf-life enhancement using micro-encapsulation. *J. Food Sci. Technol.* **2016**, *6*, 13–22.
17. Nami, Y.; Lornezhad, G.; Kiani, A.; Abdullah, N.; Haghshenas, B. Alginate-persian gum-prebiotics microencapsulation impacts on the survival rate of *Lactococcus lactis* ABRIINW-N19 in orange juice. *LWT* **2020**, *124*, 109190. [CrossRef]
18. Olivares, A.; Soto, C.; Caballero, E.; Altamirano, C. Survival of microencapsulated *Lactobacillus casei* (prepared by vibration technology) in fruit juice during cold storage. *Electron. J. Biotechnol.* **2019**, *42*, 42–48. [CrossRef]
19. Santos Monteiro, S.; Albertina Silva Beserra, Y.; Miguel Lisboa Oliveira, H.; Pasquali, M.A.d.B. Production of probiotic passion fruit (*Passiflora edulis* Sims f. *Flavicarpa* Deg.) drink using *Lactobacillus reuteri* and microencapsulation via spray drying. *Foods* **2020**, *9*, 335. [CrossRef] [PubMed]
20. Vivek, K.; Mishra, S.; Pradhan, R.C. Characterization of spray dried probiotic Sohiong fruit powder with *Lactobacillus plantarum*. *LWT* **2020**, *117*, 108699. [CrossRef]
21. Praepanitchai, O.-A.; Noomhorm, A.; Anal, A.K. Survival and behavior of encapsulated probiotics (*Lactobacillus plantarum*) in calcium-alginate-soy protein isolate-based hydrogel beads in different processing conditions (pH and temperature) and in pasteurized mango juice. *Biomed Res. Int.* **2019**, *2019*, 9768152. [CrossRef] [PubMed]
22. da Silva, T.M.; Pinto, V.S.; Soares, V.R.F.; Marotz, D.; Cichoski, A.J.; Zepka, L.Q.; Lopes, E.J.; da Silva, C.B.; de Menezes, C.R. Viability of microencapsulated *Lactobacillus acidophilus* by complex coacervation associated with enzymatic crosslinking under application in different fruit juices. *Food Res. Int.* **2021**, *141*, 110190. [CrossRef] [PubMed]

23. Rishabh, D.; Athira, A.; Preetha, R.; Nagamaniammai, G. Freeze dried probiotic carrot juice powder for better storage stability of probiotic. *J. Food Sci. Technol.* **2021**, *58*, 1–9. [CrossRef]

24. Gervasi, C.; Pellizzeri, V.; Vecchio, G.L.; Vadalà, R.; Foti, F.; Tardugno, R.; Cicero, N.; Gervasi, T. From by-product to functional food: The survival of *L. casei* shirota, *L. casei* immunitas and *L. acidophilus* johnsonii, during spray drying in orange juice using a maltodextrin/pectin mixture as carrier. *Nat. Prod. Res.* **2022**, *36*, 1–8. [CrossRef] [PubMed]

25. Massounga Bora, A.F.; Li, X.; Zhu, Y.; Du, L. Improved viability of microencapsulated probiotics in a freeze-dried banana powder during storage and under simulated gastrointestinal tract. *Probiotics Antimicrob. Proteins* **2019**, *11*, 1330–1339. [CrossRef] [PubMed]

26. Nilubol, S.; Wanchaitanawong, P. Viability of Lactobacillus plantarum TISTR 2075 in carrot tablet after fluidized bed drying. In Proceedings of the The National and International Graduate Research Conference, Khon Kaen, Thailand, 10 March 2017; pp. 155–165.

27. Srisuk, N.; Nopharatana, M.; Jirasatid, S. Co-encapsulation of *Dictyophora indusiata* to improve *Lactobacillus acidophilus* survival and its effect on quality of sweet fermented rice (Khoa-Mak) sap beverage. *J. Food Sci. Technol.* **2021**, *58*, 3598–3610. [CrossRef]

28. Hernández-Barrueta, T.; Martínez-Bustos, F.; Castaño-Tostado, E.; Lee, Y.; Miller, M.J.; Amaya-Llano, S.L. Encapsulation of probiotics in whey protein isolate and modified huauzontle's starch: An approach to avoid fermentation and stabilize polyphenol compounds in a ready-to-drink probiotic green tea. *LWT* **2020**, *124*, 109131. [CrossRef]

29. Yee, W.L.; Yee, C.L.; Lin, N.K.; Phing, P.L. Microencapsulation of *Lactobacillus acidophilus* NCFM incorporated with mannitol and its storage stability in mulberry tea. *Cienc. Agrotecnologia* **2019**, *43*, 1–11. [CrossRef]

30. Wulandari, N.; Suharna, N.; Yulinery, T.; Nurhidayat, N. Probiotication of black grass jelly [Mesona chinensis (Benth.)] by encapsulated *Lactobacillus plantarum* Mar8 for a ready to drink (RTD) beverages. *J. Agric. Sci. Technol.* **2019**, *15*, 375–386.

31. Arslan-Tontul, S.; Erbas, M.; Gorgulu, A. The use of probiotic-loaded single-and double-layered microcapsules in cake production. *Probiotics Antimicrob. Proteins* **2019**, *11*, 840–849. [CrossRef]

32. Mirzamani, S.; Bassiri, A.; Tavakolipour, H.; Azizi, M.; Kargozari, M. Fluidized bed microencapsulation of *Lactobacillus sporogenes* with some selected hydrocolloids for probiotic bread production. *J. Food Sci. Technol.* **2021**, *11*, 23–34.

33. Thang, T.D.; Hang, H.T.T.; Luan, N.T.; KimThuy, D.T.; Lieu, D.M. Survival survey of *Lactobacillus acidophilus* in additional probiotic bread. *TURJAF* **2019**, *7*, 588–592.

34. Bampi, G.B.; Backes, G.T.; Cansian, R.L.; de Matos, F.E.; Ansolin, I.M.A.; Poleto, B.C.; Corezzolla, L.R.; Favaro-Trindade, C.S. Spray chilling microencapsulation of *Lactobacillus acidophilus* and *Bifidobacterium animalis* subsp. *lactis* and its use in the preparation of savory probiotic cereal bars. *Food Bioproc. Technol.* **2016**, *9*, 1422–1428.

35. Bigdelian, E.; Razavi, S. Evaluation of survival rate and physicochemical properties of encapsulated bacteria in alginate and resistant starch in mayonnaise sauce. *Biotechnol. Bioprocess Eng.* **2014**, *4*, 1.

36. Qaziyani, S.D.; Pourfarzad, A.; Gheibi, S.; Nasiraie, L.R. Effect of encapsulation and wall material on the probiotic survival and physicochemical properties of synbiotic chewing gum: Study with univariate and multivariate analyses. *Heliyon* **2019**, *5*, e02144. [CrossRef] [PubMed]

37. Jouki, M.; Khazaei, N.; Rashidi-Alavijeh, S.; Ahmadi, S. Encapsulation of *Lactobacillus casei* in quince seed gum-alginate beads to produce a functional synbiotic drink powder by agro-industrial by-products and freeze-drying. *Food Hydrocoll.* **2021**, *120*, 106895. [CrossRef]

38. Kumar, B.V.; Vijayendra, S.V.N.; Reddy, O.V.S. Trends in dairy and non-dairy probiotic products-a review. *J. Food Sci. Technol.* **2015**, *52*, 6112–6124. [CrossRef]

39. Maciel, M.I.S.; de Souza, M.M.B. Prebiotics and Probiotics-Potential Benefits in Human Nutrition and Health. In *Prebiotics and Probiotics-Potential Benefits in Nutrition and Health*; IntechOpen: London, UK, 2020.

40. Oberoi, K.; Tolun, A.; Sharma, K.; Sharma, S. Microencapsulation: An overview for the survival of probiotic bacteria. *J. Microbiol. Biotechnol. Food Sci.* **2021**, *2021*, 280–287. [CrossRef]

41. Pech-Canul, A.d.l.C.; Ortega, D.; García-Triana, A.; González-Silva, N.; Solis-Oviedo, R.L. A brief review of edible coating materials for the microencapsulation of probiotics. *Coatings* **2020**, *10*, 197. [CrossRef]

42. Yao, M.; Xie, J.; Du, H.; McClements, D.J.; Xiao, H.; Li, L. Progress in microencapsulation of probiotics: A review. *Compr. Rev. Food Sci. Food Saf.* **2020**, *19*, 857–874. [CrossRef]

43. Frakolaki, G.; Giannou, V.; Kekos, D.; Tzia, C. A review of the microencapsulation techniques for the incorporation of probiotic bacteria in functional foods. *Crit. Rev. Food Sci. Nutr.* **2021**, *61*, 1515–1536. [CrossRef]

44. Rodrigues, F.; Cedran, M.; Bicas, J.; Sato, H. Encapsulated probiotic cells: Relevant techniques, natural sources as encapsulating materials and food applications-a narrative review. *Food Res. Int.* **2020**, *137*, 1016. [CrossRef]

45. Khalil, K.A. A review on microencapsulation in improving probiotic stability for beverages application. *Sci. Lett.* **2020**, *14*, 49–61. [CrossRef]

46. Silva, M.P.; Tulini, F.L.; Martins, E.; Penning, M.; Favaro-Trindade, C.S.; Poncelet, D. Comparison of extrusion and co-extrusion encapsulation techniques to protect *Lactobacillus acidophilus* LA3 in simulated gastrointestinal fluids. *LWT* **2018**, *89*, 392–399. [CrossRef]

47. Kim, J.U.; Kim, B.; Shahbaz, H.M.; Lee, S.H.; Park, D.; Park, J. Encapsulation of probiotic *Lactobacillus acidophilus* by ionic gelation with electrostatic extrusion for enhancement of survival under simulated gastric conditions and during refrigerated storage. *Int. J. Food Sci. Technol.* **2017**, *52*, 519–530. [CrossRef]

48. Singh, P.; Medronho, B.; Miguel, M.G.; Esquena, J. On the encapsulation and viability of probiotic bacteria in edible carboxymethyl cellulose-gelatin water-in-water emulsions. *Food Hydrocoll.* **2018**, *75*, 41–50. [CrossRef]

49. Picone, C.S.F.; Bueno, A.C.; Michelon, M.; Cunha, R.L. Development of a probiotic delivery system based on gelation of water-in-oil emulsions. *LWT* **2017**, *86*, 62–68. [CrossRef]

50. Vaishanavi, S.; Preetha, R. Soy protein incorporated nanoemulsion for enhanced stability of probiotic (*Lactobacillus delbrueckii* subsp. *bulgaricus*) and its characterization. *Mater. Today* **2021**, *40*, S148–S153.

51. Wang, L.; Song, M.; Zhao, Z.; Chen, X.; Cai, J.; Cao, Y.; Xiao, J. *Lactobacillus acidophilus* loaded pickering double emulsion with enhanced viability and colon-adhesion efficiency. *LWT* **2020**, *121*, 108928. [CrossRef]

52. Qin, X.-S.; Gao, Q.-Y.; Luo, Z.-G. Enhancing the storage and gastrointestinal passage viability of probiotic powder (*Lactobacillus Plantarum*) through encapsulation with pickering high internal phase emulsions stabilized with WPI-EGCG covalent conjugate nanoparticles. *Food Hydrocoll.* **2021**, *116*, 106658. [CrossRef]

53. Tylkowski, B.; Trojanowska, A.; Giamberini, M.; Tsibranska, I.; Nowak, M.; Marciniak, Ł.; Jastrzab, R. Microencapsulation in food chemistry. *J. Membr. Sci. Res.* **2017**, *3*, 265–271.

54. Sharifi, S.; Rezazad-Bari, M.; Alizadeh, M.; Almasi, H.; Amiri, S. Use of whey protein isolate and gum Arabic for the co-encapsulation of probiotic *Lactobacillus plantarum* and phytosterols by complex coacervation: Enhanced viability of probiotic in Iranian white cheese. *Food Hydrocoll.* **2021**, *113*, 106496. [CrossRef]

55. Timilsena, Y.P.; Akanbi, T.O.; Khalid, N.; Adhikari, B.; Barrow, C.J. Complex coacervation: Principles, mechanisms and applications in microencapsulation. *Int. J. Biol. Macromol.* **2019**, *121*, 1276–1286. [CrossRef]

56. Zhao, M.; Huang, X.; Zhang, H.; Zhang, Y.; Gänzle, M.; Yang, N.; Nishinari, K.; Fang, Y. Probiotic encapsulation in water-in-water emulsion via heteroprotein complex coacervation of type-A gelatin/sodium caseinate. *Food Hydrocoll.* **2020**, *105*, 105790. [CrossRef]

57. Arslan, S.; Erbas, M.; Tontul, I.; Topuz, A. Microencapsulation of probiotic *Saccharomyces cerevisiae* var. *boulardii* with different wall materials by spray drying. *LWT* **2015**, *63*, 685–690.

58. Jantzen, M.; Göpel, A.; Beermann, C. Direct spray drying and microencapsulation of probiotic *Lactobacillus reuteri* from slurry fermentation with whey. *J. Appl. Microbiol.* **2013**, *115*, 1029–1036. [CrossRef]

59. Raddatz, G.C.; Poletto, G.; de Deus, C.; Codevilla, C.F.; Cichoski, A.J.; Jacob-Lopes, E.; de Menezes, C.R. Use of prebiotic sources to increase probiotic viability in pectin microparticles obtained by emulsification/internal gelation followed by freeze-drying. *Food Res. Int.* **2020**, *130*, 108902. [CrossRef] [PubMed]

60. Shoji, A.S.; Oliveira, A.C.; Balieiro, J.D.C.; Freitas, O.D.; Thomazini, M.; Heinemann, R.J.B.; Favaro-Trindade, C.S. Viability of *L. acidophilus* microcapsules and their application to buffalo milk yoghurt. *Food Bioprod. Process.* **2013**, *91*, 83–88. [CrossRef]

61. Halim, M.; Mustafa, N.A.M.; Othman, M.; Wasoh, H.; Kapri, M.R.; Ariff, A.B. Effect of encapsulant and cryoprotectant on the viability of probiotic *Pediococcus acidilactici* ATCC 8042 during freeze-drying and exposure to high acidity, bile salts and heat. *LWT* **2017**, *81*, 210–216. [CrossRef]

62. Liu, H.; Cui, S.W.; Chen, M.; Li, Y.; Liang, R.; Xu, F.; Zhong, F. Protective approaches and mechanisms of microencapsulation to the survival of probiotic bacteria during processing, storage and gastrointestinal digestion: A review. *Crit. Rev. Food Sci. Nutr.* **2019**, *59*, 2863–2878. [CrossRef] [PubMed]

63. Arslan-Tontul, S.; Erbas, M. Single and double layered microencapsulation of probiotics by spray drying and spray chilling. *LWT* **2017**, *81*, 160–169. [CrossRef]

64. Haffner, F.B.; Diab, R.; Pasc, A. Encapsulation of probiotics: Insights into academic and industrial approaches. *AIMS Mater. Sci.* **2016**, *3*, 114–136. [CrossRef]

65. Sánchez-Portilla, Z.; Melgoza-Contreras, L.M.; Reynoso-Camacho, R.; Pérez-Carreón, J.I.; Gutiérrez-Nava, A. Incorporation of *Bifidobacterium sp.* into powder products through a fluidized bed process for enteric targeted release. *J. Dairy Sci.* **2020**, *103*, 11129–11137. [CrossRef] [PubMed]

66. Broeckx, G.; Vandenheuvel, D.; Claes, I.J.; Lebeer, S.; Kiekens, F. Drying techniques of probiotic bacteria as an important step towards the development of novel pharmabiotics. *Int. J. Pharm.* **2016**, *505*, 303–318. [CrossRef] [PubMed]

67. Călinoiu, L.-F.; Ştefănescu, B.E.; Pop, I.D.; Muntean, L.; Vodnar, D.C. Chitosan coating applications in probiotic microencapsulation. *Coatings* **2019**, *9*, 194. [CrossRef]

68. Beldarrain-Iznaga, T.; Villalobos-Carvajal, R.; Leiva-Vega, J.; Armesto, E.S. Influence of multilayer microencapsulation on the viability of *Lactobacillus casei* using a combined double emulsion and ionic gelation approach. *Food Bioprod. Process.* **2020**, *124*, 57–71. [CrossRef]

69. Ramos, P.E.; Cerqueira, M.A.; Teixeira, J.A.; Vicente, A.A. Physiological protection of probiotic microcapsules by coatings. *Crit. Rev. Food Sci. Nutr.* **2018**, *58*, 1864–1877. [CrossRef]

70. Colín-Cruz, M.; Pimentel-González, D.; Carrillo-Navas, H.; Alvarez-Ramírez, J.; Guadarrama-Lezama, A. Co-encapsulation of bioactive compounds from blackberry juice and probiotic bacteria in biopolymeric matrices. *LWT* **2019**, *110*, 94–101. [CrossRef]

71. Samedi, L.; Charles, A.L. Viability of 4 probiotic bacteria microencapsulated with arrowroot starch in the simulated gastrointestinal tract (GIT) and yoghurt. *Foods* **2019**, *8*, 175. [CrossRef]

72. Zaeim, D.; Sarabi-Jamab, M.; Ghorani, B.; Kadkhodaee, R. Double layer co-encapsulation of probiotics and prebiotics by electro-hydrodynamic atomization. *LWT* **2019**, *110*, 102–109. [CrossRef]

73. Shinde, T.; Sun-Waterhouse, D.; Brooks, J. Co-extrusion encapsulation of probiotic *Lactobacillus acidophilus* alone or together with apple skin polyphenols: An aqueous and value-added delivery system using alginate. *Food Bioproc. Tech.* **2014**, *7*, 1581–1596. [CrossRef]

74. Gheorghita Puscaselu, R.; Lobiuc, A.; Dimian, M.; Covasa, M. Alginate: From food industry to biomedical applications and management of metabolic disorders. *Polymers* **2020**, *12*, 2417. [CrossRef]
75. Martău, G.A.; Mihai, M.; Vodnar, D.C. The use of chitosan, alginate, and pectin in the biomedical and food sector-biocompatibility, bioadhesiveness, and biodegradability. *Polymers* **2019**, *11*, 1837. [CrossRef]
76. Pavli, F.; Tassou, C.; Nychas, G.-J.E.; Chorianopoulos, N. Probiotic incorporation in edible films and coatings: Bioactive solution for functional foods. *Int. J. Mol. Sci.* **2018**, *19*, 150. [CrossRef]
77. Mettu, S.; Hathi, Z.; Athukoralalage, S.; Priya, A.; Lam, T.N.; Ong, K.L.; Lin, C.S.K. Perspective on constructing cellulose-hydrogel-based gut-like bioreactors for growth and delivery of multiple-strain probiotic bacteria. *J. Agric. Food Chem.* **2021**, *69*, 4946–4959. [CrossRef]
78. Arepally, D.; Goswami, T.K. Effect of inlet air temperature and gum Arabic concentration on encapsulation of probiotics by spray drying. *LWT* **2019**, *99*, 583–593. [CrossRef]
79. Kwiecień, I.; Kwiecień, M. Application of polysaccharide-based hydrogels as probiotic delivery systems. *Gels* **2018**, *4*, 47. [CrossRef]
80. Lara-Espinoza, C.; Carvajal-Millán, E.; Balandrán-Quintana, R.; López-Franco, Y.; Rascón-Chu, A. Pectin and pectin-based composite materials: Beyond food texture. *Molecules* **2018**, *23*, 942. [CrossRef] [PubMed]
81. Noreen, A.; Akram, J.; Rasul, I.; Mansha, A.; Yaqoob, N.; Iqbal, R.; Zia, K.M. Pectins functionalized biomaterials; a new viable approach for biomedical applications: A review. *Int. J. Biol. Macromol.* **2017**, *101*, 254–272. [CrossRef]
82. Zhu, Y.; Wang, Z.; Bai, L.; Deng, J.; Zhou, Q. Biomaterial-based encapsulated probiotics for biomedical applications: Current status and future perspectives. *Mater. Des.* **2021**, *210*, 110018. [CrossRef]
83. Patel, J.; Maji, B.; Moorthy, N.H.N.; Maiti, S. Xanthan gum derivatives: Review of synthesis, properties and diverse applications. *RSC Adv.* **2020**, *10*, 27103–27136. [CrossRef] [PubMed]
84. Razavi, S.; Janfaza, S.; Tasnim, N.; Gibson, D.L.; Hoorfar, M. Microencapsulating polymers for probiotics delivery systems: Preparation, characterization, and applications. *Food Hydrocoll.* **2021**, *120*, 106882. [CrossRef]
85. Al-Hassan, A. Gelatin from camel skins: Extraction and characterizations. *Food Hydrocoll.* **2020**, *101*, 105457. [CrossRef]
86. Li, X.; Chen, W.; Jiang, J.; Feng, Y.; Yin, Y.; Liu, Y. Functionality of dairy proteins and vegetable proteins in nutritional supplement powders: A review. *Int. Food Res. J.* **2019**, *26*, 1651–1664.
87. Minj, S.; Anand, S. Whey proteins and its derivatives: Bioactivity, functionality, and current applications. *Dairy* **2020**, *1*, 233–258. [CrossRef]
88. Abd El-Salam, M.H.; El-Shibiny, S. Preparation and properties of milk proteins-based encapsulated probiotics: A review. *Dairy Sci. Technol.* **2015**, *95*, 393–412. [CrossRef]
89. Fathi, M.; Donsi, F.; McClements, D.J. Protein-based delivery systems for the nanoencapsulation of food ingredients. *Compr. Rev. Food Sci. Food Saf.* **2018**, *17*, 920–936. [CrossRef]
90. Dong, Q.Y.; Chen, M.Y.; Xin, Y.; Qin, X.Y.; Cheng, Z.; Shi, L.E.; Tang, Z.X. Alginate-based and protein-based materials for probiotics encapsulation: A review. *Int. J. Food Sci. Technol.* **2013**, *48*, 1339–1351. [CrossRef]
91. Nahum, V.; Domb, A.J. Recent developments in solid lipid microparticles for food ingredients delivery. *Foods* **2021**, *10*, 400. [CrossRef] [PubMed]
92. Serna-Cock, L.; Vallejo-Castillo, V. Probiotic encapsulation. *Afr. J. Microbiol. Res.* **2013**, *7*, 4743–4753.
93. Dordevic, S.; Dordevic, D.; Sedlacek, P.; Kalina, M.; Tesikova, K.; Antonic, B.; Tremlova, B.; Treml, J.; Nejezchlebova, M.; Vapenka, L. Incorporation of Natural Blueberry, Red Grapes and Parsley Extract By-Products into the Production of Chitosan Edible Films. *Polymers* **2021**, *13*, 3388. [CrossRef] [PubMed]
94. Khumpouk, P.; Saichanaphan, N.; Khimmakthong, U. The efficiency of polysaccharide microencapsulation in improving survival of probiotic bacteria. *Songklanakarin J. Sci. Technol.* **2022**, *44*, 184–190.
95. Youssef, M.; Korin, A.; Zhan, F.; Hady, E.; Ahmed, H.Y.; Geng, F.; Chen, Y.; Li, B. Encapsulation of *Lactobacillus salivarius* in single and dual biopolymer. *J. Food Eng.* **2021**, *294*, 110398. [CrossRef]
96. Riaz, T.; Iqbal, M.W.; Saeed, M.; Yasmin, I.; Hassanin, H.A.; Mahmood, S.; Rehman, A. In vitro survival of *Bifidobacterium bifidum* microencapsulated in zein-coated alginate hydrogel microbeads. *J. Microencapsul.* **2019**, *36*, 192–203. [CrossRef] [PubMed]
97. Gaudreau, H.; Champagne, C.P.; Remondetto, G.E.; Bazinet, L.; Subirade, M. Effect of catechins on the growth of oxygen-sensitive probiotic bacteria. *Food Res. Int.* **2013**, *53*, 751–757. [CrossRef]
98. Peris, M.; Rubio-Arraez, S.; Castelló, M.L.; Ortolá, M.D. From the laboratory to the kitchen: New alternatives to healthier bakery products. *Foods* **2019**, *8*, 660. [CrossRef] [PubMed]

MDPI